L. RESHETOV

# SELF-ALIGNING MECHANISMS

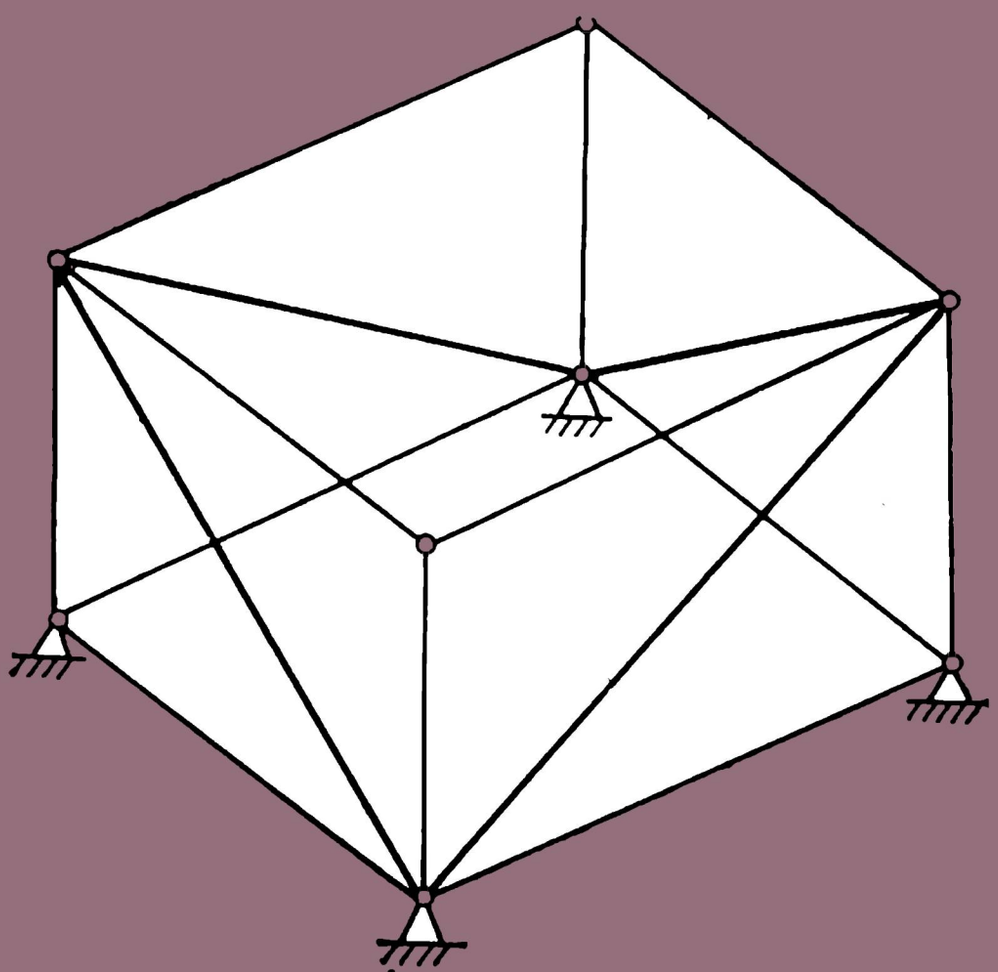

Mir Publishers Moscow

L. RESHETOV

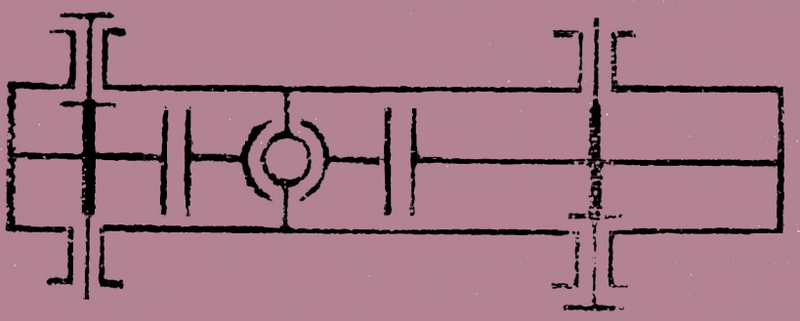

# SELF-ALIGNING MECHANISMS

Mir Publishers
Moscow

Л. Н. Решетов

# Самоустанавливающиеся механизмы

## СПРАВОЧНИК

Издательство «Машиностроение»
Москва

ИЗДАТЕЛЬСТВО
МИР

L. RESHETOV

# SELF-ALIGNING MECHANISMS

*Translated from Russian*
*by*
Leo M. Sachs

**Mir Publishers**
**Moscow**

*First published 1982*
*Revised from the 1979 Russian edition*

## The Russian Alphabet and Transliteration

| | | | | | |
|---|---|---|---|---|---|
| А а | a | К к | k | Х х | kh |
| Б б | b | Л л | l | Ц ц | ts |
| В в | v | М м | m | Ч ч | ch |
| Г г | g | Н н | n | Ш ш | sh |
| Д д | d | О о | o | Щ щ | shch |
| Е е | e | П п | p | ъ | ” |
| Ё ё | e | Р р | r | ы | y |
| Ж ж | zh | С с | s | ь | ’ |
| З з | z | Т т | t | Э э | e |
| И и | i | У у | u | Ю ю | yu |
| Й й | y | Ф ф | f | Я я | ya |

## The Greek Alphabet

| | | | | | |
|---|---|---|---|---|---|
| Α α | Alpha | Ι ι | Iota | Ρ ρ | Rho |
| Δ β | Beta | Κ κ | Kappa | Σ σ | Sigma |
| Γ γ | Gamma | Λ λ | Lambda | Τ τ | Tau |
| Δ δ | Delta | Μ μ | Mu | Υ υ | Upsilon |
| Ε ε | Epsilon | Ν ν | Nu | Φ φ | Phi |
| Ζ ζ | Zeta | Ξ ξ | Xi | Χ χ | Chi |
| Η η | Eta | Ο ο | Omicron | Ψ ψ | Psi |
| Θ θ ϑ | Theta | Π π | Pi | Ω ω | Omega |

*На английском языке*

© Издательство «Машиностроение», 1979
© English translation, Mir Publishers, 1982

# CONTENTS


Foreword . . . . . 8

*Chapter 1.* **Redundant Constraints and Mobilities in Mechanisms** . . . 9

1.1. General . . . . . 9
1.2. Checking Mechanisms for Redundant Constraints . . . . . 13
1.3. Determining Classes of Kinematic Pairs without Influence of Clearances on Their Mobility . . . . . 20
1.4. Determining Classes of Kinematic Pairs Allowing for Influence of Clearances on Their Mobility . . . . . 31
1.5. Detecting Particularly Harmful Redundant Constraints by Planar or Spherical Diagram of Mechanism . . . . . 34
1.6. Kinematic Connections with Hydraulic and Electric Restraints 38
1.7. Use of Kinematic Connections in Rational Mechanisms . . . . 40
1.8. Kinematic Connections in Electric Locomotives . . . . . 42
1.9. Typical Errors in Selection of Structural Designs of Mechanisms 47
1.10. New Method of Determining Redundant Constraints and Mobilities of Mechanisms . . . . . 51
1.11. Non-Planar Constraints and Mobilities for Investigating Structure of Mechanisms . . . . . 61
1.12. Influence of Friction Upon Self-Aligning of Mechanisms . . . . 68
1.13. Resistance to Self-Alignment in Cylindrical Pairs . . . . . 69
1.14. Resistance to Self-Alignment in Planar Pair . . . . . 70
1.15. Resistance to Self-Alignment in Spherical Pairs . . . . . 74
1.16. Resistance to Self-Alignment of Antifriction Bearing . . . . . 76
1.17. Conclusions and Suggestions . . . . . 79

*Chapter 2.* **Planar Mechanisms with Lower Pairs** . . . . . 82

2.1. Rational Designs of Fixed Connections . . . . . 82
2.2. Connection of Traction Motor with Single-Motor Bogie . . . . 93
2.3. Supports for Rotary Shafts . . . . . 94
2.4. Guideways for Linear Motion . . . . . 104
2.5. Wedge Mechanisms . . . . . 111
2.6. Screw Mechanisms . . . . . 113
2.7. Slider-Crank Mechanism . . . . . 118
2.8. Crank-and-Rocker Mechanism . . . . . 133
2.9. Parallel Crank Mechanism . . . . . 136
2.10. Link Gear Mechanisms . . . . . 140
2.11. Degeneration of Assur's Groups . . . . . 145
2.12. Structural Groups of Zero Mobility . . . . . 150

2.13. Self-Aligning Planar Structural Groups of Members of Mechanisms 156
2.14. Centrifugal Governors . . . . . 163
2.15. Valves and Gates . . . . . 170
2.16. Conclusions and Suggestions . . . . . 174

*Chapter 3.* **Three-Dimensional Mechanisms with Lower Pairs (Turning Joints)** . . . . . 177

3.1. Multiarm Groups . . . . . 177
3.2. Hydraulic Drive Mechanisms . . . . . 187
3.3. Helicopter Mechanisms . . . . . 192
3.4. Mechanisms of Gyration Crushers . . . . . 199
3.5. Universal Joints . . . . . 205
3.6. Hooke's Joints with High-Class Pairs . . . . . 213
3.7. Flexible Hooke's Joints . . . . . 217
3.8. Unconventional Double Hooke's Joint . . . . . 219
3.9. Locomotive Mechanisms . . . . . 222
3.10. Main Mechanisms of Current Collectors . . . . . 231
3.11. Current Collector with Two Mobilities . . . . . 241
3.12. Mechanisms of Lift Springs . . . . . 245
3.13. Transverse Rigidity of a Current Collector Having Two Levers on the Main Shaft . . . . . 253
3.14. Transverse Rigidity of a Current Collector with One Lever on the Main Shaft . . . . . 264
3.15. Contact System for Low Temperatures . . . . . 269
3.16. Conclusions and Recommendations . . . . . 273

*Chapter 4.* **Mechanisms with Higher Pairs** . . . . . 274

4.1. Cam Mechanisms . . . . . 274
4.2. Power Contacts of Electric Apparatus . . . . . 278
4.3. Contact Devices in Control Circuitry (Low-Current) . . . . . 280
4.4. Gear Trains . . . . . 282
4.5. Mechanisms with Single Idler . . . . . 290
4.6. Mechanisms with Two Intermediate Gears or Idlers . . . . . 304
4.7. Gearing in Load-Handling Machines . . . . . 304
4.8. Classification of Traction Drives . . . . . 314
4.9. Rational Designs of Traction Reduction Gears . . . . . 316
4.10. High-Speed Traction Drive . . . . . 322
4.11. Mechanisms with Bevel Gears . . . . . 324
4.12. Cylindrical-Bevel Reduction Gear . . . . . 327
4.13. Mechanisms of Friction Variable-Speed Drives . . . . . 331
4.14. Automotive Transmission (Gearbox) . . . . . 334
4.15. Multishift Transmissions with Return Stages . . . . . 335
4.16. Self-Alignment in Traction Gearings . . . . . 339
4.17. Conclusions and Suggestions . . . . . 341

*Chapter 5.* **Planetary Mechanisms** . . . . . 344

5.1. Mobilities in Single-Row Mechanisms . . . . . 344
5.2. Friction in Connection Mechanisms . . . . . 353
5.3. Designs of Single-Row Planetary Mechanisms . . . . . 365
5.4. Tolerances in Single-Row Mechanisms . . . . . 374

5.5. Multirow Single-Stage Reduction Gear with Straight Teeth . . . 378
5.6. Multisatellite Mechanisms . . . . . 379
5.7. Single-Row Planetary Mechanism with Six Self-Aligning Satellite Gears . . . . . 384
5.8. Positive Planetary Gearings for Big Transmission Ratios . . . . 387
5.9. Flat Planetary Mechanism with Self-Aligning Satellite Gear . . . 389
5.10. Mechanism with Free Carrier . . . . . 390
5.11. Multiple and Closed Planetary Mechanisms . . . . . 394
5.12. Reduction Gears of Wheel Motors . . . . . 401
5.13. Method of Structural Groups for Investigating Self-Alignment of Planetary Mechanisms . . . . . 410
5.14. Strain Wave Gearings . . . . . 423
5.15. Conclusions and Suggestions . . . . . 431

*Chapter 6.* **Load Handling Mechanisms** . . . . . 433

6.1. Rope Drum Drive . . . . . 433
6.2. Pulleys . . . . . 435
6.3. Grabs . . . . . 436
6.4. Crane Carriages . . . . . 439
6.5. Loading Bridges and Movable Conveyors . . . . . 441
6.6. Travelling Cranes . . . . . 443
6.7. Undercarriage of Building Cranes . . . . . 445
6.8. Cranes with Folding Boom (Portal Cranes) . . . . . 448
6.9. Elevators (Lifts) . . . . . 455
6.10. Roller Supports of Rotary Kilns and Transfer Drums . . . . . 468
6.11. Choice of Design of Shoe Brakes . . . . . 479
6.12. Bridges . . . . . 495
6.13. Bogies for Rolling Stock . . . . . 506
6.14. Conclusions and Recommendations . . . . . 520
References . . . . . 523

Index . . . . . 526

# FOREWORD

Statically indeterminate trusses have been long studied. It has been proved that it takes a redundant link for static indeterminacy to evolve. This is believed to be true of mechanisms as well. However, one encounters mechanisms with a redundant link but very rarely, and therefore their study has been considered unnecessary. It has been found, though, that static indeterminacy may take place in mechanisms having no redundant links, should their kinematic pairs impose redundant constraints, i.e. those which fail to reduce the mobility of the mechanism (at one time such constraints were also called passive). It appears that the majority of mechanisms used in machinery are subject to such constraints.

Redundant constraints do considerable harm. They call for higher accuracy in manufacture and this makes the machine considerably more costly, and more often than not such accuracy is altogether unattainable on acount of deformations. The load-bearing capacity and efficiency are reduced so the weight and size have to be increased. Therefore, in engineering design, the scientific selection of kinematic pairs (the connections of the links) must strive to eliminate redundant constraints. Mechanisms free of redundant constraints are self-aligning, which explains the title of this book. Its content is dedicated to the methods of analysis and design of such mechanisms and to their applications in various fields.

Section 1.11 was written by E. Y. Kachalova (Budyka); Sections 1.12 through 1.16 were written by N. E. Shamaidenko, Cand. Tech. Sc.; Section 4.13 was written by the author in collaboration with J. J. Gaipel; Section 5.13 was written by the author in collaboration with G. A. Chernova; Section 5.4 was written by the author in collaboration with L. L. Rusak, Cand. Tech. Sc.; the rest of the book was written by the title author with the assistance of N. L. Reshetov.

The helpful assistance and valuable suggestions on improving the manuscript made by R. V. Frolov, Corresponding Member of USSR Academy of Sciences, are greatfully acknowledged,

*L. N. Reshetov, D. Sc.,*
*Honorary Inventor of*
*the Russian Federation*

Chapter 1

# REDUNDANT CONSTRAINTS AND MOBILITIES IN MECHANISMS

## 1.1. General

In the quantity production of machines, in automotive industry in particular, the process of assembly is fairly simple, since it involves merely bringing together the components and fixing the threaded connections, with no manual adjustment required. In individual production of large-size machinery, however, notwithstanding multi-pass machining, the accuracy of the component parts more often than not is insufficient. Therefore, the assembling entails manual fitting which is extremely labor-consuming and far from readily susceptible to mechanization.

It is particularly difficult to attain the precise dimensions of links that are made up of several parts which, when connected, might have their tolerances added together beyond the permissible value. It is, therefore, very important to select the design of a mechanism so that the accuracy requirements, put before its links, should be relatively low. The said is true of statically determinate mechanisms, i.e. those devoid of redundant[1] (passive) constraints and having their links self-aligning.

*Redundant (passive) constraints are those whose elimination would not step up the mobility of a mechanism.*

The dimensions of links may vary throughout the service life on account of sagging of the foundation, of wearout and adjustments of clearance in joints, of elastic deformation (e.g. deflection of shafts), of thermal expansion, and also due to maintenance and assembling errors (for instance, if bearing inserts have been confused). The variation of the link dimensions would not affect a statically determinate mechanism. Hence, statically determinate mechanisms save labor and enhance the reliability.

Redundant constraints in a mechanism are harmful, for they increase the labor consumption in the manufacture and operation of mechanisms and affect their reliability.

[1]We will use here the expression "redundant constraints" (suggested by N. I. Kolchin) as conveying their true essence.

In a kinematic pair redundant constraints are harmless since in most cases the pair can be fabricated with adequate accuracy. Examples of such pairs are a splined joint made by broaching the hole and milling the shaft with a hob, gears with the teeth engagement factor in excess of 1.0 (modern techniques of making teeth profiles enable simultaneous operation of two pairs of teeth, a great engagement factor enhancing the gear performance), and an antifriction bearing.

The performance of kinematic pairs can be enhanced, however, by other means. Thus, rattling in four-stroke diesel engines can be kept under control by observing adequate clearances in connecting-rod ends. In two-stroke diesels, where forces in the ends do not alternate, the clearances can be not as strict for they do not influence the rattling. Unfortunately, this advantage of two-stroke diesels is not shared by two-stroke carburettor engines with their throttle control.

The required precision of gears, the dynamic loads and noise are dependent on the peripheral velocity. In some planetary gearing patterns the velocity is very high. It may be significantly reduced, however, by appropriate selection of the design, which is of essential importance for high-speed mechanisms.

When toothed and worm gearings are arranged in series, the high-speed stage should be the worm one, and the low-speed stage should be the toothed gearing. This provides a relatively low peripheral velocity of the toothed gearing, and the latter may be manufactured to a lesser precision.

Statically determinate and indeterminate systems associated with trusses have been thoroughly studied. It has been found that statically determinate systems do not yield significant advantages. The dimensions of the bars or rods are always fitted to suit job by drilling-out (in riveted structures), or by welding the members (in welded ones). Therefore, a statically determinate system associated with a truss would not bring down the accuracy requirements. One practically never encounters a case where bars are expected to perform at temperatures differing by hundreds of degrees. With the propagation of welded structures the advantages of a statically indeterminate system become more pronounced. With a great number of rivets, a loose one would affect the load-bearing capacity of a truss but slightly, whereas a loose weld would impair this capacity significantly greater. This is particularly true of a statically determinate truss where the load-bearing capacity can be reduced to the critical value.

The foregoing refers to the inner static indeterminacy of a truss. There also exists the outer static indeterminacy as, for example, in a multisupport truss. Such a truss is responsive to various degrees of sagging of the foundations of its supports. To avoid this, statically determinate Herber's and Wichert's designs are used in bridge construction.

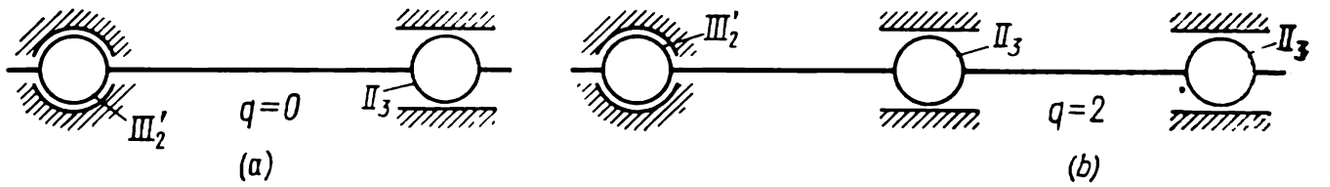


Fig. 1.1. Diagram of shaft bearings
(*a*) correct; (*b*) wrong

Now and again, mechanisms free of redundant constraints were developed by design engineers ignorant of the theory of the structure of mechanisms; more often than not they failed to eliminate all the redundant constraints.

Let us consider the advantages of mechanisms devoid of redundant constraints in two simplified exemplary cases. In a common slider-crank mechanism the lengths of the members may vary from the nominal values by several millimeters. This is used in practice for adjusting the spacing of the piston and the cover by setting an insert or spacer between the body and the end of the connecting-rod. However, in a twin mechanism, where two connecting-rods are associated with the common slider, the tolerances on the lengths of the members are measured not in millimeters, but in microns. It also takes great accuracy to ensure parallelism of the cranks.

Let us take for our second example a shaft supported by two bearings (Fig. 1.1*a*). If the bearings are made as shown in this drawing, they may be set with fairly broad tolerances (up to several millimeters). If the shaft is supported by three bearings (Fig. 1.1*b*), the required setting accuracy will be in the micron range, irrespective of the construction of the bearings.

Tolerances on the links depend on whether the mecanism is statically determinate. When the mechanism is statically determinate, the dimensions of the links all but fail to influence the forces being transmitted, and the tolerances on their dimensions may be loose, which is always desirable. With the statically indeterminate mechanism, the forces being transmitted depend on the deformation of the links. The deformation being very small (with the stress of

the material being 200 kg(f)/cm$^2$, which is often the case in practice, considering longitudinal bending, deformation of steel with $E = 2 \times 10^6$ is 0.1 mm per metre), the dimensions of the members are to be maintained with a great accuracy, lest the members intended for joint performance may strongly interfere each other in operation (in some cases the very assembling of the mechanism might prove impossible). The friction would grow considerably, and the efficiency factor would diminish. Thus, it is ill-advisable to use statically indeterminate mechanisms.

Consequently, it can be stated that for a mechanism provided with broad tolerances on the dimensions of its members to perform reliably, it should have no redundant constraints. Exceptions may be solely the cases where the links incorporate springs, or where the links are intended to work in bending with considerable deformation.

The harmful role played by redundant constraints in steam boilers is commonly known. Of particularly ill fame in this respect was the steam engine boiler. Engine-drivers were well aware of the fact that mere blow-holes in the furnace (with the grate exposed) resulted in smoke-tube leaks. This was caused by streams of the cold air reaching some of the smoke-tubes and bringing about their cooling-down, and, hence, their contraction leading to leaks. Straight smoke and flue tubes set into two rigid tube sheets present a system that is multiply statically indeterminate. As their thermal duty, and, consequently, their heat expansion cannot be the same, great strains are developed in the tubes, causing their leaking in the areas where they are secured by expansion or flaring-out. A similar phenomenon was observed in Garbe's stationary vertical water-tube boilers.

For this reason straight tubes have been replaced in present-day boilers with bent ones whose flexibility does away with the strains causing leaks. It goes without saying that even some of the tubes could not be left to remain straight.

For the same reason, V. G. Shukhov's water-tube boilers were rejected due to their straight tubes, although they had come as a breakthrough in boiler engineering and had been widely used for many years.

The first constructions of machinery had a considerable number of redundant constraints. Those were the times when the consumption of labor and time by their manufacture was of small importance. Then came the period of gradual introduction of mechanisms free of redundant constraints (Sellers's bearings, self-aligning antifriction bearings, cylindrical crossheads, etc.). Redundant constraints had

been in abundance in steam locomotives, but the trend toward reducing their number had made itself seen likewise long ago (Tate's hinged connections in boilers, axle boxes of the Tsar's system, the Hugyins ball inserts incorporated by prominent designer A. Y. Malokhovski in the "C" Series of steam locomotives). However, redundant constraints linger today in many a machine and mechanism for no reason whatsoever, complicating as they do the manufacture and operation and rising the costs involved.

It is particularly important to avoid redundant constraints in the design of mechanisms, in which some of the members are expected to operate under elevated temperatures (e.g. the regulating and control mechanisms of steam and gas turbines), for this would enhance their performance reliability and reduce friction. A major advantage of self-aligning mechanisms is the fact that the value and location of forces are independent of the tolerances, clearances and preloads.

It enables one to create mechanisms with uniform loading of the kinematic pairs—of bearings, gear teeth, brake shoes, etc. The load-bearing capacity and durability rise accordingly. Design engineers should be also aware of the fact that the design analysis of self-aligning mechanisms involves no deformation equations which are hard to solve, so the designing process is facilitated.

For numerous mechanisms, the number of redundant constraints equals that of dimensions requiring stringent tolerances; sometimes, the last-mentioned number is considerably greater than the number of redundant constraints. Therefore, it is the very presence of redundant constraints in a mechanism that is of concern, not their amount.

The examples quoted above to show the harm done by redundant constraints enable us to devise two major rules of designing self-aligning mechanisms:

—each shaft should be supported by no more than two bearings;

—twin or double mechanisms should be avoided at all costs, i.e. with the input and output links being the same, there should be no two transmitting mechanisms between them (an exception can be made solely in cases where an equalizing device is provided).

## 1.2 Checking Mechanisms for Redundant Constraints

It has been explained above that linear and angular deviations in the sizes of the members would not affect the performance of a mechanism free of redundant constraints. This gives rise to a general concept of designing rational mechanisms: a rational mechanism should be assembled without preloads and interference fits even if

the dimensions of the members deviate from nominal ones (both linear and angular). In other words, variation in the angular and linear dimensions of the members in a rational mechanism should cause no preload (meaning variation in the linear and angular dimensions of the members alone and not of the kinematic pairs).

The rule can be also applied as follows. Let us cut one of the links. The kinematics of a rational mechanism should provide the possibility of reconnecting it without a preload by bringing together the halves of the cut link by moving in the three directions and by their relative rotation around the three orthogonal axes without deformation of the links.

When the method suggested by S. A. Popov is used, the process of assembling the mechanisms should be considered. The kinematic pair in the loop, which is the last to be assembled, should be considered, and the linear bringing together of the links should be followed-up in the directions of the three orthogonal axes and by rotation about the three axes. The amount of these motions does not include the relative motion of the links yielded by the mobility of the pair itself, but they should be considered while evaluating the mobility remaining in the mechanism.

If approaching displacement of links can be performed by moving one link to another or vice versa, then one of the motions is used in assembling of the mechanism (to close the loop), while the other remains in the mechanism as a mobility. If, on the other hand, some of the motions involved in the bringing together would not be attained by the mobilities of the kinematic pairs, but solely at the cost of deformation of the members, this indicates the existence of redundant constraints.

Let us consider it in case of crank-and-rocker mechanism $OABC$ of Fig. 1.2 (the pairs are denoted by the numerator) having two rotatable pairs $O$ and $C$ and two spherical-joint pairs $A$ and $B$. The pair to be assembled last in this system is the one denoted $B$.

Let us consider the approaching motions of the links in assembling:

along $x$-axis—by rotating the crank $AO$ and the rocker $BC$; there remains the mobility—the main one in the mechanism;

along $y$-axis—by rotating the connecting-rod $AB$ about the spherical-joint pair $A$;

along $z$-axis—by rotating the connecting-rod $AB$ about the spherical-joint pair $A$;

about $x$-axis—by rotating the connecting-rod $AB$ about the spherical-joint pair $A$. When one considers the angular mobility

of the pair $B$ itself, there remains the local mobility, *viz.* the rotation of the connecting-rod about the axis $AB$;

about $y$-axis—attainable owing to the mobility of the pair $B$ itself;

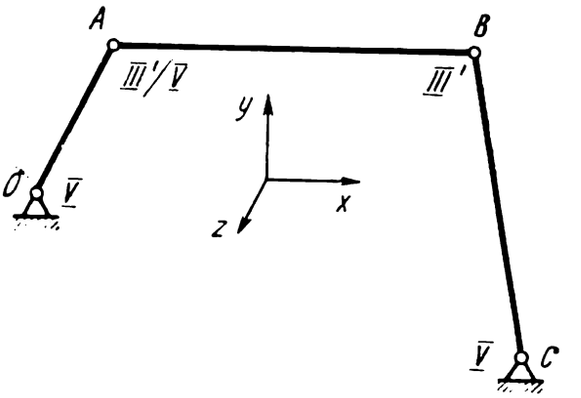


Fig. 1.2. Diagram of a four-joint mechanism for detecting preloads in assembling

about $z$-axis—attainable owing to the mobility of the pair $B$ itself.

For comparison sake, let us discuss a similar mechanism where one of the spherical joints —the pair $A$—has been replaced by a revolute or turning joint

The bringing together of the links in assembling is achieved:

along $x$-axis—by rotating the crank $OA$ and the rocker $BC$; the mobility remains—the main one in the mechanism;

along $y$-axis—by rotating the connecting-rod $AB$ about the pair $A$;

along $z$-axis—at the cost of prestraining and distorting the links.

No mobilities are required about $x$, $y$ and $z$ axes, since they are attained by the mobilities of the pair itself.

It appears expedient from the said that the last pair should be the one with the least amount of the constraint conditions, so as to reduce the number of motions involved in the assembling. An alternative way of detecting redundant constraints during assembling is the method of counting angular mobilities which is advisable in case of toothed gearings.

In the meshing of cylindrical teeth, to provide for a linear contact by self-aligning with a loading uniformly spread along the length of the tooth, one angular mobility per each engagement is required.

The number of angular mobilities in the mechanism being short of the number of engagements means that redundant constraints are present, interfering with the uniform distribution of the load longitudinally of the tooth. This will be dealt with in more detail in

Section 4. Another solution of the same problem has been suggested by A. F. Popov [29].

Besides, a mechanism may be checked for the presence of redundant constraints by counting them with the use of structural formulas. It is known that the authors of structural formulas have meant them for determination of the mobility of a mechanism, assuming the number of redundant constraints to be taken into consideration as known. The mobility of the mechanism is taken to be the number of independent parameters which should be specified to define the motion. In practice, however, it is far more easier to evaluate the mobility of a mechanism by its external inspection which is more simple and reliable than using a structural formula. It is, thus, more expedient to evaluate the mobility and introduce the value thus obtained into a structural formula, to find from the latter the number of redundant constraints. An error in evaluating the mobility is easily detectable by an unseemly number of redundant constraints (e.g. a negative one).

*There are general and local (passive) mobilities of a mechanism.* Let us call a mobility which does not influence the mobility of a mechanism, as a whole, a local mobility. Local mobilities are found in rollers (on account of their slipping), blocks, pulleys, floating bushes and pins, connecting-rods and cross-heads with spherical heads, and also in the races of antifriction bearings, if they are assembled with a slide fit (when the bearings are considered). Balls in a chute have three local mobilities in addition to the slip, i.e. rotation about the three orthogonal axes. Links with a local mobility (floating pins and bushes, flat followers in cam mechanisms) are sometimes used to provide for uniform wear of kinematic pairs.

Local mobility can be also found in a group of members. In most cases this should be avoided. We will discuss it in more detail below.

To derive a structural formula, let us make use of the classes of the kinematic pairs. We define the class of a kinematic pair as the number of constraints introduced by a given pair. The constraints in a kinematic pair are thus the restrictions to relative motion along a given axis or angular displacements about the same axis.

A limited linear displacement implies the necessity of transmitting an effort in the kinematic pair between its links, while a limited angular displacement implies the necessity of transmitting a torque between the links of the pair. Therefore, the notion of "kinematic constraints" in a structure has as counterparts the notions of "transmitted forces" or "transmitted torques" in dynamics.

It is for these forces or torques that a kinematic pair should be designed. It is solely under the condition that a pair is able to withstand this force or torque that we can state that the constraint is really imposed.

If we take the number of movable links to be $n$, they will possess $6n$ degrees of freedom (each link being free to move along the three orthogonal axes and to rotate about the three axes). To determine the mobility of a mechanism, we have to deduct from this number the constraints imposed by the kinematic pairs.

The number $p_i$ of the kinematic pairs of the $i$-th class or order imposes $ip_i$ constraints, and all the kinematic pairs impose $\sum_{i=1}^{i=5} ip_i$ constraints. However, not all of the present constraints are to be subtracted, since redundant constraints (let us denote their number as $q$) duplicate other constraints without reducing the mobility of the mechanism, but merely rendering it a statically indeterminate system. Thus, the mobility of a mechanism is defined as

$$w = 6n - \left(\sum_{i=1}^{i=5} ip_i - q\right)$$

This formula (in a slightly different form) has been suggested by A. P. Malyshev. Therefore, $q = w - 6n + \sum_{i=1}^{i=5} ip_i$, or, in the developed form:

$$q = w - 6n + 5p_{\mathrm{V}} + 4p_{\mathrm{IV}} + 3p_{\mathrm{III}} + 2p_{\mathrm{II}} + p_{\mathrm{I}} \qquad (1.1)$$

A. P. Malyshev's formula can be also derived from expressions used for evaluating both the external and internal (within the kinematic pairs) loads of a mechanism.

In a statically determinate mechanism the equations of equilibrium of links suffice for evaluating these loads. In a mechanism with redundant constraints they have to be supplemented with equations of deformation. The number of last-mentioned equations is the very number of the redundant constraints.

The number of external loads—forces or torques—equals $w + 1$, which can be easily checked with mechanisms where $w = 1, 2$, etc.

One load is always predetermined, whereby the number of unknown external loads equals $w$. Each kinematic pair of the $i$-th class transmits $i$ loads (forces and torques) which are these unknown values, and all the pairs bring in $\sum_{i=1}^{i=5} ip_i$ unknown values.

All in all, there are $w + \sum_{i=1}^{i=5} ip_i$ unknown values in a mechanism, and there are $6n$ equilibrium equations for $n$ links.

The equations that are lacking, i.e. the equations to be supplemented as deformation equations are $q = w + \sum_{i=1}^{i=5} ip_i - 6n$, i.e. Malyshev's formula once again.

It may be of interest to point out that a link with a local mobility should have the torque of the external forces about the corresponding axis equal zero. This equation can be used to check up the calculations.

Another structural formula has been proposed by O. G. Ozol [25]. He maintains the expedience of eliminating redundant constraints and offers the following formula for evaluating their number.

$$q = w + 6k - f \tag{1.2}$$

where $k$ is the number of independent loops or sequencies in a mechanism, differing from other loops by at least one link or one kinematic pair $f = p_{\mathrm{V}} + 2p_{\mathrm{IV}} + 3p_{\mathrm{III}} + 4p_{\mathrm{II}} + 5p_{\mathrm{I}}$, i.e. the sum of the mobilities of kinematic pairs.

Let us derive O. G. Ozol's formula by the method proposed by E. Yu. Budyka [5]. To assemble a single independent loop or sequence, there should be three linear mobilities and three angular mobilities about the orthogonal axes, and for all the loops the number is $6k$. The number $w$ of the mobilities of the mechanism is also to be added.

The number $q$ of redundant constraints is the difference between the number of required mobilities $w + 6k$ and the sum total $f$ of the mobilities possessed by the kinematic pairs $q = w + 6k - f$, i.e. the very same O. G. Ozol's formula.

To derive a formula for determination of $k$, let us equate formula (1.1) to formula (1.2) and introduce the value of $f$ into the equation thus obtained:

$$w - 6n + 5p_{\mathrm{V}} + 4p_{\mathrm{IV}} + 3p_{\mathrm{III}} + 2p_{\mathrm{II}} + p_{\mathrm{I}} = w + 6k - (p_{\mathrm{V}} + 2p_{\mathrm{IV}} + 3p_{\mathrm{III}} + 4p_{\mathrm{II}} + 5p_{\mathrm{I}})$$

or

$$-6n + 6(p_{\mathrm{V}} + p_{\mathrm{IV}} + p_{\mathrm{III}} + p_{\mathrm{II}} + p_{\mathrm{I}}) = 6k$$

but with

$$p_{\mathrm{V}} + p_{\mathrm{IV}} + p_{\mathrm{III}} + p_{\mathrm{II}} + p_{\mathrm{I}} = p$$

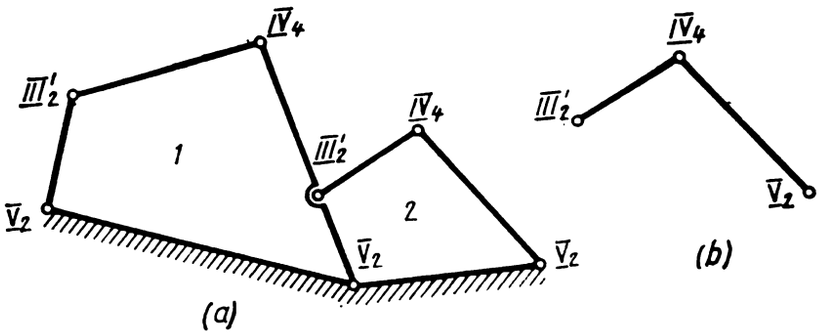


Fig. 1.3. Mechanisms
(*a*) double-loop; (*b*) double-link group

we have

$$k = p - n \tag{1.3}$$

This is the most general formula for evaluating the number of independent loops, but it is true solely of mechanisms having a fixed member. If the fixed or stationary link is lacking, the value obtained from formula (1.3) should be increased by a unity. N. E. Shamaidenko [48] has suggested to define an independent loop as the one differing from the others by at least one link or one kinematic pair.

Ja. Ja. Gaipel [8] has offered to count the number of the loops as the sum of the loops, in which one side is a fixed member (e.g. the frame of a machine), and the loops closed within the movable links. The first sum equals the number of the links connected with the fixed member but one. The other sum is easily determined by external inspection of the mechanism.

Proceeding from formula (1.2), O. G. Ozol has advanced the following generalizations which may be of help in mechanical design:

an open kinematic chain has no redundant constraints;

in a single-loop mechanism with the mobility equalling one (the dominating majority of practical cases) and in the main loop of multi-loop mechanisms the sum total of the mobilities of the kinematic pairs equals seven (if redundant constraints are absent).

These generalizations may be extended with another one: when a two-link group (Fig. 1.3*b*) is added to the main loop, the sum of the mobilities of its pairs equals six (with $q = 0$).

O. G. Ozol's and A. P. Malyshev's formulas are equivalent.

Apart from formulas (1.1) and (1.2), there is also known P. O. Somov's structural formula $w = n + f - p - 5k + q$ which can be transformed into $q = w - n + p + 5k - f$.

This formula has too many components: there are the mobilities of the mechanism, the number of the links, the number of the kine-

matic pairs, the mobilities of the kinematic pairs. For this reason its application is complicated, and it may be considered being of purely historical value. If we substitute $p - n = k$ in this formula, we shall arrive at O. G. Ozol's formula $q = w + 6k - f$.

To design mechanisms free of redundant constraints, one can follow the method of successive connection of the groups, suggested by L. V. Assur. According to him, a mechanism is formed from an initial mechanism (usually a crank) and zero-mobility groups added to it. The redundant constraints are controlled by checking the initial mechanism and the groups (before connecting) for redundant constraints.

However, the use of L. V. Assur's method may lead to errors which will be discussed in Section 2.11 below.

V. V. Solomin has suggested a table method for designing mechanisms free of redundant constraints [43]. In his tables, there are given possible combinations of kinematic pairs in dependence on the number of the links of a mechanism, out of which the most suitable one for a given application can be selected.

## 1.3. Determining Classes of Kinematic Pairs without Influence of Clearances on Their Mobility

Let us consider some kinematic pairs (Table 1.1). In the Table the classes are denoted with roman numerals *I*, *II*, *III'*, *III"*, *IV* and *V*, and the columns are denoted with arabic numerals *1* to *5*.

Let us designate each pair by the respective roman numeral with the subscript denoting the column in Table 1. Such designation will facilitate the location in the Table of the kinematic pair used in the mechanism under discussion. The forces and torques transmitted by each pair are also indicated. The Table is set to find the mobility of a kinematic pair, i.e. the number of linear and angular motions it retains between the links. In general, the sum of the class of pair and its mobility will always be six.

The simplest kinematic pair is pair $I_2$ with the point contact between the working surfaces (cf. Table 1). Let us call it "the point pair"[1]. A pair of this type is used in cam mechanisms with a barrel-shaped follower, in electric contacts with small loads and in gear teeth with a concentrated engagement spot (barrel-shaped teeth). As it will become clear from the following, this pair can be transformed by way of logical conversions into all known kinematic

[1]Accordingly, further in the text the kinematic pairs will be referred to by the type of contact between the links.

*Table 1.1*

| Class | 1 | 2 | 3 | 4 | 5 | Mobility |
|---|---|---|---|---|---|---|
| I | 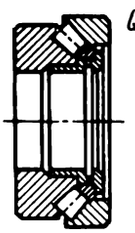  | Point $Q_z$ 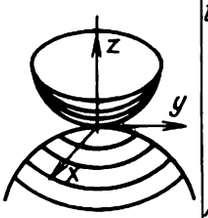 | Filamentary $Q_z$ Band $Q_z$ 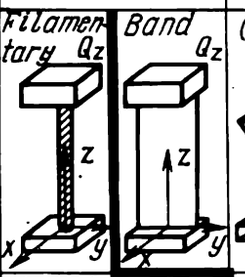 | (Land) $Q_z$ 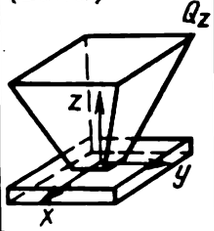 | (Line) $Q_z$ 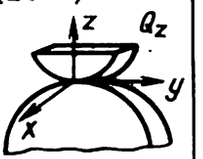 | 5 |
| II | $Q_x$ $Q_z$ 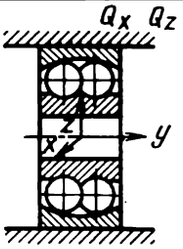 | Line $Q_z, M_y$ 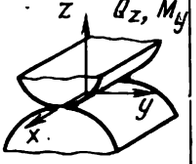 | Annular $Q_x, Q_z$ 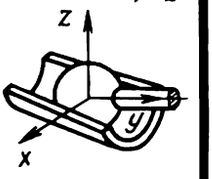 | (Annular) $Q_z, Q_x$ 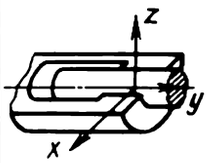 | (Strip) $Q_z, M_y$ 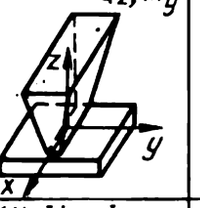 | 4 |
| III′ | $Q_x, Q_y, Q_z$ 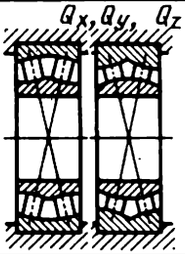 | Spherical $Q_x, Q_y, Q_z$ 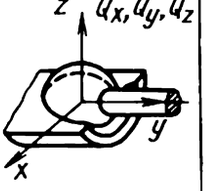 | | (Spherical) $Q_x, Q_y, Q_z$ 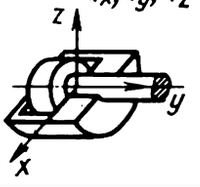 | (Helical) $Q_x, Q_z [M_y = f(Q_y)]$ 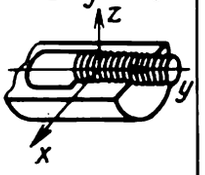 | 3 |
| III″ | $Q_z, M_x, M_y$ 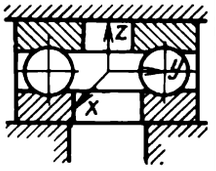 | Planar $Q_z, M_x, M_y$ 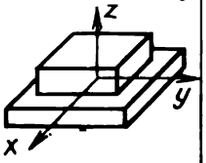 | Annular with pin $Q_x, Q_z, M_y$ 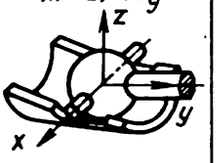 | $Q_x, Q_z, M_y$ 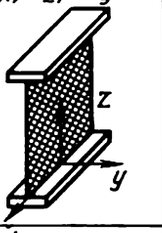 | (Spline) $Q_x, Q_z, M_y$ 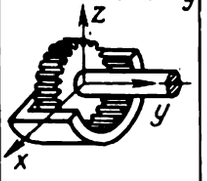 | 3 |
| IV | $Q_x, Q_z, M_x, M_z$ 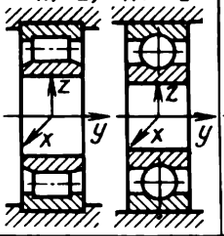 | Cylindrical $Q_x, Q_z, M_x, M_z$ 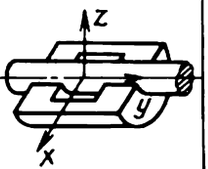 | Spherical with pin $Q_x, Q_y, Q_z, M_y$ 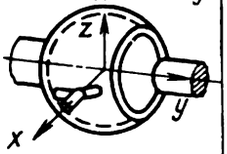 | Chain $Q_x, Q_y, Q_z, M_y$ 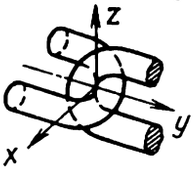 | Spline with $Q_x, Q_y, Q_z, M_y$ 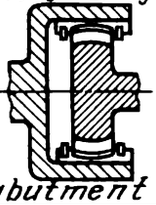 abutment | 2 |
| V | $Q_x, Q_y, Q_z, M_x, M_z$ 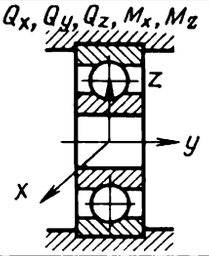 | Rotary $Q_x, Q_y, Q_z, M_x, M_z$ 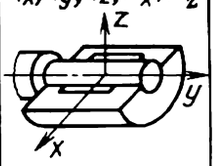 | Translatory $Q_x, Q_z, M_x, M_y, M_z$ 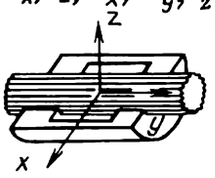 | Helical $Q_x, Q_z, M_x, M_z [M_y = f(Q_y)]$ 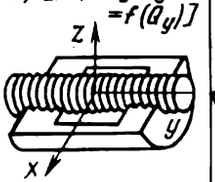 | Spiral $Q_x, Q_z, M_x, M_z [M_y = f(Q_y)]$ 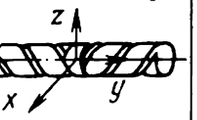 | 1 |

pairs. The point pair is a first-class one, for it opposes relative displacement and transmits a force directed along a common line normal to the working surfaces, while retaining the freedom of every other relative displacement (two displacements along the two tangents and rotation about the three axes), i.e. it presents a pair with five mobilities.

A specific case of this pair is one where one of the surfaces has degenerated into a point or spot. Let us call such a pair as a *point-and-surface pair.*

To obtain a second-class pair (two constraints imposed), two pairs of the first class are to be combined, each of them imposing one constraint condition. In general, to obtain a pair of any class, the component pairs should be connected in parallel. *The sum of the classes of the pairs combined will be the class of the pair obtained, and with redundant constraints present, the sum will equal the class of the pair obtained plus the number of the redundant constraints.*

Instead of the point contact, there may be contact over a small land or spot. In this case the number of the lands among which the load is distributed in a statically determinable manner will denote the class of the pair (at engagement under load). The spots or lands may merge into a single area. In this case the contact will be along a surface (in third- and higher-class pairs).

With several lower-class pairs connected in parallel, in general, there takes place the connection or association of these pairs, and in a specific case (or cases), a higher-class pair is produced.

Two cases of formation of second-class pairs from point pairs are of interest.

*The first case*: the planes including the engagement point and tangential to the surfaces of both point pairs coincide. Then the working surfaces of these pairs, belonging to the same link, may be combined into a single cylindrical, or even linear, surface. The resulting pair is of $II_2$ type with line contact, which we shall arbitrarily call "line". A line pair is able to transmit between the links a normally directed force and a small torque about the axis perpendicular to the normal line and to the line of engagement. This pair can impose only two constraints when the created contact is linear. Should this contact be distorted on account of one link having turned relative to the other one about the common line normal to the engaging profiles and thus shrink to a point, the pair would become a point one of the first class. The line pair $II_2$ alone displays this tendency toward "degeneration".

*The second case*: with two pairs of the "point-and-surface" type

combined, the spacing between the two points working at the two surfaces equals zero. Consequently, the point has to move simultaneously along both the surfaces, i.e. along the line of their intersection. We have now kinematic pair $II_3$, i.e. "point-and-line". Structurally, it may be a sphere moving inside a tube. Let us call this pair "annular". We shall use it later in discussion of antifriction bearings. An annular pair is able to transmit forces in two directions perpendicular to the tube axis.

There are two feasible cases of forming third-class pairs out of three point pairs. In the first case, the working surfaces of the point pairs, belonging to one link, are the parts of the same spherical surface. Then the surface of the other link may likewise be spherical (either whole or divided into three parts), and the links will contact each other along a spherical surface. Let us call this $III'_2$-pair arbitrarily *spherical* or *ball*. It restricts the displacement along all the three axes and is capable of transmitting the respective forces, while retaining the mobilities—rotation about all the three axes (a triply-mobile pair). In the second case, the working surfaces of the point pairs, belonging to one link, are parts of the same plane. Then the surfaces of the other link may also be a plane—either solid or divided into three parts, and the links will engage along a plane. Let us arbitrarily call this $III''_2$-pair as *planar*.

Still another pair $III''_3$ can be made up of an annular pair and either a point or a line one. In the latter case one redundant constraint emerges. Such a pair, to be called here *annular-with-pin*, limits displacement in two directions perpendicular to the axis of the tube and rotation about it, i.e. it may serve as a universal joint. Pair $III''_3$ is designingly unattractive. For this reason it is used in exceptional cases.

A fourth-class pair can be produced from four point pairs, provided their working surfaces are the parts of one cylindrical surface. Then the surfaces of the other link may be cylindrical, and the engagement of the links may take place along a cylindrical surface. Let us call this $IV_2$-pair *cylindrical*. It restricts relative displacements perpendicular to the shaft and transmits the respective forces, and also restricts rotation about the axes perpendicular to the shaft and transmits the corresponding torques. The pair retains mobilities—rotation about the shaft axis and displacement along the shaft axis, i.e. it is a two-mobility pair.

The cylindrical pair is advantageously different from others by the simplicity of its manufacture (with turning and grinding required for only one link, drilling and reaming for the other); moreover,

no detachable parts are to be fabricated, as the pair is disassembled by moving one of the links axially. Unfortunately, its self-alignment is impeded by friction (see Section 2.7).

Another pair $IV_3$ of the fourth class can be obtained by association of spherical pair $III'_2$ with either point pair $I_2$ or line pair $II_2$; in latter case a redundant constraint is imposed. The pair restricts displacements along the three orthogonal axes and rotation about one of them, while permitting rotation about the other two axes, i.e. it is also a doubly-mobile pair. This pair which we shall call "spherical with pin" can be met as the support of the shell of a self-aligning sliding-contact or plain bearing; unfortunately, high strains develop in pair $IV_3$ between the pin and its slot when the pair transmits a torque, while sliding results in excessive wear. Therefore, pair $IV_3$ would not be used for transmitting considerable torques and performing as a universal joint, though it is feasible kinematically. For this reason pair $IV_3$ has found very limited applications, despite highly needed in engineering design. Efforts to provide it with antifriction bearings have been so far unsuccessful. The same applies to annular pair $III''_3$ with pin.

The design of pair $IV_3$ incorporated in sewing machines is described in [19]. P. G. Mudrov has suggested instead of pair $IV_3$ a kinematic connection of spherical $III'_1$, rotary $V_2$ and planar $III''_2$ pairs. This connection is capable of transmitting considerably higher loads than pairs $IV_3$. Unfortunately, the combination of antifriction and plain bearings is unfeasible.

The third fourth-class pair $IV_4$ can be obtained if the working surfaces of four point pairs are parts of the surface of a torus. This pair is encountered in the joints of the links of welded chains. We shall, therefore, call it *chain* pair. It is structurally equivalent to the spherical pair with pin, although its construction is different. It is capable of transmitting efforts in the three directions and a torque about one axis, retaining the mobilities—rotation about two orthogonal axes.

Fifth-class pairs can be produced out of five point pairs. Of interest is the case where the working surfaces of all point pairs, belonging to the same link, are parts of a helical or screw surface. Then the surfaces of the other link may also be parts of a helical surface, and the links will engage along a helical surface. Such $V_4$-pair is commonly referred to as *helical.*

A helical or screw pair with a single-thread screw has no redundant constraints, whereas should the screw be multi-threaded, each thread (above one) shall impose five redundant constraints. Redun-

dant constraints in a helical pair are harmless, since it can be fabricated with sufficient accuracy by machining all the helical surfaces with single setting in a machine-tool.

A revolute pair $V_2$ can be obtained by joining a cylindrical pair with a planar one. This pair will have two redundant constraints, so it is important to maintain strictly the perpendicularity of the planar pair to the axis of the cylindrical pair in two directions. Such accuracy is readily attained if the end-face and cylindrical surfaces are machined with single setting in a machine-tool.

A sliding, or prismatic, pair $V_3$ can be made out of two third-class planar pairs. This pair will have one redundant constraint, whereby accurate matching of the angle between the planes in both links is essential.

It should be pointed out that when a prismatic pair is in the form of a splined joint, the number of redundant constraints can be high. However, the constraints are harmless because splined connections are usually fabricated with adequate accuracy.

When mechanisms with antifriction bearings are considered, the mobilities of the relative motion of balls, rollers, cages, sliding-fit races, etc. are usually of no interest (except the cases where the bearing itself is investigated). Therefore, there is a good reason to classify antifriction or rolling-contact bearings as kinematic pairs by the relative motion of the links they join (depending on their design and the manner of securing the races) and to include them into the kinematic pair Table (cf. Table 1.1). To simplify drawing of the diagrams of mechanisms, the bearings will be illustrated in the following pages in the same way as the kinematic pairs with sliding friction imposing the same constraints.

The first column in Table 1.1 refers to antifriction bearings: it illustrates the kinematic pairs most commonly used. Kinematic pairs presented by antifriction bearings are depicted in more detail in Table 1.2 where the transmitted force and restricted linear mobility are directed vertically, whereas free linear mobilities are directed horizontally. The manner of securing the stationary race or cup is of essential importance. Depending on the securing arrangement, one and the same bearing may be specified as a pair of two or even three different classes.

Point pair[1] $I_{1c}$ is best realized in a thrust roller bearing with spherical rollers, Type 39 000, where the outer race bears upon a

[1]Here and below the roman numeral refers to the line in Table 1.2 and the subscript to the column.

**Table 1.2**

| | 1a | 1b | 1c | 1d |
|---|---|---|---|---|
| I | 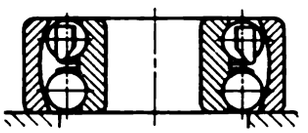 1000 | 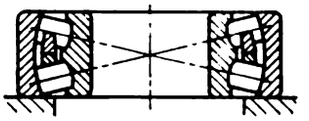 3000 | 39000 | 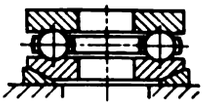 18000 |
| II | 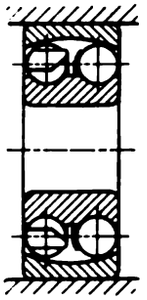 1000 | 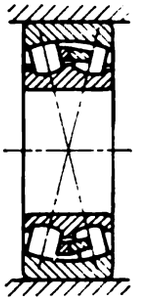 3000 | | |
| III' | 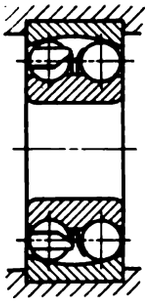 1000 | 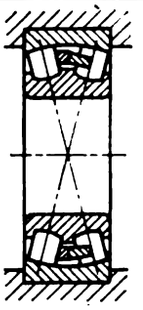 3000 | 39000 | 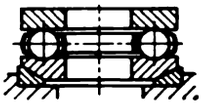 18000 |
| III'' | 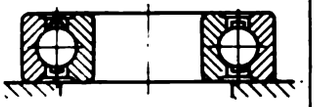 0000 | 9000 | 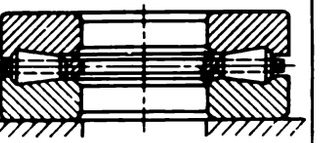 19000 | 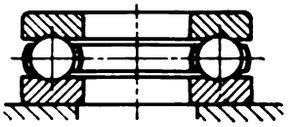 8000 |
| IV | 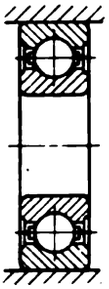 0000 | 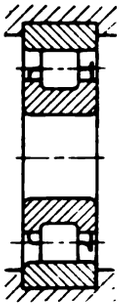 2000 | 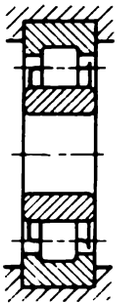 32000 | |
| V | 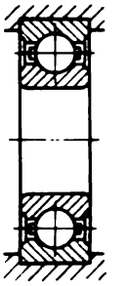 0000 | 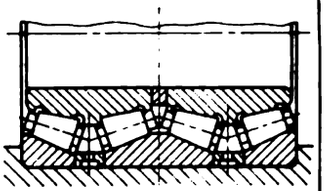 77000 | 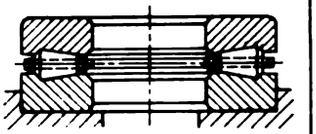 19000 | 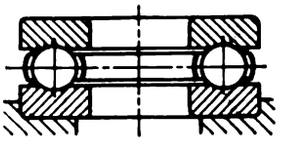 8000 |

plane. This bearing is capable of transmitting great forces while self-aligning with slight friction. When its outer race is mounted in a centering counterbore, the same bearing is a third-class pair $III'_{1c}$. A point pair $I_{1d}$ is presented by a bearing with an underlying ring, Type 18 000. Self-aligning here is associated with considerable friction, which explains why Type 18 000 is off-standard. With its outer race fixed in a centering counterbore, the same bearing is already pair $III'_{1d}$.

A point pair $I_{1a}$ can be obtained with a radial double-row self-aligning ball bearing, Type 1 000, when its stationary race bears upon a plane.

A point pair $I_{1b}$ can be likewise obtained with a radial double-row self-aligning roller bearing, Type 3 000, when its outer race bears upon a plane. Unfortunately, self-aligning bearings of the spherical type are poor transmitters of axial efforts, which makes pairs $I_{1a}$ and $I_{1b}$ suitable solely for applications where axial efforts are insignificant, e.g. for retaining the floating members of planetary gearings. The same bearings, Types 1 000 and 3 000, yield annular pairs $II_{1a}$ and $II_{1b}$ when their outer races are mounted with a movable fit; they can also yield spherical pairs $III'_{1a}$ and $III'_{1b}$ if the outer races are fixed.

Thus, either bearing, Type 1 000 or 3 000, can be made into three different kinematic pairs depending on the manner of securing the outer race.

A planar pair $III''_{1d}$ can be obtained with a thrust ball bearing, Type 8 000, when its outer race bears upon a plane.

The same bearing yields rotary pair $V_{1d}$ when its outer race bears into a centering counterbore.

Similarly, a thrust taper roller bearing, Type 19 000, can be made into planar pair $III''_{1c}$ by letting its outer race bear upon a plane. It can be also made into rotary pair $V_{1c}$ when the outer race bears into a centering counterbore.

A thrust roller bearing with cylindrical rollers, Type 9 000, is identified with planar pair $V_{1b}$. Its shortcoming is the slip between the rollers and races on account of variation of speed with different radii.

A planar pair $III''_{1a}$ can be obtained with a single-row ball bearing, Type 0 000, when the outer race bears upon a plane. This pattern is not suitable with very high angular velocities, when thrust bearings tend to perform poorly on account of jamming of the balls, caused by great centrifugal forces.

The same ball bearing, Type 0 000, can be made into cylindrical

pair $IV_{1a}$ (when the outer race is mounted with movable fit), and into rotary pair $V_{1a}$ (when the outer race is fixed).

A cylindrical pair can be obtained with a bearing with short cylindrical rollers when the outer race is fixed, *viz.* a bearing, Type 2 000, without shoulders on the outer race or cup can be made into pair $IV_{1b}$, while bearing, Type 32000, without shoulders on the inner race can be made into pair $IV_{1c}$.

Pair $IV_{1b}$ is preferable to pair $IV_{1c}$ owing to its ability of self-aligning.

It should be noted, however, that pairs $IV_{1a}$, $IV_{1b}$, $IV_{1c}$ and $V_{1a}$ are incapable of transmitting great twisting-out torques. Thus, if such torques are expected the shaft has to be mounted in two bearings, thus allowing for redundant constraints.

When loads are extremely high, four-row roller bearings, Type 77 000, are to be used to obtain rotary pair $V_{1b}$. Presently, self-aligning or spherical bearings with a spherical surface of the inner race and concave rollers are marketed abroad (cf. Table 1.1, pair $III_1'$). In most cases the outer race or cup is split for adjustment purposes. When misalignment or skewing of the outer race relative to the geometric axis of rotation is imminent, it is expedient to use bearings with the spherical surface of the outer race; if skewing of the inner race is imminent, bearings with the spherical surface of the inner race are preferred. With these conditions met, the degree of skewing may be fairly great (provided the rollers would not become offset beyond the spherical surface). If the conditions are ignored, the rollers tend to slip at skewing, and the torque tending to twist the bearing out grows with the skewing angle increasing.

When flexible connections are present (ropes, cables, transmission or conveyer belts), it is advisable to consider each of them a kinematic pair connecting rigid links and being always characterized by force closure. Therefore, when the number of the links is counted, rigid links alone should be taken into account.

Parts and components whose deformation would not practically influence the mobility will be considered here as rigid links.

On the other hand, parts and components whose deformation affects the mobility will be considered by us as flexible and classified as kinematic pairs.

The kinematic pairs described above should be further supplemented with two more, formed by flexible connections (a filament and a sheet). A filament is a first-class pair $I_3$ restricting lengthwise motion and retaining free the five remaining relative motions (pentamobile pair). A sheet (when sufficiently wide) is a third-class pair

$III_4''$. It constrains two linear motions in its plane and rotation about an axis perpendicular to this plane, retaining the rest of the motions free (triply-mobile pair).

Of particular interest is a helical pair formed by twisting a strip into a cylinder. When extended, it tends, like a screw pair, to untwist, thereby converting either translation into rotation or a force into a torque. It should be also born in mind that a flexible helical pair is made up of two strips twisted in opposite direction, i.e. it corresponds to a turnbuckle.

When the strip is untwisted, the pitch varies, whereby the pair corresponds to a variable-pitch helical one. The twisted strip is flexible, so that it is capable of transmitting but moderate transverse forces $Q_x$ and $Q_z$ and moderate torques $M_x$ and $M_z$ about the transverse axes.

Flexible connections work practically without friction, which is their substantial advantage.

By connecting filament and sheet pairs in parallel (with the constraint conditions adding up), it is possible to obtain kinematic connection of any class (cf. Table 1.3).

A combination of two parallel filament pairs yields pair $II_2$ similar to a line one; a combination of three filament pairs intersecting at one point yields pair $III_2'$ similar to a spherical one; three filament pairs connected in parallel provide pair $III_2''$ similar to a planar one; a combination of four filament pairs intersecting one straight line at two points results in pair $IV_2$ similar to a cylindrical one; a combination of a sheet pair with a parallel filament pair yields a fourth-class pair $IV_2$; a combination of a sheet pair and a filament one where they intersect the same line yields either pair $IV_4$ or pair $IV_5$ similar, respectively, to spherical-with-pin and chain pairs.

A combination of two sheet pairs imposes six constraints of which one is redundant, originating a fifth-class pair. In this case, to avoid preload, precise assembling of the sheet pairs is required.

When the sheet pairs inersect a straight line, rotary pair $V_2$ evolves (rotation about this line), which is widely known in engineering practice as the "cross joint" where the sheet pairs are usually axially offset; each pair may be connected to both links at a uniform spacing from the axis (not at the axis itself) to enhance the strength.

When the sheet pairs are parallel, this yields prismatic pair $V_3$, as is the case with the drawing calipers. Thus, all the constraint conditions may be imposed using flexible connections, which is essential in applications where friction is to be avoided.

*Table 1.3*

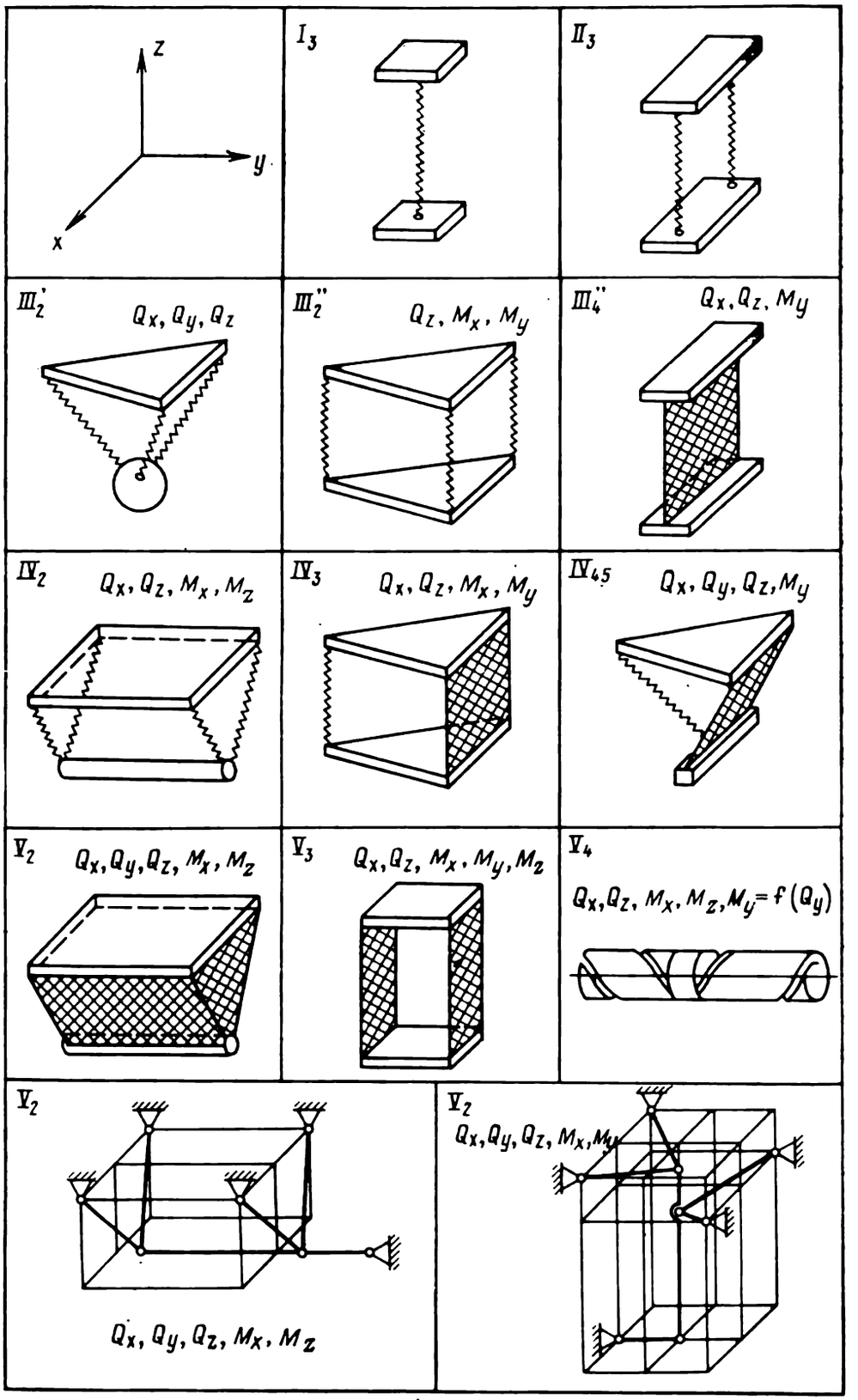
z
y
x
I3
II3
III'2
Qx, Qy, Qz
III''2
Qz, Mx, My
III''4
Qx, Qz, My
IV2
Qx, Qz, Mx, Mz
IV3
Qx, Qz, Mx, My
IV45
Qx, Qy, Qz, My
V2
Qx, Qy, Qz, Mx, Mz
V3
Qx, Qz, Mx, My, Mz
V4
Qx, Qz, Mx, Mz, My = f(Qy)
V2
Qx, Qy, Qz, Mx, Mz
V2
Qx, Qy, Qz, Mx, My

A kinematic joint of the fifth class with rotational mobility can be obtained from filament pairs exclusively—it takes five of them. Joints of this kind are of interest when evaluating the moment of inertia of suspended parts by the oscillation method.

Table 1.3 illustrates suspension patterns for oscillation about vertical and horizontal axes.

When designing such suspensions, it is essential to make sure that the filament pairs are always taut. Uniform loading of all the filament pairs may be attained by appropriate selection of the dimensions, both linear and angular.

It is expedient to consider chains as altogether flexible pairs: a plain welded chain should be seen as a filament pair, and an articulated-link one as a sheet pair. As chains would not slip on the sprockets, each length of a chain between two sprockets should be seen as a separate flexible pair. Fixed joints may be also included into the category of kinematic pairs as sixth-class ones. However, their great variety can not be accommodated in Table 1.3. Hence, we shall deal with fixed joints in a separate section.

## 1.4. Determining Classes of Kinematic Pairs Allowing for Influence of Clearances on Their Mobility

The mobility of kinematic pairs is evaluated with the clearances ignored when the kinematic pairs are in the form of antifriction bearings where clearances are negligible to a degree that a situation of prestraining may take place. With clearances present, there evolves additional mobility which in some cases is employed in operation of a mechanism [32].

For an example of employing clearances to increase the mobility, let us refer to a toothed universal joint $III_5''$ connecting in some motor vehicles the transmission with the intermediate shaft. A toothed universal joint is a splined joint of a length substantially smaller than the diameter, usually with an involute profile.

To establish which constraints can be eliminated in kinematic pairs, let us consider a turning pair with a cylindrical pin (Fig. 1.4). Owing to the clearance $\delta$, the relative translatory displacement of the links is likewise $\delta$, i.e. it is fairly small with clearances met in practice. The clearance is swiftly taken up, and then the pair transmits a force and restricts the relative translatory motion. Thus, even with the clearances present, the forces transmitted by kinematic pairs remain the same as are the translatory displacements restricted by them.

Owing to the same clearance δ, relative rotation of the links equals the angle 2 arcsin $\frac{\delta}{b}$, and the displacement of the other end of the link can be found from similarity of the triangles (cf. Fig. 1.4):

$$\frac{\frac{1}{2}S}{L} = \frac{\delta}{b}; S = 2\frac{L}{b}\delta \qquad (1.4)$$

In practice, $\frac{L}{b}$ = 10 to 100, whereby $S$ = (20 to 200) δ. This displacement can be employed in the operation of the mechanism, and also to avoid redundant constraints.

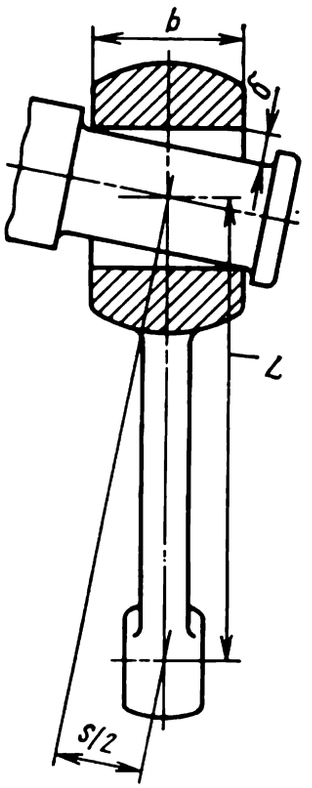


Fig. 1.4. Rotary pair with additional angular mobility owing to clearances

If $L = b$, then $S = 2\delta$, i.e. it is also small.

It seen that the presence of clearances eliminates those of the transmitted torques and restricted angular rotation in whose plane of action the kinematic pair has insignificant dimensions in comparison with the length of the link.

With clearances present, a revolute pair $V_2$ is no longer able to transmit torques $M_x$ and $M_z$ and becomes spherical pair $III'_4$; a cylindrical pair $IV_2$ fails to transmit $M_x$ and $M_z$ and becomes annular pair $II_4$; a sliding pair $V_3$ would not transmit $M_x$ and $M_z$, becoming splined pair $III''_5$ (torque $M_y$ transmitted by the meshing teeth is retained); a helical pair $V_4$ is no longer able to transmit $M_x$ and $M_z$ and becomes helical pair $III'_5$.

A planar pair $III_2'$, if it is small in comparison with the dimensions of the link, is unable to transmit torques $M_x$ and $M_y$ and becomes land pair $I_4$ of the first class. When closed geometrically, the pair presents an element of one link in the form of a plate received in the slot of the element of the other link. In this case the transmitted torques $M_x$ and $M_y$ can be eliminated only with clearances present and the pair being small in comparison with the dimensions of the link.

With force closure attained, the clearances fail to exist, i.e. they are eliminated by the closing force. Let us consider the example of land pair $I_4$ to discuss angular mobilities. As one of the links is rotated about $x$ axis, the transmitted force is shifted to the edge of the land, and an additional torque $Q\frac{b}{2}$ is produced. If the width of land $b$ is insignificant in comparison with the size of the link, this additional torque will be too small to reduce the mobility. So, what we stated above for the case of geometric closure is valid for the case of force closure, i.e., with the dimension of a force-closed kinematic pair being small in comparison with that of the link, the angular constraint is eliminated.

The above reasoning should be born in mind when considering pairs $II_5$ and $I_5$ (cf. Table 1.1).

A sheet pair transmits two forces and a torque only when the strip width is adequate. Otherwise it works merely as a filament one, i.e. imposes only one constraint $I_3$. It is from this point of view that the pairs shown in Table 1.1 beyond the bold line are those whose respective constraints have been determined with provisions for the clearances. The names of these pairs are given in brackets.

By allowing for clearances in kinematic pairs, it is far easier to design a mechanism free of redundant constraints than when the clearances are ignored. However, if there is a misalignment in a mechanism, great enough to take up the clearances, the harmful effects of the redundant constraints will be restored. Thus, a design allowing for clearances is permissible only when the dimension of a link is great in comparison with that of the kinematic pair. The method of designing by allowing for clearances is mainly used for mechanisms in which the redundant constraints would not be eliminated otherwise.

## 1.5. Detecting Particularly Harmful Redundant Constraints by Planar or Spherical Diagram of Mechanism

The most commonly met nowadays are planar mechanisms where the links move in parallel planes. Redundant constraints in these mechanisms should be determined from A. P. Malyshev's and O. G. Ozol's formulas. However, a planar diagram may also be of help when deciding which redundant constraints should be retained when their complete elimination is impossible. To do this, the projection of all the links onto a single plane can be considered, or else all the links can be brought into coincidence with one plane. The techniques are obviously artificial, for usually actual links and kinematic pairs belong to parallel planes (e.g. the crank pin and main bearings).

In a planar diagram[1] one would not find the forces acting along $z$ axis and the respective redundant constraints, nor the torque about $x$ and $y$ axes and the corresponding redundant constraints existing in planar mechanisms. The diagram enables one to study the forces along $x$ and $y$ axes, torques about $z$ axis and the respective redundant constraints which we shall denote as $q_p$.

In general, a planar diagram fails to depict completely the work of a mechanism, same as a single projection fails to reflect it in its completeness. The mobility $w_p$ of a mechanism in a planar diagram differs from the actual mobility $w$, since the planar diagram ignores rotation of the links about axes belonging to plane $xoy$ (e.g. rotation of a connecting-rod with spherical ends about its own axis).

Let us derive a formula for a planar diagram. Any mobile link in a plane has three degrees of freedom, and there are $3n$ degrees of freedom altogether.

Any rotary pair, be it (in the plane) of the fifth, fourth, third and even second class, imposes but two constraints in a planar diagram by restricting displacement along $x$ and $y$ axes. Any translatory pair, whether its class is the fifth, fourth (e.g. a trunk piston) or third, likewise imposes but two constraints in a relevant planar diagram, restricting displacement in a direction perpendicular to the displacement in this pair and restricting rotation about an axis perpendicular to the plane of the mechanism. Hence, in a planar diagram lower-class pairs impose $2p_l$ constraints[2].

[1] Here and below we shall assume that in every drawing $x$ axis runs horizontally, $y$ axis runs vertically and $z$ axis is perpendicular to the plane of the drawing.

[2] Lower (degrees of freedom) implies sliding and revolute pairs. Helical pairs are not considered since mechanisms with such pairs would not be planar.

Each higher d.o.f. pair (of the second or first class) imposes a single constraint in a planar diagram: it restricts motion along the normal line. Flexible connections (filament or sheet) also impose in a planar diagram but a single constraint condition, restricting longitudinal displacement. Consequently, we are able to view all the higher-class pairs and flexible connections together. They apply $p_h$ constraints, with $p_h$ being the sum of the higher-class pairs and flexible connections.

With provisions for redundant constraints, the mobility of a mechanism in a planar diagram is $w_p = 3n - (2p_l + p_h - q_p)$.

This expression has also been suggested first by A. P. Malyshev. By transformation

$$q_p = w_p - 3n + 2p_l + p_h \tag{1.5}$$

Let us call the expression "Malyshev's planar formula[1]". O. G. Ozol has also suggested a structural formula for a planar diagram:

$$q_p = w_p + 3k - f_p \tag{1.6}$$

where $f_p$ is the number of the mobilities of the kinematic pairs in a planar diagram.

The expression can also be derived from formula (1.5).

Prismatic and revolute pairs in a planar diagram have one mobility each, while the higher-class and flexible pairs have two mobilities.

A planar diagram is not the only one artificial diagram used for investigating mechanisms.

Spherical mechanisms met in actual life (bevel gears, universal joints) are conveniently investigated in a spherical diagram, either by considering the projection of all the links onto a single sphere, or by bringing all the links into coincidence with a single spherical surface.

The derivation of expressions for the mobility $w_s$ and the number of redundant constraints $q_s$ in a spherical diagram differs from the derivation of the respective expressions for a planar diagram solely in that flexible connections are absent, so it is not given here.

The final formulas are

$$w_s = 3n - 2p_l - p_h + q_s$$

[1]To be more exact, it's Malyshev's formula for a planar diagram. It is sometimes called "Chebyshev's formula" which is not correct, for P. L. Chebyshev has suggested the expression $3m - 2(n + v) = 1$ (where $m$ is the number of movable links, $h + v$ is the number of joints), i.e. it ignores prismatic pairs, higher-class pairs and redundant constraints, accepting solely that with the mobility equalling unity.

and

$$q_s = w_s - 3n + 2p_l + p_h \tag{1.7}$$

The above fully substantiates, as was pointed out by academician I. I. Artobolevsky, the applicability of Malyshev's planar formula to spherical mechanisms.

With the formulas for planar and spherical diagrams being thus identical, each of them can be applied to mechanisms including spur and bevel gears.

It may be deduced that, apart from projections onto a plane and sphere, projections onto other surfaces (e.g. cylindrical) can be of help in case of some mechanisms, with corresponding formulas derived.

When designing mechanisms, it is reasonable, first, to eliminate redundant constraints detected from the formula for either a planar or spherical diagram, and then (either ignoring or providing for clearances, whichever suitable in the particular case) to eliminate redundant constraints determined from formula (1.1).

In addition to formulas (1.5) and (1.6), there is known an expression for calculation of trusses, adaptable for determination of internal redundant constraints as

$$q_p = w_p - 2p_u + s + 3 \tag{1.8}$$

where $p_u$ is the number of the units of the truss; $s = n + 1$ is the number of the bars.

O. O. Galperin has suggested a formula which can be expressed in symbols adopted here:

$$q_p = w_p - n + 2k \tag{1.9}$$

The four structural formulas are equivalent for planar diagrams. In them $q_p - w_p$ is correlated to two parameters out of the six: $n$, $s$, $k$, $p_l$, $p_u$ and $f_p$.

These parameters are correlated by four expressions. The first is

$$s = n + 1 \tag{1.10}$$

As each lower pair in a plane has the mobility $1 = 3 - 2$, we derive the second expression

$$p_l = f_p \tag{1.11}$$

The third expression is formula (1.3) which, for a planar diagram without higher-class pairs, is expressed by substitution $p = p_l$ as

$$p_l - n = k \tag{1.12}$$

To derive the fourth expression, let us remember that in each unit the number of the ends of the bars is the number of the kinematic pairs plus one, and for the entirety of the units this difference equals $p_u$. Therefore,

$$p_u = 2s - p_l \tag{1.13}$$

where $2s$ is the number of the ends of bars, each bar having two ends.

By substituting $k$ from (1.12) and $f_p$ from (1.11) in Ozol's formula for a planar diagram (1.6)

$$q_p = w_p + 3p_l - 3n - p_l = w_p - 3n + 2p_l \tag{1.14}$$

By substituting $p_u$ from (1.13) and $s$ from (1.10) in (1.8)

$$q_p = w_p - 4s + 2p_l + s + 3 = w_p - 3n + 2p_l$$

By substituting $k$ from (1.12) in (1.9)

$$q_p = w_p - n + 2p_l - 2n = w_p - 3n + 2p_l$$

In every case we have obtained Malyshev's planar formula devoid of an entry containing higher pairs.

Let us see how many equivalent expressions may be obtained from the same six parameters: $C_6^2 = \frac{6 \times 5}{1 \times 2} = 15$. Two of them have to be omitted, since a structural formula cannot be obtained from $s$ and $n$, for they are correlated by expression (1.10); nor can a structural formula be obtained from $p_l$ and $f_p$, as they are equal.

Let us list these formulas:

$q_p = w_p - n + 2k$ , O. O. Galperin's formula;

$$q_p = w_p - s + 2k + 1 \tag{1.15}$$

$q_p = w_p - 3n + 2p_l$, Malyshev's "planar" formula;

$$q_p = w_p - 3s + 2p_l + 3 \tag{1.16}$$

$$q_p = w_p - 2p_u + n + 4 \tag{1.17}$$

$$q_p = w_p - 2p_u + s + 3$$

$$q_p = w_p - 3n + 2f_p \tag{1.18}$$

$$q_p = w_p - 3s + 2f_p + 3 \tag{1.19}$$

$$q_p = w_p + 3k - p_l \tag{1.20}$$

$$q_p = w_p - p_u + k + 2 \tag{1.21}$$

$q_p = w_p + 3k - f_p$—O. G. Ozol's "planar" formula;

$$q_p = w_p - \frac{3}{2} p_u + \frac{p_l}{2} + 3 \tag{1.22}$$

$$q_p = w_p - \frac{3}{2} p_u + \frac{f_p}{2} + 3 \tag{1.23}$$

Most of the above expressions have no practical importance. We have listed them here to avoid their "rediscovery".

## 1.6. Kinematic Connections with Hydraulic and Electric Restraints

Hydraulic and electric devices impose in a mechanism the same constraints as kinematic pairs. However, one should not call such devices kinematic pairs, as they, unlike the kinematic pairs, include, in excess of the two elements, intermediate elements or fluids.

Nevertheless, we shall classify them in the same way as kinematic pairs, i.e. by the number of constraints they impose.

Let us proceed with a review of some of these kinematic connections or couplings.

A hydrostatic or positive-displacement hydraulic transmission requires that the volume of the fluid contained in the pump, motor and connecting lines, is constant, i.e. $V = \text{const}$. There may be several pumps and motors: they may be machines of either the piston (single- or multi-cylinder) or the lobed type.

To maintain the constant volume, the sum of the volumes displaced by the pumps and motors should equal zero: $V_1 + V_2 + V_3 + \ldots + V_n = 0$.

As $V_1 = f_1 S_1$, where $f_1$ is the working area of the piston in a piston-type machine or the similar transformed value in a lobed machine, and $S_i$ is the stroke of the piston.

Thus

$$f_1 S_1 + f_2 S_2 + f_3 S_3 + \ldots + f_n S_n = 0 \tag{1.24}$$

The equation interrelating the displacements of pumps and motors being the only one available, it can be deduced that a positive-displacement hydraulic transmission imposes but a single constraint, i.e. it is a kinematic connection of the first class.

Hydraulic cylinders are employed in multiwheel arrangements for levelling out the loads of the wheels (instead of balance beams). Thus, the ship-carrying chamber of the Krasnoyarsk ship lift (of the 9 700 ton total mass) bears upon 78 twin-roller carriages through

hydraulic supports. To provide for self-aligning while precluding unwanted mobilities, three constraint conditions are required. Therefore, the hydraulic cylinders should be grouped into three separate hydraulic systems, with the cylinders in each system interconnected by pipelines.

A dynamic (vane-type) hydraulic transmission is not a kinematic connection, with the displacement of the motor not being proportional to that of the pump. Thus, an overloaded turbine might even halt, with the pump continuing its rotation. Nor can a pneumatic transmission be considered as a kinematic connection on account of the compressibility of air inhibiting proportionality of the displacement of the pump and motor.

An exception is a pneumatic transmission of the type used for controlling the engine of Д$^{Б}$ diesel locomotive. In this transmission the pump sets the pressure in the control line through a reducing valve, and the receiver (a spring-loaded piston) is displaced in proportion with this pressure. A pneumatic transmission of this kind is also a first-class kinematic connection.

An electric synchro or selsyn system includes two three-phase induction motors with commutator rings whose stator windings are supplied from a common source and the rotor windings are connected in parallel. If the shaft of one of the machines is rotated through some angle, that of the other machine will go through the same angle. Thus, a synchro imposes a single constraint and, hence, is a first-class kinematic connection.

With a useful resistance torque applied to the receiver, there appears a mismatch angle corresponding to the twist angle of a common-type mechanical shaft.

To reduce the mismatch angle, the rotation of the magnetic field of the stator of the synchro should be directed in opposition to the rotation of the rotor, or else a corresponding gearing can be used. Other structures of synchro systems are also in existence.

A direct-current electric transmission, even when it incorporates a motor with rigid ratings (e.g. a shunt-wound one), is not a kinematic connection as it does not ensure that the rotation of the motor is proportional to that of the generator. An alternating-current electric transmission can serve as a kinematic connection only when both the motor and generator are of the synchronous type. On account of eventual dropping out of synchronism, the last-described arrangement is met but very seldom.

A flexible shaft likewise presents a first-class kinematic connection since it imposes a single constraint—equality of the angles of rota-

tion of the driving and driven members—while allowing five other motions of the driven member (three displacements along the orthogonal axes and two rotations about the other two axes).

## 1.7. Use of Kinematic Connections in Rational Mechanisms

Elimination of redundant constraints calls for lowering the class of the kinematic pairs. It is fairly easy to lower the class of the kinematic pairs with antifriction bearings as the available bearings offer all the classes of kinematic pairs with nearly equal degree of success (cf. Table 1.1, Column 1, and Table 1.2). In other cases the lowering of the class of kinematic pairs might lead to pairs with line and even point contact, unsuitable for transmission of considerable torques and forces.

*Table 1.4*

| | (a) | (b) | (c) | (d) | (e) | (f) |
|---|---|---|---|---|---|---|
| I | $5=3+2$ $Q_z$ | $5=3+1+1$ $Q_z$ | $5=2+2+1$ $Q_z$ | $5=2+1+1+1$ $Q_z$ | $5=1+1+1+1+1$ $Q_z$ | $5=1+1+1+1+1$ $M_z$ |
| II | $4=3+1$ $Q_x, Q_z$ | $4=2+1+1$ $Q_x, Q_z$ | $4=1+1+1+1$ $Q_z, M_z$ | $4=2+2$ $Q_z, M_z$ | $4=1+1+2$ $Q_z, M_y$ | $4=1+3$ $M_x, M_y$ |
| III | $3=1+1+1$ $Q_x, Q_y, Q_z$ | $3=1+1+1$ $Q_x, Q_y, M_z$ | $3=1+2$ $Q_x, Q_z, M_z$ | $3=1+2$ $Q_y, M_y, M_z$ | $3=1+1+1$ $Q_z, M_x, M_y$ | $3=1+1+1$ $M_x, M_y, M_z$ |
| IV | $2=1+1$ $Q_x, Q_y, Q_z, M_z$ | $2=1+1$ $Q_y, Q_z, M_x, M_z$ | $2=1+1$ $Q_x, Q_y, M_y, M_z$ | $2=1+1$ $Q_x, Q_z, M_x, M_z$ | $2=1+1$ $Q_z, M_x, M_y, M_z$ | |

This can be avoided by replacing kinematic pairs by kinematic connections made up of several serially-arranged kinematic pairs. S. S. Arutyunov has developed a considerable number of such connections. However, elimination of redundant constraints was not his goal, therefore his Table is not given here.

As N. E. Shamaidenko has found, with pairs connected in series, their mobilities add up [48]. This enables one to obtain kinematic connections with one, two, three and four constraints resulted from pairs with the surface contact of the fifth, fourth and third classes. For the sake of comparison, let us recall that with pairs connected in parallel, the constraints imposed by them add up.

E. Yu. Budyka has elaborated the law of series connection of kinematic pairs in a different form [41]. Namely, with kinematic pairs connected serially, there remain only the constraints they commonly share, because when a pair has a corresponding mobility, it would not transmit a constraint of this kind and direction. This law applies to a case where the centres of the kinematic pairs coincide, which is most often the case with electric locomotive constructions (cf. Section 1.8). When the centres of the pairs do not coincide, the situation is complicated on account of linear mobility being replaced by angular mobility (cf. Section 1.10).

Series connections are illustrated in Table 1.4, whereas connections not included there and having either local mobility or line contact are illustrated in Fig. 1.5. Each line of the Table corresponds to the class of the connection, that is to the number of constraints it imposes, while the columns are denoted by letters, to distinguish from the notation of kinematic pairs of Table 1.1.

The directions of the orthogonal axes are the same in every diagram: $x$—toward the reader; $y$—to the right, and $z$—upward. The top right-hand corner of each diagram offers the listing of the forces and torques transmitted by the connection, while the left-hand top corner contains the symbol (Table 1.1) of the pair which this connection replaces. Some of the diagrams lack this symbol, which means that there is no single kinematic pair capable of transmitting the same combination of forces and torques. This underlines the advantage of a kinematic connection over a kinematic pair.

As I. I. Artobolevski has proved, a kinematic pair would not transmit exclusively torques with no forces transmitted. A kinematic connection can do it, as illustrated by $I_f$, $II_f$, $III_f$. The Table of kinematic connections include revolute $V_2$, cylindrical $IV_2$, spherical $III'_2$, planar $III''_2$ and partly sliding $V_3$ pairs. The latter are used but seldom, since with several such pairs the connection becom-

es poor from the construction point of view ($III_e$, $III_f$ and $IV_e$). Therefore, they are employed only when motions along the orthogonal axes are required (e.g. in machine-tools). Furthermore, prismatic pairs would not yield rotary mobilities, so that a connection cannot have more than three of them.

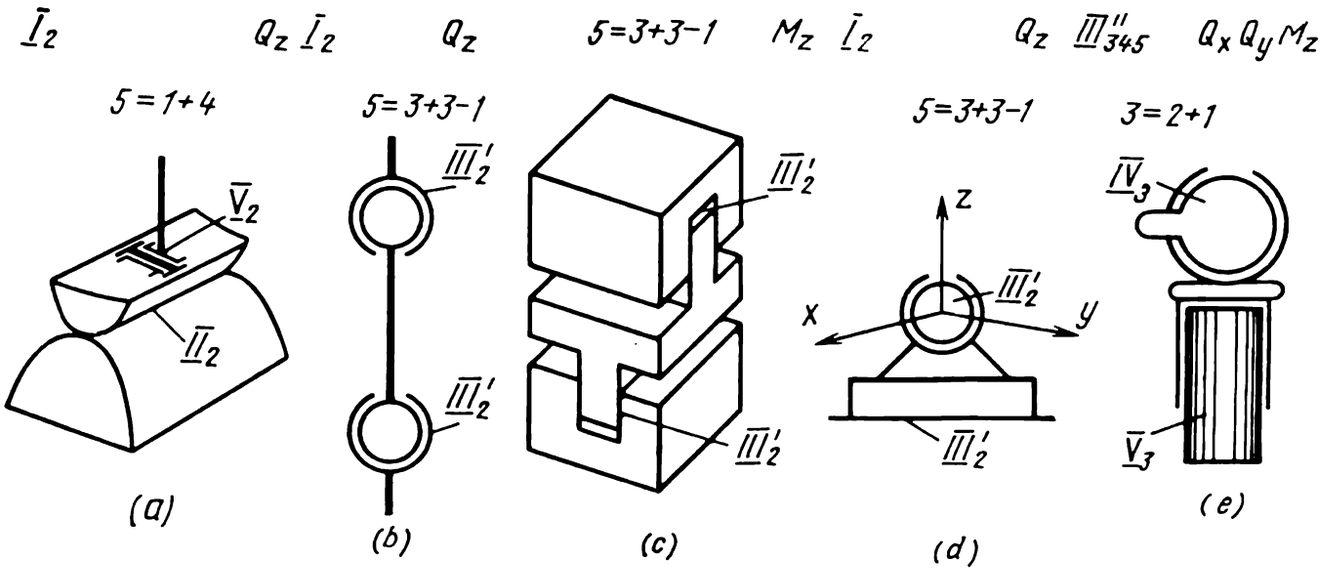


Fig. 1.5. Kinematic connections with local mobility or line contact

With kinematic pairs connected in series, each pair transmits the full force (or torque). Let us recall once again that with pairs connected in parallel, the constraints they are to impose add up, while the transmitted forces (or torques) are distributed among the pairs and can be thus substantially reduced. This is the advantage of a parallel connection.

## 1.8. Kinematic Connections in Electric Locomotives

The running gear mechanisms of an electric locomotive are under the action of forces as great as 10 to 15 t(f) (ton-force), and at certain points even 30 t(f) and greater. This renders the use of higher pairs in electric locomotives impossible, opening way to broad employment of kinematic connections.

A kinematic connection with one constraint (five mobilities) is used in the ЧС-2 passenger-train electric locomotive for transmitting the traction effort from the bogie to the body (the pivot assembly). Its longitudinal section[1] is shown in Fig. 1.6.

[1]Here and in the pages to follow, the longitudinal direction is one running along the track, and the transverse direction—perpendicular to the track.

The vertical mobility is required to eliminate redundant constraints, as the pivot assembly would not transmit the weight of the body. The transverse mobility is intended to reduce the action upon the track (to enable the cradle arrangement to perform). There is no longitudinal mobility, for it is this direction in which the traction effort is transmitted. The mobility about the vertical axis is needed for rotation of the bogie; the mobility about the transverse axis provides for proper distribution of the load among the axles (the wheels); the mobility about the longitudinal axis eliminates redundant constraints.

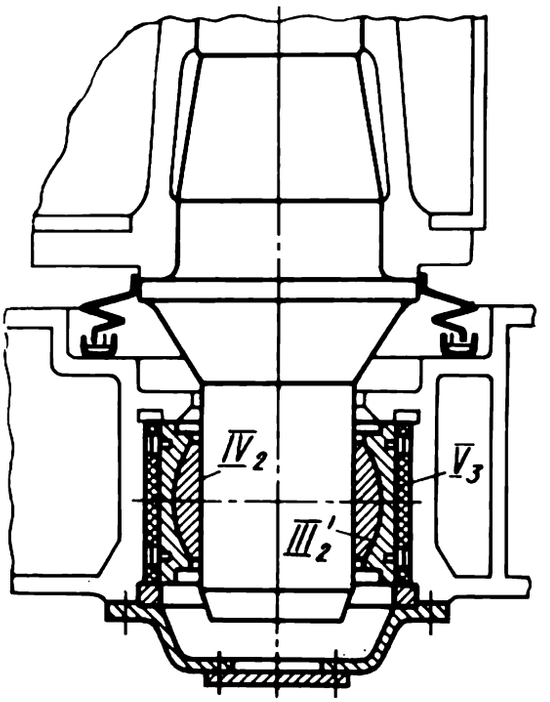


Fig. 1.6. First-class kinematic connection — pivot assembly of ЧС-2 electric locomotive

The pivot pin is fast with the body, forming pairs $IV_2$ with an intermediate part—the sphere. The sphere defines pair $III_2'$ with the successive link or member—the socket made of two parts bolted together. The socket defines translatory pair $V_3$ with the box in the bogie. The sphere possesses a local mobility (a harmless one) — rotation about the vertical axis.

Thus, the total mobility is $2 + 3 + 1 - 1 = 5$, as required.

A similar connection is incorporated in electric locomotives, Series К, ВЛ80 and ВЛ10.

In present-day electric locomotives, the weight of the body is transmitted to the bogies via side supports (the slide assemblies) which are likewise kinematic connections with a single constraint.

The side support of the ЧС-2 electric locomotive is shown in Fig. 1.7. It is a connection of a spherical pair $III_2'$ and a planar one $III_2''$. The intermediate member possesses a local mobility (harmless)—rotation about the vertical axis as far as the abutments will let it.

The mobility of the connection is $3 + 3 - 1 = 5$.

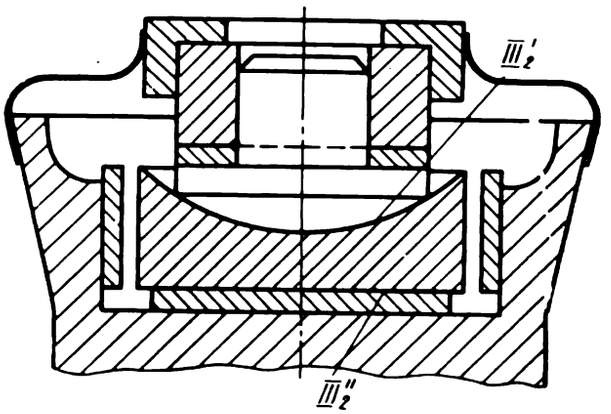


Fig. 1.7. First-class kinematic connection—side support of ЧС-2 electric locomotive

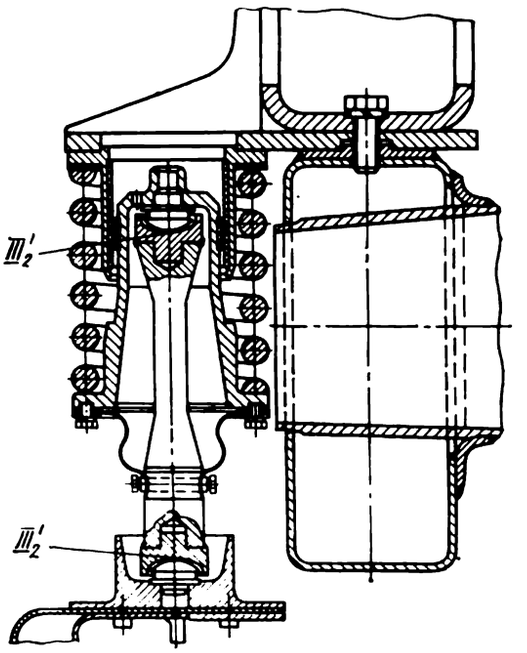


Fig. 1.8. First-class kinematic connection—side support of Ф electric locomotive

The side support of the Ф-type electric locomotive is illustrated in Fig. 1.8. The side support of the ВЛ60к locomotive is of a similar design, with two spherical pairs $III_2'$. A harmless local mobility—rotation of the rod about its axis—is present, too. The side support of the Ф-type electric locomotive is not free from a shortcoming: its body is in unstable equilibrium. This has been the reason for providing the return springs. With the bogie turning, this support develops practically no friction, thus giving rise to a yaw tendency.

First-class kinematic connections are used for interconnection of the bogies of the ЧС-2 and К electric locomotives. They are intended to transmit exclusively vertical forces, which is essential for proper distribution of the load among the bogies (wheels).

The interconnection of the bogies of the ЧС-2 locomotive is shown in plan view of Fig. 1.9. It includes a cylindrical pair $IV_2$, a spherical pair $III_2'$ and another cylindrical pair $IV_2$. With one bogie moving transversely relative to the other one, the opposition

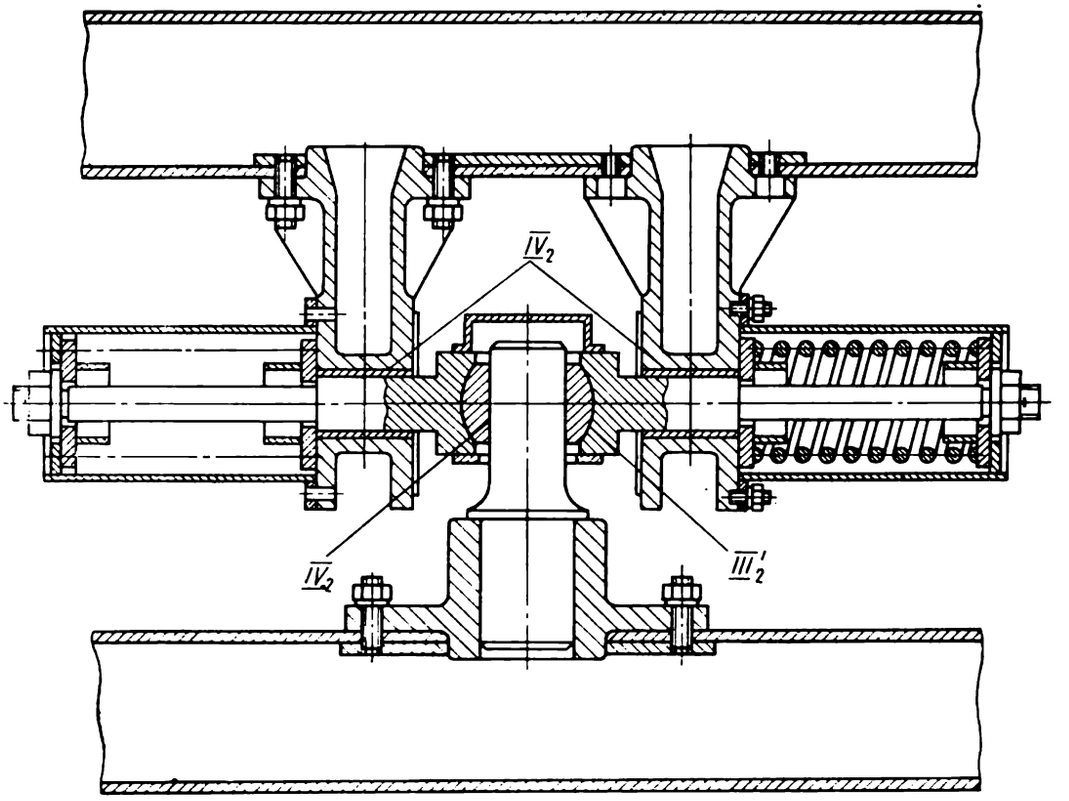


Fig. 1.9. First-class kinematic connection—joint of bogies of ЧС-2 electric locomotive

of the return springs has to be overcome, but it does not affect the mobility. The connection has two harmless local mobilities—rotation of the sphere about the longitudinal axis and rotation of the socket about the transverse one.

The mobility of the connection is $2 + 3 + 2 - 2 = 5$.

Second-class kinematic connections are used for jointing the bogies of the ВЛ8 and ВЛ23 electric locomotives (Fig. 1.10). The connection is made up of a cylindrical pair $IV_2$ and a spherical one $III_2'$ and possesses one harmless local mobility—rotation of the sphere. The mobility is $2 + 3 - 1 = 4$. It restricts longitudinal motion (transmits the traction effort) and transverse displacement of one bogie relative to the other one.

The last-mentioned constraint is redundant and strongly affects the track. For this reason the ВЛ8 locomotive is now out of production, and the locomotives still in operation have a lower speed limit.

Third-class kinematic connections are not used in the rolling stock, as three constraints are adequately provided by lower-class pairs, *viz.* spherical $III_2'$ and planar $III_2''$.

Fourth-class kinematic pairs—spherical with pin $IV_3$ and chain $IV_4$—are the higher-class ones and regarding their design features,

are unsuitable for the railway rolling stock. Hence, they have to be replaced with parallel connections of kinematic pairs.

Connection of the above-spring bar with the body of the СД electric motor coach is shown in Fig. 1.11. It includes a spherical

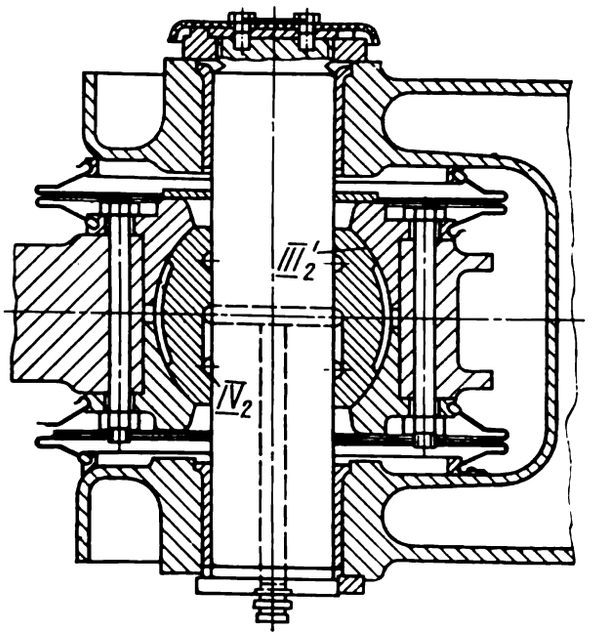


Fig. 1.10. Second-class kinematic connection—joint of bogies of ВЛ8 electric locomotive

pair $III''_2$ of the pivot assembly (three constraints imposed) and four convex rollers (one constraint each). The weight of the body is taken up by the spherical pair. To avoid a redundant constraint, a 2-6 mm clearance is set between the body and the rollers.

With one roller working, there will be no redundant constraints ($3 + 1 = 4$).

A design with two side rollers of a large diameter is used in some cranes. If the vertical load is transmitted to these rollers, a structure with no redundant constraints will result. Low friction in this connection is of no concern in case of cranes, as the low speeds make the yaw hazard non-existent.

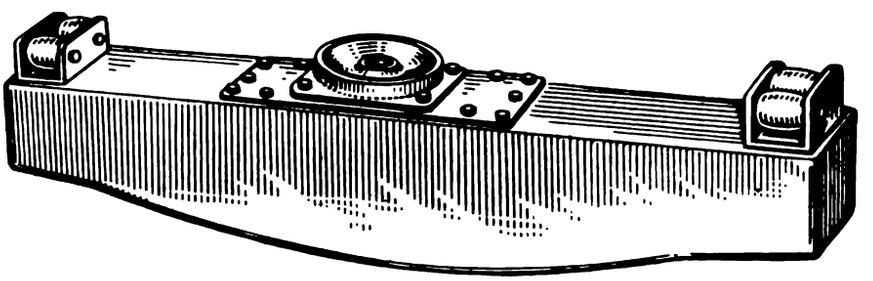

Fig. 1.11. Above-spring bar of СД electric motor coach (with elements of fourth-class kinematic connection clearly visible)

## 1.9. Typical Errors in Selection of Structural Designs of Mechanisms

Three major errors are possible while designing the structure of a mechanism.

The first error is to lose the mobility of the mechanism. The eventuality of such an error and the ways of making good are well known to design engineers. Moreover, the first error is unrelated to elimination of redundant constraints, and for this reason we shall not discuss it.

The second error is associated with the appearance of a harmful mobility. This affects the determinability of the motion, and the mechanism fails to operate. It may be brought about by improper elimination of redundant constraints: by either lowering the classes of the kinematic pairs or by introducing additional pairs. It might happen that the constraints eliminated were not those which should have been actually avoided, with redundant constraints remaining and unwanted extra mobilities gained. The matter is complicated by the fact that neither structural formula would yield the values of the redundant constraints and mobilities separately, while giving solely their difference.

To illustrate the point, let us consider the truss (Fig. 1.12*a*) described by I. M. Rabinovich, which is free of redundant constraints

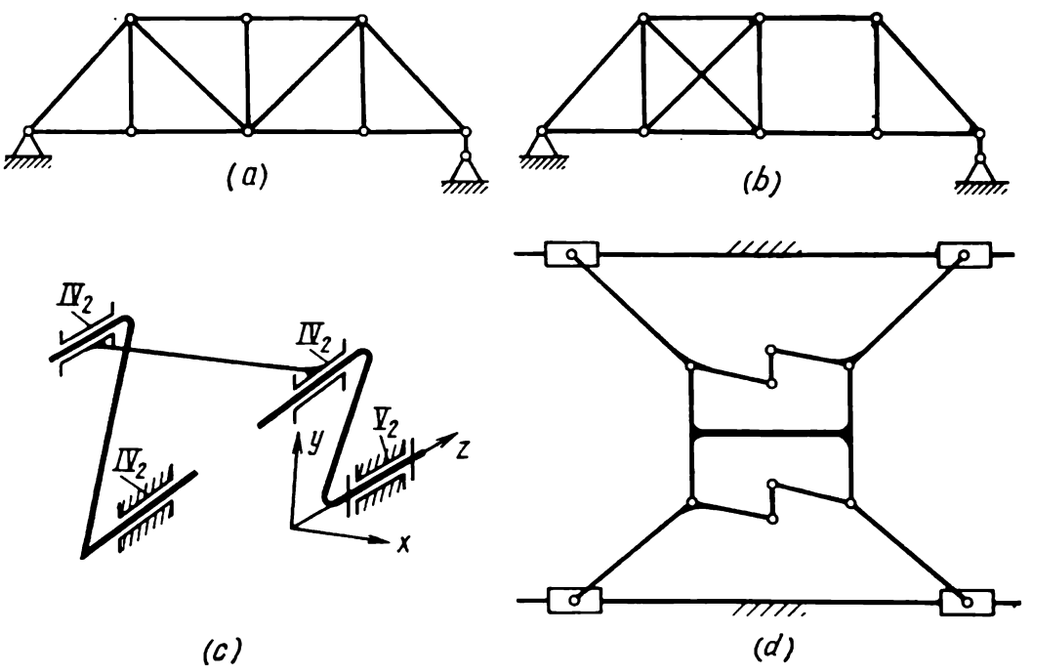


Fig. 1.12. Wrong designs of planar mechanisms with harmful local mobilities and redundant constraints

and extra mobilities, as it can be ascertained using either Malyshev's or Ozol's formulas for a planar diagram. When one link or member is repositioned (Fig. 1.12*b*), the same number of the links ($\eta = 14$) and pivots ($p_l = 21$) yields a harmful mobility $w_p = 1$ in the right-hand half and a redundant constraint $q_p = 1$ in the left-hand one, which can be substantiated by using expression (1.5), i.e. $1 = 1 - 3 \times 14 + 2 \times 21$. Thus, the first technique of detecting such faults evolves. The mechanism shall be investigated part-wise (the left-hand and right-hand parts are considered as separate entities in the example described), and mobilities and redundant constraints shall be detected in these parts.

In another example, the crank-and-rocker mechanism (Fig. 1.12*c*) comprises one rotary pair $V_2$ and three cylindrical ones $IV_2$. This mechanism, however, would not work. The rocker and the connecting-rod both have a mobility along the axis and so might fall off in operation. Thus, the mobility of the mechanism includes the main mobility and local mobilities of the connecting-rod and rocker directed axially, i.e. $w = 3$. From formula (1.1) $q = 3 - 6 \times 3 + 5 \times 1 + 4 \times 3 = 2$.

In some cases, the defects of a structure can be detected only by considering the mechanism as a whole. As an example, Fig. 1.12*d* shows a wrong planar diagram of a construction crane on four trolleys (schematically shown as slides). Each pair of the crane legs here is able to rotate through the same angles in opposite directions, which is provided for by the pivot joints connecting them. On account of this, the crane (shown as an I-beam) is able to move transversely of the trackway, which displacement is a superfluous, harmful mobility.

The pivot joints or mechanisms permit only translatory motion of the crane relative to the trackway, and with the rails being non-parallel a strain occurs. The design can be made good by interconnecting through pivot mechanisms the legs of the trolleys, bearing upon either rail.

A wrong design of a pantograph (the current collector of an electric locomotive) is illustrated in Fig. 1.13. It has an extra mobility (the local group one), with the top frame tending to fall. The mechanism is devoid of redundant constraints ($q = 0$), therefore the redundant mobility can be also found from structural formula (1.1). In the mechanism shown in Fig. 1.13 the mobility $w = 8$ (raising, six rotations of the connecting-rods about their axes, one slanting of the top frame). By entering the mobilities into (1.1), $q = 8 - 6 \times 8 + 5 \times 2 + 3 \times 10 = 0$.

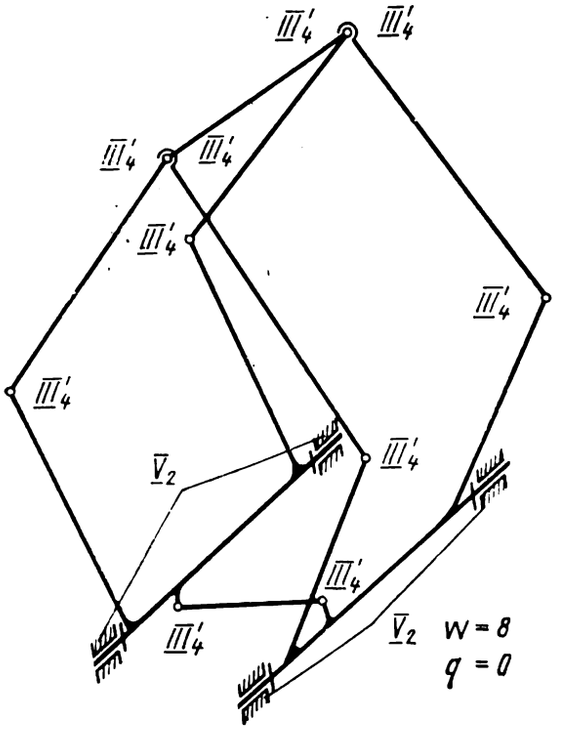


Fig. 1.13. Wrong structure of current collector mechanism with harmful group mobility

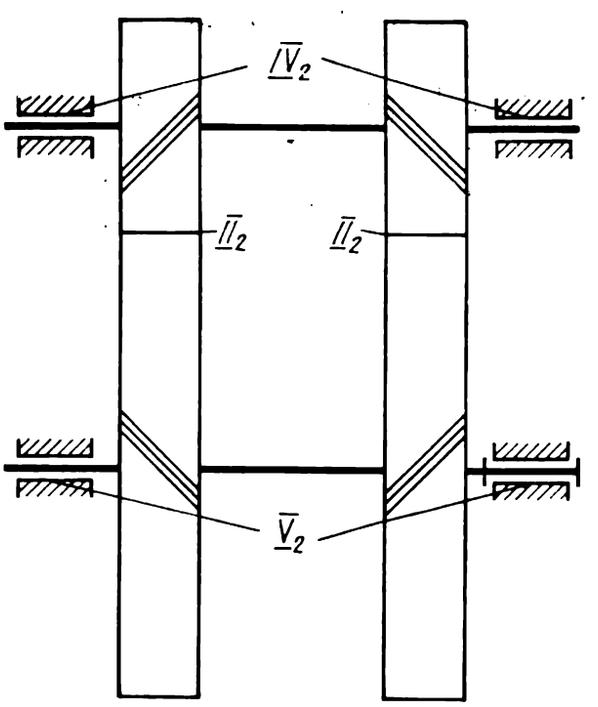


Fig. 1.14. Two-side helical gearing

An extra mobility can be detected by considering the assembling of the mechanism: this should be done part-wise. First, let us consider the mechanism of the bottom frames with the connecting rod. The latter is set in place without prestraining. This retains a local mobility—rotation of the rod about its own axis, which is harmless. Apart from it, there is the main mobility—raising of the pantograph.

When assembling the top frames, while the horizontal rod is set, the bringing together can be attained by rotating either the left-hand or right-hand pairs of these frames. The top frames retain a redundant mobility rendering the mechanism unworkable. A remedy is to provide a diagonal rod at one of the top frames.

A group mobility in a load-handling device is particularly hazardous, as it might result in dropping the load. A case is on record of an iron flue having fallen while being hoisted. This could not be caused by a broken rope, for the rope load is at the maximum with the flue down, whereas the emergency occurred when the flue was all but completely hoisted. Hence, particular care should be devoted to detecting and eliminating group mobility.

The third error in designing the structural pattern of a mechan-

ism may be the failure to ensure self-aligning of the mechanism, on account of friction. Let us illustrate the point using a two-side or double helical gearing (Fig. 1.14). Self-aligning here is provided for by axial displacement of either shaft, with a corresponding clearance ensured in its bearings.

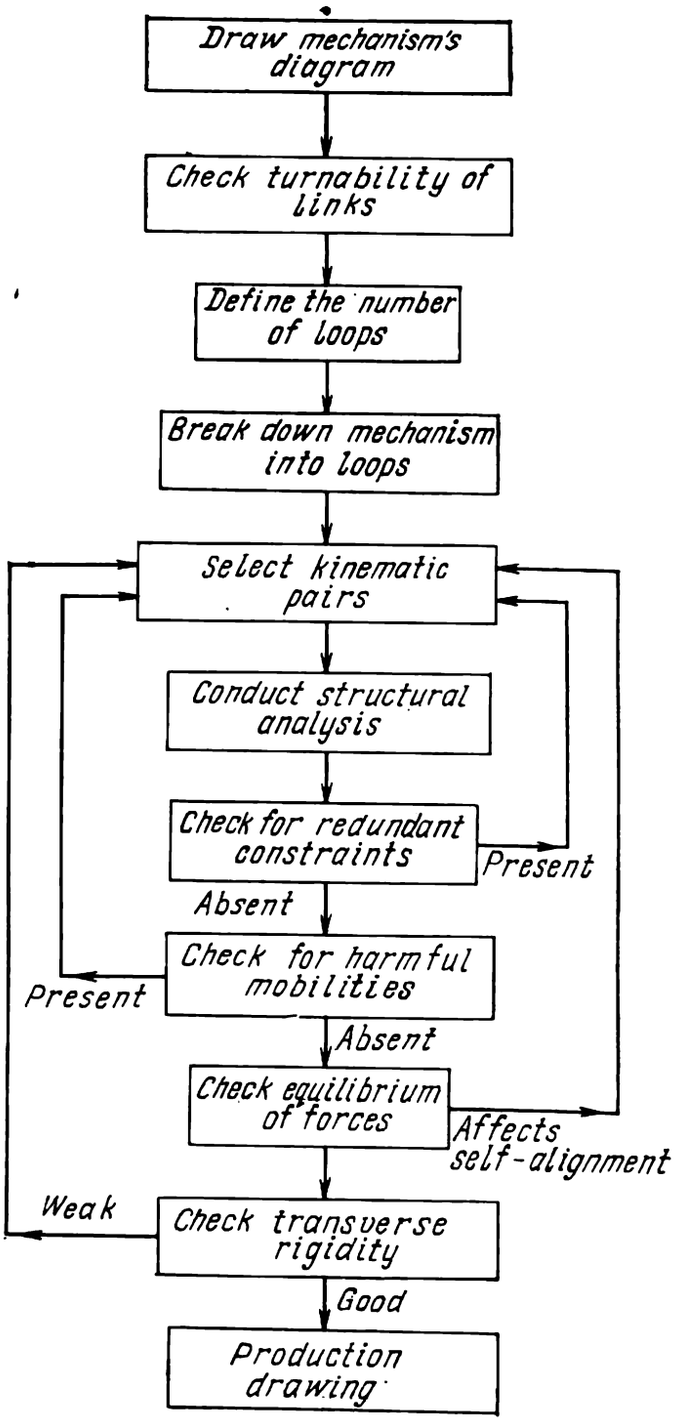


Routine of designing self-aligning mechanisms

With non-uniform distribution of the load, caused by erroneous setting of gear either axially or circumferentially, the mechanism self-aligns during the first revolutions by helical motion of the gear set with the axial clearance. This would take place even with the helix angle being short of the angle of friction, as friction here, acting in a plane perpendicular to the axis of rotation, would not affect the axial forces.

Should the non-uniformity of the forces be caused, however, by slanting or skewing of one of the gears, the gear with axial mobility would continuously slide axially with a period equalling one revolution of the skewed gear, and friction would affect the forces: no self-aligning would occur with small helix angles of the teeth. Once again, two cases of self-alignment are clearly seen here, namely: one at the commencing of motion, which we shall call "single-time" (unaffected by friction), and the other in the course of further motion of machine, which we shall call "continuous" (where friction forces should be taken into account). The theory of influence of

friction upon self-alignment will be extended in Sections 1.12 through 1.16.

When redundant constraints are absent, the tolerances for the dimensions of the links may be considerably increased, which would lead to distortion of the law of the motion of the driven link or part. More often than not such distortion is of no practical significance, e.g. when the piston of a compressor moves according to a law which is not strictly harmonical. In some cases, however, the distortion of the law of the motion might affect the operation of a mechanism. The degree of the influence of the distortion can be checked by calculation [20].

The recommended routine of designing self-aligning mechanisms (devoid of redundant constraints) is well illustrated by the above chart suggested by J.J. Gaipel.

## 1.10. New Method of Determining Redundant Constraints and Mobilities of Mechanisms

It is essential, while designing self-aligning mechanisms, to be able to determine in a given mechanism (i.e. with the kinematic pairs and their arrangement known) where and what mobilities and redundant constraints take place.

Malyshev's structural formula and the equivalent Ozol's formula yield just one correlation between structural parameters of a mechanism out of many, which is not sufficient for a unique decision on the selection of the mechanism's parameters. The solution of the problem resides in the investigation of mobilities in a loop of the mechanism, to be described below [36].

At present, loops in a mechanism have been exploited by O. G. Ozol and N. E. Shamaidenko [49].

From formula (1.2) we find $f = 6k + w - q$, where $q =$ redundant constraints; $w =$ mobility including the local one; $k = p - n$ is the number of independent loops; $f =$ the sum of mobilities.

To solve the equation, let us break down the sum $f$ of the mobilities of kinematic pairs by coordinate axes. As $f$ is an arithmetic sum of the mobilities, the breakdown also contains an arithmetic sum:

$$f = f'_x + f'_y + f'_z + f''_x + f''_y + f''_z$$

where $f'_x$ is the sum of linear mobilities along $x$ axis, and $f''_x$ is the sum of angular mobilities about $x$ axis, and so on.

A substantial merit of this correlation is its applicability to various coordinate systems. An orthogonal system may be used,

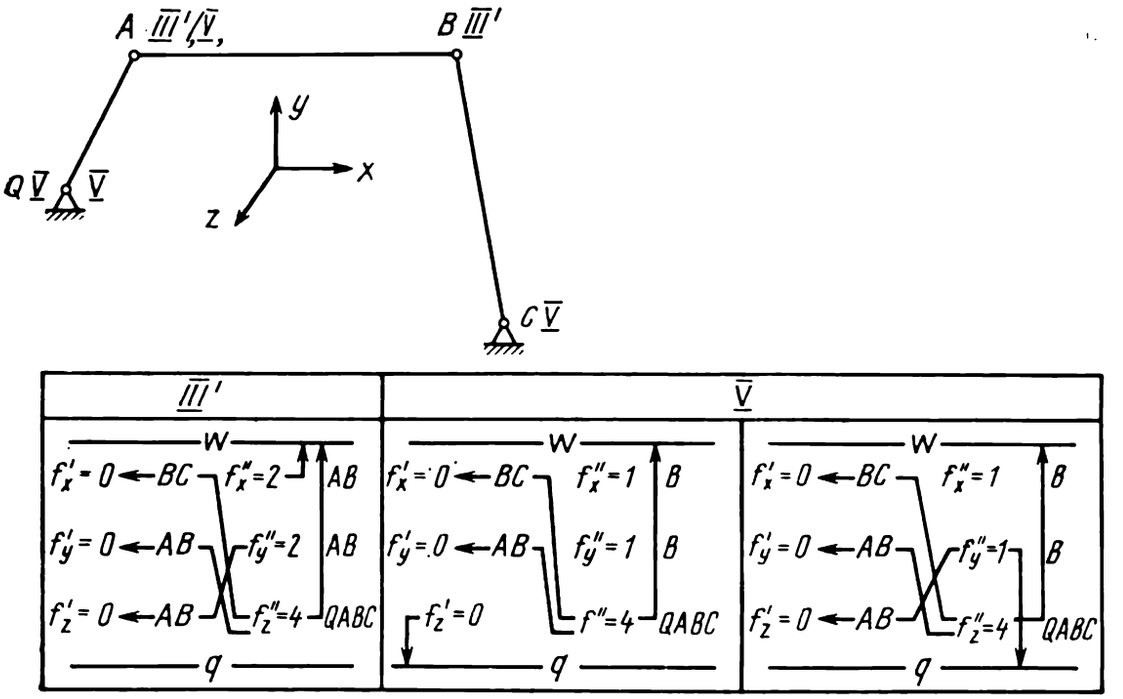


Fig. 1.15. Mobilities in the loop of a four-pivot mechanism

as well as an oblique-angle one, but the three axes should not be, however, in the same plane, otherwise mobility in the direction perpendicular to this plane will not be provided. Either the same or different coordinate axes can be taken for the linear and angular mobilities, and a mobility can be considered at an angle to a given coordinate axis (different from 90° in any case) for a mobility to have a resultant along this axis.

*For a single-loop mechanism, the presence of all the three angular mobilities is a necessary condition for the loop to close without prestrain, i.e.* $f''_x \geqslant 1$; $f''_y \geqslant 1$; $f''_z \geqslant 1$.

The absence of even one such mobility brings about prestrain and a redundant constraint.

With extra angular mobilities, a similar condition would not be necessary for linear mobilities, as linear approach displacement of links while assembling can be done not only owing to the linear mobility of the kinematic pairs, but also by rotating the links about an axis perpendicular to the direction of linear mobility (cf. Fig. 1.15). *Therefore, linear mobility can be replaced by angular mobility about an axis perpendicular to the direction of the linear mobility*; the mechanism, however, should be checked to establish a link which would move linearly in the required direction as a result of such rotation, and make certain that this capability is unaffected in certain positions, e.g. at dead centres. To illustrate the

point, let us apply this method to a four-pivot mechanism with a spherical pair $III'$ at point $A$ (cf. Fig. 1.15, the left-hand part of the Table where the kinematic pairs are denoted by the numerator). Let $x$ axis extend along the connecting-rod $AB$. In the mechanism, the linear mobilities of the kinematic pairs along the three orthogonal axes equal zero. The spherical pairs at points $A$ and $B$ have each a single angular mobility about $x$ axis. They also have angular mobilities about $y$ axis, i.e. the sum of the angular mobilities is two. All the four pairs have angular mobilities about $z$ axis.

The kinematic pairs whose linear mobilities are entered into the Table of Fig. 1.15 are to be found in the left-hand column of the Table, while the pairs, whose angular mobilities are also there, are to be found in the right-hand column.

The replacement of a linear mobility with an angular one is indicated with a zig-zag arrow leading from the angular mobility to the linear one. The arrow denotes the link that rotates at such replacement. The first in the symbol is the kinematic pair whose angular mobility is used for the replacement (as suggested by E.Y. Budyka). This is essential to avoid exploiting a single link twice by rotation about the same axis (although a link may be rotated about different axes, for example, link $AB$ in Fig. 1.15 is rotatable about $y$ and $z$ axes).

Let us see the destination of the angular mobilities.

We start with $f''_z$. One mobility is retained for closing the loop, two are spent on replacement of $f'_x$ and $f'_y$, and one remains as the mobility of the mechanism. In the Table, this distribution is illustrated with zig-zag arrows, each symbolizing a unit of mobility. One mobility, $f''_y$, is retained for closing the loop, another is used to replace $f'_z$, which is quite feasible since link $AB$ is rotatable about $y$ axis; $f''_x$ —one mobility is retained for closing the loop, and another is the local mobility (rotation about $x$ axis) of the connecting-rod $AB$. Thus, with the kinematic pairs denoted in Fig. 1.15 by the denominator, the mechanism has general mobility and a local mobility (rotation of the connecting rod about its own axis) and is free from redundant constraints.

Another system of building the chart—the "line-by-line" one—has been suggested by E.Y. Budyka [40].

For comparison sake, let us discuss the same mechanism, but having a rotary pair at point $A$ (Fig. 1.15—central part of the Table, where the kinematic pairs are denoted by the denominator); only angular mobilities $f''_x$ and $f''_y$ will change, each equalling unity as there is now but a single spherical pair instead of two. All the three

linear mobilities still are absent. The condition $f_z''' = 4$ remains, same as the distribution of these mobilities. Mobility $f_z'$ equals zero, and there is nothing to replace it, as $f_x''' = 1$ and $f_y''' = 1$, and they are used for closing the loop, and, hence, they cannot be spent on replacing the linear mobility. Consequently, there is no mobility along $z$ axis, and the mechanism is characterized by prestrain and a redundant constraint, which is indicated with the corresponding arrow in the Table. There is no local mobility, as $f_x'' = 1$, and there is no extra angular mobility. Thus, with the kinematic pairs denoted in Fig. 1.15 by the denominator, the mobility of the mechanism equals one, and there is one redundant constraint—the prestrain along $z$ axis. To eliminate the constraint, the turning pair in pivot $A$ is to be replaced with a fourth-class cylindrical pair.

The prestrain along $z$ axis brings about loading effort $P$ in kinematic pair $B$ and torque in pair $A$, as well as in pairs $Q$ and $C$. If one imagines that pair $A$ is made up of two bearings spaced apart by distance $b$, then the load of each bearing caused by prestrain $P$ will equal $P\frac{L_{AB}}{b}$, i.e. it is far greater than $P$. Therefore, the decisive factor brought about by the redundant constraint is the torque, not force. In Fig. 1.15 (the right-hand part of the Table) the lacking linear mobility $f_z'$ is replaced by the angular one $f_y'''$. Then there is no angular mobility $f_y'''$ available for closing the loop, and there will appear a redundant constraint causing prestrain in the form of a torque. It so appears that a redundant constraint in a loop causes prestrain practically in the form of a torque. This has enabled postgraduate student V. Ja. Akulov to suggest calling such redundant constraints "loop" ones, and calling redundant constraints in a group of loops, capable of causing force prestrain, "group" ones. The classification seems to be more to the point than that by V. V. Dobrovolski who divides the redundant constraints into genetic and individual ones, which is of no help to an engineer in evaluating the effects of these constraints.

The suggested method is also applicable to the two-loop mechanisms. If the floating link is an intermediate one, both loops can be considered simultaneously, with the number of the required mobilities along the orthogonal axes and about the axes being doubled. On the other hand, each loop can be considered separately, and the mobilities of the kinematic pairs belonging to both loops should be distributed among them. A mobility should be allocated to the loop where it eliminates prestrain, and not the loop where it remains as a local mobility.

The method of mobilities in a loop is further applicable to multi-loop mechanisms. It is expedient to consider the loops starting with the major mechanism and proceeding with associated groups. While considering the mobilities of the first-discussed loop, one can allocate the mobilities of all the pairs it includes. If redundant constraints are detected in it, they will remain as redundant constraints of the mechanism, as no successive loop is of help in eliminating them. The total mobility of this loop will be the mobility of the mechanism.

Local mobility is quite another case: it depends on which link it belongs to. If the local mobility is possessed by a link included in the next loop, it will be included into the number of the mobilities of this loop and can be utilized for eliminating its redundant constraints. Should the local mobility, however, be possessed by a link not included into the next loop, it would remain as a local mobility of the mechanism. Let us take as an example a mechanism with a knuckle connecting rod (Fig. 1.16).

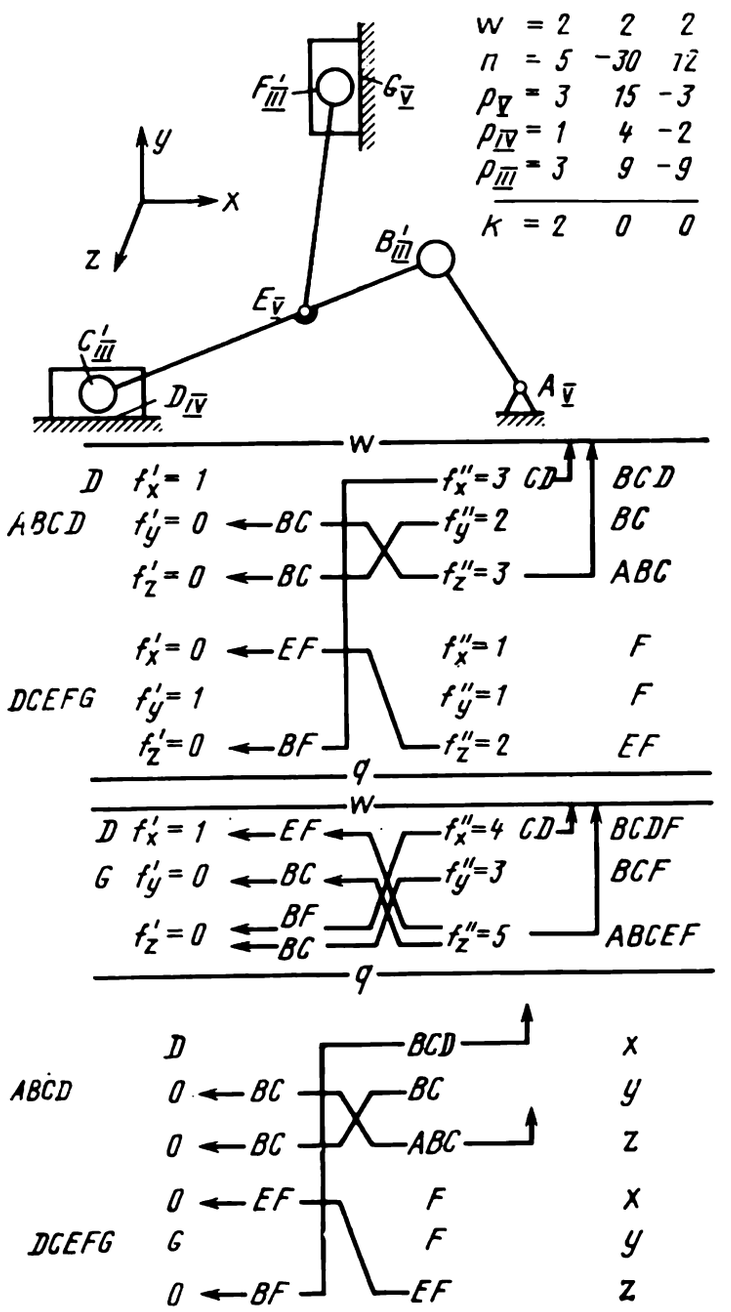


Fig. 1.16. Mobilities in a double-loop mechanism

The Table in the top right-hand corner is one of calculation by structural formulas, with the constraint conditions by Malyshev's formula in the central column, and mobilities by Ozol's formula in the right-hand column. We are going to use similar tables or charts in the pages to follow.

Let us take the first loop as the one including the main connecting crank, the connecting rod and the horizontal slide, and the second loop as including the vertical slide, the knuckle connecting rod and the horizontal slide. In the first loop, angular mobilities $f''_y$ and $f''_z$ are used for replacing linear mobilities $f'_z$ and $f'_y$ and for closing the loop. The remaining angular mobility $f''_z$ is the general mobility of the mechanism. Out of the three angular mobilities $f''_x$ one is used for closing the loop, another—the mobility of the cylindrical slide—remains as a local mobility of the mechanism, and the third—rotation of the connecting rod about its own axis—passes to the second loop to be used for replacement of linear mobility $f'_z$. In the second loop, one angular mobility $f''_z$ replaces linear mobility $f'_x$ for closing the loop.

Thus, by proceeding from one loop to another, we are able to investigate the entire mechanism.

In complex mechanisms, e.g. in planetary gearings, the number of the loops may be as high as 12 or even higher. Therefore, it is important to simplify the solution, which is attainable in three ways.

**The first way.** Two links are connected by several kinematic pairs arranged parallel to one another. Then the constraints they impose add up. By the sum of the constraints, a substituting pair should be selected, providing, of course, for the possibility of appearing of redundant constraints. The number of the loops is thus reduced in accordance with formula (1.3).

For instance, three point pairs can be considered to exist between a wheel pair and the rails: two contacts of the tapering portions of the tyre and the engagement of the flanges. On the other hand, the engagement of a wheel pair with the rails may be considered as a single third-class pair, which means that the number of the loops per each wheel pair is reduced by 2. This technique is used in Section 6.13 below. We can go still further. When there are several first-class dogs between two links, each imposing a single constraint (cf. 3.1), they can be substituted by a single dog of a higher class. We shall use this technique in the case of current collector mechanisms (3.10).

**The second way.** A block made up of several links may be considered separately. Thus, in planetary gearings it may be expedient to consider a block including the central or sun wheel, the internal or ring gear, the carrier and the planetary pinions interconnecting them, and to evaluate the redundant constraints and mobilities in this block. Then the constraints will be included into the number of the redundant constraints of the entire mechanism, while the

mobilities will be added to the number of the mobilities of the kinematic pairs in the remaining loops, whose number, reduced by the number of the loops considered in the block, will be fairly small. This technique will be used in Section 5.7. A similar technique may be used when dealing with multilink pivot mechanisms, where it may be expedient to consider a planar structural group (cf. 2.11 below).

**The third way.** Mobilities may be considered in several groups simultaneously. This technique is illustrated by the central Table in Fig. 1.16. Quite obviously, the number of the mobilities required for closing the loops would grow in proportion to the number of the loops. The detection of local mobilities and redundant constraints is in this case more complicated than when the loops are considered separately (cf. Section 5.13).

Furthermore, the task of distributing the mobilities of the pairs belonging to several loops among the loops may be simplified. Instead of allocating the mobilities to the first loop and passing the remaining mobilities to the successive loops, they can be distributed among the loops at the very beginning, using the following rule: *a mobility is to be allocated to a loop where it eliminates a redundant constraint and not to one where it yields local mobility.* When distributing the mobilities, it may be useful to begin with kinematic pairs belonging to a single loop. We shall denote these pairs in the following pages with a dot above the letter. This will show more clearly where the mobilities of the rest of the pairs should be allocated.

The pattern of mobilities in loops may be substantially simplified (cf. bottom Table in Fig. 1.16). Bearing in mind that linear mobilities along given orthogonal axes are entered into the left-hand column, and angular mobilities are in the right-hand column, it is expedient to write down the alphabetic symbols of the kinematic pairs yielding the corresponding mobility instead of the mobility numbers, with each letter standing for one mobility. There is no necessity then to write such symbols as $f'_x$, $f'_y$, and so on; it suffices to put to the right the symbols of the respective coordinate axes (and with a single system of the coordinate axes even this can be omitted). The remaining redundant constraints should be indicated with the arrows pointing down, and the mobilities—with the arrows pointing up (suggested by J. J. Gaipel). Lines $w$ and $q$ are not needed then any longer. It is easy to denote in this chart the kinematic pairs associated with the mobility being considered. In the following pages both ways of illustrating mobilities will be used.

All the kinematic pairs take part in the general mobility, whe-

reas usually two pairs define a local mobility. Out of the two mobilities of the latter pairs one is employed for closing the loop (for the assembly), while the other one extends from the loop as the local mobility. It is useless, if possible at all, to distinguish between the two mobilities. In a chart or diagram, they should be interconnected with a bracket, with the arrow indicating the local mobility extending from this bracket. This set signifies one local mobility and one mobility employed for closing the loop (cf. Section 6.13). Local mobilities evolve in self-aligning mechanisms when one of the loops possesses extra mobilities apart from those required for the general mobility and elimination of redundant constraints. These mobilities are brought about either by stepping up the mobility of the kinematic pairs or by addition of new pairs. In some cases a single kinematic pair is added, but it takes at least two pairs to define local mobility.

When a local mobility involves adjacent kinematic pairs, in most cases (but not always) it is harmless. If the pairs are not adjacent, the local mobility is a group one, and it is essential to check whether it is harmless. When couples participating in local mobility adjoin a fixed member, in most cases the group mobility is harmful.

The abovesaid should be born in mind whenever the local mobility of one loop is employed to eliminate the redundant constraints of another one.

Let us consider a single toothed gearing with line contact of the teeth ($II_2$) and one of the shafts supported by cylindrical pair $IV_2$ (Fig. 1.17). In this case $x$ axis preferably extends tangentially of the tooth, $y$ axis—along the normal, and $z$ axis—along the axis of rotation of the gears.

Linear mobilities in this gearing are found: along $x$ axis—slipping of teeth, $f'_x = 1$; along $y$ axis—normal to the tooth, $f''_y = 0$; along $z$ axis—axial slipping of the teeth and axial mobility of pair $IV_2$, $f'_z = 2$. Angular mobilities are found: about $x$ axis, $f'_x = 0$; about $y$ axis — relative rotation about the normal, $f''_y = 1$[1]; and about $z$ axis in every kinematic pair, $f''_z = 3$.

The distribution of the mobilities is as follows: $f'_x$ is used for closing the loop; $f'_z$—for closing the loop and for a local mobility of the mechanism (a harmful one); $f''_x = 0$ causes a redundant constraint—non-uniform distribution of the load along the tooth; $f''_y = 1$—for

[1]We assume that line contact of the teeth is retained, which is permissible because calculations [34] show that even with the greatest practical non-parallelism of the axes the clearances at the ends of a tooth are a fraction of the deformation of the teeth.

closing the loop; $f_z'' = 3$—for closing the loop, for replacing $f_y'$ and for the main mobility of the mechanism.

The mechanism under discussion is inoperable, as it has mobilities other than required: it retains axial mobility of one of the shafts (the gears would move apart in operation) and a redundant

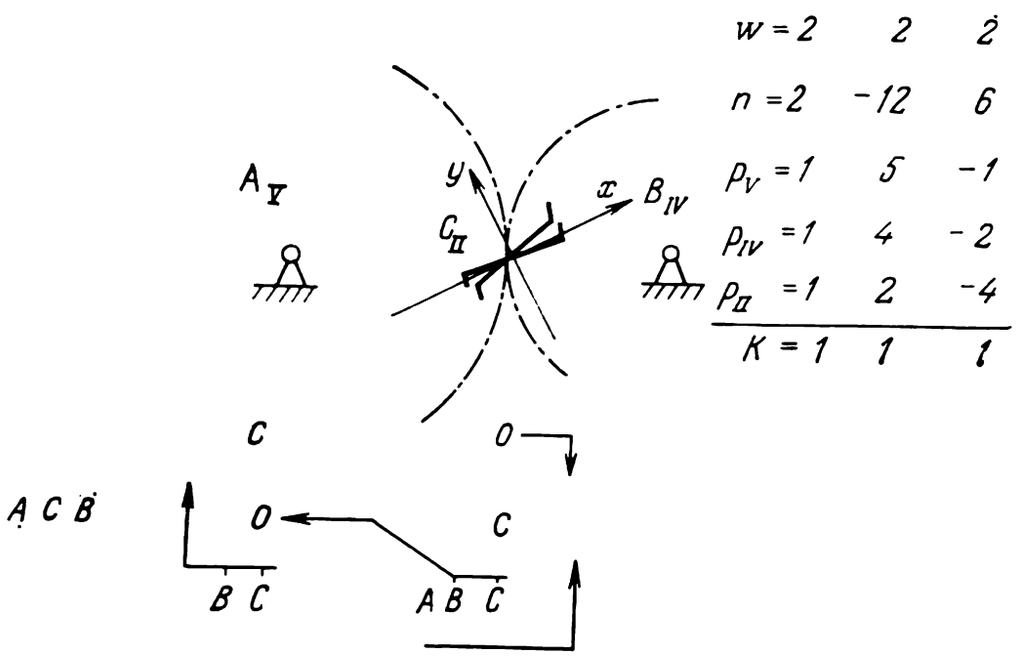


Fig. 1.17. Mobilities in loop of spur toothed gear train with harmful mobility

constraint causing non-uniform distribution of the load along the tooth.

The proposed method is applicable also in cases where the mobility of a kinematic pair (either linear or angular) is at an angle to the coordinate axes which is not always avoidable even by using coordinate axes extending at oblique angles. The mobilities then should be related to one of the axes—the one where a mobility is usable and which is defining with the mobility a small angle. This is natural, as it is only along a single coordinate axes that the motion is independable, while along the other axis the motion is associated with the tangent of the inclination angle. The situation is similar to that of a helical pair characterized by both linear and angular motions of which only one is independent, so that the pair is considered a single-mobility one.

Let us consider as another example a double universal-joint mechanism without a spline joint (Fig. 1.18). Let $x$ axis be directed along the intermediate shaft. All the kinematic pairs are fifth-class revolutes devoid of linear mobility, so that the three linear mobilities

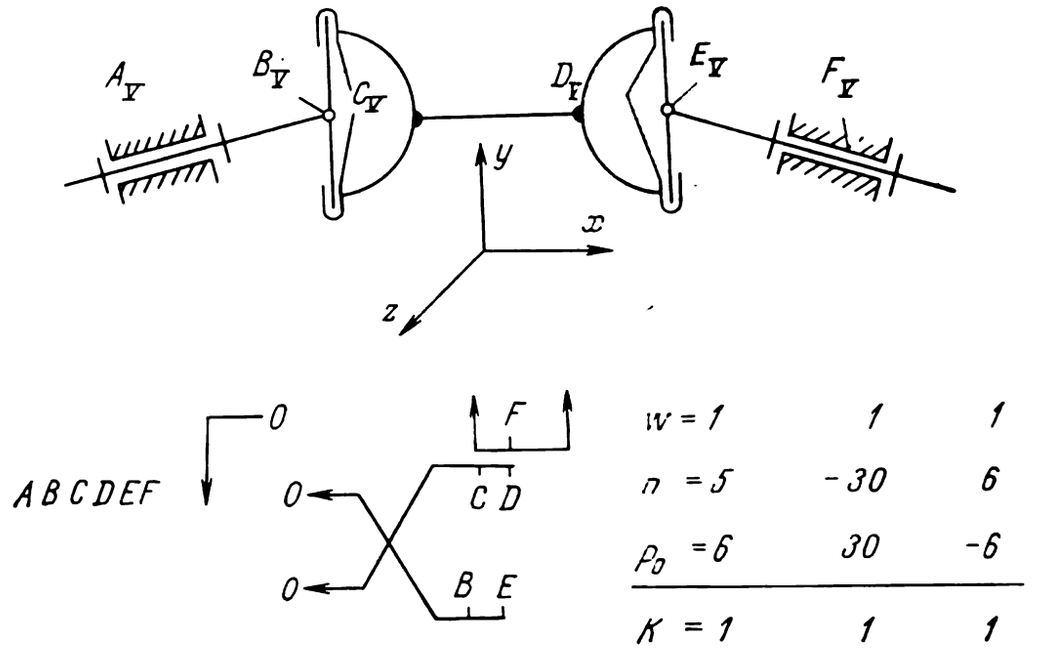


Fig. 1.18. Mobilities in loop of double universal-joint mechanism

$f'_x$, $f'_y$ and $f'_z$ equal zero. For the above-mentioned reasons, let us relate the angular mobilities of the driving and driven shafts to $x$ axis, so that $f''_x = 2$. To evaluate angular mobilities about $y$ and $z$ axes, it is possible either to direct $y$ and $z$ axes parallel to the pivot axes of the universal joints, or else to consider the mechanism in a position where the jaws of the universal joints on the intermediate shaft align with the plane of the two axes, or to relate the mobilities in the pivots of the universal joints to one of the two coordinate axes. In any case, we shall come to $f''_y = 2$ and $f''_z = 2$.

There is no mobility along $x$ axis ($f'_x = 0$). It cannot be replaced by an angular mobility, as the mechanism is devoid of a link perpendicular to $x$ axis, whose rotation could yield the respective motion; neither has the mechanism any extra angular mobilities. Therefore, there appears a redundant constraint causing prestrain along the intermediate shaft, which is indicated with the arrow in chart of Fig. 1.18.

The lacking mobilities $f'_y$ and $f'_z$ are replaced by angular mobilities $f''_z$ and $f''_y$ which abound in the mechanism owing to the intermediate shaft being perpendicular to $y$ and $z$ axes and capable of corresponding rotation.

The second mobility $f''_x$ about $x$ axis is retained as the mobility of the mechanism.

Thus, a double universal-joint mechanism with the kinematic pairs shown in Fig. 1.18 has one mobility and one redundant con-

straint prestraining the shaft axially. To eliminate it, the shaft should be provided with a spline joint.

Independent determination of redundant constraints and mobilities in a mechanism can be done using the graph method. A method of this kind has been developed and suggested by L.A. Pavlova [26].

## 1.11. Non-Planar Constraints and Mobilities for Investigating Structure of Mechanisms

The complete method of detecting redundant constraints in mechanisms—the method of mobilities in loops—has been described in the preceding Section. The method enables one to detect redundant constraints in any planar and three-dimensional mechanism.

With the number of the loops being relatively small, the method provides for evaluating all the mobilities and redundant constraints in a mechanism in a fairly simple procedure. With a considerable number of the loops, the solution is far more complicated. To simplify the solution, the following method is suggested.

Let us assume that all the possible constraints and mobilities of the kinematic pairs of a planar mechanism are in the form of two groups, *viz.* those belonging to the plane of the mechanism (to be more exact, those acceptable to its planar diagram), or in short, planar constraints and mobilities $s_p = s'_x + s'_y + s''_z$ and $f_p = f'_x + f'_y + f''_z$; and those in planes perpendicular to the plane of the mechanism, or, in short, non-planar constraints and mobilities $s_{np} = s''_x + s''_y + s'_z$ and $f_{np} = f''_x + f''_y + f'_z$.

It is easy to prove that mechanisms having no passive links (as is the situation with the vast majority of planar mechanisms) are devoid of planar redundant constraints, i.e. $q_p = q'_x + q'_y + q''_z = 0$, and, therefore, such mechanisms can be investigated solely for detection of non-planar redundant constraints $q_{np} = q''_x + q''_y + q'_z$.

This shortened method, as compared with the full one, significantly reduces the time required for detecting redundant constraints in planar mechanisms. With this method, the diagram of the mobilities is cut by one half, and, which is even more important, the number of replacements of lacking mobilities—the most effort-consuming part of the investigation—is reduced to a fraction. There are avoided the most frequent replacements of planar mobilities $f'_x$ and $f'_y$, while the mobility $f'_z$ to be considered according to the shortened method is absent but rarely, e.g. owing to axial mobility along $z$ axis (in toothed gearing and cam-and-follower mechanisms).

The shortened method is also applicable to planar mechanisms with exclusively prismatic pairs, i.e. to the so-called wedge mechanisms, but here each loop would include, in addition to $q_{np}$, one planar redundant constraint $q''_z$.

Before applying the shortened method to planar mechanisms having passive links imposing redundant constraints, the passive links should be eliminated. The easiest way to determine the absence of passive links is breaking down the diagram of the mechanism to Assur's structural groups and the group of initial links, which is elementary simple. Planar mechanisms with passive links are, in general, a rarity.

To illustrate the point, let us determine the redundant constraints in a planar mechanism shown in Fig. 1.19 by the complete and shortened methods. The number of the independent loops of the mechanism $k = p - n = 13 - 9 = 4$. For completeness of the analysis, there is also shown in Fig. 1.19 the diagram of planar mobilities yielding $q_p = 0$.

With the shortened method, let us register non-planar mobilities in the chart in a single column, from top down: $f''_x$, $f''_y$, $f'_z$.

It is clear from comparing the mobility charts that the chart of the shortened method is half as big as the complete-method one, and, moreover, the shortened method involves but one replacement, while the complete one requires nine replacements. The eight replacements are required by the planar diagram.

The table or chart of mobilities in Fig. 1.19 could be further clarified by separating all the mobilities and constraints into linear and angular ones.

Let us show the necessary additions to the planar formulas of A. P. Malyshev and O. G. Ozol.

Table 1.5 gives the numbers of the mobilities of kinematic pairs for the three-dimensional, planar and non-planar diagrams of a mechanism, reflecting the orientation of these pairs relative to the plane of the planar mechanism, which has not been done before. In the Table, for each class, in top lines (*a*) the kinematic pairs are depicted in the most common orientation, i.e. they are arranged in the plane of the mechanism. In bottom lines (*b*) the pairs are turned through 90° relative to this plane, which can be encountered in numerous mechanisms, e.g. in planetary gear trains, as well as in mechanisms where redundant constraints are eliminated by addition of kinematic pairs. Helical pairs do not belong to planar mechanisms.

We should be aware of the fact that a kinematic pair of one and the same class has different numbers of planar and non-planar con-

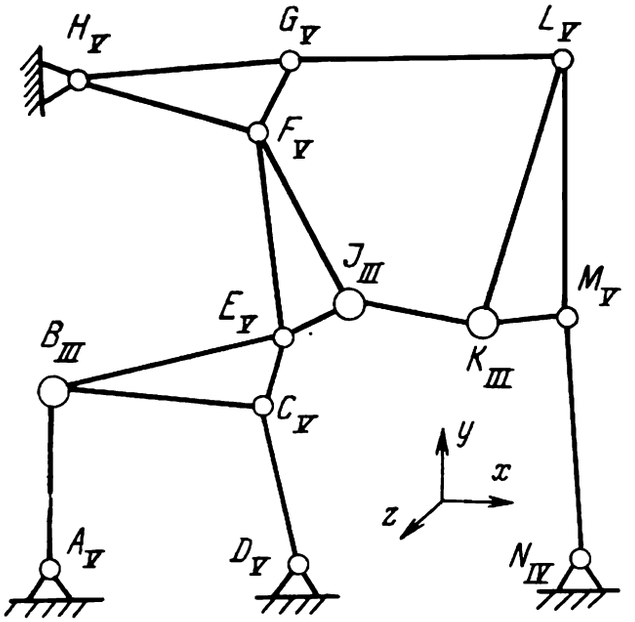


| | Three-dimensional | | Planar | | Non-planar | |
|---|---|---|---|---|---|---|
| | M | O | M | O | M | O |
| w | 2 | 2 | 1 | 1 | 1 | 1 |
| n = 9 | -54 | 24 | -27 | 12 | -27 | 12 |
| $p_V = 9$ | 45 | -9 | 18 | -9 | 27 | 0 |
| $p_{IV} = 1$ | 4 | -2 | 2 | -1 | 2 | -1 |
| $p_{III} = 3$ | 9 | -9 | 6 | -3 | 3 | -6 |
| K = 4 | 6 | 6 | 0 | 0 | 6 | 6 |
| | q | | | | | |

| Loops | Three-dimensional | Planar | Non-planar |
|---|---|---|---|
| DCEFṄ | 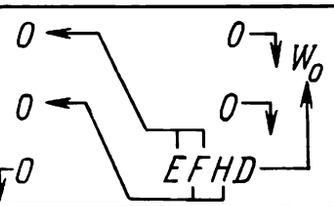 | 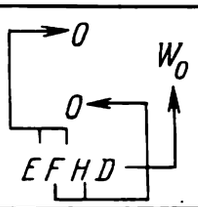 | 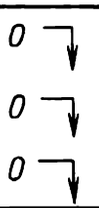 |
| DCḂÀ | 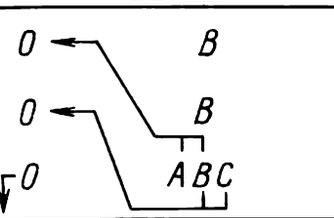 | 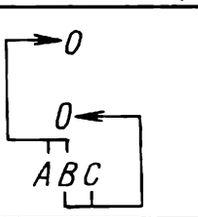 | 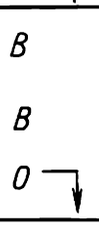 |
| JFĠL̇K | 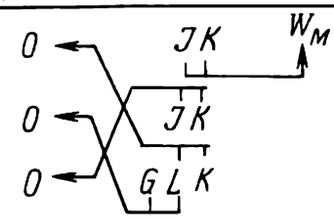 | 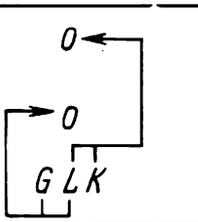 | 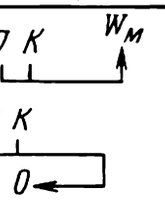 |
| DEJKṀṄ | 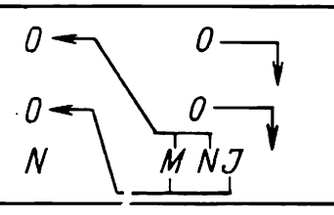 | 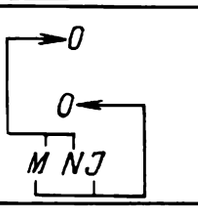 | 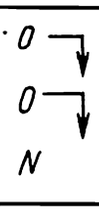 |
| q | q = 6 | $q_p = 0$ | $q_{np} = 6$ |

Fig. 1.19. Planar mechanism and its analysis for nonplanar constraints and mobilities

*Table 1.5*

| Class of Pair | | Three-dimensional | | Planar | | Non-planar | |
|---|---|---|---|---|---|---|---|
| | | $S_f$ | $f$ | $S_p$ | $f_{np}$ | $S_{np}$ | $f_{np}$ |
| (a) $I_1\ I_2\ I_3\ I_4\ I_5$ | 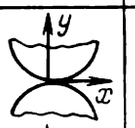 | 1 | 5 | 1 | 2 | 0 | 3 |
| (b) | 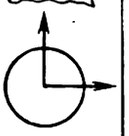 | 1 | 5 | 0 | 3 | 1 | 2 |
| $II_2\ II_5$ | 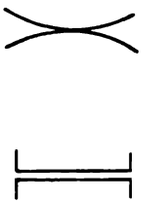 | 2 | 4 | 1 | 2 | 1 | 2 |
| $II_1\ II_3$ $II_4$ | 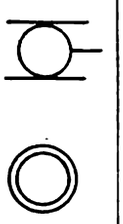 | 2 | 4 | 2 | 1 | 0 | 3 |
| $III_1'\ III_2''$ $III_4'$ | 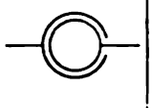 | 3 | 3 | 2 | 1 | 1 | 2 |
| $III''\ III_2''$ | 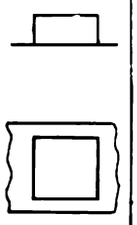 | 3 | 3 | 0 | 3 | 3 | 0 |
| $III_3''\ III_4''\ III_5''$ | 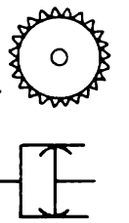 | 3 | 3 | 3 | 0 | 0 | 3 |
| | | 3 | 3 | 1 | 2 | 2 | 1 |
| $IV_3\ IV_4$ $IV_5$ | 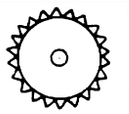 | 4 | 2 | 3 | 0 | 1 | 2 |
| $IV_1\ IV_2$ | 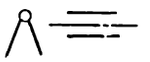 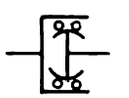 | 4 | 2 | 2 | 1 | 2 | 1 |
| $V_1\ V_2$ | | 5 | 1 | 2 | 1 | 3 | 0 |
| $V_3$ | 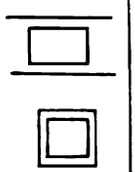 | 5 | 1 | 3 | 0 | 2 | 1 |

straints and mobilities, depending on its orientation, i.e. depending on whether it is in (*a*) or (*b*) lines of the Table. For instance, the spline pair of class $III_5''$, in top line (*a*) has $s_p = 3$ and $f_p = 0$ (in a planar diagram), whereas in bottom line (*b*) the same pair has $s_p = 1$ and the number of mobilities $f_p = 2$, which is also true of the pairs of other classes. Non-planar constraints and mobilities are in a similar situation. However, in the column corresponding to a three-dimensional diagram the values of $s$ and $f$ are independent of the orientation of the pairs, i.e. of the line in the Table. Let us analyze the work of the structural formulas of the mechanisms in the light of Table 1.5.

As far as Ozol's planar formula (1.6) is concerned, the available sources do not contain indications as to how the number of planar mobilities $f_p$ included in the formula can be evaluated, therefore the formula may lead to errors, if the orientation of the pairs is not taken into account.

To obtain proper results when using Ozol's planar formula (1.6), mobility $f_p$ should be selected from Table 1.5: columns for planar diagrams of mechanisms, row (*a*) or (*b*) in strict compliance with the orientation of the pair.

The available sources give no structural formula for evaluating the number of non-planar redundant constraints of planar mechanisms.

Finally, let us remember that there exists a specific group of multiplane mechanisms (see below) for which all the structural formulas of planar mechanisms require corrections.

Let us fill in the gaps left by the existing structural formulas for planar mechanisms.

In accordance with the logic of deriving Malyshev's formula (1.1), the latter can be used both with the three-dimensional diagram of a mechanism and with a purely planar or non-planar one.

Let us write down formula (1.1) for three-dimensional mechanisms:

$$q = w - 6n + 5p_{\mathrm{V}} + 4p_{\mathrm{IV}} + 3_{p\mathrm{III}} + 2p_{\mathrm{II}} + p_{\mathrm{I}}$$

Let us further give formula (1.6)—Malyshev's planar formula—in the developed form:

$$q_p = w_p - 3n + s^p_{\mathrm{V}} p_{\mathrm{V}} + s^p_{\mathrm{IV}} p_{\mathrm{IV}} + s^p_{\mathrm{III}} p_{\mathrm{III}} + s^p_{\mathrm{II}} p_{\mathrm{II}} + s^p_{\mathrm{I}} p_{\mathrm{I}}$$

By subtraction, we derive a structural formula for non-planar redundant constraints, or the non-planar formula:

$$q_{np} = w_{np} - 3n + s^{np}_{\mathrm{V}} p_{\mathrm{V}} + s^{np}_{\mathrm{IV}} p_{\mathrm{IV}} + s^{np}_{\mathrm{III}} p_{\mathrm{III}} + s^{np}_{\mathrm{II}} p_{\mathrm{II}} + s^{np}_{\mathrm{I}} p_{\mathrm{I}} \qquad (1.25)$$

where

$$q_p + q_{np} = q; \quad s^p_{IV} + s^{np}_{IV} = 4: \quad s^p_{II} + s^{np}_{II} = 2$$

$$s^p_V + s^{np}_V = 5; \quad s^p_{III} s^{np}_{III} = 3; \quad s^p_I + s^{np}_I = 1$$

We select coefficients to formula (1.25) from Table 1.5 depending on the orientation of kinematic pairs.

In the plane of the mechanism, $w_{np}$ practically equals $w_m$.

Malyshev's three-dimensional and planar formulas (1.1) and (1.5) take into account the number of links and kinematic pairs. Ozol's formulas (1.2) and (1.6) are built upon the number of the loops $k$, and of mobilities $f$. Non-planar formula (1.25) is based on Malyshev's formula. It is useful to derive a non-planar formula from Ozol's one.

Let us write down formula (1.2) in the developed form:

$$q = w + 6k - p_V - 2p_{IV} - 3p_{III} - 4p_{II} - 5p_I$$

Also formula (1.6)—Ozol's planar formula—in the developed form:

$$q_p = w_p + 3k - f^p_V \; p_V - f^p_{IV} p_{IV} - f^p_{III} p_{III} - f^p_{II} p_{II} - f^p_I \; p_I$$

Hence, by subtraction, we obtain a structural formula for non-planar redundant constraints, or a non-planar structural formula based on Ozol's formula:

$$q_{np} = w_{np} + 3k - f^{np}_V p_V - f^{np}_{IV} p_{IV} - f^{np}_{III} p_{III} - f^{np}_{II} p_{II} - f^{np}_I p_I \quad (1.26)$$

where

$$q_p + q_{np} = q; \quad f^p_{IV} + f^{np}_{IV} = 2; \quad f^p_{II} + f^{np}_{II} = 4$$

$$f^p_V + f^{np}_V = 1; \quad f^p_{III} + f^{np}_{III} = 3; \quad f^p_I + f^{np}_I = 5$$

Coefficients to formula (1.26) are selected from Table 1.5 depending on the orientation of kinematic pairs.

Also illustrated in Fig. 1.19 is a compact pattern of recording the calculations by Malyshev's (M) and Ozol's (0) structural formulas and formulas (1.25) and (1.26)—for three-dimensional, planar and non-planar diagrams of a mechanism. The Table lists all the summands with their signs and their sums, i.e. the values of $q$ for these formulas.

The above formulas can also be used in case of three-dimensional mechanisms, when one of the planes of a three-dimensional mechanism dominates. This plane can be taken as basic, and the mechanism can be analyzed with respect to this calculation plane by the planar and non-planar formulas.

In a planar mechanism, the calculation plane may be not only that of the motion, but also some other plane.

The above refinements of the planar formulas by A.P. Malyshev and O.G. Ozol enable one to arrive at correct results in some of the mentioned practically important cases. In its turn, the newly derived non-planar formula can be of help to a designer for a rapid check-up of the analysis by the shortened method, for better understanding of the nature of redundant constraints of planar mechanisms to be eliminated.

The somewhat complicated form of the newly derived formulas reflects their deeper penetration into the laws of construction of mechanisms.

There exists a specific group of planar mechanisms for which a direct calculation of the number of redundant constraints from the structural formulas for their planar and non-planar diagrams yields erroneous results. However, formulas for three-dimensional mechanisms, if applied, give a correct amount of the redundant constraints.

Each mechanism of this group is arranged in several parallel planes, with motion being successively transmitted from one plane into an adjacent one via floating connection parts or links. The group is exemplified by a train of planetary gearings with floating carriers and some linkages, e.g. the articulated mechanism of a straw shaker. A detail analysis by the method of mobilities in a loop would reveal that each floating link of such a mechanism either transfers to, or substitutes two angular mobilities from the non-planar diagram into two linear mobilities in the planar diagram of the mechanism, where mobilities are added up and the number of the planar redundant constraints is reduced to zero. However, if the number of redundant constraints is calculated by any structural formula separately for the planar and nonplanar diagrams of the mechanism, the structural formulas not responding to the substitution of the mobilities will yield wrong results.

Therefore, in case of a mechanism with floating links, *two* should be subtracted from the number of redundant constraints calculated from any planar structural formula per each floating link.On the other hand, *two* should be added, per each floating link, to the number of redundant constraints calculated from a non-planar formula.

As these corrections to the structural formulas do not prove any inadequacy of these formulas, they should only be taken as required for calculation of the value of $q$ in above-mentioned group of mechanisms.

## 1.12. Influence of Friction Upon Self-Aligning of Mechanisms

The influence of friction forces upon the ability of the parts of mechanisms to self-align should be taken into account due to the following considerations:

the friction forces can deprive the kinematic pairs of a mechanism of some of the mobilities, so that the mechanism devoid, by its design, of redundant constraints may, in fact, become statically indeterminate;

the friction forces are capable of causing additional strain and deformation;

the friction forces affect the accuracy of the self-alignment of links, which in some cases plays the decisive role.

Let us define "resistance to self-alignment" as the force (or torque) spent on the additional motion required for a mechanism to self-align. With continuous self-aligning, the resistance affects the distribution of forces in and among the kinematic pairs, which fact should be taken into account. With single self-alignment, the resistance acts only during the first revolutions and then ceases to affect the distribution of the forces.

Numerous mechanisms have several statically determinate structural designs with different resistance to self-alignment; this should be considered while selecting the structural design. The value of the resistance to self-alignment may play a decisive role in selecting the structure of kinematic pairs.

To be able to evaluate the resistance to self-alignment of the parts of actual mechanisms, let us compute the resistances for most common kinematic pairs with several mobilities in relation to the ratio of the velocities of the main relative motion of the parts to the rate of their self-aligning. The expressions derived below fit the cases of friction with dry, semidry and semifluid lubrication. It should be remembered, however, that in numerous mechanisms the velocities of the relative motion of the links of a pair are relatively low, whereas the reactions in the pairs are substantial and more often than not have alternating values and directions. Under such conditions even the elements of pairs with surface contact of the links work in the mode of semidry friction or friction with semifluid lubrication. The elements of kinematic pairs of all mechanisms work under similar conditions at starting moments when self-aligning is greatly opposed. And, finally, it is the present-day practice to widely introduce new synthetic materials into the manufacture of

the elements of kinematic pairs subject to friction, to provide for normal performance of mechanisms with little or no lubrication.

The theory dealt with in Sections 1.13 through 1.15 takes no account of dependence of the friction coefficient on the velocity and specific pressure. Thus, strictly speaking, it applies exclusively to semidry friction. However, the velocity or rate of self-aligning is in practice insignificant in comparison with the velocity of sliding in a kinematic pair. Consequently, self-aligning would not alter significantly the working duty of the pair, i.e. the friction coefficient, and so the theory is applicable with some approximation to all types of friction.

## 1.13. Resistance to Self-Alignment in Cylindrical Pairs

A cylindrical pair possesses two mobilities, *viz.* a prismatic one along the axis of the pair at velocity $v_t$ and a revolute—about the axis of the pair—at angular velocity $\omega$. Then the full velocity of relative sliding of the contacting elements of the pair is

$$v = \sqrt{(\omega R)^2 + (v_t)^2} \tag{1.27}$$

where $R$ is the nominal radius of the pin.

At some areas of contact between the elements of the pair the vectors of the elementary friction forces $dF$ are directed in opposition to vector $v$. Under these conditions it is possible to determine the force of resistance to the translatory and rotary relative motions of the links.

In case of a pair with a clearance which has not been run-in, and the contact of the links can therefore be taken as line one, the full force of friction $F = Qf/\sqrt{1 + f^2}$, where $Q$ is the load applied to the pin; $f$ is the coefficient of friction between the pin and insert.

With $f = 0.2$, $\sqrt{1 + f^2} = 1.02$. Thus, we are going to ignore the value of $f^2$.

Then the force of resistance to translatory motion

$$F_t = Qf \frac{v_t}{\sqrt{\omega^2 R^2 + v_t^2}} \tag{1.28}$$

and that to rotary motion

$$F_r = Qf \frac{\omega R}{\sqrt{\omega^2 R^2 + v_t^2}} \tag{1.29}$$

For a run-in pair (taking the wear of the insert in the direction of the resultant of the normal reactions to be constant), let us denote the angle of engagement of the pin by the insert as $2\varphi_e$. Then the forces of resistance to the translatory motion and rotation, obtained by integration of the corresponding equations, are

$$F_t = Qf \frac{2 \sin \varphi_e}{\varphi_e + \frac{1}{2} \sin 2\varphi_e} \cdot \frac{v_t}{\sqrt{\omega^2 R^2 + v_t^2}} \tag{1.30}$$

$$F_r = Qf \frac{2 \sin \varphi_e}{\varphi_e + \frac{1}{2} \sin 2\varphi_e} \cdot \frac{\omega R}{\sqrt{\omega^2 R^2 + v_t^2}} \tag{1.31}$$

with $2\varphi_e = \pi$

$$F_t = Qf \frac{4v_t}{\pi \sqrt{\omega^2 R^2 + v_t^2}} \tag{1.32}$$

$$F_r = Qf \frac{4\omega R}{\pi \sqrt{\omega^2 R^2 + v_t^2}} \tag{1.33}$$

In statically determinate mechanisms, a cylindrical pair can perform the functions of either a revolute pair or a sliding one. The major motion then is the relative rotation or translation of the parts, whereas the self-aligning motion is, respectively, translation or rotation.

If the links or parts of the pair self-align by the translatory motion, the force of resistance to self-alignment by the forces of friction equals the corresponding component of the friction force: $F_s = F_t$.

If rotation is the motion of self-aligning, the moment of the friction forces equals $M_s = F_r R$.

It should be pointed out that expressions (1.28) through (1.33) for the forces of friction in a cylindrical pair are the most general ones. By substituting $v_t = 0$, or $\omega = 0$, we would derive the known formulas of friction in a rotary and translatory pair, respectively.

## 1.14. Resistance to Self-Alignment in Planar Pair

**Case One.** The main relative motion of the links is translatory, at velocity $v_m$, and the motion of self-aligning is translatory at velocity $v_s$, perpendicular to the main one (Fig. 1.20*a*). With the uniform distribution of the pressure over the area of the contact of the slide

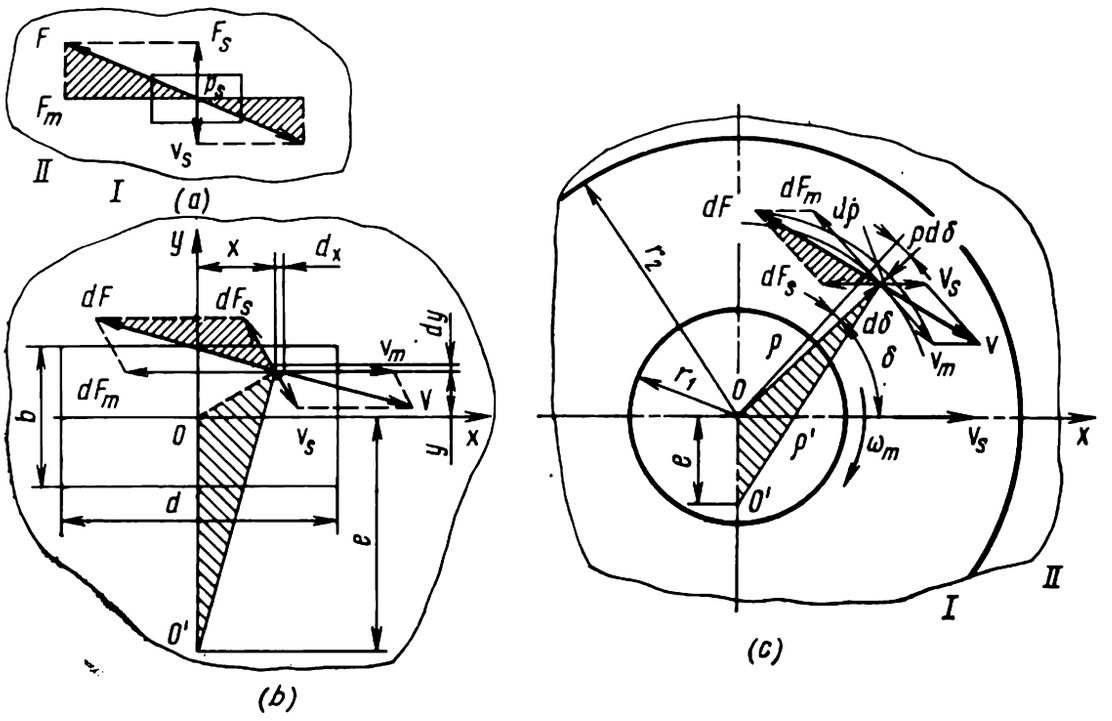


Fig. 1.20. Friction forces and velocities in planar pair
(*a*) with linear self-aligning of rectilinearly moving planar pair; (*b*) with angular self-aligning of rectilinearly moving planar pair; (*c*) with linear self-aligning of rotating planar pair

with the fixed plane, we may assume that the resultant $F$ of friction forces is applied at centre $O$ of the slide. Then, from the similarity of the shaded triangles we find that the force of resistance to the self-aligning motion of the slide

$$F_s = Nf \frac{v_s}{\sqrt{v_m^2 + v_s^2}} \tag{1.34}$$

where $N$ is the normal load applied to the slide.

**Case Two.** The main motion of the parts is translatory, at velocity $v_m$; the self-aligning motion is rotation about geometric centre $O$ of the slide at angular velocity $\omega_s$. In this case the torque of resistance to self-alignment $M_s$ is the sum of all the elementary torques $dM_s$ of forces $dF_s$ acting at elementary lands $ds = dxdy$ in directions opposite to the linear velocities of self-aligning of these lands (Fig. 1.20,*b*), i.e. $M_s = \int\int_S dM_s$. Let us denote: $a$ and $b$—geometric dimensions of the working area of the slide; $x$ and $y$—coordinates of an elementary contact area or land; $e = \frac{v_m}{\omega_s}$—distance from instant centre $O'$ of rotation of the slide to its geometric centre $O$.

By determining from the similitude of the shaded triangles

$$dF_s = dF \frac{\sqrt{x^2+y^2}}{\sqrt{(y+e)^2+x^2}}\ ;\ dM_s = dF_s \sqrt{x^2+y^2}$$

we derive

$$M_s = \frac{Nf}{ab} \int_{-\frac{a}{2}}^{+\frac{a}{2}} \int_{-\frac{b}{2}}^{+\frac{b}{2}} \frac{x^2+y^2}{\sqrt{x^2+(y+e)^2}}\, dxdy \tag{1.35}$$

The expression (1.35) enables one to evaluate the torque $M_s$ of resistance to self-aligning of the slide for the case of uniform distribution of the normal specific pressure over the entire surface of engagement of the slide and the supporting surface. With different laws of distribution of the pressure, similar expressions can be derived.

The integral included in the formula would not be expressed in elementary functions. For small values of $\omega_s$ it can be assumed with justifiable approximation that

$$\sqrt{x^2+(y+e)^2} \approx y+e \tag{1.36}$$

Then

$$M_s = \frac{Nf}{ab} \int_{-\frac{a}{2}}^{+\frac{a}{2}} \int_{-\frac{b}{2}}^{+\frac{b}{2}} \frac{x^2+y^2}{y+e}\, dxdy$$

or

$$M_s = \frac{Nf}{ab} \left[ \left( \frac{a^2}{12} + e^2 \right) \ln \frac{2e+b}{2e-b} - be \right] \tag{1.37}$$

**Case Three.** The main motion is rotary with angular velocity $\omega_m$; the self-aligning motion is translatory with velocity $v_s$.

Let us denote: $dF$—full friction force over an elementary land; $e = \frac{v_s}{\omega_m}$ — distance from centre $O$ of the thrust bearing or pivot to centre $O'$ of instant rotation; $q$—pressure upon the surface of the pivot; $\rho'$—radius of instant rotation of the elementary land; $\rho$—radius of the major rotation of the elementary land; $\delta$—angular coordinate of the land; $r_1$ and $r_2$—respectively, the inner and outer radii of the annular pivot.

In this case the pair is usually made in the form of an annual pivot bearing upon a plane. The force $F_s$ of resistance to self-alignment equals the sum total of all the elementary forces $dF_s$ acting at the elementary lands $dS = \rho d\rho d\delta$ in directions opposite to the self-aligning velocity (Fig. 1.20*c*); $F_s = \int_S dF_s$.

From the similitude of the shaded triangles:

$$dF_s = dF \frac{e}{\rho'}$$

But $dF = qfds = qf\rho d\rho d\delta$ and $dF_s = qfe\frac{\rho}{\rho'} d\rho d\delta$.

In its general form, the solution would not be expressed in elementary functions.

However, with values of $v_s$ being small, we can assume with approximation $\rho' \approx \rho$

Then

$$F_s = fe \int_S \int q d\rho \, d\delta \tag{1.38}$$

In a fresh pivot, the normal pressure uniformly distributed over the contact area can be found from expression

$$q = \frac{N}{\pi (r_2^2 - r_1^2)} \tag{1.39}$$

In a run-in pivot

$$q = \frac{N}{\pi (r_2 - r_1) \rho} \tag{1.40}$$

With the above expressions in view, the self-alignment force for a fresh pivot

$$F_s = \frac{Nfe}{\pi (r_2^2 - r_1^2)} \int_{r_1}^{r_2} \int_0^{2\pi} d\rho \, d\delta$$

or

$$F_s = \frac{2Nfe}{r_2 + r_1} = \frac{2Nfv_s}{(r_2 + r_1)\omega_m} \tag{1.41}$$

For a run-in pivot

$$F_s = \frac{Nfe}{2\pi (r_2 - r_1)} \int_{r_1}^{r_2} \int_0^{2\pi} \frac{d\rho \, d\delta}{\rho}$$

or

$$F_s = \frac{Nfe \ln \frac{r_2}{r_1}}{r_2 - r_1} = \frac{Nf \ln \frac{r_2}{r_1}}{r_2 - r_1} \frac{v_s}{\omega_m} \tag{1.42}$$

## 1.15. Resistance to Self-Alignment in Spherical Pairs

A spherical pair admits three relative rotations of the parts it connects. Therefore, the main relative motion of its members and the self-aligning action will always be rotation at respective angular velocities $\omega_m$ and $\omega_s$, the axes of these rotations being perpendicular.

The full relative angular velocity $\omega = \sqrt{\omega_m^2 + \omega_s^2}$.

As the vector of friction torque $M$ opposes vector $\omega$, we are able to split it into vectors $\omega_m$ and $\omega_s$, obtaining

$$\frac{M_s}{M} = \frac{\omega_s}{\omega}$$

whereby

$$M_s = M \frac{\omega_s}{\sqrt{\omega_m^2 + \omega_s^2}} \tag{1.43}$$

Friction torque $M$ in a spherical joint would not be expressed in elementary functions. To solve the problem, N.E. Shamaidenko has found by approximation the functions offering the accuracy sufficient for practical purposes.

If a spherical joint is manufactured to a higher precision than the third class, i.e. with a sufficiently small initial clearance, it can be presumed that following running-in the pin and the insert engage along a semisphere with central angle $\alpha = \frac{\pi}{2}$. The distribution of the pressure loads over the surface of the semisphere is determined from assumption that the total wear of the pin and insert in the direction of the resultant of normal reactions is a permanent value.

Then friction torque

$$M = \frac{8}{\pi (3 + \cos 2\gamma)} QRf \tag{1.44}$$

where $\gamma$ is the angle defined by the transmitted force and the axis of rotation.

The members of a run-in spherical joint manufactured to a precision not higher than the third class normally engage along the surface of a spherical segment, the central angle of which is preferably taken as 120°.

Then friction torque

$$M = \frac{5.62}{\pi (2.5 + \cos 2\gamma)} QRf \tag{1.45}$$

A spherical pivot and a spherical journal present the most common spherical joint. The problem of friction in a spherical joint of this type can be solved with a higher accuracy. A spherical joint acts as a pivot when the angle between the direction of action of the load upon the pin and the latter's axis of rotation equals zero.

A spherical pivot is made usually as a washer, with the working surface being that of the spherical belt, with a solid angle $\alpha_m$ being higher than angle $\alpha_1$. Thus, for a run-in spherical pivot friction torque

$$M = \frac{QRf\,(\sin^2 \alpha_m - \sin^2 \alpha_1)}{\alpha_m - \alpha_1 + \frac{1}{2}(\sin 2\alpha_m - \sin 2\alpha_1)} \tag{1.46}$$

When the pin and the insert engage over a semisphere with angles $\alpha_m = \frac{\pi}{2}$ and $\alpha_1 = 0$

$$M = \frac{2}{\pi} QRf \tag{1.47}$$

When a spherical joint works as a journal, $\gamma = \frac{\pi}{2}$ and the insert in most cases is a spherical belt with angular width $2\alpha_m$ and the angle of engaging the pin $2\varphi_m$. Then

$$M = \frac{2 \sin \varphi_m \left(\alpha_m + \frac{1}{2} \sin 2\alpha_m\right) QRf}{\left(\varphi_m + \frac{1}{2} \sin 2\varphi_m\right) \sqrt{\left(\alpha_m + \frac{1}{2} \sin 2\alpha_m\right)^2 + (2f \sin \alpha_m)^2}} \tag{1.48}$$

If $\varphi_m = \frac{\pi}{2}$,

$$M = \frac{4 \left(\alpha_m + \frac{1}{2} \sin 2\alpha_m\right) QRf}{\pi \sqrt{\left(\alpha_m + \frac{1}{2} \sin 2\alpha_m\right)^2 + (2f \sin \alpha_m)^2}} \tag{1.49}$$

And, finally, if the pin and insert engage over a semisphere

$$M = \frac{4QfR}{\pi \sqrt{1 + \frac{16}{\pi^2} f^2}} \tag{1.50}$$

## 1.16. Resistance to Self-Alignment of Antifriction Bearing

When statically determinate mechanisms are designed, broad use is made of spherical ball and roller bearings which in such cases present a spherical pair. The rolling of the rolling bodies along the races of an antifriction spherical bearing under load is accompanied by resilient and geometric slip. However, quite a number of experimentally checked calculations prove, that, with even slight geometric slip present, resilient slip can be neglected. As the axis of relative rotation of the races of a spherical bearing at self-alignment is usually perpendicular to the axis of their main relative motion (i.e. the bearing axis), the self-aligning of the races can take place exclusively on account of their slipping along the rolling bodies. Hence, the evaluation of the resistance to self-alignment of spherical rolling-contact bearings amounts to decomposition of the full force of sliding friction of the races along the rolling bodies by the directions of geometric slip in the main motion and of slip in the self-aligning motion.

It is impossible to calculate the resistance torque with high accuracy; even its approximated calculation involves too many assumptions and bulky expressions. The torque of resistance to self-alignment of spherical ball and roller bearings can be determined from formula

$$M_s = \frac{3QR_s f}{4} c \left[ (2+c^2)^2 \ln \frac{1+\sqrt{1+c^2}}{c} \sqrt{1+c^2} \right] \qquad (1.51)$$

For ball bearings

$$c \approx 1\,050 \operatorname{tg} \varphi \sqrt[3]{\frac{d_b^4 z^2}{Q^2 \cos \beta}} \qquad (1.52)$$

and for roller bearings

$$c \approx 310 \frac{R_s^2 \operatorname{tg} \varphi}{R_s - d_r} \sqrt[3]{\frac{d_r z^2}{Q^2 \cos \beta}} \qquad (1.53)$$

where $\operatorname{tg} \varphi = \frac{\omega_s}{\omega}$ ; $R_s$ is the radius of the sphere of the spherical race of the bearings; $d_b$ and $d_r$ are, respectively, the diameters of the ball and roller in centimetres; $z$ is number of the balls or rollers in a single row of a double-row bearing; $2\beta$ is the central included angle of the two rows of the rolling bodies of the bearing; $Q$ is the load upon the bearing, kg(f).

The expression (1.51) has been experimentally tested while investigating ball bearings, Types 1 506 and 1 308, and roller bearings,

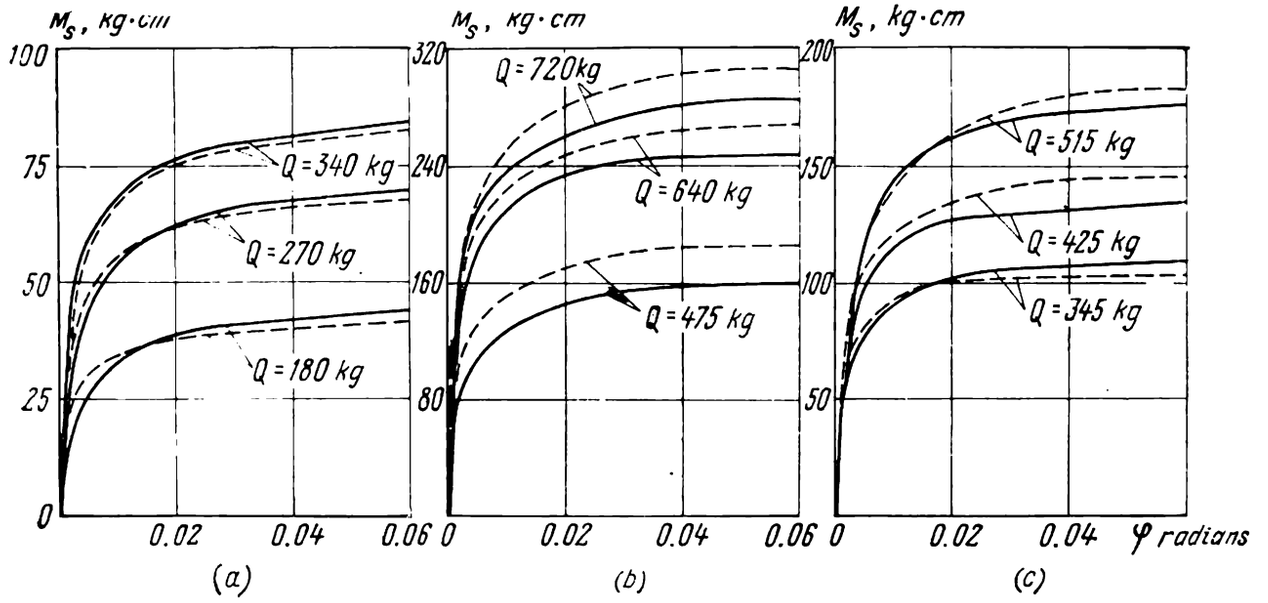


Fig. 1.21. Self-alignment torques of bearings vs. slanting angles
(*a*) ball bearing, Type 1506; (*b*) roller bearing, Type 3611; (c) ball bearing, type 1308

Type 3 611. The testing was performed in a unit enabling the outer race of the bearing under investigation to rotate at 250 r.p.m. with various angles of slanting of the races and various loads applied to the bearings. The torque of self-alignment of the bearing was measured at its stationary inner race with the aid of a Tokar-type dynamometer. The testing proved that in operation of a bearing under similar conditions, torque $M_s$ is practically uninfluenced by the type of lubricant used and the wear of the bearing. The experimentally obtained values of torque $M_s$ for these bearings, as functions of the angle at various loads, are shown in Fig. 1.21 as solid lines. The dash lines illustrate curves calculated from expression (1.51). The friction coefficient of ball bearings was taken to be 0.08, and for roller ones—0.07, since the rolling speeds in the latter are greater, and the pressure values are smaller, thus enhancing the lubrication conditions. At portions where angle $\varphi$ is within 20′ to 30′, the theoretically obtained values of $M_s$ sometimes differ from those obtained by experiment by as much as 25%. It may be assumed that with small slanting angles the final action is significantly influenced by resilient slip omitted in the theoretical calculations. On the other hand, there is hardly any practical reason to use spherical bearings with the slanting angles that small, since single-row ball bearings offer sufficiently fine performance under these conditions.

With the value of angle $\varphi$ increasing further, the difference between the theoretical and practical values of $M_s$ is within 15% of experi-

mentally obtained values of $M_s$. By altering the friction coefficient, this difference can be reduced. What is important is that the calculated and experimental curves are close. At any rate, the suggested expression can be used for evaluating the self-alignment torque $M_s$ in various spherical antifriction bearings practically as accurately as it is done in preliminary friction design calculations.

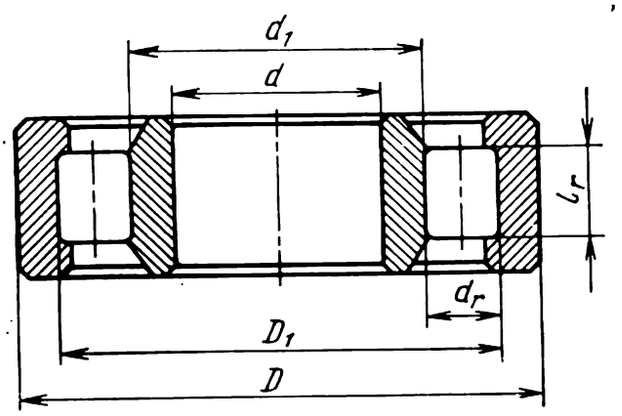


Fig. 1.22. Dimensions of a bearing with cylindrical rollers

$D_1$ and $d_1$ — diameters of the rolling surfaces, respectively, of the outer and inner races; $d_r$ — roller diameter; $l_r$ — roller length

If the main relative motions of the members of a cylindrical pair is rotation, it can be substituted in statically determinate mechanisms by a series of roller bearings permitting relative axial motion of the races within specified limits. As such bearings are working in their main motion, the rolling bodies roll along the races, whereas the self-aligning motion of the connected parts is possible solely due to the slippage of the rolling bodies along the races.

With the rolling bodies in cylindrical roller bearings having a cylindrical shape, no geometric slip takes place, and the rolling is accompanied exclusively by resilient slip which undoubtedly influences the force of resistance to relative axial displacement of the races, i.e. the force of resistance to their self-alignment. However, it is extremely difficult to assess this influence theoretically, for the problem of resilient slip of rolling bodies has not yet been solved fully, even assuming that no lateral slip takes place.

To evaluate the resistance to self-alignment of the races of cylindrical roller bearings (the geometric parameters of such bearings are illustrated in Fig. 1.22), some empirical expressions can be suggested. With the rolling bodies slipping axially along the inner race of the bearing, the force of resistance to self-alignment equals

$$F_s = f\left\{\left[0.92 + 0.37 \operatorname{arctg} \frac{140 v_s}{(D+3d)(\omega_i - \omega_o)}\right] Q - \frac{5\lambda z (D-d)^2}{64}\right\} \quad (1.55)$$

When the rolling bodies slip along the outer race,

$$F_s = f\left\{\left[0.92 + 0.37 \operatorname{arctg} \frac{140 v_s}{(3D+d)(\omega_o - \omega_i)}\right] Q - \frac{5\lambda z (D-d)^2}{46}\right\} \quad (1.56)$$

where $f$ is the friction coefficient of rolling bodies along the races of the bearing; $D$ and $d$ are, respectively, the outer and inner diameters of the bearing, centimeters; $\omega_0$ and $\omega_i$ are the angular velocities, respectively, of the outer and inner races of the bearing, $s^{-1}$, $v_s$ is the self-alignment rate, i.e. the velocity of relative axial displacement of the rings, cm/s; $Q$ is the load of the bearing, kg(f); $z$ is the number of the rollers in the bearing; $\lambda$ is the ratio of the length of the roller to its diameter.

We have to point out in all fairness that these expressions have been obtained from an experimental study of the resistance to the sideslip of loaded rollers in operation, but they have not been experimentally checked in their final form with bearings.

The study of the resistance to the sideslip of loaded rollers has shown that the slip is primarily dependent on the ratio $\delta$ of the slippage rate to the total rolling velocity of the rollers, this dependence being particularly pronounced with $\delta < 0.05$. With $\delta > 0.05$, the resistance to the sideslip of the rollers varies but slightly and approximates the sliding friction force between the rollers. Therefore, expressions (1.55) and (1.56) can be recommended with sufficiently low rates of self-aligning of the bearing rings. Otherwise, to evaluate the force of resistance to self-aligning of the races of cylindrical roller bearings, one should use the formula

$$F_s = fP \quad (1.57)$$

where $P \approx 1.46Q$ is the arithmetic sum of reactions applied to the rollers of the bearing with $10 < z < 20$.

It should be further pointed out that with very small loads exerted on antifriction bearings, the force of resistance to self-aligning of their races is affected to a great degree, by various random factors and tends to be highly unstable. Hence, one should use expressions (1.51), (1.55) and (1.56) exclusively, in the cases where the load on the bearings is more than one-fifth of their nominal load capacity at a given r.p.m. number.

## 1.17. Conclusions and Suggestions

Self-aligning mechanisms (i.e. those free of redundant constraints) are worth using in all practical cases, owing to their advantages.

A mechanism devoid of redundant constraints can be assembled without preloading even when the dimensions of parts deviate from the nominal values, which facilitates designing.

Redundant constraints can be determined from either Malyshev's or Ozol's structural formulas. This technique facilitates checking a selected structure.

Particularly harmful redundant constraints can be detected from the structural formulas for a planar or spherical diagram of a mechanism. This technique is advantageous in complicated cases, enabling one to sort out the redundant constraints.

Redundant constraints may be determined by considering mobilities in a loop, which are preferably broken down along the three coordinate axes. It takes six mobilities to close any loop, *viz.* three linear ones and three angular ones. A linear mobility can be substituted by an angular mobility about an axis perpendicular to the flat surface, if angular mobility is in abundance and there is a part or link whose rotation enables this substitution, i.e. a part directed either along the third coordinate axis or at a small angle to it.

The absence of one of the mobilities indicates preloading and a redundant constraint. The presence of two mobilities of the same kind indicates a mobility in the mechanism—either general or local.

The selection of kinematic pairs in complex planar mechanisms is facilitated by employing self-aligning planar structural groups. The internal pairs of such a group (more often than not, they are fifth-class revolute pairs) retain the links in a single plane.

The group itself is guided by three spherical pairs connecting it to either a fixed member or an external driver.

If known kinematic pairs fail to satisfy a design engineer, kinematic connections of pairs can be used, connected either serially or in parallel.

With serial connection, the mobilities of the kinematic pairs are added up, with each pair transmitting the full load (a force or a torque).

With parallel connection, the constraints imposed by kinematic pairs are added up, with the load distributed among the pairs, which makes their performance easier.

A usual hydrostatic transmission imposes the condition of the permanence of the volume of the liquid in the receiver and transmitters, i.e. it imposes a single constraint and is a first-class kinematic connection. A similar first-class kinematic connection is defined by some electric devices, e.g. synchro systems.

A major error in designing self-aligning mechanism is the appearance of a harmful mobility.

A redundant constraint and a harmful mobility in the same structural formula compensate for each other and may thus remain undetected.

The method of mobilities in a loop can be used for separate evaluation of mobilities and redundant constraints.

Friction (self-braking) may hinder self-alignment. Therefore, a cylindrical pair is suitable for rotary motion only in applications where a full revolution takes place. The same pair can be used in all cases of translatory motion.

Chapter 2

# PLANAR MECHANISMS WITH LOWER PAIRS

## 2.1. Rational Designs of Fixed Connections

Fixed connections are used for securing machinery on foundations, for interconnecting individual units and for fixing detachable parts. If devoid of redundant constraints, such connections take significantly less labor for their manufacture; even in cases of manufacturing inaccuracies, tightening of the bolts would not result in deformation of the components and resulting strain. Neither would the strain be brought about by sagging foundations and thermal expansion of the parts. Fitting-in (whenever required) is far simpler with statically determinate connections than with indeterminate ones, with the former clearly showing where a pad should be inserted or surplus metal is to be removed. The pad has to be provided in one place only, with no need to worry about the distribution of the loads between the several supports. And, finally, the connection can be designed to facilitate arriving at the required dimension in the course of fitting-in (e.g. parallelism of gear axes).

A statically determinate fixed connection shall impose six constraints; i.e. restricting motion along the three coordinate axes and restricting rotation about the three orthogonal axes. To have six constraints, it takes two to six kinematic pairs depending on their class, with the constraints they impose being added up.

In connections made of six kinematic pairs the latter should be first-class ones. Bosses can be used as the $I_4$ pair of this class, with the connected member bearing upon them. It is essential, though, that the size of the boss should be small in comparison with that of the member, and that the contact strain should not be excessive. Furthermore, the fastening bolts should be set with sufficient gaps left, so as to avoid imposing redundant constraints (not shown in the drawings).

It would take six ($6 = 1 + 1 + 1 + 1 + 1 + 1$) first-class pairs (Fig. 2.1, *a*, *b*, *c* and *d*). One member of the connection is shown in the drawing, the other members being shown conventionally with dash lines.

In Fig. 2.1*a* two bosses are set on each coordinate plane, to restrict motion along $x$ axis (on $yoz$ plane), rotation about $x$ axis (on $xoy$ plane), motion along $y$ axis (on $xoz$ plane), rotation about $y$ axis (on $yoz$ plane), motion along $z$ axis (on $xoy$ plane) and rotation about $z$ axis (on $xoz$ plane).

Different arrangement of the bosses is possible, provided they restrict motion along the three coordinate axes and rotation about these axes. It is possible, for instance, to set three bosses on one plane, two of them on the other and one on the third plane (Fig. 2.1*b*). However, more than three bosses should not be set on one plane as it may result in a statically indeterminate system evolves, with one redundant constraint and one mobility violating the fixed connection. The connection illustrated in Fig. 2.1*b* is of a smaller height than that of Fig. 2.1*a*. This connection offers very convenient checking and adjustment of the setting along $x$ axis (one boss), but less convenient checking and adjustment of the setting angle about $x$ and $y$ axes (the interrelated ones) and the setting along $z$ axis (three bosses). In Fig. 2.1*a* the line connecting the $I_4$ pairs on each coordinate plane is parallel with one of the coordinate axes, e.g. in case of $xoy$ plane, the line is parallel with $oy$. This arrangement, however, is not imperative. The line may extend at an angle to the respective coordinate axis, e.g. at 45° (Fig. 2.1*c*), provided the three lines are not intersecting at one point (cf. Fig. 2.6*a*) as one redundant constraint and a harmful rotational mobility will evolve.

The arrangement of $I_4$ pairs may be different, e.g. the pairs may be arranged at the corners of a rectangle (Fig. 2.1*d*): one pair at each of two corners and two pairs at each of the remaining two corners. This pattern matches well a machine or unit of a rectangular shape.

There are altogether four versions of connections made of six pairs. Connections with six first-class pairs are particularly advisable when matching in place is expected.

Connections made of five kinematic pairs (Fig. 2.2*a*, *b*, *c*, *d*) can be obtained by using one second-class pair and four first-class ones ($6 = 2 + 1 + 1 + 1 + 1$). $II_5$ strip pair can be used as the second-class one, with the members engaging each other along a narrow straight strip (Fig. 2.2, *a*, *b* and *c*). The strip can be either parallel with one of the coordinate axes (Fig. 2.2, *a* and *b*) or extend at an angle to the axis (Fig. 2.2, *d*).

Each coordinate plane may accommodate two first-class pairs (Fig. 2.2*a* and *d*), or else one of them may accommodate three such pairs (three being the limit), another plane accommodating one pair (Fig. 2.2*b*).

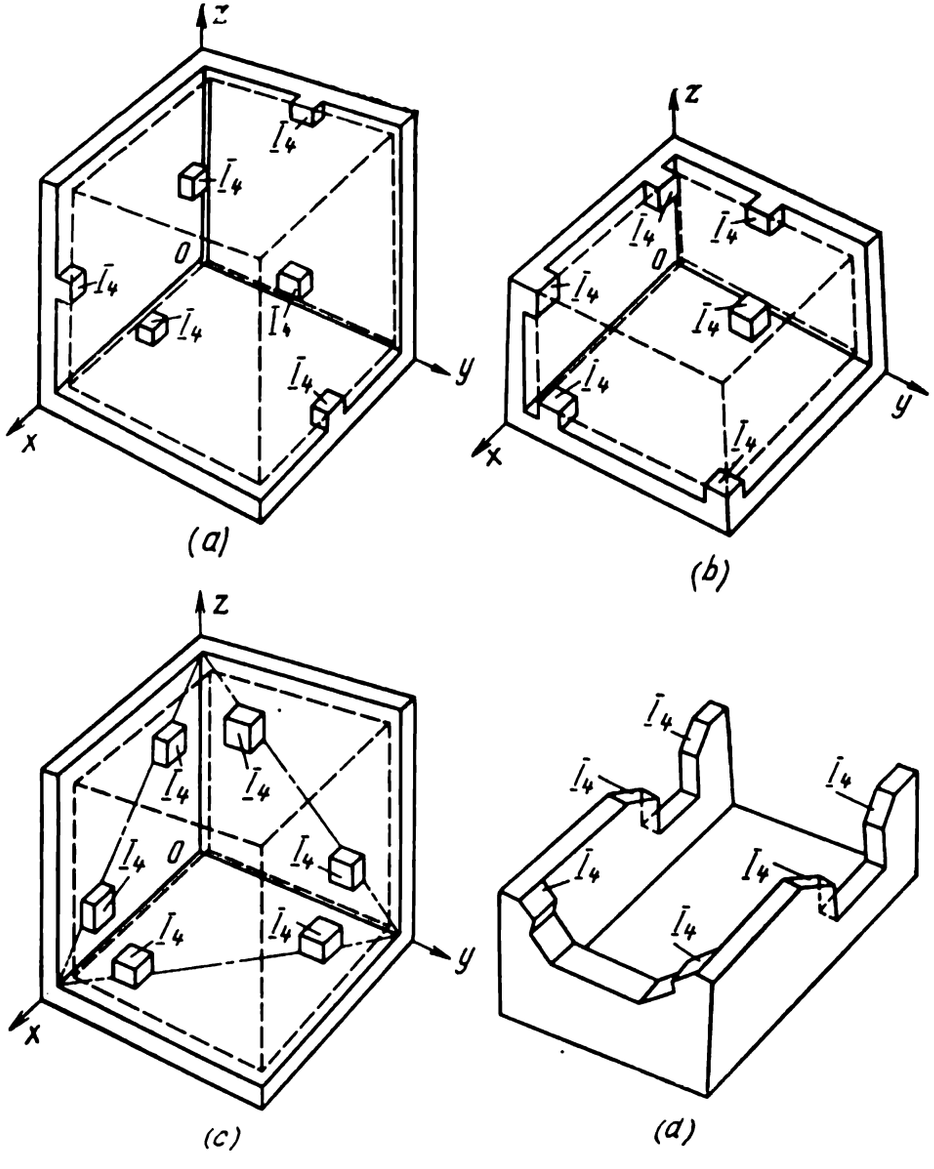


Fig. 2.1. Fixed connections made of six first-class pairs (land ones)

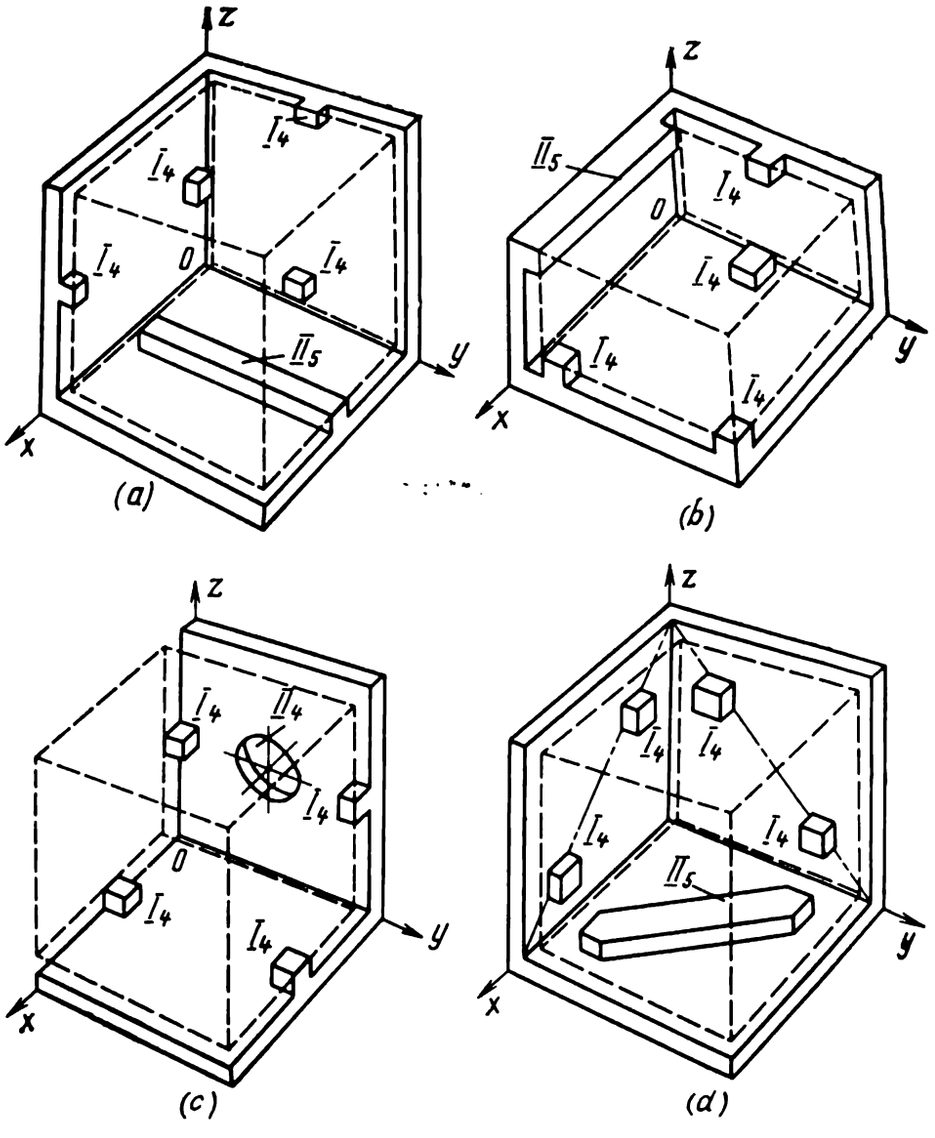


Fig. 2.2. Fixed connections made of five pairs: one second-class pair and four first-class ones

A connection including $II_4$ annular pair, with the members engaged along a narrow cylindrical surface (Fig. 2.2*c*) is advisable for large machines (electric motors, centrifugal pumps, fans) with reducers, in which case the torque (reactive moment) is transmitted from the machine's stator directly by the bosses on the *xoy* plane and will not load the bearing shields. The position of the axis of the machine along *z* and *y* axes need not be adjusted, while horizontality of the machine axis (i.e. its position relative to *y* axis) can be adjusted with aid of the bosses on *xoy* plane, and the direction of the machine axis in the horizontal plane (about *z* axis) can be adjusted with aid of the bosses on *yoz* plane.

The five pairs have yielded four versions of connections. The merits and drawbacks of the different patterns of arranging these pairs remain the same as with six first-class pairs.

Fixed connections made of four kinematic pairs (Fig. 2.3*a-e*) may be formed by two second-class pairs and two first-class ones ($6 = 2 + 2 + 1 + 1$). It is also possible to use one third-class pair (Fig. 2.3*f*) and three first-class pairs ($6 = 3 + 1 + 1 + 1$).

The second-class pairs can be two $II_5$ strip ones (Fig. 2.3*a* and *b*). These designs are different from those of Fig. 2.1, *a*, *b* in that the four $I_4$ first-class pairs have been replaced by two $II_5$ ones. Connections expected to transmit considerable efforts may benefit from the last-mentioned patterns owing to the greater engagement surface. Thus, the pattern shown in Fig. 2.3*a* is expedient with great forces along *y* and *z* axes. By varying the height of the bosses on *yoz* plane, it is easy to adjust the position along *x* axis and the angular setting about *y* axis. The remaining angular and linear settings, though, are harder to adjust, since the greater surface of the $II_5$ couples has to be machined.

By using one $II_5$ strip pair and one $II_4$ annular pair, we have two versions of fixed connections (Fig. 2.3*c* and *d*). They differ from the pattern of Fig. 2.2*c* in that two $I_4$ pairs have been replaced by one $II_5$ pair. The advantages and drawbacks are the same as those of the pattern of Fig. 2.2*c*. The patterns can be recommended for connecting a large machine with a reducer.

With two annular pairs used (cf. Fig. 2.3*e*), the axes of the $II_4$ pairs coincide (although this is not obligatory). The planes of the first-class pairs should be arranged at an angle to avoid a redundant constraint and a harmful mobility that may appear to violate the fixed connection. This type of a connection is convenient from the point of machine design as the kinematic pairs are arranged at the corners of a rectangle.

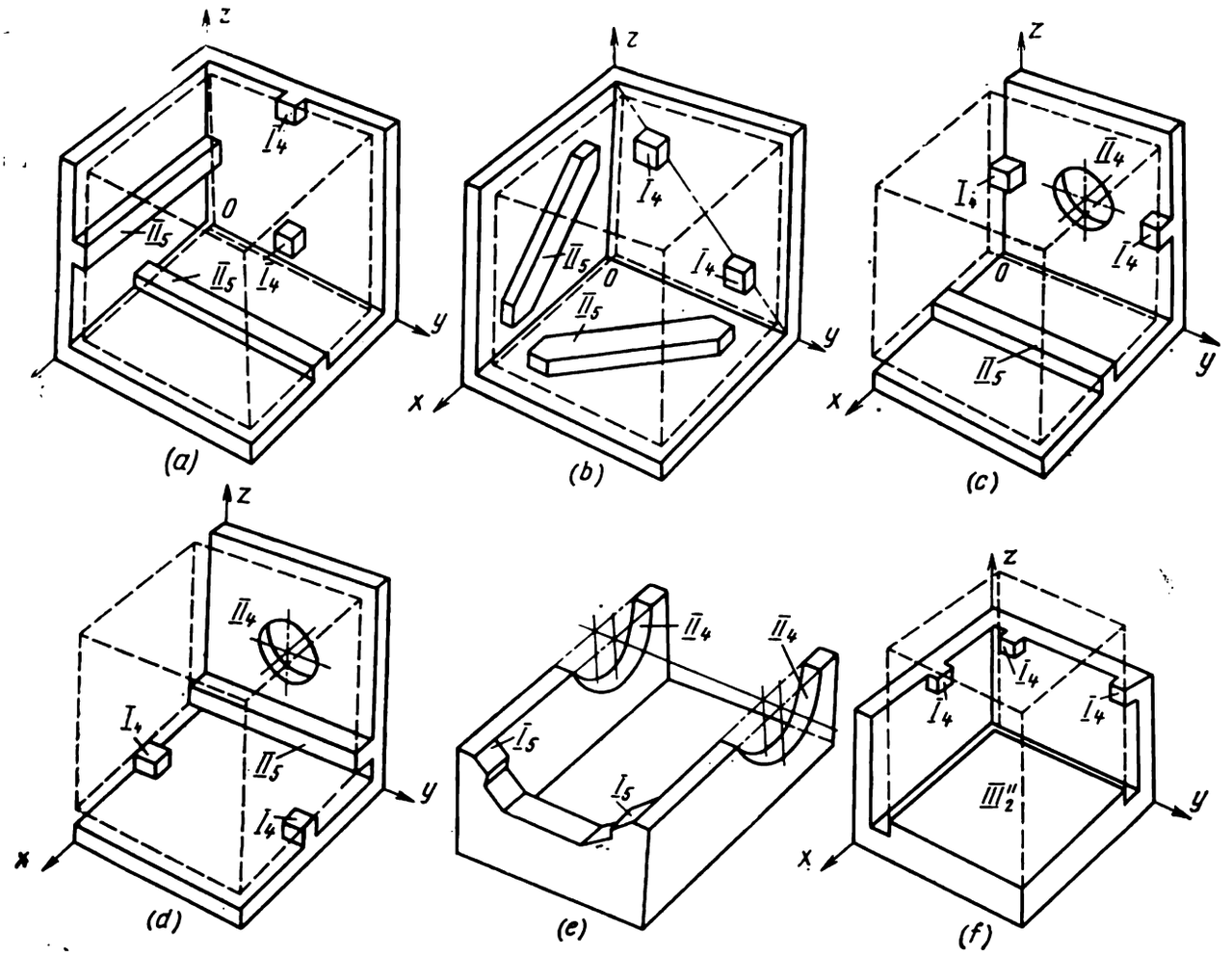


Fig. 2.3. Fixed connections made of four pairs
(*a*)-(*e*) two second-class pairs and two first-class ones; (*f*) one third-class pair and three first-class ones

In the fixed connection including one third-class pair and three first-class ones (Fig. 2.3*f*), the first pair is $III_2''$ planar one; it may be, however, a spherical pair $III_2'$. The latter is far more difficult in manufacture than a planar pair, for which reason it is ill-advisable for a fixed connection and not illustrated in the drawings.

The pattern of Fig. 2.3*f* is expedient in a case where the forces acting in one direction (and loading the third-class pair) are significantly greater than the forces acting in two other directions.

It is expedient to arrange the first-class pairs in the plane of action of horizontal forces, although they may be arranged considerably lower than this plane (to save space).

Thus, connections made of four pairs may be in seven versions (counting the connection with a spherical pair, too).

To have a connection made of three kinematic pairs is not as simple as it might appear at the first glance. Three points of one part

must not bear upon the plane of the other part as this arrangement imposes but three constraints, with three mobilities of the member on the plane remaining. True enough, these mobilities could be eliminated by friction forces brought about by tightening the bolts. However, this structure calls for readjustment following any disassembling, for the parts would not occupy precisely the previous places. Furthermore, there is the eventuality of the parts shifting in operation, which might result in a serious hazard. Tightly fit bolts may not be set at the three points, as three constraints would emerge at each one of them bringing about three redundant constraints.

Therefore, connections made of three pairs should be formed on the basis of the general theory, by counting the number of the constraints.

One can use:

$6 = 3 + 2 + 1$ for a third-, a second- and a first-class pair (Fig. 2.4, *a-c*);

$6 = 2 + 2 + 2$ for three second-class pairs (Fig. 2.4, *d* and Fig. 2.5, *a-e*);

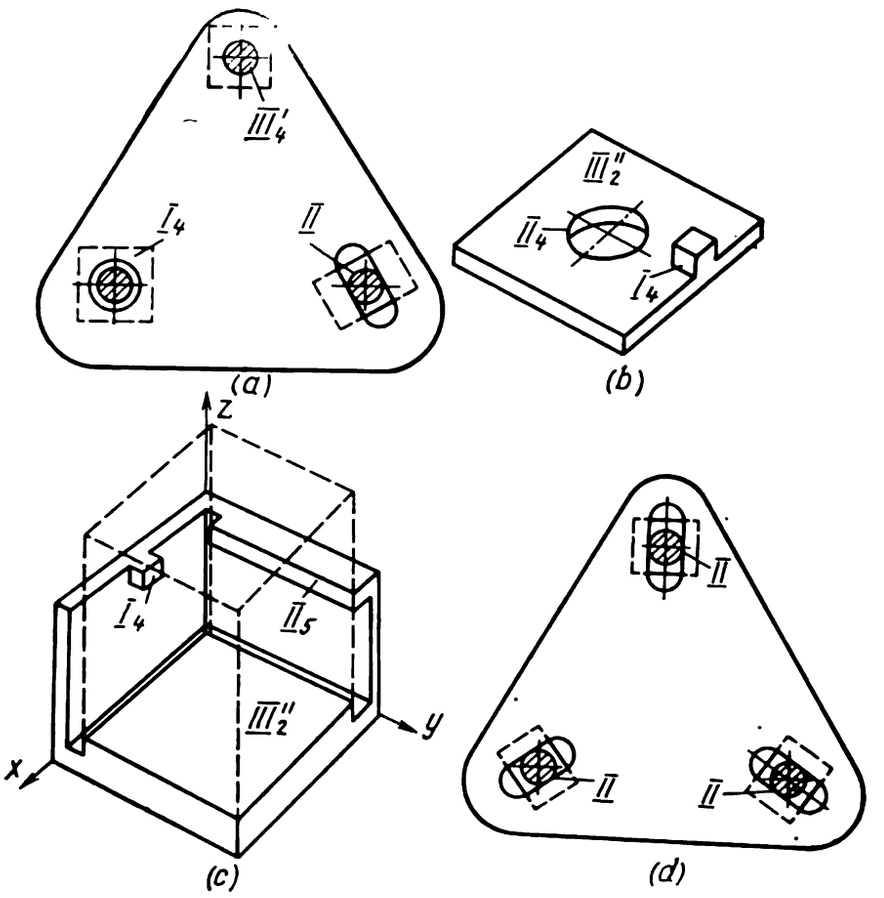


Fig. 2.4. Fixed connections made of three pairs
(*a*)-(*c*) one third-, one second- and one first-class pair; (*d*) three second-class pairs

$6 = 4 + 1 + 1$, one fourth-class pair and two first-class ones.

In the connection shown in Fig. 2.4*a* one part is set onto three bosses made integral with the other part. One bolt set without a gap (into a tightly reamed opening) forms, together with its boss, a $III'_4$ pair imposing three constraints. Another bolt extends through a slot in the part and imposes two constraints with its boss. The third bolt extends through the part with a gap left, forming together with its boss a $I_4$ pair imposing as it does a single constraint. Six constraints altogether—exactly what is needed.

In Fig. 2.4*a* the axis of the slot of the second bolt extends through the centre of the first bolt, although it is not obligatory. There may be an angle between the two directions, provided it is not 90°.

This connection was successfully used by V. N. Kalikhovich for securing the casing of the toothed gearing of an electric locomotive.

In another connection (Fig. 2.4*b*) there are used a planar $III''_2$ pair, an annular $II_4$ pair and a land $I_4$ one. This connection is expedient in applications where the planar pair dominates.

A similar connection, where $II_5$ pair with engagement along a narrow strip replaces the annular pair, is shown in Fig. 2.4*c*.

The three pairs may be identical, e.g. three second-class $II_4$ annular pairs, or else each pair may be in the form of a boss and a bolt received in a slot (Fig. 2.4*d*). In the drawing, all the three slots are directed toward the centre, which is not obligatory: the slots may deviate from this direction, although not by a great angle.

It is advisable to arrange the first- and second-class kinematic pairs in the plane of action of the horizontal forces. However, they may be situated much closer to the planar $III''_2$ pair (to save space); although this results in a non-uniform distribution of the load of $III''_2$ pair this can be neglected.

The connections illustrated in Fig. 2.4*b* and *c* may have their third-class planar $III''_2$ pair replaced, as an exception, by a spherical $III''_2$ one.

A connection with three $II_5$ second-class pairs engaging along a strip (cf. Fig. 2.5*a*) is similar to that of Fig. 2.1*a*, although here the engagement area is greater, therefore the connection is advisable where a significant force is to cope. In this connection the pair on *xoy* plane restricts the displacement of the part along *z* axis and rotation about *x* axis; the pair on *xoz* plane—along *y* axis and about *z* axis; the paire on *yoz* plane—along *x* axis and about *y* axis, respectively.

The three second-class pairs may be arranged at an angle to the coordinate axes (Fig. 2.5*b*), the pattern of their arrangement being

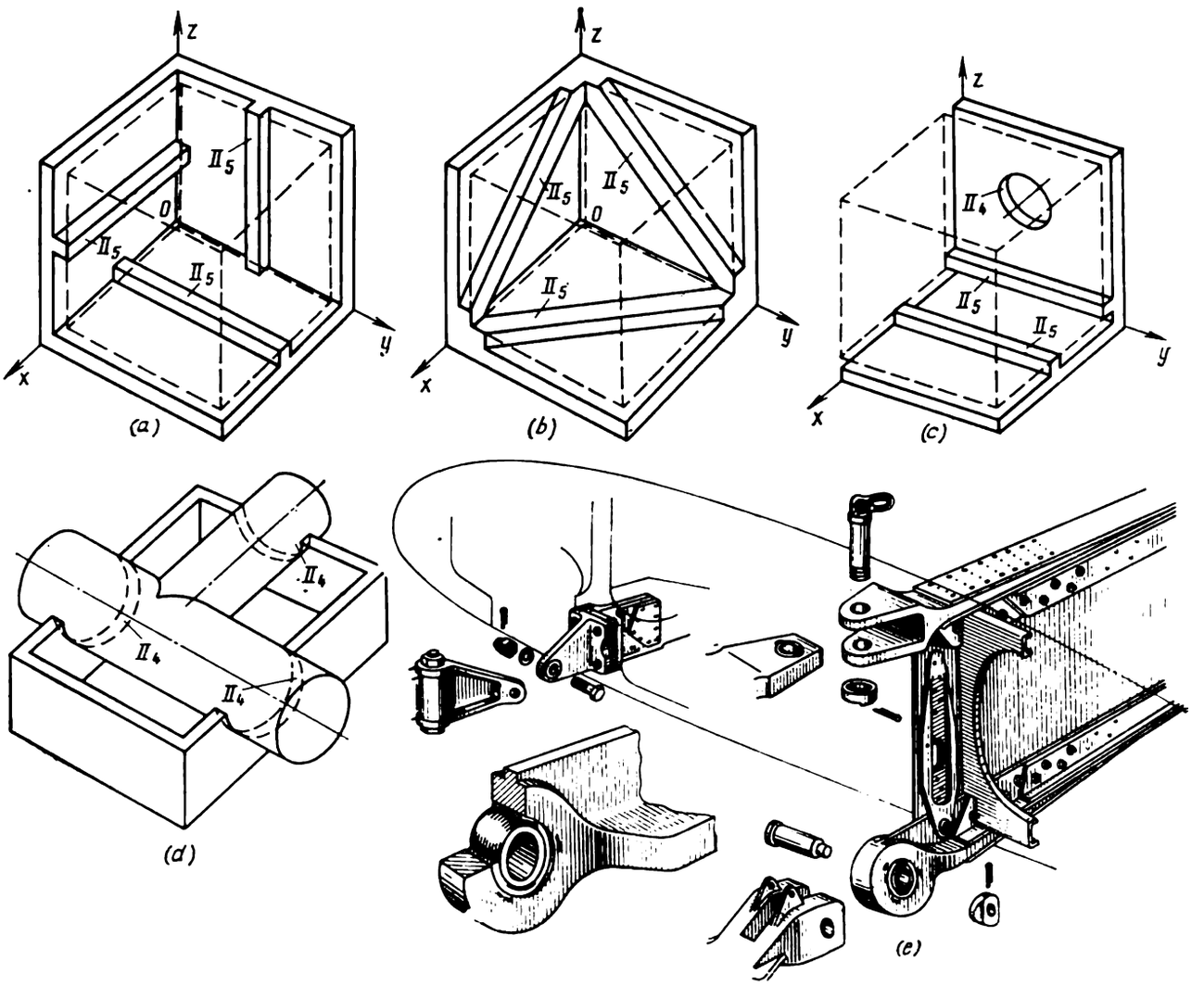


Fig. 2.5. Fixed connections with three second-class pairs

similar to that of Fig. 2.1*c*. However, the three line $II_5$ pairs should not have their respective engagement lines intersecting a single straight line (Fig. 2.6*a*), for this would result in a redundant constraint and a harmful mobility about this line.

Neither should the engagement lines of these pairs be parallel (Fig. 2.6*b*): this would yield a harmful mobility—rotation about a line parallel with *ox*, whereas rotation about *z* axis would be restricted by two pairs, which amounts to a redundant constraint.

Similar defective designs made of first-class pairs are shown in Fig. 2.6*c* and *d*.

A connection with three second-class pairs may also include two $II_5$ pairs with engagement along a strip and one $II_4$ pair with engagement along a narrow cylindrical surface (cf. Fig. 2.5*c*). It has much in common with the connections illustrated in Figs. 2.2*c* and 2.3*c*

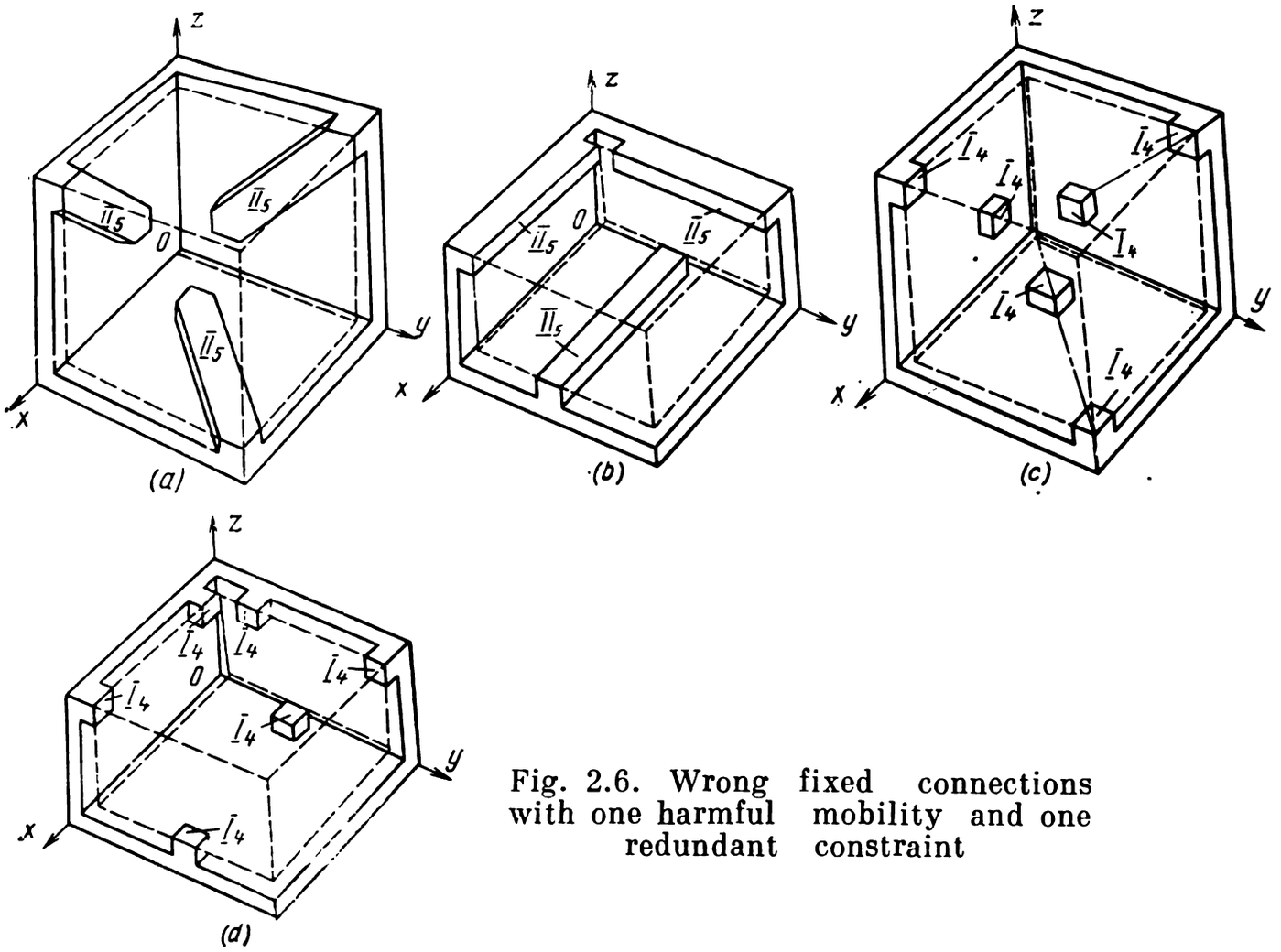


Fig. 2.6. Wrong fixed connections with one harmful mobility and one redundant constraint

and *d*; likewise, it is advisable for connecting large machines with reducers. The engagement area here is larger than that in 2.2*c*, whereby the design of 2.5*c* is recommended to cope with great forces. The height of the machine axis and its position along *y* axis are likewise inadjustable.

The horizontality of the machine axis is adjusted with the kinematic pair on *xoy* plane; the position of the machine along *x* axis and the angular position in a horizontal plane about *z* axis are adjustable with the pair on *yoz* plane, which in Fig. 2.5*c* is at the bottom. However, it may also be arranged either at the top or at the centre of the machine.

In the fixed connection with three annular $II_4$ pairs with engagement along a narrow cylindrical surface (Fig. 2.5*d*) the axes of the pairs intersect at right angles (although this is not obligatory). They may intersect at any angle, e.g. 120°; they also may cross one another. This connection is advisable in case of relatively small components, particularly, when the movable component is retained

by its own weight (it is essential that the component should set itself at once and accurately where it belongs).

On account of their line contact, annular pairs work with considerable contact stress, which makes them practically unsuitable for particularly strained structures, e.g. those in aircraft.

In such cases, $II_4$ pair should be substituted by a connection of $IV_2$ and $III_2'$ pairs (Fig. 2.5*e*), e.g. in a detachable joint of the airplane wing with the centre section [52].

A fixed connection with three kinematic pairs may have one fourth-class pair and two first-class ones ($6 = 4 + 1 + 1$). In this case the first-class pairs facilitate adjustment of the detachable part along the axis of the cylindrical pair and of its angular position about the same axis. It is advisable to employ this connection with relatively small components and with parts intended for repeated detachment.

Thus, three kinematic pairs yield eleven versions of fixed connections (including two designs with spherical pairs and one with a cylindrical pair).

Connections with two kinematic pairs can be composed of a fifth-class pair and a first-class one ($6 = 5 + 1$), or else of a fourth-class pair and a second-class one ($6 = 4 + 2$).

A fixed connection cannot be made of any combination of two third-class pairs (a $III_2'$ spherical pair and a $III_2''$ planar one), because they will always impose one redundant constraint, with one mobility remaining uneliminated.

A connection made of a revolute $V_2$ and a $I_2$ pair (Fig. 2.7*a*) is used for tram-type suspension of the traction motors of freight electric locomotives, the motor bearing upon the axle of the wheel through the revolute pair $V_2$. The reactive moment is transmitted via the tip ($I_2$ pair and the spring crosspiece) to the bogie. Flange-mounted electric motors are secured in a similar manner, but their $V_2$ pair is in the form of a flange with a centering ring.

Connections made of a prismatic pair $V_3$ and a $I_2$ pair are used with detachable handles and levers, the translatory pair being either square or splined one.

Connections with a helical or screw pair $V_4$ and a $I_2$ pair have been lately used for securing detachable handles, with the force closure ensured by the transmitted torque. Such a connection, however, transmits the torque in one direction only, as with the handle rotated in the opposite direction, it gets unscrewed.

A fixed connection made of a $IV_2$ cylindrical pair and a $II_4$ annular pair (Fig. 2.7*b*) has a lot in common with the connection illustrated in Fig. 2.5*d*, its applications being likewise similar. When being

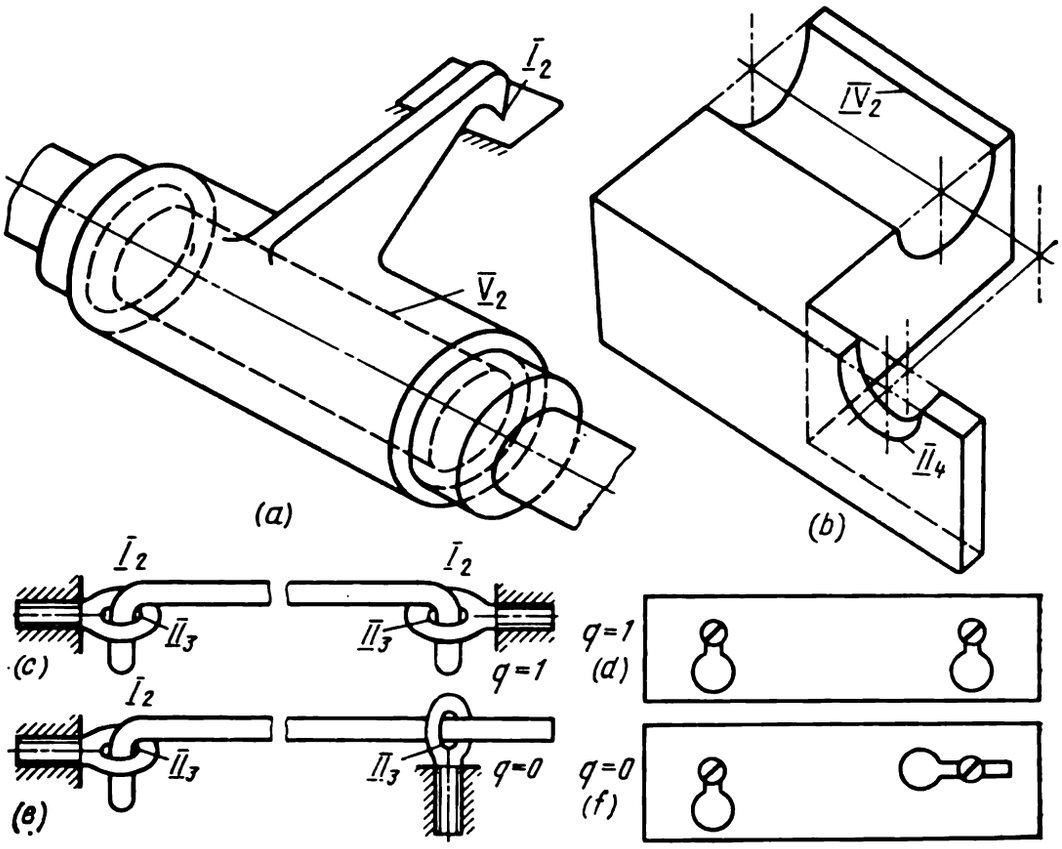


Fig. 2.7. Fixed connections made of two pairs

(*a*) of $V_2$ and $I_2$ pairs; (*b*) of $IV_2$ and $II_4$ pairs; (*c*) and (*e*) used for securing curtain wires (*c* — wrong, with $q = 1$; *e* — correct, with $q = 0$); (*d*) and (*f*) used for securing destination plates on railway cars (*d* — wrong, with $q = 1$; *f* — correct, with $q = 0$)

assembled, the parts (cf. Fig. 2.5*d* and 2.7*b*) can be brought together vertically.

A cylindrical pair may be a closed one, with the parts being brought together axially when assembled. The cutout of the annular pair should extend axially of the cylindrical pair. If the cutout is arranged as shown in Fig. 2.7*b*, the members of the pair have to be connected in two movements—by moving axially and turning.

The securing of curtain wires can be conventionally regarded as a connection with two pairs (Fig. 2.7*c* and *d*), same as the securing of destination plates on railway cars (Fig. 2.7*e* and *f*). In most cases, a curtain suspension wire is bent at the ends into a cramp inserted into two loops (Fig. 2.7*c*), each loop defining two pairs $II_3$ and $I_2$ which can be considered as a single $III_2$ pair. One redundant constraint remains—the strain along $x$ axis—which requires that the length of the cramp should precisely equal the spacing between the loops. In practice, this requirement is hard to meet, and even when it is met, more often than not the cramps are mixed up, which results in the loops being wrenched out.

The redundant constraint may be eliminated by bending the wire into a hook (Fig. 2.7*d*). In this case, one loop is made up of $II_3$ and $I_2$ pairs which we consider as a single $III'_2$ pair. The other loop forms a $II_3$ pair, so the redundant constraint has been eliminated. The mobility about $x$ axis is harmless, since it takes place within the limits of the gaps.

The same is true of the two patterns of securing a destination plate to the outer wall of a railway car. Fig. 2.7*e* shows a wrong design with a redundant constraint requiring a precise distance between the screws in accordance with the spacing of the holes in the plate. Fig. 2.7*f* shows a proper pattern where this precision is uncalled for. Thus, we have six varieties of connections made of two kinematic pairs.

All in all, we have arrived at 32 varieties of fixed connections devoid of redundant constraints: four made of six kinematic pairs, four made of five pairs, seven made of four pairs, eleven made of three pairs and six connections made of two pairs. This variety will always provide a version fitting any practical case.

## 2.2. Connection of Traction Motor with Single-Motor Bogie

In a fixed connection with six constraints each link or member can be deformed independently of the other connected member.

In the case of an electric locomotive, this means that the frame of the traction motor would not take part in the transmission of torques deforming or straining the bogie, and it is common knowledge that the frame of the motor is a large steel casting serving as a part of the magnetic circuit and possessing great strength. The said particularly applies to single-motor bogies where a high-power motor is arranged at the centre of the bogie and is prone to take up some of the forces acting on it.

Specifically hazardous to a bogie are two kinds of deformations: the twisting and slanting (in the latter case the bogie is distorted into a parallelogram in plan view). The forces produced by these deformations are relatively small, owing to the limited rigidity of the bogie with respect of these deformations. Therefore, the construction might stand some limited strain. Thus, in the connection of the motor with the bogie, it is expedient to increase the number of the constraints by two, i.e. to have eight constraints. To avoid twisting of the bogie, the motor should be supported by four feet (Fig. 2.8), and to have eight constraints, each foot should be secured

with a second-class pair. The pair usually includes a trapezoidal prism fast with one member and received in the trapezoidal groove of the other member.

In ЧС-4 electric locomotives the securing pattern uses three brackets, i.e. the frame of the motors takes no part in enhancing the

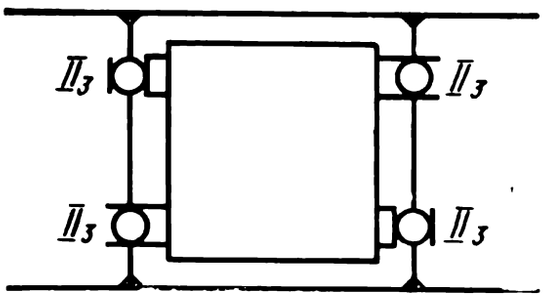

Fig. 2.8. Rational connection of a traction motor with a single-motor bogie

strength of the bogie. The brackets are secured to the motor and to the bogie by fifth-class translatory pairs. This yields six redundant constraints, two per each bracket, which results in twisting of the bracket about two axes and has caused numerous bracket failures.

## 2.3. Supports for Rotary Shafts

Each rotating part of a machine should be supported by two bearings, then the accuracy of the radial setting of each bearing will be determined by tolerable skewing of the shaft axis. Should the shaft be supported by three bearings, the third one must be centered relative to the axes of the other two with a high precision. Therefore, setting each rotary member on two bearings and not on their greater number should be the law of engineering design. For the same reason, doors and wings should be mounted on two hinges—not three. The slot for the catch of the lock should be 8-10 mm wider than the catch, to avoid the sagging of the building interfering with the performance of the lock. By the way, the hinges should be positioned with the pins facing down and not up. Then the lubricant will not flow so easily out of the cap, and the hinge will perform better. Quite naturally, the hinge "half" with the pin should be attached to the door itself, not to its frame.

Elongated shafts should be tubular, for rigidity sake (as in bridge cranes), or else of a split structure, with their parts interconnected through twin universal joints (preferably toothed or flexible). This construction is used in steam turbine power units where the shafts of every housing and the generator shaft are supported each by its

two bearings and interconnected through couplings corresponding to a twin universal joint.

Another approach is to have all the bearings in the housing of a machine devoid of inserts and shells, and to machine them in a single setting of the working tool. This provides for alignment of the axes, and in the structural formula the bearings may be regarded as a single kinematic pair. This technique is used with motor vehicle engine crankshafts. A shortcoming of this technique, however, is that it would not provide for using self-aligning bearings.

Axially, a shaft should be retained in one bearing only, lest a redundant constraint would be imposed, and the temperature strain may overload and even burn the thrust bearings.

A split shaft can be retained either as a whole or with each split part retained separately, but in the latter case the parts should be connected by couplings providing for axial mobility. The latter technique is preferred, as it significantly reduces axial displacement under temperature strain.

In multicylinder piston-type machines, the main shaft may be supported by two bearings. With several cylinders, this can be attained by arranging the cylinders into a star. This pattern is widely used in aircraft engines, and it is also suitable for other applications, e.g. in compressors. With three cylinders, the arrangement may be W-type, and with two cylinders, V-type. Angle compressors may serve as an example of the last-mentioned pattern, with their single-crank shaft being supported by two bearings and the electric motor rotor being mounted in the cantilever fashion. The same crank drives the connecting rods of the vertical and horizontal cylinders, i.e. one crank acts as two. The mechanism is well-balanced, and the space between the horizontal and vertical cylinders is well-suited for mounting inter-stage coolers, with the minimized length of the connection lines.

With cylinders arranged in-line, the shaft may be supported by two bearings only when the number of the cylinders is small. With two cylinders, this pattern is generally used (motorcycle motors). There is even known a design of a four-cylinder in-line engine with the shaft journalled in two bearings (CT3 15/30 engine), but the shaft proved to be excessively heavy. With a high compression ratio (in diesel engines), this pattern is impossible.

In horizontal double-cylinder steam engines and compressors, the design with the cranks at the end of the shaft supported by two bearings is widely used. The driving pulley or the rotor of the electrical machine is arranged between the two bearings. This pattern is

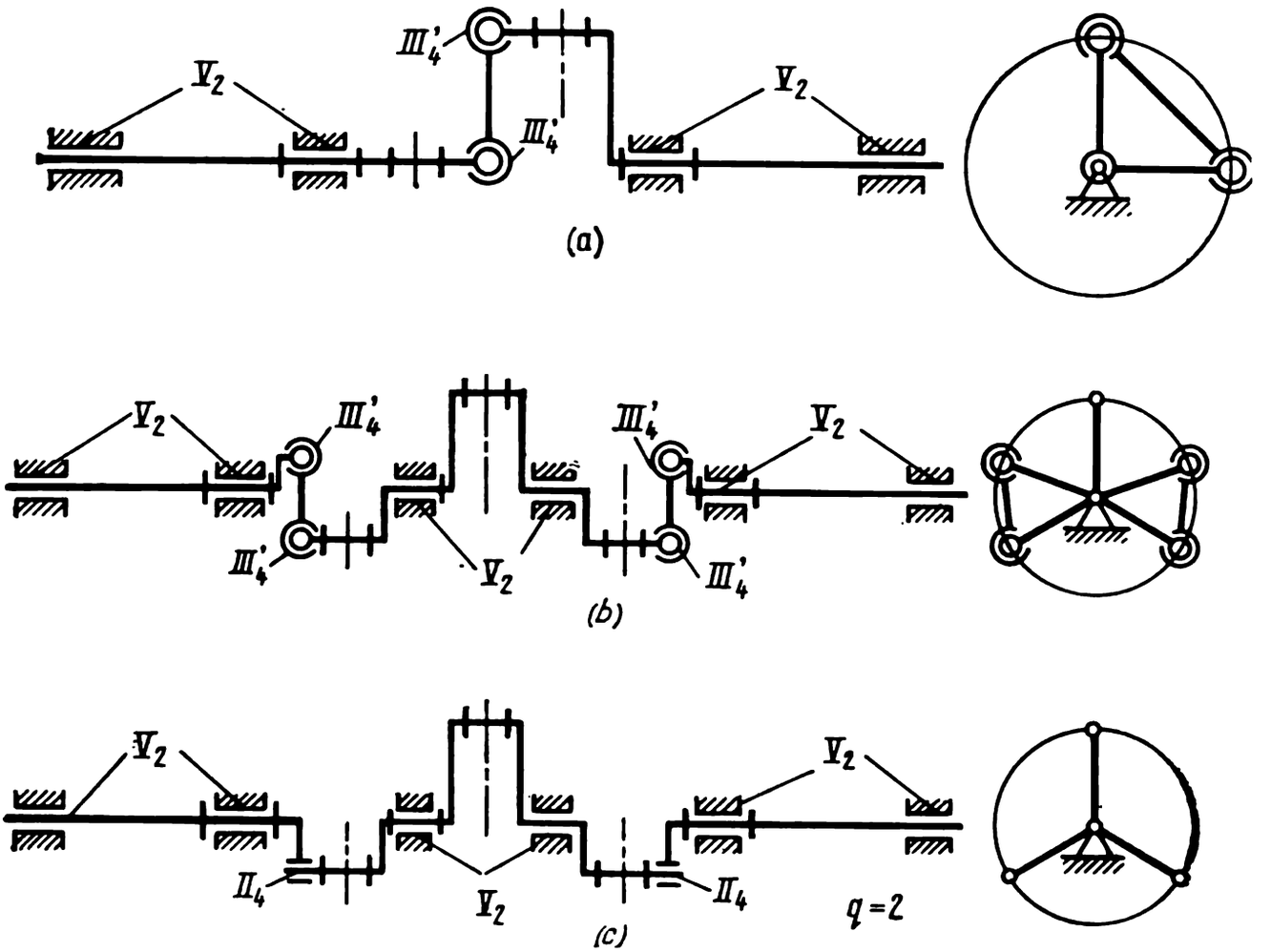


Fig. 2.9. Rational patterns of multi-bearing crankshafts used in paddle-wheel ships

not suited for river boats and ships where paddle-wheels are mounted at the ends of the shaft; in this case, with a double-cylinder engine, the shaft is supported by at least four bearings: two mounted in the engine frame, and two mounted in the ship hull next to the wheels.

If this shaft is of a solid structure, there evolves a statically indeterminate system with a great number of redundant constraints. The design was used in river steamboats, and the displacement of the bearings in service used to cause breakdown of the shafts. To avoid this, split shafts are used (Fig. 2.9*a*). Each half of the shaft is supported by two bearings—one mounted in the engine frame and the other in the ship hull next to the paddle wheel. Each half carries the crank of the respective cylinder, the two cranks being interconnected by a coupler with spherical heads: either $III'_2$ or $III'_4$. This design has eliminated the redundant constraints, i.e. the assembly procedure has been facilitated, and shaft breakage has been avoided.

A similar pattern can be incorporated in a three-cylinder machine (the triple-expansion type), with the shaft made of three parts being interconnected by two couplers (Fig. 2.9*b*). Here, the redundant constraints have been eliminated completely.

With three cranks, the design with partly eliminated redundant constraints (Fig. 2.9*c*) is used, where the central crank is solid. In the endmost cranks the crank pin has fixed connection with one web and a movable connection with the other web (the pin freely extends through the opening provided in the web). If this connection is regarded even as a $II_4$ pair, two redundant constraints will remain, calling for precise centering of the frame-mounted bearings. However, less precision is required to position the bearings at the paddle-wheels. With an unsplit shaft, the construction imposes eight redundant contraints.

In the old design of screw-propeller vessels, the engine used to be arranged near midship. The propeller shaft was correspondingly long (about half the ship length), with numerous bearings. In hot seasons, the above-water part of a motor vessel hull is heated in the daytime more than the under-water one, so that the hull (and the propeller shaft, too) is bent in one direction. At night, the above-water part is cooler than the under-water one, and the shaft tends to bend in the opposite direction. This has been avoided by accommodating the power plant at the stern, thus eliminating the lengthy propeller shaft line. The pattern had been initially used in diesel-electric ships where the propeller-driving motors were positioned exclusively at the stern; then its use was extended to tankers and dry cargo motor ships; and now it is used in passenger ships as well.

The bearings should preferably be self-aligning ones (Fig. 2.10). This design enables one to avoid the hard problem of aligning their axes and maintaining the uniform distribution of the load lengthwise of the insert or shell, as sagging or deflecting of axes develops.

Self-aligning shells may be supported by a spherical pair (Fig. 2.10*a*). Rotation of the shell is prevented by a pin received in the longitudinal slot of the shell. Thus, the connection of the shell with the fixed member becomes a $IV_3$ pair—spherical with a pin. The position of the pin is of no importance, but usually it is situated at the top, so that to remove the bottom shell by turning out, without lifting the shaft.

Axially, the shaft is retained in one bearing ($V_2$ pair), the other bearing being a cylindrical pair $IV_2$. To simplify the manufacture, the spherical pair may be replaced by a $II_4$ annular one with the engagement along a narrow cylindrical belt (Fig. 2.10*b*), in which

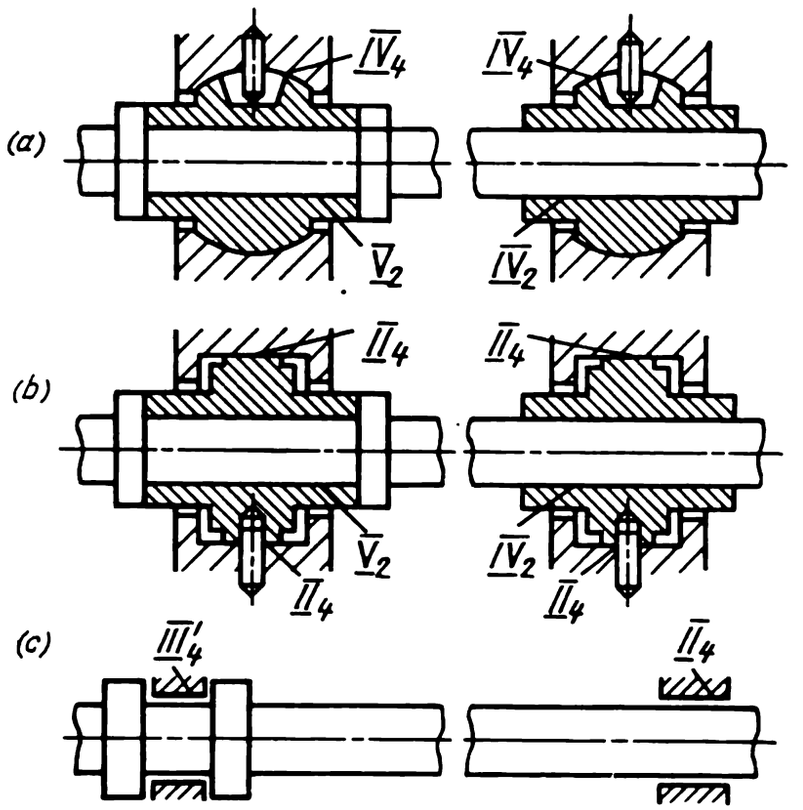


Fig. 2.10. Rational patterns of two-bearing shafts with plain bearings

case the pin prevents the shell from both rotation and longitudinal displacement, for which end the pin should be received in a bore provided in the shell, i.e. should form another $II_4$ pair.

To enhance self-aligning of the shell, friction is to be reduced by positioning the pin at the bottom (at the loaded side), so that with the shell turning, its sliding path is shorter. However, in this case the bottom shell would not be removed without lifting the shaft. To avoid a breakdown with the pin sheared off, the housing of the bearing should in all cases have shoulders to arrest the axial displacement of the shell (cf. Fig. 2.10*b*).

Same as in the previously discussed case, one bearing should be a rotary $V_2$ pair, and the other one—a cylindrical $IV_2$ pair. In both cases, there will be no redundant constraints, which can be ascertained by using formulas (1.1) or (1.2).

With small loads and short inserts, the bearings may be regarded as pairs $III'_4$ and $II_4$ (Fig. 2.10*c*).

The supports illustrated in Fig. 2.10*a* and *b* are not fit to transmit considerable axial loads, particularly, when the entire axial force is taken up by the pin (Fig. 2.10*b*).

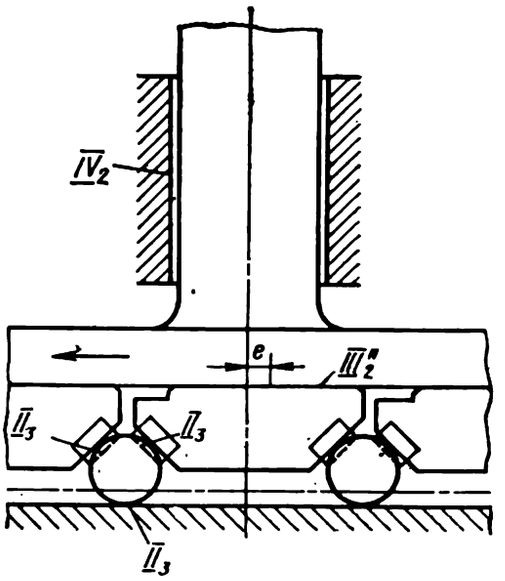


| | | | |
|---|---|---|---|
| $w = 1+3i$ | $1+3i$ | $1+3i$ |
| $\eta = 1+2i$ | $-6-12i$ | $6+12i$ |
| $p_{IV} = 1$ | $4$ | $-2$ |
| $p_{III} = i$ | $3i$ | $-3i$ |
| $p_{II} = 3i$ | $6i$ | $-12i$ |
| $p_I = 1$ | $1$ | $-5$ |
| $K = 1+2i$ | $0+0$ | $0+0$ |

**Fig. 2.11. Thrust bearing with self-aligning segments**

To cope with higher axial forces, the Mitchell-type thrust bearings with self-aligning segments, are used. The equalizing mechanism should ensure the uniform distribution of the load among the segments and its proper distribution over a segment (to form an oil wedge). The mechanism has to be free of redundant constraints, or the deformation will affect the distribution of the forces. One such mechanism is shown in Fig. 2.11. Conventionally, the radial bearing $IV_2$ is shown above the thrust bearing, although in most cases it is beneath the thrust bearing. The load is transmitted via balls received in the trough in the fixed member ($II_3$ pair) and in the troughs provided in the segments ($II_3$ pairs, too). The balls level out the load applied to the segments.

The required load distribution along a segment is attained by offsetting the centre of the segment relative to the middle of the distance between the balls ($e$ = 0.05-0.1 of the segment length). Alternatively, this may be attained by different inclination of the front and rear troughs of the segment.

To avoid rotation of the segments with the balls, one of them has to be connected to the fixed member by a first-class pair. The number of the segments, $i$, may be from 4 to 16, depending on the thrust bearing dimensions. Then, no redundant constraints are present, which can be proved by using formula (1.1). It has to be remembered, though, that owing to the sliding, each ball can have three local mobilities, i.e. rotation about the three axes.

A. Shibel pointed out that thrust bearings with self-aligning segments offered the load bearing capacity which was sixfold to eight-

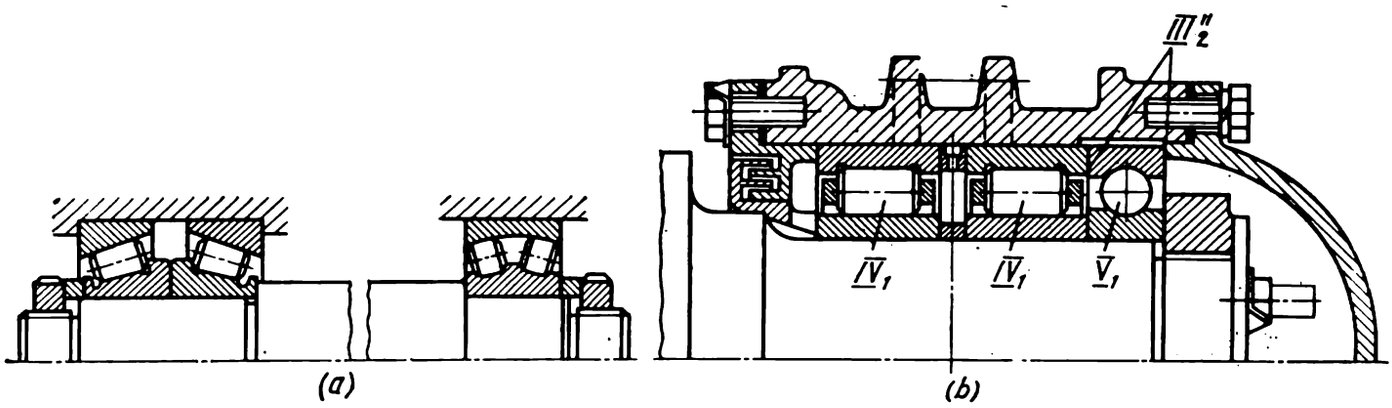


Fig. 2.12. Double-support shaft with roller bearings, for high axial loads

fold that of thrust bearings with solid rings, whereas the friction was 10 to 20 times smaller. It was for this reason that bearings with solid rings were made of a comb-like structure. Thus, we have another proof of the expedience of having mechanisms without redundant constraints.

In bearing supports with rolling-contact bearings redundant constraints are avoided by using self-aligning radial spherical double-row ball and roller bearings. These also include sliding-contact bearings manufactured to the antifriction-bearing standards to function as spherical bearings.

Once again, a shaft should be supported by two bearings. In one of the bearings both races have to be secured ($III'_1$ pair), whereas the other bearing should have its outer race mobile ($II_1$ pair).

Should it be necessary to journal a shaft in four antifriction bearings, each pair of bearings should be combined in a self-aligning housing. Two spherical bearings may be mounted between the housing and the shaft. Such a housing can be examplified by the axle box casing of locomotives and railway cars. The housings should be preferably unsplit. One of the four bearings should have its both races fixed to retain the shaft axially, with the outer races of the three remaining bearings being mounted with sliding fit.

In the case of three bearings, two of them are combined in a self-aligning housing, while the third one is connected directly to the fixed member. Only one of the three bearings should be axially retained.

Should it be necessary to provide for the gap adjustments and to cope with high axial loads, one end of a shaft may be supported by tapered roller bearings (Fig. 2.12*a*). The bearings should be positioned so that the lines normal to the centre of the line of contact of a

roller with the outer race should intersect the axis at the same point, in which case the remaining redundant constraints are the least harmful, and the bearings correspond to a $III_1'$ pair. The gaps and strain should be adjusted with the aid of the outer rings (the adjustment device is not shown in Fig. 2.12*a*).

The other end of the shaft should be supported by a spherical bearing with a mobile outer race ($II_1$ pair).

There has been designed a construction where the shaft is supported by three bearings. Shown in Fig. 2.12*b* is the axle box of the electric locomotive developed by ВЭЛНИИ. The point is that bearings with short cylindrical rollers, Types 62 000 or 92 000 poorly withstand axial loads, whereas radial single-row ball bearings, Type 0000 are fit for high axial loads. Therefore, it is expedient to transmit radial loads to roller bearings while transmitting axial loads to single-row radial ones. To avoid the necessity of precisely centering the ball bearing relative to the axis of the roller bearings, the former's outer race should be radially movable (i.e. set with a gap relative to the housing).

To relieve the roller bearings of the axial loads, they have no shoulders on their inner race of the 32 000 Type, i.e. they define fourth-class kinematic pairs.

The mobility of this support equals two: the rotation of the shaft and the rotation of the outer race of the ball bearing.

Using formula (1.1) we find: $q = 2 - 6 \times 2 + 5 + 4 \times 2 + 3 \times 1 = 6$.

Although redundant constraints are numerous, they are not harmful, since the mounting surfaces for all three bearings are machined at a single setting in the machine tool. Similarly, the mounting surfaces for the bearings in an axle box housing are machined at a single setting, so misalignment and skewing are avoided. The detected redundant constraints are equivalent to those in a kinematic pair, and thus are not harmful.

A specific case of a support for rotary motion is a bearing support of an exceptionally small axial size, although having a large diameter (Fig. 2.13,*a*). A rational design in this case is afforded by planar $III_2'$ and annular $II_1'$ pairs. Using formula (1.1): $q = 1 - 6 \times 1 + 3 \times 1 + 2 \times 1 = 0$.

This bearing support is useful as the guide of the work table of a vertical lathe and of a vertical gear-hobbing machine [6].

In older designs (Fig. 2.13*b*) there were numerous redundant constraints. Two tapering cast-iron circular guideways $III_2'$, i.e. a single Y-shaped one, were used. Mounted at the centre were an adjustable

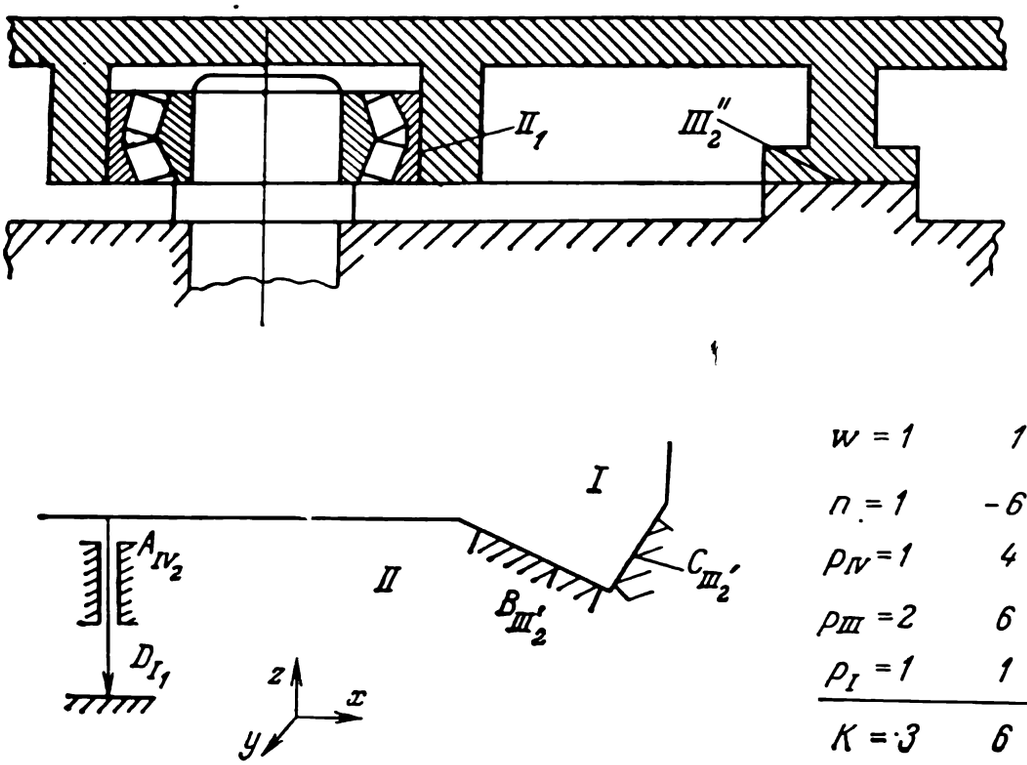


| | | | |
|---|---|---|---|
| $w = 1$ | 1 | 1 |
| $n = 1$ | −6 | 18 |
| $p_{IV} = 1$ | 4 | −2 |
| $p_{III} = 2$ | 6 | −6 |
| $p_I = 1$ | 1 | −5 |
| $K = 3$ | 6 | 6 |

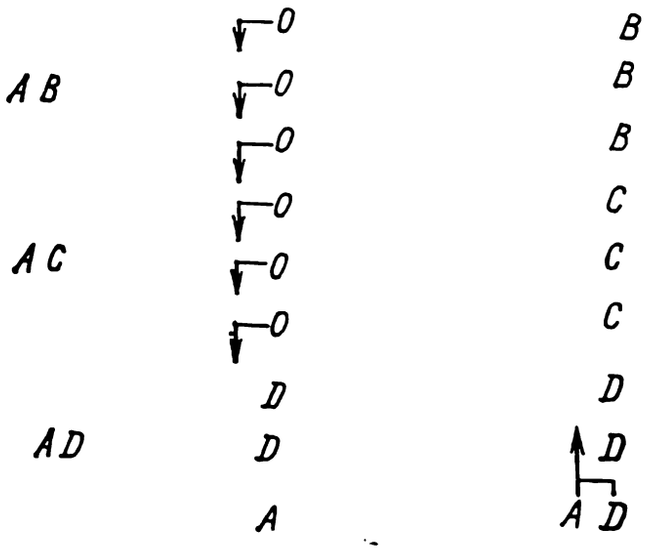


Fig. 2.13. Supports of vertical lathe work table

*top* — free of redundant constraints; *bottom* — obsolete with redundant constraints

cylindrical plain bearing $IV_2$ and an axial spherical bearing $I_1$, to relieve the circular guideways. Even if each tapering guide is considered as a spherical pair $III_2'$, formula (1.1) will yield: $q = 1 - 6 \times 1 + 4 \times 1 + 3 \times 2 + 1 \times 1 = 6$.

The following loops have been selected:

$AB$—framework, $IV_2$ pair, $III_2'$ pair, framework;

$AC$—framework, $IV_2$ pair, the other $III_2'$ pair, framework;

$AD$—framework, $IV_2$ pair, $I_1$ pair, framework.

The redundant constraints are linear ones, directed along the three coordinate axes.

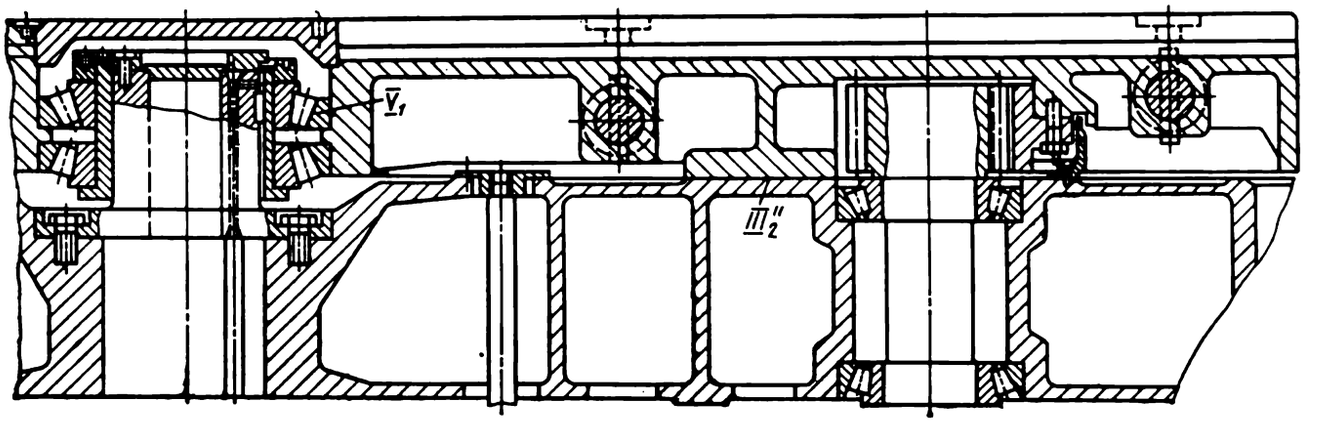


Fig. 2.14. Support of vertical lathe (Consolidated-Bats) with three redundant constraints

The work table is centered along $x$ axis by $IV_2$ pair and two $III_2'$ pairs. One constraint is necessary, while the remaining two are redundant.

The same pairs center the work table along $y$ axis, and two redundant constraints are imposed once again.

The $I_1$ pair and the two $III_2'$ pairs retain the work table along $z$ axis: once more, two constraints are redundant.

The redundant constraints used to affect the precision of the machine's operation. To cut down their number, a 0.05-0.08 mm gap was introduced into one of the tapering guideways $III_2'$, whereby one of the $III_2'$ pairs was excluded from the operation, while the number of the redundant constraints was reduced by three.

The drawbacks brought about by redundant constraints have made design engineers switch over to constructions of the kind illustrated in Fig. 2.13*a*.

Fig. 2.14 shows the guideways of the vertical lathe manufactured by Consolidated-Bats, with the faceplate 4 750 mm in diameter. A single planar guideway $III_2''$ is used here, but the faceplate is centered not by a $II_3$ pair, but by two tapered roller bearings which should be regarded as a $V$ pair. A spherical barrel-shapped roller bearing is not used here, obviously, for the reason that it does not provide for the tightening force essential for the machining accuracy. However, a spherical roller bearing with concave rollers could have been used to provide for the required tightening.

Let us use formula (1.1): $q = 1 - 6 \times 1 + 5 \times 1 + 3 \times 1 = 3$. One of the redundant constraints—linear in the vertical direction—produces the preload relieving the planar guideways, which is intentionally adjustable. Thus, this constraint cannot be regarded as harmful.

The other two redundant constraints are angular about $x$ and $y$ axes.

Provided that each member of this rotary motion support is machined at a single setting of the machine tool, skewing is precluded, and the angular redundant constraints will not result in a strain. What is more important, the temperature-induced deformation of the faceplate produces in this case neither strain nor harmful mobilities, same as in the design of Fig. 2.13*a*. So, the last-discussed design is to be regarded as a successful one. A similar construction has been incorporated by the Kolomna Heavy-Duty Machine Tool Factory in their Model 1540 lathe with a faceplate of 4 000-mm diameter.

## 2.4. Guideways for Linear Motion

Guideways for rectilinear motion may be circular like a cylindrical pair $IV_2$. In this case rotation about the axis of the pair is precluded by respective connections in the mechanism (e.g. in a slider-crank mechanism). In other cases the guideways themselves impose constraints that prevent such rotation, i.e. they impose five restraint conditions.

The first-mentioned case has a typical illustration in a trunk piston (i.e. a crosshead-free one) of either an internal-combustion engine or a simple-action compressor. The construction is proper, being devoid of redundant constraints.

Quite another case is presented by a crosshead with detachable shoes (Fig. 2.15*a*). In it, the connections of the body with the shoes are rotary pairs $V_2$. Let us consider the crosshead together with the piston which, owing to the gaps commonly present, can be regarded as a $II_4$ pair. We disregard the seal, for it may be designed as a floating type not to influence the restraint conditions.

The guideways of the crosshead are cylindrical, so that they define with the shoes cylindrical pairs $IV_2$. We have here five pairs and three movable members, so that two loops are formed. Let us assign the mobility of the piston (a $II_4$ pair) to the first loop, so that the mobility table takes the pattern of Fig. 2.15*a*.

In the first loop, the second linear mobility $f'_x$ along $x$ axis is the main mobility of the mechanism. The second angular mobility $f''_x$ about $x$ axis compounds the second mobility of the mechanism. The second angular mobility $f''_y$ about $y$ axis closes the loop along $z$ axis, since there is the member—the piston with its rod—whose rotation results in such closure.

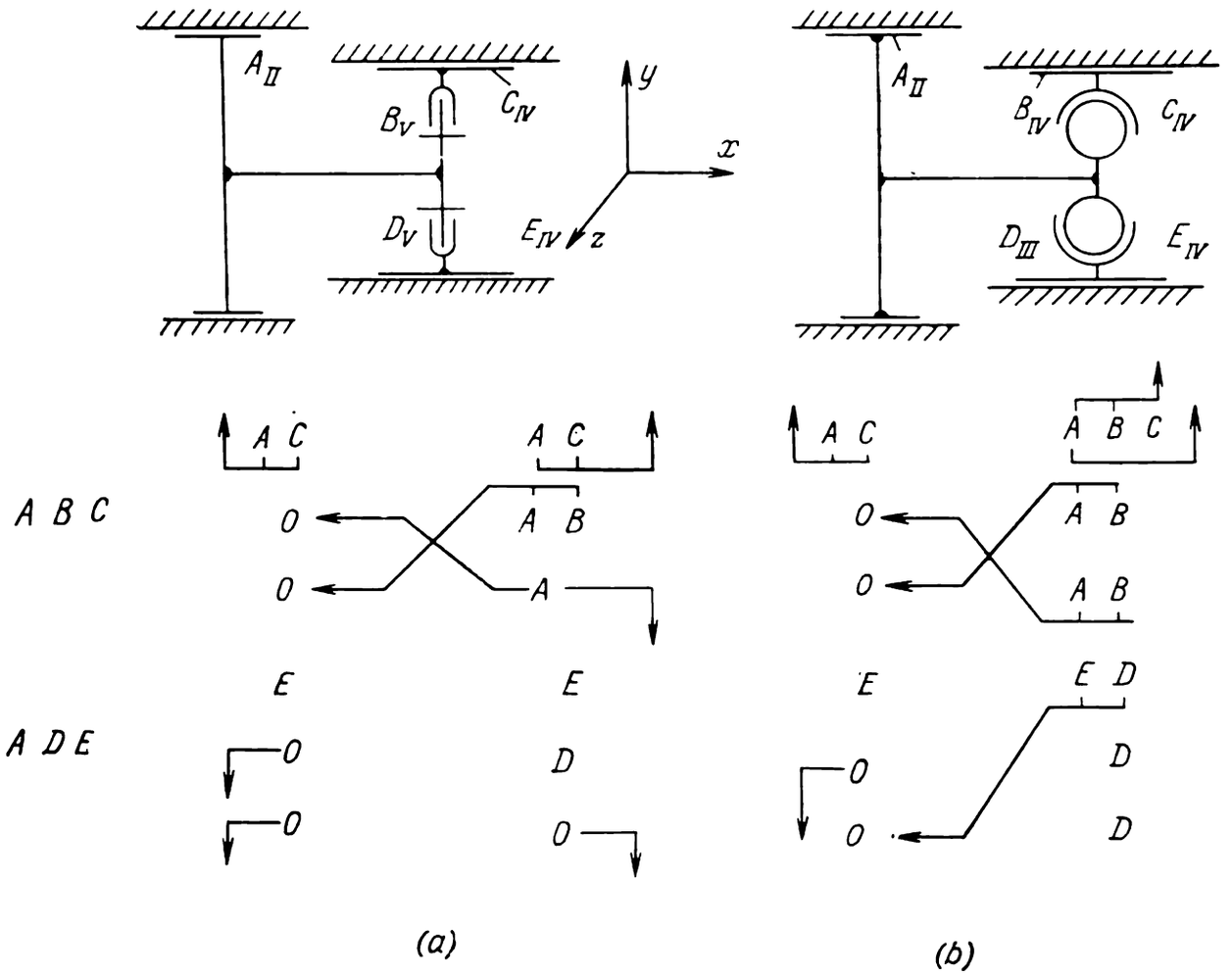


Fig. 2.15. Crossheads with cylindrical guideways
(*a*) wrong construction; (*b*) correct construction

The loop is closed along $y$ axis by rotation of the piston with the rod about $z$ axis. As there is no second mobility ($f''_z$) here, there is imposed a redundant constraint, which might, on account of manufacturing inaccuracies, cause nonuniform distribution of the load applied to the top shoe in the longitudinal direction. A similar redundant constraint will be imposed on the other shoe, on account of the second loop having no angular mobility ($f''_z$) about $z$ axis. The second loop having no linear mobilities ($f'_y$ and $f'_z$) along $y$ and $z$ axes, there will be imposed two corresponding redundant constraints and preloads, of which the first one—urging the second shoe—is unavoidable, while the other results in uneven load distribution in the transverse direction.

This construction had been used in steam engines, and there were even attempts to employ it in high-pressure compressors for the chemical industry.

In large steam machines there was sometimes used the crosshead construction (Fig. 2.15*b*) developed by Sulzer, where the shoes were joined to the housing through spherical pivots, with the male part of these pivots belonging to the housing, and the female part, to the shoe. However, the opposite would have been better. Then the centre of the pivot would be closer to the working surface of the shoe, and the distribution of forces would provide better conditions for forming an oil wedge.

Let us consider this crosshead together with the piston. It also forms two loops. The table of mobilities is given in Fig. 2.15*b*. The distribution of the mobilities in the first loop is as follows: $f'_x$—for closing the loop and for the main mobility; $f''_x$—for closing the loop, for the second mobility and for the substitute for $f'_z$, as there is a member (the shoe) perpendicular to $x$ and $z$ axes; $f''_z$—for closing the loop and for the substitute for $f_{II}$, as there is a member (the piston with its rod) directed along the third axis $x$.

The distribution of the mobilities in the second loop is: $f''_x$—for closing the loop and for substituting for $f'_z$, as there is a member (the second shoe) directed along the third axis; $f'_y = 0$—generating a redundant constraint—urging the second shoe (unavoidable).

The first loop retains one free angular mobility about $y$ axis, i.e. rotation of the piston with the crosshead body about $y$ axis including the centre of the piston, with simultaneous rotation of the two shoes about $x$ axis in opposite directions. If a slider-crank mechanism employs fifth-class pairs, this mobility will even be useful as it may reduce the number of redundant constraints.

In large diesels there are generally used sliders with flat guideways. A rational design of such a mechanism can be obtained with a double-side crosshead (Fig. 2.16*a*), by connecting the crosspiece with the shoes by spherical pivots $III'_2$ or $III'_4$. With a short piston usually associated with four-stroke diesels of the simple action, its connection with the cylinder can be regarded as an annular pair $II_4$.

When determining the number of restraint conditions, we may assume that only those planes are operating which are urged at a given moment, i.e. two prismatic pairs $V_3$ are present.

From formula (1.1): $q = 1 - 6 \times 3 + 5 \times 2 + 3 \times 2 + 2 \times 1 = 1$.

This redundant constraint is imposed by the urging of the shoulders of both sliders and requires strict parallelism of both guideways. This redundant constraint can be avoided by having one slider made with two shoulders and the other slider with none, while restraining the excessive mobility by stops.

The longer piston of two-stroke diesels, that closes off the scavenging and exhaust ports, is to be considered a cylindrical pair $IV_2$. To avoid redundant constraints, it should be connected to the rod by a spherical-with-pin pair $IV_3$, the connection being shown at the top of Fig. 2.16*a*. A spherical pair cannot be used, since the joints of the

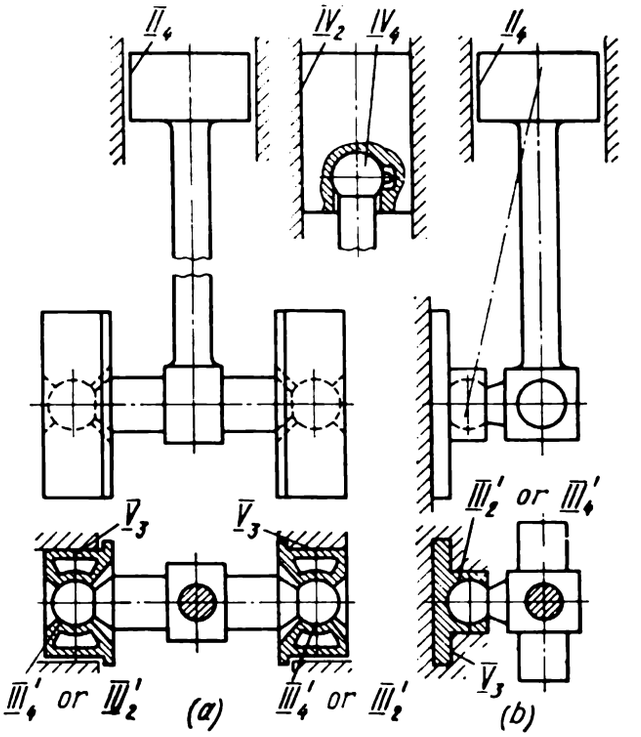


Fig. 2.16. Rational structures of diesel sliders
(*a*) double-side; (*b*) single-side

piston rings will not then travel over the bridges of the scavenging and exhaust ports.

Unfortunately, the use of this construction is complicated if the piston is cooled via the rod.

With a single-side slider, redundant constraints can be eliminated by connecting the shoe with the crosspiece by a spherical pair $III_2'$ (Fig. 2.16*b*). The arrangement of this pivotal joint between the rod and the working plane of the shoe enhances the formation of an oil wedge, with the slider engaging the guideways over two narrow planes. The pressure in this case is very high, hence, the ensuring of adequate conditions for forming an oil wedge is essential.

With the slider sliding along the guideway by its entire major engagement area, the specific engagement pressure is significantly lower, so that the arrangement of the spherical joint shown in Fig. 2.16*b* is quite permissible. In this mechanism, in addition to the main mobility (the translation), there is also the rotation about the inclined axis including the centre of the piston and the centre of the spherical pair (cf. Fig. 2.16*b*). This mobility is eliminated by the

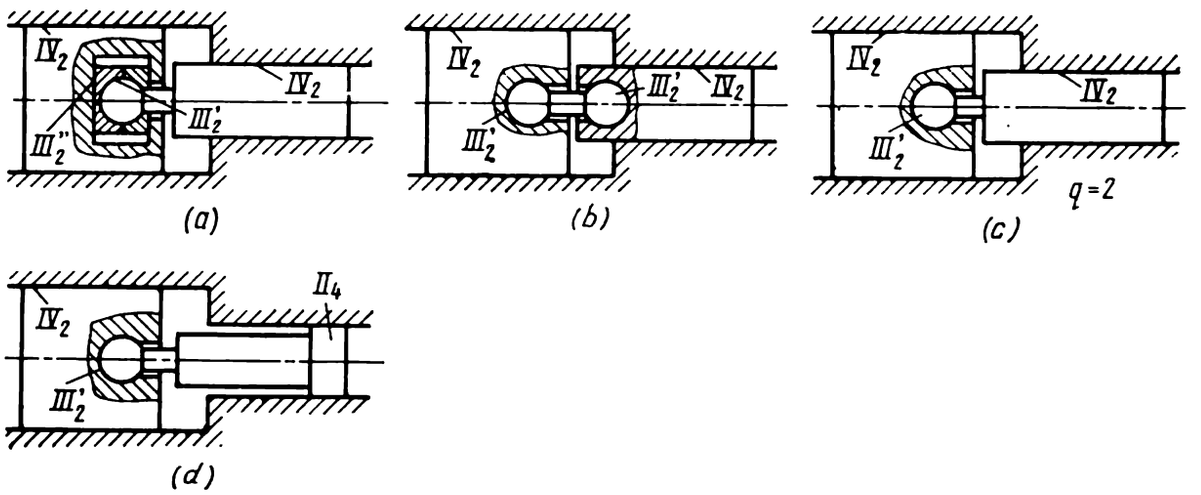


Fig. 2.17. Piston connections in multi-stage compressors

constraints of the slider-crank mechanism (same as in the trunk piston), which adds to the elimination of redundant constraints in the mechanism, so that they are absent in the slider with a spherical joint, i.e. $q = 2 - 6 \times 2 + 5 \times 1 + 3 \times 1 + 2 \times 1 = 0$. With a longer piston (two-stroke engines), an additional $IV_3$ pivotal joint on the rod is required, as it has been explained in connection with the double-side crosshead.

Multistage pistons are widely used in high-pressure compressors for chemical plants. With a wrong design, numerous redundant constraints may be easily imposed.

Let us consider a two-stage piston. With the pistons rigidly connected, there are imposed four redundant constraints, and precise axial alignment becomes a must. To avoid this, a mobile connection should be introduced through a planar pair $III_2''$, an intermediate link and a spherical pair $III_2'$ (Fig. 2.17*a*), or else, through two spherical pairs $III_2'$ and an intermediate link (Fig. 2.17*b*). The other structure is preferable by having less friction. In both patterns, the mobility equals four: the rectilinear motion and the rotation of both pistons and of the intermediate link. If independent rotation of the pistons is intolerable (as is the case with the cylinders having inlet ports in which the piston ring joints travel over port-to-port spaces), spherical-with-pin pairs $IV_3$ can be used.

Using a single spherical joint (Fig. 2.17*c*) is impractical, for two redundant constraints would remain. If, however, the smaller piston is so short that its connection with the cylinder can be regarded as a second-class $II_4$ pair, the redundant constraints can be avoided. In practice, though, a high-pressure piston cannot be so short on account of the multiple piston rings; besides, a reduction of the piston

body diameter increases the dead space of the previous stage, which is likewise undesirable, as it brings down the capacity of the compressor. Neither is a single planar $III_2''$ pair adequate, as it leaves two redundant constraints, although less harmful than in the case with a spherical joint.

In machine-tool and instrumentation engineering the guideways impose five constraints, leaving a single mobility, that of the rectilinear motion. These guideways can be in the form of a spline connection—a $V_3$ pair. Although it has redundant constraints, the latter are harmless, acting as they do within the kinematic pair and not within the mechanism as a whole. Moreover, a spline connection can be manufactured fairly accurate—the bore by broaching and the shaft, by milling with a hob.

A spline connection is employed in case of movable gears in gearboxes and transmissions. However, it does not provide for adjusting the gap and thus cannot ensure the high rigidity of the connection required in machine-tools. Neither is its use advisable in cases where the direction of the transmitted efforts is constant (in sliders), since the working planes cannot be arranged perpendicularly to this direction.

Thus, in some cases it is expedient to have guideways made of several kinematic pairs (Fig. 2.18). Five relevant constraints can be imposed by a cylindrical pair $IV_2$ and a spot one $I_2$ or $I_4$ (Fig. 2.18*a*). This connection is suitable for instruments where the forces are small. Its another advantage is that the slider can be swung aside by turning about the axis of the cylindrical pair, facilitating inspection, repairs, and so on. With greater forces, a pair with the spot engagement is inadequate and it should be replaced by a kinematic connection of pairs of the fifth, fourth or third class, offering engagement over a surface.

To have five mobilities (same as in a first-class pair), one should have two fourth-class pairs and a fifth-class one. A slider with this connection is shown in Fig. 2.18*b*.

It is also possible to use one spherical $III_2'$ or $III_4'$ pair and a single planar pair $III_2''$. We have here a local (passive) mobility—the rotation of the cylindrical block about the vertical axis between the abutments, which is harmless. This slider is shown in Fig. 2.18*c*.

With the spherical pair replaced by a rotary $V_2$ one, the local mobility vanishes, but one redundant constraint emerges, which biases the connection and steps up the friction in case of non-parallelism of pairs $IV_2$ and $III_2''$ (Fig. 2.18*d*). Since this non-parallelism

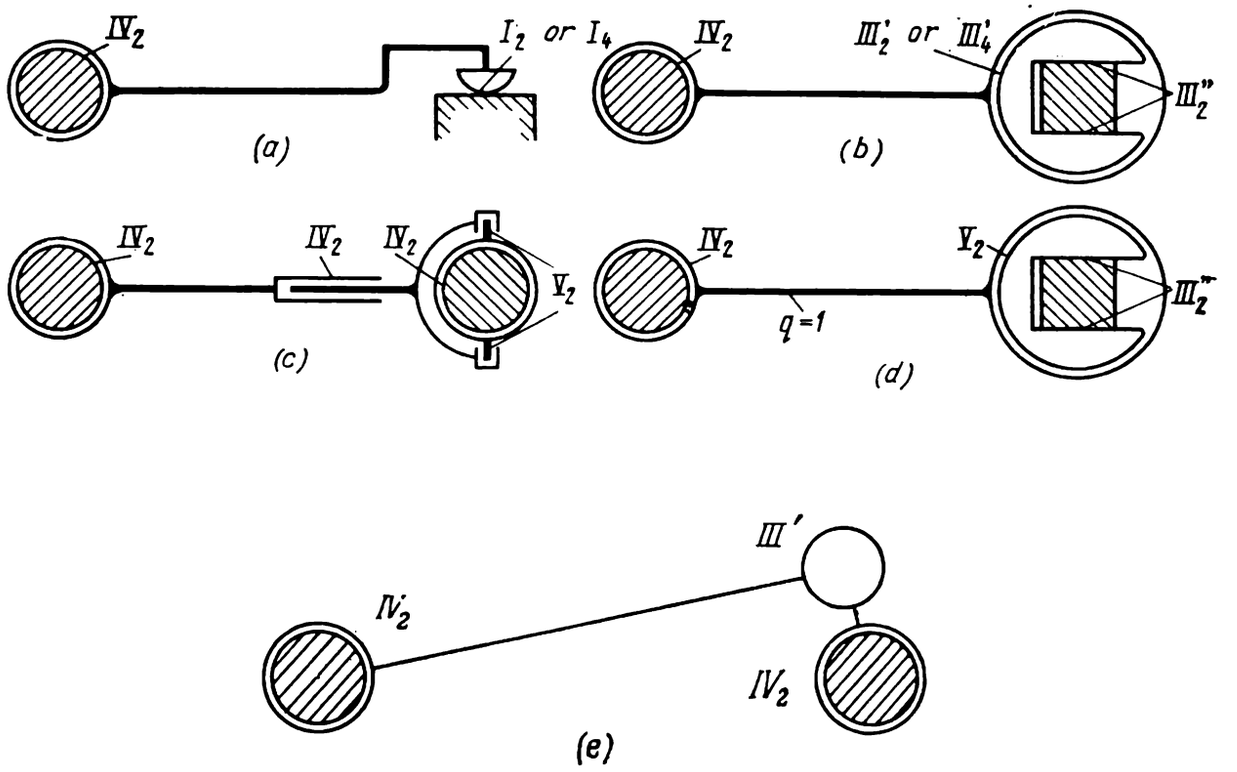


Fig. 2.18. Guideways made of several kinematic pairs

is generally insignificant, and the gaps are present, this redundant constraint in some cases can be tolerated.

There is one more way to attain seven mobilities in the loop by connecting the two sliders by a *III'* pair. With small tolerances of the skewing angle, the pair can be of $III_4'$ type, and it would not be costly. Care should be taken, however, that its offsetting relative to the axis of the guide is insignificant in comparison with the length of the slider.

In case of machine-tool guideways, the requirements of the precision and rigidity of the connection are very high. The guideways are made with a higher accuracy than those of other machines. Thus, redundant constraints could be tolerable. A proper design includes a wedge-shaped slider and a flat one (Fig. 2.19*a*). If the engagement surfaces or planes are regarded as $II_5$ pairs, there is one redundant constraint. When these surfaces intersect along non-parallel lines, the redundant constraint results in uneven loading in the longitudinal direction. In practice, this non-parallelism is prevented by machining the three planes at a single setting in the machine-tool. All three pairs of the planes operate simultaneously, precluding skewing of the slider.

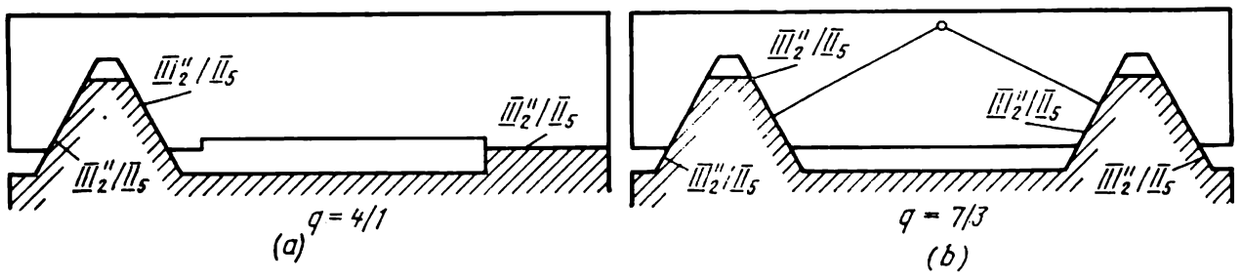


Fig. 2.19. Machine-tool guideways

If, however, the planes are regarded as pairs $III''_2$, there will be four redundant constraints which, on account of eventual manufacturing inaccuracy, lead to uneven loading of these planes in the transverse direction. The same is true of trapezoidal guideways which are used in many cases to facilitate the gap adjustment.

A wrong design with two wedge-shaped sliders is shown in Fig. 2.19*b*. It has numerous redundant constraints, therefore, in this case, not four, but two planes are working (the four planes would work only under the condition of extra-high machining accuracy and the absence of thermal expansion). With the two planes working (we consider them $II_5$ pairs), there are four restraint conditions instead of five. This means that the slider attains the second mobility, i.e. rotation about the instant rotation centre $P$ (with the inner planes working) until the third pair of the planes abuts. This mobility affects the size of the article being machined, for which reason guideways with two wedge-shaped sliders are ill-advisable for incorporation in machine-tools.

## 2.5. Wedge Meehanisms

A wedge mechanism comprises two wedges and three kinematic pairs (Fig. 2.20), i.e. $n = 2$, $p_{\text{V}} + p_{\text{IV}} + p_{\text{III}} = 3$, as pairs of the second and first class are not present.

With $q = 0$ and $w = 1$, from formula (1.1) we arrive at: $0 = 1 - 12 + 5p_{\text{V}} + 4p_{\text{IV}} + 3p_{\text{III}} + 2p_{\text{II}} + p_{\text{I}}$.

Thus, $5p_{\text{V}} + 4p_{\text{IV}} + 3p_{\text{III}} + 2p_{\text{II}} + p_{\text{I}} = 11$.

The equations are satisfied with $p_{\text{IV}} = 2$ and $p_{\text{III}} = 1$, i.e. $f = 7$ (Fig. 2.20, *a*). This construction can be seen in clamping devices of machine-tools and their attachments.

Let us determine the mobilities and redundant constraints in this mechanism by considering the mobilities in the loops: here, $p = 3$; $n = 2$, then $k = 1$. Let us draw the coordinate axes $x_1$ and $y_1$ along the axes of the wedges, $x_2$—in the engagement plane of the wedges,

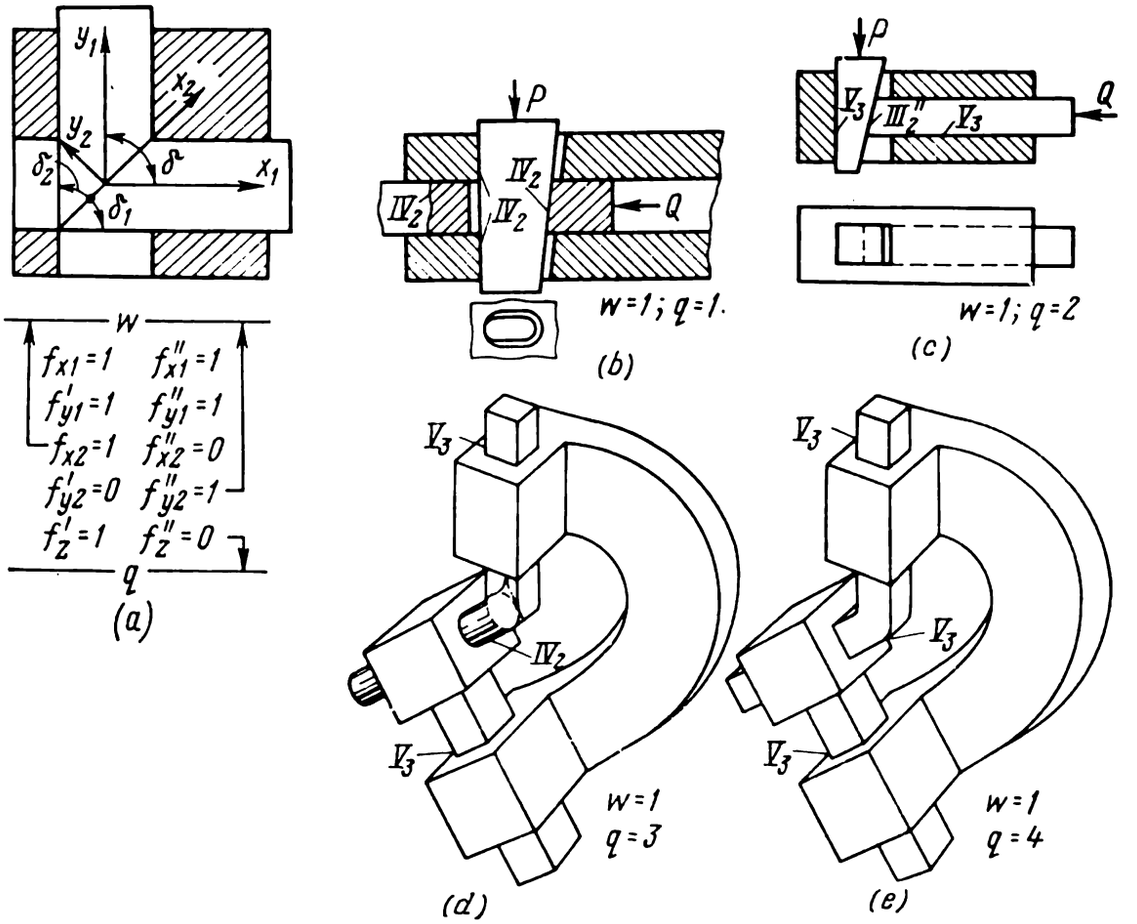


Fig. 2.20. Wedge mechanism structures

(*a*) the best; (*b*) tolerable, with one redundant constraint; (*c*) wrong, with two redundant constraints; (*d*) and (*e*) inadmissible, with four redundant constraints

$y_2$—perpendicularly to this plane, and $z$ axis—perpendicularly to the plane of the drawing. Linear mobilities along $x_1$ and $y_1$ axes are the sliding motions of the wedges, $f'_{x_1} = 1$ and $f'_{y_1} = 1$; along $x_2$—relative sliding of the wedges in the planar pair in the plane of the drawing $f'_{x_2} = 1$, and along $z$ axis—perpendicularly to the plane of the drawing $f'_z = 1$; along $y_2$ axis—perpendicularly to the planar pair; there can be no sliding, here, and $f'_{y_2} = 0$.

There are linear mobilities along the axes $x_1$, $y_1$ and $z$ not belonging to the same plane, which is sufficient for closing the loop. The fourth mobility $f'_{x_2}$ provides for the motion of the mechanism.

The angular mobilities: about $x_1$ and $y_1$ axes—rotation of the wedges in the fourth-class cylindrical pairs $f''_{x_1} = 1$ and $f''_{y_1} = 1$, and rotation about the normal $y_2$ to the planar pair between the wedges, $f''_{y_2} = 1$. Angular mobilities about $x_2$ and $z$ axes belonging to the plane of the planar pair are absent, $f''_{x_2} = 0$ and $f''_z = 0$. There have evolved angular mobilities about $x_1$, $y_1$ and $x_2$ axes belonging to the same plane, which will not close the loop in the absence of angular

mobility about $z$ axis, so a redundant constraint is imposed. There remains one as yet unused angular mobility which can be spent on the other mobility of the mechanism, i.e. the rotation of the wedges. Thus, in the mechanism under consideration $w = 2$ and $q = 1$. The redundant constraint causes uneven loading of the planar pair of the engaging wedges. Only when $\delta_1 + \delta_2 < \delta$, the wedges will self-align through rotation about their respective axes, and in this case $y_2$ axis leaves the plane of the drawing. Then $x_1$, $y_1$ and $y_2$ axes belong no longer to the same plane, and their corresponding mobilities suffice for closing the loop. Here, $w = 1$ and $q = 0$. The less attractive construction shown in Fig. 2.20,*b* is used for connecting the rod with the slider. Here, $p_{IV} = 3$: all the three kinematic pairs are cylindrical ones.

From formula (1.1): $q = 1$, i.e. one redundant constraint is imposed, requiring the strict accuracy of one dimension, i.e. the angle of the wedge should correspond to that of the rod. There is no need to ensure that the axes of the guideways of the wedge in the rod and in the slider belong to the same plane, since these directions would align by rotation of the rod; if the axes of the guideways and of the wedge do not align with the axis of the rod, this will result merely in some limited turning of the wedge.

A wrong design with two prismatic pairs $V_3$ and one planar pair $III_2'''$ is shown in Fig. 2.20*c*. It has two redundant constraints which necessitate precise manufacturing (or fitting) of two angles of one of the wedges.

In a wedge mechanism with two $V_3$ pairs and one $IV_2$ pair (Fig. 2.20*d*), $w = 1$ and $q = 3$. In a wedge mechanism with three sliding pairs $V_3$ (Fig. 2.20*e*), $w = 1$ and $q = 4$.

The multitude of redundant constraints calling for precise machining of numerous dimensions renders the two last-mentioned designs implausible, they only serve as examples of wrong concepts.

## 2.6. Screw Mechanisms

In screw mechanisms, the driving member (the lead screw) is generally rotatable relative to a fixed member (the bearings—a $V_2$ pair), whereas, the driven one (the nut) is movable through a rectilinear translatory motion (the guideways—a $V_3$ pair). If the screw and the nut are made as a $V_4$ pair (Fig. 2.21), the introduction into (1.1) of $w = 1$, $n = 2$, $p_V = 3$ yields $q = 1 - 6 \times 2 + 5 \times 3 = 4$.

The four redundant constraints call for accurate alignment of the nut axis and screw axis in the vertical and horizontal planes,

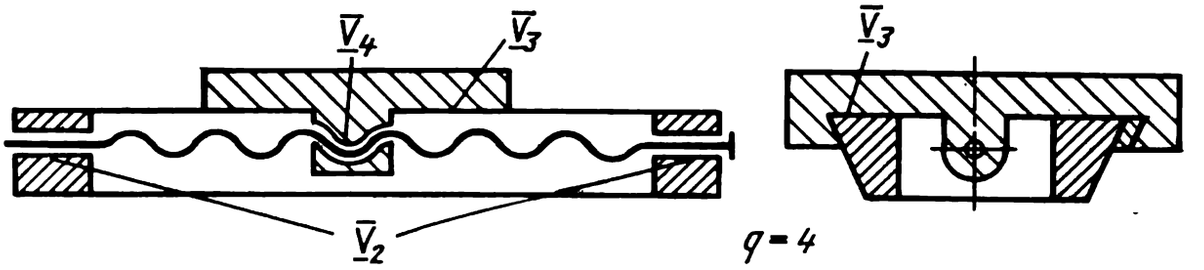


Fig. 2.21. Impractical structure of lead screw mechanism with four redundant constraints

and also for parallelism of the screw axis and the guideways in the vertical and horizontal planes. Even when these requirements are met at the manufacturing stage, the wear of the guideways and their resulting adjustment would practically inadvertently result in offsetting of the nut axis from the screw axis, so that subsequent operation is made possible owing to the clearance or at the expense of deflection of the screw. Thus, this design (which is used in practice in machine tool engineering) is characterized by high friction and high lost motion. The redundant constraints may be avoided by increasing the number of the members and of the kinematic pairs. There is, for instance, a design where the nut is connected with a slider by a cylindrical $IV_2$ pair. The number of the redundant constraints is thus less by two.

The design of Fig. 2.21 can be improved by having the screw supported by one end in a single bearing. Then the nut would serve as the other bearing. Then, with gaps afforded and with the lengths of the bearing and of the nut being small as compared to that of the screw, they may be regarded as $III_4'$ and $III_5'$ pairs.

Then from (1.1): $q = 1 - 6 \times 2 + 5 + 3 \times 2 = 0$.

This construction is used in the tail spindle mechanism of the tailstock of lathes.

The condition of having no redundant constraints is advisable to find from formula (1.2): $q = w + 6k - f$, since in (1.1) the number of restraints varies with the number of the members. In case of single-screw mechanisms (single-loop, $k = 1$), with $q = 0$, the required number of mobilities of the kinematic pairs $f = 6 + w$. When $w = 1$, $f = 7$, i.e. seven mobilities are required.

The screw mechanisms in use are of two kinds: with separately made guideways (cf. Fig. 2.22) and with the guideways in the form of screws. The latter is used in screw hoists. In mechanisms with separate guideways, the screw and the guideway jointly yield two

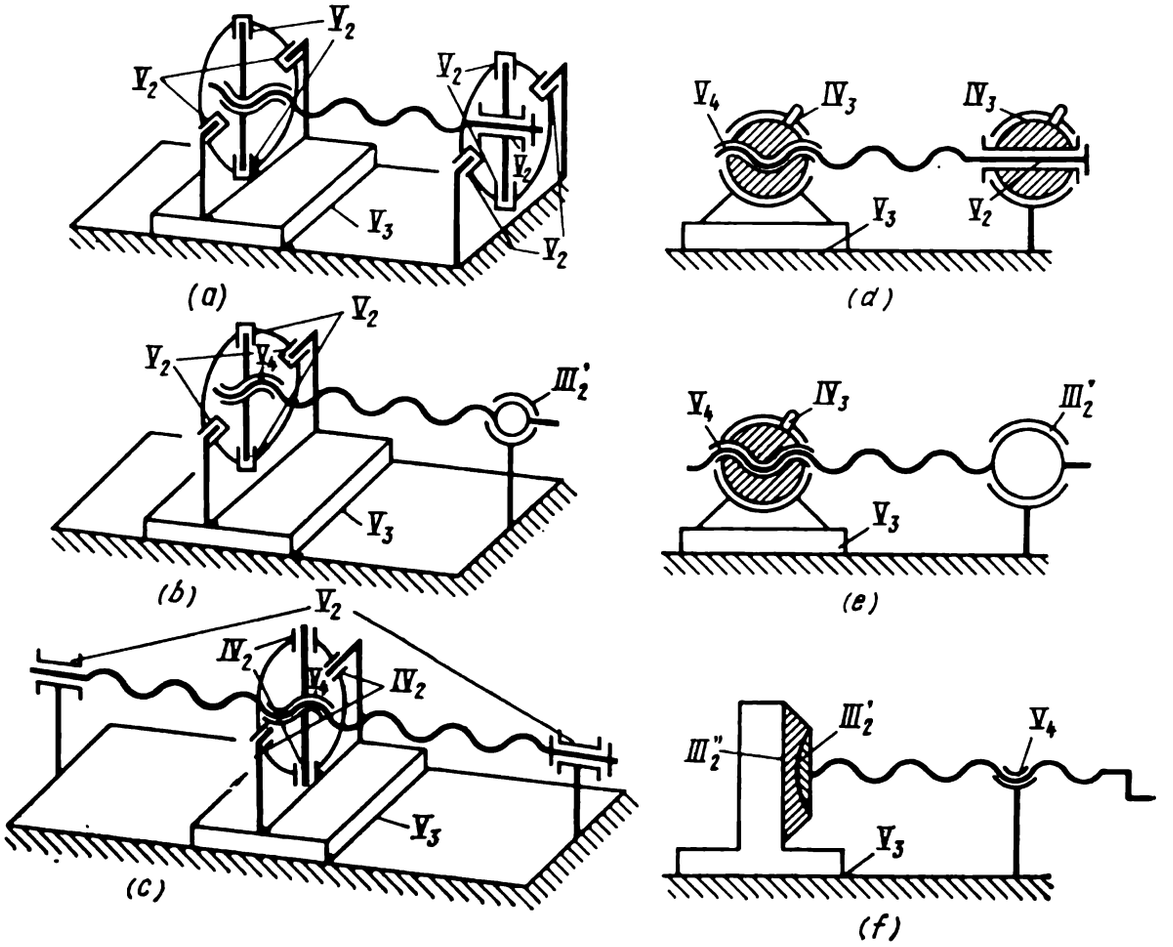


**Fig. 2.22. Rational structures** of screw mechanisms

mobilities as fifth-class pairs. Five mobilities (out of seven) then fall onto the rest of the pairs.

If fifth-class (single-mobility) pairs are used, it will take five pairs (Fig. 2.22*a*). For clarity, in this drawing the translatory pair $V_3$ (slider-guideways) is shown below the screw. In reality, it should be arranged symmetrically with respect of the screw. The same is true of other designs of Fig. 2.22.

In Fig. 2.22,*a* the nut is connected with the slider through two pivots $V_2$, while the screw is connected with the fixed member through three pivots $V_2$. Alternatively, the nut may be connected with the fixed member through three pivots, with the screw connected with the slider through two pivots, which yields an absolutely equivalent structure.

If one spherical three-mobility pair $III_2'$ is used, two single-mobility fifth-class pairs should be added to the screw and the guideway to yield seven mobilities (Fig. 2.22*b*). This structure may be altered: the spherical bearing $III_2'$ may be connected with the slider, and

the nut may be connected with the fixed member through two $V_2$ pivots.

Another possibility is using two cylindrical $IV_2$ pairs (Fig. 2.22*c*). Let us determine the mobilities in the loop $f = 7 = (1 + 1) + 2 + + 2 + 1$. Here, in addition to the screw and the guideways, another single-mobility $V_2$ pair is required (the bearings of the screw).

The structure of Fig. 2.22*c* is simpler than that of 2.22*a* in that it has five pairs instead of seven. Besides, in this structure the screw is solely rotatable, which simplifies its drive.

If two spherical-with-pin $IV_3$ pairs are used (Fig. 2.22*d*), we have the structure widely employed in bench vices. In the vice, however, it is not the prismatic pair $V_3$ which connects the movable jaw with the fixed member, but a rotary $V_2$ one.

A similar structure, although with two $IV_4$ chain pairs, was used in screw couplings of railway cars. The construction, however, used to be excessively strained, since the weight of the coupling was limited by the muscular effort of coupler's hands. If it had had redundant constraint the construction would have been inoperable.

It is further possible to have a single spherical pair $III'_2$ (three-mobility) and a single spherical-with-pin (two-mobility) pair $IV_3$ (Fig. 2.22*e*). In this case, the number of mobilities $f = 7 = (1 + 1) + 3 + 2$.

With two three-mobility pairs $III'_2$ and $III''_2$ (Fig. 2.22*f*), $f = (1 + 1) + 3 + 3 = 8$.

We have now the seven mobilities plus one, which indicates a local mobility—the rotation of the spacer between the screw and the slider. This structure is sometimes used in hand-operated presses where the screw works in longitudinal bending. However, if the arrangement of the members is altered the screw may work in tension.

In hoists (or jacks) where the screw itself serve as the guides, it is easier to avoid redundant constraints. In a single-screw hoist (Fig. 2.23) this is attained by using a self-aligning thrust ball bearing, i.e. a first-class pair. In hoists of this kind the nut is usually rotatable, while the screw reciprocates, the screw having a keyway and being guided in a sleeve with a key. Here, $p_V = 2$ and $p_I = 1$, whereby $f = 7$.

From (1.1): $q = 1 - 6 \times 2 + 5 \times 2 + 1 \times 1 = 0$.

If a not self-aligning ball bearing pair is used, i.e. a third-class pair, then $q = 2$. The two redundant constraints require accurate machining of the end face surfaces of the nut and the sleeve, perpendicularly to the screw axis. Then the end face surface of the nut should be machined and its thread should be cut at a single setting in

the machine tool, while the machining of the end face of the sleeve and the boring of its opening should be likewise performed at a single setting in the machine tool.

If the point of application of a load is not aligned with the axis of the screw of a single-screw hoist, the screw is subjected to a ben-

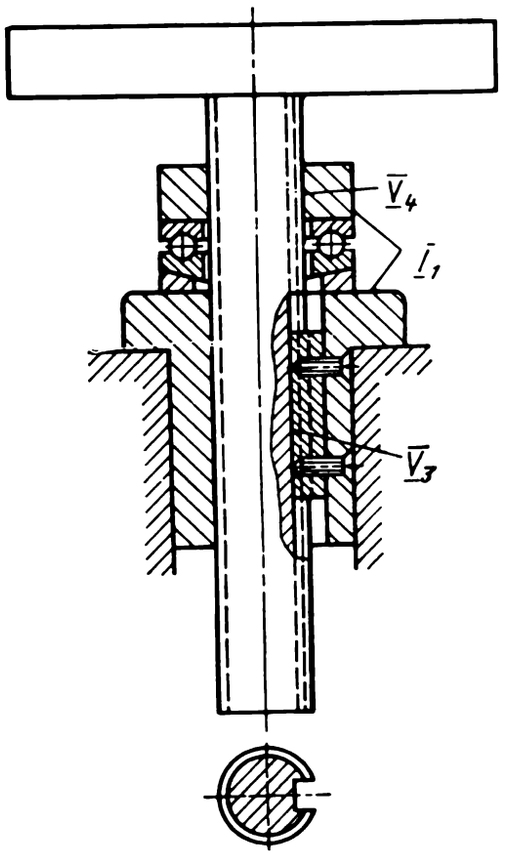


Fig. 2.23. Rational structure of single-screw hoist

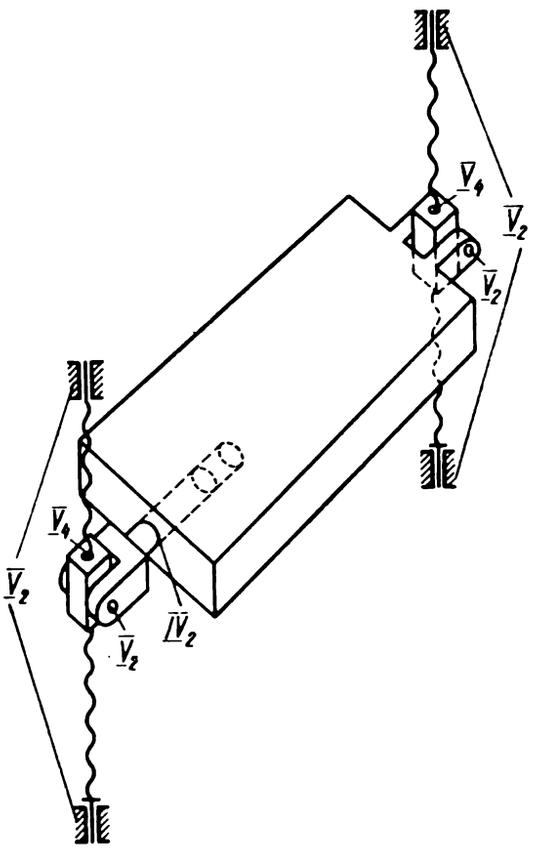


Fig. 2.24. Rational structure of double-screw hoist

ding load, which is a shortcoming of the mechanism.

A double-screw hoist (Fig. 2.24) can be likewise designed with no redundant constraints. In most cases, the screws of such hoists are driven from a single drive. However, mechanisms devoid of redundant constraints should also provide for separate drives, i.e. $w = 2$. Let us consider this case so as not to include the drive mechanism into our calculations. The nuts of the hoisting screws should not be fast with the platform. Preferably, one of them is connected via a revolute pair $V_2$ and a cylindrical $IV_2$ pair, and the other one via a revolute pair $V_2$. Then from (1.1): $q = 2 - 6 \times 6 + 5 \times 6 + 4 \times 1 = 0$.

With no redundant constraints, this mechanism is capable of faultless operation even with broad tolerances in manufacture, as-

sembly and service (e.g. sagging of the foundation). It is also operable when the platform is to be tilted in addition to being hoisted.

In a double-screw hoist the screw is not subjected to bending if the load is aligned with the axis of the platform, i.e. the situation is better than with a single-screw hoist.

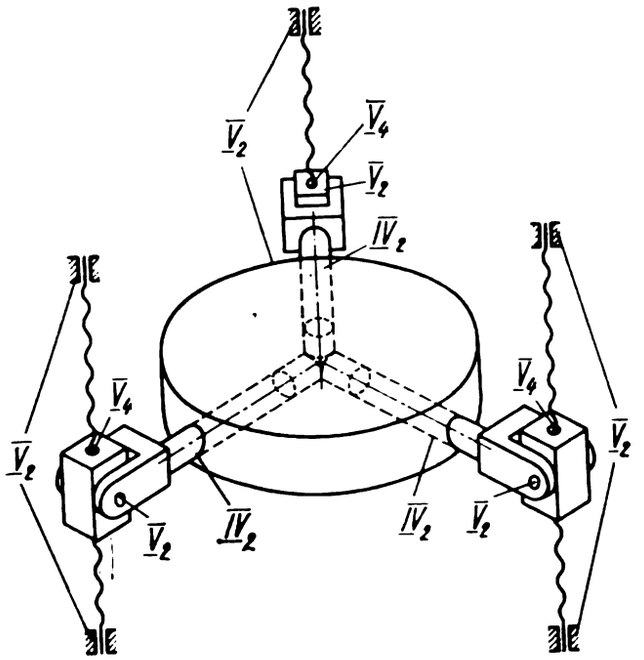


Fig. 2.25. Rational structure of triple-screw hoist

Avoiding completely the bending torques applied to the screws is feasible with a triple-screw hoist (Fig. 2.25), which design is recommended with a large platform. In this hoist the screws are operable with either an individual or a common drive.

Let us discuss the case with the individual drives, i.e. with $w = 3$. In this hoist the nuts of the three hoisting screws should be connected with the platform via revolute and cylindrical pairs. Then, from (1.1): $q = 3 - 6 \times 10 + 5 \times 9 + 4 \times 3 = 0$. The design can be used when the platform is to be hoistable and rotatable about two axes.

Hoists with the number of the screw in excess of three require specific balancing arrangements to avoid redundant constraints, and, therefore, are impractical.

## 2.7. Slider-Crank Mechanism

A slider-crank mechanism is commonly used to convert rotary motion into reciprocation and vice versa. It includes pairs with surface contact; it is of simple structure and capable of transmitting great ef-

forts; it enables the shaft to turn through a complete revolution, which makes it usable with continuous rotation.

In a planar diagram, irrespectively of the classes of the kinematic pairs, from formula (1.5) the mechanism is devoid of redundant constraints: $q_p = 1 - 3 \times 3 + 2 \times 4 = 0$.

If all the pairs are of class $V$, from (1.1): $q = 1 - 6 \times 3 + 5 \times 4 = 3$. This means that any manufacturing inaccuracy would result in the last-assembled pair being either strained or preloaded in three ways. If this last-assembled pair is a slider-crank, the preloading will be, as follows: the first strain develops when the slider would not fit the guideways axially of the shaft (in the direction perpendicular to the shaft axis the slider can be always set into the guideways, owing to the mobilities of the connecting-rod ends); the second and third strains result from misalignment of the guideways in two planes parallel with the shaft axis—the horizontal and vertical ones (in the plane perpendicular to the shaft axis this alignment can always be reached owing to the mobilities of the connecting-rod ends).

These redundant constraints call for high manufacturing and assembling accuracy, which is particularly hard to attain when the mechanism is of big dimensions.

The condition of the absence of redundant constraints is derived from formula (1.1) by having there $n = 3$, $w = 1$ and $q = 0$:

$$1 - 3 \times 6 + 5p_{\mathrm{V}} + 4p_{\mathrm{IV}} + 3p_{\mathrm{III}} = 0;$$

or else $5p_{\mathrm{V}} + 4p_{\mathrm{IV}} + 3p_{\mathrm{III}} = 17$, i.e. the sum of the classes of the kinematic pairs (the number of the restraints imposed) should equal seventeen. First- and second-class pairs are absent in the formula because they are not used in mechanisms of this kind.

The condition of the absence of redundant constraints can be expressed in other way from formula (1.2): $q = w + 6k - f$.

By introducing $q = 0$, $w = 1$ and $k = 1$ (the number of the loops), we have $f = 7$, i.e. the sum of the mobilities of the kinematic pairs should equal seven.

The numerals 17 and 7 thus obtained are true only with mobility $w = 1$. With other values of the mobility, they would equal [from formulas (1.1) and 1.2)], respectively:

| | | | |
|---|---|---|---|
| $w$ | 1 | 2 | 3 |
| $\Sigma i p_i$ | 17 | 16 | 15 |
| $f$ | 7 | 8 | 9 |

In rational structures of a slider-crank mechanism it is expedient to use spherical $III_1'$ pairs which may be spherical ball- and roller-

bearings with the secured outer race, or else pairs with plain bearings $III_2'$. The construction of such a pair, employed in internal combustion engines, is shown in Fig. 2.26, *a*, and that employed in presses is shown in Fig. 2.27.

In diagrams to follow, we will designate a spherical pair with a circle of a diameter greater than the diameter of a circle designating a revolute pair. Spherical-with-pin pairs will be likewise designated by a circle of an enlarged diameter, with the pin arbitrarily directed askew. In reality, the pin should be directed along the longitudinal axis of the pivot.

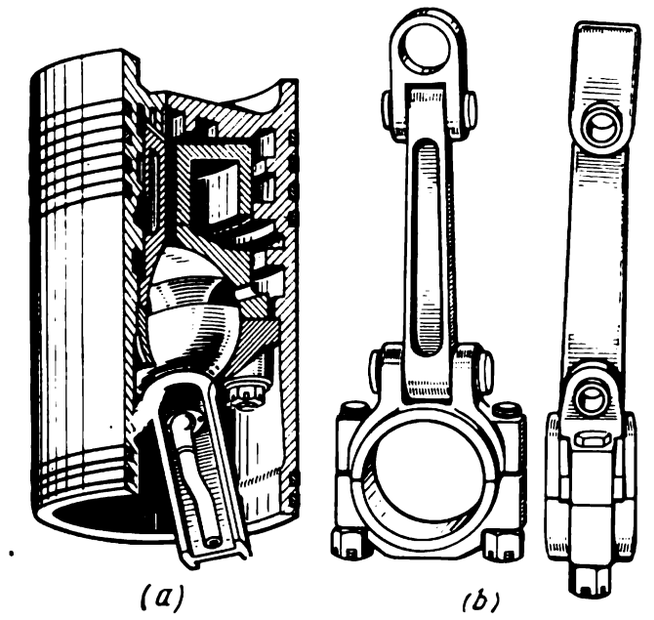


Fig. 2.26. Connecting-rods of rational slider-crank mechanisms used in I. C. engines

(*a*) with spherical pair; (*b*) with additional joints, suggested by V.S. Salenko for the engine of Moskvich car

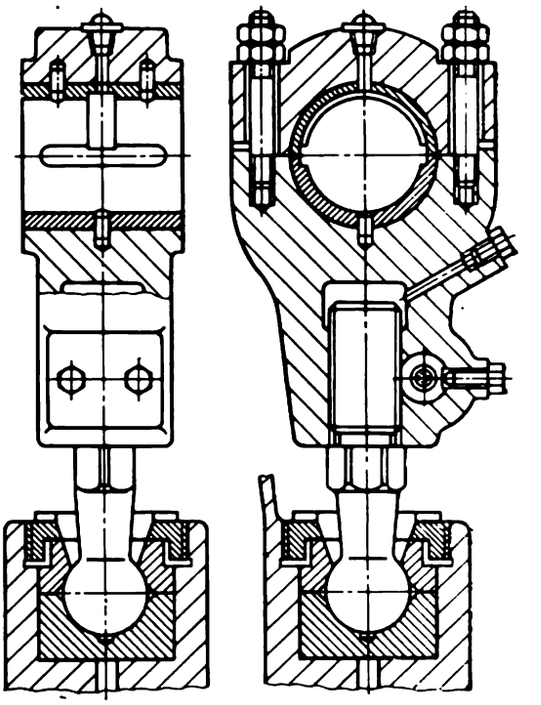

Fig. 2.27. Rational structure of connecting-rod with spherical pair, used in presses

Pairs $II_3$ or $II_1$ will not be considered, as an annular pair $II_3$ is unsuitable for great forces on account of its line contact, whereas pair $II_1$ with its high friction of the outer race cannot be used in cases where the self-alignment motion is periodical, i.e. is unsuitable for connecting-rod ends. Quite obviously, a pair $II_1$ can be used jointly with a pair $III_1$ in association with the crankshaft where they form a pair $V_1$ as the latter is designated in the diagrams.

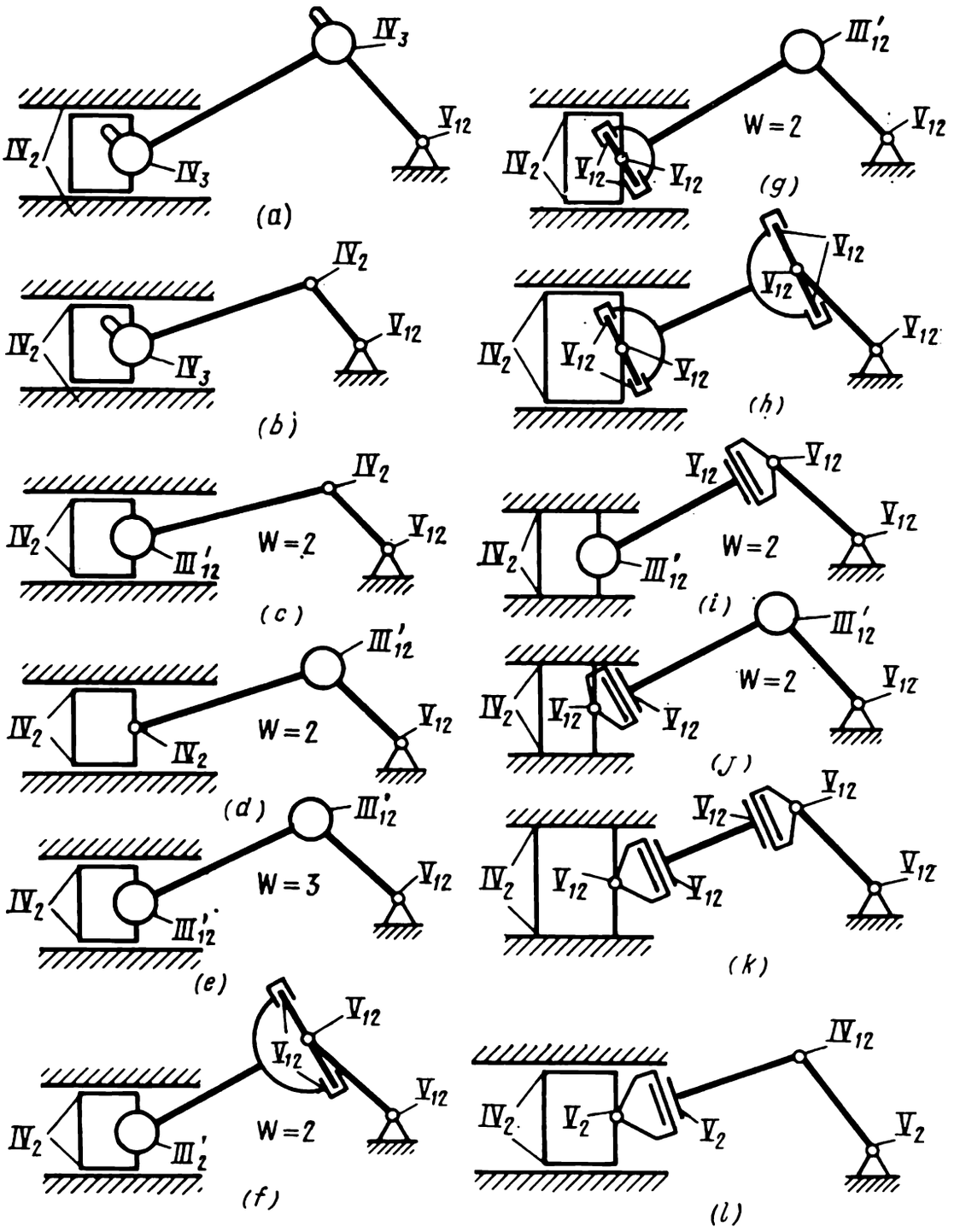


Fig. 2.28. Rational structures of slider-crank mechanism with cylindrical slider

In slider-crank mechanisms the slider can define either a cylindrical pair $IV_2$ (Fig. 2.28, *a-l*) or a prismatic pair $V_3$ (Fig. 2.29*a-k*). We will designate conventionally a cylindrical pair $IV_2$ as a trunk piston, whereas a prismatic pair $V_3$ will be designated as a single-side slider (in similarity with a steam locomotive construction).

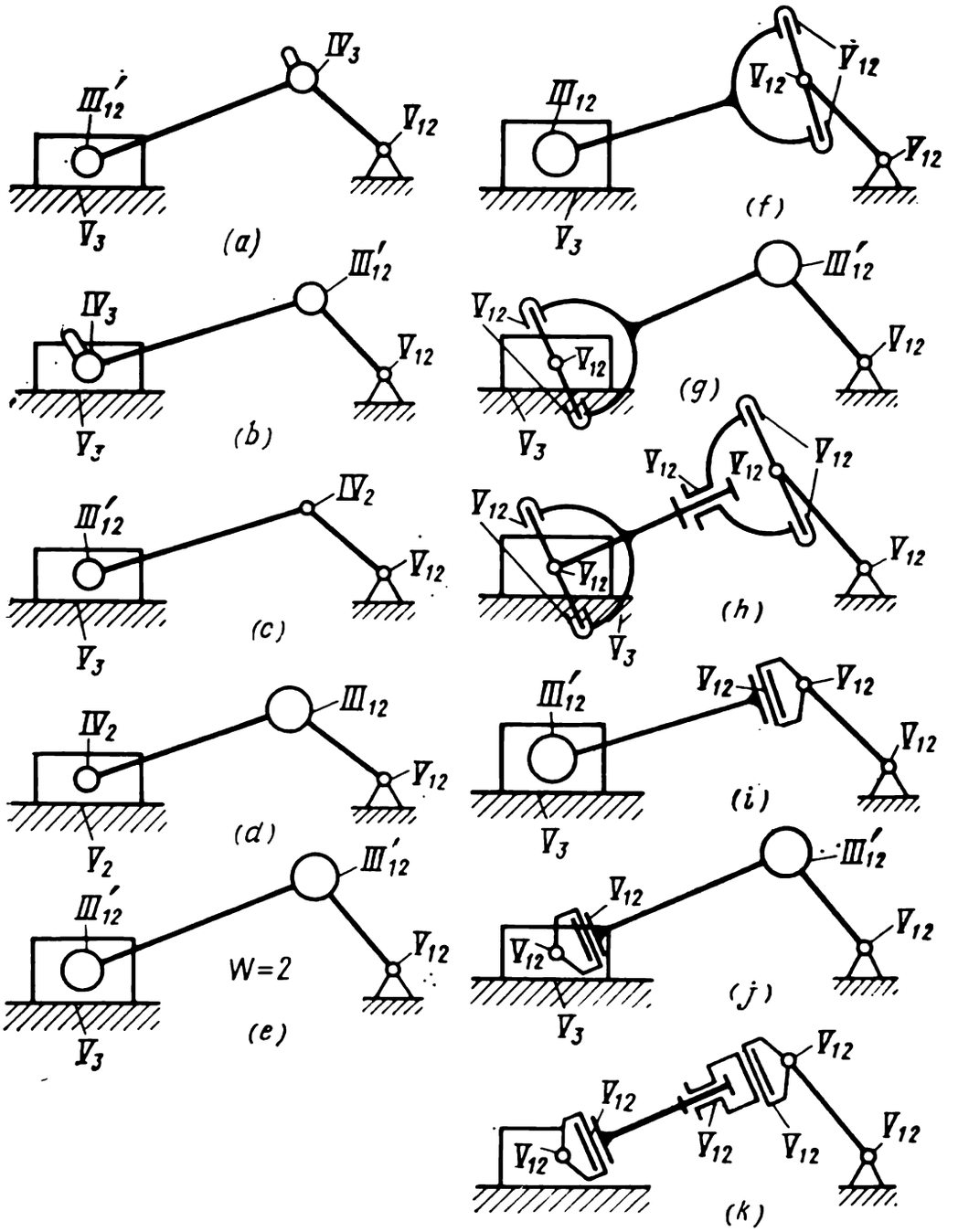


Fig. 2.29. Rational structures of slider-crank mechanism with translatory slider

The above discussed condition of a rational structure (17 restraints) is satisfied by one pair $V_{12}$* and three fourth-class pairs (Fig. 2.28*a*, *b*). There should not be, however, two cylindrical $IV_2$ pairs with parallel axes, or one harmful local mobility and one redundant constraint will occur.

The same condition is met by two pairs $V_{12}$ and $V_3$, $IV_3$ and $III'_{12}$ (Fig. 2.29*a*, *b*).

*Pair $V_{12}$ means a fifth-class pair from Columns 1 or 2 (Table 1.1).

A spherical-with-pin pair $IV_3$ has line contact rendering it unsuitable for transmitting great forces. Moreover, it can hardly be made up of antifriction bearings. For this reason it is replaced by a pair $IV_2$ (Fig. 2.29*c*—presses; Fig. 2.29*d*—steam locomotives with antifriction bearings). Note that in the mechanism of Fig. 2.28*a* the two

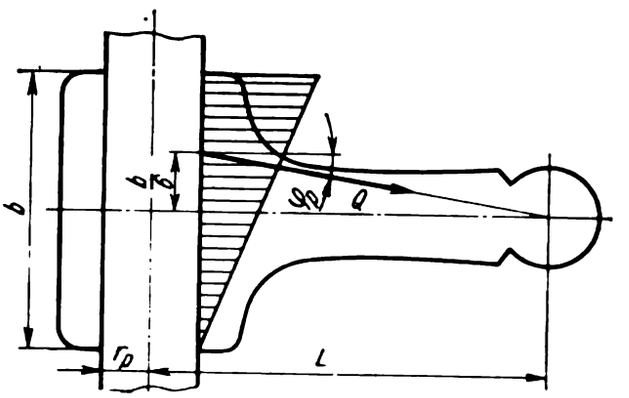


Fig. 2.30. Diagram of force acting upon connecting-rod from crank with cylindrical pair

$IV_3$ pairs cannot be replaced by two $IV_2$ pairs as one redundant constraint and one intolerable local mobility (the self-detachment of connecting-rod from the mechanism) will be brought in.

With cylindrical pairs $IV_2$ used, self-alignment is attained owing to axial sliding in the pair. It is essential that the sliding should be made possible and not eliminated on account of self-braking.

Let us consider a mechanism with a cylindrical pair $IV_2$ on the crank pin (see Fig. 2.28*c* or Fig. 2.29*c*). To provide for axial sliding, the load of the cylindrical pair should be non-uniform. Presuming the loading diagram over the length of the pair is a triangle (Fig. 2.30), the gravity centre of the load triangle will be $b/6$-distant from the connecting-rod axis. The force $Q$ transmitted by the connecting-rod should pass through this gravity centre and the centre of the spherical end, and, to provide for the sliding, it should define with the normal the friction angle $\varphi_p$.

Then,

$$b > 6\, L \operatorname{tg} \varphi_p \tag{2.1}$$

Knowing that $\operatorname{tg} \varphi_p = f_p = \frac{4}{\pi} f$ ($f_p$ being the reduced friction coefficient in the formula for worked-in journals), by introducing this value of $f_p$ into (2.1) we obtain:

$$b > \frac{24}{\pi} fL \tag{2.2}$$

Formula (2.2) yields fairly large dimensions of the kinematic pairs: thus, with $f = 0.1$, $b > 0.76\ L$.

This situation requires that the antifriction bearing should have its axial mobility provided by the slide fit of the outer race. Therefore, in many cases this design is impractical. Roller bearings having no shoulder on one of the races, Types 2000 or 32 000, should be used.

With sliding-contact bearings, the necessary length $b$ of the bearing may be much smaller if the relative axial displacement is accompanied by relative rotation. In this case, the friction force directed in opposition to the full relative speed attains a more favourable direction, with the reduction of its axial component $F_p$ defining the friction angle in formula

$$\operatorname{tg} \varphi_p = \frac{F_p}{Q}$$

By introducing from (1.32) the value

$$F_p = Q \frac{4}{\pi} f \frac{v_p}{\sqrt{\omega^2 r_p^2 + v_p^2}}$$

we arrive at

$$\operatorname{tg} \varphi_p = \frac{4}{\pi} f \frac{v_p}{\sqrt{\omega^2 r_p^2 + v_p^2}} = \frac{\frac{4}{\pi} f}{\sqrt{\left(\frac{\omega r_p}{v_p}\right)^2 + 1}} \tag{2.3}$$

As the speed of the axial sliding (i.e. of self-aligning) is very small in comparison with circumferential velocity $\omega r_p$, we may neglect the unity under the radical sign. Then

$$\operatorname{tg} \varphi_p = \frac{4}{\pi} f \frac{v_p}{\omega r_p} \tag{2.4}$$

By substituting it into (2.1), we obtain:

$$b > \frac{24}{\pi} \frac{L}{r_p} f \frac{v_p}{\omega} \tag{2.5}$$

To define tolerances for permissible skewing of the members of the mechanism, let us find from (2.5)

$$\frac{s}{2\pi} = \frac{v_p}{\omega} < \frac{\pi}{24} \frac{b}{L} \frac{r_p}{f} \tag{2.6}$$

We see that the relative motion in the cylindrical pair of the connecting-rod is helical, with the maximum pitch $s$ defined by the friction conditions (with jamming avoided) calculated from formula (2.6). This pitch is dependent on the friction coefficient $f$ and on the diagram of load distribution along the journal (the triangle).

With $L = 565$, $r_p = 77.5$ and $b = 100$ (6 Ч 23/30 engine, crank end):

$$s_c = \frac{\pi^2}{12}\frac{b}{L}\frac{r_p}{f} = \frac{\pi^2}{12}\frac{100}{565}\frac{77.5}{0.1} = 113\,\text{mm}$$

For comparison sake, let us find the friction circle radius in the same end:

$$\rho_c = \frac{4}{\pi} fr_p = \frac{4}{\pi} 0.1 \times 77.5 = 9.9\,\text{mm}$$

For a piston end with $L = 565$, $r_p = 45$ and $b = 92$,

$$s_c = \frac{\pi^2}{12}\frac{b}{L}\frac{r_p}{f} = \frac{\pi^2}{12}\frac{92}{565}\frac{45}{0.1} = 60.2\,\text{mm}$$

and the friction circle radius is $\rho_p = \frac{4}{\pi} fr_p = 0.1 \times 45 = 5.73$ mm.

To determine tolerances for skewing of the members, let us find what skewing in the crank end still makes possible this terminal helical motion with pitch $s$.

Let us consider a slider-crank mechanism wherein the crank pin is skewing at angle $\gamma$ (Fig. 2.31). In this case, the maximum axial displacement of the crank end per one side is $k = L \operatorname{tg} \gamma$.

Assuming that the relative axial displacement is governed by the harmonic law and writing for the angle of rotation of the shaft, we define current displacement $x = k \sin \delta = L \operatorname{tg} \gamma \sin \delta$, and velocity $v = \omega L \operatorname{tg} \gamma \cos \delta$.

The maximum velocity (the most hazardous one) is $v_p = \omega L \operatorname{tg} \gamma$.

Now we find

$$\frac{s_c}{2\pi} = \frac{v_p}{\omega} = L \operatorname{tg} \gamma$$

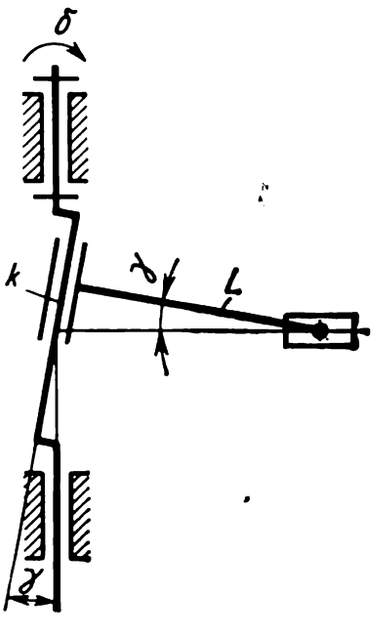


Fig. 2.31. Slider-crank mechanism with crank pin skewing at $\gamma$

Solving this equation for the skew angle of the crank pin, we arrive at

$$\operatorname{tg} \gamma = \frac{s_c}{2\pi L} \qquad (2.7)$$

For the engine (Type 6Ч 23/30) already considered as an example:

$$\operatorname{tg} \gamma = \frac{113.0}{2\pi\, 565} = 0.0318, \text{ and } \gamma = 1.8°$$

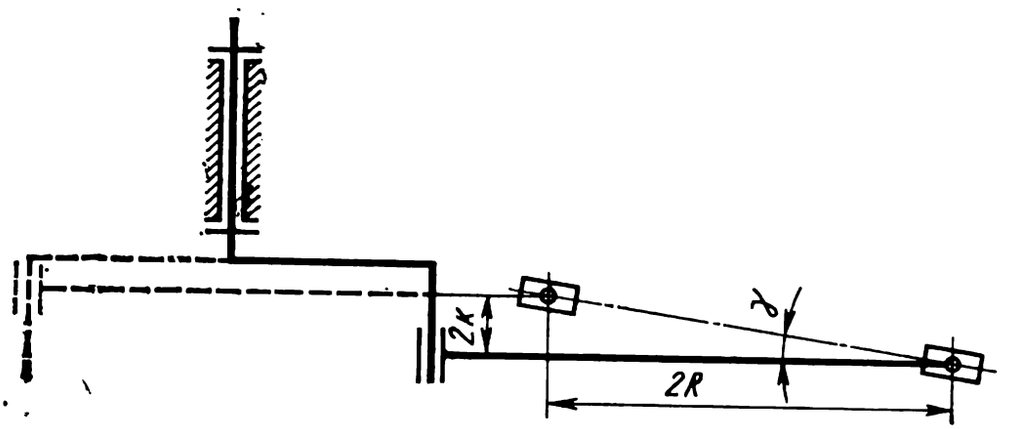


Fig. 2.32. Slider-crank mechanism with skewing guideways

Let us now consider the case of the guideways skewing at angle $\gamma$ (Fig. 2.32), i.e. when guideways are not perpendicular to the main shaft. Here, $2k = 2R \operatorname{tg} \gamma$.

Assuming the harmonic law of the axial sliding: $x = k \sin \delta = R \operatorname{tg} \gamma \sin \delta$; $v = \omega R \operatorname{tg} \gamma \cos \delta$; $v_p = \omega R \operatorname{tg} \gamma$; and $\frac{s_c}{\pi} = \frac{v_p}{\omega} = R \operatorname{tg} \gamma$. We still neglect here the angular velocity of the connecting-rod, being negligible in comparison with the angular velocity of the crank.

From the last-written expression:

$$\operatorname{tg} \gamma = \frac{s_c}{2\pi R} \tag{2.8}$$

For the same Type 6Ч 23/30 engine ($R = 150$):

$$\operatorname{tg} \gamma = \frac{113.0}{2\pi\, 150} = 0.12; \quad \gamma = 6.8^\circ$$

With the crank end of the connecting-rod skewing, it will become displaced axially through a permanent distance. Thus, the friction force in this end will be directed circumferentially, i.e. in opposition to the sliding velocity.

There will be no axial friction force, and, hence, self-braking will be precluded. Ordinary self-alignment will take place, for which reason we are not going to discuss this situation.

Let us now turn to a mechanism where the cylindrical pair $IV_2$ is mounted on the slider (cf. Fig. 2.28, *d* and Fig. 2.29*d*). Let us consider the situation where the pin in the slider is skewing at $\gamma$ in the horizontal plane including the axis of the main shaft (Fig. 2.33). The figure shows plan view of the mechanism in three positions: at the two dead centres and with the crank extending vertically.

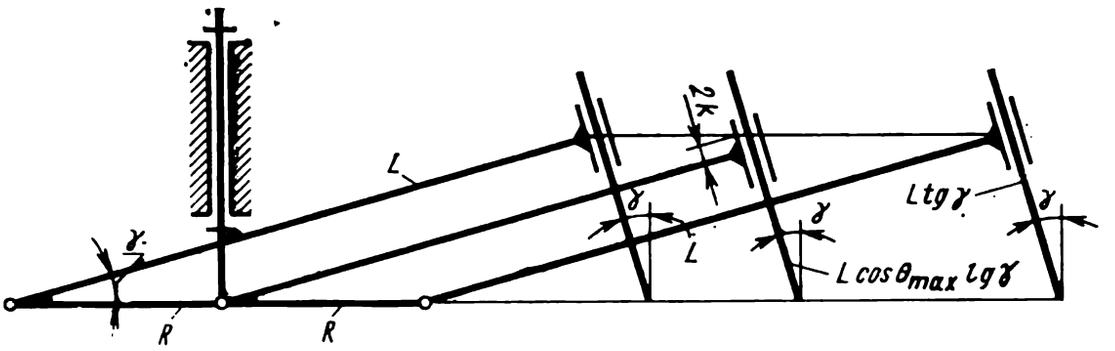


Fig. 2.33. Slider-crank mechanism with skewing piston pin

At the dead centres, the piston end of the connecting-rod will be offset by the value $L$ tg $\gamma$—the very value that should be taken into account for calculating the necessary tolerances.

In the intermediate position, the connecting-rod is inclined at an angle $\theta_{max}$ (Fig. 2.34), its projection onto a horizontal plane being $L \cos \theta_{max}$, and the displacement of the piston end being $L \cos \theta_{max} \operatorname{tg} \gamma$.

The difference between the displacement in these position yields the value of the longitudinal sliding of the piston end:

$$2k = L \operatorname{tg} \gamma - L \operatorname{tg} \gamma \cos \theta_{max} = 2L \operatorname{tg} \gamma \sin^2 \frac{\theta_{max}}{2} \tag{2.9}$$

In a slider-crank mechanism (Fig. 2.34)

$$\sin \theta = \frac{R}{L} \sin \delta$$

Differentiation of the last expression for $t$ yields

$$\omega_{c\text{-}r} \cos \theta = \omega \frac{R}{L} \cos \delta$$

or

$$\omega_{c\text{-}r} = \omega \frac{R}{L} \frac{\cos \delta}{\cos \theta} \tag{2.10}$$

If $\delta = 90°$, we have $\sin \theta_{max} = R/L$.

Fig. 2.34. Planar diagram of slider-crank mechanism

Since in most cases $\frac{R}{L} < \frac{1}{3.5}$ and $\theta_{max} < 17°$, assuming

$$\sin \frac{\theta_{max}}{2} \approx \frac{R}{2L}$$

and substituting in (2.9):

$$k = \frac{R^2}{4L} \operatorname{tg} \gamma \tag{2.11}$$

If we assume that the displacement of the piston end along the pin follows the harmonic law, it is bound to be the second-order harmonic $x = k \cos 2\delta$.

Thus, the velocity (with the sign omitted):

$$v = 2\omega k \sin 2\delta = \omega \frac{R^2}{2L} \operatorname{tg} \gamma \sin 2\delta$$

Dividing this expression by (2.10):

$$\frac{v}{\omega_{c\text{-}r}} = R \operatorname{tg} \gamma \cos \theta \sin \delta$$

With $\delta = 90°$; $\theta = \theta_{max}$ and $v = v_p$:

$$\frac{s_p}{2\pi} = \frac{v_p}{\omega_{c\text{-}r}} = R \operatorname{tg} \gamma \cos \theta_{max}$$

Hence,

$$\operatorname{tg} \gamma = \frac{s_p}{2\pi R \cos \theta_{max}} \tag{2.12}$$

For the abovecited example, considering that the expression (2.12) includes the pitch $s_p$ of the piston end which is smaller than that of the crank end:

$$\sin \theta_{max} = \frac{R}{L} = \frac{150}{565}\ ;\ \theta_{max} = 15.4°$$

From (2.12):

$$\operatorname{tg} \gamma = \frac{60.2}{2\pi\, 150 \cos 15.4°} = 0.0664, \text{ and } \gamma = 3.8°$$

It is reasonable to consider also the case of the piston pin skewing in the longitudinal vertical plane (Fig. 2.35), although this case is possible only with the guides being a fifth-class pair. Should the guideways be a fourth-class cylindrical pair (the trunk piston case), the angle would be eliminated by self-alignment. In Fig. 2.35, $k = R \sin \gamma$. Assuming the axial sliding velocity varying in accordance with the harmonic law, we have $v = \omega k \cos \delta = \omega R \sin \gamma \cos \delta$.

Let us define $\frac{v}{\omega_{c-r}}$ by dividing the above expression by (2.10):

$$\frac{v}{\omega_{c-r}} = L \sin \gamma \cos \theta$$

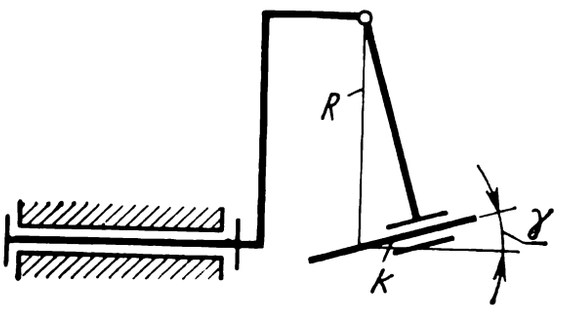


Fig. 2.35. Mechanism with translatory slider and skewed piston pin (end view)

The maximum value of this expression with $\delta = 0$ and $\theta = 0$:

$$\frac{s_p}{2\pi} = \frac{v_p}{\omega_{c-r}} = L \sin \gamma \tag{2.13}$$

hence

$$\sin \gamma = \frac{s_p}{2\pi L} \tag{2.14}$$

Let us further discuss the case of the guideways skewing at $\gamma$, i.e. where the guideways are not perpendicular to the main shaft (Fig. 2.36). Here, $k = R \sin \gamma$.

We still assume the axial sliding law being the harmonic one. However, with $\delta = 0$, $x = k$, with $\delta = 90°$, $x = 0$, and with $\delta = 180°$, $x = -k$.

These conditions are satisfied by expression $x = k \cos \delta$, or $x = R \sin \gamma \cos \delta$.

By differentiating and omitting the sign:

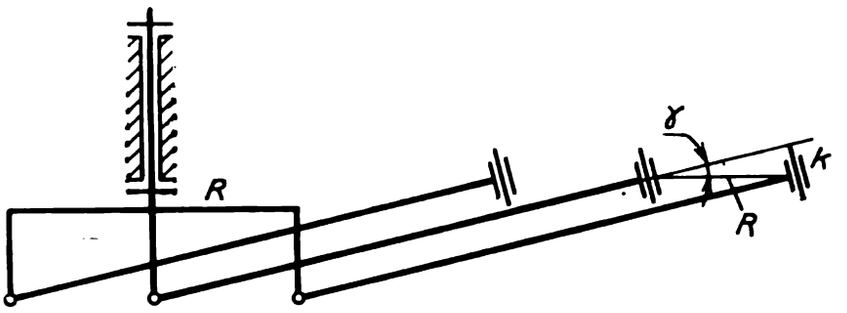


Fig. 2.36. Mechanism with cylindrical pair on slider and skewing guideways

$v = \omega R \sin\gamma \sin\delta$. By dividing this by $\omega_{c-r}$ from (2.10):

$$\frac{r}{\omega_{c-r}} = L\cos\theta \operatorname{tg}\delta \tag{2.15}$$

The maximum value with $\delta = 90°$:

$$s_p = 2\pi \frac{v_p}{\omega_{c-r}} = \infty \tag{2.16}$$

The expression indicates that self-alignment is impossible here. Therefore, a cylindrical pair must be always mounted on the crank, and the spherical pair must be mounted on the slider (a cylindrical pair must not be mounted on the slider).

By generalizing the data obtained for all the abovediscussed mechanisms, we can draw a conclusion that a cylindrical pair $IV_2$ should be mounted only where it goes through a full revolution.

It is useful to generalize the expressions for different cases of skewing. With the $IV_2$ pair on the crank pin, for the crank pin skewing we have from (2.6) and (2.7):

$$\operatorname{tg}\gamma < \left(\frac{\pi}{24}\frac{1}{f}\frac{b}{L}\right)\frac{r_p}{L}$$

for the guideways skewing we have from (2.6) and (2.8):

$$\operatorname{tg}\gamma < \left(\frac{\pi}{24}\frac{1}{f}\frac{b}{L}\right)\frac{r_p}{R}$$

With the pair $IV_2$ on the piston end, for the piston pin skewing in a horizontal plane we have from (2.6) and (2.12):

$$\operatorname{tg}\gamma < \left(\frac{\pi}{24}\frac{1}{f}\frac{b}{L}\right)\frac{r_p}{R\cos\theta_{\max}}$$

and for the piston pin skewing in the vertical axial plane we have from (2.6) and (2.13)

$$\sin\gamma < \left(\frac{\pi}{24}\frac{1}{f}\frac{b}{L}\right)\frac{r_p}{L}$$

and the skewing of the guideways $\gamma = 0$.

The calculations have proved that in a mechanism devoid of redundant constraints the tolerances for skewing may be proved to be excessive. It should be remembered, however, that they have been found from the condition of the triangular law of the loading of the journal. It is expedient to have the tolerance for skewing somewhat smaller, to enhance the working conditions of the kinematic pairs.

When the cylindrical pair $IV_2$ incorporates antifriction bearings, roller bearing without shoulders on one of the races should be used (Types 2 000 or 32 000). When the requirement is to withstand high

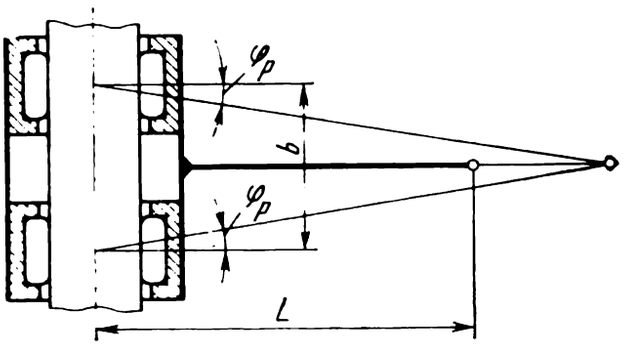


Fig. 2.37. Schematic view of connecting-rod with crank end on needle bearings

loads at low speeds, needle bearings may be recommended (Fig. 2.37).

In this case

$$L < \frac{b}{2 \operatorname{tg} \varphi_p} \tag{2.17}$$

If the inner race has no shoulders, then to determine $\operatorname{tg} \varphi_p = F_p/Q$, $F_p$ should be found from

$$F_p = f \left\{ \left[ 0.92 + 0.37 \operatorname{arctg} \frac{140 v_p}{(D+3d)\,\omega} \right] Q - \frac{5\lambda z (D-d)^2}{64} \right\}$$

and when it is the outer race that has no shoulders, $F_p$ should be found from

$$F_p = f \left\{ \left[ 0.92 + 0.37 \operatorname{arctg} \frac{140 v_p}{(3D+d)\,\omega} \right] Q - \frac{5\lambda z (D-d)^2}{46} \right\}$$

where $D$ and $d$ are, respectively, the diameters of the outer and inner races (cf. Fig. 1.21); $z$ is the number of the rollers in the bearing, $\lambda$ is the ratio of the roller length to its diameter.

Comparing the two expressions, we see that in the last-mentioned case the friction is smaller since $3D + d > D + 3d$. Thus, it is more expedient to use bearings with the shoulderless outer race (Type 2 000).

With a cylindrical slider, the spherical-with-pin pair can be completely avoided by being replaced by a spherical pair $III''_{12}$ (cf. Fig. 2.28*c*). This yields a single local mobility—rotation of the piston about its axis ($w = 2$). The mobility is harmless in four-stroke engines; in two-stroke engines it is impermissible, for in these engines the joints of the pistons may not align with the intake and exhaust ports.

A spherical pair $III'_{12}$ should be mounted on the piston end of the connecting-rod (cf. Fig. 2.28*c*). It is hazardous to mount it on the

crank end (Fig. 2.28*d*), because at a dead position the connecting-rod with the piston may be turned about the crank end $III'_{12}$, and with the machine being started, a breakdown will occur. It is yet another proof that a cylindrical pair $IV_2$ must not be mounted on the slider.

A cylindrical pair $IV_2$ restricts the capacity for self-alignment. Therefore, it is preferably replaced on the piston end by a spherical pair $III'_{1\ 2}$ (cf. Fig. 2.28*e* and Fig. 2.29*e*). This would bring about a local mobility, i.e. rotation of the connecting-rod about its axis (between the abutments). The pattern is unsuitable for two-stroke engines, enabling as it does the alignment of the joints of the piston rings with the intake and exhaust ports, which is impermissible.

Another way to avoid pairs $IV_3$ and $IV_{1\ 2}$ is their replacement by a kinematic connection $IV_a$ (see Table 1.4 and Figs. 2.28*f*, *g* and 2.29*f*, *g*). In Fig. 2.29*f*, *g* it is immaterial on which one of the connecting-rod ends the spherical pair $III_{1\ 2}$ and the kinematic connection of two pairs $V_{1\ 2}$ will be mounted. In the design shown in Fig. 2.28*f* the mounting of the spherical pair on the crank end is as hazardous as in Fig. 2.28*d*.

In cases where the tolerances for the dimensions of the members are particularly great, the additional angular mobilities offered by spherical bearings may prove insufficient. If so, the spherical pairs $III_{1\ 2}$, too, should be replaced by a kinematic connection $III_a$ (Table 1.4, Fig. 2.29*c*). The third $V_{12}$ pair transmits an axial effort alone, so it is offset from the intersection points of the axes to simplify the structure.

With a cylindrical slider $IV_2$, it is expedient to have both connecting-rod ends as fourth-class connections ($IV_a$, Fig. 2.28*c*). This design is used in the control mechanisms of steam turbines.

In kinematic connections illustrated in Figs. 2.28*f*, *g*, *h* and 2.29*f*, *g*, *h*, the axes of the rotational pairs intersect. This design is the very best from the theory view-point, but the actual structure becomes too cumbersome. Therefore, the design is practically employed for such applications as steam turbines where the displacements of the members, caused by thermal extension, are particularly great. Where such displacements are relatively small (e.g. in internal combustion engines), it is more reasonable to use designs in which the axes of the rotational pairs in the kinematic connections are crossing (cf. Fig. 2.28*i*, *j*, *k* and Fig. 2.29*i*, *j*, *k*).

The design illustrated in Fig. 2.28*k* was proposed by V. S. Salenko who reconstructed the engine of "Moskvich" car accordingly. The new construction of the connecting-rod is shown in Fig. 2.26*b*.

The tests showed that the friction in the mechanism was reduced, particularly, the take-off torque. This was what had to be expected, for in the mechanism with no redundant constraints the prestraining was absent. Piston-skewing was eliminated, enhancing the sealing properties. All these resulted in significantly better starting of the engine.

No tests concerned with the wear of the piston and cylinder have been conducted as yet, but there are all the reasons to expect improvements in this area, too. All in all, the design has bright prospects opened up before it. Even better prospects seem to be in store for the design shown in Fig. 2.28*l*, since it is simpler than that of 2.28*k* and easier in manufacture than those of Figs. 2.28*c*, and 2.28*a*.

## 2.8. Crank-and-Rocker Mechanism

The planar diagram of a crank-and-rocker mechanism is illustrated in Fig. 2.38*a*. When checked against the formula (1.5) or (1.6), it yields $q_p = 0$, i.e. the absence of particularly harmful redundant constraints. To have no redundant constraints at all, let us substitute in (1.1) $q = 0$, $w = 1$ and $n = 3$, and, considering that the mechanism is free of first- and second-class pairs ($p_{\mathrm{I}} = 0$ and $p_{\mathrm{II}} = 0$), we arrive at the expression for the number of the restraint conditions of the kinematic pairs of this mechanism: $5p_{\mathrm{V}} + 4p_{\mathrm{IV}} + 3p_{\mathrm{III}} = 17$.

The same condition expressed as the number of the mobilities can be obtained by similar substitution in (1.2). We will arive then at $f' = 7$ for the number of the mobilities of the kinematic pairs of the closed loop.

These conditions are met by two $V_2$ pairs, one $IV_3$ pair and one $III_2'$ pair (Fig. 2.38*b*). Unfortunately, the $IV_3$ pair—the spherical-with-pin one—features the linear contact of the members at the pin and is unsuitable for great efforts, leaving the design of Fig. 2.38, *b* for lightly loaded mechanisms exclusively. The $IV_3$ pair can be avoided by being replaced by a spherical pair $III_2'$ (Fig. 2.38*c*). The mobility of the mechanism is thus stepped up to two by the appearance of a harmful local mobility—the rotation of the connecting-rod about its axis. This design is exemplified in the broadly popular and well-proven steering linkage of an automobile.

The design is also to be found in biological mechanisms. The highly responsible mechanism in a human organism—the transmission from the tympanic membrane to the middle ear—is built about spherical joints. The transmission in question consists of a crank (the hammer), a connecting-rod (the anvil) and a rocker (the stirrup)

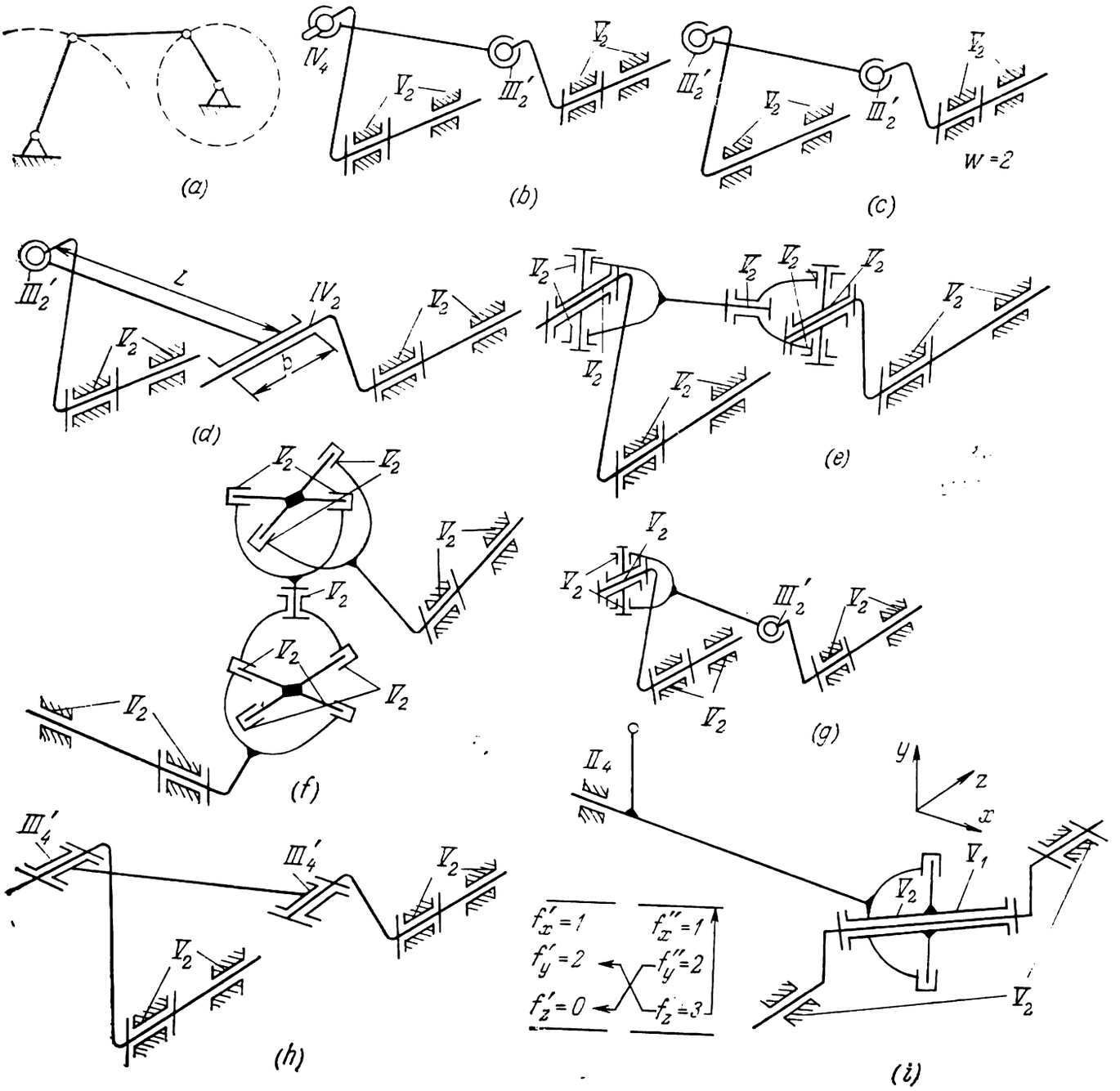


Fig. 2.38. Rational designs of crank-and-rocker mechanism

integral with the internal ear. The terms "hammer" and "anvil" used in the medical science are a gross misrepresentation of the mechanism. Should the mechanism actually have had gaps, with one member striking against the other, a human being would have heard nothing but rattling noise drowning away every other sound.

Particularly recommendable is the design of Fig. 2.38*c* incorporating spherical pairs in the form of spherical (self-aligning) antifriction bearings.

Quite naturally, both spherical pairs should be at the ends of the connecting-rod. With either one of them included between the crank and the fixed member, the local mobility would result in the crank with the connecting-rod "falling down", and the mechanism would be inoperable.

Another path toward a rational mechanism is the replacement of the spherical-with-pin pair $IV_3$ by a cylindrical one $IV_2$ (Fig. 2.38*d*). Self-alignment is attained here owing to the longitudinal sliding of the pair. This self-alignment is, however, opposed by friction. Therefore, the pair should be mounted on the crank and not on the rocker. A self-alignment check may be conducted with approximation by using the expressions drawn above for the slider-crank mechanism.

The third way to arrive at self-aligning mechanisms is using kinematic connections (see Table 1.4) instead of pairs $IV_3$ and $III_2'$ (cf. Fig. 2.38*e*). The pair $IV_3$ is replaced by a connection $IV_a$ including two rotational pairs $V_2$, and the pair $III_2'$ is replaced by a connection $III_a$ made up of three pairs $V_2$. This yields a mechanism of seven pairs (seven mobilities in the loop) and seven members (the fixed member included).

The mechanisms of Fig. 2.38*c* and *e* can also be used when the crank axes are perpendicular (Fig. 2.38*f*), which design is sometimes employed in regulators of steam turbines. However, the commonly used designs have no rotational pair on the connecting-rod axis, thus leaving a redundant constraints.

It is also possible to replace only the pair $IV_3$ by a kinematic connection, retaining the spherical pair $III_2'$. We have then a mechanism with four rotational pairs $V_2$ and a single spherical one $III_2'$ which also yield seven mobilities per loop (cf. Fig. 2.38*g*).

Finally, when the dimensions of the members are particularly great in comparison with those of the kinematic pairs (50 times greater or even more), the pairs on the pins of the crank and rocker, with the gaps taken into account, may be considered spherical ones $III_4'$, so that the design of Fig. 2.38*h* is likewise practical.

A peculiar four-pivot mechanism is used in mowers (Fig. 2.38*i*). The mechanism converts rotation of the main shaft into oscillation about an axis perpendicular to the shaft axis and intersecting the latter. This mechanism is well-suited to a mower where it actuates the cutting device. To avoid redundant constraints, one bearing should be a second-class pair (preferably, $II_4$), since the direction of this shaft practically does not vary. The mobilities in the loop are indicated in Fig. 2.38*i*. The angular mobility at the crank pin is related

here to $z$ axis, for the angle between them does not affect the closing of the loop.

## 2.9. Parallel Crank Mechanism

In the majority of mechanisms the mobility is the same in any position. A parallel crank mechanism, however, is an exception (cf. Fig. 2.39), being as it is a particular case of a crank-and-rocker mechanism where the mobility in the dead position increases by a unity. To avoid alignment of the lines, the connecting-rod $AB$ and fixed member $OC$ are conventionally shown in the drawing as U-shaped, whereas in reality they are straight.

Let us consider the mobilities of this mechanism in the dead position. Assuming that rotational pairs $V_2$ are set at points $O$ and $C$, and spherical pairs $III_2^1$ are set at points $A$ and $B$, then the linear mobilities along the three axes are equal zero, i.e. $f'_x = 0$, $f'_y = 0$ and $f'_z = 0$. Angular mobilities about $x$ and $y$ axes will be possessed only by the spherical pairs at points $A$ and $B$, i.e. $f''_x = 2$ and $f''_y = 2$, and all the four pairs will have angular mobilities about $z$ axis, i.e. $f''_z = 4$.

Let us now consider the distribution of the angular mobilities: $f''_x = 2$ are spent on closing the loop and a local mobility—rotation of the connecting-rod about its axis; $f''_y = 2$ will be used for closing the loop and for substitution of the linear mobility $f'_z$. This is possible owing to the presence of a member (the connecting-rod) directed along $x$ axis, i.e. along the third coordinate axis perpendicular to both $y$ and $z$; $f''_z = 4$ will close the loop, substitute the linear mobility $f'_y$ (owing to the connecting-rod extending along $x$ axis) and afford the two mobilities which are the mobilities of the mechanism.

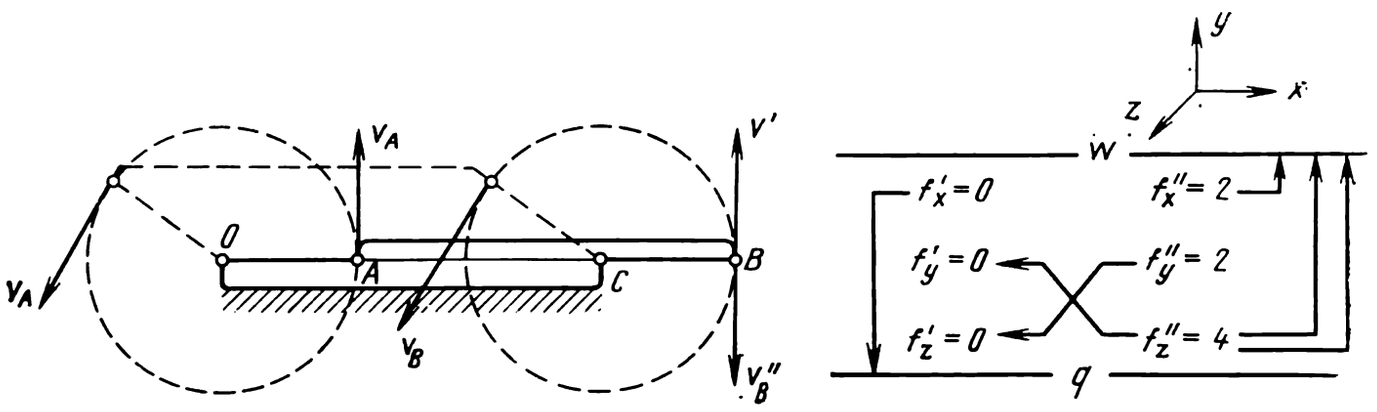


Fig. 2.39. Parallel crank mechanism in dead position (solid lines) and in arbitrary position (dash lines)

There is no linear mobility along $x$ axis ($f'_x = 0$), and it cannot be substituted by an angular mobility about $z$ axis, since no member is parallel with $y$ axis. Thus, we have one redundant constraint $q = 1$ and the total mobility $w = 3$.

In any position except the dead points (the members are shown with dash lines in Fig. 2.39) the mobility is composed of two elements: the main mobility and the rotation of the connecting-rod. With $V_A$ present, speed $V_B$ is quite determinate and equals $V_A$.

At the dead centre $V_B$ is no longer determined and it may either become equal to $V'_B$, so that the parallel crank mechanism is retained, or opposite to $V''_B$, making the mechanism an antiparallelogram. Thus, for the motion at the dead centre to be determinable, not only the velocity of point $A$ should be preset, but also the velocity of point $B$, then the mobility is increased by a unity. Characteristically, not only members $OA$ and $AB$ become aligned, but members $OC$ and $BC$ align simultaneously, i.e. the position is a double dead centre one.

The increasing mobility involves the appearance of redundant constraints, which follows from expression (1.5).

With the mobility $w_p$ increasing by a unity in a mechanism with no redundant constraints, we will have $q_p = 1$, as all the other components in the expression remain intact.

One can arrive at the same conclusion from formulas (1.1) or (1.2).

The redundant constraint in the parallel crank mechanism requires that the condition $OA + AB = OC + CB$ should be accurately observed.

If the transition is to be realized through both dead centres, then the second precondition will be the accuracy of $OC + OA = AB + CB$.

By addition, subtraction and conversion of the two equations we arrive at $OA = CB$ and $AB = OC$.

In locomotive transmissions where a twin parallel crank mechanism is used for transition through the dead centre, i.e. when the main rule of designing is devised, a redundant constraint will be present in any position of the mechanism. As a result, this mechanism, once widely employed in steam locomotives, is no longer incorporated in present-day locomotives. In single-motor electric locomotive bogies it has been replaced by a toothed gearing with an idler pinion.

The number of redundant constraints in the pin mechanism of the parallel crank type included in planetary-eccentric gearing for transmitting rotation from a satellite to the driven shaft is too high.

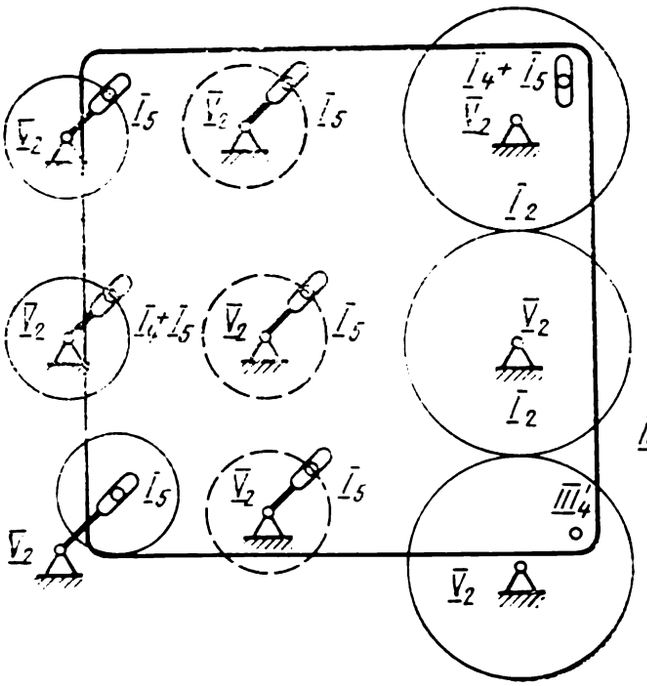

Fig. 2.40. Mechanism for multispindle head with idler pinion

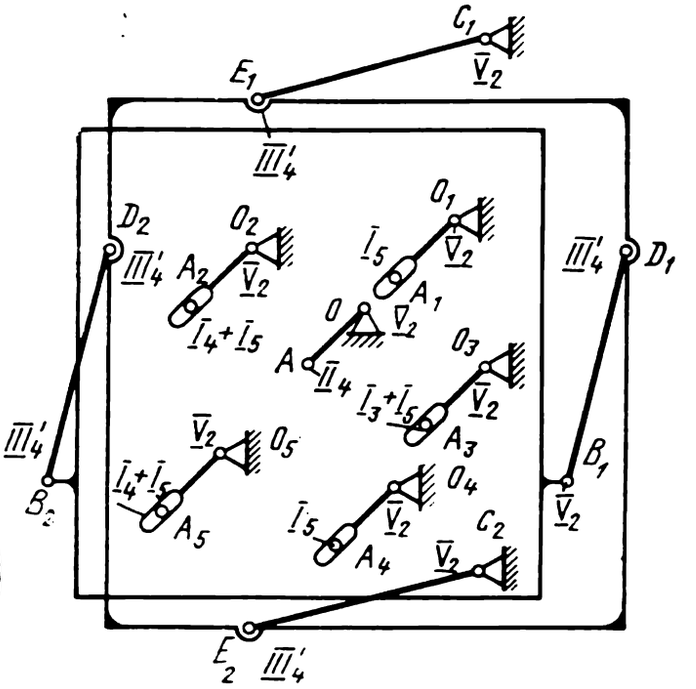

Fig. 2.41. Mechanism for multispindle head with parallelogram linkages

With the commonly used number of the pins (6-8) the number of the redundant constraints is 5 to 7, which is excessive and involves a high manufacturing accuracy. Moreover, as V. N. Kudryavtsev has pointed out, the location of the pin mechanism in the satellite presents difficulties in case of involute gearing, so that either pins of a very small diameter or large-diameter bores have to be used.

These drawbacks have been eliminated in the reducer with a double-slider rolling-contact coupling suggested and tested by Yu. A. Grin.

Application of the double crank mechanism in multispindle drilling heads has been likewise inhibited by the enormous amount of redundant constraints (one constraint for each spindle). Instead, mechanisms with numerous idler pinions are used, although a double crank mechanism could significantly simplify the construction.

The redundant constraint can be eliminated by replacing the sleeve (Fig. 2.40) in one of the pivots of the crank by a groove. In the dead positions this would preclude the redundant constraint, and in the rest of the positions the mobility would increase by a unity, with the variable mobility eliminated, but with an excessive mobility—eventual rotation of the connecting-rod in the plane of the mechanism—appearing. This one can be eliminated by introducing additional restraints. In the design shown in Fig. 2.40 the toothed gearing with an idler pinion is used for the purpose, and the design of

Fig. 2.41 incorporates a mechanism made of parallelograms $C_1E_1E_2C_2$ and $B_1D_1D_2B_2$ which is generally employed in T-squares of drawing boards. Other parallel motion mechanisms can also be used, e.g. the Oldham coupling.

In the mechanism of Fig. 2.41 all the axles can be associated with drilling spindles, and in the mechanism shown in Fig. 2.40 the same applies to every axle except that of the idler pinion, as the latter rotates in opposition to the rotation of the rest of the heads.

The mechanism illustrated in Fig. 2.40 is more simple as it has only one idler pinion while the mechanisms built about toothed wheels have several of them. Besides, the mechanism constructed in accordance with Fig. 2.40 enables one to easily vary the spacing of the centres of the bores, which is impossible with a mechanism with toothed wheels.

When designing a mechanism in accordance with Fig. 2.40, one should remember that the connecting-rod (the plate) must be secured at three points. Thus, three pins ($III_4'$, $I_4 + I_5$ and $I_4 + I_5$) should have shoulders, and the rest of the pins should have no shoulders to avoid redundant constraints.

Similarly, the connecting-rod (the plate) shown in Fig. 2.41 must be retained at three points in the direction perpendicular to the plane of the drawing. Therefore, pins $A_2$, $A_3$ and $A_5$ should have shoulders, and the rest of the pins should be shoulder-free. To enhance the retaining accuracy, the shoulders are preferably provided on the most remote pins (cf. Fig. 2.41). Similarly, the frame $E_1D_1E_2D_2$ should be retained at the three broadly remote points $E_1$, $D_1$ and $E_2$ in the direction perpendicular to the plane of the drawing. This is attained by having the pivots $C_1$, $B_1$ and $C_2$ in the form of rotational pairs $V_2$. The rest of the pivots ($B_2$, $D_2$, $E_1$, $E_2$ and $D_1$) should be spherical pairs $III_4'$. Member $B_2D_2$ thus has a local mobility—rotation about its axis. Therefore, the total mobility of the mechanism $w = 2$.

It is possible to have another pattern of the kinematic pairs of the mechanism illustrated in Fig. 2.41. Thus, if the plate and the frame are associated with planar guideways ($III_2''$ pairs), all the pins should be shoulder-free, and all the drivers should have spherical pairs $III_4'$.

Another way of elimination of redundant constraints is illustrated in Fig. 2.42. To avoid redundant constraints, the connecting-rod is a split one, with the two parts connected by a cylindrical pair $IV_2$. The extremities of the connecting-rod are connected to its ends by pivots $V_2$. The pairs may be of the simplest kind, as the relative

motion there is negligible. Thus, the pair $V_2$ may be in the form of a roller, with the pair taking place of the several bolts used for connecting the parts in a statically indeterminate mechanism. Thus, the elimination of redundant constraints in the mechanism of Fig. 2.42 should not raise its cost. The excessive mobility is avoided by con-

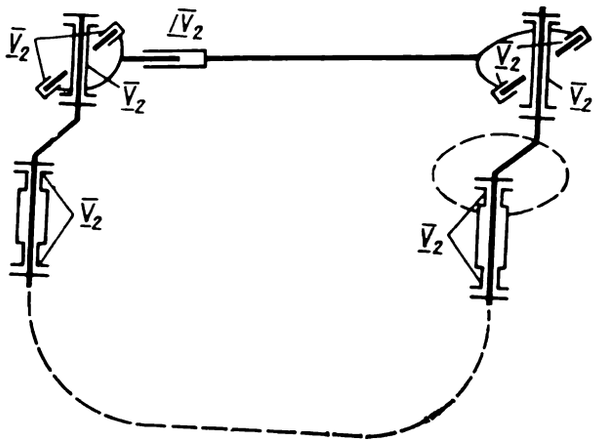


Fig. 2.42. Parallel crank mechanism with independently driven cranks

necting the two cranks through worm gearing and an intermediate shaft from which both cranks are rotated (conventionally shown with dash lines).

To check the absence of redundant constraints by formula (1.1), these gearings are not taken into account, assuming that the cranks are driven independently, i.e. assuming $w = 2$. Unfortunately, this technique of avoiding constraints cannot be used when the parallel crank mechanism is expected to transmit a driving torque (e.g. the twin crank mechanism of a locomotive).

## 2.10. Link Gear Mechanisms

Depending on the motion of the member carrying the slide block pin and the motion of the link, planar link gear mechanisms may be divided into three types:

crank-and-link mechanisms with either revolving or oscillating link—both members are rotating (cf. Fig. 2.43);

sine-link mechanisms—the pin is on the rotating member, and the link moves rectilinearly (Fig. 2.44, *a* — *c*);

tangent-link mechanism—the pin is on the rectilinearly moving member, and the link rotates (Fig. 2.44, *d*—*g*).

Let us consider the crank-and-link mechanism with the revolving (or oscillating) link. The planar diagram of this mechanism is shown in Fig. 2.43*a*. If the crank radius exceeds the distance between the centres ($OA > O_1O_2$) the link will be driven through full revolutions

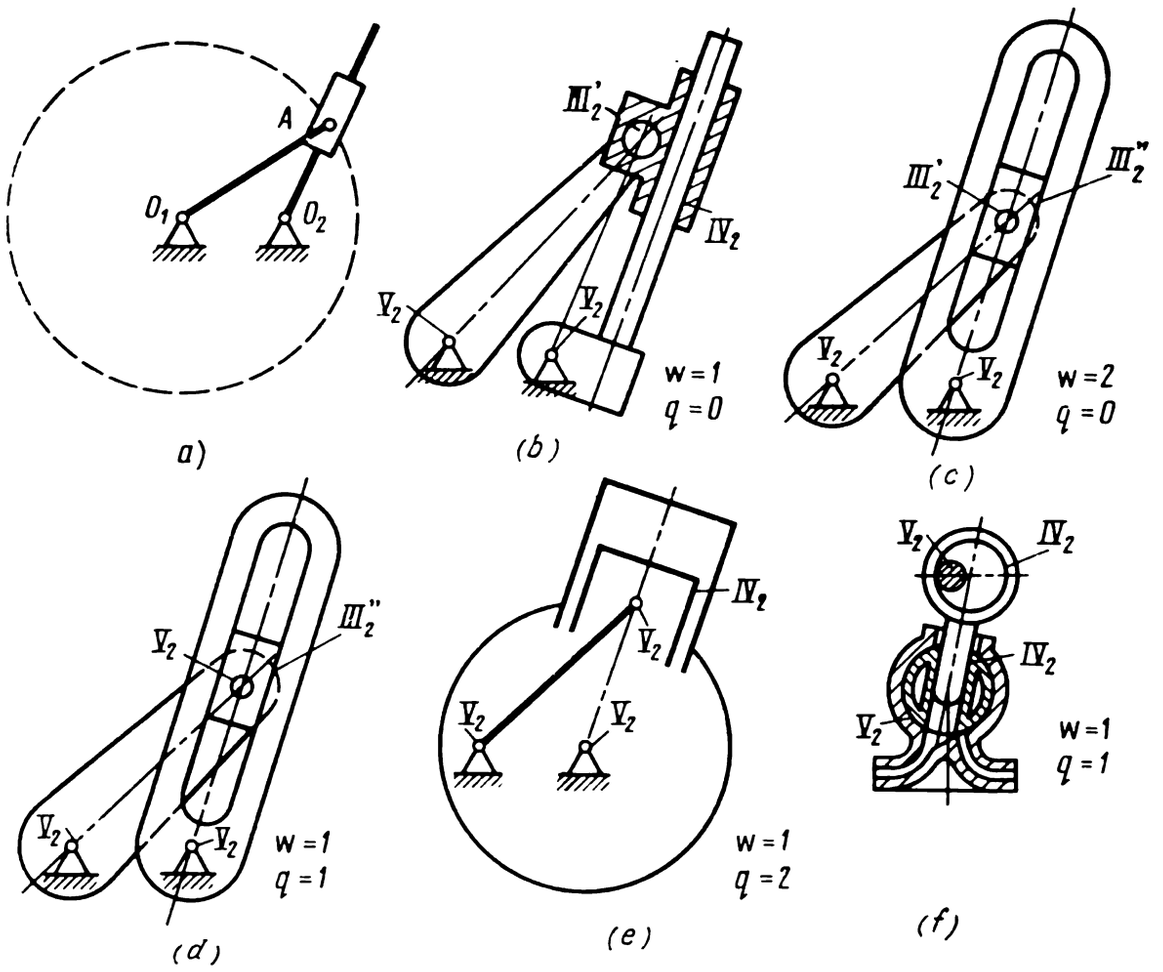


Fig. 2.43. Designs of mechanisms with either revolving or oscillating link

(it revolves), and if $OA < O_1O_2$, it will be driven through a part of a revolution (it oscillates).

Redundant constraints are the same in both cases, and thus we shall consider them concurrently. When checked against expressions (1.5) or (1.6), the planar diagram reveals no redundant constraints.

When real-life mechanisms devoid of redundant constraints are considered, the relationships drawn above for a slider-crank mechanism remain valid, as they have been defined for the same number of the members and kinematic pairs, i.e. $5p_V + 4p_{IV} + 3p_{III} = 17$; $p_V + p_{IV} + p_{III} = 4$. Added to these relationships is the condition $p_V \geqslant 2$ arising from the necessity of retaining axially the driving and driven shafts. The conditions are met with $p_V = 2$, $p_{IV} = 1$ and $p_{III} = 1$ (Fig. 2.43*b*).

This design of the mechanism is attractive both in manufacture and in operation, however, it uses an offset slide block (the centre of the spherical pin on the crank does not lie on the axis of the cylind-

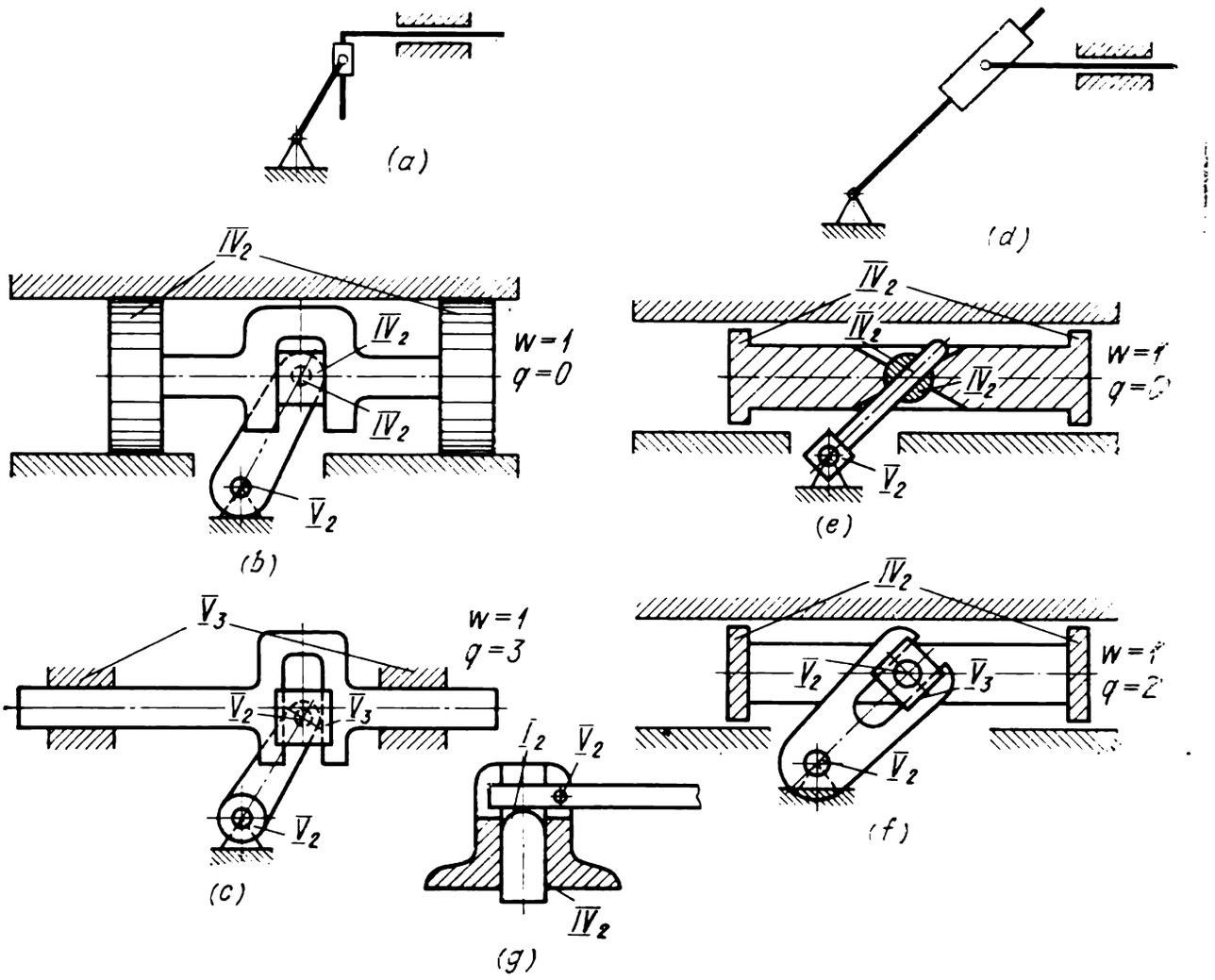


Fig. 2.44. Designs of link-gear mechanisms (*a*)-(*c*) sine-link; (*d*)-(*g*) tangent-link

rical pair of the link). The actual design should be aimed at minimizing this offset.

A simple structure with no redundant constraints is obtained with $p_V = 2$, $p_{III} = 2$ and $w = 2$ (Fig. 2.43*c*). This is the case of a single local mobility—rotation of the slide block about the spherical pin. It is practically harmless, for the angle of rotation is limited by the corresponding abutments.

A design with a single redundant constraint is used in machine-tools (Fig. 2.43*d*). In this structure $p_V = 3$, $p_{III} = 1$ and $w = 1$. From (1.1), $q = 1$. This redundant constraint requires strict parallelism of the axes of the rotational pairs with the planar pair (the engagement plane of the link and slide block) in any position of the mechanism.

A mechanism with a revolving link was employed in star-shaped (radial) aircraft engines with rotating cylinders (Fig. 2.43*e*). In this structure $p_V = 3$ and $p_{IV} = 1$. From (1.1) $q = 2$. The redundant constraints can be eliminated by having spherical ends of the connecting-rod. This, however, would bring about two local mobilities—rotation of the piston and rotation of the connecting-rod about their axes.

An oscillating-link mechanism is used in oil pumps with an oscillating cylinder (Fig. 2.43*f*). In this mechanism $p_V = 2$ and $p_{IV} = 2$. Formula (1.1) yields $q = 1$. This redundant constraint calls for strict parallelism of the axes of the shaft, the cylinder oscillation axis and of the eccentric axis in any position of the mechanism.

A sine-link mechanism (the one with an infinite-length connecting-rod) produces the maximum torque by the crank at the middle of the stroke and the minimum torque at the ends of the stroke, if the effort applied to the slider is constant. This torque curve is beneficial for electric apparatus, as it precludes the jamming of the apparatus in intermediate positions. The planar diagram of this mechanism (Fig. 2.44*a*) reveals no redundant constraints when checked against formulas (1.5) or (1.6). The design includes two prismatic pairs and two rotational ones. It may also use three cylindrical pairs with mutually perpendicular axes, when $p_V = 1$ and $p_{IV} = 3$. This will yield neither local mobilities (present with the parallel axes), nor redundant constraint. The design is illustrated in Fig. 2.44*b*.

A wrong, although popular, design with exclusively fifth-class pairs is shown in Fig. 2.44*c*. The design imposes three redundant constraints, leaving very narrow tolerance for a number of dimensions. Designs can be met, in which one or two pairs are of the cylindrical type, with the number of the redundant constraints being respectively lower. However, to eliminate the redundant constraints completely, three cylindrical pairs should be used, as shown in Fig. 2.44*b*.

A tangent-link mechanism, with a permanent efforts applied to the slider, produces the maximum torque at the link (the shaft) at the ends of the stroke, and the minimum torque at the middle. This torque curve is well-suited for a ship steering engine, as it approximates the curve of torques required at the rudder shaft. The planar diagram of this mechanism (Fig. 2.44*d*) reveals no redundant constraints determined from (1.5). The mechanism may have three cylindrical pairs with non-parallel axes ($p_V = 1$, $p_{IV} = 3$, $w = 1$, $q = 0$). The design (Fig. 2.44*e*) suggested by A. N. Ivanov is used nowadays in the actuators of the reverse controls, brake switches and voltage switches of electric motor cars.

An example of the wrong design (Fig. 2.44*f*) has one cylindrical pair (the slider—guideways), the rest of the pairs being fifth-class ones. From formula (1.1) the design imposes two redundant constraints, requiring strict perpendicularity of the axes of the cylinder and of the shaft, and the accuracy of positioning the cylinder along the shaft axis.

There are also designs where two cylindrical pairs and two fifth-class ones are used. They have one redundant constraint necessitating strict perpendicularity of the cylinder axis and the shaft.

In sanitary devices, there is a tangent-link mechanism (the float-controlled valve of the flush tank) illustrated in 2.44*g*. In the mechanism $p_V = 1$, $p_{IV} = 1$ and $p_I = 1$—redundant constraints are non-existent. A shortcoming of this mechanism is the first-class pair with the spot contact, whose low load capacity renders the mechanism unsuitable for considerable loads. Owing to the extended sliding and a high friction coefficient (operation in water), the mechanism performs very poorly in the flush tanks. It is possible, however, to select the dimensions so that with the valve closed there would be no sliding of the arm against the actuator. This, however, would involve undoing the rivet of the arm pivot.

A more simple approach is to select the length of the valve so that in the closed position the arm would be inclined by the angle of friction. Then the valve guides would be relieved, and jamming would be prevented (tested by the author).

Let us compare a sine-link mechanism (Fig. 2.44*b*) with a tangent-link one (Fig. 2.44*e*). They differ solely in the direction of the axis of the cylindrical pair connecting the slide block with the shaft. In case of a sine-link mechanism this axis is parallel with the shaft, i.e. it defines with the shaft axis an angle equalling 0°, and in a tangent-link mechanism the angle is 90°. Any intermediate pattern is possible between the two extreme positions (proved by modelling), to attain a characteristic intermediate between the sine- and tangent-link mechanisms. If the angle is made adjustable, the characteristic could be adjustable, accordingly.

The sole drawback of such a mechanism is that it is a three-dimensional one, and the theory governing it is far more complicated than the theory of a planar mechanism.

A mechanism with an intermediate characteristic has been explored by A. A. Kasamanyan. When $a$ is the spacing of the shaft and slider axes, $\alpha$ is the angle defined by the shaft and the axis of the cylindrical pair connecting the slide block and the shaft, $\delta$ is the

angle of rotation of the shaft, and $\beta$ is the corresponding angle of rotation of the slider (the forced one), we may write down $\beta = \alpha - \text{arctg}\ (\text{tg}\ \alpha \cos \delta)$.

The displacement of the slider from the central position: $x = a \times \sin^2 (\alpha - \beta)\ \text{tg}\ \delta + a \cos^2 (\alpha - \beta) \sin \delta$.

With $\alpha = 0$ and $\beta = 0$, $x = a \sin \delta$—the mechanism becomes a sine-link one.

With $\alpha = 90°$ and $\beta = 0$, $x = a\ \text{tg}\ \delta$—the mechanism becomes a tangent-link one.

## 2.11. Degeneration of Assur's Groups

The theory elaborated by L. V. Assur is used for designing complex linkages. According to this theory, a mechanism or linkage is made up of zeromobility groups, i.e. of groups which, when connected to a fixed member, yield a zero mobility and reveal no redundant constraints in a planar diagram ($q_p = 0$).

It is not always so, however. With certain arrangement of the arms, a group may attain a mobility and, hence, a redundant constraint. This violates the main precondition—the zero mobility, and the group degenerates. If such cases are not provided for, we might arrive at mechanisms with harmful mobilities and redundant constraints. Let us consider such cases.

**Two-arm group.** In the dead-centre position, there appear a mobility and a corresponding redundant constraint. This situation can take place in a parallel crank mechanism which has been discussed in detail in Section 2.9 (see Fig. 2.39).

**Three-arm group.** The three arms intersect in a single point (Fig. 2.45*a*). This point $P$ is the centre of instant rotation of the member. As the third arm extends through this point, it will not eliminate the mobility, but will yield a redundant constraint instead.

**Three-arm group with the three arms parallel** (Fig. 2.45, *b*). With three arms having the same length and extending in the same direction, even finite displacement is possible. The group is reduced then to a parallel crank mechanism with three cranks. In this design all the three pivots of the basic member move with same velocities having the same direction (perpendicular to the arms), i.e. the motion is translatory. Therefore, the third arm cannot oppose this motion, so it imposes a redundant constraint.

**Three-arm group with two arms extending along a single straight line** (Fig. 2.45*c*). The point of intersection of this line with the third

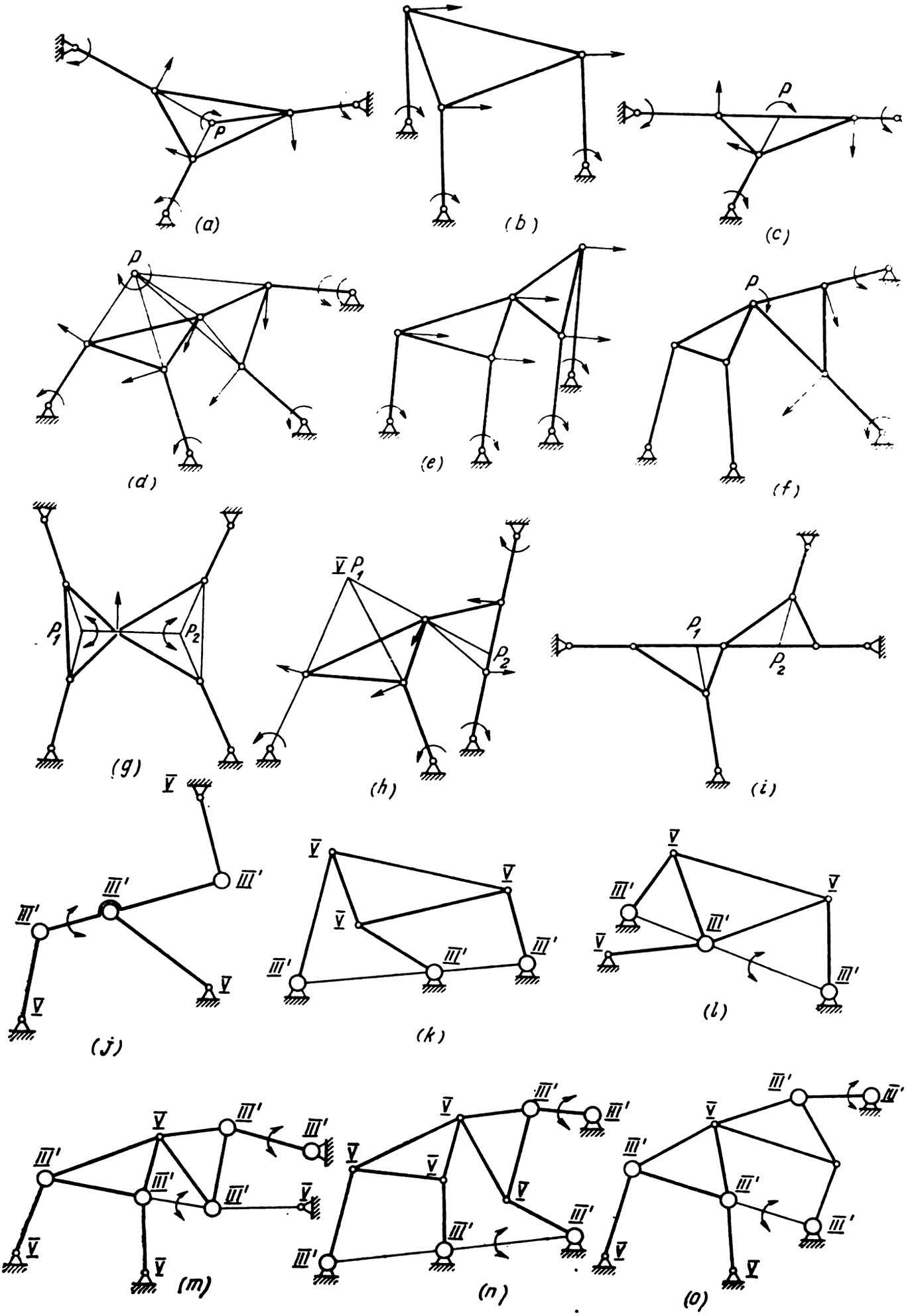
P
(a)
(b)
P
(c)
P
(d)
(e)
P
(f)
P1
P2
(g)
V P1
P2
(h)
P1
P2
(i)
V
III'
III'
III'
V
V
(j)
V
V
V
V
III'
III'
(k)
V
III'
V
III'
III'
III'
(l)
V
III'
III'
III'
III'
V
V
V
(m)
V
III'
III'
V
V
III'
III'
III'
(n)
III'
III'
V
V
III'
III'
III'
(o)

arm (or its extension) will be the centre of instant rotation, with the corresponding mobility.

This may be checked for three-arm groups by using structural formula (1.5) for the planar diagram:

$$q_p = 1 - 3 \times 4 + 2 \times 6 = 1.$$

**Four-arm group with the four arms intersecting in one point** (Fig. 2.45*d*). The point will be the centre of instant rotation for the block of the two basic members.

**Four-arm group with the four arms parallel** (Fig. 2.45*e*). In this case the block of the two basic members is movable in a translatory manner in a direction perpendicular to the arms.

**Four-arm group with two arms of one basic member intersecting at the centre of the pivot connecting the basic members** (Fig. 2.45*f*). This point of intersection of the two arms will be the centre of instant rotation of their basic member, with the pivot between the basic members not opposing this rotation, but imposing a redundant constraint.

**Four-arm group with points $P_1$ and $P_2$ of intersection of the arms of each basic member belonging to the same line with the pivot interconnecting the basic members** (Fig. 2.45*g*). In this case the basic members are rotatable about their centres of instant rotation $P_1$ and $P_2$. The pivot connecting the basic members will move in a direction perpendicular to the line $P_1P_2$ without opposing this motion, but imposing merely a redundant constraint.

With a four-arm group, should two arms extend along a single straight line, degeneration would occur if the arms are connected to one and the same basic member (Fig. 2.45*h*), with their centres of instant rotation $P_1$ and $P_2$ belonging to the straight line including the pivot connecting the basic members (similar to the diagram of Fig. 2.45*g*). On the other hand, should the arms extending along a single line belong to different basic members (Fig. 2.45*i*), degeneration would occur under one additional condition—the line should include the pivot connecting the basic members.

For four-arm groups, the results obtained may be checked using structural formula (1.5).

Fig. 2.45. Degeneration of Assurs's groups—advent of mobility and redundant constraint

(*a*), (*b*), (*c*) three-arm in planar diagram; (*d*), (*e*), (*f*), (*g*), (*h*), (*i*) four-arm in planar diagram; (*j*), (*k*), (*l*) three-arm in three-dimensional diagram; (*m*), (*n*), (*o*) four-arm in three-dimensional diagram

For mechanisms of Fig. 2.45 *d*, *e*, *f*: $q_p = 1 - 3 \times 6 + 2 \times 9 = 1$. Likewise, from formula (1.6) for the diagrams of Fig. 2.45, *a* and *b*: $q_p = 1 + 3 \times 2 - 1 \times 6 = 1$; and for those of Fig. 2.45, *d e*, *f*: $q_p = 1 + 3 \times 3 - 1 \times 9 = 1$.

Formula (1.1) may be also used for the checking.

It is worth pointing out that the number of the loops for a two-arm group is one; for a three-arm group—two; and for a four-arm group—three; i.e. **the number of the loops equals the number of the arms minus one.**

The redundant constraints in the planar diagram (Fig. 2.45*a-i*) bring about additional longitudinal stresses (extension or compression) of the arms, bending stresses of the basic members (of the levers) and linear stresses of the rotational pairs. The rotational pairs have no angular stresses about axes belonging to the plane of the mechanism on account of $q_p$, since these torques are not considered for a planar diagram.

A planar diagram fails to give an exhaustive answer to the problem of the structure of the mechanism, as this diagram leaves some mobilities and redundant constraints unexplored. A full answer can be given by A.P. Malyshev's and Ozol's three-dimensional structural formulas.

The arms can be associated with third-, fourth- and fifth-class pairs. Depending on their combinations, a zero-mobility group with one basic member may be two-, three-, four-, five- or six-arm one. Let us discuss out of them only the three-arm version as the simplest and most commonly used. In it, to avoid redundant constraints, each arm should carry one rotational pair *V* and one spherical pair *III'*. Their preferable arrangement can be determined by the force analysis. It should be remembered that if two spherical pairs *III'* are mounted on a single arm, the latter would attain a local mobility—rotation about its axis, and, correspondingly (cf. the structural formula) one redundant constraint would be imposed.

Let us consider a more hazardous situation where three spherical pairs belong to a single line. If the spherical pairs are mounted on the basic member (Fig. 2.45*j*), the latter is reduced to a straight line, and there occurs a local mobility (although harmless)—rotation about the axis of the member, and, naturally, a redundant constraint is incurred. This may be the case with the Evans straight-motion linkage design. It is worse when the three spherical pairs are on the fixed member and belong to the same line (Fig. 2.45*k*). The basic member would then collapse about this line, jointly with the arms, i.e. a harmful local mobility takes place.

The same is true of the spherical pairs carried both by the basic member and the fixed one, should they belong to the same line (Fig. 2.45*l*). Here, the basic member with two arms would collapse about this line, i.e. the occurring local mobility is a harmful one. Thus, with a three-arm group the three spherical pairs *III'* should not belong to a single line. A similar condition can be drawn for a four-arm group.

From Malyshev's formula: with $n = 6$ and $q = 0$, assuming the presence of fifth- and third-class pairs only owing to their better design characteristics, we obtain $0 = w - 6 \times 6 + 5p_{\text{V}} + 3p_{\text{III}}$, and $5p_{\text{V}} + 3p_{\text{III}} = 36 - w$, but $p_{\text{V}} + p_{\text{III}} = 9$.

The equations are satisfied with $w = 1$, $p_{\text{V}} = 4$ and $p_{\text{III}} = 5$ (Fig. 2.45*m*). The basic members have to be connected here by a $V_2$ rotational pair; three arms have to carry pairs *V*, *III'*—they will guide the basic members in the given plane; the fourth arm (the supporting one) should carry two spherical pairs *III'*, *III'*. It will have one local (harmless) mobility—rotation about its axis.

In case of a four-arm group with such pairs, in addition to the situations illustrated as planar diagrams in Fig. 2.45,*d*, *e*, *f*, *g*, *h*, *i*, there is yet another situation where a local mobility and a redundant constraint are brought about (Fig. 2.45*m*): three spherical pairs of the guide arms align along a single line, irrespectively whether these arms are at the side of the basic members (Fig. 2.45*m*), on the fixed member side (Fig. 2.45*n*), or at both sides (Fig. 2.45*o*). The basic members will collapse either alone or together with the arms. This is not affected by the arrangement of the spherical pairs of the supporting arm, since it is not the guide one. The redundant constraints imposed by the alignment of the three spherical pairs along a straight line will cause additional transverse (bending) stresses in the arms and complex loading of the basic members. The spherical pairs then become additionally loaded by forces perpendicular to the plane of the mechanism, and the rotational pairs—by torques about axes perpendicular to the arms and belonging to the plane of the mechanism.

The harmful mobilities and redundant constraints of the mechanisms of Fig. 2.45,*j*—*o* may be superimposed upon those of the designs of Fig. 2.45,*a*—*i*, which would impair the performance of the mechanisms still further.

## 2.12. Structural Groups of Zero Mobility

At present, Assur's theory presents the following zero-mobility groups: the two-arm one without the basic member, the three-arm one with a single basic member and a four-arm one with two basic members.

We are going to show that these are but specific cases of zero-mobility groups, and that in general the number of the arms may be from two to seven. Here and in the narration to follow only statically determinate groups are being dealt with.

The point is that the amount of the restraints imposed by each arm depends on the classes of its kinematic pairs. Thus, the arms may be single-, double, triple- and quadruple-restraining. To determine the number of these restraints, one may assume that when the kinematic pairs are serially connected, their mobilities add up, as

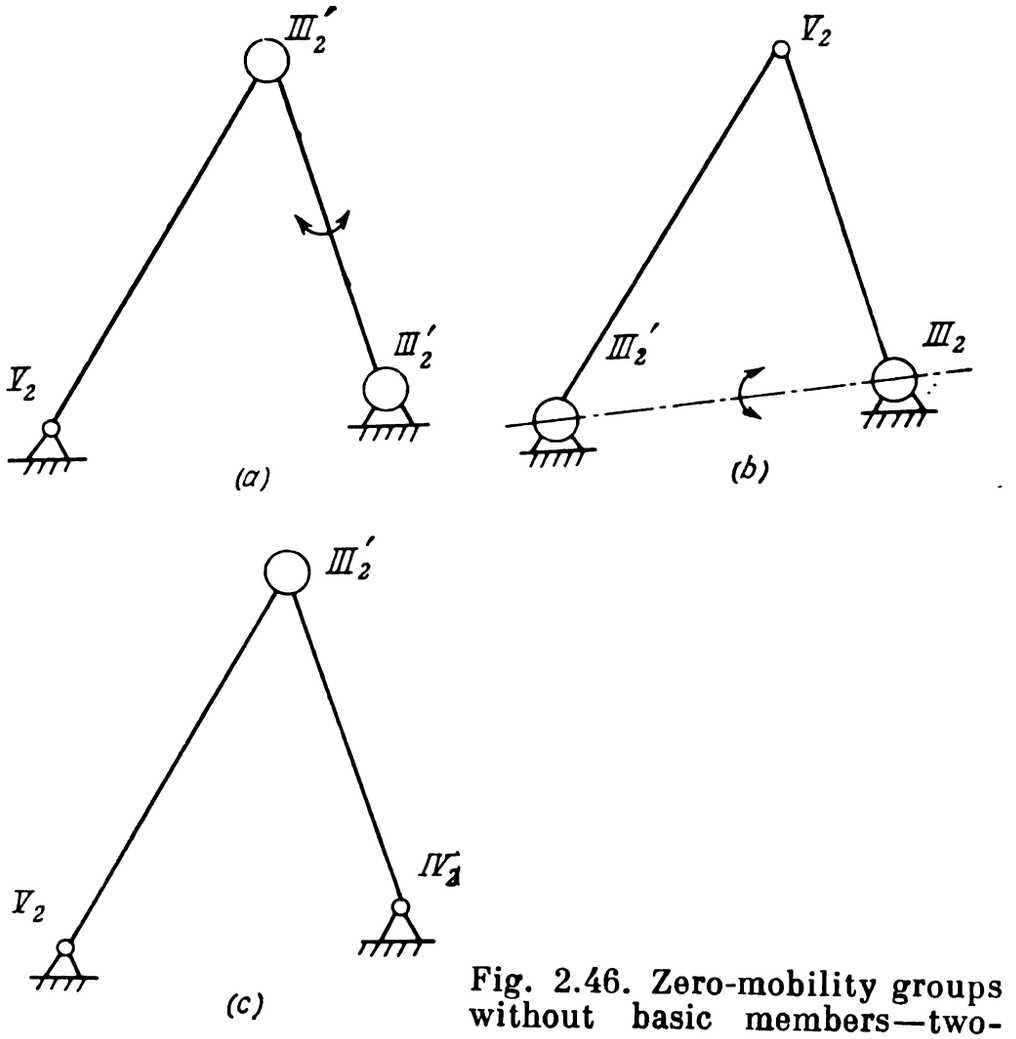


Fig. 2.46. Zero-mobility groups without basic members—two-arm ones

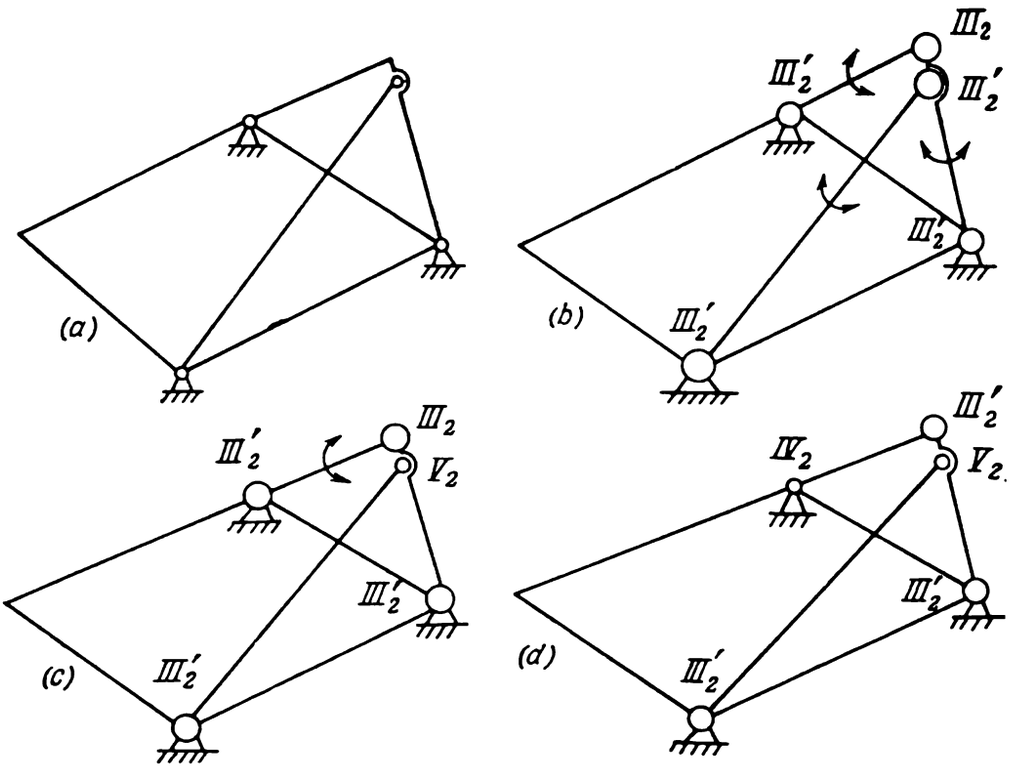


Fig. 2.47. Zero-mobility groups without basic members—three-arm ones

suggested by N.E. Shamaidenko, or else that only those restraints are retained, which are incurred by all the serially connected kinematic pairs, as suggested by E.Y. Budyka.

A single-restraining arm is one with pairs either *III'* and *III'*, or else *III'* and *IV*, the first-mentioned case leaving one local mobility—rotation of the arm about its axis. A double-restraining arm is one with pairs *III'* and *V*, or *IV* and *IV*. A triple-restraining one is with pairs *IV* and *V*, and a quadruple-restraining arm is one with pairs *V* and *V*. Let us consider groups without basic members. In planar mechanisms, these will be solely two-arm groups. To attain self-alignment, such a group should have one fifth-group pair $V_2$ and two spherical pairs $III'_2$ (Fig. 2.46*a*). It will have one local mobility—rotation of the arm $III'_2III'_2$ about its axis, which is usually harmless. Pairs $III'_2III'_2$ must be avoided on the fixed member (Fig. 2.46*b*), lest the groups might collapse—the mobility being harmful. This diagram may be used solely when this harmful mobility is eliminated by other kinematic pairs.

It is possible to use one rotational pair $V_2$, one cylindrical pair $IV_2$ and one spherical pair $III'_2$ (Fig. 2.46*c*). The relative arrangement of the pairs is of no importance. It should be ascertained, however, that friction in pair $IV_2$ would not inhibit self-alignment (the axial

mobility). In most cases this amounts to the advisability of using the pair $IV_2$ solely where it is driven through a full revolution.

In three-dimensional mechanisms a zero-mobility group without basic members may be a two-arm one, as shown in Fig. 2.46, or a three-arm one (Fig. 2.47*a*). To ensure self-alignment, the latter may have spherical pairs $III'_2$ exclusively (Fig. 2.47*b*), although it will

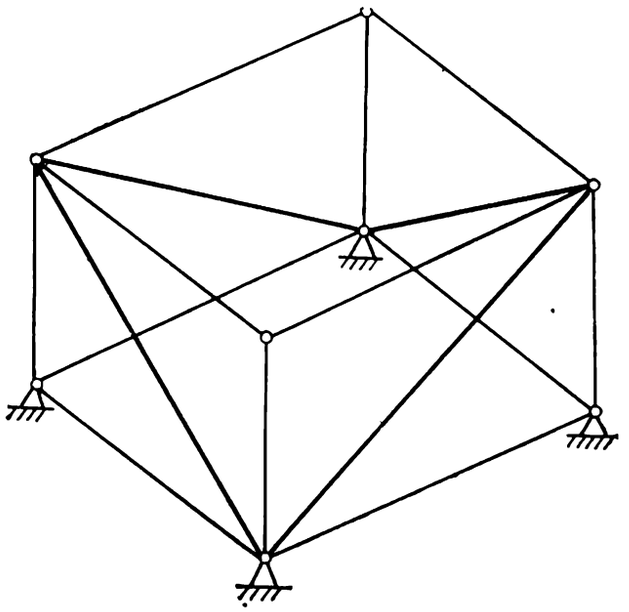

Fig. 2.48. Framework of building free of redundant constraints, made up of zero-mobility groups

possess then three harmless local mobilities—rotation of the three arms about their axes. Two local mobilities can be removed by connecting the arms with a pair $V_2$ instead of the pair $III'_2$ (Fig. 2.47*c*).

The last remaining local mobility can be removed by using a cylindrical pair $IV_2$ instead of pair $III'_2$ (Fig. 2.47*d*). Obviously, it should be checked whether friction could not impair self-alignment. Three-arm three-dimensional groups are well suited, among other applications, for railway current collectors (Figs. 3.42 and 3.43*a*).

Let us discuss an example of designing the framework of a building (Fig. 2.48).

**Selection of the number and arrangement of braces.** Let us consider a framework of two three-arm groups (shown with bold lines) and add to it two more three-arm groups (hair lines).

**Groups with a single basic member.** To ensure zero-mobility, the arms should so define the mobility of the connection of the basic member with the fixed one that 6 restraints will be incurred. The following cases are possible:

(a) $6 = 4 + 2$
(b) $6 = 4 + 1 + 1$
(c) $6 = 3 + 3$

(d) $6 = 3 + 2 + 1$
(e) $6 = 3 + 1 + 1 + 1$
(f) $6 = 2 + 2 + 2$
(g) $6 = 2 + 2 + 1 + 1$
(h) $6 = 2 + 1 + 1 + 1 + 1$
(i) $6 = 1 + 1 + 1 + 1 + 1 + 1$

Cases (a) and (c) are two-arm ones. Unfortunately, we are not sure that the case (c) is practical, so that case (a) alone remains. Cases

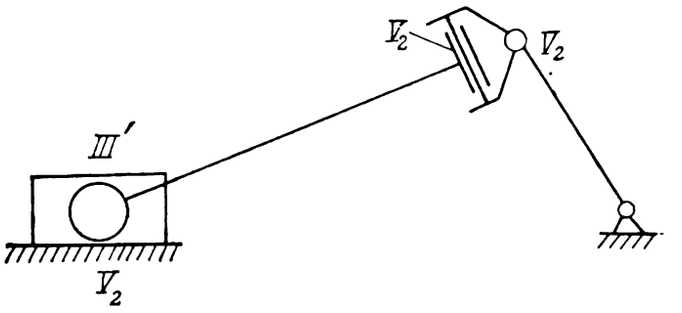


Fig. 2.49. Two-arm group with one basic member—in self-aligning slider-crank mechanism

(b), (d) and (f) are the known three-arm groups; cases (e) and (g) are four-arm groups, case (h) is a five-arm group, and case (i) is a six-arm one.

The above cases are employed in engineering practice. Let us prove it for (a), (f), (g), (h) and (i).

Case (a) is illustrated in Fig. 2.49. Here and in the following illustrations the multiarm group is shown with bold lines, while the rest of the members of the mechanism and auxiliary structures are shown with hair lines. Case (a) has been already suggested in Fig. 2.29*f* for eliminating redundant constraints in a slider-crank mechanism, with the connecting-rod connected to the crank by a $V_2V_2$ arm, and to the fixed member by a $III'V_3$ arm. Although we cannot trace here the kinematics of Assur's theory, the zero mobility and static determinacy are ensured.

Case (f) illustrated in Fig. 2.50. It is widely known and needs no further explanation.

Let us take case (g) as an example of a four-arm group, commonly known as Stephenson double-eccentric link gear, Fig. 2.51. There are two double-restraining arms—the forward-run eccentric rod (the bottom one) $III'_2V_2$ and the suspended rod $III'_4V_2$, and two single-restraining arms—the reverse-run eccentric rod (the top one) $III'_2III'_2$ and the slide block with the slide valve and pairs $V_2III'_4IV_2$. The latter, although having three kinematic pairs, imposes only one restraint, i.e. it is a single-restraining arm. All the four arms are required to retain the groove member of the link. Thus, if the slide

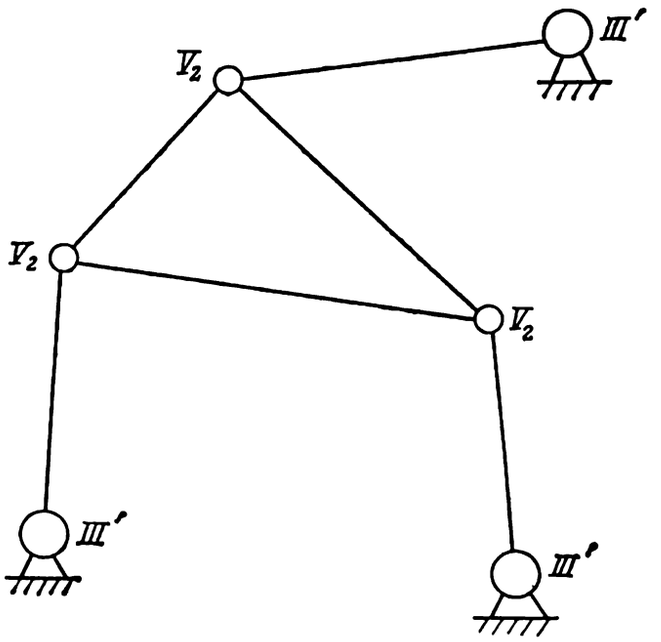


Fig. 2.50. Three-arm group with one basic member—self-aligning

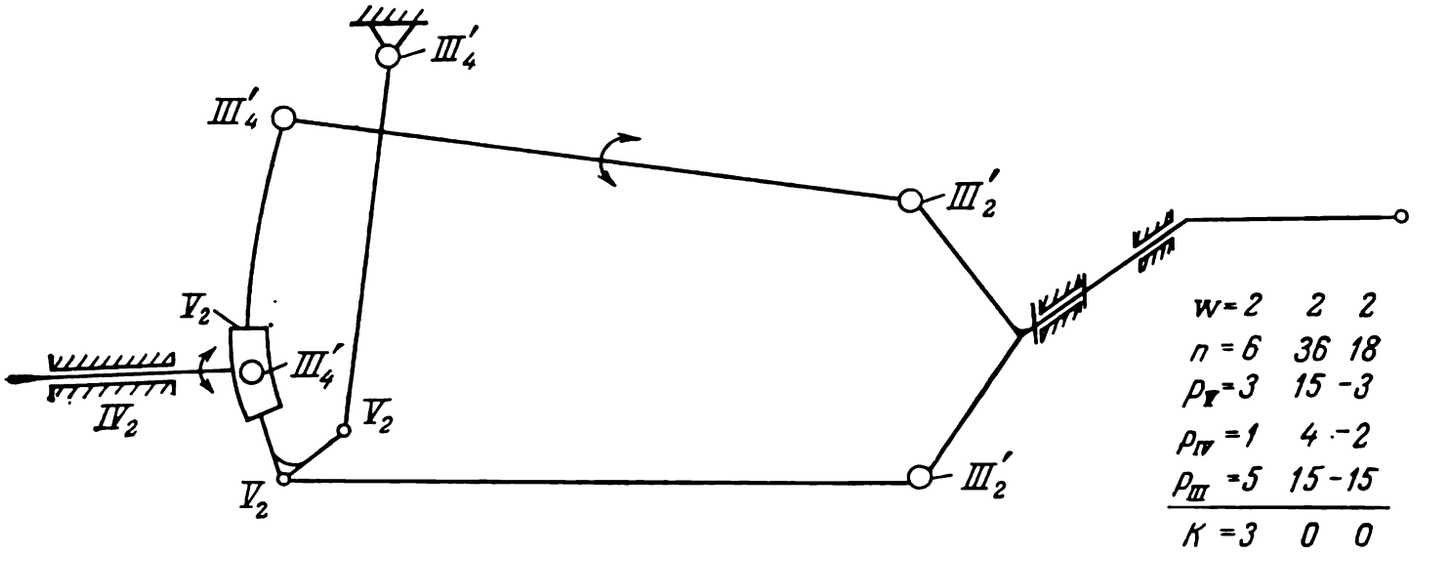


Fig. 2.51. Four-arm group with one basic member—in Stephenson link gear

block with the slide valve are removed, the groove member will collapse about the rotation axis. As an example of a five-arm group (h), let us recall the triple-eccentric Stephenson link gear illustrated in Fig. 2.52. Linkages of this kind had been used in large marine steam engines. There is one double-restraining arm $III'_4V_2$ and four single-restraining ones: three eccentric rods $III'_2III'_4$ and the slide

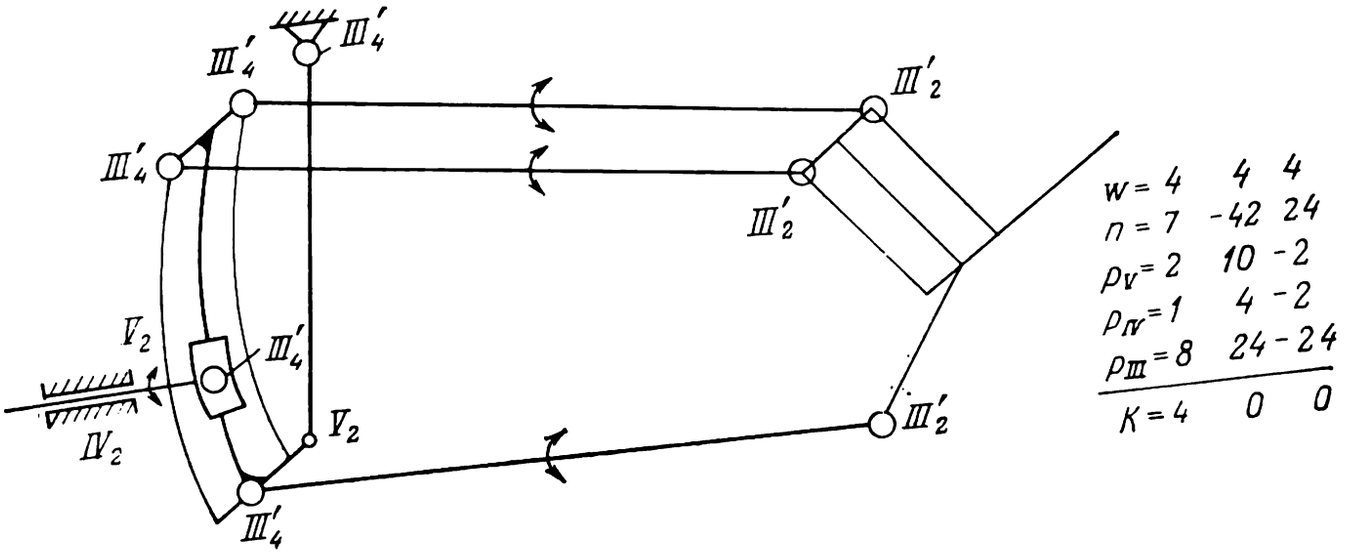


Fig. 2.52. Five-arm group with one basic member—in triple-eccentric Stephenson link gear (formerly used in large marine steam engines)

block with the slide valve and pairs $V_2III'_4IV_2$. For an example of case (i)—a five-arm group—let us consider top frames of a statically determinate current collector, Fig. 2.53. There are six single-restraining arms $III'_4III'_4$ including four longitudinal ones and two diagonal ones, supporting the base of the top carriage $III'_4III'_4$.

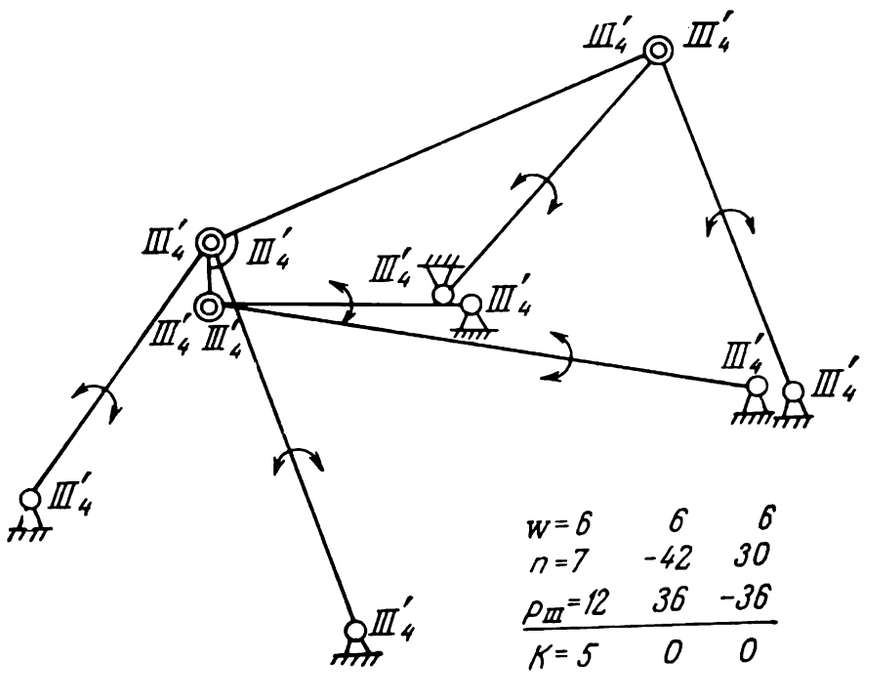


Fig. 2.53. Six-arm group with one basic member—upper frame of current collector (USSR Inventors' Certificate No. 333 080, inventors L. N. Reshetov and V. V. Solomin)

**Groups with two basic members.** Let us discuss only the case where the basic members are connected by a $V_2$ pair, with the mobility equalling one. To arrive at zero mobility, the arms should impose seven restraints. The following cases are possible:

(a) $7 = 4 + 3$
(b) $7 = 4 + 2 + 1$
(c) $7 = 4 + 1 + 1 + 1$
(d) $7 = 3 + 3 + 1$
(e) $7 = 3 + 2 + 2$
(f) $7 = 3 + 2 + 1 + 1$
(g) $7 = 3 + 1 + 1 + 1 + 1$
(h) $7 = 2 + 2 + 2 + 1$
(i) $7 = 2 + 2 + 1 + 1 + 1$
(j) $7 = 2 + 1 + 1 + 1 + 1 + 1$
(k) $7 = 1 + 1 + 1 + 1 + 1 + 1 + 1$

The groups are described as: (a)—two-arm; (b), (d), (e)—three-arm; (c), (f), (h)—four-arm; (g), (i)—five-arm; (j)—six-arm; (k)—seven-arm.

In practice, only four-arm groups are used. The complexity of other cases deems them interesting solely from a theoretical viewpoint. If the basic members are connected by a spherical pair *III'*, the maximum number of the arms will be nine. Therefore, this design is usable in exceptional cases only.

## 2.13. Self-Aligning Planar Structural Groups of Members of Mechanisms

The most universal solution to technical problems is offered by spherical pairs *III'* which we shall conventionally denominate by a large-diameter circle. They are incorporated in the simplest manner by having both ends of the connecting-rod spherical. However, this solution is not the absolutely best one, introducing as it does a local mobility—rotation of the connecting-rod about its axis—that should be checked for harmlessness. And, which is also important, this mobility arises from the extra spherical pairs which are not essentially necessary—and a spherical pair is more costly than a fifth-class rotational one.

A practical problem may be set as follows.

A multimember planar mechanism diagram is given (e.g. one of those shown in Figs. 2.56, 2.57, 2.58 and 2.59). The solution should suggest at what points rotational pairs $V_2$ should be provided, and at what points there should be spherical pairs $III'_2$ to render the mechanism self-aligning.

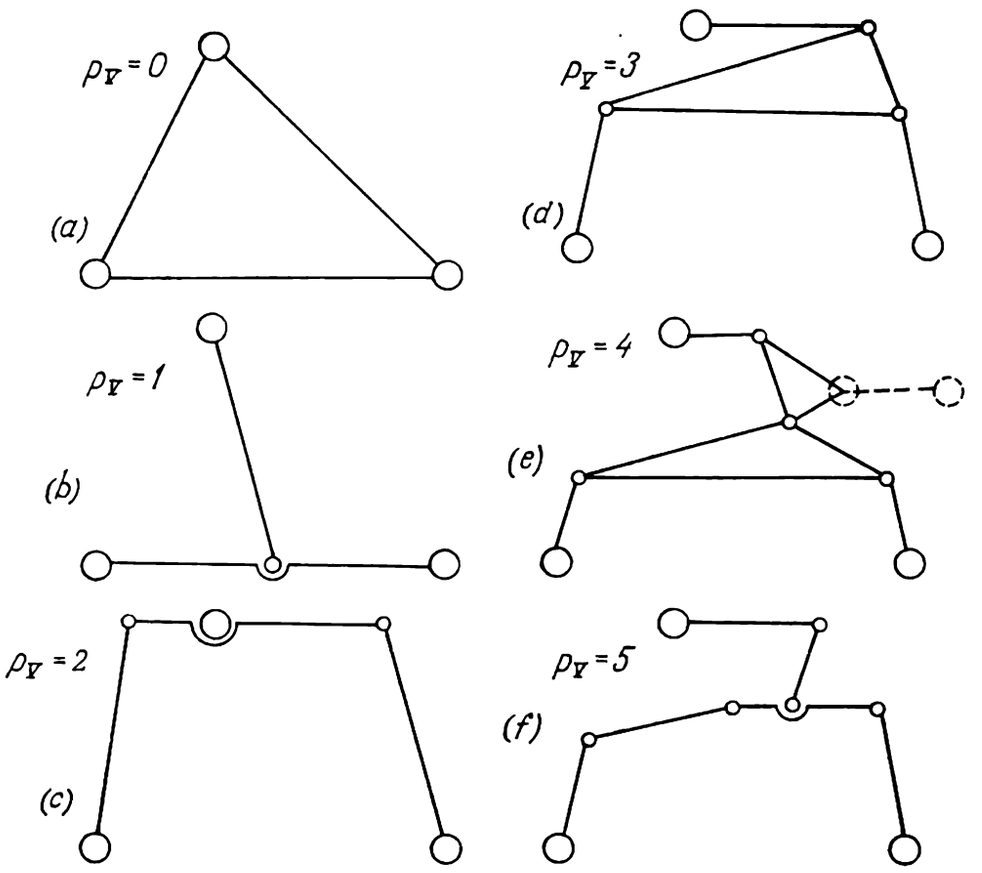


Fig. 2.54. Self-aligning planar structural groups
(*a*) without inner pairs; (*b*) with one inner pair; (*c*) with two inner pairs; (*d*) with three pairs; (*e*) with four pairs; (*f*) with five pairs

Using Assur's groups is not the simplest approach, for it does not consider the classes of kinematic pairs, but solely the planar diagram as such. If the classes of kinematic pairs are taken into account, the basic member in a zero-mobility group would be associated with 2 to 6 arms, and the number of spherical pairs could be minimized with the aid of self-aligning planar structural groups—SAPS groups.

Let us define a structural group as a group of the members of a mechanism, united by a certain law and intended for investigating the structure. Assur's groups are those structural groups whose mobility in a planar diagram equals zero.

Let us define a self-aligning planar structural (SAPS) group as one of members connected by such kinematic pairs whose restraints retain all the members of the group in a single plane (Fig. 2.54); as the position of a plane is determined by three points, a SAPS group should be connected to a mechanism by three spherical pairs. For higher rigidity, these pairs should be spaced from one another

as far as possible. In addition to these three pairs fixing the plane of a SAPS group, depending on its mobility and the mobility of the mechanism, the SAPS group may be connected to the mechanism by "free arms", i.e. those having solely pairs *III'* (Figs. 2.58, 2.59).

The most attractive is the case where the connecting pairs are rotational pairs $V_2$ with the axes perpendicular to the plane of the group; however, sliding pairs $V_3$ and planar pairs $III''_2$ may be also employed.

In general, referring to the work by E.Y. Kachalova, we can claim that kinematic pairs within SAPS groups should have exclusively planar mobilities and should be devoid of non-planar ones. A group of this kind would be different from an Assur's group and would have a different number of mobilities.

Let us consider an open (not closed) kinematic chain made up of fifth-class rotational pairs with the axes perpendicular to the plane of the mechanism, which, as Ozol has proved, has no redundant constraints. A group of this kind may be either unidirectional or branching-off. The fifth-class pairs will hold all the members in a single plane. To fix the position of this plane, three points are required, provided, quite naturally, that they neither belong to the same line nor—even worse—coincide with one another. At these points spherical pairs $III'_2$—to be called by us the support ones—are to be provided. The number of the rotational pairs may be various.

It may equal zero (Fig. 2.54*a*), with the group reduced to a single member of three spherical pairs. If the number is one (Fig. 2.54*b*), the group consists of two members connected by a rotational pair. If it is two (Fig. 2.54*c*), the members are connected by two pairs; if three (Fig. 2.54*d*), four members are interconnected by three rotational pairs. We have here a three-arm Assur's zero-mobility group. There may also be four rotational pairs (Fig. 2.54*e*), then five members will be connected by four rotational pairs: this arrangement differs from a four-arm group solely in that the fourth arm (shown with dash lines in Fig. 2.54*e*) is not considered. This arm should be made with spherical pairs, and takes no part in fixing the plane of the group.

The number of rotational pairs in a SAPS group may be higher than four (Fig. 2.54*f*). In a SAPS group, two spherical pairs must not be provided at the ends of the connecting-rod to avoid a local mobility and the resulting redundant constraint. This is not true, however, of the member with three pairs as in Fig. 2.54*a*, since here the third pair restrains the rotation. Obviously enough, the

mechanism may have fifth-class rotational pairs outside the SAPS group.

SAPS groups can be produced of Assur's groups by addition of the corresponding number of arms. The arms may have $III'_2$ and $V'_2$ pairs. They will incur two restraints, and we shall conventionally call them the guide ones. They may be arms with $III'_2III'_2$ pairs, and, if they impose one restraint, they will have a local mobility—rotation about their axes—and we shall call them the free ones. A SAPS group is produced in the simplest way of a three-arm group, as the number of arms equals there the number of the supporting pairs. If the three-support (spherical) pairs are arranged at the external ends, a SAPS group of Fig. 2.54*d* or 2.55*d* is produced automatically, including the basic member and the three arms. It has three inner rotational pairs. The three-support pairs may be situated at the inner ends of the arms, and the SAPS group is reduced to a three-pair member of Figs. 2.54*a* and 2.55*a* which should be connected by three guide arms not included in the SAPS group. The latter is shown here and in the following drawings with bold lines, and the external arms are shown with hair lines. Two support pairs may be situated at the inner ends of the arms, with the third one provided at the external end (Fig. 2.55*b*). The SAPS group will include then the basic member and one arm, the other two arms being external guide ones.

Another possibility is to have one support pair at the inner end of an arm and two support pairs at the external ends (Fig. 2.55*c*). In this case, the SAPS group includes the basic member and two arms, with the third arm serving as the external free one. The situation is somewhat different with a four-arm group (with four inner rotational pairs). There are but three-support spherical pairs (Fig. 2.55*d*), and they would leave out one arm. Therefore, the latter has to be made the free one with spherical pairs, as shown with dash lines in Fig. 2.54*e*. The SAPS group includes here two basic members and three arms. The arrangement of the support pairs at the inner and external ends of the arms may be varied, as it has been shown for three-arm groups, to arrive at four versions of the diagram.

A group with five inner rotational pairs requires already as many as two free arms (not shown in Fig. 2.54*f*). A SAPS group may also include a closed loop, but in this case the redundant constraints in it must be eliminated by including either two $III'_2$ pairs (with one local mobility appearing), or else one $IV_2$ pair and one $III'_2$ pair.

Before selecting kinematic pairs, the planar diagram of the mechanism is to be worked out and assumed as a given one. One should

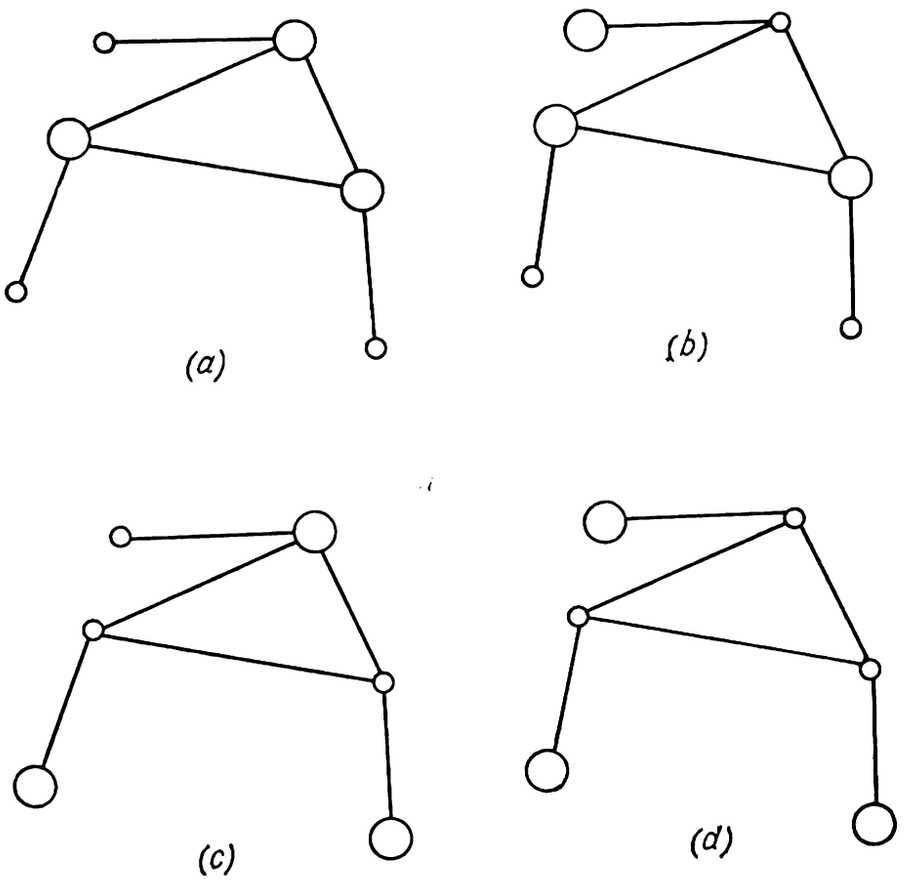


Fig. 2.55. Forming SAPS groups of Assur's three-arm groups

remember, however, that the position of the plane of a SAPS group is defined by three points. The points should be as remote from one another as possible (thus, selecting the points adjoining a straight line would be a mistake); moreover, the points should offer the most rigid linear connection in a direction perpendicular to the plane of the SAPS group. The support spherical pairs should be situated either at these points or close to them. To check up, the following relationship can be used: the sum of the mobilities of the rotational pairs of a SAPS group—the inner and rotational pairs of its guide arms—equals three plus the number of free arms (we suggest you check it using the diagrams of Fig. 2.55).

**Example 1.** A mechanism with a coupled connecting-rod (Fig. 2.56). The main connecting-rod $BC$ and the coupled one $EF$ may be considered a SAPS group $BCEF$ with the support points $B$, $C$, $F$ (in similarity to Figs. 2.54*b* and 2.55*b*), where pairs $III_2'$ are provided, and a single pivot $E$ with a pair $V_2$.

**Example 2.** The link gear mechanism of a planing machine, Fig. 2.57. Let us select as the SAPS group $DBCEF$ with the support

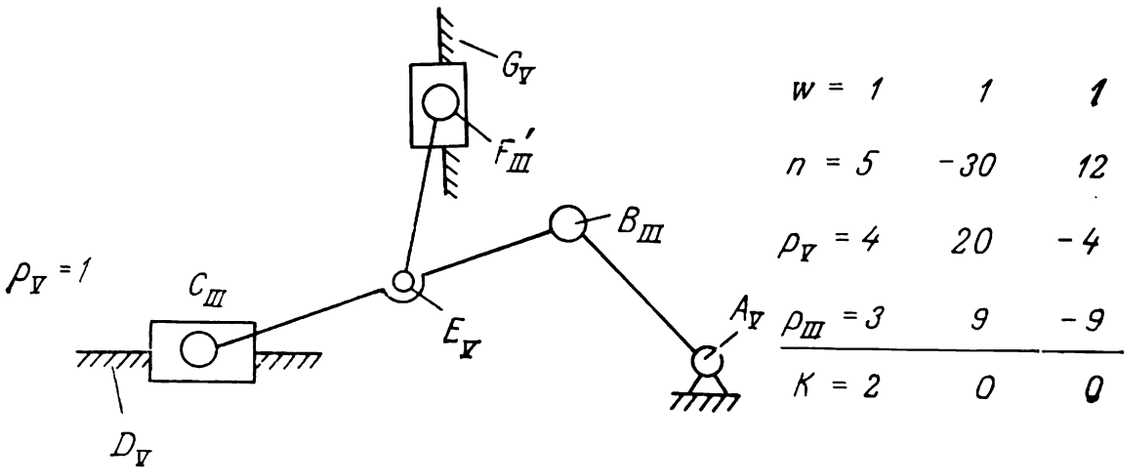


Fig. 2.56. SAPS group with one inner pair in a coupled connecting-rod mechanism

points $D$, $B$, $F$ where pairs $III'$ are provided, and inner pairs $C$ and $E$ where pairs $V_3$ and $V_2$ are situated, in similarity to Figs. 2.54*c* and 2.55*c*.

**Example 3.** Stephenson link gear, Fig. 2.58. Let us consider the structural group *BDFGEC*. The support points are to be selected where the restraints of the mechanism inhibit linear mobilities perpendicularly to the plane of the SAPS group. These points would be the eccentrics $B$ and $C$ and the slide valve pivot $G$, where pairs $III'$ are to be situated (in similarity to Figs. 2.54*d* and 2.55*d*). Pairs $D$, $F$, $E$ are to be regarded as inner ones, so that they will be of the fifth class. The arm $JK$ will be not included into the SAPS

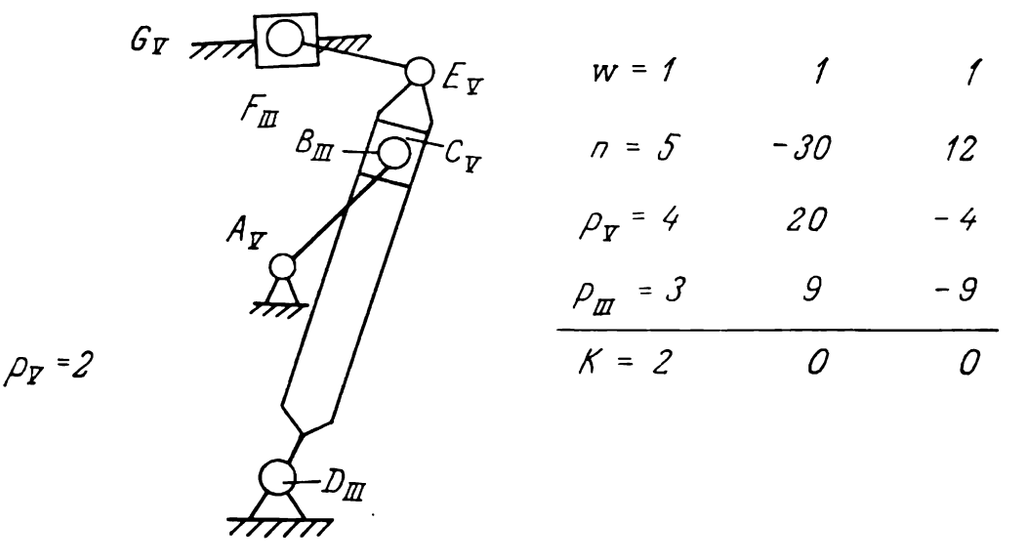


Fig. 2.57. SAPS group with two inner pairs in a planing machine mechanism

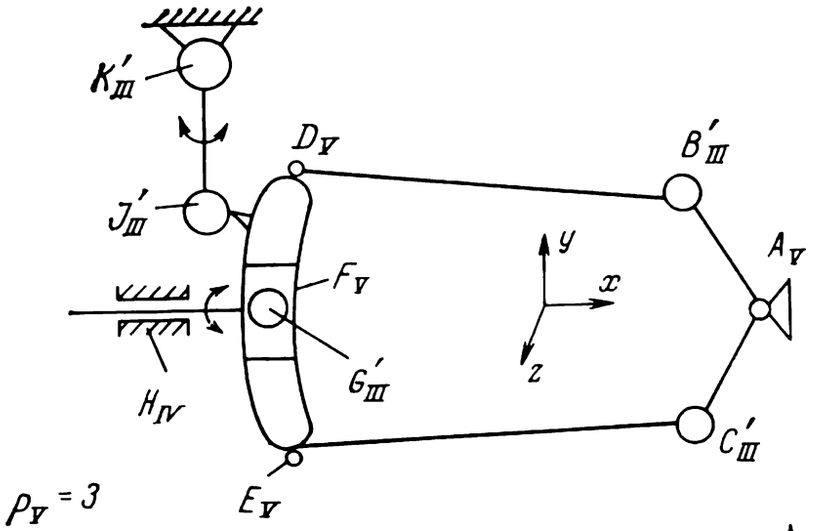


| | | |
|---|---|---|
| $W = 3$ | 3 | 3 |
| $n = 7$ | −42 | 18 |
| $\rho_V = 4$ | 20 | −4 |
| $\rho_{IV} = 1$ | 4 | −2 |
| $\rho_{III} = 5$ | 15 | −15 |
| $K = 3$ | 0 | 0 |

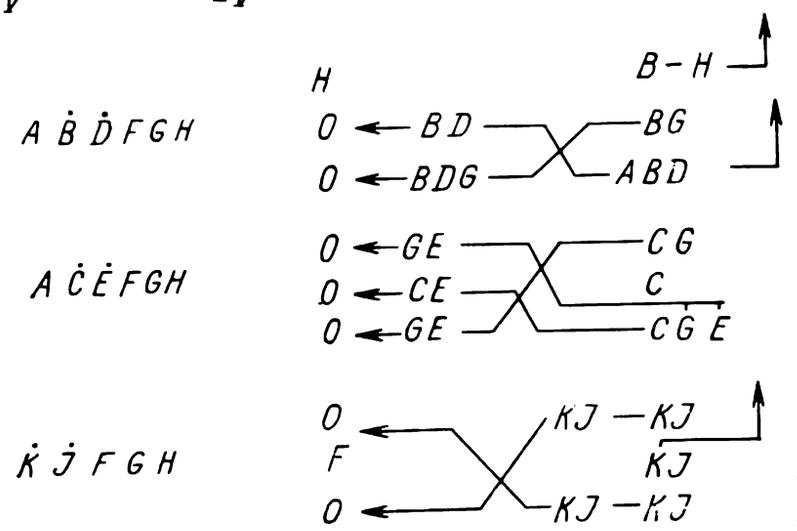


Fig. 2.58. SAPS group with two inner pairs in Stephenson link gear mechanism

group and will be made as a free one with pairs *III'*, however it will have a harmless local mobility—rotation about its axis.

**Example 4.** Wahlshart-Heusinger link gear, Fig. 2.59. In the four-arm group with basic members *HL* and *HG* and arms *LM*, *JK*, *GF* and *QR* (similar to Fig. 2.54*e*) we shall select the points *M*, *J* and *G* as the support ones with *III'* pairs. Point *R* will not suit, as it is closer to the line *GJ* than point *M*, and its selection will impair the retaining of the SAPS group. Therefore, the arm *QR* will be not included in the SAPS group and will be made a free one with spherical pairs. The members *L* and *H* will be connected by fifth-class pairs. An alternative solution is possible: the point *L* is taken as the support one instead of *M*, with a pair *III'* installed there, while a pair *V* is provided at the point *M*. The two solutions are equivalent. Outside the SAPS group, as it could be expected, local mobilities remain—rotation of the connecting-rods *QR*, *BD* and *CN*.

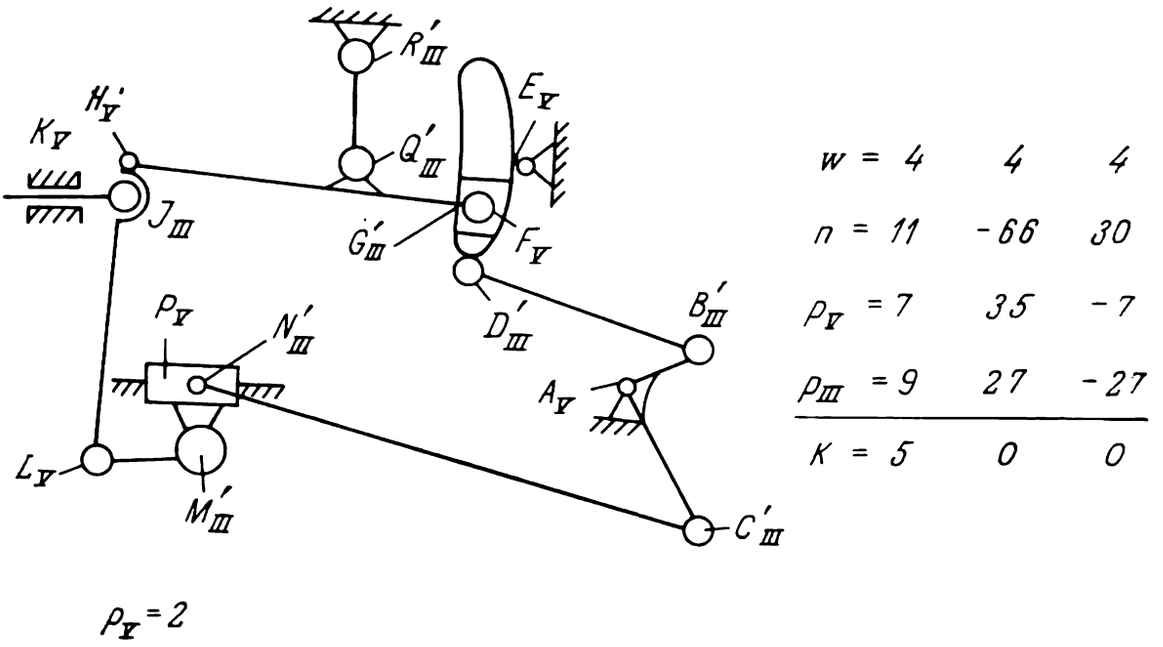


Fig. 2.59. SAPS group with two inner pairs in Wahlshart-Heusinger link gear mechanism

The spherical pairs $III'$ need not be actually spherical. They may be in the form of pairs $III'_4$—cylindrical with gaps and a short sleeve. The rotational pairs are preferably those with two spaced sleeves, with the respective arm being bifurcated, as it is usually the case in practical designs.

## 2.14. Centrifugal Governors

Elimination of redundant constraints in centrifugal governors, in addition to the abovediscussed general merits, reduces friction, and, hence, the deadband of governors, which is of essential importance.

Let us discuss some standard patterns of present-day centrifugal governors. The governors generally include two fly-weights and, correspondingly, two transmission linkages from the weights to the coupling sleeve. The existence of the two mechanisms would not affect static determinacy, as each mechanism transmits its own centrifugal force (a twin mechanism inadmissible on account of its redundant constraints is one where the motion of one member is transmitted to other by two parallel linkages).

In the conical governor (Fig. 2.60*a*, where it is shown without the weight and springs associated with the coupling sleeve) the weight arms are connected to the shaft by rotational pairs $V_2$ transferring

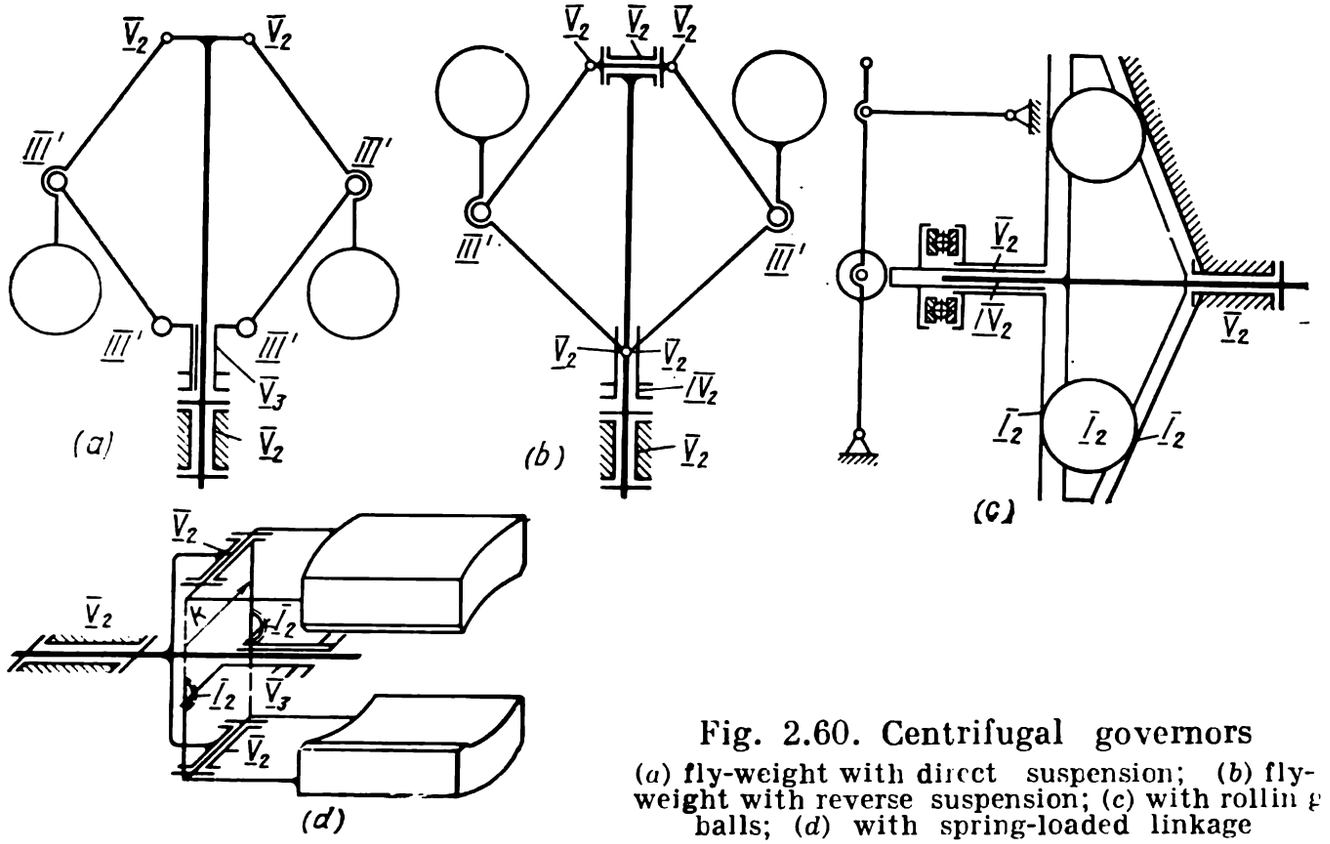


Fig. 2.60. Centrifugal governors
(*a*) fly-weight with direct suspension; (*b*) fly-weight with reverse suspension; (*c*) with rolling balls; (*d*) with spring-loaded linkage

the moment of inertia forces to the weights as the speed of the machine varies. For this moment to cause minimized friction, the journals of these pairs should be made as long as possible. In many practical structures, this is attained by the weight arms having wide bifurcated ends encompassing the journals.

The sleeve of the governor is movable along the shaft with aid of a translatory pair $V_3$ (a keyway connection). To connect the weight arms with the sleeve without stresses, rods with spherical pairs $III'_1$, $III'_2$ or $III'_4$ should be used. In the last-mentioned case the journals are preferably made very short, with gaps left.

The structures of governor mechanisms can be investigated in two ways:

—by considering the entire mechanism of a governor, including its shaft bearings (in this case there will be two general mobilities—rotation of the governor and motion of the sleeve—beside the local ones);

—by regarding the housing of the governor as a fixed member and considering only the displacement of the sleeve (in this case mobility equals one).

Let us follow the first way.

The mobility of the governor under investigation includes rotation of the shaft, motion of the sleeve and local mobilities (rotation of the two rods about their axes), i.e. $w = 4$.

From (1.1): $q = 4 - 6 \times 6 + 5 \times 4 + 3 \times 4 = 0$.

The design of Fig. 2.60*a* is suitable for any conical governor with direct suspension of the fly weights—be the rods open or crossing, be the arms straight or curving. With the reverse suspension of the weights, the design is operable solely with straight arms. Should the arms be bent, the local mobilities would be harmful, as the rotation of the arms about their axes would affect the proper positioning of the weights.

Conical weight governors are usable only with a vertical shaft, whereas conical spring governors can be associated both with vertical and horizontal shafts. With a horizontal shaft, the gravity force of the weight is alternatively added to the centrifugal force (in the bottom position of the weight) and subtracted from it (with the weight in the top position), i.e. the weight is acted upon by an alternating force causing continuous relative displacement of the members of the governor. This motion opposes friction and thus lowers the deadband of the governor. With the shaft extending vertically, the resultant of the gravity and centrifugal forces is of a permanent value and direction (relative to the governor shaft) and will not cause displacements opposing friction. And this is where a horizontal governor is essentially more attractive than a vertical one.

The centrifugal forces developed by the two weights of a governor may be unequal on account of the tolerances on the mass of the weights and dimensions of the members. These centrifugal forces, when transmitted to the sleeve, apply to it a horizontal force and a torque about an axis perpendicular to the plane of the drawing (a twisting torque). This steps up the friction and the deadband of the governor. The twisting torque, however, can be eliminated. This can be attained by superimposing the points of connection of the rods to the sleeve (Fig. 2.60*b*), i.e. the rods should be in the form of bifurcated members engaging the sleeve and connected to it with the aid of two journals defining a rotational $V_2$ pair. To avoid redundant constraints, the design should be somewhat developed: another pivot $V_2$ should be added at the top of the governor, and the keyway connection of the sleeve should be removed (to render it a cylindrical $IV_2$ pair), as in this design the sleeve is rotated by the rods of the weights, the key would have merely imposed a redundant constraint. The horizontal roller serves as an equalizing mechanism in transmission of the torque.

From (1.1): $q = 2 - 6 \times 7 + 5 \times 6 + 4 \times 1 + 3 \times 2 = 0$.

The design of Fig. 2.60*b* is operable with reverse suspension of the weights and curving arms, which is just what is shown in Fig. 2.60*b*. Care should be taken, however, of the equality of the centrifugal forces, e.g. by employing weights of a simple shape so that the dimensions should be smaller and the mass more accurate. The weights should be prechecked by weighing, and the governor should be balanced with and without the weights.

In a governor with rolling balls (Fig. 2.60*c*) the latter are accommodated between a stationary tapering disc and a movable flat one. The balls are driven by a cage (a cross) coupled to the engine shaft. The movable disc is spring-loaded either directly or through an arm and is capable of two motions: the axial one (as the speed varies) and rotation (by the friction of the rolling balls). The governor is in fact a planetary gearing where the balls are the satellites and the cage is the carrier. The movable disc is rotated at about twice the angular speed of the cage, the latter being associated with a thrust bearing transmitting its axial motion to the regulating mechanism. As the speed varies, the balls roll along the discs, following helical paths, so that the slip is minimal and the friction is low.

Let us consider the structure of this governor, less the transmission arms. Let us assume it has six balls (governors of this kind have two to six balls). The mobility of the mechanism: main rotation, rotation of the disc, of the sleeve and of the six balls about the three coordinate axes on account of the slip, axial displacement of the sleeve; altogether, $w = 22$.

From (1.1): $q = 22 - 6 \times 9 + 5 \times 2 + 4 \times 1 + 18 = 0$. Thus, the design is proper and requires no changes.

In a linkage governor (Fig. 2.60*d*, with springs omitted) longitudinal springs are used to act upon the sleeve or upon the transmission arms, or else transverse springs are used to act directly on the fly weights. Longitudinal springs are widely employed in diesel engines of vehicles, owing to the simplicity of adjustment of their tension for speed control. Transverse springs, on the other hand, enable one to minimize the forces in the kinematic pairs of the governors, i.e. to reduce the friction and to enhance the deadband, provided the effort of the spring is directed through the gravity centre of the weight. Thus the major forces—the centrifugal force and the effort of the spring—are directly counterbalanced and would not be transmitted to the pivots. For this reason governors with transverse springs are used in stationary installations, particularly, in steam turbines, where the accuracy of control action is essential.

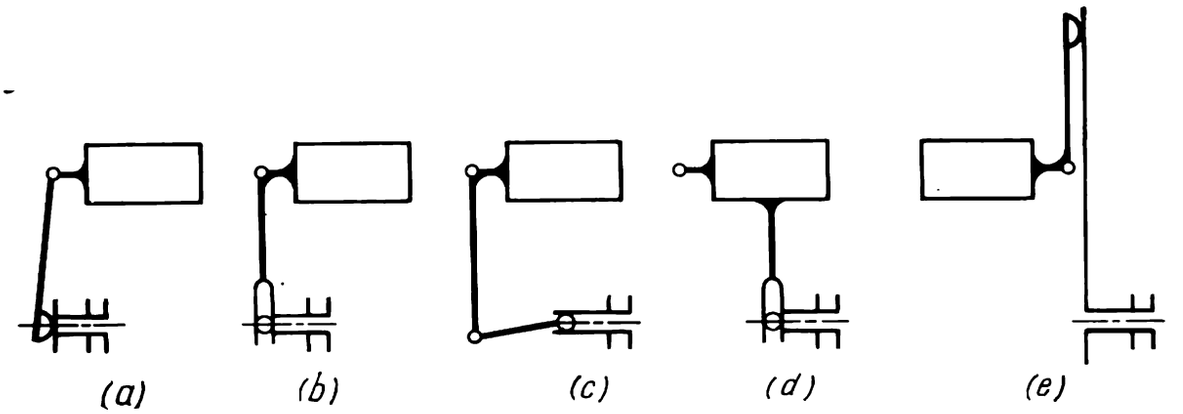


Fig. 2.61. Diagrams of connection of weight arm with sleeve
(*a*)-(*c*) correct; (*d*) and (*e*) wrong

The weights are connected with the sleeve through either sine (Figs. 2.60*d* and 2.61*a*) or tangent-link (Fig. 2.61*b*) mechanisms, or else a slider-crank mechanism (Fig. 2.61*c*).

In the link mechanisms the sliding in the link is greater than in a slider-crank mechanism, and the friction is correspondingly higher. Therefore, link mechanisms are commonly used in vehicle engines, and slider-crank ones are incorporated in stationary installations. To reduce friction in a link mechanism, the latter should be designed for the sliding velocity in the link to approach zero at the central position of the weights. Thus, the designs of Fig. 2.61*a* and *b* are correct ones and that of Fig. 2.61*d* is the wrong one. Another way to reduce friction is to mount a follower onto the pin of the link mechanism.

With longitudinal springs, the centifugal force of the weights moves the sleeve in one direction, while the spring moves it in the opposite direction. Thus, one may use an open-slot link mechanism (Figs. 2.60*d* and 2.61*a*). With transverse springs, it is the weights which move the sleeve in both directions, and the link has to be a closed-slot one (Fig. 2.61*b* and *d*).

If the contact or engagement of the weight arm and the link is considered a point one (an $I_2$ pair), there will be no redundant constraints: $q = 2 - 6 \times 4 + 5 \times 4 + 1 \times 2 = 0$.

Even with line contact ($II_2$ pair) redundant constraints are not hazardous, for they may result solely in non-uniform distribution of the force along the line of contact.

Uneven centrifugal forces may subject the sleeve to a twisting torque increasing the friction and affecting the sensitivity of the governor. To reduce this torque, distance $k$ (cf. Fig. 2.60*d*) should be

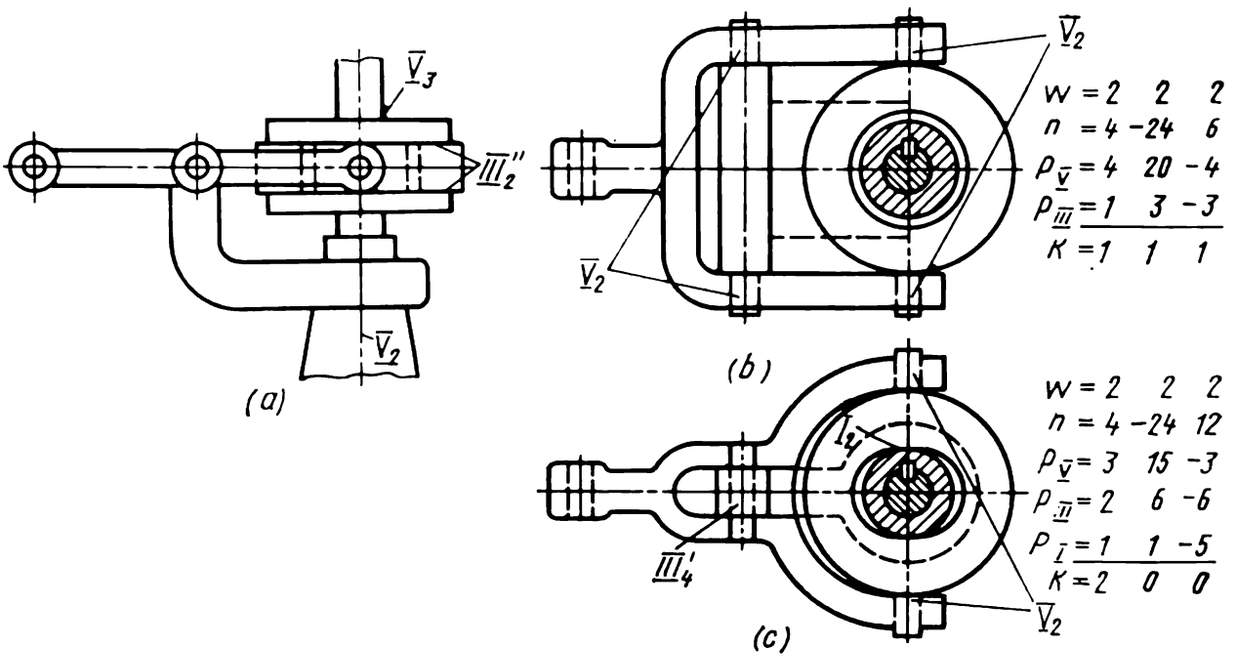


Fig. 2.62. Transmission from sleeve to control arm

minimized and the identity of the weights checked. Thus, designs are preferred where the sleeve is not on the governor shaft, but on a specifically provided bearing, which makes it possible to position the weight arms close to each other. A structure with the weight arm extending outwardly (Fig. 2.61*e*) is patently wrong, as the arm length $k$ is excessive.

A twin mechanism must be avoided by all means (dash lines in Fig. 2.60*d*), to avoid redundant constraints. If the link is of the open type, only one mechanism out of two will operate, and if it is slot-operated, any manufacturing inaccuracy should produce stresses and sharply increase friction.

Redundant constraints in a transmission mechanism between the sleeve and the control arm (Fig. 2.62*a*) cause non-uniform loading of the planar pair $III_2''$ and its untimely wear. This is particularly important for exposed constructions where adequate lubrication is always a problem. Such was the case in designs where the arm was connected to a fixed member by a rotational pair $V_2$ (steam engines, Fig. 2.62*b*). A proper structure is illustrated in Fig. 2.62*c*, with the arm connected to the fixed member through a spherical pair $III_4'$, and the excessive mobility precluded by the ring abutting against the sleeve—pair $I_2$. In the design shown, the ring has an oblong opening, which is not mandatory. A similar structure can be recommended for disengagement of a friction clutch.

In hydraulic turbines, governors with flexible connections are used to practically avoid friction and reduce the deadband of the governor to zero. Governors of this type usually are called the pendulum ones. There are known an involute band pendulum (shown as Rozov's design) and a rhombic band pendulum (Fig. 2.63) developed by a Leningrad enterprise. In the fabricated construction the transverse pivot $V_2$ at the bottom of the mechanism is not included. This design is not unlike the conical governor, with the arms and rods replaced by flexible links—the sheet pairs $III_4''$.

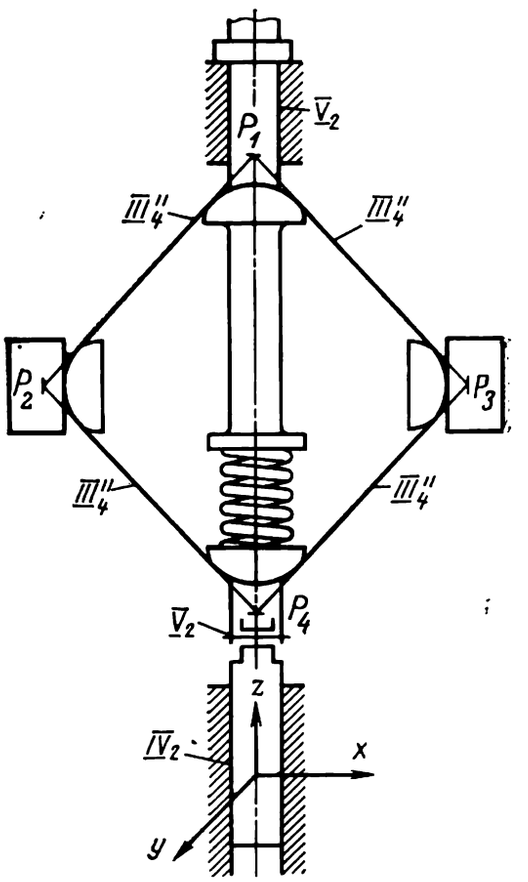


Fig. 2.63. Rhombic band pendulum of Leningrad Metal Works

The mobility of the governor $w = 4$: rotation, motion of the sleeve and the local mobility of the two weights (rotation about the points $P_2$ and $P_3$ of intersection of the sheet pairs). For stability sake, the gravity centres of the weights must be situated outwardly of these points.

From (1.1): $q = 4 - 6 \times 4 + 5 + 4 + 3 \times 4 = 1$.

The redundant constraint amounts to non-uniformity of the loading of the two flexible sheets—the bands. To eliminate it, a rotational pair should be provided on one of the central members in the plane of the drawing. Then: $q = 4 - 6 \times 5 + 5 \times 2 + 4 + 3 \times 4 = 0$.

In this governor the sleeve (which is the spool valve of the hydraulic servomotor) rotates in a stationary bore, with the friction directed circumferentially and having practically no axial components. Owing to this, the deadband of the governor is practically at the zero level.

The necessity of having the horizontal pivot between the bottom corner of the rhomb and the sleeve (the spool valve) can be also derived from the condition that the mechanism could be assembled without prestressing. Let us assume that the last pair to be assembled is a $IV_2$ pair made up of the spool valve and the bore. To align these two members, the spool valve has to be rotated about two coordinate axes and displaced twice along these axes. No rotation about $z$ axis

and displacement along it are required, as the spool valve-bore pair itself provides them. Rotation about $x$ axis is controlled by the horizontal pivot, and about $y$ axis—by the centre $P_4$ of instant rotation.

Displacement along $x$ axis is provided by the centres $P_1$ and $P_4$ of instant rotation, and displacement along $y$ axis, by twisting of the bands $P_1P_2$ and $P_1P_3$ (then the two other bands are less deformed) and by rotation of the bottom assembly about $x$ axis. For this rotation not to be transmitted to the spool valve, the horizontal pivot has been incorporated.

Thus, the rotation about $x$ axis and the displacement along $y$ axis are independent only when the horizontal pivot is provided. With this pivot omitted in the design of the mechanism, the independence becomes non-existent, causing prestressing and uneven performance of the flexible bands. With this redundant constraint eliminated, the governor becomes the best one among the existing designs, and its use should be spread into other fields. The cost of the additional pivot is negligibly small.

An involute pendulum has two redundant constraints, while the number of redundant constraints in the pendulum designed by A.G. Rozov is even greater. Their elimination involves considerable complication of the governors, for which reason these mechanisms are not discussed here.

## 2.15. Valves and Gates

Swinging-disc valves are installed in pipelines (as check valves) and in chemical apparatus as leakproof closures of ports; they are also used as closures of steam boilers and flues. In the past, they were used in hand-operated fire-fighting pumps, but their redundant constraints resulted in their poor performance, particularly, with polluted water, which eventially prohibited their use altogether.

An old design of a check valve for a pipeline is shown in Fig. 2.64.

The working surface of the valve member—the disc—is planar ($III_2''$ pair), and the pivot is a $V_2$ pair. In the closed position, $w = 0$, $n = 1$. From (1.1): $q = 0 - 6 \times 1 + 5 \times 1 + 3 \times 1 = 2$.

The two redundant constraints cause skewing of the valve disc about the vertical and horizontal axes, which impairs the tightness of the closing action. The remedy can be found in three ways.

I. A $III_4'$ pivot is provided at the axis of the valve disc to ensure self-aligning. In the closed state $w = 1$—rotation of the valve disc has been added, though small. It is included, however, in the structural formula: $q = 1 - 6 \times 2 + 5 \times 1 + 3 \times 2 = 0$ (Fig. 2.65).

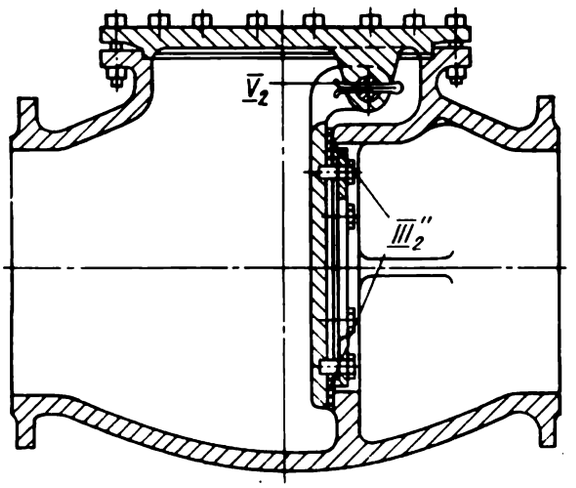


Fig. 2.64. Swinging-disc check valve (wrong design of the past, with redundant constraints)

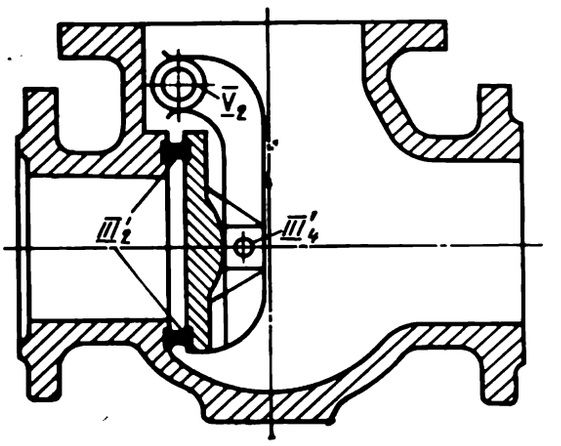


Fig. 2.65. Swinging-disc check valve with self-aligning disc ($q = 0$)

II. The valve disc is mounted on two arms with pivots $III_4'$ (Fig. 2.66). In the closed state $w = 3$—rotation of the two arms about their axes and the general mobility in a plane parallel with the working plane. The mobilities are negligible, and being confined within the gaps in the pivots, they are harmless. Redundant constraints $q = 3 - 6 \times 3 + 3 \times 5 = 0$.

III. The bores in the pivot $V_2$ (Fig. 2.64) are replaced by a horizontal groove (preferably, in the stationary part) which provides for self-aligning.

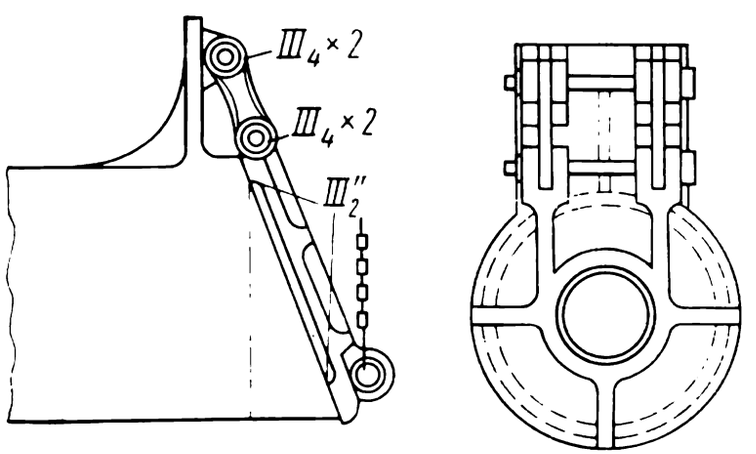


Fig. 2.66 Swinging-disc check valve with disc on two arms, without redundant constraints

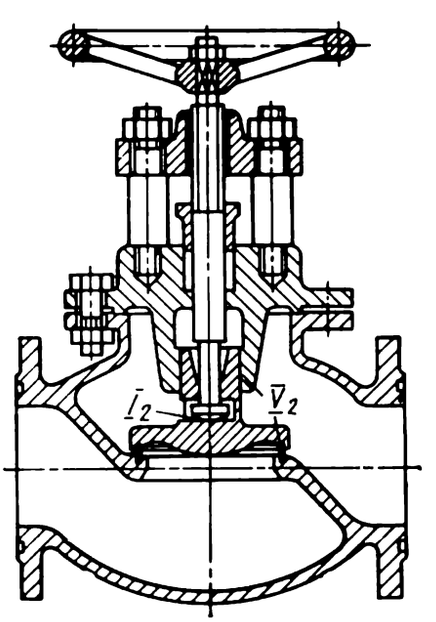


Fig. 2.67. Control valve with self-aligning valve plate, owing to gaps in the guides

Lift plate valves are used in closure-control valves of pipelines (Fig. 2.67). The plate is the closure member of the valve; it is guided either by ribs—top or bottom, or by a central bar. In the closed state, the guiding device forms with the working surface a $V_2$ rotational pair. To provide for self-alignment and to eliminate redundant constraints, a first-class $I_2$ pair should be provided between the control stem and the lift plate, e.g. with the end stem being spherical and bearing upon the planar surface of the valve plate.

In the closed state $w = 1$—rotation of the valve plate. Redundant constraints $q = 1 - 6 \times 2 + 5 \times 2 + 1 \times 1 = 0$.

In small water-main faucets there is employed a similar design without guides. Then the kinematic pair defined by the plate valve and the valve seat should be seen as a planar $III_2''$ pair. To avoid harmful mobilities, a spherical pair $III_2'$ is included between the valve plate and the stem. Redundant constraints are absent, i.e. $q = 1 - 6 \times 2 + 5 \times 1 + 3 \times 2 = 0$.

Gate valves have been recently widely employed as pipeline control fittings, due to their pressure loss values being considerably lower than those of either swinging-disc or lift valves. A wedge-gate valve of an old system with redundant constraints is shown in Fig. 2.68. Calculations using formulas (1.1) and (1.2) are given to the right of the drawing (the screw mechanism is not considered).

Notwithstanding the movable con-

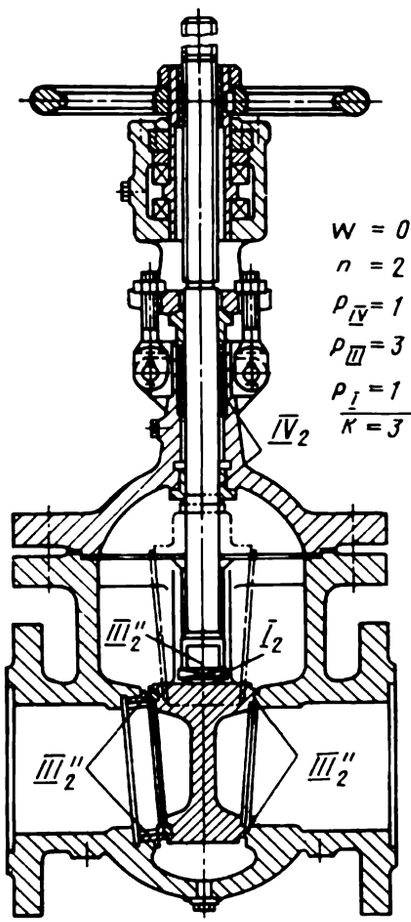


| | | | |
|---|---|---|---|
| $w$ | 0 | 0 | 0 |
| $n$ | 2 | −12 | 18 |
| $p_{IV}$ | 1 | 4 | −2 |
| $p_{III}$ | 3 | 9 | −9 |
| $p_I$ | 1 | 1 | −5 |
| $K$ | 3 | 2 | 2 |

Fig. 2.68. Gate valve (wrong design of the past, with two redundant constraints)

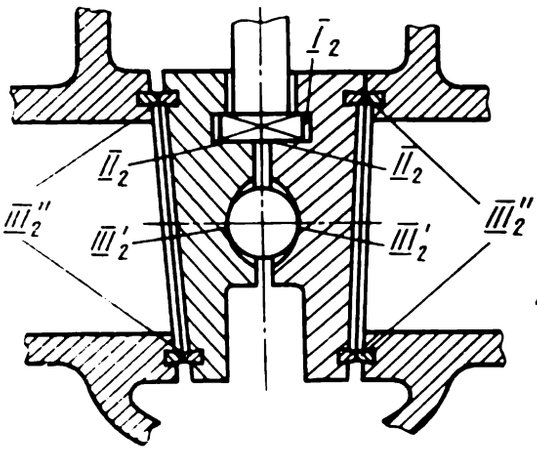


| | | | |
|---|---|---|---|
| $w$ | 4 | 4 | 4 |
| $n$ | 4 | −24 | 24 |
| $p_{IV}$ | 1 | 4 | −2 |
| $p_{III}$ | 4 | 12 | −12 |
| $p_{II}$ | 2 | 4 | −8 |
| $p_I$ | 1 | 1 | −5 |
| $K$ | 4 | 1 | 1 |

Fig. 2.69. Diagram of removing redundant constraints affecting tightness of gate valve

nection of the wedge to the stem, made up of two pairs ($III_2''$ and $I_2$), the gate valve has two redundant constraints which require strict equality of the angles of the wedge and valve housing in the two axial planes—the vertical and horizontal ones. The required accuracy is practically unattainable, whereby one pair of the working surfaces out of two operates at any given moment, depending on the flow direction.

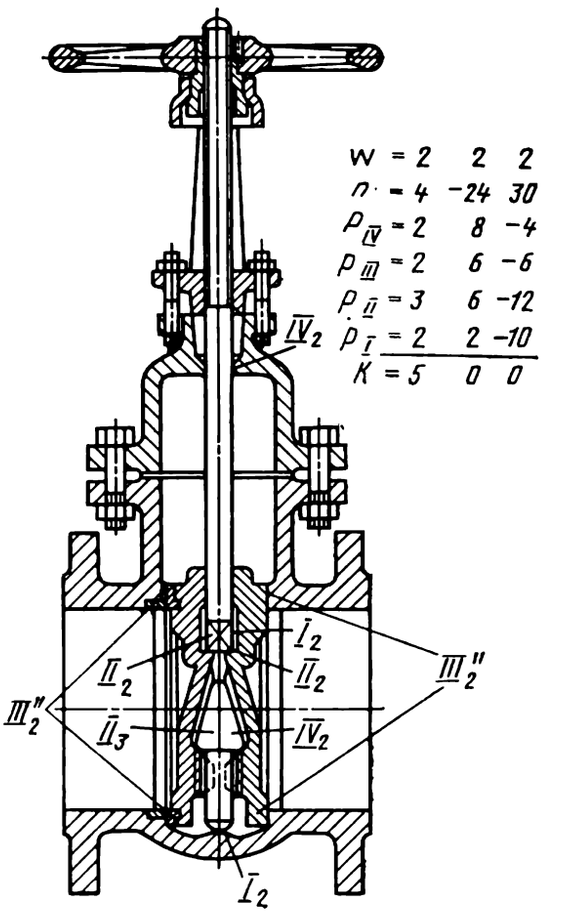


Fig. 2.70. Ludlow's gate valve with no redundant constraints

To avoid redundant constraints, the wedge is made up of two parts with a steel ball interposed (Fig. 2.69*), with the stem engaging both halves of the wedge. Let us place a $II_2$ pair between the stem and one half, and pairs $II_2$ and $I_2$ between the stem and the other half, as the wedges are supposed to oppose rotation of the stem. The calculation of mobilities and redundant constraints from formulas (1.1) and (1.2) is given on the right of the drawing. There are four mobilities in this mechanism: rotation of the ball about the three coordinate axes and transverse displacement of the two wedges in the housing (against their respective abutment surfaces). The redundant constraint $q = 1$ causes non-uniform distribution of the load between the stem and the two halves, but it does not impair the tightness of the closing action.

A gate valve with parallel working surfaces of Ludlow's general design is illustrated in Fig. 2.70. The discs are pressed against their seats at the end of the closing motion by a spreading wedge arranged centrally. The calculation according to the structural formulas is given on the right of the drawing.

To avoid redundant constraints and attain complete self-alignment, let us presume that a $IV_2$ pair exists between the spreading wedge and one disc, and a $II_3$ pair is between the wedge and the other disc.

*The stem guide, pair $IV_2$, is not shown.

There are two mobilities in the gate valve mechanism—transverse displacement of the two discs with the spreading wedge toward abutting against the seats, and rotation of the wedge about its axis. Then redundant constraints are non-existent, i.e. $q = 0$.

## 2.16. Conclusions and Suggestions

Self-aligning fixed connections reduce considerably the time of replacing machinery units. Thirty two such connections have been described.

For self-alignment sake, a shaft should be supported by two bearings and not by a greater number. In piston-type machines this is attained by the radial design, in bridge cranes the use of tubular shafts is suggested, and in motor vessels the power plant should be positioned close to the stern to avoid a lengthy propeller shaft. The rotary work tables of machine tools (e.g. vertical lathes, boring mills, gear-hobbing machines) should be supported by a planar pair and a central annular pair.

In crossheads of piston-type machines, self-alignment requires that the blocks should be connected to the crosshead body by spherical pairs. With several pistons operated by a single crosshead, they should be interconnected by an arm with two spherical pairs. Guideways in machine tools should have a wedge-shaped slider and a flat one.

A wedge mechanism is preferably made up of cylindrical wedges with a planar pair connection.

The screw mechanisms used are of two kinds: those with separately provided guideways and those where the screw itself acts as the guide. In single-screw mechanisms with separate guideways, the screw and the guideways afford two mobilities. Self-alignment requires that the rest of the pairs should yield five mobilities (out of seven).

Mechanisms with guide screws may be of the single-, double- and triple-screw types. The single-screw type is the simplest, but it affords solely the translatory motion, with the screw subjected to a bending strain as the load displaces in either direction. A double-screw mechanism is more complicated. With the screws separately driven, the mechanism affords, in addition to the translatory motion, the slanting of the platform about one axis. Displacement of the load along the platform would not cause bending strain of the screws. A triple-screw mechanism is the most complicated one. With the screws driven independently, the mechanism enables the platform,

in addition to its translation, to incline about two axes (i.e. about any axis). The screws are not subjected to bending strain altogether.

A slider-crank mechanism with a cylinder-shaped slider (a piston) has two redundant constraints. Their elimination enhances starting the engine and reduces the wear of the piston rings and cylinder sleeves. The elimination of the redundant constraints is attained either by incorporating two additional pivots on the connecting-rod, or by replacing the $V_2$ pair by a $III_2'$ one on the piston and the $V_2$ pair by a $IV_2$ pair on the crank pin, or by combining the two techniques.

A cylindrical $IV_2$ pair should be situated solely where it is operated through a full revolution, and the length of its lining should be checked for self-alignment.

In a crank-and-rocker mechanism, self-alignment requires that the kinematic pairs with the exception of the crank and rocker bearings should afford five mobilities. This is attained by having additional pivots (e.g. in steam distribution mechanisms of turbines with a high level of thermal expansion), by using spherical pairs, etc.

In a parallel crank mechanism, an additional mobility takes place in the dead centre position, usually a harmful one, and a redundant constraint, too. The harmful mobility may be eliminated by using an additional mechanism, and the redundant constraint is removed by an additional pair affording linear mobility along one of the members.

In link gear mechanisms (of the sine- and tangent-link types), redundant constraints are efficiently removed by using three cylindrical $IV_2$ pairs, with only the main shaft bearings being retained as $V_2$ pairs.

When designing self-aligning multiarm mechanisms, the use of Assur's theory is significantly complicated for the following reasons: there are numerous cases where Assur's groups have non-zero mobility and a redundant constraint; groups with a single basic member may be not only the three-arm ones, but also those with two, four, five or six arms. The case of two basic members is even more complicated.

There is one more technique of investigating a structure: the one of breaking down the mobilities and restraints into planar and non-planar ones. The formulas for the planar diagram of a mechanism are valid for planar restraints and mobilities. For non-planar restraints and mobilities (directed perpendicularly to the plane of the motion of a mechanism), there are formulas suggested by E.Y. Ka-

chalova and disclosed in this Chapter. They offer an efficient way of detecting redundant constraints which more often than not are non-planar.

An assembling routine may be suggested so that strains and harmful mobilities should be avoided.

Self-alignment of centrifugal governors reduces friction and, hence, the deadband of the governor. The latter may be also enhanced by using a horizontal governor shaft instead of a vertical one, by replacing pivots by flexible bands and by avoiding the twisting or slanting torque at the sleeve, or else by replacing the sleeve by a spool or slide valve rotatable in a fixed bore.

Self-alignment of valves and gates improves their sealing properties.

Chapter 3

# THREE-DIMENSIONAL MECHANISMS WITH LOWER PAIRS (TURNING JOINTS)

## 3.1. Multiarm Groups

When statically determinate mechanisms are designed, the most difficult task is to select the structural pattern of a multiarm group, particularly, if the latter is three-dimensional. It may so happen that one part of the group evolves redundant constraints, while the other part has harmful mobilities.

Let us explore multiarm groups having the basic member and several arms. Let us consider, first, only the arms imposing one restraint, which we shall call, in similarity to kinematic pairs, first-class arms. Such arms can be made of a rod with two third-class spherical pairs or we may as well take first-class kinematic pairs—either filamentary or spot ones. An arm imposing several restraints may be considered as several first-class arms.

The basic member may have six degrees of freedom. To eliminate them, it takes six arms. Thus, a zero-mobility group in space is a six-arm one. Similarly, a group having one mobility would be five-arm one, and so on. A group with five mobilities would be a single-arm one. As it has been already shown in Section 1.3 above, each restraint is either a force or a torque being transmitted. Therefore, using the force method for investigating mobilities and restraints is reasonable.

There are six equations of statics concerning a basic member:

$$\Sigma Q_x = 0; \quad (3.1) \qquad \Sigma M_x = 0; \quad (3.4)$$

$$\Sigma Q_y = 0; \quad (3.2) \qquad \Sigma M_y = 0; \quad (3.5)$$

$$\Sigma Q_z = 0; \quad (3.3) \qquad \Sigma M_z = 0; \quad (3.6)$$

The coordinates may be either rectangular or oblique. Torques may be regarded with respect to the same axes as the forces; they may be also considered with respect to other coordinate axes.

One of the equations of statics being reduced to an identity indicates the corresponding mobility. The number of the equations is

reduced accordingly, and the number of the arms has to be reduced to retain static determinability.

If, on the other hand, the equations of equilibrium would not suffice to determine forces in the arms, they have to be supplemented with deformation equations, which indicates the existence of redundant constraints.

Let us consider a single-arm group with the arm extending along $y$ axis. Equations (3.1), (3.3), (3.4), (3.5) and (3.6) become identities, which means that the total mobility equals five. Equation (3.2) remains, out of which but a single force can be found. This yields the first condition of static determinability which is also valid for a multiarm group: *not more than one arm may extend along a single line*. Neither should any resultant of the forces acting upon other arms extend along this arm. This condition is illustrated in Table 3.1 where conditions of the arrangement of the arms, necessary for self-alignment, are given for different numbers of arms.

*Table 3.1*

| Condition | Arrangement of arms (of forces to be determined) | | Maximum permissible number of arms |
|---|---|---|---|
| 1 | In a plane | Along one line | 1 |
| 2 | | In one plane, parallel | 2 |
| 3 | | In one plane, including the same point | 2 |
| 4 | | In one plane, in general | 3 |
| 5 | In space | Parallel | 3 |
| 6 | | Including the same point | 3 |
| 7 | | In parallel planes, intersecting the line perpendicular to this plane | 4 |
| 8 | | Intersecting two crossing lines | 4 |
| 9 | | In parallel planes | 5 |
| 10 | | Intersecting a line, or parallel to this line | 5 |
| 11 | | In general | 6 |

Let us consider a two-arm group with the arms extending parallel with $y$ axis (Fig. 3.1*a*). Equations (3.1), (3.3), (3.4) and (3.5) become identities. Therefore, there are four mobilities indicated in the

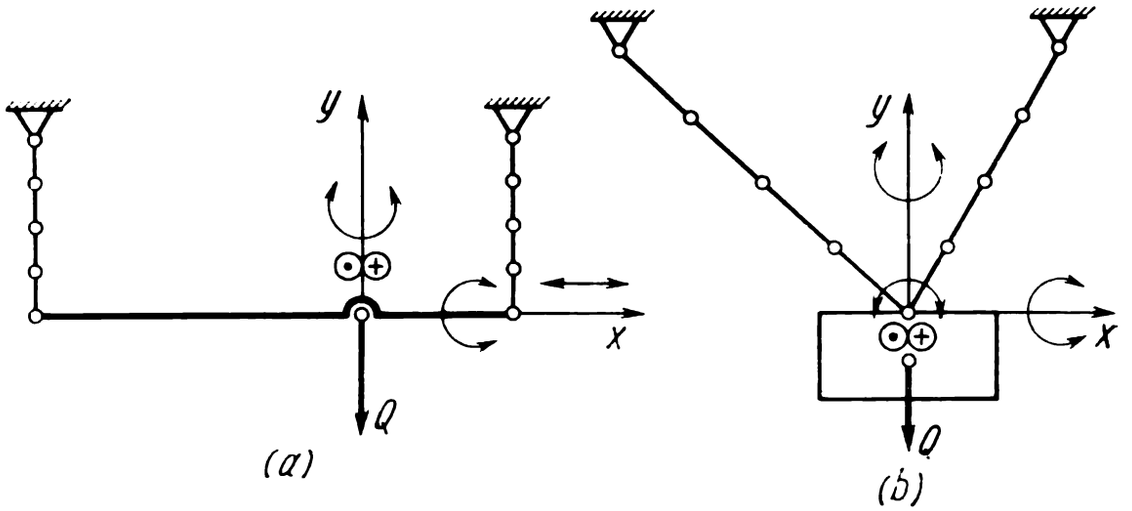


Fig. 3.1. Two-arm groups of four mobilities

drawing with arrows (the mobility perpendicular to the plane of the drawing is indicated with an encircled cross—the tail of the demonstrating arrow, or with an encircled point—the point of the arrow). Two equations $\Sigma Q_y = 0$ and $\Sigma M_z = 0$ remain, out of which but two forces can be determined.

Thus, in addition to the first condition, the second condition has to be satisfied as well (cf. Table 3.1): *not more than two parallel arms may belong to one plane.*

Let us consider a two-arm group with the arms intersecting at one point the line of action of the given force (Fig. 3.1*b*). Equations (3.3), (3.4), (3.5) and (3.6) become identities. Thus, there are four mobilities indicated in the drawing with arrows. Two equations $\Sigma Q_x = 0$ and $\Sigma Q_y = 0$ remain, out of which but two forces may be determined. Consequently, beside the first condition, the third one has to be satisfied, too (cf. Table 3.1): *not more than two arms intersecting a given force at a single point may belong to one plane.*

Considering a three-arm group with the arms belonging to a single plane (Fig. 3.2*a*) we see that equations (3.3) to (3.5) become identities, yielding three mobilities indicated with arrows in the drawing. Three equations $\Sigma Q_x = 0$, $\Sigma Q_y = 0$ and $\Sigma M_z = 0$ remain, enabling determination of but three forces. Thus, apart from the previous three conditions, the fourth one has to be satisfied: *not more than three arms may belong to one plane* (provided they are not parallel and do not include the same point).

Let us consider a three-arm group with three parallel arms (Fig. 3.2*b*). A similar group with three point or spot pairs (spheres bearing upon a plane) is shown in Fig. 3.2*c*.

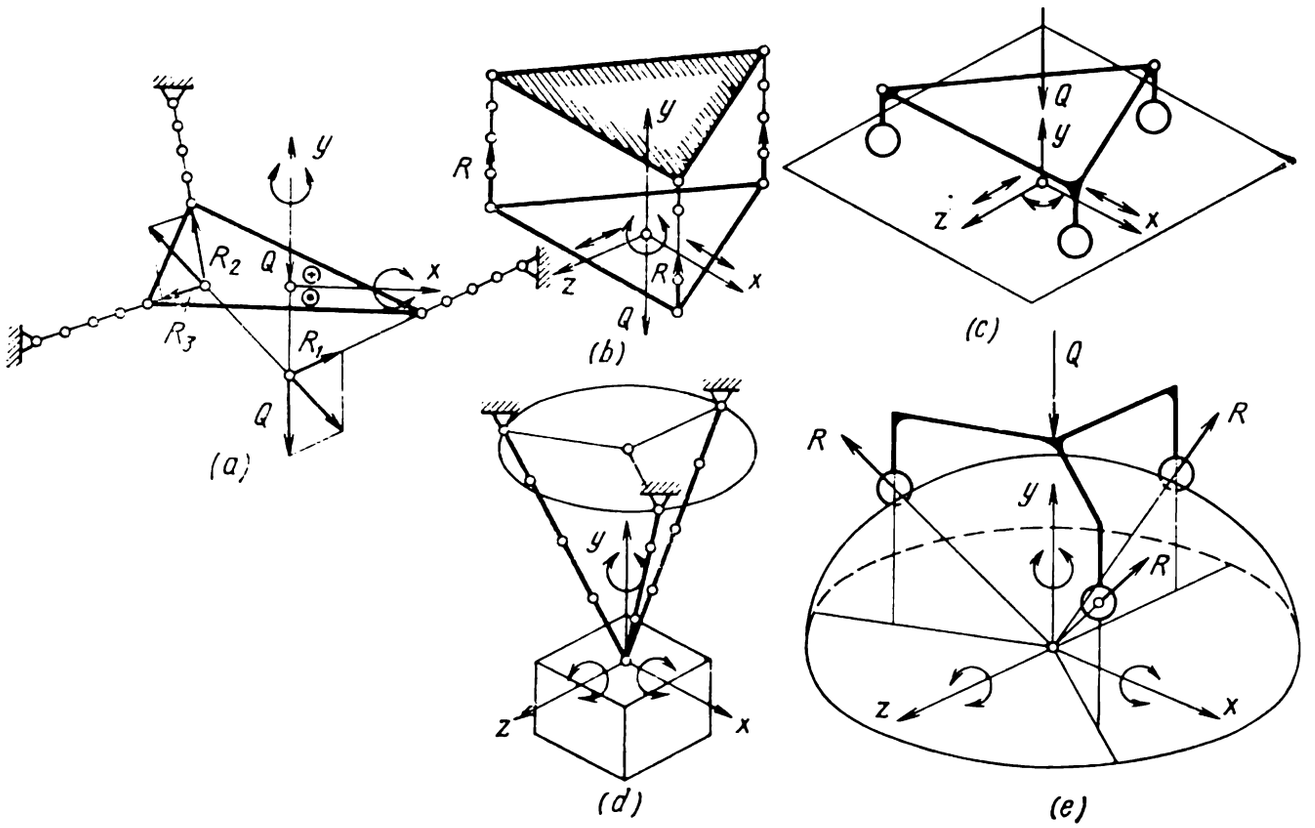


Fig. 3.2. Three-arm groups of three mobilities

Equations (3.1), (3.3) and (3.5) become identities, yielding three mobilities indicated in the drawing with arrows. Three equations remain: $\Sigma Q_y = 0$, $\Sigma M_x = 0$ and $\Sigma M_z = 0$, out of which but three forces may be determined. Hence, the fifth condition has to be satisfied (cf. Table 3.1): *not more than three arms may extend parallel to one another* (provided they do not belong to the same plane).

Let us further consider a three-arm group with the arms intersecting at one point (Fig. 3.2*d*). A similar group with point or spot pairs (balls bearing on a sphere) is illustrated in Fig. 3.2*e*. Equations (3.4), (3.5) and (3.6) become identities, leaving us three mobilities indicated with arrows. The three remaining equations $\Sigma Q_x = 0$; $\Sigma Q_y = 0$ and $\Sigma Q_z = 0$ enable one to determine but three forces.

The sixth condition can be derived: *not more than three arms may intersect at one point* (provided they do not belong to the same plane).

Let us now consider a four-arm group with the arms belonging to parallel planes and intersecting a line perpendicular to these planes (Fig. 3.3*a*).

A similar group with point or spot pairs (spheres bearing upon a cylinder) is shown in Fig. 3.3*b*. It has been developed by the author to ensure that each end of a helical spring uniformly urges four

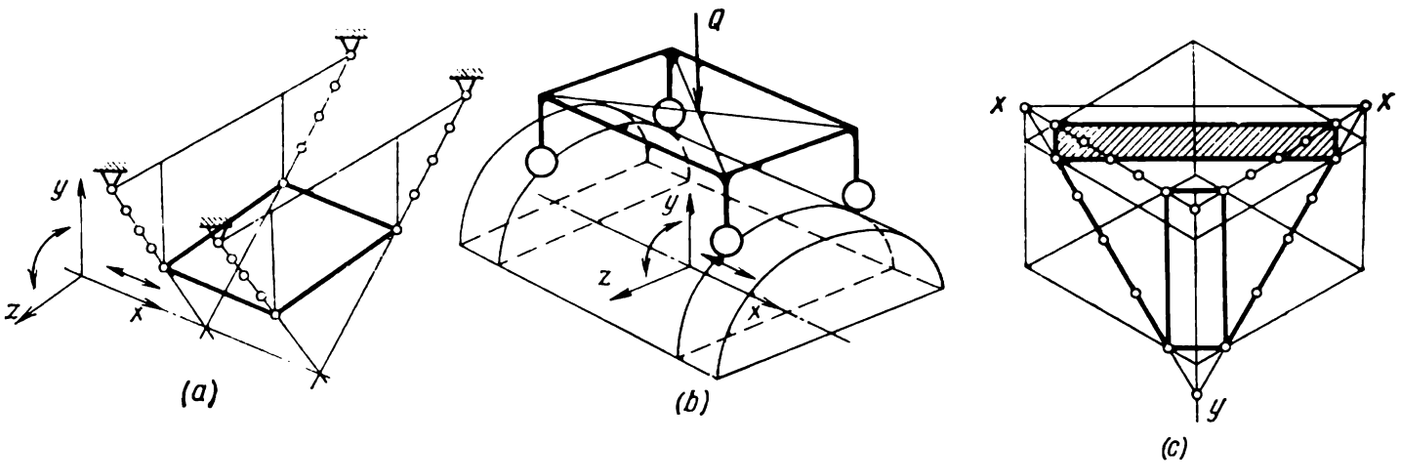


**Fig. 3.3. Four-arm groups of two mobilities**

contacts. Similarly, the designs of Fig. 3.2*c* and *e* can be used to ensure uniform urging of three contacts by a single spring. Equations (3.1) and (3.4) become identities, leaving two mobilities indicated with arrows. The four remaining equations $\Sigma Q_y = 0$, $\Sigma Q_z = 0$, $\Sigma M_y = 0$ and $\Sigma M_z = 0$ enable one to determine but four forces. Thus, the seventh condition may be formulated (cf. Table 3.1): *with arms belonging to parallel planes and intersecting a line perpendicular to these planes, not more than four such arms are permissible to provide for self-alignment.*

Let us consider a four-arm group with all the arms intersecting two crossing lines *xx* and *yy* (Fig. 3.3*c*). The equations of torques about these axes are reduced to identities, leaving four equations out of which not more than four forces may be determined. This yields the eighth condition of arriving at a multiarm group devoid of redundant constraints: *with arms intersecting two crossing lines, not more than four such arms are permissible.* It goes without saying that a four-arm group is expected to satisfy the conditions derived for single-, two- and three-arm groups.

Let us consider now a five-arm group with the arms belonging to parallel planes (Fig. 3.4*a*). A similar group with point or spot pairs is shown in Fig. 3.4*b*. Equation (3.3) becomes an identity. Thus, there is the single mobility indicated with an arrow. The remaining five equations enable one to determine but five forces, which results in the ninth condition of self-alignment (cf. Table 3.1): *with arms belonging to parallel planes, not more than five such arms are permissible.*

Now, let us consider a five-arm group with the arms either intersecting a line or extending parallel with the line. A group of this kind with point or spot pairs bearing upon the surface of a body of revolution is shown in Fig. 3.4*c*. In this group some pairs may bear

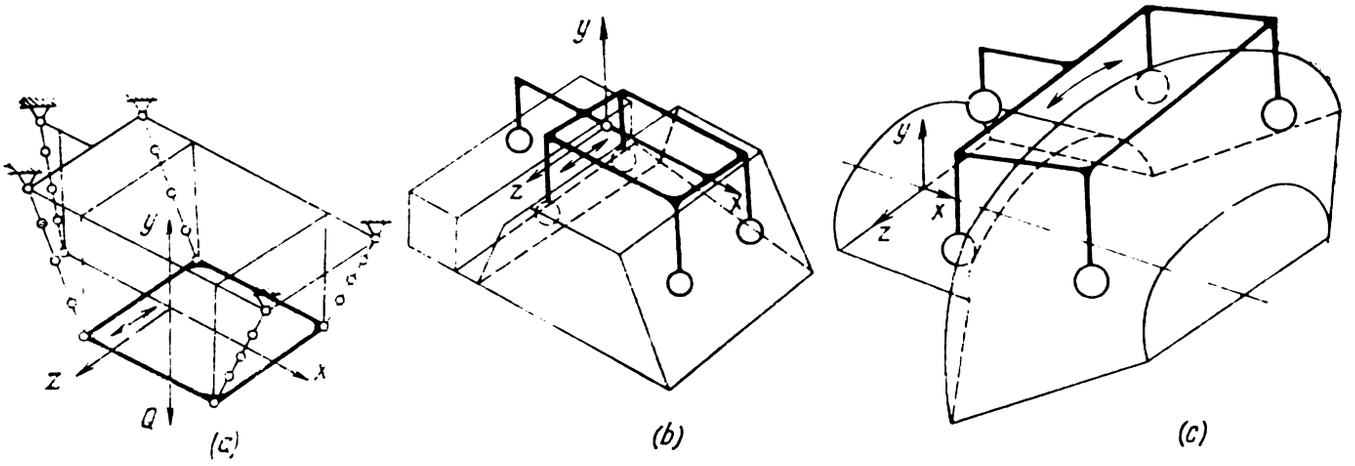


Fig. 3.4. Five-arm groups of a single mobility

upon planes perpendicular to the abovementioned line. Equation (3.4) becomes an identity. The five remaining equations enable one to determine five forces at the most. Hence, the tenth condition: *with arms either intersecting a straight line or parallel with this line, not more than five such arms are permissible.*

With arms extending along normals to a helical surface, equation (3.4) is equivalent to equation (3.1); equation (3.6) is equivalent to equation (3.3), so that two more equations are lost and only three remain. Thus, with arms extending along normals to a helical surface, not more than three such arms are permissible. It is obvious that a five-arm group shall satisfy the conditions derived for group with a smaller number of arms.

Let us consider a six-arm group. For the group to be statically determinate and to have no harmful mobilities, it has to satisfy all the ten conditions derived for groups with a smaller number of arms. which can be explained by the fact that parts of a six-arm group can be regarded as groups with less arms. A group of this kind is shown in Fig. 3.5*a* (with arms) and 3.5*b* (with point pairs). In this case all the six equations of statics are valid, so that forces applied to the six arms can be determined.

Instead of checking a six-arm group for satisfaction of the above ten conditions, it may be explored using the six equations of statics, i.e. to check whether any one of the equations is reduced to an identity.

Among other applications. multiarm groups are used for securing gas-turbine engines [24], [52]. Freedom of redundant constraints is of essential importance in this case, for deformations of the aircraft not to be transmitted to the engine, lest, with the diminutive clear-

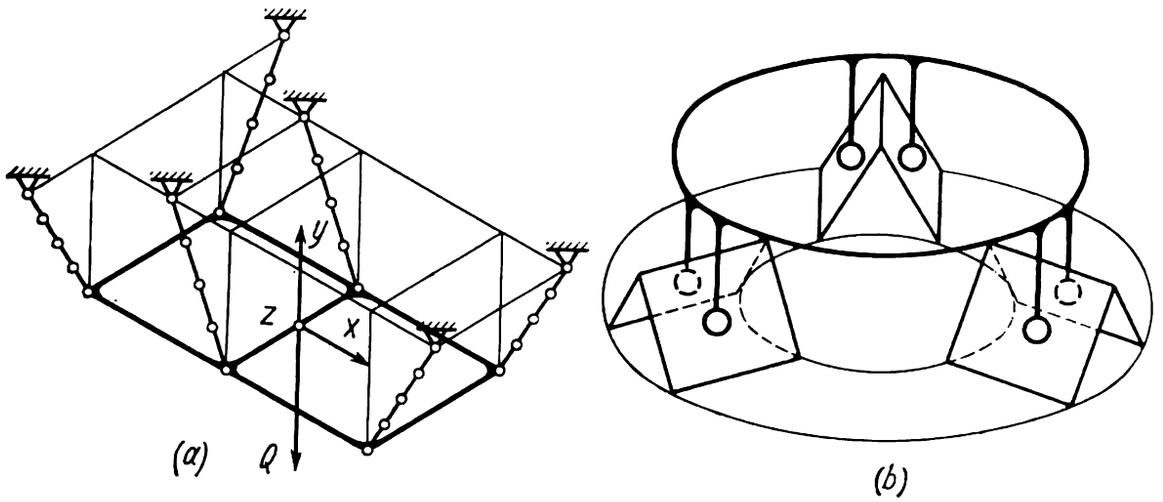


Fig. 3.5. Six-arm groups of zero mobility

ances between the rotary and stationary blades, any deformation of the engine might result in a complete breakdown.

Let us discuss possible designs of multiarm attachment without redundant constraints (Fig. 3.6). With the securing pattern being symmetrical with respect to the axis of the engine (Fig. 3.6*a* and *b*) all the arms may be chosen identical, and the pairs $III_4'$ by which they are connected to the airframe and the engine may be combined in pairs (Fig. 3.6*a*). This will be the general pattern of the arrangement of the arms, similar to the pattern of Fig. 3.5*b*. Three arms may be arranged in a single plane, and the three remaining arms may intersect at one point (Fig. 3.6*b*), or, if required, the latter may be arranged in parallel.

With the rectangular arrangement of the arms (Fig. 3.6*c*) four arms may intersect a single line, and the two remaining arms may be arranged separately. This pattern, however, is deficient in that its lateral rigidity is inadequate. The attachment of the arms to the engine may be arranged in two planes which are perpendicular to the axis of revolution (Fig. 3.6*d*). This pattern has seven arms. To avoid redundant constraints, two of the arms are interconnected by a balance arm. Thus, the efforts applied to the arms are less likely to deform the engine casing.

It is also possible to use a combination attachment pattern including a kinematic pair $III_2'$ and arms. A case of this kind with a spherical pair is illustrated in Fig. 3.6*e*. With this attachment three arms are required, which are arranged in this pattern in a single plane. The attachment with a single revolute $V_2$ pair is shown in Fig. 3.6*f*, in which case one arm will suffice, although shown in the pattern are two arms and a balancing mechanism distributing the

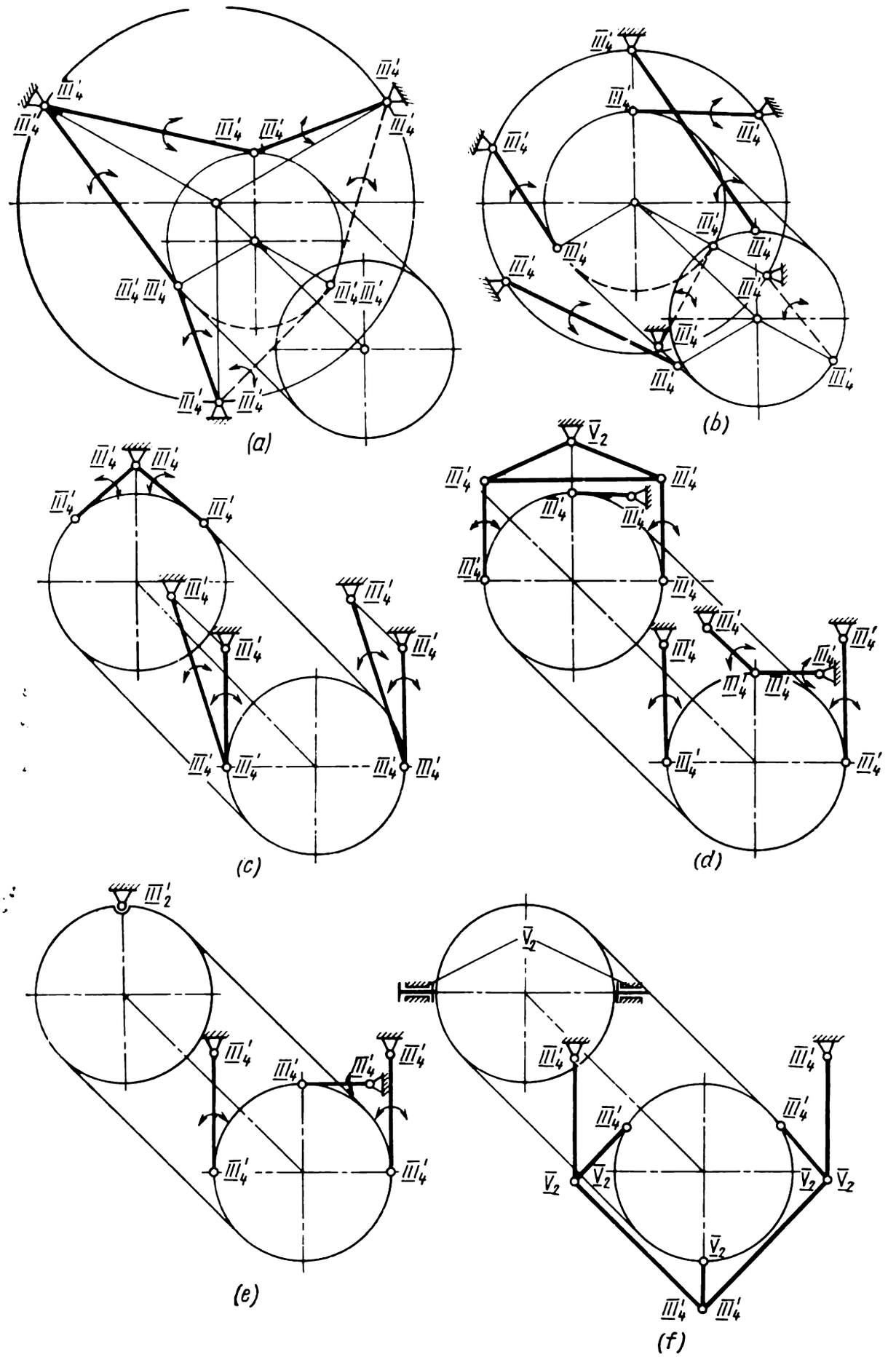
(a)
(b)
(c)
(d)
(e)
(f)

forces among three points of the engine, which, naturally, enhances its working conditions. Multiarm groups are also employed in mechanisms of the adjustable nozzle of turbojet engines [38].

To have a multiarm group without redundant constraints, the conditions of Table 3.1 should be met. With a six-arm group all these conditions have to be satisfied. With a group with less arms the conditions pertaining to this group are to be satisfied, same as the conditions concerning groups with a smaller number of arms which can be considered as parts of the bigger group.

The exploration of static determinacy of a multiarm group has come to resolving a given force applied to the basic member into forces acting along the arms, i.e. to resolution of a force along predetermined lines of action. The number of such forces may vary from one to six, depending on the arrangement indicated in Table 3.1.

The arms discussed above have been solely those with pairs $III'_2$, i.e. those imposing a single restraint. By using pairs of other classes it is possible to have arms imposing a greater number of restraints. Thus, a second-class arm can be obtained by using, respectively, one third-class pair and one fifth-class pair (Fig. 3.7*a*); a third-class arm—with one fourth-class pair and one fifth-class pair (Fig. 3.7*b* and *c*); or a fourth-class arm—with two fifth-class pairs (Fig. 3.7*d*).

Shown in the top right-hand corner of every drawing in Fig. 3.7 are the forces and torques transmitted by the arm because of the restraints. Depending on the number of the restraints imposed by the arms, the quantity of the arms in a zero-mobility group varies. A group with a single basic member would be a three-arm one exclusively with second-class arms. In general, the number of the arms may vary from two to six. Shown in Fig. 2.29 *f* above were two arms $V_{1\,2}$, $V_{1\,2}$, and $III'_{1\,2}$, $V_3$ (connecting-rod—the basic member). Fig. 2.58 illustrates a Stephenson link with four arms: two second-class ones $V_2III'_4$ and $V_2III'_4$ (the eccentric ones) and two first-class ones $III'_4$, $III'_4$ and $V_2III'_4IV_2$ (the suspension and the spool valve).

Big steamships used to incorporate a triple-eccentric Stephenson link gear mechanism. It was a five-arm one. A six-arm group is used in the current collector of electric locomotives. Thus, it would be

---

Fig. 3.6. Suspension patterns of turbojet engines, free of redundant constraints (*a*) with symmetrical arrangements of rods; (*b*) with three rods in one plane perpendicular to an axis and with three rods either intersecting at one point or parallel; (*c*) with four rods intersecting a line perpendicular to an axis and two arms arranged separately; (*d*) with a lever balancing the forces acting upon two points of the engine; (*e*) with a spherical pair $III'_2$ and three rods in a plane perpendicular to an axis; (*f*) with a revolute $V_2$ and a balancing mechanism for ensuring equality of forces acting upon three points of the engine

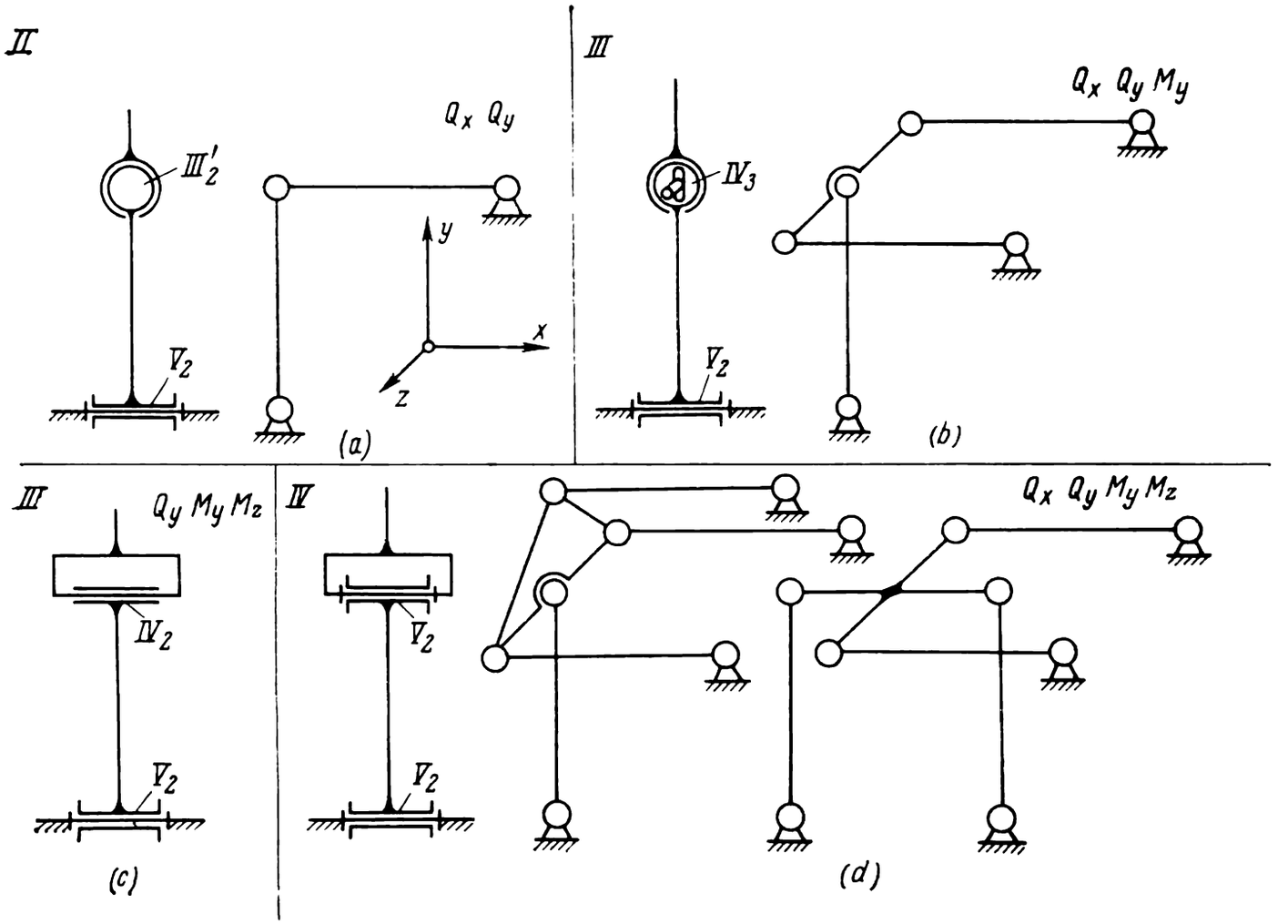


Fig. 3.7. Multiconnected arms
(*a*) second-class; (*b*), (*c*) third-class; (*d*) fourth-class

wrong to presume that zero-mobility groups with a single basic member are always three-arm ones. With groups having two basic members the situation with the number of arms is even more complex, since such groups are not always four-arm ones.

When designing a multiarm group with multiconnected arms, the equations of statics (3.1)—(3.6) should be consulted, same as with single-connected ones.

Multiconnected arms may be substituted by a corresponding number of properly arranged single-connected ones.

Each arm transmits a force (i.e. imposes a linear restraint) along its axis. Two parallel arms, in addition to a force, transmit a torque (i.e. impose an angular restraint) about an axis perpendicular to the plane of these arms (cf. Fig. 3.7*b*). Thus, arms are capable of transmitting a torque only when they transmit a force. Therefore, with the arms being of the first class, the number of transmitted torques

would not be greater than the number of transmitted forces. Hence, a third-class arm (cf. Fig. 3.7*c*) transmitting two torques and one force cannot be replaced by three first-class arms.

When selecting replacement arms, one should start with force-transmitting arms. In Fig. 3.7*a*, *b* and *d* forces $Q_x$ and $Q_y$ are transmitted. Consequently, there should be an arm directed along $x$ axis and an arm directed along $y$ axis.

To transmit a torque, second arms should be introduced, running parallel with the force-transmitting arms. In Fig. 3.7*b* and *d*, the second arm should be added along $x$ axis to transmit a torque $M_y$. An arm extending along $y$ axis would not do, since it is incapable of creating a torque about this axis. In Fig. 3.7*d*, to transmit a torque $M_z$, one should introduce either an arm parallel with $x$ axis (the central diagram) or an arm parallel with $y$ axis (the right-hand diagram).

## 3.2. Hydraulic Drive Mechanisms

Systems of automatic control make wide use of positive-displacement or hydrostatic drives consisting of a hydraulic pump discharging working fluid under a high pressure and a hydraulic motor powered by this fluid. The angular speed (or frequency) may be varied either by controlling the output of the pump or by influencing the hydraulic motor. We are going to discuss below pumps with axial arrangement of the cylinders (three-dimensional pumps). Common-type pumps in aircraft systems operate at 3 000-4 000 r.p.m., and some operate even at a speed 20 000-30 000 r.p.m. The output pressure of common-type pumps is about 210 to 350 kgf/cm$^2$, and that of the unique ones may be as high as 700 kgf/cm$^2$. The power rating of unique hydraulic drives is up to 4 000 kW [2]. In most cases the pump and the motor are of the same construction.

For simplicity sake, let us discuss only the pumps.

An axial-plunger hydraulic pump with a stationary cylinder block is shown in Fig. 3.8. It includes a cylindrical (axial) cam whose followers are the plungers in the cylinders (their number usually equals seven). Force closure is effected either by springs acting upon the plungers or by the pressure of oil (the working fluid) supplied into the hydraulic pump by a special booster pump. To reduce friction, instead of roller followers commonly used in cam mechanisms, the working part of the cam, i.e. the swash-plate, is rotatable on antifriction bearings.

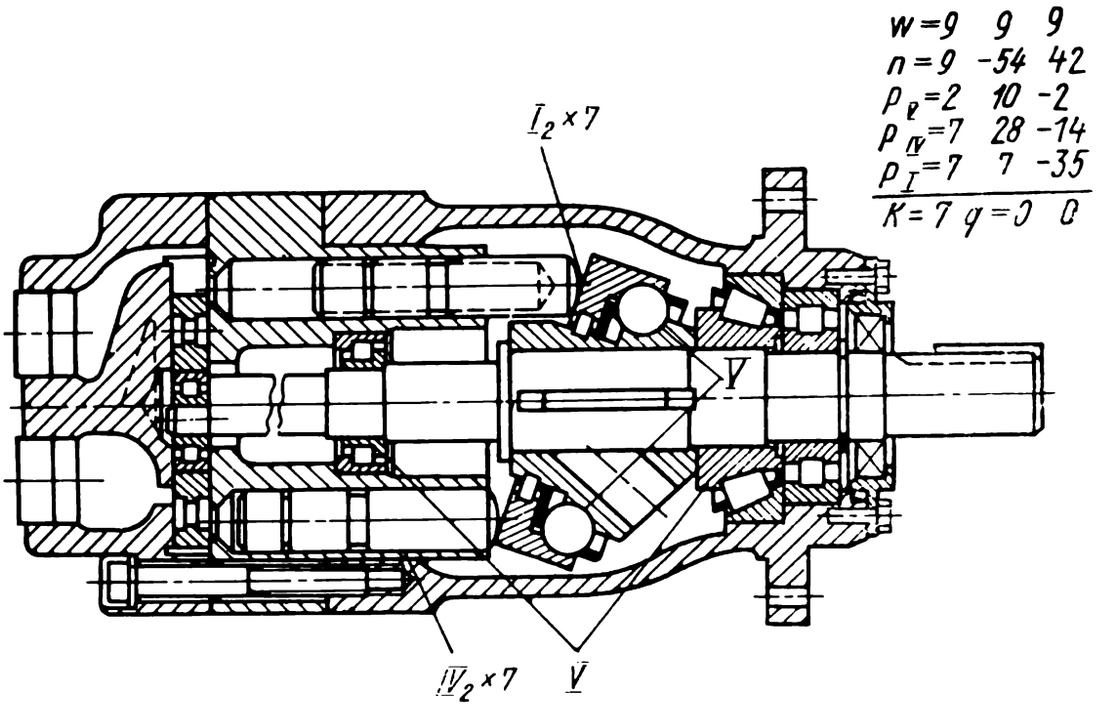


Fig. 3.8. Pumps (nonregulated) with plungers and stationary cylinder block and with self-aligning distribution valve

Oil is distributed by a circular flat valve actuated by a crank mounted on the end of the drive shaft. This valve has a harmless local mobility—rotation about the crank pin.

Let us count redundant constraints in the distributing valve mechanism. For simplicity sake, let us regard the drive as stationary. Then $w = 1$; $n = 1$; $p_{III} = 1$; $p_{II} = 1$; $q = 1 - 6 + 3 + 2 = 0$, i.e. self-aligning of the valve is ensured.

In the main mechanism, the mobility is made up of the main one—the slipping of the swash-plate and of rotation of the seven plungers, i.e. $w = 9$.

The calculation of redundant constraints is given in Fig. 3.8: $q = 0$. Therefore, the mechanism is a self-aligning one, free of redundant constraints.

The drawbacks are the point contact of the plungers with the swash-plate and the lateral efforts acting upon the cylinder walls, causing non-uniform wear of the cylinder walls and of the plungers and a torque transmitted to the cylinder block. To eliminate this torque, plungers are connected to the swash-plate through connecting-rods with spherical ends (Figs. 3.9 and 3.12) $III_2'$ and $III_2'$. To avoid a harmful mobility, this design requires a kinematic connection between the cylinder block and the swash-plate: in Fig. 3.9 it is effected with aid of a universal joint $III_5''$, and in the design

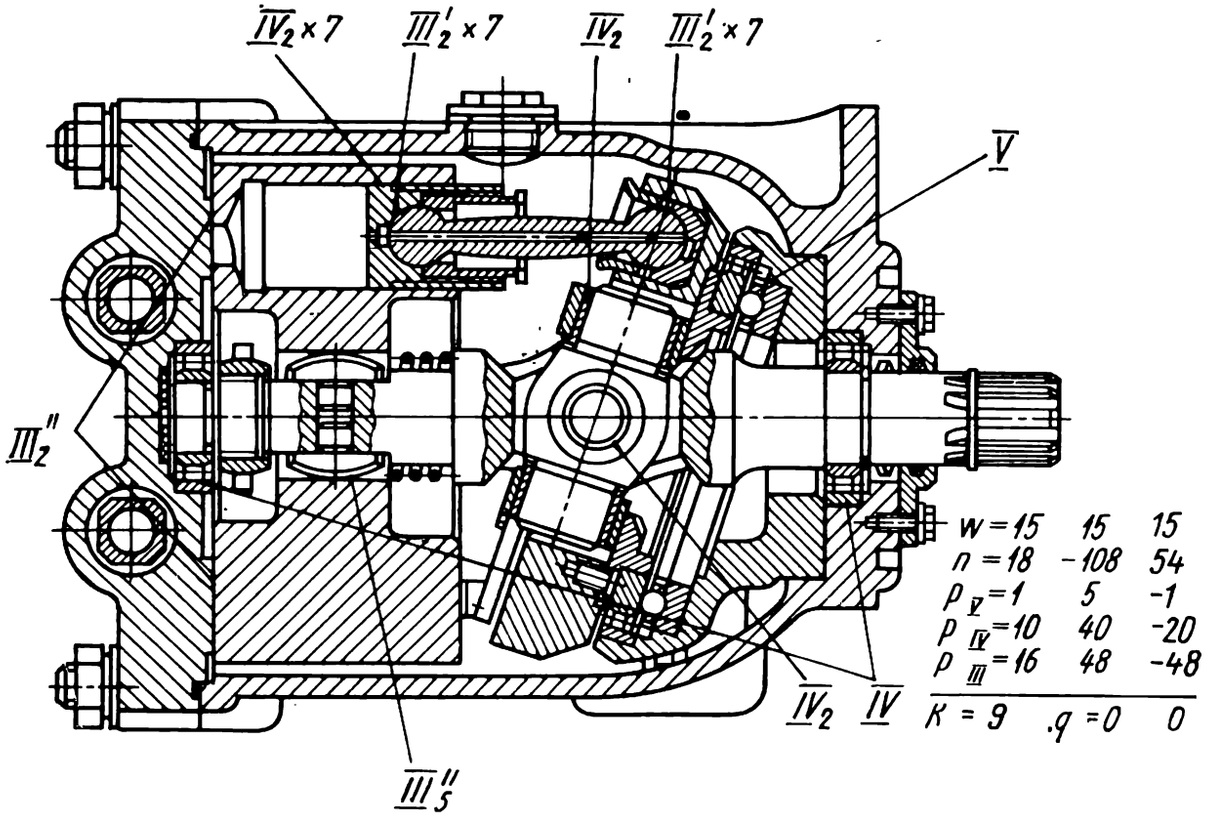


Fig. 3.9. Pump with connecting-rods and rotating cylinder block—nonregulated, with self-aligning valve

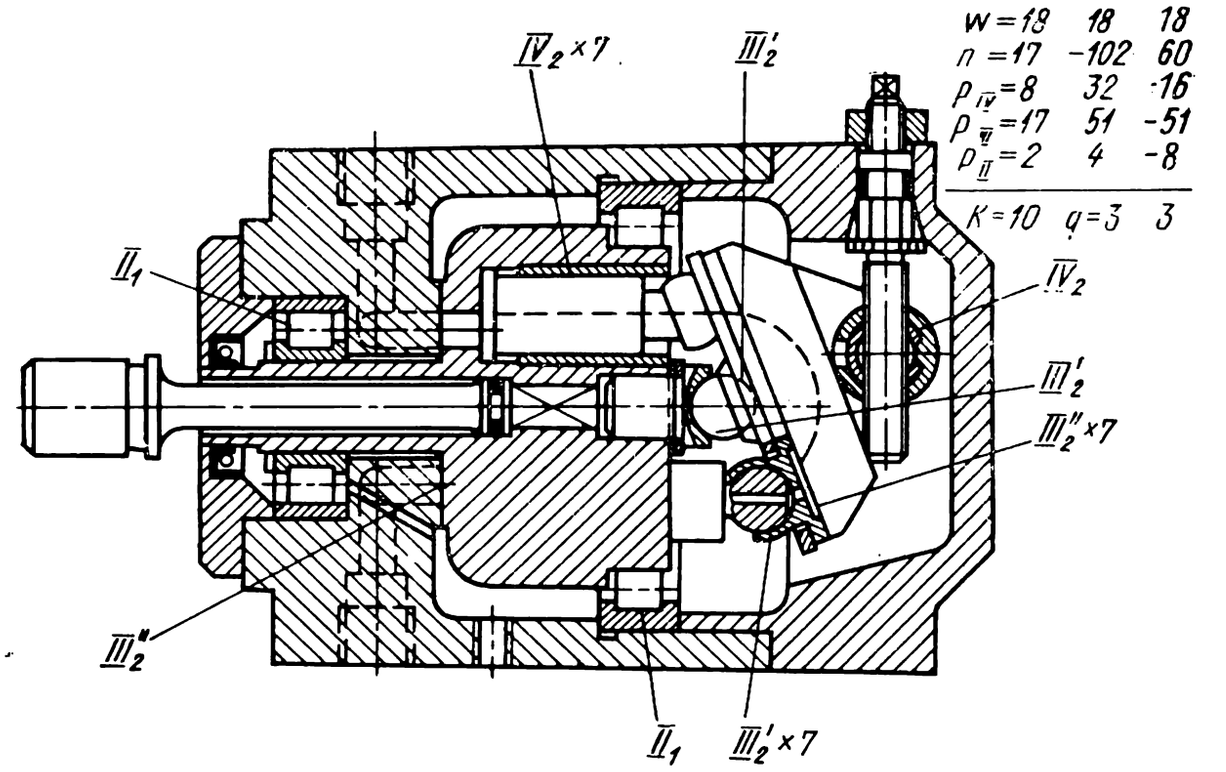


Fig. 3.10. Pump with shoes and rotating cylinder block (controlled by varying swash-plate tilting. The valve is not self-aligning)

of Fig. 3.12 the connection is provided by the connecting-rods abutting against the plungers which are elongated. With several plungers redundant constraints are inavoidable, but they are not harmful because the mechanism would be operable even when the circumferential force is transmitted by a single plunger. The inclination of the connecting-rods in this design is insignificant, so that the pressure against the walls of the cylinders and the torque transmitted to the cylinder block are practically close to zero.

The design with shoes (Fig. 3.10) possesses intermediate properties. The pairs $III_2'$ and $III_2''$ have surface engagement, but the load applied to the cylinder walls and the torque transmitted to the cylinder block are not eliminated. This design is simpler than the one with connecting-rods, for no kinematic connection of the cylinder block with the swash-plate is required. The shoe design is ingenious in that oil from the cylinder is fed to the shoe through a duct in the plunger to relieve the shoe and thus to step up the efficiency factor and to reduce the wear of the mechanism.

The mechanism of Fig. 3.8 is nonregulated. Making it regulated would have been a difficult task since it would involve varying the parameters of the rotating swash-plate on the run. Therefore this mechanism is usually used as hydraulic motor. To make the mechanism regulated, there are used hydraulic pumps with a rotating cylinder block and a stationary swash-plate (Figs. 3.10 and 3.11). The control action is effected by varying the inclination of the swash-plate which is equivalent to varying the parameters of the cam, and with the swash-plate being immobile, this is easily attained. The cylinder block itself acts as the distributing valve in this mechanism, engaging in its rotation the valve face—either flat (Figs. 3.10 and 3.11) or spherical (Fig. 3.12). Self-alignment of a valve (the absence of redundant constraints) is essential for its fluid-tight sealing. The designers of steam-powered machinery were well aware of this fact and made all the flat valves self-aligning. Self-aligning distribution valves are used in all designs of railway air brakes. In hydraulic drives, however, this requirement is not always met.

In Fig. 3.9 the cylinder block is retained by the planar pair $III_2''$ and the toothed universal joint $III_5''$ (the connecting-rods and plunger take no part in retaining the cylinder block in its position). From (1.1): $q = 0 - 6 \times 1 + 3 \times 2 = 0$, i.e. redundant constraints are none; self-alignment and reliable performance are provided for.

In Fig. 3.10 the cylinder block rotates in two bearings which may be regarded as pairs $II_1$ and a planar pair $III_2''$. From (1.1): $q = 1 - 6 \times 1 + 3 \times 1 + 2 \times 2 = 2$. Thus, there are two redund-

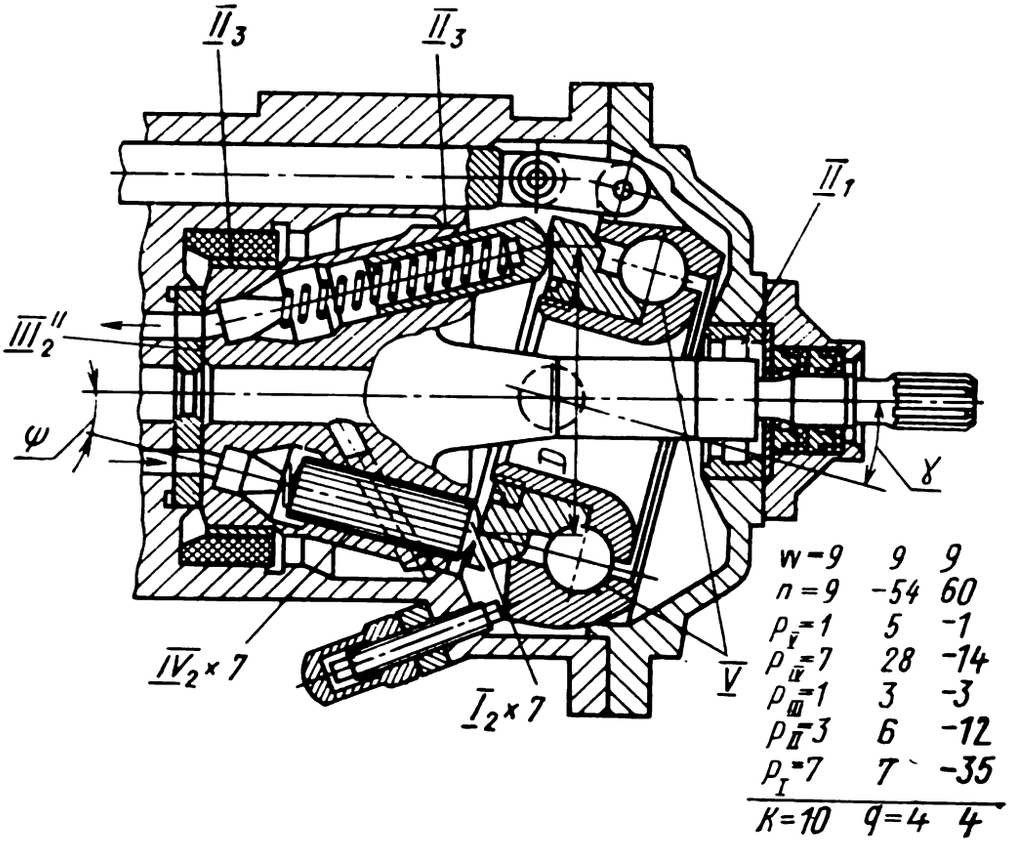


Fig. 3.11. Pump with plungers and rotating cylinder block (regulated by varying swash-plate tilt)

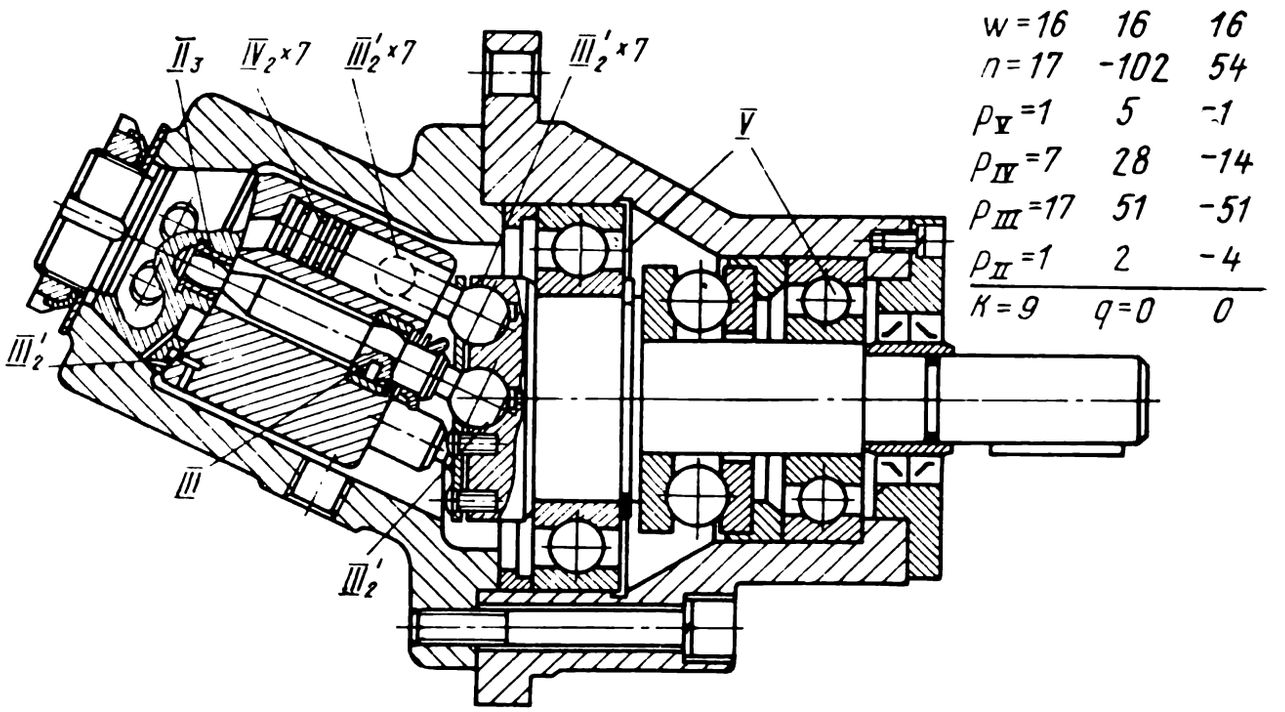


Fig. 3.12. Nonregulated pump with connecting-rods, rotating cylinder block and driven swash-plate. The valve is self-aligning

ant constraints. Proper sealing of the distribution valve can be attained exclusively by its high-precision lapping and is easily impairable.

To correct the design, one of the bearings has to be eliminated. Moreover, the design of Fig. 3.10 does not explain clearly what member takes up the reaction of the shoes to the swash-plate as the screw acting as a cantilever beam could not in all probability sustain this force.

In Fig. 3.11 the cylinder block rotates in as many as three bearings $II_3$, $II_3$ and $II_1$ and one planar $III_2''$ pair. Four redundant constraints are imposed, so that two bearings are superfluous.

In a mechanism with connecting-rods and a rotating cylinder block the working torque is transmitted to the swash-plate, not to the block. Thus, it is expendient to have the swash-plate connected to the drive (cf. Fig. 3.12) and to arrange the axis of the cylinder block at an angle. To adjust the output, the angle is varied by turning the cylinder block about a transverse hollow shaft through which oil is supplied.

The valve face is spherical.

Let us consider the cylinder block jointly with the central rod.

From (1.1): $q = 1 - 6 \times 2 + 3 \times 3 + 2 \times 1 = 0$, i.e. self-alignment of the valve is provided for, and performance is enhanced.

## 3.3. Helicopter Mechanisms

The most sophisticated element of a helicopter structure is the wobble plate mechanism. It was invented in 1911 by B.N. Yuriev—then a student, later an academician. It was he who also invented a helicopter with a single lifting rotor and a single steering tail rotor—the design most widely used nowadays.

The wobble plate mechanism may have different structures, but its operating principle is the same. Both the lifting and steering rotors of a helicopter are variable-pitch rotating-blade ones, and rotation of the blades is what the wobble plate mechanism controls.

Blades of the lifting rotor are usually connected with the hub by horizontal and vertical pivoting joints (Fig. 3.13). Owing to them, the blade self-aligns along the resultant of aerodynamic force and centrifugal and tangential inertia forces, which eliminates a bending moment applied at the root of the blade. This is an interesting case of mobility reducing strain, contrary to the commonly shared opinion that the opposite is true. This principle should be employed in other designs, e.g. in locomotives.

The wobble plate mechanism controls not only the general pitch of the blades, which is essential for controlling the vertical motion of the helicopter; it also controls the cyclic pitch, i.e. the pitch varying with the angle of rotation of the rotor.

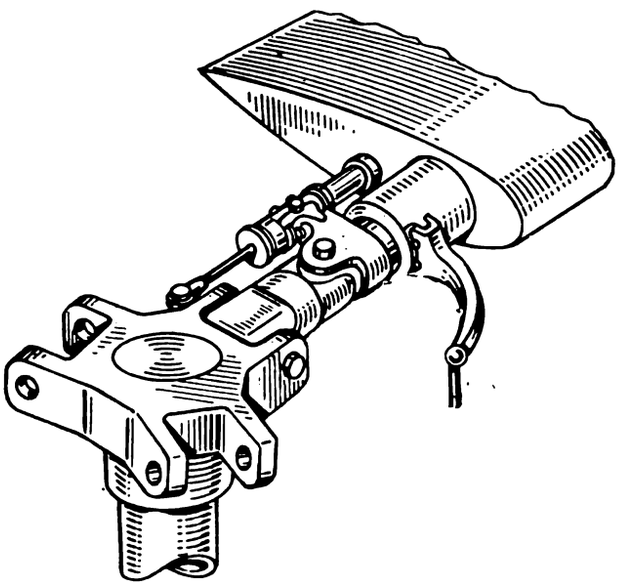

Fig. 3.13. Movable connection of a lifting rotor blade with the hub

For the helicopter to move forward, it is necessary that the pitch of a rear blade should be greater than that of a leading one, which produces the resultant forward force. The "longitudinal" cyclic pitch is controlled by longitudinal motion of the control stick.

For helicopter to bank to the left, the pitch of a right-hand blade has to be greater than that of a left-hand one. The "transverse" cyclic pitch is controlled by moving the stick transversely.

The control member of the mechanism may extend through a hollow shaft, and the structure is called "the spider" for its shape (Figs. 3.14, 3.15, 3.16*a* and *b*). It may alternatively be arranged externally, and then the structure is called annular (Figs. 3.17*a*, *b*, *c* and 3.18). The control member has three mobilities in accordance with its control functions being concerned with the general pitch, the longitudinally variable pitch and the transversely variable pitch. The actuating spider mechanism is illustrated in Fig. 3.14, with $q = 2$.

Let us consider the spider wobble plate mechanism of Fig. 3.14 with a three-blade rotor. The spider has three rigid feet. The feet are connected to the blades through arms $III_2'$, $V_2$. The spider rotates jointly with the rotor. We are going to disregard this rotation, same as the mobilities of the blades owing to their pivotal connection to the hub for the sake of simplicity, since these mobilities are irrelevant for eliminating the redundant constraints.

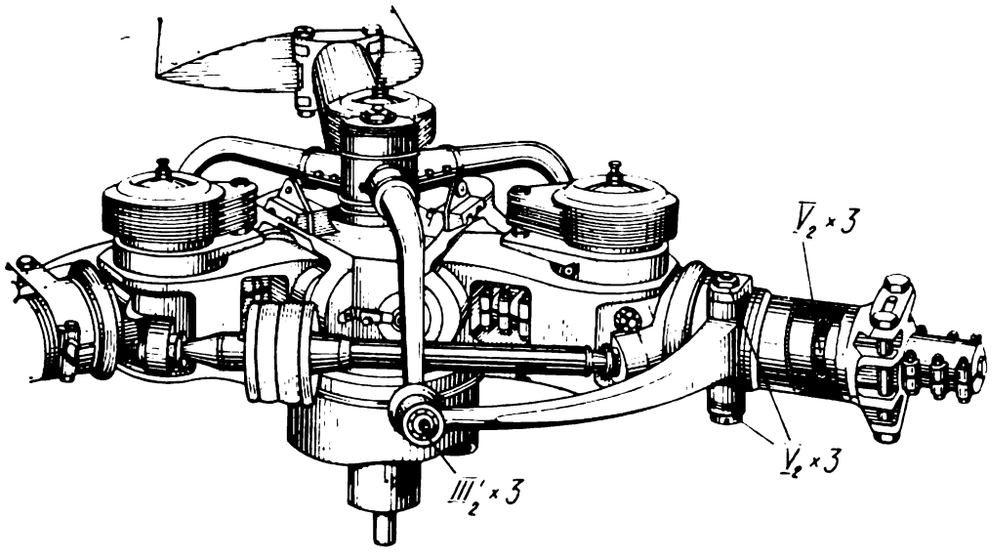


| | | |
|---|---|---|
| $w = 4$ | 4 | 4 |
| $n = 17$ | -66 | 36 |
| $p_V = 6$ | 30 | -6 |
| $p_{IV} = 1$ | 4 | -2 |
| $p_{III} = 10$ | 30 | -30 |
| $K = 6$ | 2 | 2 |

Fig. 3.14. "Spider" wobble-plate mechanism—a real-life structure with $q = 2$

Let us consider only the mobilities involved in the control action, namely, controlling the general pitch by raising the spider and controlling the longitudinal and transverse cyclic pitch by rotating the spider about two horizontal axes.

To simplify our task, we shall consider the three control rods $III_2' III_2'$ as fixed ones, and then we shall substitute the control mobilities in the structural formula by the local mobilities (rotation about their proper axes) of the three rods. In some cases, other local mobilities will be added, e.g. in Figs. 3.14 and 3.16*a* there is the local mobility of the guide sleeve $III_2'IV_2$ of the spider.

The spider is guided by the sleeve made up of the serial connection of two pairs $III_2'$ and $IV_2'$ (not shown in the drawings of Figs. 3.14 and 3.16*a*), while this connection imposes two restraints and yields one local mobility—rotation of the connecting bushing. Thus, $w = 4$.

The calculation of redundant constraints is given in the Table of Fig. 3.14, with $q = 2$, i.e. the mechanism is operable owing to strain and deformation of the members. Another drawback is the limited length of the $V_2$ joints transmitting the torque, which adds to the strain of their operation.

The mechanism rotating the blade includes a lever with pairs $III_2'V_2$ and a joint providing for rotation of the blade $V_2$. The lever extends perpendicularly to the force transmitted by the pair $III_2'$ and is bent by the moment of this force. Let us determine the mobility of the kinematic connection between the spider and the body of the

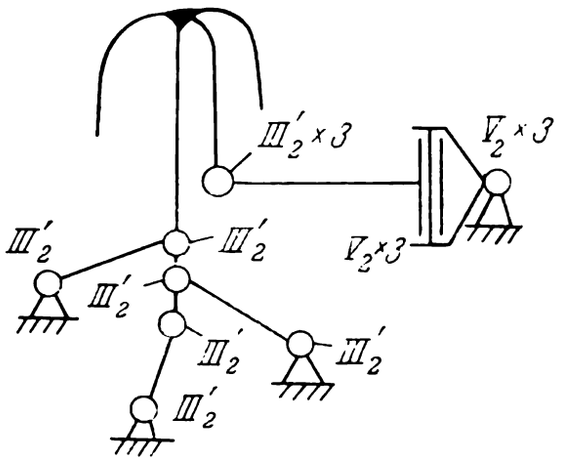


| $w$ = 3, rotations of control rods = 3 | | |
|---|---|---|
| $w = 3$ | 3 | 3 |
| $n = 10$ | − 60 | 30 |
| $p_V = 6$ | 30 | − 6 |
| $p_{III} = 9$ | 27 | 27 |
| $K = 5$ | 0 | 0 |

Fig. 3.15. "Spider" wobble-plate mechanism—the simplest self-aligning design with 10 members

rotor by summing up the mobilities of the serially connected kinematic pairs: 3 + 1 + 1 = 5, while the imposed restraint: 6 — 5 = 1. The three control rods may be single-restraint arms. Thus, the spider is supported by six first-class arms, which is exactly what is needed by a self-aligning mechanism (similar to designs of Figs. 3.5*a* and 3.6*a*, *b* and *c*). The central guide made of pairs $III'_2$ and $IV_2$ is superfluous, its presence merely imposing redundant constraints. Therefore, it should be eliminated, as shown in Fig. 3.15 (this has been checked with a scale model). The mechanism is the simplest one, counting but ten members including the control rods.

Another real-life mechanism with a spider is shown in Fig. 3.16*a*. The blade-rotating mechanism includes a first-class arm $III'_2III'_2$ and a joint $V_2$ providing for rotation of the blade. These kinematic connections would not rotate the spider. To transmit rotation, there has been incorporated the splined joint mechanism of two members and pairs $V_2$, $III'_2$ and $V_2$.

The above considered wobble plate mechanism is a self-aligning one with $q = 0$.

Its advantage is the capability of handling any amount of the blades, although it is more complicated with its 13 members. It may be simplified, however, by removing the splined joint, which can be done with one of the first-class arms being replaced by a second-class one with pairs $III'_2V_2$. It works in extension and compression, with the pair $V_2$ transmitting only random torques, in which the arm differs from the lever $III'_2V_2$. This design retains the advantage of being operable with any number of the blades. One may go even further and have all the three arms of the second class. Then

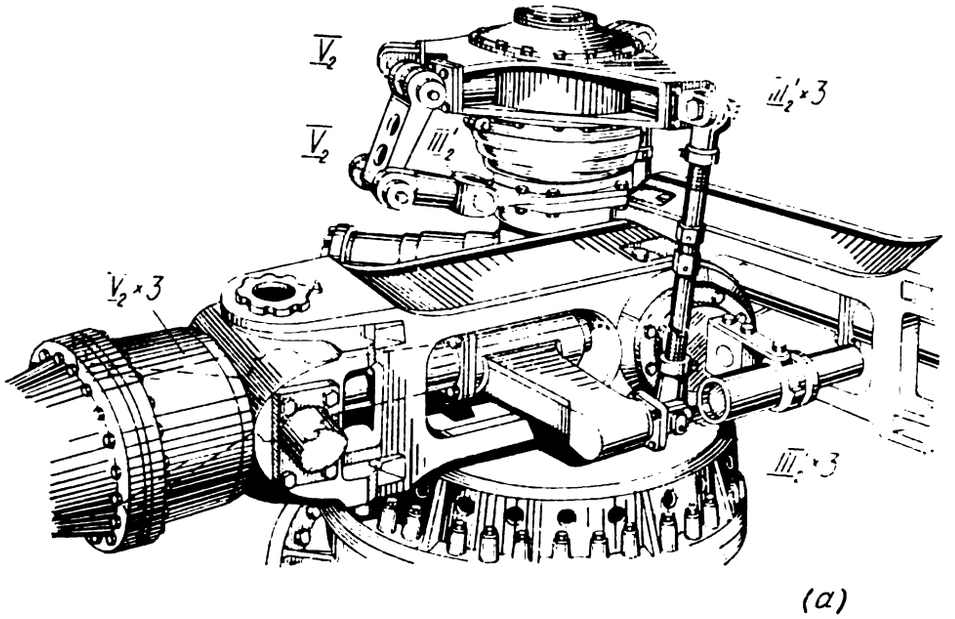


(a)

| | | |
|---|---|---|
| $w = 7$ | 7 | 7 |
| $n = 13$ | -78 | 42 |
| $p_V = 5$ | 25 | -5 |
| $p_{IV} = 1$ | 4 | -2 |
| $p_{III} = 14$ | 72 | 42 |
| $K = 7$ | 0 | 0 |

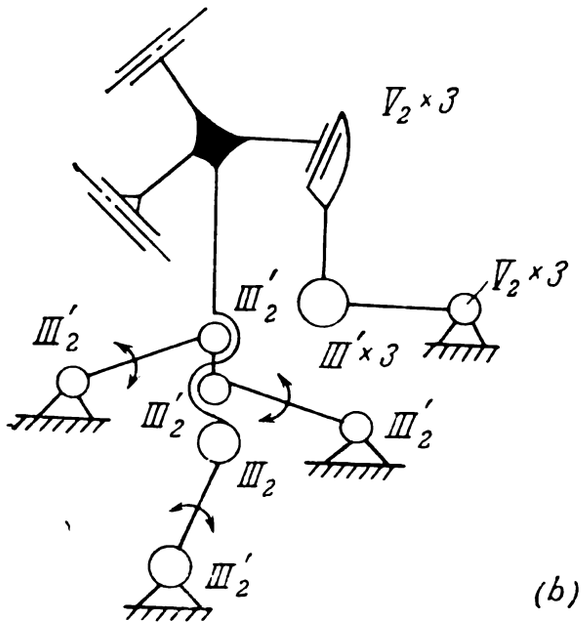


(b)

| | | |
|---|---|---|
| $w = 3$ | 3 | 3 |
| $n = 10$ | -60 | 30 |
| $p_V = 6$ | 30 | -6 |
| $p_{III} = 9$ | 27 | -27 |
| $K = 5$ | 0 | 0 |

Fig. 3.16. "Spider" wobble-plate mechanisms

(*a*) real-life design free of redundant constraints but having 13 members; (*b*) another simplest design with arms not subjected to bending and free of redundant constraints, with 10 members

the central guide may be eliminated (Fig. 3.16*b*), and the design becomes similar to that of Fig. 3.15 by also having 10 members. It is suitable for a six-blade rotor, in which case three arms should be of the second class and the three remaining arms of the first class. In general, a second-class arm replaces two first-class ones, while being considerably simpler with its two pairs $V_2$ and $III_2'$. If compared

with four spherical pairs $III_2'$, the use of second-class arms may significantly simplify the mechanism.

A real-life design of a wobble plate mechanism of the annular type is shown in Fig. 3.17*a*. It is fairly complicated with its 16 members.

In a wobble plate mechanism with a spider the control rods are connected by joints arranged at the axis of its rotation. In an annular structure this is impossible, so that one more ring has to be used—the bottom one which is not rotatable and, therefore, connected to the housing by a splined joint. In the design of Fig. 3.17*a* first-class arms are used, and the second splined joint has to be incorporated to provide for rotation of the top ring. This design, however, may be significantly simplified—see Fig. 3.17*b*.

By connecting the blades with the top ring by second-class arms $V_2III_2'$, the top splined joint and the central guide are eliminated. By connecting the control rods with the bottom ring also by second-class arms $V_2III_2'$, the bottom splined joint may be eliminated, too. Although in this design the top and bottom rings are to be connected to form a planar pair $III_2''$, this is quite feasible with the use of sliding-contact bearings.

If antifriction or rolling contact bearings are preferable, it would be better to have here a turning pair $V_1$; then two second-class arms should be replaced by first-class ones—see Fig. 3.17*c*. It does not matter whether this replacement takes place at the bottom or at the top. The design is also suitable for six-blade rotors, in which case three of the blades should be furnished with first-class pairs. In principle, it is suitable for any number of the blades, provided the numbers of the first- and second-class arms are properly selected.

There also exists a wobble plate mechanism (Fig. 3.18) where the bottom ring is supported by a double Hooke's joint instead of a splined joint (as is the case with the design of Fig. 3.17*a*). Although somewhat simpler, it is, nevertheless, complicated enough with its 15 members.

One should remember, though, that a ball joint has considerable sliding friction which is to be overcome in the control action, thus complicating the pilot's task. A wobble plate mechanism with a Hooke's joint is free from this drawback. The design of tail rotors is simpler than that of lifting rotors, since the angle of inclination of blades in the former is constant during one revolution, and we shall not discuss it.

**Summary.** The application of the self-alignment principle to the wobble plate mechanism of a helicopter enables one to simplify it by reducing the number of members from 16 to, in some cases,

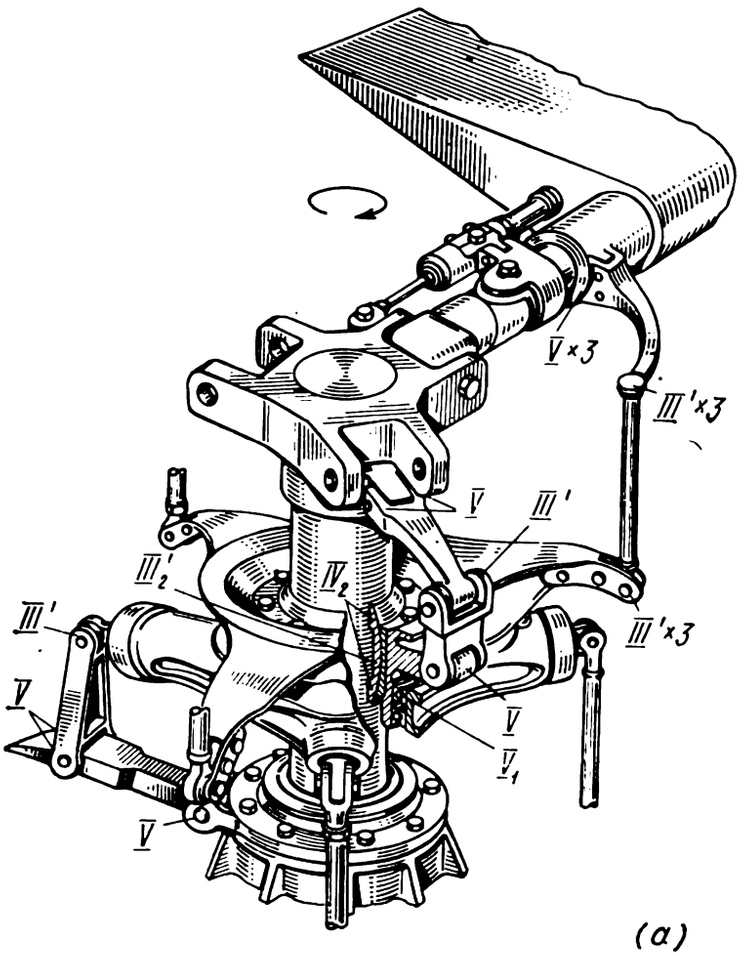


(a)

| Rotation of control rods (3)<br>Rotation of I-class arms (3)<br>Rotation of block (1) | | w=7 |
|---|---|---|
| w = 7 | 7 | 7 |
| n = 16 | -96 | 48 |
| $p_V$ = 8 | 40 | -8 |
| $p_{IV}$ = 1 | 4 | -2 |
| $p_{III}$ = 15 | 45 | -45 |
| K = 8 | 0 | 0 |

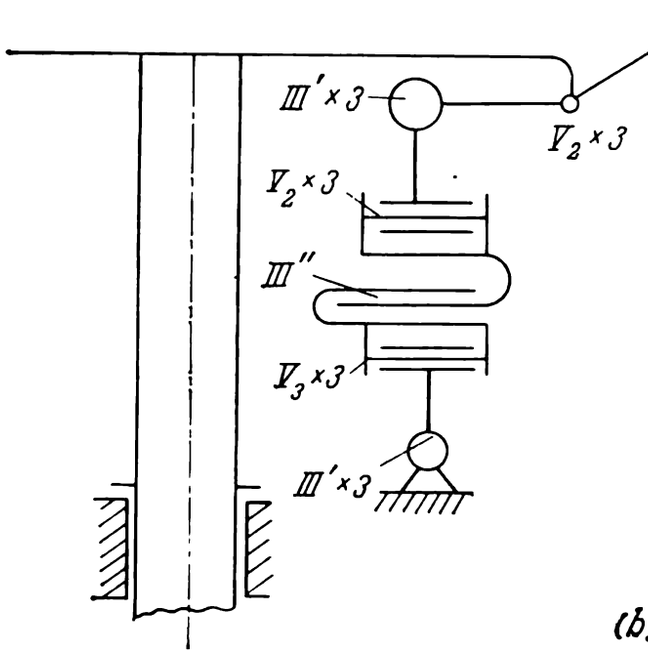


(b)

| | | |
|---|---|---|
| w = 0 | 0 | 0 |
| n = 11 | -66 | 30 |
| $p_V$ = 9 | 45 | -9 |
| $p_{III}$ = 7 | 21 | -21 |
| K = 5 | 0 | 0 |

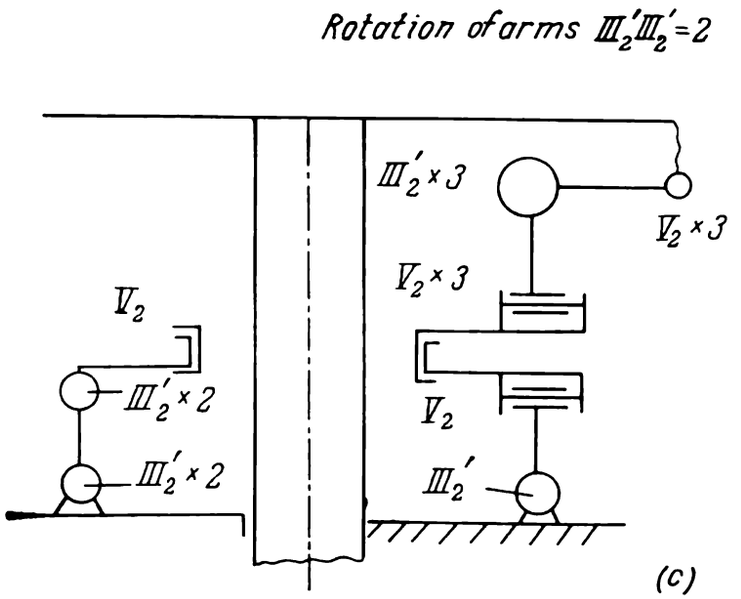


| | | | |
|---|---|---|---|
| $w = 2$ | 2 | 2 |
| $n = 11$ | -6 6 | 30 |
| $p_V = 8$ | 40 | -8 |
| $p_{III} = 8$ | 24 | -24 |
| $K = 5$ | 0 | 0 |

Fig. 3.17. Annular wobble-plate mechanisms

(*a*) complicated real-life design with 16 members; (*b*) design free of redundant constraints with 11 members (not counting control rods and levers); (*c*) design free of redundant constraints, with $V_1$ revolute pair between top and bottom rings, also with 11 members

11 members, to say nothing of the structure becoming correspondingly lighter (which is essential in an aircraft), and the manufacturing accuracy requirement being less strict.

## 3.4. Mechanisms of Gyration Crushers

A gyration crusher consists of two cones between which the product is crushed. The fixed cone has the inner working surface lined with slabs made of wear-resistant steel. The movable cone is installed within the fixed cone and has the outer working surface also lined with slabs. The axis of the movable cone describes during its movement a conical surface (with the vertex at the crusher axis), or a cylindrical surface. The movable cone rotates freely about its axis, that is it has a local mobility.

In primary crushers there is a statically indeterminate mechanism (Fig. 3.19). The movable cone shaft is supported at its upper end by the spherical support $III_2'$ which also takes up its weight. The lower end of the shaft is received in an inclined bore of a sleeve to form therewith the cylindrical pair $IV_2$.

The sleeve coupled to a fixed member by means of the rotational pair $V_2$ receives rotation from a drive (generally with bevel gears). The sleeve causes the movement of the movable cone, the cone axis moving along a conical surface.

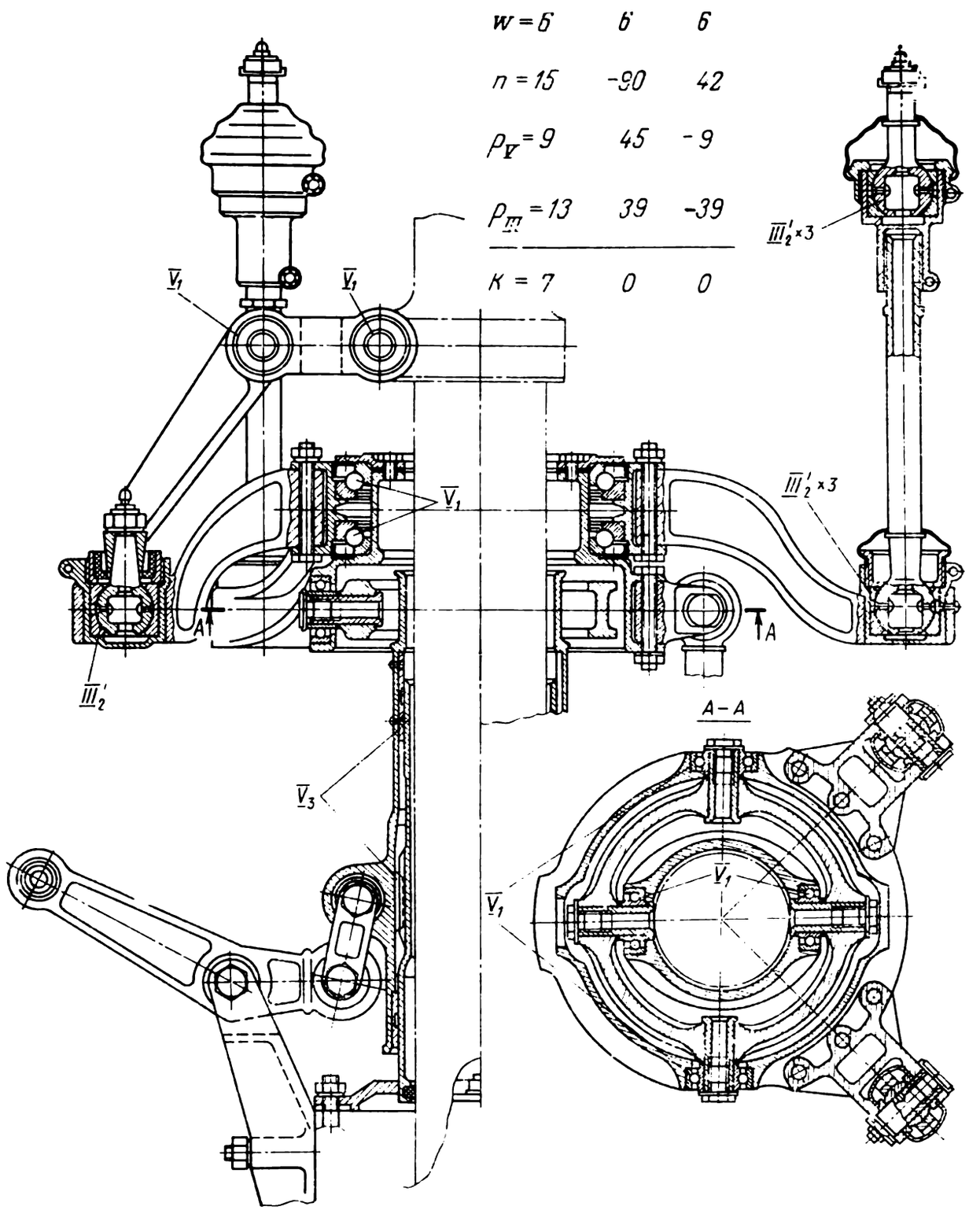


Fig. 3.18. Wobble-plate mechanism with bottom ring on a double Hooke's joint—free of redundant constraints, with 15 members

In such mechanism $n = 2$, $w = 2$ (the main mobility and cone rotation about its axis).

Therefore from (1.1), $q = 2 - 6 \times 2 + 5 + 4 + 3 = 2$.

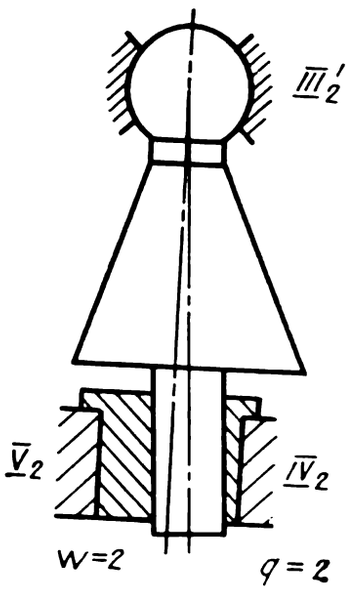


Fig. 3.19. Gyration crusher with two redundant constraints (incorrect design)

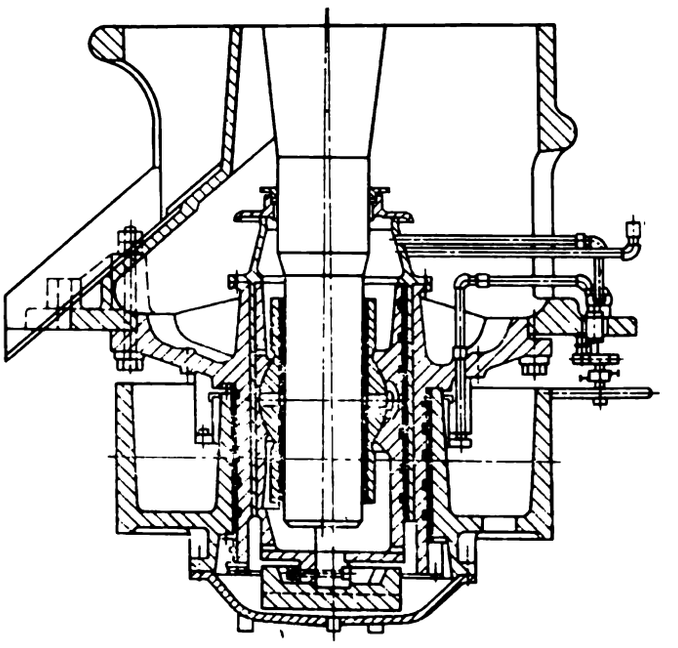

Fig. 3.20. Kennedy crusher (lower support with an additional spherical joint to eliminate redundant constraints)

Two redundant constraints require that the axis of the inclined bore of the sleeve should always extend through the centre of the spherical pair. For that purpose, it is necessary to comply accurately with many dimensions. In addition, members of the crusher are deformed under the action of enormous forces acting during operation, which also disrupts uniformity of load in kinematic pairs and accelerates their wear. This disadvantage can be eliminated if the spherical pair $III_2'$ (Fig. 3.20) is provided between the movable cone shaft and the sleeve, in addition to the cylindrical pair $IV_2$. The Figure shows only the lower support and the drive pulley. The upper bearing is made spherical. It should be noted that here one unharmful local mobility is added: rotation of a spherical insert about the axis of the movable cone, so that $n = 3$, $w = 3$, and $q = 3 - 6 \times 3 + 5 + 4 + 3 \times 2 = 0$.

This mechanism is applicable to small-size crushers. It is difficult to accommodate the spherical joint within the sleeve of large-size crushers.

A very simple mechanism (without redundant constraints) may be obtained when the movable cone axis is caused to move along a cylindrical surface (rather than along the conical surface) (Fig. 3.21). The sleeve is eccentric and is rotating about a fixed axis on the rotational $V_2$ pair. The movable cone rotates freely on the sleeve

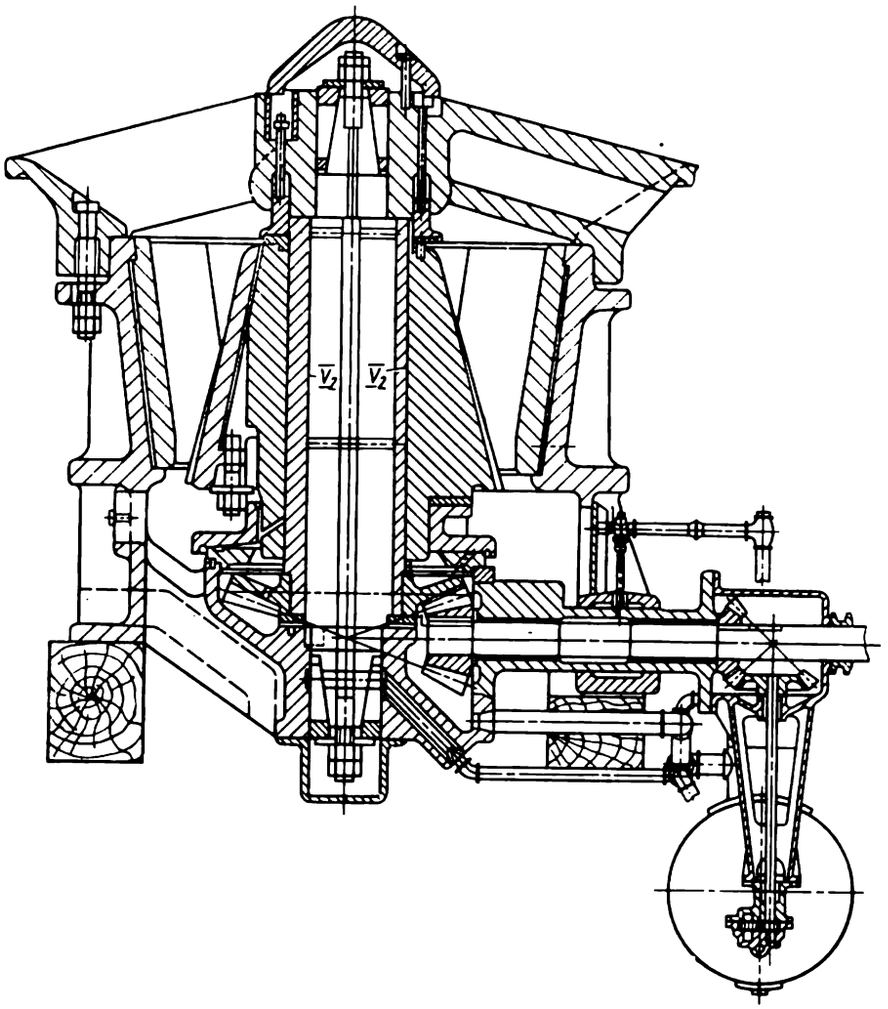


Fig. 3.21. Tellsmith crusher for primary crushing (simple design without redundant constraints with a large size of rotational pairs)

(by means of the rotational pair $V_2$). In this case $q = 2 - 6 \times 2 + 5 \times 2 = 0$.

The same mechanism can enable the movable cone movement not only along the cylindrical surface, but also along the conical surface. For that purpose, the sleeve should have a conical bore and appropriately-machined end faces. The angle of taper is, however, small.

The surfaces of rotational pairs in such mechanism are very large which is very important under heavy loads so as to reduce wear.

A simple mechanism suitable for all applications may be obtained in case the cylindrical sleeve of the mechanism shown in Fig. 3.19 is replaced by a spherical sleeve $III_2'$ (Fig. 3.22*a*). Here $n = 2$, $w = 2$, and $q = 2 - 6 \times 2 + 4 + 3 \times 2 = 0$.

The spherical sleeve has only one rotary motion since the two remaining rotational mobilities are eliminated by the coupling to

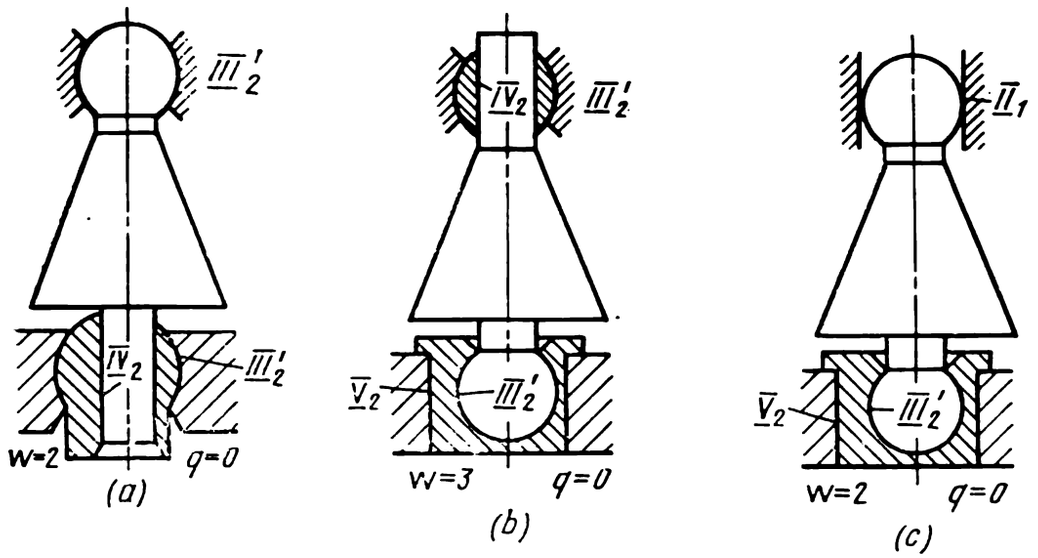


Fig. 3.22. Rational designs of gyration crushers

the movable cone shaft. Therefore, a drive gear may be installed on the spherical sleeve similarly to the cylindrical sleeve.

The above-discussed design (see Fig. 3.20) is deficient in that the sleeve is large in diameter because it must accommodate both the cylindrical pair $IV_2$ and the spherical pair $III'_2$. The diameter of the sleeve may be reduced if the cylindrical pair is transferred into the upper spherical support $III'_2$ (Fig. 3.22*b*). In such case the cone weight is transmitted to the lower sleeve so as to make the upper part of the crusher more lightweight.

The mobility in Fig. 3.22*b* is $w = 3$ (the main one and two rotations of the members), $n = 3$, and $q = 3 - 6 \times 3 + 5 + 4 + 3 \times 2 = 0$.

The design may be simplified if the upper support is made as a spherical rolling-contact bearing (Fig. 3.22*c*) with the loose fit of the outer ring, so that the support transforms into a $II_1$ pair. Then there is no need in the cylindrical pair.

In this mechanism $n = 2$, $w = 2$, and $q = 2 - 6 \times 2 + 5 + 3 + 2 = 0$.

With a greater angle of the movable cone which is always the case in secondary crushers, the spherical pair $III'_2$ of the conventional design (Fig. 3.23*a*) is disposed under the movable cone, and the movable cone is coupled to the sleeve by means of a tapered dowel (for greater strength), that is by means of the rotational pair $V_2$, rather than cylindrical. The sleeve is coupled to the fixed member by means of the rotational pair $V_2$, and the sleeve also receives rotation from the

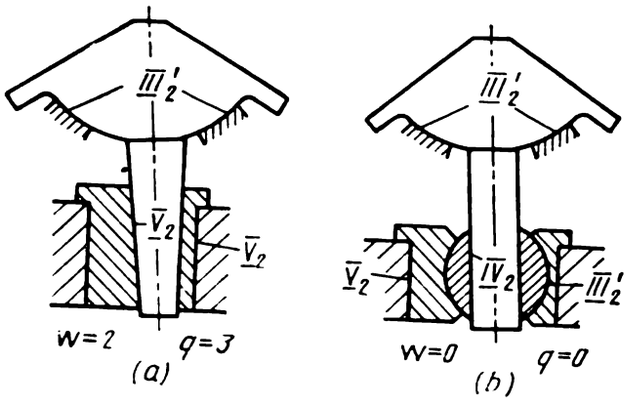


Fig. 3.23. Secondary crusher designs
(*a*) incorrect design with three redundant constraints; (*b*) without redundant constraints

drive similarly to the sleeve in Fig. 3.19. In the mechanism of Fig. 3.23*a*, $n = 2$ and $w = 2$, i. e. $q = 2 - 6 \times 2 + 5 \times 2 + 3 = 3$.

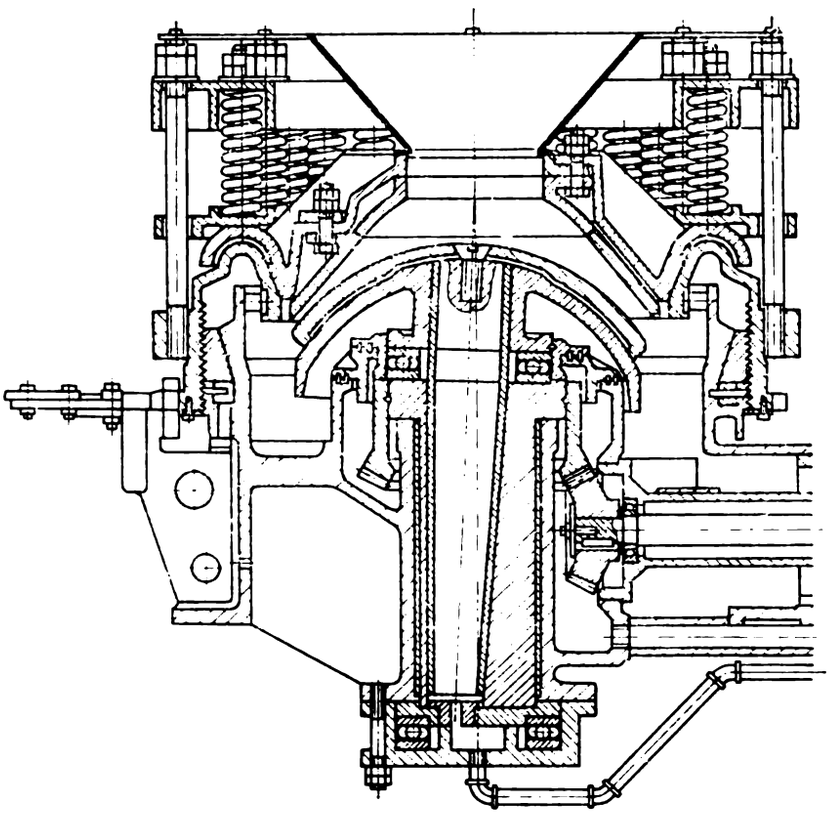

Fig. 3.24. Tellsmith crusher for secondary crushing (rational design without redundant constraints)

These redundant constraints require that the axis of the conical bore of the sleeve always extend through the centre of the spherical pair (two constraints). In addition, it is necessary to maintain a correct distance from the sleeve to the spherical pair (the third redundant constraint). The redundant constraints may be eliminated by coupling the end of the movable cone to the sleeve by means of a

cylindrical $IV_2$ pair and spherical $III_2'$ pair (Fig. 3.23*b*). There is one general and two local mobilities here, $n = 3$, $w = 3$, and $q = 3 - 6 \times 3 + 5 + 4 + 3 \times 2 = 0$.

A very simple structure can be obtained if the spherical pivot is dispensed with in the mechanism of Fig. 3.23*a*, and the load is transmitted to the sleeve (Fig. 3.24). The sleeve, in this case is installed in rolling-contact bearings. The increased sleeve diameter should cause no special concern since, owing to a large angle of the movable cone, mainly axial forces are applied to the movable cone shaft. There are only two rotational pairs here, and $q = 2 - 6 \times 2 + 5 \times 2 = 0$.

## 3.5. Universal Joints

One of such mechanisms is the Hooke's (Cardan) joint shown in Fig. 3.25. All kinematic pairs but one in this mechanism are rotational $V_2$ pairs with cylindrical rims. The coupling between the yoke and spider should be regarded as one kinematic pair, since the two elements are believed to have been manufactured at one setting of the tool providing adequate alignment of their axes.

The last $II_4$ pair is an annular one, and it is generally made as a spherical rolling-contact bearing whose outer ring has a loose fit. In such mechanism $w = 1$, $n = 3$, $p_V = 3$, $p_{II} = 1$, and $q = 1 - 6 \times 3 + 5 \times 3 + 2 = 0$, that is there are no redundant constraints.

In a Hooke's joint made up of sliding-contact bearings, the kinematic pair $II_4$ may be made, in case of low loads, as a cylindrical pair without rims but with clearances, provided that it is sufficiently spaced from the centre of the joint (5-10 radii of the yoke) and the insert is sufficiently short (not exceeding the shaft diameter).

Clearances in the kinematic pairs increase angular mobilities and do not influence linear mobilities. Therefore, the clearances provided in the cylindrical pair $IV_2$ transform it into the $II_4$ pair.

In case a spherical $III_2'$ pair is used to replace a $II_4$ pair, a mechanism with one redundant constraint is obtained in which distances from the centre of the sphere to the centre of the spider on the fixed member and that on the driven shaft should be exactly the same. In case a cylindrical $IV_2$ pair (without rims) is used to replace a $II_4$ pair, a mechanism with two redundant constraints is obtained. The axes of cylinders should be exactly aligned on the fixed member and on the output shaft (two dimensions).

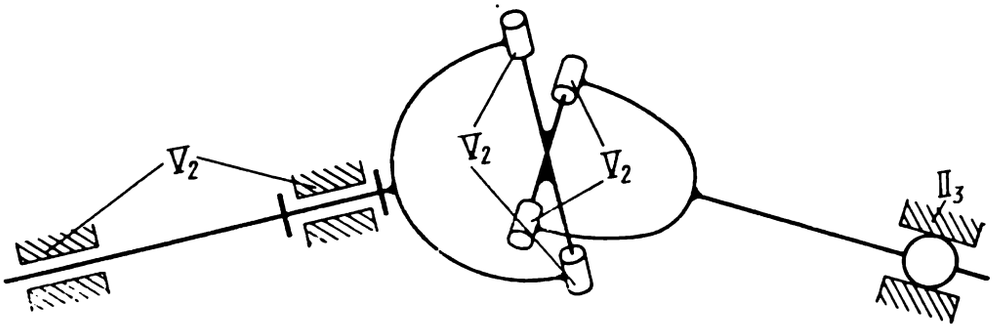


Fig. 3.25. Single Hooke's joint

In case a $II_4$ pair is replaced by a rotational $V_2$ pair, a mechanism with three redundant constraints is obtained. Then three dimensions should be exactly the same on the fixed member and output shaft: alignment of the axes of cylinders and equal distance from the pair to the centre of the spider. The accuracy requirement makes the manufacture of such a mechanism more expensive and lowers its reliability in operation since, upon a change in dimensions caused, for example by heating or settlement of the foundation, the mechanism is loaded with additional forces which result in increased friction and may cause failure of members. Consequently Hooke's joints with redundant constraints should never be used.

In practice it may occur that rotational pairs $V_2$ are necessary on both the drive and the driven shafts, it means that a $II_4$ pair cannot be installed on either shaft (when oscillations of the shaft are not permitted). In such case the use may be made of a double Hooke's joint or a Hooke's joint with a cube (Fig. 3.26*a*). This mechanism tolerates an angle between the directions of the shafts when there is an axial play between the cube and the yoke. The same result is obtained by chamfering the cube corners. The admissible angle depends on the play or on the amount of chamfering of the cube corners. In such a mechanism the mobility is $w = 2$ since, in addition to the main mobility (rotation), there is an axial mobility of the cube within the clearances, and there are no redundant constraints, that is $q = 2 - 6 \times 3 + 5 \times 2 + 3 \times 2 = 0$ from (1.1).

This mechanism has not been used so far in the function of Hooke's joint, and it was regarded as applicable only to parallel axles, that is as the Oldham coupling. The Oldham coupling even in its conventional form may be used as the Hooke's joint in case an axial play is provided. This is due to the fact that the planar $III_2'$ pair inserted between the spider and yoke permits relative rotation, that is it can replace the rotational pair.

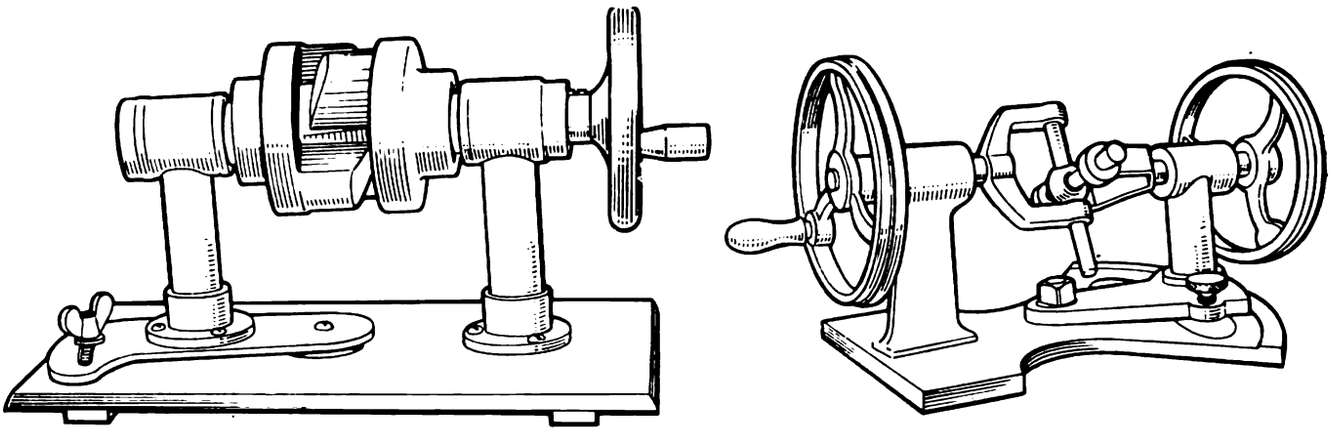

(*a*) (*b*)

**Fig. 3.26.** Hooke's joints (models from the Laboratory of Mechanisms of the Baumann Higher Technical School)
(*a*) with a cube; (*b*) with the pairs $IV_2$

The Hooke's joint with a cube is kinematically identical with the conventional single Hooke's joint, that is it gives a varying transmission ratio with the coefficient of non-uniformity which is approximately equal to the square of the angle between the axes (in radians).

The mechanism with one pair $V_2$ and three pairs $IV_2$ (Fig. 3.26*b*) does not have redundant constraints, that is $q = w - 6n + 5p_V + 4p_{IV} + \ldots = 1 - 6 \times 3 + 5 \times 1 + 4 \times 3 = 0$.

It cannot, however, be used as the Hooke's joint since in case there is a misalignment of the axes or an angle between them, the shaft with the pair $IV_2$ performs oscillations along the axis at the double frequency. The amplitude may be controlled by displacing the axes or by changing the angle between them. The mechanism can, therefore, be used for transforming rotary motion into reciprocations in case where the amplitude control is required, but the amplitude is yet very low.

Double Hooke's joints are used in practice. In case a mechanism is composed of two Hooke's joints (Fig. 3.27*a*), it is necessary to have a free splined joint (the translatory pair $V_3$) on one of the shafts (drive, driven, or intermediate shaft). The intermediate shaft should not have bearings. In case these conditions are fulfilled, there are no redundant constraints, that is $q = w - 6n + 5p_V + \ldots = 1 - 6 \times 6 + 5 \times 7 = 0$, and the mechanism functions reliably. In case there is no splined joint, one redundant constraint remains which generally results in failure of such mechanisms.

The splined joint may be dispensed with in case one or two Hooke's joints are universal joints, that is where they enable the axial

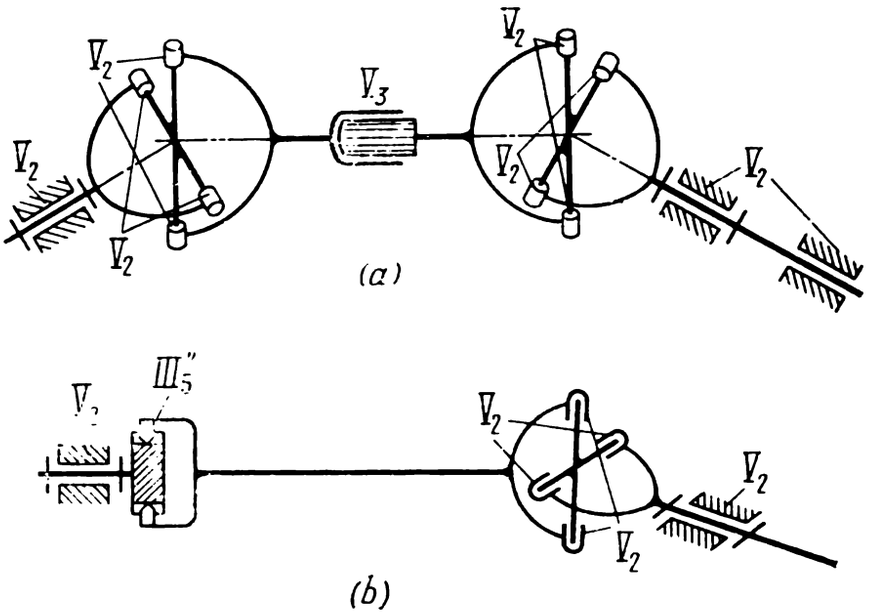


Fig. 3.27. Hooke's joints
(*a*) double; (*b*) double with one universal toothed joint

mobility (Fig. 3.27*b*). In this case one of the Hooke's joints is a toothed joint. Thus $q = 1 - 6 \times 4 + 5 \times 4 + 3 \times 1 = 0$, that is there are no redundant constraints.

One should be warned against using bearings on the intermediate shaft of the double Hooke's joint mechanism since they strongly increase the number of redundant constraints.

A noteworthy solution was used to eliminate redundant constraints in the Trakt mechanism (Fig. 3.28*a*). From the kinematic point of view, this mechanism comprises a double Hooke's joint having four movable members, rather than six. The spiders of the joint are interconnected directly through a planar $III_2'$ pair, rather than through two intermediate members and the rotational, prismatic, and rotational pairs, so that three relative mobilities are retained. The planar pair is made in the form of a deep recess in one member which receives a plate provided at the end of the other member. This pair enables the same relative movement of the members (spiders) as in the conventional double Hooke's joint. For assembly of the rotational pairs $V_2$ their surfaces are sawn off. For assembly, the journals are turned through 90°. There are no redundant constraints in the mechanism, that is $q = w - 6n + 5p_{\mathrm{V}} + 3p_{\mathrm{III}} = 1 - 6 \times 4 + 5 \times 4 + 3 \times 1 = 0$.

The Trakt mechanism is very interesting in its concept. It is, however, difficult to realize this mechanism using rolling-contact bearings. Special jigs are required for machining its members, because

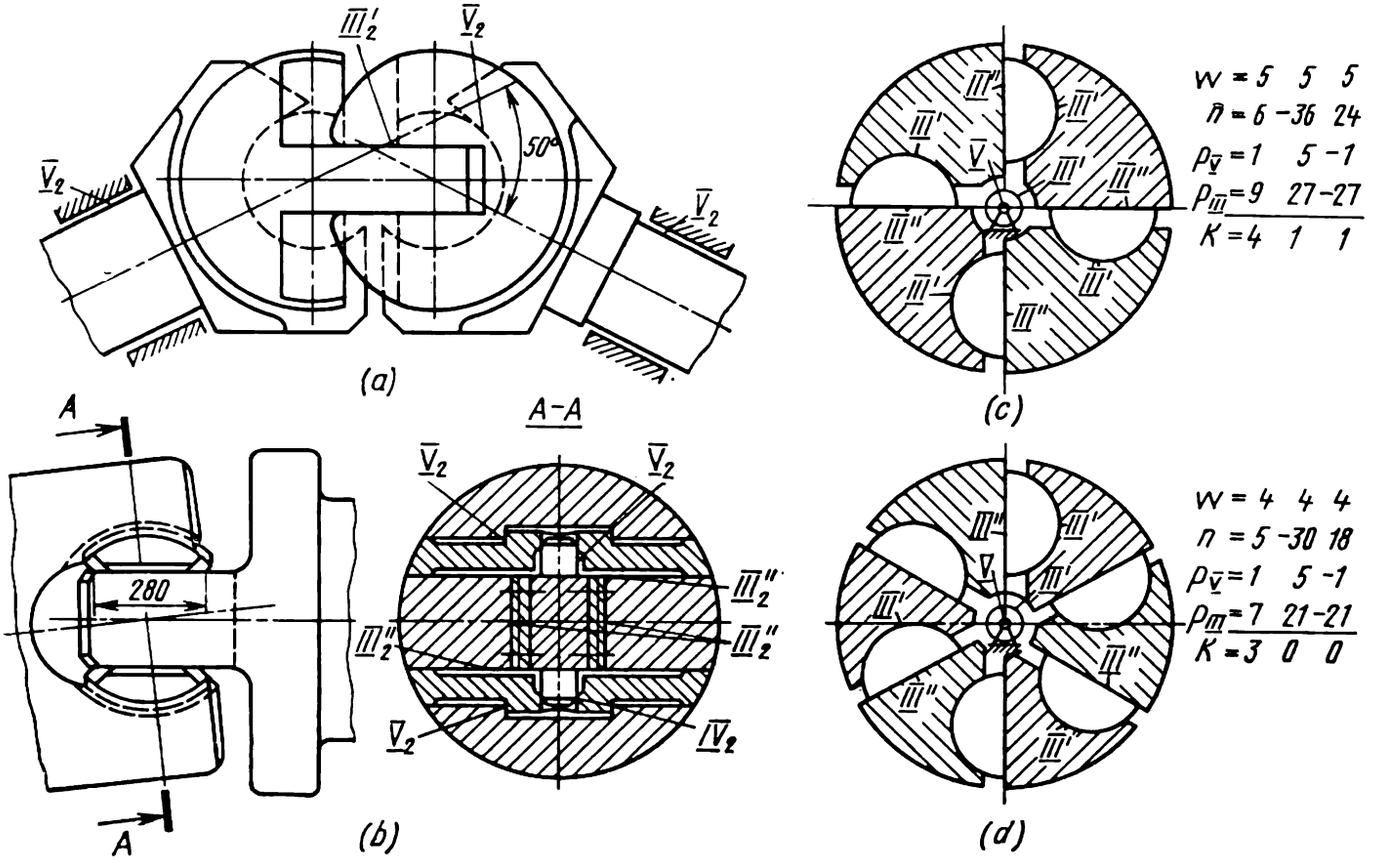


**Fig. 3.28. Hooke's joints with planar III″ pairs**
(*a*) Tract's double joint; (*b*) rolling mill-type; (*c*) one used in pilgrim rolling mills; (*d*) recommended joint without redundant constraints

otherwise it is difficult to fix the members on the machine tool so that the mechanism is unsuitable for individual manufacture. In addition, it is difficult to obtain a large angle between axes in this mechanism.

Consider next the Hooke's joint used in rolling mills (Fig. 3.28*b*), universal. The torque is transmitted through two inserts in the form of cylindrical segments having rims. The other side of the insert defines with the driven yoke the planar pair $III_2'$. In order to prevent the driven yoke from moving out in the radial direction, there is provided a slide block in the form of a parallelepiped coupled to the inserts by means of rotational pairs. As the slide block can only be fixed axially by one of these pairs which is the pair $V_2$, the second pair is the pair $IV_2$. Support bearings (when the single joint is considered) should be the pairs $V_2$ and $III_2'$ (not shown in Fig. 3.28*b*). The number of redundant constraints is determined by the formula $q = 1 - 6 \times 5 + 5 \times 4 + 4 \times 1 + 3 \times 4 = 7$.

The slide block should be rotatable about the inserts, that is five restraints should be provided between them, while there are 5 +

$+ 4 = 9$. Four among them are redundant, and they can cause non-uniform loading of two dowels in two planes. It is, therefore, necessary to ensure the alignment of axes of the insert holes and alignment of axes of the slide block dowels. The latter condition can readily be fulfilled by turning the axles in centres. The other three redundant constraints may cause non-uniform loading of the planar pairs $III_2'$ between the inserts and yoke and between the slide block and yoke. Therefore, the manufacturing process should be well prepared to ensure appropriate parallelism and perpendicularity of planes. The yoke thickness should correspond to the inserts spacing.

The large number of redundant constraints is a serious disadvantage of the rolling mill Hooke's joint. The Hooke's joint used in pilgrim rolling mills is free from this disadvantage (Fig. 3.28*c*, cross-section). The yokes of the drive and driven shafts shown with left- and right-hand hatching, respectively, are received in one another. The torque is transmitted through four spherical segments: two for the forward rotation and two for the reverse. With the forward rotation, the segments for the reverse align the yokes. They should, therefore, be biased which causes the appearance of one redundant constraint (see calculation in Fig. 3.28*c*) which does not, however, disrupt the self-alignment and uniform distribution of load between the friction surfaces so that the adverse effect of this constraint is minimized. This constraint may be eliminated by using a Hooke's joint having six segments (Fig. 3.28*d*) with three segments for the forward rotation and three segments for the reverse. With the forward rotation, the three segments will adequately center the Hooke's joint, while the reverse segments may not touch one another so that no redundant constraints appear (see calculation in Fig. 3.28*d*).

Double Hooke's joints are generally used in rolling mills. It should be born in mind that the intermediate shaft is axially movable within clearances. Therefore $w = 2$ for calculations.

Hooke's joints have been made so far with the rotational pairs $V_2$ (except for one support). In case the spherical joints $III_2'$ are used, new designs of Hooke's joint mechanisms may be obtained (Fig. 3.29). The universal joint, that is the joint that transmits torque between shafts about the shaft axis and forces along the axes extending at right angle to the shaft axis consists of two triple yokes interconnected by three rods. Fig. 3.29 shows a double three-arm Hooke's joint of the ЦНИИМПС design with rubber blocks which should be regarded as the pairs $III'$. The pins of this pair are connected to the yokes and the bushings to the arms. V. N. Yermak has connected the bushings to the yokes (flanges), and the pins to the carriers (Fig. 3.30). The

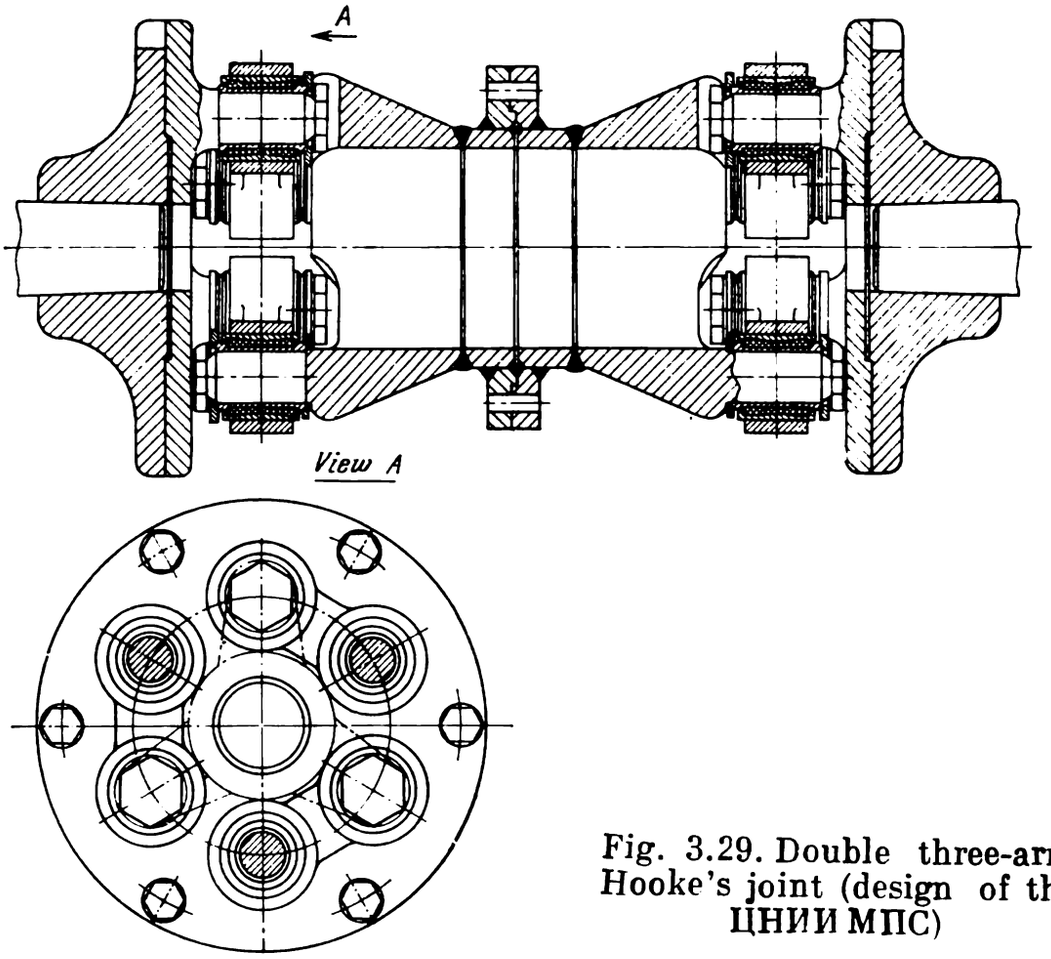


Fig. 3.29. Double three-arm Hooke's joint (design of the ЦНИИ МПС)

arms are two plates whic is not hazardous in view of the flexibility of the rubber blocks. Moments bending the pins are reduced and moments at the clamping points of the pins are eliminated. The flanges are closer to one another so that the axial dimension of the Hooke's joint is reduced which is very important for locomotives.

The mechanism is especially advantageous for the railway applications in case joints are made with silent-blocks (with rubber). With small angles between the axes, they may also be made with spherical rolling-contact bearings. Fig. 3.29 shows the double three-arm joint. Supports of the drive and driven shafts—the pairs $V_2$—are not shown. Connecting rods have local mobilities—rotation about their own axes—which gives six mobilities. In addition, there is an axial mobility of the intermediate shaft within clearances and the main mobility—rotation of the mechanism. Therefore $w = 8$. By formula (1.1), $q = 8 - 6 \times 9 + 5 \times 2 + 3 \times 12 = 0$, that is there are no redundant constraints. The load on the joints is one and a half times lower than in the conventional Hooke's joint.

The kinematics of the three-arm joint was studied by M. A. Fakhriev [46]. He has found that the centre of the driven yoke describes a circle of the radius

$$\rho = \frac{1}{4} R\gamma^2$$

where $R$ is the radius of the yoke; $\gamma$ is the angle between the axes. The centre of the yoke describes this circle three times during one revolution of the Hooke's joint. Therefore, the three-arm Hooke's joint is unbalanced. It is suitable for electric locomotives where the angle $\gamma$ between the axes is very small, and it cannot be used in automobiles where this angle is much greater.

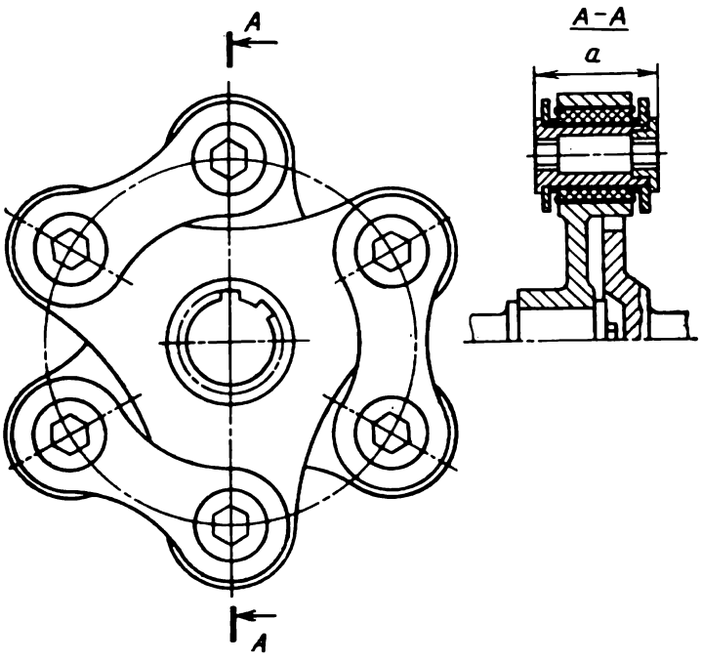


Fig. 3.30. Three-arm Hooke's joint by V. N. Yermak

The angle of rotation of the driven shaft is

$$\varphi = \alpha - \frac{\pi}{3} + \frac{1}{4\sqrt{3}} \gamma^2$$

where $\alpha$ is the angle of rotation of the drive shaft. The third term in the formula shows that the driven shaft receives an additional angle of rotation which is proportional to the square of the angle $\gamma$ between the axes.

Therefore, with $\gamma$=const, which is generally the case, the transmission ratio is constant.

The conventional Hooke's joint realizes four restraints between the shafts: torque and forces along the three coordinate axes. Four connecting rods are, therefore, required. The rods and yokes should

be located in different planes because otherwise a statically indeterminate structure is formed, and the redundant mobility appears along the shaft axis (Fig. 3.31).

With the correct arrangement, $w = 1 + 4 = 5$ (four local mobilities of the rods), and there are no redundant constraints, that is $q = 5 - 6 \times 6 + 5 \times 1 + 3 \times 8 + 2 \times 1 = 0$.

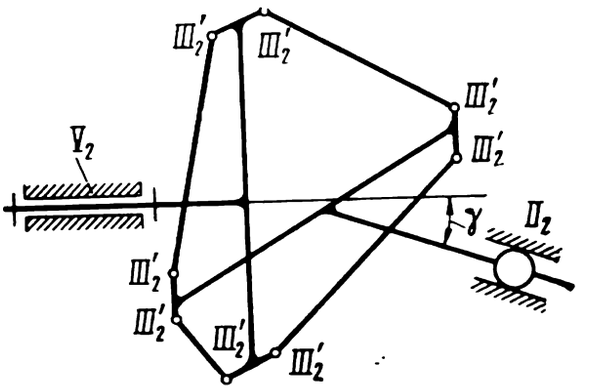


Fig. 3.31. Four-arm Hooke's joint

In the four-arm Hooke's joint the load on the joints is almost two times lower, as compared with the conventional Hooke's joint.

## 3.6. Hooke's Joints with High-Class Pairs

Recently shaft couplings have come into use in which forces are transmitted through balls. A constant transmission ratio is easily obtained in such mechanisms. The structure of such mechanisms features, however, a large number of redundant constraints.

In the Weiss mechanism (Fig. 3.22*a*) forces from the drive yoke are transmitted to the driven yoke through a pair of balls running along circular grooves made in the yokes, rather than through a spider. The two other balls are used to transmit torque in the reversed direction, and they do not function during the forward torque transmission so that they may be ignored. The middle ball serves for centering the yokes. Owing to the symmetry of the mechanism with respect to the drive and driven yokes, their angular velocities are identical so that the transmission ratio is constant and equal to unity. The number of movable members (two yokes and three balls) is $n = 5$. In determining the mobility, it should be borne in mind that each ball has local (passive) mobilities owing to a possible slippage—rotation about three coordinate axes, so that $w = 1 + 3 \times 3 = 10$.

Coupling of the balls by means of a groove forms the kinematic pair $II_3$ (the annular pair). The central ball defines with the yokes the spherical pairs $III_2'$. According to (1.1), $q = 10 - 6 \times 5 + 5 \times 2 + 3 \times 2 + 2 \times 4 = 4$.

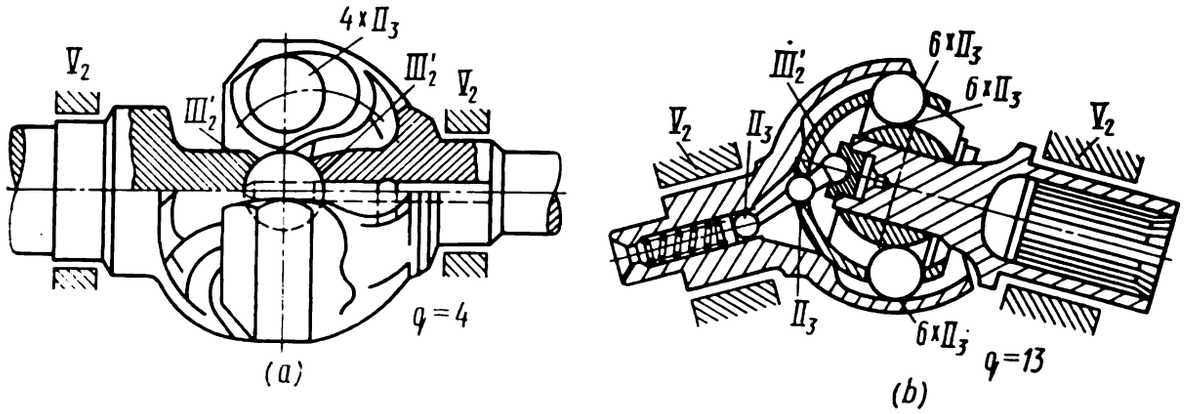


Fig. 3.32. Joints with constant transmission ratio
(*a*) Weiss; (*b*) Rzepp

The mechanism may be improved by replacing the double yokes with triple yokes and transmitting the torque through three balls. Let us set three balls out of the centre instead of one central ball and lateral balls. Then the load on the ball is reduced one and half times: the middle ball can be dispensed with as the three balls can align the yokes by themselves.

One of the kinematic pairs $V_2$ is to be replaced with the pair $III'_2$ (spherical pair). In this mechanism, $w = 1 + 3 \times 3 = 10$ and $n = 5$; $q = 10 - 6 \times 5 + 5 \times 1 + 3 \times 1 + 2 \times 6 = 0$.

This mechanism has been developed by V. V. Smirnov.

The Rzepp mechanism (Fig. 3.32*b*) consists of spherical members having grooves for balls in the axial plane (meridional grooves). One of the members has the outer spherical surface and the other member has the inner spherical surface. Balls (generally six balls) are inserted in the grooves and are held by means of a retainer cage and an indexing mechanism within the plane which divides the angle between the axes into halves. The mobility of the mechanism is composed of the main mobility, local mobility of the six balls, and local mobility (rotation) of the lever of the indexing mechanism. Therefore $w = 1 + 6 \times 3 + 1 = 20$.

Each ball is connected to the retainer cage and to the heads of drive and driven shafts by means of three annular pairs $II_3$. Two similar pairs are disposed between the indexing lever and the head and between the lever and retainer cage. The support bearings can be regarded as the pair $V_2$. The number of redundant constraints $q = 20 - 6 \times 10 + 5 \times 2 + 3 \times 1 + 2 \times 20 = 13$.

With such an enormous number of redundant constraints, the mechanism can only function with a very precise manufacture.

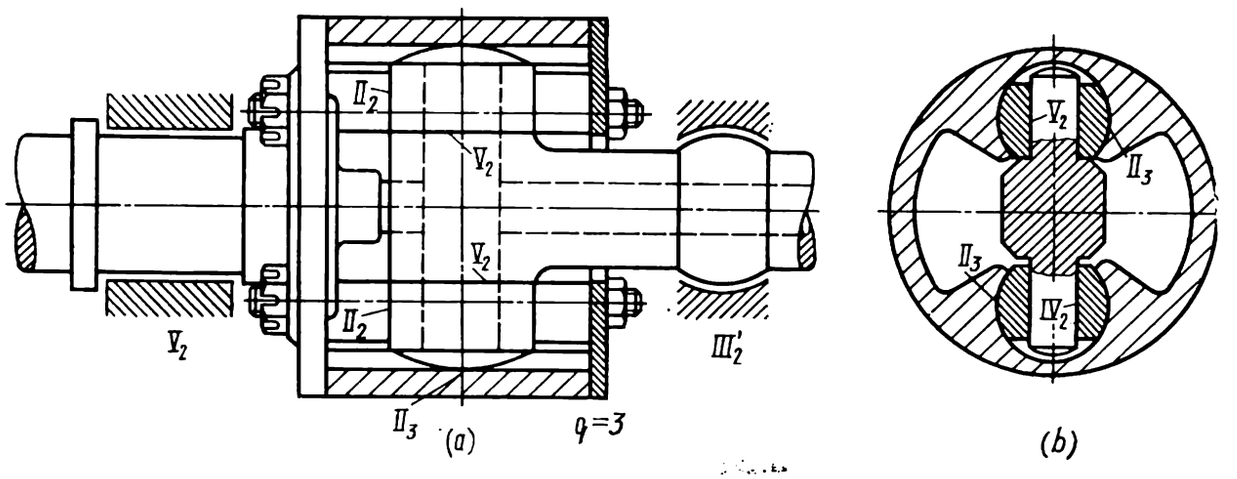


Fig. 3.33. Universal bell-type joints:
(*a*) with three redundant constraints; (*b*) without redundant constraints

A bell-type Hooke's joint (Fig. 3.33*a*) is a universal joint, that is it enables axial movement of the axles. Consequently it does not require axial mobility in bearings. The latters are made as follows: one bearing is in the form of the rotational pair $V_2$ and the other is the spherical pair $III_2'$. Each roller works over two surfaces: a plane and cylinder, and the roller itself has cylindrical and spherical working surfaces. These portions should, therefore, be regarded as individual pairs $II_2$ and $II_3$. Only one roller can be radially biased, and both rollers are biased in the circumferential direction, so that $p_{II} = 3$.

The mobility of the mechanism (the main mobility and slippage of the two rollers) is $w = 3$. From (1.1) $q = 3 - 6 \times 4 + 5 \times \times 3 + 3 \times 1 + 2 \times 3 = 3$.

Redundant constraints may cause non-uniform distribution of loads over the generatrix of the roller and over the spherical surface. The precise manufacture of the mechanism is, therefore, necessary. It is difficult to eliminate these constraints. The rollers may be made spherical (Fig. 3.33*b*), and the working surfaces of the bell, in the form of two parallel cylinders. Then the number of the purely kinematic pairs of the $II_3$ type (annular pairs) is $p_{II} = 2$.

The kinematic pair between one roller and the arm should be regarded as a $V_2$ pair, and that between the other roller and the arm as the pair $IV_2$, since the arm can be radially biased only against one roller. Similarly to any universal joint, the support bearings are formed as follows: one $V_2$ and the other $III_2'$. Redundant constraints $q = 3 - 6 \times 4 + 5 \times 2 + 4 \times 1 + 3 \times 1 + 2 \times 2 = 0$, i.e. there are no redundant constraints. Unfortunately, the arm cannot be accurately centered in this mechanism in case there is an angle between the axes, so that the mechanism is unbalanced.

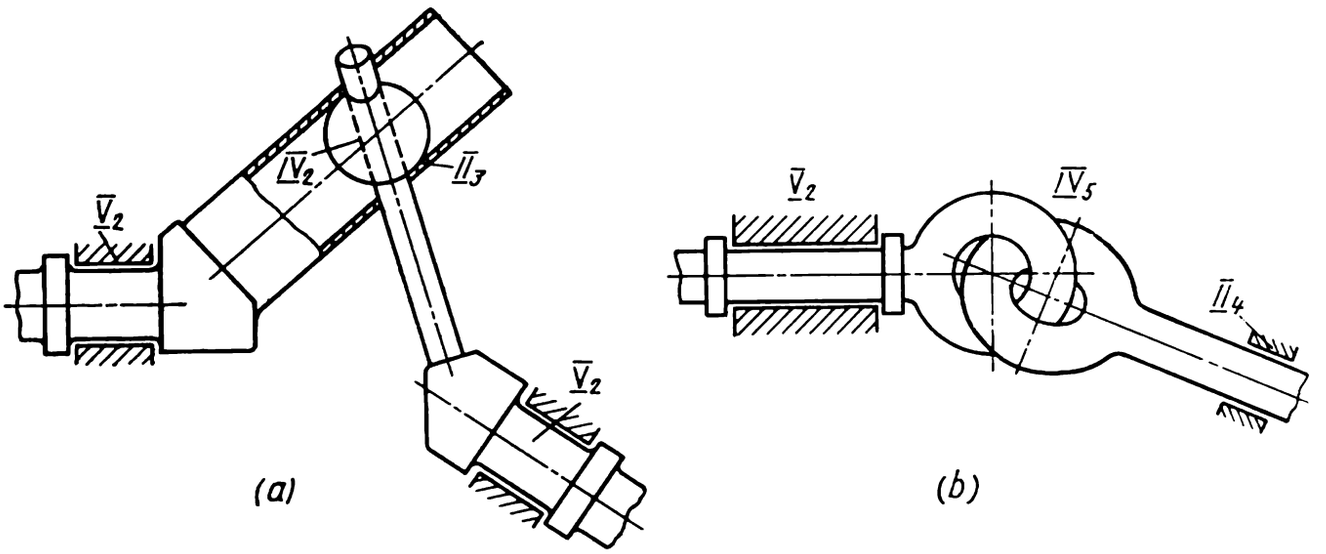


Fig. 3.34. Hooke's joints
(*a*) proposed by M. I. Lysov; (*b*) with the chain pair

The mechanism developed by M. I. Lysov also does not have redundant constraints. The roller of the mechanism is spherical and its respective groove is cylindrical. The mechanism transmits only a force (one restraint), so that the supports of both shafts are made with the use of the rotational pairs $V_2$ (Fig. 3.34*a*). The mobility is $w = 2$ (main mobility and roller slippage). Redundant constraints $q = 2 - 6 \times 3 + 5 \times 2 + 4 \times 1 + 2 \times 1 = 0$. The bearings in this mechanism are loaded with the circumferential force.

In order to eliminate redundant constraints (in applications with a small angle between axes), the use of a toothed Hooke's joint is very convenient. A splined coupling with its short length receives additional angular mobilities owing to large plays, that is it becomes the coupling $III_5''$, rather than $V_3$, which is required for the universal joint. Involute gearing is used in the toothed Hooke's joints to facilitate the manufacture. The inner crown is made by the gear hobbing method. A barrel-shaped toothing is provided on the outer crown. It should be, however, noted that load in the toothed clutch is distributed among a large number of teeth, that is a statically indeterminate distribution of forces with many redundant constraints arises. They are, however, the redundant constraints in the kinematic pair which can be manufactured very accurately so that such redundant constraints are not harmful, and there is no need in calculating them. Redundant constraints in the mechanism are regarded as harmful where dimensions of many members influence the distribution of loads and where manufacturing errors can be accumulated. Therefore, the gearing should be regarded in calculations as the kine-

matic $III_5''$ pair. In determining the mobility of the double-toothed Hooke's joint, the axial play of the coupling should be taken into account, so that $w = 2$. There are no redundant constraints within the mechanism, that is $q = 2 - 6 \times 3 + 5 \times 2 + 3 \times 2 = 0$.

Unfortunately, the toothed Hooke's joint permits only a small angle between the axes, that is 1°30′ at the largest.

The chain pair $IV_4$ which gives the necessary four restraints can also serve as a Hooke's joint (Fig. 3.34*b*). Owing to poor contacts and large plays, this joint is unsuitable for a mechanical drive; it can only be used for a manual drive (for opening doors, shutters, louvers). The $IV_3$ pair—the spherical pair with the pin—can also serve the same purposes.

## 3.7. Flexible Hooke's Joints

Flexible shaft couplings that do not require lubrication and have the immunity to contamination and wear have recently come into use. When properly designed, such couplings are failure-proof in operation. Fig. 3.35*a* shows a double flexible Brown-Bovery Hooke's joint used in electric locomotives [51]. The joint shaft extends within a hollow shaft of an electric motor. This is the reason of an unconventional arrangement of supports. The double Hooke's joint is used in electric locomotives. For the sake of simplicity, let us consider a single joint, with the shaft bearings being regarded as the pairs

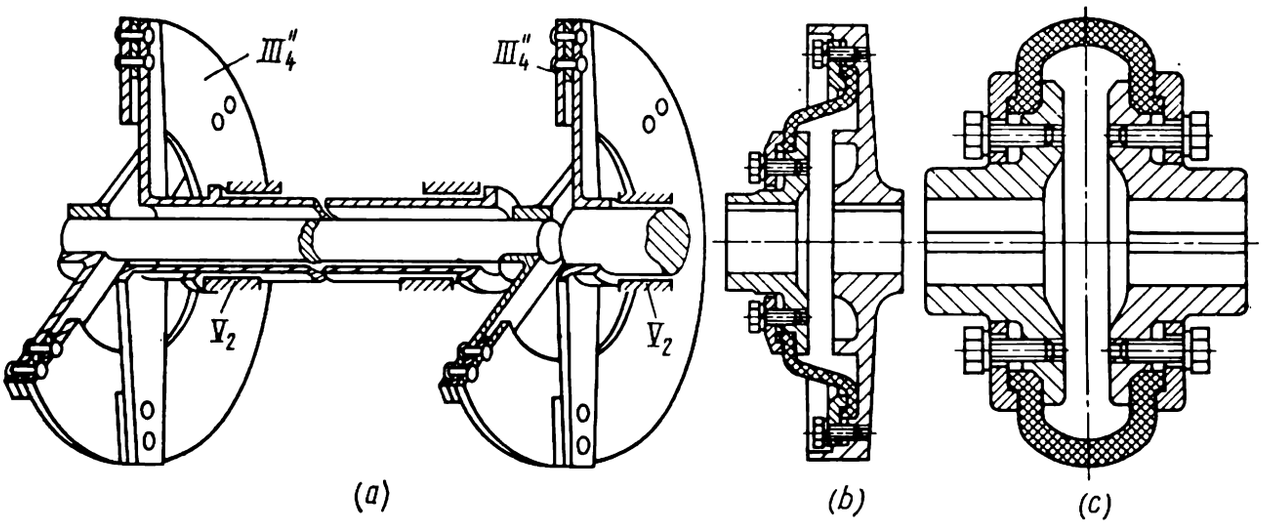


Fig. 3.35. Flexible Hooke's joints
(*a*) double, Brown-Bovery; (*b*) single, rubber; (*c*) double, of the "tyre" type

$V_2$ and $III_2'$ similarly to any Hooke's joint. The joint consists of a flexible steel plate to which are secured yokes of the drive and driven shafts. The plate imposes three restraints, that is it constitutes the pair $III_4''$ which is needed for the universal joint. The redundant constraints $q = 1 - 6 \times 2 + 5 \times 1 + 3 \times 2 = 0$, which attests to the correct design.

A flexible Hooke's joint Secheiron is used in electric locomotives ЧС-1. In this joint, 12 plates are used instead of one sheet, and each plate may be regarded as a flexible plate (the pair $III_4''$). The ends of the plates should be regarded as rigid members. They are connected to the yokes by means of journals (the pairs $V_2$). Therefore, the Secheiron Hooke's joint has a large number of redundant constraints. It requires a very accurate manufacture and assembly. This is a very important information for operators dealing with the repair and replacement of parts of this mechanism.

Both Secheiron and Brown-Bovery Hooke's joints are used in electric locomotives in the form of double joints. They are installed on a high-speed shaft, the cardan shaft being disposed within the hollow shaft of the traction electric motor. The flexible Hooke's joints are not enclosed. The angle between the axes is small which contributes to a longer life of the mechanism inspite of its high speed and large transmitted torques.

Flexible rubber shaft couplings are also used: in the form of a plate (Fig. 3.35*b*) or a "tyre" (Fig. 3.35*c*). The latter design corresponds to a double joint of the former type. The mobility in this case can be easily found on the basis of the fact that the mobilities of series connected kinematic pairs are added. It should be borne in mind that the axial mobility is defined by both joints, and one common axial mobility is obtained, that is $3 \times 2 - 1 = 5$, i. e. 3 displacements along the coordinate axes and two rotations about two axes perpendicular to the shaft axis. The imposed restraints $1 = 6 - 5$ correspond to the torque transmitted about the shaft axis.

The mechanism shown in Fig. 3.35*c* is made with bearings which represent the rotational pairs $V_2$. There are no redundant constraints here, that is $q = 1 - 6 \times 2 + 5 \times 2 + 1 \times 1 = 0$.

Unfortunately, this Hooke's joint exhibits a very high rigidity with respect to transverse linear mobilities. This became clear during operation of ЭР cars (failures of bearings of the drive gear and non-uniform load along the tooth length). Therefore, it is unwarranted to expect transverse linear mobilities in such a mechanism, hence, the "tyre"-type Hooke's joint should only be used in the form of the single, rather than double, joint.

## 3.8. Unconventional Double Hooke's Joint

The following rules are commonly adopted for Hooke's joints:
—in order to obtain a constant transmission ratio in the double Hooke's joint, the yokes of both joints should be in one and the same plane on the intermediate shaft;

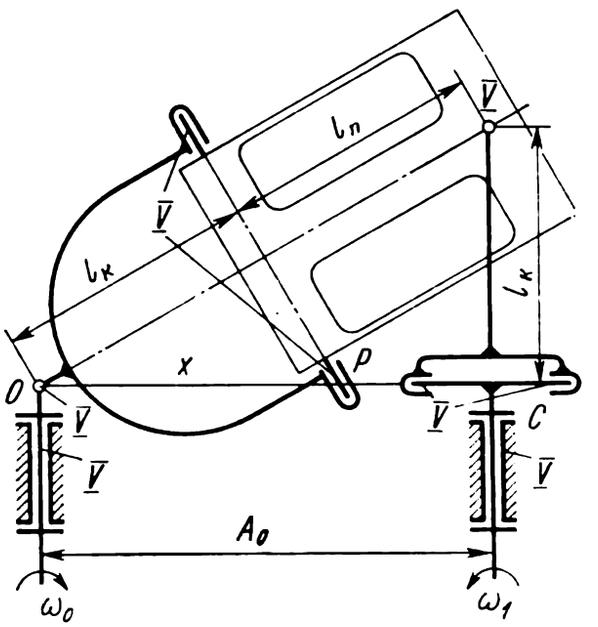


Fig. 3.36. Double Hooke's joint used in mixers

—the angle between the axes in each joint should not exceed 45°, and at any rate this angle cannot be 90°.

The exception from this rule is the mechanism of a mixer made by the Swiss firm Willy A. Bahoffen (WAB) that was shown at the International Chemical Exhibition in Moscow in 1966 (Fig. 3.36).

The angle between the axes of the mechanism is 180°, that is 90° per each Hooke's joint. The yokes of both joints are at an angle of 90° on the intermediate shaft of the length $l_n$. The mechanism is formed as a three-dimensional frame within which is installed a drum (not shown) containing a material being mixed. A complicated movement of this member contributes to good mixing. Spiders of both joints are made with crossing axes with the distance $A_0$ between the axes. There is no splined coupling on the intermediate shaft. Therefore, there is only one redundant constraint in the mechanism. This can be shown by using formula (1.1): $q = 1 - 6 \times 5 + 5 \times 6 = 1$.

Strains caused by this constraint may be eliminated in case the driven shaft is installed on a movable (rotatable) frame, so that the mechanism can work with varying distance between the shaft axes, or, otherwise, to form the support of one shaft as the pair $IV_2$, as proposed by Ovakimyan.

Let us determine non-uniformity of rotation of the driven shaft. The angular velocities $\omega_1$ and $\omega_2$ attain their peak values when one of the yokes of the intermediate shaft coincides with the plane of the axes. One of such positions is shown in Fig. 3.36. The transmission ratio will be determined using the contact point $P$ which is found at the point of intersection of the axis of the yoke joint with the centre line $OC$:

$$\frac{\omega_1}{\omega_0} = \frac{OP}{CP} = \frac{x}{A_0 - x}$$

After rotation through 90°, when the axis of the other yoke of the intermediate shaft coincides with the plane of the axes, we can write:

$$\frac{\omega_2}{\omega_0} = \frac{A_0 - x}{x}$$

The coefficient of non-uniformity

$$\delta = \frac{\omega_1 - \omega_2}{\omega_0} = \frac{\omega_1}{\omega_0} - \frac{\omega_2}{\omega_0}$$

or, after substitution of angular velocity values,

$$\delta = \frac{x}{A_0 - x} - \frac{A_0 - x}{x} = \frac{1}{\frac{A_0}{x} - 1} - \left(\frac{A_0}{x} - 1\right)$$

It can be seen from Fig. 3.36 that

$$A_0^2 = (l_s + l_i)^2 - l_s^2 = (2l_s + l_i)\, l_i$$

From the similarity of the triangles in Fig. 3.36:

$$\frac{l_i}{x} = \frac{A_0}{l_s + l_i}$$

By multiplying the ratio $\frac{l_s}{x}$ by $\frac{A_0}{l_s}$ and substituting in this product the value of $A_0^2$, we obtain:

$$\frac{A_0}{x} = \frac{A_0^2}{l_s (l_s + l_i)} = \frac{l_i}{l_s} \frac{2l_s + l_i}{l_s + l_i} = \frac{l_i}{l_s} \frac{2 + \frac{l_i}{l_s}}{1 + \frac{l_i}{l_s}}$$

Let us denote $\frac{l_i}{l_s} = y$. Then

$$\frac{A_0}{x} = \frac{y(2+y)}{1+y} = \frac{2y + y^2}{1+y}$$

$$\frac{A_0}{x} - 1 = \frac{2y + y^2 - 1 - y}{1+y} = y - \frac{1}{1+y}$$

By substituting this value in the formula for $\delta$, we obtain:

$$\delta = \frac{1}{y - \dfrac{1}{1+y}} - \left(y - \frac{1}{1+y}\right)$$

With $\delta = 0$, $y = \dfrac{l_i}{l_s} = \sqrt{2} \approx 1.41$.

With $y = 1$, $\delta = 1.5$.

This coefficient of non-uniformity is possible since even with $\omega_2 = 0$, $\delta = 2$, and in case $\omega_2 < 0$, that is when the driven shaft periodically receives a reverse rotation, $\delta > 2$.

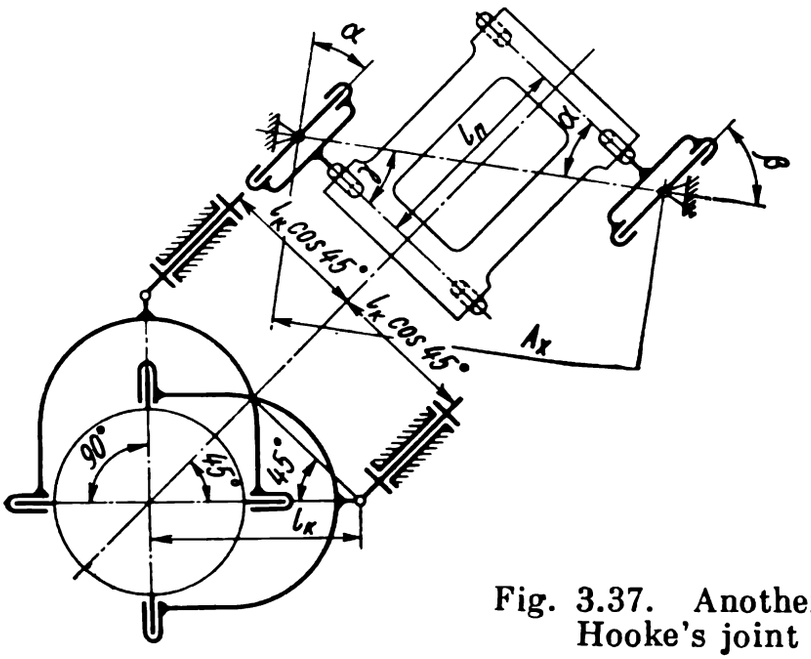


Fig. 3.37. Another position of the Hooke's joint used in mixers

In order to find how the centre distance varies, let us consider the mechanism in the position where the yokes of the drive and driven shafts run in parallel (Fig. 3.37). The figure shows the projection to the plane extending at right angles to the axes, and the second projection is shown to the plane extending at right angles to the axis of the intermediate shaft.

Let us consider two parallel planes perpendicular to the axes of joints of the drive and driven yokes. They are perpendicular to the plane of the top projection (Fig. 3.37) and their traces on this plane are straight lines. The image of the length of spiders in this projection is $l_s \cos 45°$ (see the triangle in the bottom projection).

The axis of the intermediate shaft is perpendicular to these planes as it is perpendicular to two straight lines (axes of the joints) in these planes. It is, therefore, parallel with the upper plane of the

projections, and its image in the top projection is perpendicular to the traces of the two parallel planes.

By projecting the above straight lines to the horizontal, we obtain

$$A_x = l_i \sin \alpha + 2l_s \cos 45° \cos \alpha$$

or

$$\frac{A_x}{l_s} = y \sin \alpha + \sqrt{2} \cos \alpha$$

The angle $\alpha$ can be found from the triangle in Fig. 3.37:

$$\operatorname{tg} \alpha = \frac{\frac{l_i}{2}}{l_s \cos 45°} = \frac{y}{\sqrt{2}}$$

Then $\frac{A_x}{l_s}$ should be determined from the former formula. The change in the centre distance may be found by comparing this value with the ratio $A_0/l_s$, which is found from the formula for $A_0^2$ by transforming it into the form:

$$\frac{A_0}{l_s} = \sqrt{(2+y)\, y}$$

The equality of the ratios $\frac{A_x}{l_s}$ and $\frac{A_0}{l_s}$ is obtained at $y = 1$; in this case the angle $\alpha = 35.3°$ and $\delta = 1.5$.

With $y = 1.40$ and the coefficient $\delta = 0.034$ (close to zero), the change in the centre distance is $0.19l_s$, that is it is high enough, and the bearing for supporting the driven shaft on the oscillating frame cannot be dispensed with.

It is worthy of note that the period of the change in the centre distance in this mechanism is 1/4 of the revolution, whereas in the three-arm Hooke's joint the period of the shaft displacement is 1/3 of the revolution. In the mechanisms obtained from the Oldham coupling the period of displacement is 1/2 of the revolution, and in conventional planar mechanisms with low-class pairs, one revolution.

Unfortunately, these considerations are of only theoretical value so far, since the amplitude of these oscillations is too small for practical applications.

## 3.9. Locomotive Mechanisms

Owing to increasing speeds of passenger train locomotives, there is now a need to reduce the unsprung weight. The tramway type suspension of the traction motor, in which one half of the weight is trans-

mitted to the axle through the motor and axle bearings of the motor, has become inadequate. Now the motor is attached to the bogie with the transmission of rotation to the axle through a joint mechanism. This mechanism is necessary to permit the locomotive to oscillate on the springs. The mechanism should transmit the torque about the

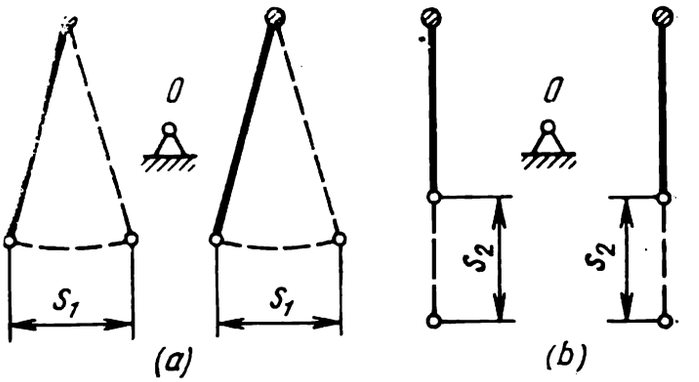


Fig. 3.38. Relative displacements in the mechanism of a locomotive drive
(*a*) horizontal; (*b*) vertical

wheel axis, while leaving the remaining mobilities free: the displacements along the three coordinate axes and rotation about two axes perpendicular to the wheel axis, that is the mechanism should have the same mobilities as the double universal Hooke's joint (see Table 1.4*f*).

The double Hooke's joint is widely used for that purpose in the cars of the series Д and E for the underground railway, in electric trains ЭР, in electric locomotives Skoda (ЧС-1, ЧС-2, ЧС-3 and ЧС-4), and in the Jaquemain drives of the French locomotives. All of them have no redundant constraints and therefore comply with the above conditions. The double Hooke's joint is well balanced. The Oldham coupling (with prismatic kinematic pairs) has not come into wide use owing to high friction and rapid wear. In addition, it is not balanced which is a very serious disadvantage for high-speed electric locomotives.

Drive mechanisms with the rotational pairs proved completely adequate and have found widespread application. Torque is transmitted in such mechanisms through two rods extending in the plane perpendicular to the axis of rotation (Fig. 3.38). The rods are provided with spherical joints (pairs $III_2'$). Owing to this, the driven member has two angular mobilities with respect to the drive member—rotations about the axes extending in the plane of the drawing. These joints also provide for two linear mobilities: one along the wheel axis (perpendicularly to the plane of the drawing) and one horizontal mobility $S_1$ (Fig. 3.38*a*) in this position of the mechanism.

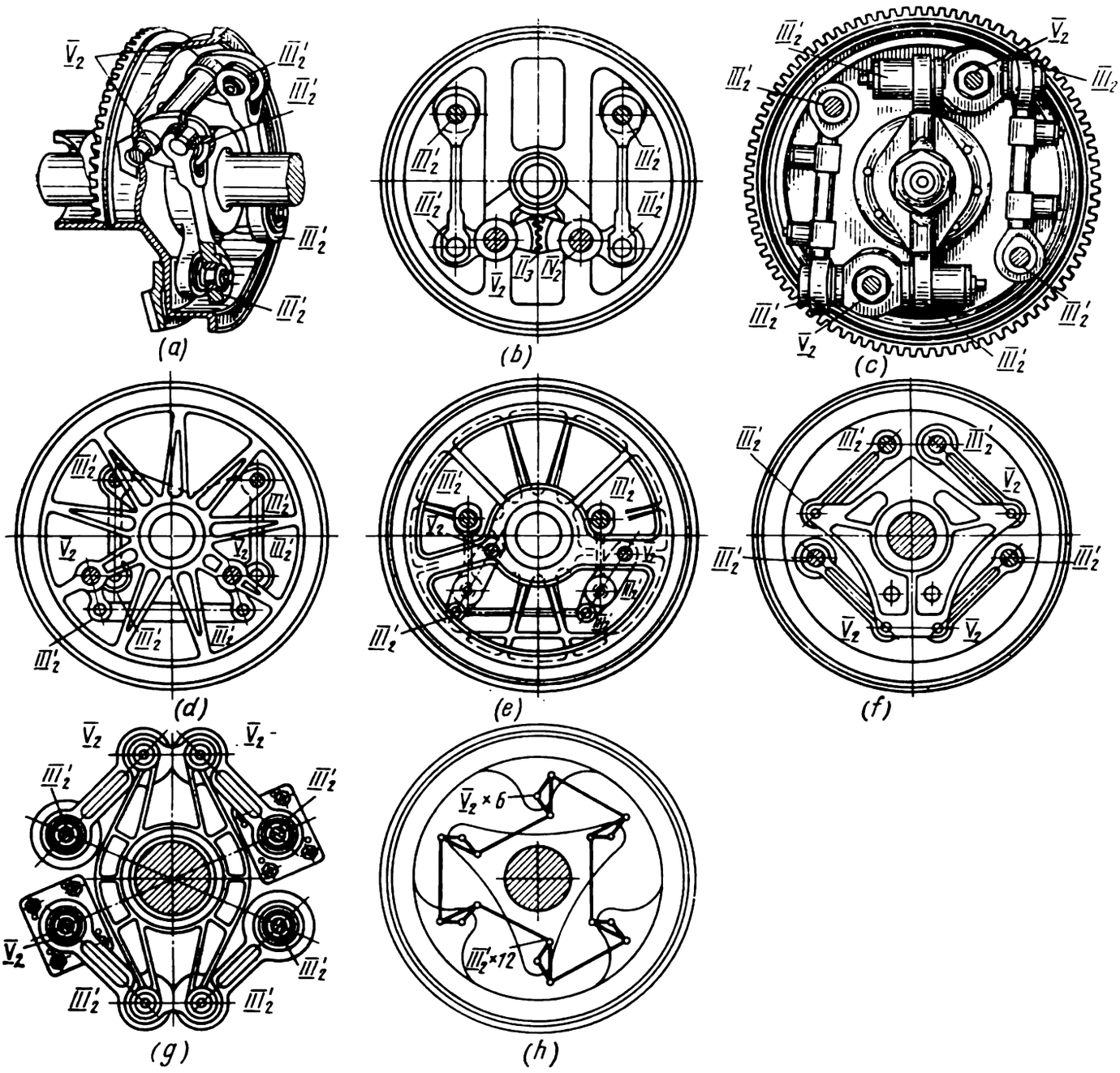


Fig. 3.39. Locomotive drives

(*a*) Siemens-Schuckert; (*b*) Buhley (Brown-Bovery); (*c*) Oerlikon-I; (*d*) Ganz; (*e*) Skoda; (*f*) Kravchenko; (*g*) Alsthom; (*h*) Yermak

In order to ensure the vertical mobility (in this position), the rods should be connected to the driven member by means of a mechanism which would enable their displacement only through equal distances $S_2$ (Fig. 3.38*b*) with respect to this member. Unequal displacements $S_2$ cannot be permitted since in such a case the driven member would turn with respect to the drive member.

The mechanism for such a coupling may be in the form of: a shaft with two cranks—the Siemens-Schuckert mechanism (Fig. 3.39*a*),

two arms interconnected by means of a gearing (Fig. 3.39*b*), two straight levers interconnected by means of a rod (Fig. 3.39*c*), two angle levers interconnected by means of a rod (Fig. 3.39*d*), two oblique levers interconnected by means of a rod (Fig. 3.39*e*), a mechanism of parallel crank by Kravchenko (Fig. 3.39*f*), an antiparallelogram Alsthom mechanism (Fig. 3.39*g*).

An interesting multiple-arm mechanism has been proposed by V. N. Yermak. This mechanism may be made with four, six (Fig. 3.39*h*) and even greater number of arms (but only the even number should be used) so that loads in the joints are reduced.

In all these diagrams, the joints connected to the driven member are shown with the lefthand hatching, and those connected to the drive member with the righthand hatching. It should be noted that the terms drive and driven members are purely conventional in this case and they can be reversed (if this is more convenient for the design purposes). All the above-mentioned mechanisms are at the same time equalizing mechanisms, that is they equalize the loads in the rods. Owing to this, only torques are transmitted to the drive and driven members, and additional loads on the bearings are eliminated.

The Siemens-Schuckert mechanism (see Fig. 3.39*a*) is the simplest among them. Of six members, five are movable. It may be easily made without redundant constraints. For that purpose, the rods are made with spherical heads $III_2'$, and the remaining pairs may be the rotational pairs $V_2$. The bearings of the drive and driven shafts (the pairs $V_2$) are not shown in Fig. 3.39. The mobility of the mechanism is $w = 3$ (the main plus two local mobilities—rotations of the rods about their axes), and the number of redundant constraints is $q = 3 - 6 \times 5 + 5 \times 3 + 3 \times 4 = 0$ from formula (1.1).

Forces in the joints are small and they are approximately equal to the forces transmitted by the rods. The mechanism can be readily balanced: it is sufficient to install balance weights on an equalizing shaft. The only disadvantage of such a mechanism resides in a torque transmitted by the equalizing shaft.

The Buhley mechanism (Fig. 3.39*b*) is more complicated; it has seven members and six of them are movable. In order to avoid redundant constraints with the line contact between teeth (pair $II_2$), which is very important owing to large forces, one of the levers should be supported by means of the pair $IV_3$. It is not necessary to make this pair in the form of the spherical pair with a pin, for that purpose. The lever may be supported by a spherical support, and the redundant mobility may be eliminated by providing projections in the casing to limit the displacement of the rim along the axis: from formu-

la (1.1) $q = 3 - 6 \times 6 + 5 \times 3 + 4 \times 1 + 3 \times 4 + 2 \times \times 1 = 0$.

It is more preferred to use an arch tooth—the pair $II_3$, and one of the arms should be installed by means of the pair $IV_2$.

If both arms are supported by the rotational pairs $V_2$, the teeth should have a point contact (pair $I_2$) to eliminate redundant constraints, which is disadvantageous owing to large forces. The forces transmitted by the teeth of the equalizing mechanism are about equal to the forces in the rods (with the same radii). Forces on the pivots of such levers are twice as great (in case centrifugal forces are ignored), which is disadvantageous. The mechanism can be readily balanced.

The mechanisms Oerlicon-1, Ganz, Skoda, Kravchenko and Alsthom have eight members and seven among them are movable.

In the Oerlicon-I mechanism (Fig. 3.39*c*), to eliminate redundant constraints, the ends of all three rods are made with spherical supports (pair $III_2'$), and the lever supports with the rotational pairs $V_2$; from formula (1.1) $q = 4 - 6 \times 7 + 5 \times 4 + 3 \times 6 = 0$

Forces in the spherical pairs are equal to the forces in the rods, and forces in the rotational pairs are twice as great (without taking into account the centrifugal forces). The mechanism is well balanced. It does not require balance weights with correct dimensioning.

The Ganz mechanism (Fig. 3.39*d*) should have the same kinematic pairs as the mechanism Oerlicon-I in order to eliminate redundant constraints. Forces in the spherical pairs are equal to the forces in the rods (with the same arm lengths), and forces in the rotational pairs are 1.4 ($\sqrt{2}$) times greater than the forces in the rods. The mechanism can be balanced. For that purpose, angle levers should be provided with balance weights.

The Skoda mechanism (Fig. 3.39*e*) should have the same kinematic pairs as the Oerlicon-I and Ganz mechanisms. Forces in the kinematic pairs depend on the ratio of arm lengths and angle of inclination of the levers. They are about equal to the forces in the Ganz mechanism. It is more difficult to balance this mechanism compared to the Ganz mechanism as the balance weights installed on the levers may extend beyond the overall dimensions.

In the mechanisms by A. I. Kravchenko (see Fig. 3.39*f*) and Alsthom (see Fig. 3.39*g*) the torque is transmitted through a floating frame suspended on arms. For the frame to remain in a pre-set plane, it must be guided by three arms since the position of the plane is defined by three points. The fourth arm should not be the guide arm so as to avold redundant constraints. It must, therefore,

have the spherical pairs $III_2'$ at both ends. There is only one local mobility here—rotation about its own axis. Each guide arm should have one rotational pair $V_2$ and one spherical support point $III_2'$. For a better guidance of the floating frame, the support points should be spaced from one another as much as possible. Accordingly, the rotational and spherical pairs are arranged appropriately in Fig. 3.39, *f* and *g*. According to (1.1), $q = 2 - 6 \times 7 + 5 \times 5 + 3 \times 5 = 0$.

In case these mechanisms are made with rubber blocks which, while being cylindrical in shape, enable a certain amount of rotation with respect to two other axes owing to rubber deformation, all joints are made identical. Forces transmitted by the kinematic pairs in the mechanisms shown in Figs. 3.39*f* and 3.39*g* are small. In the Alsthom mechanism all four rods are tensioned or compressed, and in the mechanism by Kravchenko two rods are tensioned and two compressed, which contributes to a smoother operation. The Alsthom mechanism exhibits a certain non-uniformity of the transmission ratio, which is practically imperceptible. The transmission ratio in the mechanism by Kravchenko is strictly constant. The mechanisms by Kravchenko and Alsthom are unbalanced. In case of misalignment of the axes, the floating frame moves along a circle of a diameter equal to the amount of the misalignment (similarly to the Oldham coupling). The centre of gravity of the frame moves twice around the circle during one revolution of the wheel. This results in an enormous centrifugal force in high-speed electric locomotives.

The centrifugal force in the French electric locomotives that set up the speed record 300 km/h was as high as 7.5 tf. It is practically impossible to balance these mechanisms, since balance weights should be installed on the extensions of the arms, that is beyond the overall outlines. In addition, the inertia forces of the balance weights would increase the loads in the kinematic pairs here to such an extent that it would be impossible to realize such pairs.

The mechanism by V. N. Yermak (Fig. 3.39*h*) consists of equal-arm angle levers. One half of the levers are supported by the drive shaft by means of the pairs $V_2$ and the others are supported by the driven shaft by means of similar pairs. The levers are interconnected by means of the arms $III_2'$, $III_2'$. The mechanism is well balanced. The transmission ratio in the mechanism is constant. Forces in the joints are small, and they can still be diminished by increasing the number of arms. The mechanism has also a local group mobility—

rotation of all levers about their pivots. In order to make this mobility unharmful, appropriate stops should be provided.

With $i$ arms, the mobility is $w = 1 + i + 1$ (the main mobility, plus rotation of $i$ arms, plus the group mobility). From (1.1), $q = (2 + i) - 6(2 + 2i) + 5(2 + i) + 3 \times 2i = 0$. The analysis of the above-described mechanisms has shown that certain designs are well balanced but exhibit large forces in the joints, while others, on the contrary, exhibit small forces in the joints but are poorly balanced.

In the process of design, the engineer should correctly assess the prevailing importance of one of these factors and make the choice of the mechanism design based on this assessment.

It is interesting to make the comparison of the above-discussed mechanisms (see the Table).

| | Siemens-Schuckert | Buhley | Oerli-con-I | Ganz | Skoda | Kravc-henko | Alsthom | Yermak with 3 arms | Double Hook's joint |
|---|---|---|---|---|---|---|---|---|---|
| Number of movable members | 5 | 6 | 7 | 7 | 7 | 7 | 7 | 14 | 6 |
| Number of kinematic pairs | 7 | 9 | 10 | 10 | 10 | 10 | 10 | 20 | 7 |
| Maximum load | $Q$ | $2Q$ | $2Q$ | $\sqrt{2}Q$ | $\sqrt{2}Q$ | $Q$ | $Q$ | $0.578Q$ | $Q$ |
| Total load | $6Q$ | $9Q$ | $10Q$ | $8.8Q$ | $8.8Q$ | $8Q$ | $8Q$ | $7.46Q$ | $8Q$ |
| Balancing | 1/2 | 1/2 | 1 | 1/2 | 1/2 | 0 | 0 | 1 | 1 |

The comparison starts with the generally known parameters such as the number of teeth and the number of kinematic pairs. A very important parameter is the maximum load in the kinematic pair, since not unfrequently it is difficult to accommodate a kinematic pair of an appropriate size in the traction gearings.

The next line represents the total load in kinematic pairs. This characterizes the mechanism in a much better manner than the number of pairs; moreover, it is indicative of friction losses in the first approximation.

The last line characterizes the balancing. Completely balanced mechanisms are marked with *1*. The mechanisms that can be readily balanced are marked with *1/2*, and the mechanisms for which the ways of balancing them are unknown to the author are marked with 0.

The mechanisms of Oerlicon-I, Yermak and double Hooke's joint are completely balanced. They should be used in the most high-speed locomotives.

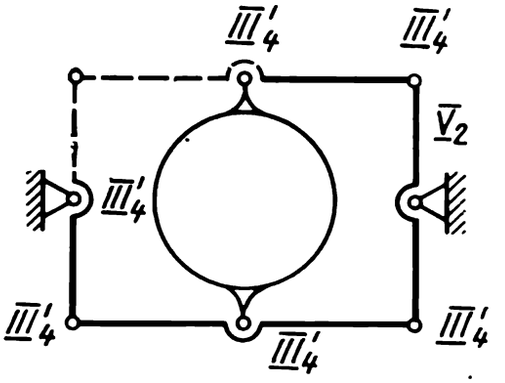


Fig. 3.40. False king bolt mechanism (members eliminated to avoid redundant constraints are shown with dash lines)

The Yermak mechanism is the best from the viewpoint of maximum load: $0.578Q$, then comes the double Hooke's joint, while the Oerlicon-I and Buhley are the worst—$2Q$. The large number of teeth used in the Yermak mechanism is therefore warranted for the locomotives.

The Siemens-Schuckert mechanism is the simplest one. It is interesting to note that the same mechanism was used by the French engineer Jaquemain (see Fig. 3.39) where the rotational pair connecting the cardan shaft to the drive shaft was turned at 90°.

All the above-discussed mechanisms ensure the linear movement of the drive member with respect to the driven member (in the plane perpendicular to the axis of rotation), which is similar to the movement in an artioulated drawing board. Therefore, the value of these mechanisms goes far beyond the sphere of the locomotive drives. For example, they can be used for guiding the drive plate in a gang drill head.

A false king bolt mechanism is employed in locomotives (Fig. 3.40) which is used for coupling the bogie to the body in applications where the place for installation of the king bolt is occupied by other devices (such as a traction motor). The Foight mechanism comprises a parallelogram (a part of its members are shown with dotted lines in Fig. 3.40). The middle parts of the transverse levers are connected to the body (which is conventionally regarded as fixed). The middle

parts of the longitudinal levers are coupled to the bogie (conventionally shown in the form of a circle).

According to (1.5), $q_n = 1 - 3 \times 5 + 2 \times 8 = 2$.

Two redundant constraints cause two strains (in the assembly of the parallelogram with the body and its coupling to the bogie), and they result in non-uniform loading of the transverse and longi-

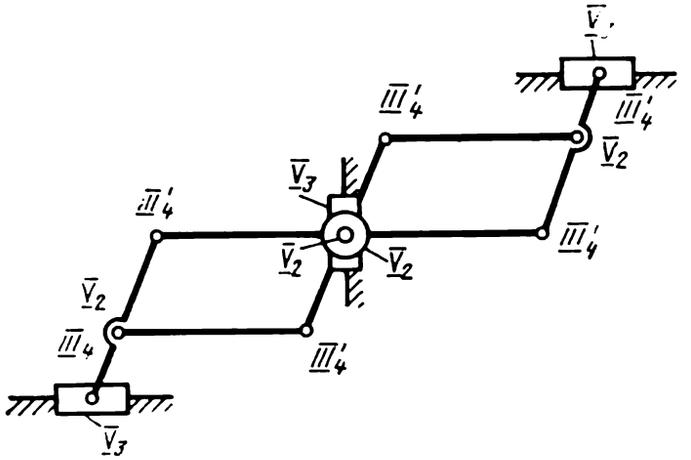


Fig. 3.41. Mechanism for a shaftless gas generator

tudinal levers. In order to eliminate the strains, the portions of the levers shown with dotted lines and one joint should be discarded. Then, according to (1.5), $q_n = 1 - 3 \times 5 + 2 \times 7 = 0$.

There are no especially harmful redundant constraints now. In order to eliminate the redundant constraints altogether, the kinematic pairs shown in Fig. 3.40 should be used.

Mobilities of the mechanism are rotations of the bogie about three axes, vertical displacement (spring plays), and rotations of three members about their axes (pairs $III'_4$). There are seven mobilities in total.

The number of redundant constraints according to (1.1): $q = 7 - 6 \times 5 + 5 \times 1 + 3 \times 6 = 0$.

Diesel locomotives with a pneumatic transmission which is simpler, less expensive and more lightweight compared to the electrical transmission are now coming into use in the USSR in accordance with the concept proposed by Prof. A. N. Shelest.

Pescar proposed shaftless gas generators which are now used in diesel locomotives. Pistons of the shaftless gas generator should move towards one another at the same speed, hence they travel through identical distances. This is ensured by an equalizing linkage (Fig. 3.41). There are other systems, such as toothed systems. The complicated design of the equalizing mechanism is due to a small size, hence, large angles of rotation of rocker arms (180°), so that a twin link gear cannot be used.

In order to avoid particularly harmful redundant constraints, the central joint should be self-aligning in the vertical direction on the slide (as shown in Fig. 3.41). According to (1.5), $q_n = 1 - -3 \times 9 + 2 \times 13 = 0$. In the Pescar shaftless gas generator the most harmful redundant constraints remain.

To eliminate redundant constraints in the structural design of a mechanism (in choosing classes of the kinematic pairs), it is necessary to avoid strains in closing-up the loops of the mechanisms.

Pistons of the shaftless generator are the translatory pairs $V_3$ as eccentric piston rods hamper their rotation. An auxiliary slider can be installed in the translatory pair $V_3$, the rotational pairs $V_2$ can be provided on the rocker arms, and the sliders can be coupled to the rocker arms by means of SAPS groups $III_4'$, $III_4'$, $V_2$, $III_4'$ shown in Fig. 2.54*b*.

The mechanism can be checked for redundant constraints by formula (1.1): $q = 1 - 6 \times 9 + 5 \times 7 + 3 \times 6 = 0$.

## 3.10. Main Mechanisms of Current Collectors

The pantograph collector is a complicated three-dimensional mechanism. With deviations of dimensions of the members from nominal ones caused by manufacturing tolerances and skewing of the pantograph base during assembly on the roof, friction substantially increases in conventional types of pantograph collectors. It is therefore difficult to keep the pre-set difference in pressures on the contact wire during the lifting and lowering of the pantograph collector.

In order to facilitate the manufacture and operation of the pantograph collector, its mechanism is to be so designed that deviations of dimensions should not cause an increase in friction. This condition is fulfilled in mechanisms free of redundant constraints. Main shafts of pantograph collectors are coupled by means of an antiparallelogram mechanism enabling vertical movement of the collector strip [44].

The pantograph collector is a guide mechanism ensuring the straight-line contact shoe movement in the vertical direction. The direction of this movement may be adjusted by varying the length of the rod interconnecting the main shafts. With an increase in the length, the straight line is caused to turn to the right and with a decrease, to the left (Fig. 3.42*b*).

The antiparallelogram mechanism is made with one or two rods. With one rod, the coupling mechanism have no redundant constraints. Owing to this, small deviations in dimensions of the rod,

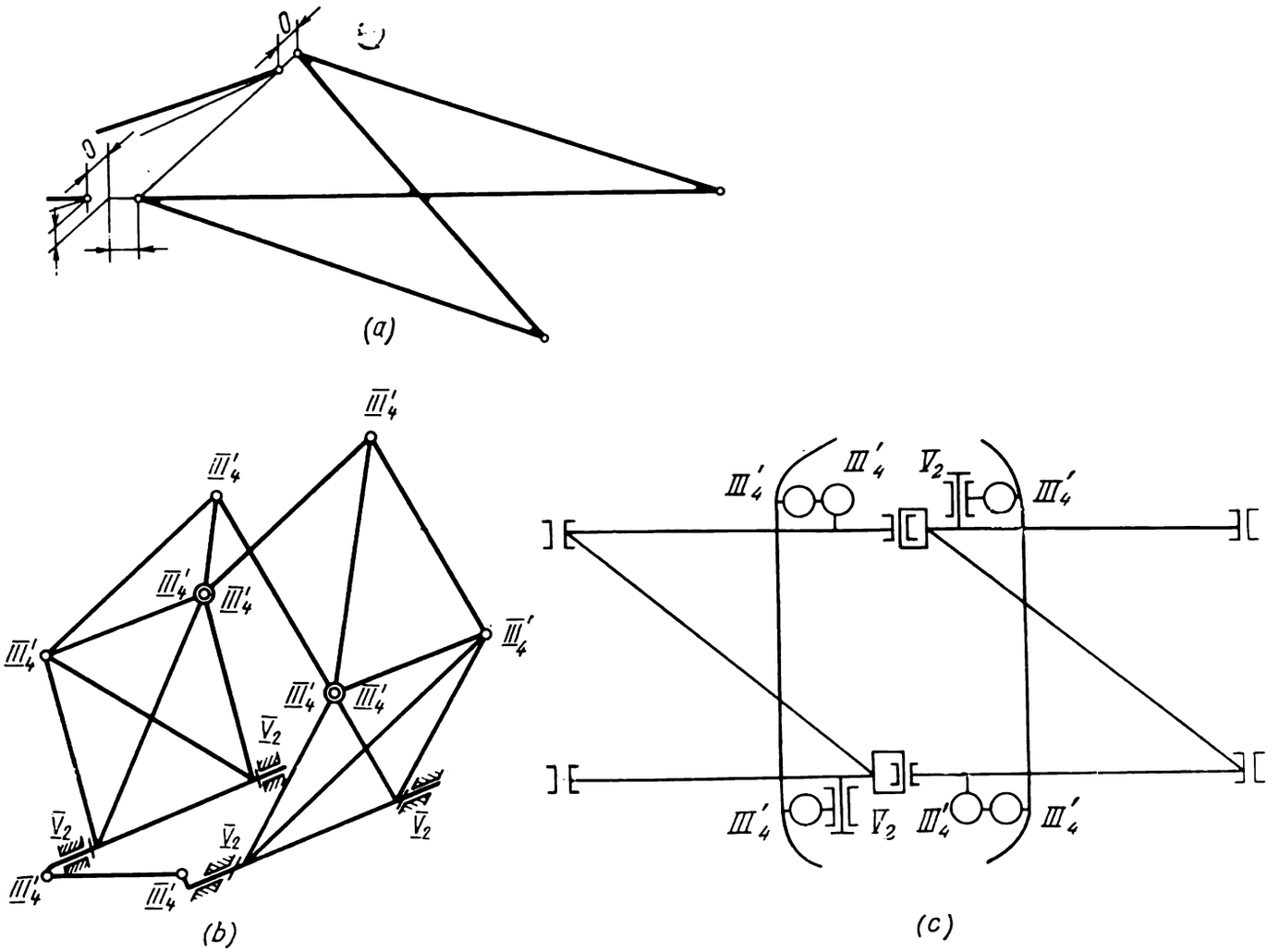


Fig. 3.42. Two-shoe pantograph collector

*a*) strains in the assembly of the main mechanism composed of rigid frames; (*b*) design of the main mechanism without redundant constraints; (c) design of the upper carriage without redundant constraints; *v* is the vertical and *h* horizontal dimension in (*a*)

centre distances between axes of the main shafts, and radii of cranks have no effect on friction. With two rods, owing to the presence of redundant constraints, dimensional deviations cause overload of the joints. Therefore, the main shafts of the pantograph collector should be interconnected by one rod, rather than two. Breakage of the rod is not dangerous, since in some instances the coupling rods are made of wood and serve as protective members which fail in case the pantograph collector interferes with the contact system; other, more expensive parts, remain intact. With a correct design of the pantograph collector, the protective member is necessary. The best way is to insert the protective member into the coupling rod. It is inexpedient to use the rod itself for this purpose, since it is tensioned when the train moves in one direction and subjected to buckling when the train moves in the opposite direction.

So that the force under which the rod would break when the train moves in one direction strongly differs from the force under which this rod would break when the train moves in the opposite direction.

Let us discuss the main mechanism. As shown by the theory, there are three redundant constraints in the pantograph collector ДЖ-4. They can be detected in assembling the pantograph (Fig. 3.42*a*). After the upper frames are connected to the lower frames which are installed on the pantograph base, the upper frames having their dimensions different from nominal ones should be interconnected with a certain amount of strain resulting in an increased friction since one of the joints is axially misaligned (*o* in Fig. 3.42*a*), and the other joint is also misaligned in the horizontal (*h*) and vertical (*v*) directions.

In order to diminish the harmful effect of these strains, they should be eliminated or reduced at the middle of the working height.

To eliminate the axial misalignment of the joints *o*, washers should be placed under one of the insulators, and the parallelism of the main shafts should be broken to eliminate the horizontal misalignment *h* of the joints. To eliminate the vertical misalignment *v* of the joints, the upper frames should be bent (twisted). The alignment of the joints can be, however, achieved only within a narrow range, and the result can be obtained in one position of the pantograph collector only. The strain may be eliminated by using the design of the main pantograph collector mechanism shown in Fig. 3.42*b*. Here the upper frames are made in the form of two "tripods" with the legs supported by the joints of the lower frames. The "tripods" which comprise structural groups with zero mobility according to Fig. 2.47 may be assembled without strain with any deviations of dimensions of their members from nominal values. The distance between the joints in the coupling of the upper frames is, however, also different from the nominal dimension and may prove different at different positions of the mechanism (different height of contact shoes). These joints cannot, therefore, be interconnected by means of rigid rods as a redundant constraint can be caused in such case. The latter condition can be hardly fulfilled in a single-shoe pantograph collector since the contact shoe itself generally provides such a joint.

In operation of such pantograph collectors, in order to eliminate increased friction caused by the strain (that is if the characteristic of the pressure on the contact wire is not kept constant), the upper carriage should be removed and constant distances between the

joints of the upper frames coupling should be obtained in different positions of the mechanism. This distance should correspond to the carriage length, which is achieved by placing spacers on one of the insulators, so that the mechanism could be assembled without strains, and this can be achieved either by varying the length of oblique rods or by skewing the pantograph base which may require an enlargement of holes for bolts securing the base to the insulators.

On the contrary, this condition is readily fulfilled in two-shoe pantograph collectors. For this purpose, the carriage should be so constructed that each contact shoe be axially (transversely) movable relative to one "tripod" and fixed relative to the other "tripod". Accordingly, one lever $V_2III'_5$ supporting the shoe should be retained, and the other lever should be replaced by a plate $III'_4III'_4$ which does not hamper the axial movement of the contact shoe owing to plays in the joints.

These joints are conventionally shown as spherical joints in Fig. 3.42*c*, and the contact shoes themselves are turned through 90°. The carriage brackets are not shown.

Redundant constraints in single-shoe pantograph collectors may be eliminated by dispensing with one of oblique rods of the upper frames. This design is used in pantograph collectors WVSS-54 (Austria) and DBS-54 (West Germany). It is deficient in that the lateral rigidity is ensured only by one half of the mechanism, the other only making the pantograph heavier. This design restricts the use of such pantograph collectors only to the high-speed rolling stock where the light-weight and lateral rigidity are especially important. Therefore, the design with the upper frames composed of two "tripods" is not suitable for the single-shoe pantograph collector. Let us consider this design (Fig. 3.43*a*). The upper frames should form a zero mobility group, that is if their lower joints are connected to a fixed member, the system must be fixed. We will discuss it in this (simplified) form. Certainly, in case the upper frames are coupled to the lower frames, the system obtains the mobility owing to the lower frames mobility.

The horizontal transverse rod which serves as the upper carriage base is supported by six arms: four longitudinal rods and two diagonal rods. Unfortunately, all six arms intersect the axis of the rod, that is the tenth condition of Table 3.1 is not fulfilled. The system becomes statically indeterminate, and a local mobility—rotation of the carriage base about its axis (transverse rod) appears.

To eliminate this mobility, link mechanisms are provided in the pantograph collector 1OPP. For correcting the design, at least one

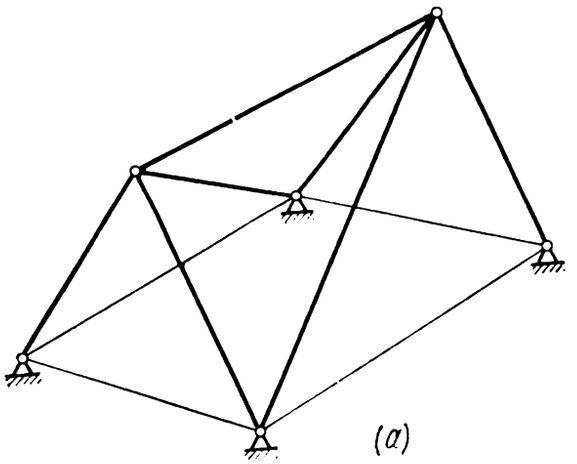

(a)

Fig. 3.43. Upper frames of a single-shoe pantograph collector
(*a*) with a redundant constraint; (*b*) without redundant constraints

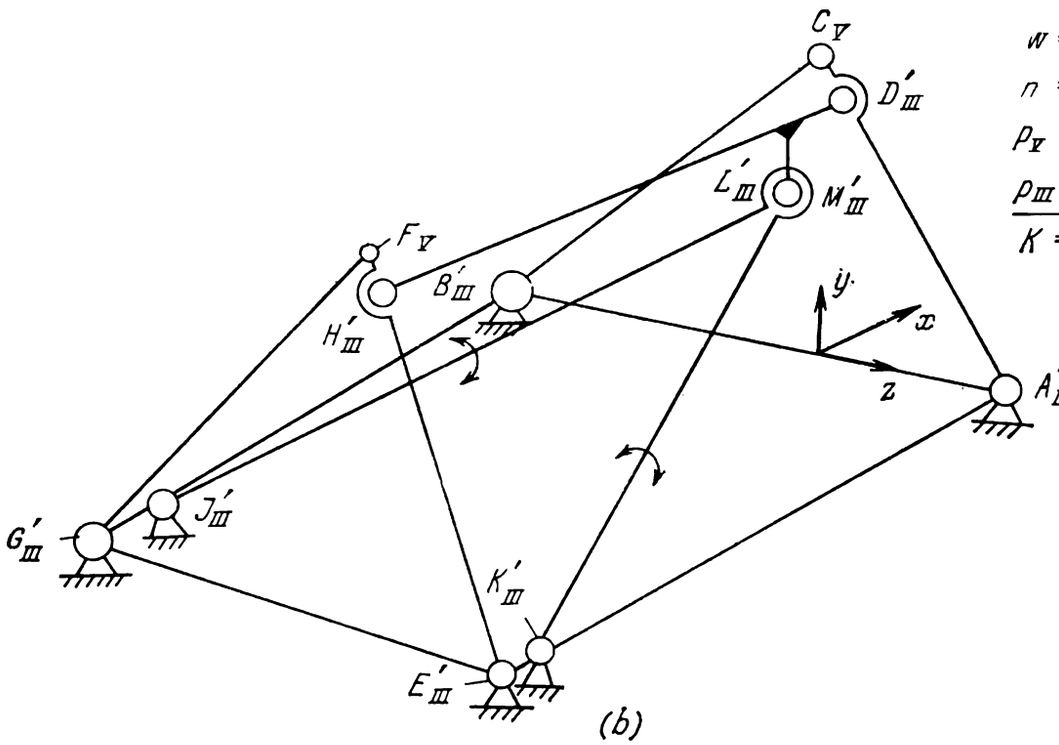


(b)

| | | | |
|---|---|---|---|
| $w = 2$ | 2 | 2 |
| $n = 7$ | -42 | 30 |
| $p_V = 2$ | 10 | -2 |
| $p_{III} = 10$ | 30 | -30 |
| $K = 5$ | 0 | 0 |

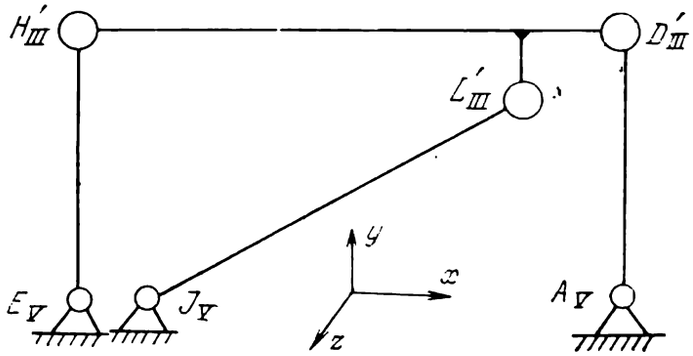


| | | | |
|---|---|---|---|
| $w = 0$ | 0 | 0 |
| $n = 4$ | -24 | 12 |
| $p_V = 3$ | 15 | -3 |
| $p_{III} = 3$ | 9 | -9 |
| $K = 2$ | 0 | 0 |

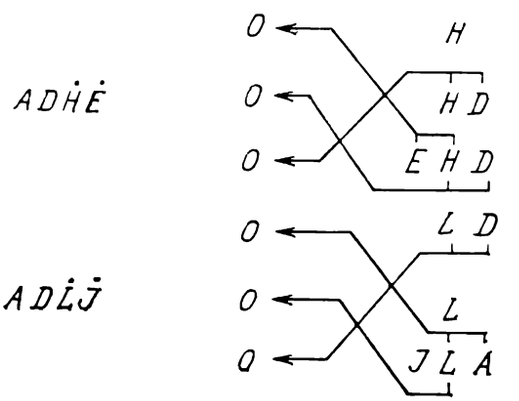


(c)

arm (two for the sake of symmetry) should be offset with respect to the axis of the transverse rod. The diagonal rods should be used as such arms, and they are to be displaced downwards, since the place over the transverse rod is occupied by the contact strip. The direction of one of the diagonal rods should also be changed by making both diagonal rods to extend toward one upper joint (Fig. 3.43*b*). Otherwise a mobility (rotation of the transverse rod with simultaneous transverse displacement) and a strain would remain owing to the presence of the second diagonal rod.

For the contact strip to move vertically without lateral displacement, the lower ends of the diagonal rods should be coupled to the lower frames, rather than to the upper ones, with an appropriate choice of the connection point. Link mechanisms for guiding the upper carriage can then be dispensed with. Such pantograph collectors have been manufactured at the Electric Locomotive Depot Moskva III according to the design by the Undergraduate Design Office of the Baumann Higher Technical School. A part of single-row ball bearings were replaced by spherical double-row bearings. The doubled friction force reduced to the contact strip was substantially reduced from 2.5-3 kgf to 0.8-0.9 kgf and became independent of the operation dimensions (such as of the insulator height), the repair was substantially simplified, and the check of the characteristic became superfluous.

In Fig. 3.43*b* the kinematic pairs $C$ and $D$, as well as $F$ and $H$, are spaced apart for the sake of clarity. In the real structure they coincide with one another. Redundant constraints are calculated in the Table in this Figure. There are 5 loops. Let us show how the number of loops can be reduced by way of the example of this mechanism. For that purpose, the first class arms are united into pairs and considered as the second class arms of Figure 3.43*c*. The arms $AC$ and $CB$ define a triangle rotating about the axis $AB$ which is regarded as the fifth class pair. The pair $D$ is retained, and the arm $AD$ is obtained.

Similarly, the second class arm $LJ$ is obtained from two first class arms $LJ$ and $MK$, and the arm $EH$ is obtained from the arms $FE$ and $FG$.

The number of loops is reduced to two (see the Table of mobilities in Fig. 3.43*c*), which considerably simplifies the study. The diagram of mobilities in these loops is shown in the same Figure.

To summarize the above, a conclusion may be drawn that in selecting the design of a single-strip pantograph collector, the diagonal rods should be directed toward one and the same upper

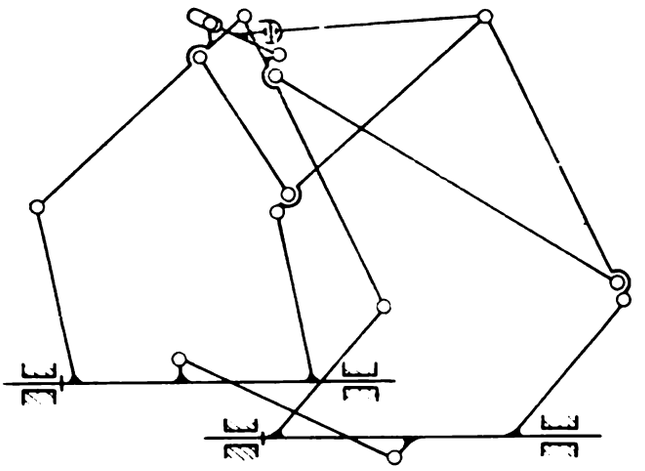

Fig. 3.44. Design of a pantograph collector with diagonal rods directed toward one upper joint

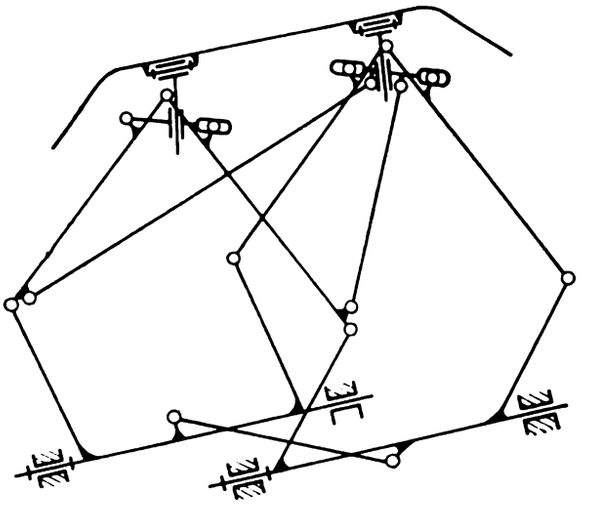

Fig. 3.45. Design of a pantograph collector with diagonal rods coupled to the base of the upper carriage

joint (Fig. 3.44), and two other conditions should be fulfilled as well: a mobility should be introduced to eliminate strains and the equality of loads of the diagonal rods should be achieved under the action of the lateral force applied to the strip.

Both these conditions are fulfilled in the above-discussed mechanism with the use of the transverse rod (the upper carriage base) when the oblique rods are coupled below its axis.

In the current collectors П-1 and П-3, the upper carriage base is coupled to the upper frames by means of grooved members installed on stub shafts. In this case the oblique rods should be directed toward one and the same upper joint (Fig. 3.45) and they should be coupled to the base of the upper carriage, rather than to the longitudinal rods. In this design the mobility is obtained owing to displacements in the grooves, and equal loads in the rods are ensured due to the symmetrical arrangement of forces acting on the upper carriage base. Still two other solutions of the same problem are possible (Figs. 3.46 and 3.47—the oblique rods are not shown).

In the design shown in Fig. 3.46 the mobility is achieved owing to the axial (transverse) displacement in the joint interconnecting the upper frames.

Uniform distribution of loads caused by the lateral force is achieved owing to a lever with a groove installed on a stub shaft, the upper carriage base being coupled to the middle of the lever.

In Fig. 3.47 the longitudinal rods of the upper frames are interconnected by means of two crossing rods having spherical heads. Owing to the spherical heads, the longitudinal rods acquire relative

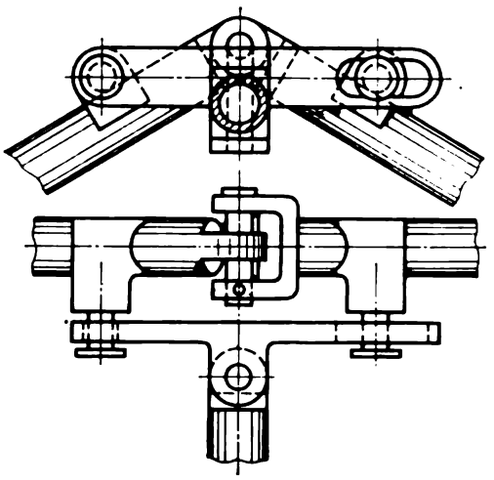

Fig. 3.46. Design of the main upper joint with an axial spacing of the longitudinal rods

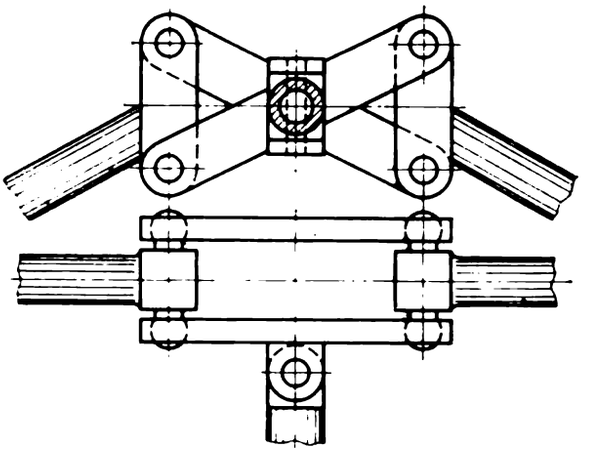

Fig. 3.47. Design of the main upper joint with crossing rods

mobility in the axial direction. One of the crossing rods is used as a lever equalizing the loads of the oblique rods, caused by the lateral force. The point of intersection of the oblique rods is centre of instant rotation of one longitudinal rod with respect to the other.

The designs shown in Figs. 3.45, 3.46 and 3.47 were tested by the author, using models at the Baumann Higher Technical School.

The mobility intended to eliminate the strain may be directed lengthwise the locomotive (see Figs. 3.43*b* and 3.45), or transversely (Figs. 3.46 and 3.47) which is practically of no difference.

It is much easier to eliminate redundant constraints in an asymmetrical pantograph collector (Fig. 3.48) which came recently in use for alternating current electric locomotives. Owing to high voltage, the current consumed by the electric locomotive is 7-8 times lower compared to the direct current. The two-shoe pantograph collectors of the heavy weight series became thereof obsolete. An asymmetrical current collector (semi-pantograph) belongs to the pantograph collectors of the light-weight series. It consists of a lower tubular frame *VV* in the form of an I-beam and an upper frame in the form of a trapezium. The rod $III'_4III'_4$ provides the movement of the upper frame.

The kinematics of this mechanism should provide for the straight-line vertical movement of the contact shoe, that is the mechanism is a straightening gear (similarly to the symmetrical pantograph).

Such a mechanism may be designed similarly to a gantry crane with a rigid brace (see Figs. 6.20 and 6.21).

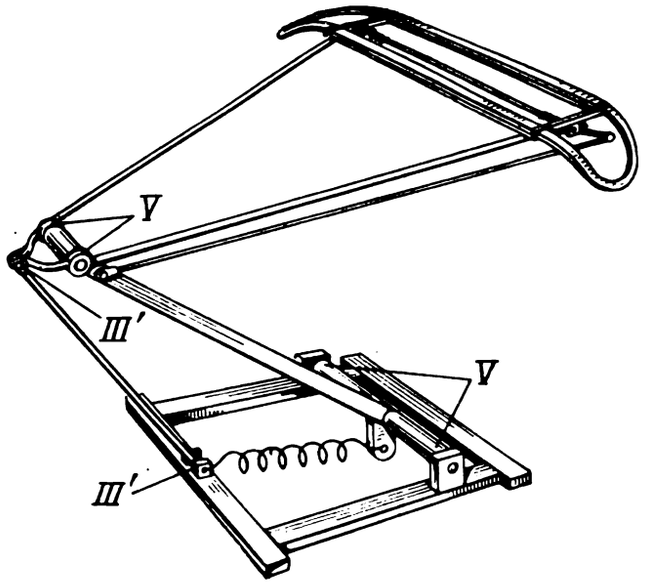


Fig. 3.48. Main mechanism of an asymmetrical pantograph (semi-pantograph)

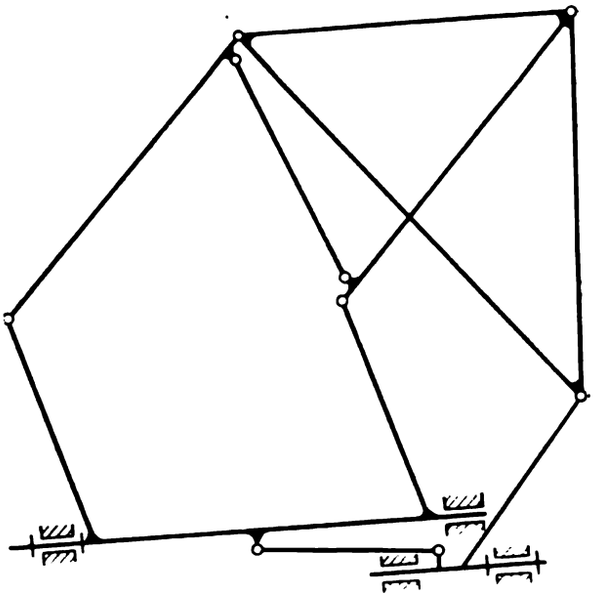

Fig. 3.49. Half-symmetrical (three-lever) current collector

In calculating redundant constraints, added to the main mobility is the rotation of the rod $III_4'III_4'$ about its axis, so that, according to (1.1), $q = 2 - 6 \cdot 3 + 5 \cdot 2 + 3 \cdot 2 = 0$.

A half-symmetrical (three-lever) pantograph collector (Fig. 3.49) takes an intermediate position between the symmetrical (four-lever) pantograph and semi-pantograph (single-lever pantograph). One half of this pantograph is absolutely the same as in the four-lever current collector, and the other half consists of a lower single-lever frame and an upper triangular frame. The base of this current collector is fixed by means of three insulators.

Slots are made instead of holes to eliminate redundant constraints (fixed coupling according to Fig. 2.4*d*), which makes it possible to avoid strains and damage to insulators during assembly of the pantograph collector. Compared to the semi-pantograph, the joints of this mechanism are considerably less loaded.

Current collectors of modern passenger train locomotives should ensure reliable current collection at a speed of 200 km/h. The mass of the current collector reduced to the contact strip is very important at such a speed. In order to lower this mass, I. A. Belyaev proposed a "self-controlled" current collector, which consists of an upper pantograph which is movable under the pressure of the contact wire, and a lower pantograph actuated by a pneumatic cylinder. The upper pantograph controls the admission and discharge of compressed air in the cylinder. The upper pantograph is very

small in size, and its reduced mass was lowered respectively. Let us consider the design of a self-controlled current collector in which the redundant constraints are completely eliminated (Fig. 3.50). The lower gear of the current collector is a parallel crank gear. Each crank consists of a lower shaft and two levers. It is connected

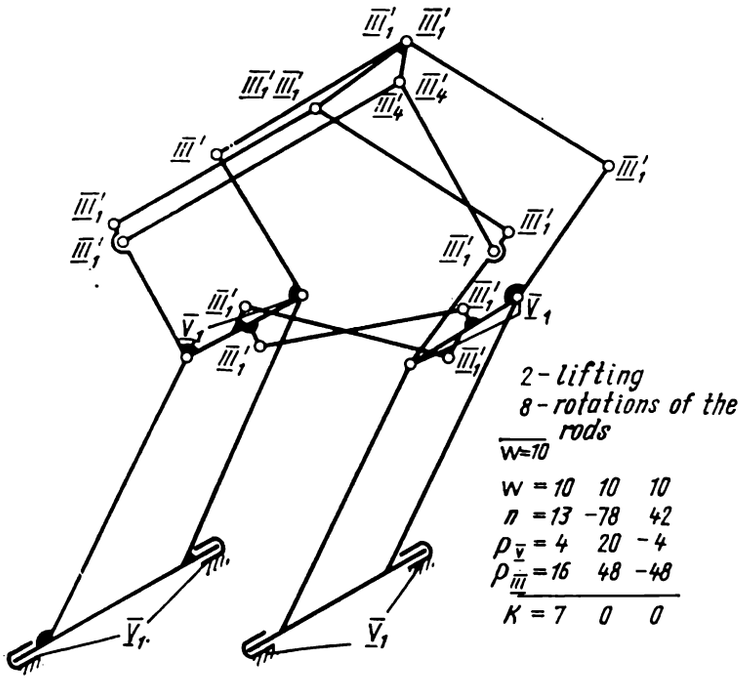


Fig. 3.50. Self-controlled current collector

by means of the pair $V_1$ to the base and by means of the pair $V_1$ to the main shaft of the upper pantograph. The lower gear is actuated by the pneumatic cylinder through a crank gear which is not shown in Fig. 3.50, as such a mechanism was discussed above (see Fig. 2.28). The upper mechanism is symmetrical pantograph (pentagon). Redundant constraints can be eliminated by using one of the above described designs shown in Figs. 3.43, 3.45, 3.46, and 3.47 (the design of Fig. 3.43 is used in Fig. 3.50).

To eliminate redundant constraints, the base (frame) of the upper pantograph is replaced with another mechanism of antiparallelogram which connects the main shafts.

Dimensions of the members of the antiparallelograms should be chosen based on the condition of maximum accuracy of the transmission ration (unity) according to the theory by V. V. Solomin [44], because otherwise the distance between the main shafts would vary. Calculations show that with the correct choice of dimensions, a change in the centre distance is fractions of millimetre. It has been found experimentally that the consumption of contact inserts,

in a self-controlled current collector was reduced several times The wear of the contact wire is expected to be reduced.

The current collector shown in Fig. 3.50 has two disadvantages: first, it is complicated (two pneumatic cylinders); second, the asymmetrical lower mechanism prevents its use in both directions. But these disadvantages have been eliminated. †

## 3.11. Current Collector with Two Mobilities

A contact system represents a multiple-mass system with many degrees of freedom, whose movement is very complicated. For simplicity, assume (after B. Fink, I. Beyer, F. Knithammer, and

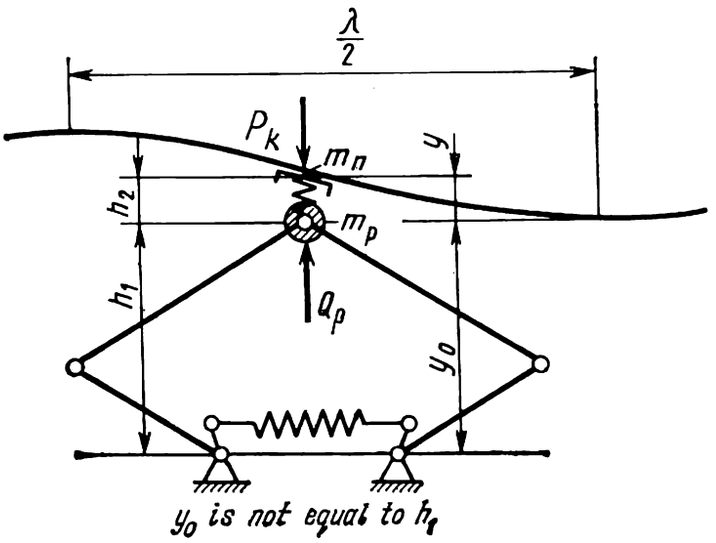


Fig. 3.51. Current collector with two mobilities

I. A. Belyaev) that the contact strip moves along a sinusoid (Fig. 3.51):

$$y = y_{max}(1 - \cos \omega t)/2 \tag{3.7}$$

Here ω is the angular velocity of the vector, the vertical projection of which gives the displacement of the contact strip:

$$\omega = 2\pi v/\lambda \tag{3.8}$$

where λ is the wavelength.

Let us denote the contact strip mass as $m_s$; the mass of the movable frames reduced to the upper joint, which is assumed constant, as $m_f$; the elastic force of lift springs reduced to the upper frame joints as $Q_f$ which is also assumed constant. This condition is met

† Here and elsewhere this symbol implies the availability of a relevant USSR Inventory Sertificate.

especially accurately in pantograph collectors with a chain transmission between the lift springs and the main shaft.

Let us denote the height of the upper joint over the pantograph base as $h_1$ (a variable), and the height of the carriage as $h_2$, that is the distance from the upper joint to the contact strip (also a variable). Then

$$h_1 + h_2 = y_0 + y \tag{3.9}$$

where $y_0$ is the minimum height of the wire over the current collector base.

Let us denote the height of the carriage in the neutral state as $h_{2n}$ and the stiffness of the carriage springs as $c_s$.

Then the equation for the movement of the mass $m_f$ will have the following form:

$$\frac{d^2h_1}{dt^2} m_f = Q_f - (h_{2n} - h_2)\, c_s - m_f g = h_2 c_s + Q_f - h_{2n} c_s - m_f g$$

By substituting the value obtained from (3.7) and (3.9)

$$h_2 = y_0 + \frac{y_{\max}}{2} (1 - \cos \omega t) - h_1 \tag{3.10}$$

we obtain

$$\frac{d^2h_1}{dt^2} m_f = y_0 c_s + \frac{y_{\max}}{2} c_s - \frac{y_{\max}}{2} c_s \cos \omega t - h_1 c_s + Q_f - h_{2n} c_s - m_f g$$

or

$$\frac{d^2h_1}{dt^2} + h_1 \frac{c_s}{m_f} = -\frac{y_{\max}}{2} \frac{c_s}{m_f} \cos \omega t + \frac{c_s}{m_f} \left( y_0 + \frac{y_{\max}}{2} - h_{2n} \right) + \frac{Q_f}{m_f} - g \tag{3.11}$$

According to observations by I. A. Belyaev, free oscillations are rapidly damped and only forced oscillations remain. Therefore let us consider only forced oscillations. Let us represent the movement of the main frames in the form of the equation

$$h_1 = B_1 \cos \omega t + C_1 \tag{3.12}$$

wherefrom

$$\frac{dh_1}{dt} = -\omega B_1 \sin \omega t$$

and

$$\frac{d^2h_1}{dt^2} = -\omega^2 B_1 \cos \omega t$$

[1] $g$ is the gravity acceleration.

By substituting these values in (3.11), and equating the coefficients at cos $\omega t$, we obtain

$$-B_1\left(\omega^2-\frac{c_s}{m_f}\right)=-\frac{y_{\max}}{2}\frac{c_s}{m_f}$$

wherefrom

$$B_1=-\frac{y_{\max}c_s}{2\,(c_s-\omega^2 m_f)} \tag{3.13}$$

and, by equating the constant terms, we obtain

$$C_1=y_0+\frac{y_{\max}}{2}-h_{2n}+\frac{Q_f}{c_s}-\frac{gm_f}{c_s} \tag{3.14}$$

Substituting $h_1$ from (3.12) and $B_1$ and $C_1$ from (3.13) and (3.14) into (3.10) gives:

$$h_2=y_0+\frac{y_{\max}}{2}-\frac{y_{\max}}{2}\cos\omega t+\frac{y_{\max}c_s}{2\,(c_s-\omega^2 m_f)}\cos\omega t-y_0$$

$$-\frac{y_{\max}}{2}+h_{2n}-\frac{Q_f}{c_s}+\frac{gm_f}{c_s}=B_2\cos\omega t+C_2$$

wherefrom

$$B_2=\frac{y_{\max}\omega^2 m_f}{2\,(c_s-\omega^2 m_f)} \tag{3.15}$$

and

$$C_2=h_{2n}-\frac{Q_f}{c_s}+\frac{gm_f}{c_s} \tag{3.16}$$

Let us find the contact pressure $P_c$. For that purpose, using d'Alembert's principle, let us consider the projections to the vertical of all forces acting on the contact strip: the contact pressure $P_c$, the weight $m_s g$, the carriage springs force

$$c_s\,(h_{2n}-h_2)=c_s h_{2n}-B_2 c_s\cos\omega t-C_2 c_s$$

the force of inertia of the contact strip $-m_s\frac{d^2y}{dt^2}$

We can write:

$$-P_c-m_s g+c_s h_{2n}-B_2 c_s\cos\omega t-C_2 c_s-m_s\frac{d^2y}{dt^2}=0$$

By determining $P_c$ and substituting $\frac{d^2y}{dt^2}$ from (3.7), $B_2$ from (3.15), and $C_2$ from (3.16), we obtain

$$P_c=-m_s g+c_s h_{2n}-\frac{y_{\max}\omega^2 m_f c_s}{2\,(c_s-\omega^2 m_f)}\cos\omega t-c_s h_{2n}+Q_f$$

$$-m_f g-\omega^2 m_s\frac{y_{\max}}{2}\cos\omega t$$

Then

$$P_c = Q_f - \omega^2 \frac{y_{max}}{2} \cos \omega t \left[ \frac{m_f c_s}{c_s - \omega^2 m_f} + m_s \right] - (m_s + m_f) g \quad (3.17)$$

With $c_s = \infty$ (rigid carriage without springs)

$$P_c = Q_f - \frac{\omega^2 y_{max}}{2} (m_s + m_f) \cos \omega t - (m_s + m_f) \quad (3.18)$$

At critical velocity $\omega_c$, when $c_s - \omega_c^2 m_f = 0$

$$\omega = \omega_c = \sqrt{\frac{c_s}{m_f}} \quad (3.19)$$

the values $h_1$, $h_2$, and $P_c$ will tend to $\infty$ (friction being ignored).

With $\omega < \omega_c$, it will be apparent from formulas (3.15) and (3.13) that the frames move in phase with the contact strip.

With $\omega > \omega_c$, the frames move in antiphase with the contact strip. It will be apparent from (3.17) that with

$$\frac{m_f c_s}{c_s - \omega_0^2 m_f} + m_s = 0$$

the contact pressure $P_c$ is constant, or

$$m_f c_s + m_s c_s - \omega_0^2 m_f m_s = 0$$

Then

$$\omega_0 = \sqrt{c_s \frac{m_f + m_s}{m_f m_s}} \quad (3.20)$$

or, dividing by (3.19), we get

$$\frac{\omega_0}{\omega_c} = \sqrt{\frac{m_f}{m_s} + 1} \quad (3.21)$$

Since generally $m_f \approx 2m_s$, it follows that

$$\frac{\omega_0}{\omega_c} \approx 1.73 \quad (3.22)$$

The idea of making a pantograph collector operating at a speed above the critical speed, and especially with $P_c = \text{const}$, is very attractive since an improved current collection at high speeds should be expected. Therefore, the work by O. I. Pozdnyakov and V. P. Mikheev who developed a pantograph collector with a highly flexible carriage and obtained a good result is worthy of note [28]. They worked at speeds above the critical speed and close to $\omega_0$.

Similar results were obtained in France with current collectors having a very large stroke of the upper carriage.

## 3.12. Mechanisms of Lift Springs

The function of this mechanism is to maintain a constant bias of the contact strip against the contact wire at any position.

In a symmetrical pantograph collector (Fig. 3.52), the spring generally acts on the cranks of both main shafts and consequently remains horizontal. This simplifies the calculation and makes it possible to obtain the analytical solution [37].

In the lift spring mechanism, the radius of the crank $r$ and the angle of rotation of the main shaft $2\delta$ are assumed pre-set. The following values are unknown: spring tension in the lower position $T_l$ (maximum), stiffness of the half of the spring $c_h$ (since one main shaft and one half of the spring will be considered), and the angle of the crank in the middle position $\varphi$. To find these values, we take three equations of moments for pre-set values of forces: in the lowermost position $M_l$, in the middle position $M_m$, and in the uppermost position $M_u$, that is the calculation is made at three points:

$$M_l = T_l r \sin(\varphi - \delta) \tag{3.23}$$

$$M_m = \{T_l - c_h r [\cos(\varphi - \delta) - \cos\varphi]\} r \sin\varphi \tag{3.24}$$

$$M_u = \{T_l - c_h r [\cos(\varphi - \delta) - \cos(\varphi + \delta)]\} r \sin(\varphi + \delta) \tag{3.25}$$

From (3.23) we find

$$T_l = \frac{M_l}{r \sin(\varphi - \delta)} \tag{3.26}$$

from (3.24)

$$T_l = \frac{M_m}{r \sin\varphi} + c_n r [\cos\varphi \cos\delta + \sin\varphi \sin\delta - \cos\varphi] \tag{3.27}$$

from (3.25)

$$T_l = \frac{M_u}{r \sin(\varphi + \delta)} + c_h r 2 \sin\varphi \sin\delta \tag{3.28}$$

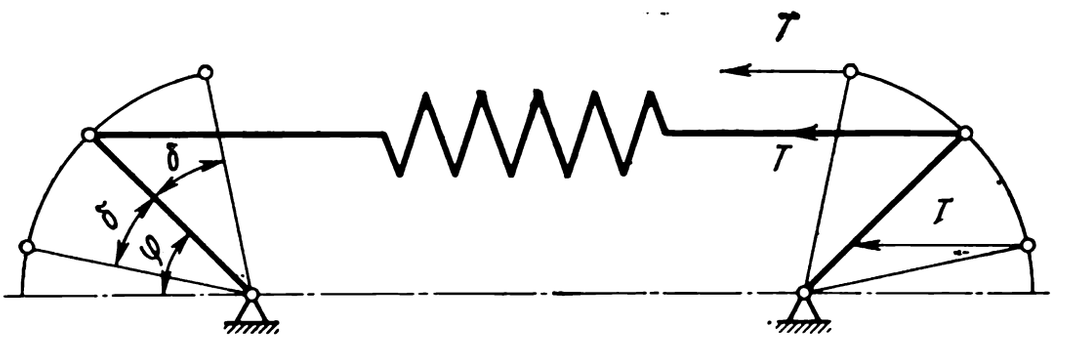


Fig. 3.52. Mechanism of lift springs of a symmetrical pantograph collector

By substituting the value of $T_l$ from (3.26) in (3.27) and (3.28) and transforming the formula, we obtain

$$\frac{M_l}{r\sin(\varphi-\delta)}-\frac{M_u}{r\sin\varphi}=c_h r\left[\sin\varphi\sin\delta-2\cos\varphi\sin^2\frac{\delta}{2}\right]$$

and

$$\frac{M_l}{r\sin(\varphi-\delta)}-\frac{M_u}{r\sin(\varphi+\delta)}=c_h r 2\sin\varphi\sin\delta \tag{3.29}$$

These formulas are divided into one another to cancel out $c_h$:

$$\frac{M_l\sin\varphi-M_m\sin(\varphi-\delta)}{M_l\sin(\varphi+\delta)-M_u\sin(\varphi-\delta)}=\frac{\sin\varphi}{\sin(\varphi+\delta)}\times\frac{\sin\varphi\sin\delta-2\cos\varphi\sin^2\frac{\delta}{2}}{2\sin\varphi\sin\delta}$$

After transformation, we obtain:

$$\frac{M_l\sin\varphi-M_m\sin\varphi\cos\delta+M_m\cos\varphi\sin\delta}{M_l\sin\varphi\cos\delta+M_l\cos\varphi\sin\delta-M_u\sin\varphi\cos\delta+M_u\cos\varphi\sin\delta}=\frac{\frac{1}{2}\sin\varphi-\frac{1}{2}\cos\varphi\,\mathrm{tg}\frac{\delta}{2}}{\sin\varphi\cos\delta+\cos\varphi\sin\delta}$$

or, by multiplying by 2 and dividing the numerator and denominator of both terms by $\cos\varphi$. we obtain:

$$\frac{2M_l\,\mathrm{tg}\,\varphi-2M_m\,\mathrm{tg}\,\varphi\cos\delta+2M_m\sin\delta}{M_l\,\mathrm{tg}\,\varphi\cos\delta+M_l\sin\delta-M_u\,\mathrm{tg}\,\varphi\cos\delta+M_u\sin\delta}=\frac{\mathrm{tg}\,\varphi-\mathrm{tg}\frac{\delta}{2}}{\mathrm{tg}\,\varphi\cos\delta+\sin\delta}$$

By eliminating the denominator, we obtain

$$\begin{aligned}&2M_l\,\mathrm{tg}^2\varphi\cos\delta-2M_m\,\mathrm{tg}^2\varphi\cos^2\delta+2M_m\,\mathrm{tg}\,\varphi\sin\delta\cos\delta\\&+2M_l\,\mathrm{tg}\,\varphi\sin\delta-2M_m\,\mathrm{tg}\,\varphi\sin\delta\cos\delta+2M_m\sin^2\delta\\&=M_l\,\mathrm{tg}^2\varphi\cos\delta+M_l\,\mathrm{tg}\,\varphi\sin\delta-M_u\,\mathrm{tg}^2\varphi\cos\delta\\&+M_u\,\mathrm{tg}\,\varphi\sin\delta-M_l\,\mathrm{tg}\,\varphi\cos\delta\,\mathrm{tg}\frac{\delta}{2}-M_l\sin\delta\,\mathrm{tg}\frac{\delta}{2}\\&+M_u\,\mathrm{tg}\,\varphi\cos\delta\,\mathrm{tg}\frac{\delta}{2}-M_u\sin\delta\,\mathrm{tg}\frac{\delta}{2}\end{aligned}$$

that is, a quadratic equation of the following form:

$$A\,\mathrm{tg}^2\varphi+B\,\mathrm{tg}\,\varphi+C=0 \tag{3.30}$$

Here

$$A=2M_l\cos\delta-2M_m\cos^2\delta-M_l\cos\delta+M_u\cos\delta$$

or

$$A = (M_l - 2M_m \cos\delta + M_u)\cos\delta \tag{3.31}$$

$$B = 2M_m \sin\delta\cos\delta + 2M_l \sin\delta - 2M_m \sin\delta\cos\delta - M_l \sin\delta$$
$$- M_u \sin\delta + M_l \cos\delta \operatorname{tg}\frac{\delta}{2} - M_u \cos\delta \operatorname{tg}\frac{\delta}{2}$$

or

$$B = (M_l - M_u)\left(\sin\delta + \cos\delta \operatorname{tg}\frac{\delta}{2}\right)$$
$$= (M_l - M_u)\frac{\sin\delta\cos\frac{\delta}{2} + \cos\delta\sin\frac{\delta}{2}}{\cos\frac{\delta}{2}}$$

Then

$$B = (M_l - M_u)\frac{\sin\frac{3}{2}\delta}{\cos\frac{\delta}{2}} \tag{3.32}$$

$$C = 2M_m \sin^2\delta + M_l \sin\delta \operatorname{tg}\frac{\delta}{2} + M_u \sin\delta \operatorname{tg}\frac{\delta}{2}$$

or

$$C = 2M_m \sin^2\delta + 2(M_l + M_u)\sin^2\frac{\delta}{2} \tag{3.33}$$

It will be apparent from (3.32) that $B$ influences $M_l$ and $M_u$, that is the angle of inclination of the force characteristic of the current collector. Similarly, it will be apparent from (3.31) that $A$ influences its concavity. Hence, by varying $A$ and $B$, the characteristic parameters may be changed.

In designing a mechanism, the angle $\varphi$ should be found from (3.30), maximum tension of the spring from (3.26), and stiffness from (3.29), that is

$$c_h = \frac{\dfrac{M_l}{\sin(\varphi - \delta)} - \dfrac{M_u}{\sin(\varphi + \delta)}}{2r^2 \sin\varphi \sin\delta}$$

Of the two solutions of the quadratic equation (3.30), the solution at which the stiffness $c_h$ is more suitable from the design point of view should be taken.

For checking, it is preferable to determine the values of moments from (3.23) through (3.25) and to compare them with the pre-set values.

It should be noted that formula (3.29) includes $c_n r^2$ so that it is not necessary to pre-set the value of $r$, and an appropriate radius $r$ may be chosen for a pre-set stiffness of the spring.

**Example.** Let us consider the current collector П-1 (the reduced weight of the members is assumed constant). The pre-set values: $M_l = 4\,890.8$ kgf cm, $\delta = 18°45'$, $M_m = 4\,421.4$ kgf cm, $r = 10$ cm, $M_u = 3\,493.5$ kgf cm.

Find $A = (4\,890.8 - 2 \times 4\,421.4 \cos 18°45' + 3\,493.5) \cos 18°45 = 10.21$ from (3.31), $B = (4\,890.8 - 3\,493.5) \dfrac{\sin 28°7'}{\cos 9°23'} = 667.6$ from (3.32), and $C = 2 \times 4\,421.4 \sin^2 18°45' \times (4\,890.8 + 3\,493.5) \sin^2 9°23' = 1\,136.1$ from (3.33).

We find from (3.30)

$$\operatorname{tg}\varphi = \frac{-B \pm \sqrt{B^2 - 4AC}}{2A} = -\frac{p}{2} \pm \sqrt{\frac{p^2}{4} - q}$$

$$= \frac{p}{2}\left(1 \pm \sqrt{1 - \frac{q}{\left(\frac{p}{2}\right)^2}}\right)^{1)}$$

where

$$\frac{p}{2} = \frac{B}{2A} = \frac{667.6}{2 \times 10.21} = 32.7$$

$$q = \frac{C}{A} = \frac{1\,136.1}{10.21} = 111.2$$

$$\operatorname{tg}\varphi = -32.7\left(1 \pm \sqrt{1 - \frac{111.2}{(32.7)^2}}\right)$$

$$\varphi_1 = 115°26' \text{ and } \varphi_2 = 90°54'$$

Since the first value results in a very disadvantageous value of the spring stiffness, it is discarded, and $\varphi = 90°54'$ is taken. From (3.29), the stiffness of half of the spring

$$c_h = \frac{\dfrac{M_l}{\sin(\varphi - \delta)} - \dfrac{M_u}{\sin(\varphi + \delta)}}{2r^2 \sin\varphi \sin\delta}$$

$$= \frac{\dfrac{4\,890.8}{\sin(90°54' - 18°45')} - \dfrac{3\,493.5}{\sin(90°54' - 18°45')}}{2 \times 10^2 \sin 90°54' \sin 18°45'} = 22.2 \text{ kgf/cm}$$

[1] The formula is given here bekause it proved very convenient for calculations with the use of microcalculators.

Since two springs are used in the current collector П-1, the stiffness of each spring is $\frac{22.2}{4} = 5.5$ kgf/cm. Maximum tension of each spring from (3.23) is

$$\frac{T_l}{2} = \frac{M_l}{2r \sin(\varphi - \delta)} = \frac{4\,890.8}{2 \times 10 \sin(90°54' - 18°45')} = 258 \text{ kgf}$$

There is one main shaft in the asymmetrical current collectors. Therefore, the second end of the spring cannot be connected to

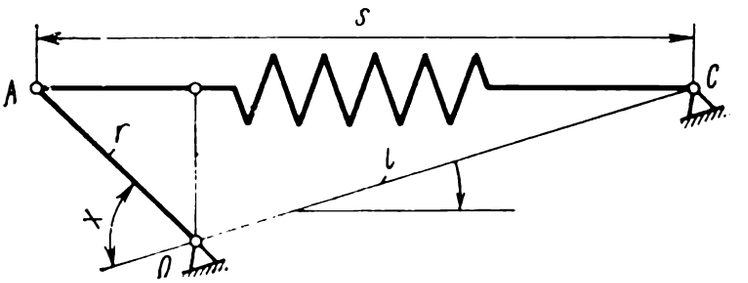


Fig. 3.53. Mechanism of lift springs for an asymmetrical pantograph collector ($p$ is the vertical dimension)

a second crank, but to a fixed point (Fig. 3.53). This mechanism is also used in symmetrical current collectors, e.g. in the current collector M7. Here the spring changes its direction during the lifting of the pantograph so that relationships for its length $s$ and arm length $p$ prove more complicated, and the calculation of the mechanism is preferably made by the trial and error method.

Similarly to the symmetrical current collector, the calculation is made at three points:

lower with $x_l = \varphi - \delta$ and $s = s_l$;

middle with $x_m = \varphi$ and $s = s_m$;

upper with $x_u = \varphi + \delta$ and $s = s_u$.

Let us find the stiffness of the spring in the zone between the lowermost and middle positions:

$$c_l = \frac{T_l - T_m}{s_l - s_m} \tag{3.34}$$

and in the zone between the middle and upmost positions

$$c_u = \frac{T_m - T_u}{s_m - s_u} \tag{3.35}$$

These stiffnesses should be equal to one another, and this is preferably used for choosing the value of the angle $\varphi$.

From the triangle $OAC$ (see Fig. 3.53) we find

$$s = \sqrt{r^2 + l^2 + 2rl \cos x}$$

For a slide rule, this expression should be transformed as follows:

$$s = \sqrt{r^2 + l^2}\sqrt{1 + \frac{2rl}{r^2 + l^2}\cos x}$$

or

$$s = \sqrt{A}\sqrt{1 + B\cos x} \tag{3.36}$$

where the values

$$A = r^2 + l^2 \text{ and } B = \frac{2rl}{r^2 + l^2}$$

are computed once for all values of the angle.

It is obvious that $s$ may be determined using any formula for solving a triangle with two sides and one angle given. The area of the triangle $OAC$ is

$$\frac{1}{2}ps = \frac{1}{2}rl\sin x$$

wherefrom

$$p = \frac{rl\sin x}{s}$$

The force of the spring

$$T = \frac{M}{p} \text{ or } T = \frac{Ms}{rl\sin x} \tag{3.37}$$

For choosing the stiffness, $s_l$, $s_m$ and $s_u$ should be found by (3.36) for arbitrary values of φ, and $T_l$, $T_m$ and $T_u$ should be found by formula (3.37). Subsequently $c_l$ and $c_u$ should be found from (3.34) and (3.35). A curve for relationship of these stiffnesses versus the angle φ should be plotted. This makes it possible to detect the errors of calculation and accelerates the solution of the problem.

In case $c_l > c_u$, the angle φ should be increased, and if $c_l < c_h$, reduced.

Lift springs which generally act on the cranks connected to the main shafts (Fig. 3.54) should ensure a constant bias of the collector strip to the contact wire. For that purpose, the design of the pantograph collector provides not only the adjustment of the average pressure force, but also of the force at individual points. Two sets of springs are provided for such adjustment in the pantograph collector ДЖ-4 (Fig. 3.54*a*). Cranks of the outer springs are secured at a greater angle compared to the inner springs. Owing to such a design, the effort may be increased at higher position of the panto-

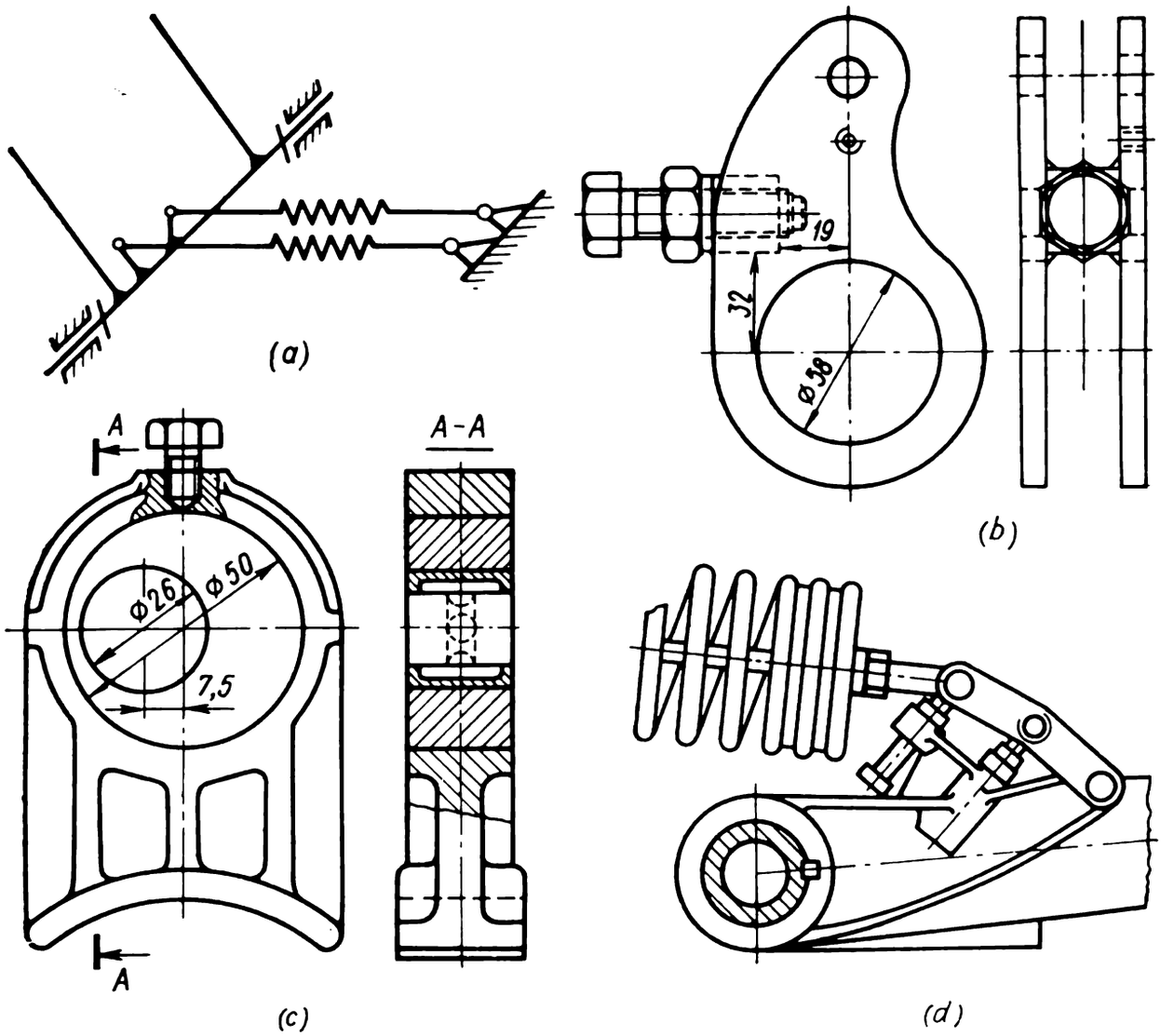


Fig. 3.54. Mechanisms used for the adjustment of contact pressure at individual points within the working height of the pantograph collectors
(*a*) ДЖ-4; (*b*) П-7; (*c*) П-3А; (*d*) 9PP and 10PP

graph collector by tensioning the outer springs, the tensioning of the inner springs being used at lower positions of the pantograph.

The pantograph collectors П-7 use a somewhat different adjustment: here the force of the spring and the angle of the crank may be adjusted (Fig. 3.54*b*) (the design by V. A. Shiyan).

In the pantograph collector П-3А (Fig. 3.54*c*) the crank pin is installed on an eccentric which is turned to vary the angle of installation. The eccentric is locked by a bolt. The constant pressure force is achieved by the trial and error method. This is more difficult compared to the pantograph collector ДЖ-4, the more so that with the eccentric turned not only the angle, but also the radius

of the crank, is changed which also affects the collector strip pressure force.

Adjustment at three points is provided in the pantograph collectors 9PP and 10PP of the Czechoslovakian electric locomotives of the ЧС-1, ЧС-2 and ЧС-3 series (Fig. 3.54*d*). Here a chain transmission is provided between the spring and the main shaft. The pressure force at the upmost point of the working height is adjusted by changing the spring tension; a first bolt setting up the arm of spring force is used for adjustment at the middle of the working height; and a second bolt is used for adjustment at the lowermost point of the working height [1].

The only disadvantage of this mechanism is its complicated structure.

The adjustment by changing the stiffness of the spring by screwing plates and changing the number of effective turns (similarly to centrifugal governors) has not found application in pantograph collectors.

In order to achieve a constant pressure contact, not only the lift spring mechanism should be correctly designed, but it should also be adjusted properly so as to eliminate the effect of all tolerances inevitable in the manufacture. Mechanisms for such adjustment are described above (see Fig. 3.54).

The reference is now made to the mechanism of the pantograph collector П-7 (see Fig. 3.54*b*) in which the angle $\varphi$ can be adjusted. This makes it possible to adjust effort at two points, generally at the upmost and lowermost points (since two parameters—spring force and angle $\varphi$ —are controlled). If the adjustment of the spring stiffness by screwing and unscrewing plates is added, the adjustment at three points is obtained, which is quite adequate.

Let us refer to the characteristics of the pantograph collector, that is relationship of the pressure force versus height, taking into account the point at which an overload occurs, hence where the moment is greater than the design moment. Therefore, an overload may occur at the top (upmost), at the bottom (lowermost), and at the middle (medium) points.

The uppermost overload can be eliminated either by increasing the angle $\varphi$ (unscrewing the screw for adjustment of the angle) or by increasing the stiffness of the spring by reducing the number of effective turns by way of screwing-in the plates. The lowermost overload can be remedied by reducing the angle $\varphi$ through screwing-in the screw for adjustment of the angle or through unscrewing the spring plates (stiffness decrease).

The calculations showed that the middle overload can be eliminated by increasing the angle φ (by unscrewing the screw) with concurrent reduction of the spring stiffness (by unscrewing the plates). The crank screw and the spring plates should be screwed-in in case of the middle underload.

For adjustment, tables should be compiled to give all adjustment parameters for deviation of the contact pressure at a given point.

Therefore, a complicated chain transmission may be dispensed with, and the adjustment of characteristics at all three points may be achieved.

### 3.13. Transverse Rigidity of a Current Coollector Having Two Levers on the Main Shaft

The transverse rigidity should be determined for evaluating the period of fundamental oscillations of pantograph collectors which is especially important at high speeds. The problem was discussed in a paper [59] published twenty years ago. It dealt with levers of a constant cross-section which varies substantially in modern pantograph collectors. Thus the moment of inertia of the section at the end of the arm of the pantograph collector П-5 is 1.09 $cm^4$ compared to 27.9 $cm^4$ at the fulcrum.

The deformation of the main shaft was not taken into account correctly, the coefficient of 1/2 was used for torsion, and the force from the longitudinal rod of the upper frame was ignored in bending. These factors did not permit to find the position in which the rigidity was at its minimum. A. V. Plaks has solved this problem in a more accurate manner.

Let us consider the rigidity of current collectors in which the lower frame consists of the main shaft (generally hollow) and two levers in the form of conical tubes. The rods of upper frames are only tensioned and compressed, their deformations are negligible.

Thus, a pipe 30/28 mm, 1 800 mm long would expand under the load of 1 kgf at

$$f = \frac{Ql}{EF} = \frac{1 \times 180}{2 \times 10^6 \times \pi \times 2.9 \times 0.1} = 0.0001 \text{ cm} = 0.001 \text{ mm}$$

Therefore, the upper frames are generally considered as an absolutely rigid system, and the deformation of the lower frames only is taken into account.

There are lower frame levers (Fig. 3.55) with the cross-section formed of two half-rings with the mean diameter $d$ and the thickness $\delta$

and two rectangular spacers $h \times \delta$ (the pantograph collector 10PP). Most widely used are levers in the form of a hollow conical pipe of a constant thickness $\delta$.

Owing to a small thickness $\delta$, approximate formulas for the moment of inertia of the ring may be used.

The moment of inertia of the section with respect to the $y$ axis

$$J_y = \frac{\pi}{8} \delta d^3 + 2h\delta \left(\frac{d}{2}\right)^2$$

or

$$J_y = \frac{\pi}{8} \delta d^3 + \frac{h}{2} \delta d^2 \tag{3.38}$$

Let us determine the moment of inertia with respect to the $x$ axis.

Moments of inertia of the half-ring are:

$\frac{1}{2}\frac{\pi}{8}\delta d^3$ with respect to the diameter;

$\frac{1}{2}\frac{\pi}{8}\delta d^3 - \frac{\pi d}{2}\delta\left(\frac{d}{\pi}\right)^2$ with respect to the centre of gravity;

$\frac{1}{2}\frac{\pi}{8}\delta d^3 - \frac{\pi d}{2}\delta\left(\frac{d}{\pi}\right)^2 + \frac{\pi d}{2}\delta\left(\frac{h}{2}+\frac{d}{\pi}\right)^2$ with respect to the middle axis.

The total moment of inertia of the section consisting of two half-rings and two rectangles is

$$J_x = \frac{\pi}{8}\delta d^3 + \pi d\delta\left[\left(\frac{h}{2}+\frac{d}{\pi}\right)^2 - \left(\frac{d}{\pi}\right)^2\right] + 2\frac{\delta h^3}{12}$$

or

$$J_x = \frac{\delta h^3}{6} + \frac{\pi}{4}\delta h^2 d + \delta h d^2 + \frac{\pi}{8}\delta d^3 \tag{3.39}$$

A subscript 1 will be used for the dimensions of the end section and a subscript 2 for the dimensions of the fulcrum section. Further discussion will apply to bending in both planes so that the subscripts $x$ and $y$ will not be used in this sense; the $x$ axis will extend along the lever, and the $y$ axis will extend in the direction of deflection.

With a straight-line generatrix, the dimension $d$ changes linearly with the lever arm length:

$$d = d_1 + cx \tag{3.40}$$

The dimension $h$ changes proportionally with $d$.

It will be apparent from (3.38) and (3.39) that the sum of the powers for $d$ and $h$ is equal to three for all terms. Therefore, the moments of inertia are proportional with the third power of the diameter, that is

$$\frac{J}{J_1} = \left(\frac{d}{d_1}\right)^3 = \left(\frac{d_1 + cx}{d_1}\right)^3$$

For a round section and for sections in which the outlines of the middle line are similar, this relationship is exact, the relationship

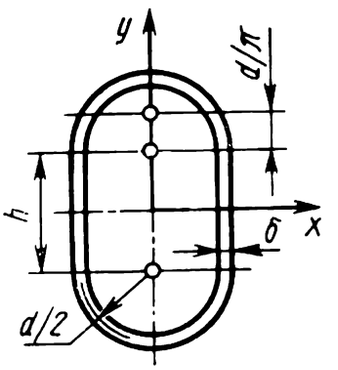


Fig. 3.55. Cross-section of the lower frame lever of the current collector

being approximate for other sections.

Let us determine the deformation of a cantilever beam with a section as shown in Fig. 3.55. The differential equation of the elastic line $EJ_y'' = Qx$, or, after substitution of the value of $J$,

$$EJ_1 \left(\frac{d_1 + cx}{d_1}\right)^3 y'' = Qx$$

Then

$$y'' = \frac{Qd_1^3}{EJ_1} \frac{x}{(d_1 + cx)^3}$$

Integration gives

$$y' = \frac{Qd_1^3}{EJ_1} \frac{1}{c^2} \left[ -\frac{1}{d_1 + cx} + \frac{d_1}{2(d_1 + cx)^2} \right] + C_1$$

With $x = l$, $y' = 0$ and $d_1 + cx = d_2$, so

$$C_1 = \frac{Qd_1^3}{EJ_1 c^2} \left[ \frac{1}{d_2} - \frac{d_1}{2d_2^2} \right]$$

After the second integration, we obtain

$$y = \frac{Qd_1^3}{EJ_1 c^2} \left[ -\frac{1}{c} \ln (d_1 + cx) - \frac{d_1}{2c} \frac{1}{d_1 + cx} \right] + C_1 x + C_2$$

With $x = 1$, $d = d_1 + cx = d_2$; $y = 0$.

Then

$$C_2 = \frac{Qd_1^3}{EJ_1c^2}\left[\frac{1}{c}\ln d_2 + \frac{1}{2c}\frac{d_1}{d_2} - \frac{l}{d_2} + \frac{d_1 l}{2d_2^2}\right]$$

With $x = 0$ $y = f$, so

$$f = \frac{Qd_1^3}{EJ_1}\frac{1}{c^2}\left[\frac{1}{c}\ln d_2 + \frac{1}{2c}\frac{d_1}{d_2} - \frac{l}{d_2} + \frac{d_1 l}{2d_2^2} - \frac{l}{c}\ln d_1 - \frac{1}{2c}\right]$$

or

$$f = \frac{Qd_1^3}{EJ_1c^2}\left[\frac{1}{c}\ln\frac{d_2}{d_1} - \frac{1}{2c}\frac{d_2-d_1}{d_2} - \frac{l}{d_2} + \frac{d_1 l}{2d_2^2}\right]$$

With $x = l$, $d = d_2$, we obtain from (3.40)

$$c = \frac{d_2-d_1}{l} \tag{3.41}$$

By substituting this expression in formula for $f$, we obtain

$$f = \frac{Qd_1^3}{EJ_1}\frac{l^2}{(d_2-d_1)^2}\left[\frac{l}{d_2-d_1}\ln\frac{d_2}{d_1} - \frac{l}{2d_2}\left(3 - \frac{d_1}{d_2}\right)\right] \tag{3.42}$$

For the sake of convenience, the reduced moment of inertia is determined, that is the moment of inertia of a constant-section beam having the same deflection

$$f = Ql^3/3EJ$$

By substituting this value in (3.42), we obtain

$$J = \frac{J_1\left(\frac{d_2-d_1}{d_1}\right)^3}{3\left[\ln\frac{d_2}{d_1} - \frac{d_2-d_1}{2d_2}\left(3-\frac{d_1}{d_2}\right)\right]} \tag{3.43}$$

By denoting

$$\sqrt{\frac{J_2}{J_1}} = \frac{d_2}{d_1} = k \tag{3.44}$$

and substituting the value of $k$ in (3.43), we obtain

$$J = \frac{J_1(k-1)^3}{3\left[\ln k - \frac{1}{2}\left(1-\frac{1}{k}\right)\left(3-\frac{1}{k}\right)\right]} \tag{3.45}$$

The formulas (3.44) and (3.45) will be used to calculate the bending of levers in both planes.

Let us find certain regularities in case where forces are transmitted through an absolutely rigid mechanism.

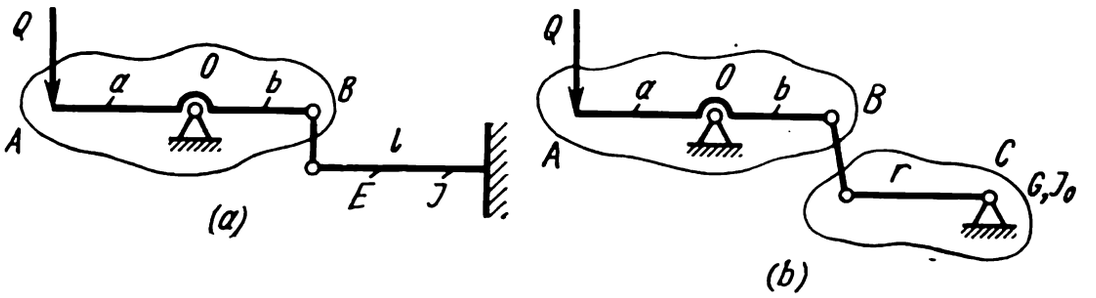


Fig. 3.56. Action of force on a deformed member through an absolutely rigid lever

(*a*) with bending deformation; (*b*) with torsional deformation

The upper frames are regarded as absolutely rigid mechanism owing to negligible deformations, which transmits forces to the lower frames (deformable) and transforms deformations of the lower frames into transverse displacements of the upper joint.

Let us start with a simplified example of a transmission mechanism in the form of a lever $AOB$ and with a deformable member in the form of a cantilever beam (Fig. 3.56*a*) or a torsion bar (3.56*b*).

The force at point $B$ is $Q\frac{a}{b}$.

Deformation at point $B$ is $Q\frac{a}{b}\frac{l^3}{3EJ}$.

Deformation at point $A$ is

$$Q\frac{a}{b}\frac{l^3}{3EJ}\frac{a}{b}=\frac{Ql^3}{3EJ}\left(\frac{a}{b}\right)^2$$

but as $\frac{a}{b}=u$ is the transmission ratio, the deformation at point $A$ is

$$f_A=\frac{Ql^3}{3EJ}u^2$$

The length of a torsion bar is denoted as $l$. The torque at point $C$ (see Fig. 3.56*b*) is $Q\frac{ar}{b}$. Angular deformation of the torsion bar is $Q\frac{ar}{b}\frac{l}{GJ_0}$, where $J_0$ is the polar moment of inertia of its section.

Deformation at point $A$ is

$$f_A=Q\frac{ar}{b}\frac{l}{GJ_0}\frac{ra}{b}=\frac{Ql}{GJ_0}\left(\frac{ar}{b}\right)^2$$

Here $ar/b$ may be conventionally referred to as a "transmission ratio" (though it has a linear rather than zero dimension) so as not to introduce new terms.

Then

$$f_A = \frac{Ql}{QJ_0} u^2$$

This relationship can also be proved in the general form: a transmission mechanism transforms a force by $u$ times, and then transforms the deformation of an elastic (deformable) member by $u$

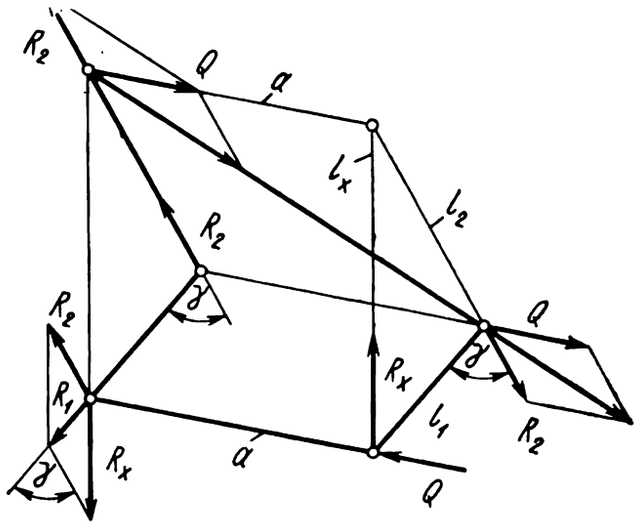


Fig. 3.57. Diagram of forces acting on frames of the current collector (loaded members are shown with bold lines)

times which gives the total of $u^2$. The transmission ratio may be determined both from the ratio of forces (certainly without taking into account friction) and from the inverted ratio of displacements. The use of forces is more preferable.

Let us consider one upper frame and one lower frame (Fig. 3.57), the angle between the frame planes being denoted by $\gamma$. For a conventional four lever pantograph, this is one half of the mechanism, and the actual rigidity will be two times greater.

For current collectors WVSS-54 (Austria) and DBS-54 (West Germany) this will be the actual rigidity.

From the similarity of triangles shown in Fig. 3.57

$$\frac{R_2}{Q} = \frac{l_2}{a} \tag{3.46}$$

The force bending the lever in the end plane is $R_2 \sin \gamma$. The transmission ratio is

$$\frac{R_2 \sin \gamma}{Q} = \frac{l_2 \sin \gamma}{a}$$

Let us denote the reduced moments of inertia of the lever section as $J_x$ and $J_y$. Then, on the basis of the derived relationship, the dis-

placement of the upper joint from this deformation is $\frac{Ql_1^3}{3EJ_x}\left(\frac{l_2 \sin\gamma}{a}\right)^2$; and for two levers the displacement is

$$f_1 = \frac{2}{3} Q \frac{l_1^3 l_2^2 \sin^2\gamma}{EJ_x a^2} \tag{3.47}$$

The force bending the lever in the axial plane is $Q$, that is the transmission ratio is equal to unity. Therefore, the displacement of the upper joint is

$$f_2 = Q \frac{l_1^3}{3EJ_y} \tag{3.48}$$

The torque twisting the main shaft is $M_t = R_2 l_1 \sin\gamma$.

The transmission ratio is $\frac{R_2 l_1 \sin\gamma}{Q} = \frac{l_1 l_2 \sin\gamma}{a}$.

By denoting the polar moment of inertia of the main shaft section with $J_0$, we obtain the displacement of the upper joint caused by torsion of the main shaft:

$$f_3 = \frac{Qa}{GJ_0}\left(\frac{l_1 l_2 \sin\gamma}{a}\right)^2 = \frac{Ql_1^2 l_2^2}{GJ_0 a} \sin^2\gamma \tag{3.49}$$

To find the force $R_1$ bending the main shaft, we take moments of the forces acting in the lower frame plane

$$R_1 = Q \frac{l_1}{a} \tag{3.50}$$

This force may be found in a different way, by adding the force $R_2$ and the force $R_x$ acting on the main shaft bearing. The force $R_x$ can be found from the condition of balance of external forces for both frames:

$$R_x = Q \frac{l_x}{a} \tag{3.51}$$

The force $R_2$ acting on the end of the lever may be replaced by the same force acting on the main shaft and a torque $M_t = R_2 l_1 \sin\gamma$ twisting the main shaft (the torque was taken into account above).

The resultant of the forces $R_2$ and $R_x$ bends the main shaft. This force is found from the parallelogram of forces in Fig. 3.57. Let us take triangles with the sides $R_x$, $R_1$, $R_2$ and $l_x$, $l_1$ and $l_2$ ($R_x \parallel l_x$, $R_2 \parallel l_2$) and obtain, using (3.51) and (3.46):

$$\frac{Q}{a} = \frac{R_x}{l_x} = \frac{R_2}{l_2}$$

that is the sides are proportional. The triangles are hence similar, that is $R_1 \parallel l_1$ and

$$\frac{Q}{a} = \frac{R_x}{l_x} = \frac{R_2}{l_2} = \frac{R_1}{l_1}$$

wherefrom $\frac{R_1}{Q} = \frac{l_1}{a}$, that is the same formula (3.50) is obtained. The transmission ratio here is $\frac{l_1}{a}$.

By denoting the moment of inertia of the main shaft section with $J_s$, we obtain the displacement of the upper joint caused by the bending of the main shaft:

$$f_4 = \frac{Qa^3}{3EJ_s}\left(\frac{l_1}{a}\right)^2 = \frac{Qal_1^2}{3EJ_s} \tag{3.52}$$

The transverse displacement of the upper joint caused by the force $Q$ is

$$f = f_1 + f_2 + f_3 + f_4$$

From this formula, the displacement per 1 kgf is obtained by substituting the values of deformations from (3.47) through (3.49) and (3.52):

$$\frac{f}{Q} = \frac{2}{3}\frac{l_1^3 l_2^2}{EJ_x a^2}\sin^2\gamma + \frac{l_1^3}{3EJ_y} + \frac{l_1^2 l_2^2}{GJ_0 a}\sin^2\gamma + \frac{al_1^2}{3EJ_s} \tag{3.53}$$

The most important is the maximum displacement which occurs at $\gamma = 90°$, that is in case where the upper and lower frames are at right angle to one another. In such a case

$$\frac{f_{max}}{Q} = \frac{2}{3}\frac{l_1^3 l_2^2}{EJ_x a^2} + \frac{l_1^3}{3EJ_y} + \frac{l_1^2 l_2^2}{GJ_0 a} + \frac{al_1^2}{3EJ_s} \tag{3.54}$$

**Example 1.** The pantograph collector П-5: $a = 113.5$ cm; $l_2 = 175.8$ cm; $\delta = 0.15$ cm; $l_1 = 122.0$ cm, but the lever is installed on the main shaft horn so as to reduce the deformable length by 19.5 cm. Therefore, in calculating the bending, $l_1$ is assumed 101.5 cm, and the lever has the diameter $d_1 = 2.5 + 0.15 = 2.65$ cm, $d_2 = 7.65 + 0.15 = 7.80$ cm, and the main shaft has $D = 8.83$ cm, $d = 7.5$ cm.

First find

$$J_1 = \frac{\pi}{8}\delta d_1^3 = \frac{\pi}{8}0.15 \times 2.65^3 = 1.095 \text{ cm}^4$$

$$J_2 = \frac{\pi}{8}0.15 \times 7.80^3 = 27.9 \text{ cm}^4$$

Find from (3.44)

$$k = \sqrt[3]{\frac{J_2}{J_1}} = \sqrt[3]{\frac{27.9}{1.095}} = 2.94$$

$$\frac{1}{k} = 0.340; \quad 1 - \frac{1}{k} = 0.660$$

from (3.45) we obtain

$$J = \frac{1.095 \times 1.94^3}{3\left(\ln 2.94 - \frac{1}{2}\, 0.660 \times 2.66\right)} = 13.32 \text{ cm}^4$$

For comparison, we find $\frac{J_1 + J_2}{2} = \frac{1.095 + 27.9}{2} = 14.5$ cm$^4$.

Find for the main shaft

$$J_s = \frac{\pi}{64}(D^4 - d^4) = \frac{\pi}{64}(8.83^4 - 7.5^4)$$

$$= \frac{\pi}{64}(6\,085 - 3\,160) = 143.5 \text{ cm}^4$$

$$J_0 = 2J_s = 287 \text{ cm}^4$$

Tangential bending of the levers from (3.54) is

$$\frac{f_1}{Q} = \frac{2}{3}\frac{l_1^3 l_2^3}{EJ_x a^2} = \frac{2}{3}\frac{101.5^3 \times 175.8^2}{2 \times 10^6 \times 13.32 \times 113.5^2} = 0.0629 \text{ cm/kgf } (65.8\%)$$

axial bending of the lever:

$$\frac{f_2}{Q} = \frac{l_1^3}{3EJ_y} = \frac{101.5^3}{3 \times 2 \times 10^6 \times 13.32} = 0.0131 \text{ cm/kgf } (13.7\%)$$

shaft torsion

$$\frac{f_3}{Q} = \frac{l_1^2 l_2^2}{GJ_0 a} = \frac{122^2 \times 175.8^2}{8 \times 10^5 \times 287 \times 113.5} = 0.0176 \text{ cm/kgf } (18.4\%)$$

shaft bending

$$\frac{f_4}{Q} = \frac{a l_1^2}{3EJ_0} = \frac{113.5 \times 122^2}{3 \times 2 \times 10^6 \times 143.5} = 0.0020 \text{ cm/kgf } (2.1\%)$$

maximum bending for one half of the pantograph collector

$$\frac{f_{max}}{Q} = 0.0956 \text{ cm/kgf } (100\%)$$

Since the calculation was made for one half, for two halves it will be

$$\frac{f_{max}}{Q} = \frac{0.0956}{2} = 0.0478 \text{ cm/kgf}$$

**Example 2.** The pantograph collector 10 PP, $a = 110$ cm; $l_1 = 120$ cm; $l_2 = 180.1$ cm; $\delta = 0.2$ cm. The arm cross-section as shown in Fig. 3.55: $d_1 = 2.6$ cm; $d_2 = 5.8$ cm; $h_1 = 2.0$ cm; $h_2 = 4.0$ cm; main shaft dimensions: $D = 7.4$ cm, $d = 4.8$ cm.

Find from (3.38):

$$J_{y1} = \frac{\pi}{8} 0.2 \times 2.6^3 + \frac{2 \times 0.2 \times 2.6^2}{2} = 1.381 + 1.354 = 2.735 \text{ cm}^4$$

$$J_{y2} = \frac{\pi}{8} 0.2 \times 5.8^3 + \frac{4 \times 0.2 \times 5.8^2}{2} = 15.30 + 13.46 = 28.76 \text{ cm}^4$$

from (3.44) we obtain:

$$k_y = \sqrt[3]{\frac{28.76}{2.735}} = 2.19; \quad \frac{1}{k_y} = 0.456;$$

$$1 - \frac{1}{k_y} = 0.544$$

from (3.45) we obtain:

$$J_y = \frac{2.735 \times 1.19^3}{3\left(\ln 2.19 \frac{1}{2} 0.544 \times 2.544\right)} = 16.8 \text{ cm}^4$$

for comparison, we find:

$$\frac{J_{y1} + J_{y2}}{2} = \frac{2.735 + 28.76}{2} = 15.7 \text{ cm}^4$$

From (3.39) we obtain:

$$J_{x1} = \frac{0.2 \times 2^3}{6} + \frac{\pi}{4} 0.2 \times 2^2 \times 2.6 + 0.2 \times 2 \times 2.6^2$$

$$+ \frac{\pi}{8} 0.2 \times 2.6^3 = 0.267 + 1.633 + 2.710 + 1.382 = 5.992 \text{ cm}^4$$

$$J_{x2} = \frac{0.2 \times 4^3}{6} + \frac{\pi}{4} 0.2 \times 4^2 \times 5.8 + 0.2 \times 4 \times 5.8^2$$

$$+ \frac{\pi}{8} 0.2 \times 5.8^3 = 2.13 + 14.6 + 26.9 + 15.30 = 58.9 \text{ cm}^4$$

from (3.44) we obtain:

$$k_x = \sqrt[3]{\frac{58.9}{5.99}} = 2.143; \quad \frac{1}{k_x} = 0.466; \quad 1 - \frac{1}{k_x} = 0.534$$

from (3.45) we obtain:

$$J_x = \frac{5.99 \times 1.143^3}{3\left(\ln 2.143 \frac{1}{2} 0.534 \times 2.534\right)} = 35.1 \text{ cm}^4$$

for comparison, we obtain:

$$\frac{J_{x1}+J_{x2}}{2}=\frac{5.99+58.9}{2}=32.44 \text{ cm}^4$$

The moment of inertia of the main shaft is

$$J_s=\frac{\pi}{64}(D^4-d^4)=\frac{\pi}{64}(7.4^4-4.8^4)=\frac{\pi}{64}(2\,999-530.8)=121 \text{ cm}^4$$

Polar moment of inertia $J_0 = 2$ cm$^4$; $J_s = 242$ cm$^4$. From (3.54) we obtain

the tangential bending of the levers

$$\frac{f_1}{Q}=\frac{2}{3}\frac{l_1^3 l_2^2}{EJ_x a^2}=\frac{2}{3}\frac{120^3}{2.10\times10^6\times35.1}\left(\frac{180.1}{110}\right)^2=0.0440 \text{ cm/kgf (51.5\%)}$$

the axial bending of the lever

$$\frac{f_2}{Q}=\frac{l_1^3}{3EJ_y}=\frac{120^3}{3\times2\times10^6\times168}=0.0172 \text{ cm/kgf (20.1\%)}$$

the shaft torsion

$$\frac{j_3}{Q}=\frac{l_1^2 l_2^2}{GJ_0 a}=\frac{120^2\times180.1}{8\times10^5\times242\times110}=0.0220 \text{ cm/kgf (25.8\%)}$$

the shaft bending

$$\frac{f_4}{Q}=\frac{al_1^2}{3EJ_s}=\frac{110\times120^2}{3\times2\times10^6\times121}=0.0022 \text{ cm/kgf (2.6\%)}$$

the maximum bending for one half of the pantograph

$$f_{max}/Q = 0.0854 \text{ cm/kgf (100.0 \%)}$$

the maximum bending for the whole pantograph

$$\frac{f_{max}}{Q}=\frac{0.0854}{2}=0.0427 \text{ cm/kgf}$$

For current collectors (see Fig. 3.43*b*) in which the point of connection of oblique rods to the base of the upper carriage is displaced down by $b = 120$ mm (to eliminate redundant constraints), the deformation of the transverse rod will be considered (Fig. 3.58). The force bending the transverse rod is $Q\frac{b}{a}$, and the transmission ratio is $\frac{b}{a}$.

The displacement of the upper joint caused by bending of the transverse rod is

$$f_5=\frac{Qa^3}{3EJ_t}\left(\frac{b}{a}\right)^2=\frac{Qab^2}{3EJ_t} \qquad (3.55)$$

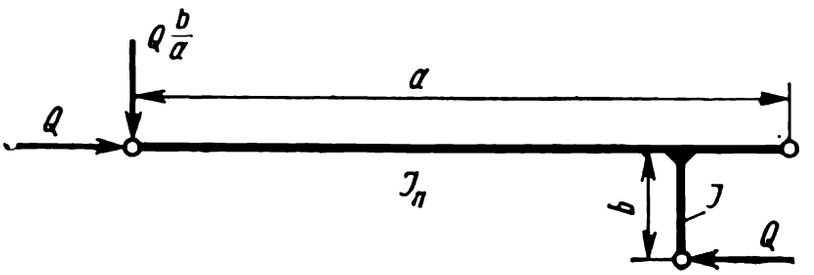


Fig. 3.58. The base of the upper carriage (transverse rod) of the current collector shown in Fig. 3.43*b* ($J_п$ *stands for* $J_t$ *and* $J$ *for* $J_c$)

The displacement of the upper joint caused by bending of the vertical rod can be found in a simpler manner as the bending force is equal to $Q$, and the transmission ratio is unity, that is

$$f_6 = \frac{Qb^3}{3EJ_c} \tag{3.56}$$

Let us calculate these displacements. The moment of inertia is identical for both transverse and vertical rods:

$$J_t = J_c = \frac{\pi}{64}(D^4 - d^4) = \frac{\pi}{64}(2.14^4 - 1.6^4) = 0.708 \text{ cm}^4$$

From (3.55):

$$\frac{f_5}{Q} = \frac{110 \times 12^2}{3 \times 2 \times 10^6 \times 0.708} = 0.00373 \text{ cm/kgf}$$

from (3.56)

$$\frac{f_6}{Q} = \frac{12^3}{3 \times 2 \times 10^6 \times 0.708} = 0.00041 \text{ cm/kgf}$$

The resultant values are very small inspite of the fact that the parts increasing the rigidity of both transverse and vertical rods have been ignored in the calculation. Therefore, the transverse rigidity remains normal upon elimination of redundant constraints.

## 3.14. Transverse Rigidity of a Current Collector with One Lever on the Main Shaft

Lower frames with one lever on each main shaft (Fig. 3.59) are used in asymmetrical current collectors, as well as in certain types of symmetrical current collectors such as ТЛ13у, ТЛ-14М, and П-7. The lower frame of such current collectors consists of a main shaft with the dimensions $2l_l$ and moment of inertia $J_l$ and a middle shaft which is shorter and has the dimension $2l_m$ and moment of

inertia $J_m$, the shafts being interconnected by means of a lever generally of a constant cross-section, with a dimension $l_1$ and moment of inertia $J_1$.

The upper frame is generally trapezoidal. In Fig. 3.59, similarly to Fig. 3.57, the loaded elements are shown with bold lines and non-loaded elements and auxiliary lines are shown with thin lines.

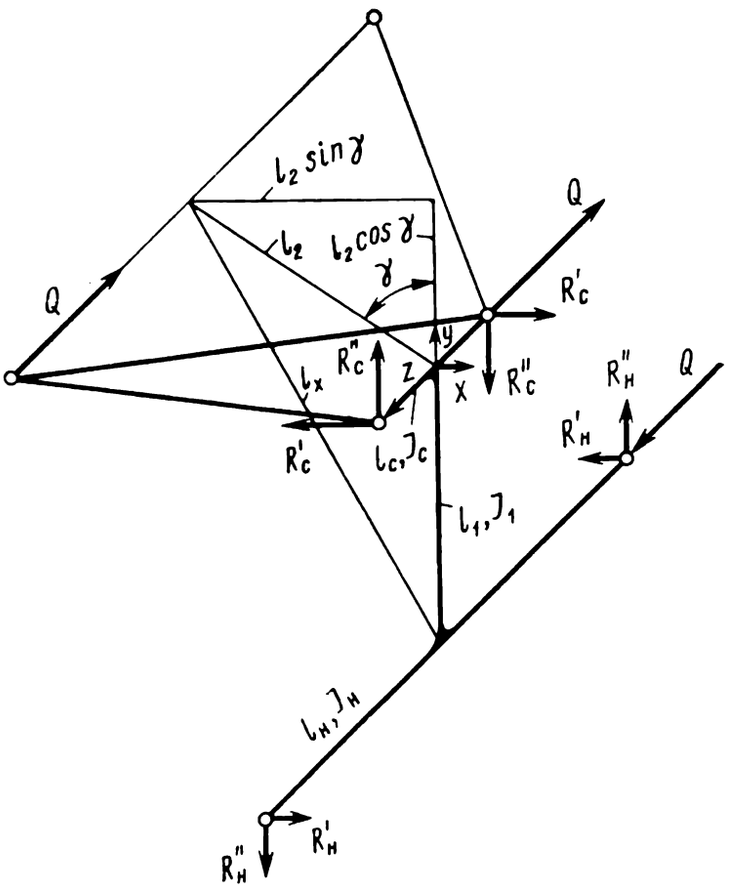


Fig. 3.59 .Forces in the current collector with the lower frame having one lever ($R_C$ stands for $R_m$ and $R_H$ for $R_l$)

The position of coordinate axes is shown in Fig. 3.59. Axes $y$ and $z$ are in the plane of the lower frame, and axis $x$ is perpendicular to this plane. Let us show the forces acting on the lower frame. Take the sum of moments of forces acting on the upper frame with respect to the $y$ axis: $Ql_2 \sin\gamma - R'_m 2l_m = 0$.

Then

$$R'_m = Q \frac{l_2 \sin\gamma}{2l_m} \tag{3.57}$$

On the basis of this formula, the displacement of the upper joint caused by bending deformation of the two ends of the middle shaft is

$$f'_m = 2 \frac{Ql_m^3}{3EJ_m} \left( \frac{l_2 \sin\gamma}{2l_m} \right)^2 = \frac{Ql_m l_2^2 \sin^2\gamma}{6EJ_m} \tag{3.58}$$

The sum of moments with respect to the $x$ axis:

$$Q_2 l_2 \cos\gamma - R''_m 2l_m = 0$$

Then

$$R''_m = Q\frac{l_2 \cos\gamma}{2l_m} \tag{3.59}$$

The length $l_m$ is small and cannot be increased as this would increase the reduced mass and drag. Therefore, the forces $R'_m$ and $R''_m$ prove to be very large and may cause breakage of bearings. This is an important drawback of such a design.

The torque twisting the lever is

$$M_t = R'_m 2l_m = Ql_2 \sin\gamma$$

The corresponding displacement of the upper joint is

$$f_c = \frac{Ql_1}{G2J_1}(l_2 \sin\gamma)^2 \tag{3.60}$$

Here $2J_1$ is the polar moment of inertia of the lever section.

The sum of moments of the forces acting on the lower frame with respect to the $x$ axis is

$$R'_m 2l_m - R'_l 2l_l = 0$$

Then

$$R'_l = R'_m \frac{l_m}{l_l} = Q\frac{l_2 \sin\gamma}{2l_l} \tag{3.61}$$

The displacement of the upper joint caused by bending of the two halves of the lower shaft in the plane $xoz$ is

$$f'_l = 2\frac{Ql_l^3}{3EJ_l}\left(\frac{l_2 \sin\gamma}{2l_l}\right) = \frac{Ql_l l_2^2 \sin^2\gamma}{6EJ_l} \tag{3.62}$$

The sum of moments of the forces acting on the lower frame with respect to the $x$ axis is

$$Ql_1 + R''_m 2l_m - R''_l 2l_l = 0$$

or, taking into account (3.59),

$$Ql_1 + Ql_2 \cos\gamma - R''_l 2l_l = 0$$

Then

$$R''_l = Q\frac{l_1 + l_2 \cos\gamma}{2l_l} \tag{3.63}$$

The displacements of the upper joint caused by bending of the middle and lower shafts in the plane $yoz$ can be found using the derived general relationship involving the second power of the transmission ratio.

Using (3.59), we obtain displacement for the two ends of the middle shaft

$$f''_m = 2\frac{Ql_m^3}{3EJ_m}\left(\frac{l_2\cos\gamma}{2l_m}\right)^2 = \frac{Ql_m l_2^2\cos^2\gamma}{6EJ_m} \tag{3.64}$$

Using (3.58) and (3.62), we obtain

$$f_m = f'_m + f''_m = \frac{Ql_m l_2^2}{6EJ_m} \tag{3.65}$$

Using (3.63), we obtain for the two ends of the lower shaft

$$f''_l = 2\frac{Ql_l^3}{2EJ_l}\left(\frac{l_1 + l_2\cos\gamma}{2l_l}\right)^2 = \frac{Ql_l(l_1 + l_2\cos\gamma)^2}{6EJ_l} \tag{3.66}$$

Using (3.62) and (3.66), we obtain

$$f_l = f'_l + f''_l = \frac{Ql_l}{6EJ_l}[l_2^2\sin^2\gamma + (l_1 + l_2\cos\gamma)^2]$$

or

$$f_l = \frac{Ql_l}{6EJ_l}[l_1^2 + l_2^2 + 2l_1 l_2\cos\gamma] = \frac{Ql_l l_x^2}{6EJ_l} \tag{3.67}$$

It is more difficult to take into account the lever bending in the plane *yoz*. The lever is a cantilever beam, the force $Q$ and the moment $M = Ql_2\cos\gamma$ acting on the beam end. They cause a deflection which is transmitted directly to the upper joint:

$$f_s = \frac{Ql_1^3}{3EJ_1} + \frac{Ml_1^2}{2EJ_1} = \frac{Ql_1^3}{3EJ_1} + \frac{Ql_1^2 l_2\cos\gamma}{2EJ_1} \tag{3.68}$$

Moreover, $Q$ and $M$ cause rotation of the upper section of the lever through the angle $\theta$ about the $x$ axis and a corresponding rotation of the upper frame which causes a lateral displacement of the upper joint through

$$f_u = \theta l_2\cos\gamma$$

By substituting the value of $\theta$ calculated by conventional formulas for beam bending in the latter formula, we obtain

$$f_u = \left(\frac{Ql_1^2}{2EJ_1} + \frac{Ml_1}{EJ_1}\right) l_2\cos\gamma = \frac{Ql_1^2 l_2\cos\gamma}{2EJ_1} + \frac{Ql_1 l_2^2\cos^2\gamma}{EJ_1} \tag{3.69}$$

The total displacement of the upper joint per 1 kgf can be found from (3.60), (3.65), (3.67) through (3.69):

$$\frac{f}{Q} = \frac{f_m + f_l + f_s + f_u + f_c}{Q}$$

or

$$\frac{f}{Q}=\frac{l_m l_2^2}{6EJ_m}+\frac{l_l l_x^2}{6EJ_l}+\frac{l_1^3}{3EJ_1}+\frac{l_1^2 l_2\cos\gamma}{EJ_1}$$
$$+\frac{l_1 l_2^2\cos\gamma}{EJ_1}+\frac{l_1 l_2^2\sin^2\gamma}{2GJ_1} \qquad (3.70)$$

or, by joining the terms relating to the lever bending, we have

$$\frac{f}{Q}=\frac{l_1 l_2^2\sin^2\gamma}{2GJ_1}+\frac{l_1^3}{EJ_1}\left[\frac{1}{3}+\left(\frac{l_2}{l_1}\cos\gamma\right)+\left(\frac{l_2}{l_1}\cos\gamma\right)^2\right]$$
$$+\frac{l_l l_x^2}{6EJ_l}+\frac{l_m l_2^2}{6EJ_m} \qquad (3.71)$$

For determining the maximum, substitute the value of $l_x^2 = l_1^2 + l_2^2 + 2l_1 l_2\cos\gamma$ by (3.67) into (3.70). Then we can write

$$\frac{f}{Q}=\frac{l_m l_2^2}{6EJ_m}+\frac{l_l\,(l_1^2+l_2^2+2l_1 l_2\cos\gamma)}{6EJ_l}+\frac{l_1^3}{3EJ_1}$$
$$+\frac{l_1^2 l_2\cos\gamma}{EJ_1}+\frac{l_1 l_2\cos\gamma}{EJ_1}+\frac{l_1 l_2^2\sin^2\gamma}{2GJ_1} \qquad (3.72)$$

By differentiating (3.72), we obtain

$$\frac{d\left(\frac{f}{Q}\right)}{d\gamma}=-\frac{l_l l_1 l_2\sin\gamma}{3EJ_l}-\frac{l_1^2 l_2\sin\gamma}{EJ_1}$$
$$-\frac{l_1 l_2^2\,2\cos\gamma\sin\gamma}{EJ_1}+\frac{l_1 l_2^2\sin\gamma\cos\gamma}{GJ_1}=0$$

The first solution $\sin\gamma = 0$ and $\gamma = 0$ gives the maximum deflection; by cancelling out $l_1 l_2\sin\gamma$ and transforming the equation, we obtain

$$-\frac{l_l}{3EJ_l}-\frac{l_1}{EJ_1}-\frac{2l_2\cos\gamma}{EJ_1}+\frac{l_2\cos\gamma}{GJ_1}=0$$

which is multiplied by $\frac{EJ_1}{l_2}$ to get

$$-\frac{1}{3}\,\frac{l_l J_1}{l_2 J_l}-\frac{l_1}{l_2}-2\cos\gamma+\frac{E}{G}\cos\gamma=0$$

Then

$$\cos\gamma=\frac{\frac{1}{3}\,\frac{l_l}{l_2}\,\frac{J_1}{J_l}+\frac{l_1}{l_2}}{\frac{E}{G}-2}$$

With $\frac{E}{G} = 2.5$; $J_1 = J_l$ and $\frac{l_l}{l_2} = \frac{1}{4}$; $\frac{l_1}{l_2} = 0.7$

$$\cos\gamma = \frac{\frac{1}{3}\times\frac{1}{4}+0.7}{2.5-2} = \frac{0.78}{0.5} > 1,$$ which is impossible.

One solution $\gamma = 0$ remains: since this value cannot be achieved, it should be assumed that maximum deformation occurs with the uppermost working position of the collector strip.

## 3.15. Contact System for Low Temperatures

Central areas of Siberia are most remote from the ocean. There are no places in the world, except for the USSR, which are so distant from sea. Therefore, the climate along the Siberian railways is the most continental with the greatest temperature difference. The contact system should be designed to withstand such difference. A weak element in the system is the insulator, and more particularly, the joint between the porcelain and the cap. At low temperatures, the cap contracts stronger (owing to a high coefficient of expansion of steel compared to that of porcelain) and causes a fatigue failure of porcelain. During severe frost periods, such failures have become a real disaster. A radical solution resides in dispensing with the caps altogether. This solution was known long ago for suspended insulators and it is used in the saddle-type and Hewlett-type insulators. These insulators should be used at low temperatures. Certain disadvantages of such insulators may be eliminated by increasing the number of insulators in the string. These insulators have one very important advantage: in case of failure of the insulator the contact system does not fall and remains suspended.

If the conventional type of suspended insulator is still more preferable, the cap should be of the self-aligning type (Fig. 3.60). For that purpose, the bearing surface of the porcelain should be tapered, with the angle of taper greater than the angle of friction. The cap should be, however, made composite of two halves covered by a hood as shown in Fig. 3.60, or another similar design should be used.

The problem is more difficult for a stick insulator, since it functions with both compression, tension and bending. Bending can be avoided by providing pivot joints at the ends of the insulator. Tension may be avoided by using an appropriate span design of the contact system (Fig. 3.61). Here, the insulated rotatable cantilever is used, and the insulator has pivot joints: a spherical joint *III'*

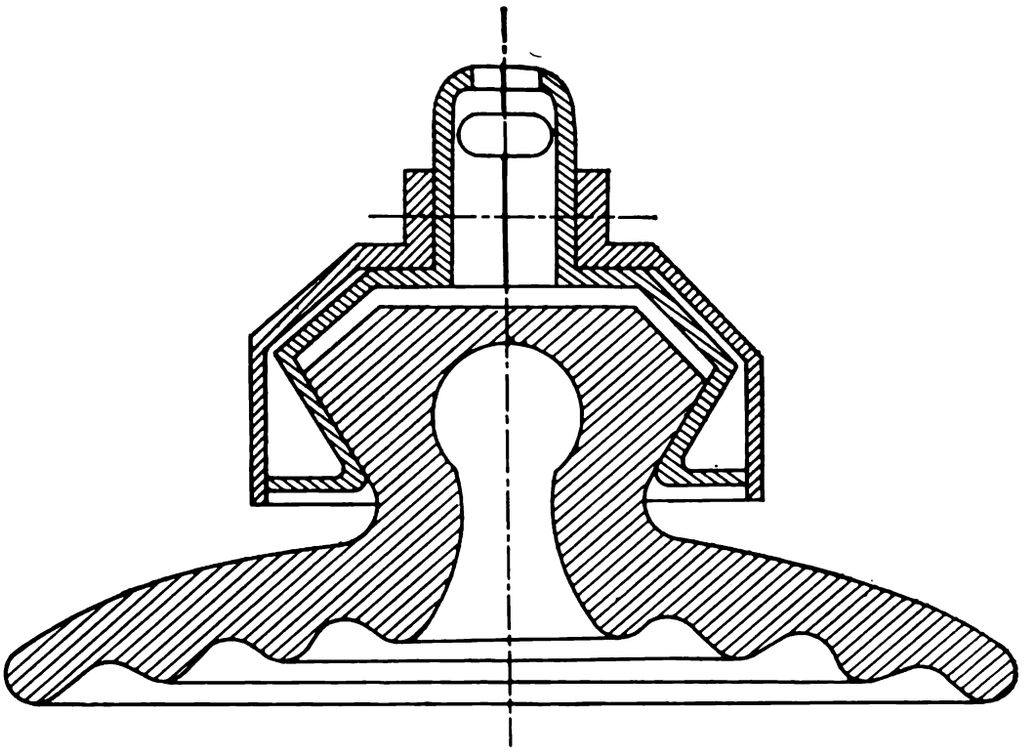

3.60. Self-aligning cap of suspended insulator precluding crushing of porcelain

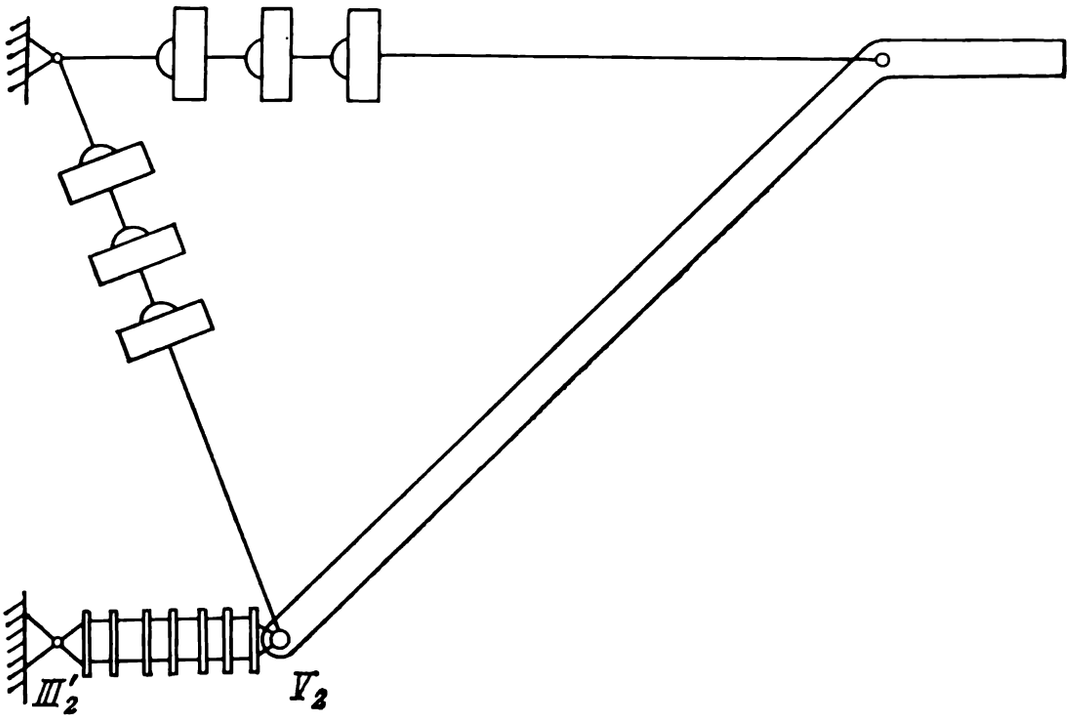


3.61. Cantilever precluding bending of stick insulator

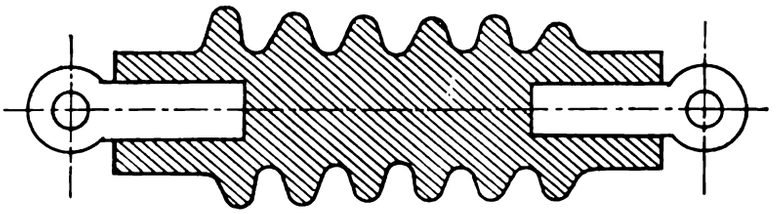

**3.62.** Stick insulator with pin replacing caps

and a pivot joint $V_2$. Then pins may be used to replace caps (Fig. 3.62). Such an insulator can function appropriately since, owing to the joints, it is almost completely free from bending. Bending is caused only by the wind load in the longitudinal direction. To avoid bending completely, two stick insulators should be installed in the triangular configuration in the horizontal plane. The only requirement is to choose the parameters of the span structure of the contact system in such a manner that the stick insulator should never be subjected to tension. A radical solution resides in completely dispensing with the use of stick insulators. Three ways of doing this may be given for double-track railways. An earthed cantilever may be used. (Fig. 3.63), with a lower transverse bracing rope. Braces should be connected to the rope using inclined bracing posts or bracing angle bars as shown in Fig. 3.63. The cantilever will be high because of two suspended insulators. However, with a compensated suspension, these insulators impart a sufficient mobility to the bearer cable, so that the cantilever may be fixed thus making it simpler.

A flexible span structure may be used as shown in Fig. 3.64, with inclined bracing posts. The upper bracing cable is preferably dispensed with. This design provides for longitudinal mobility

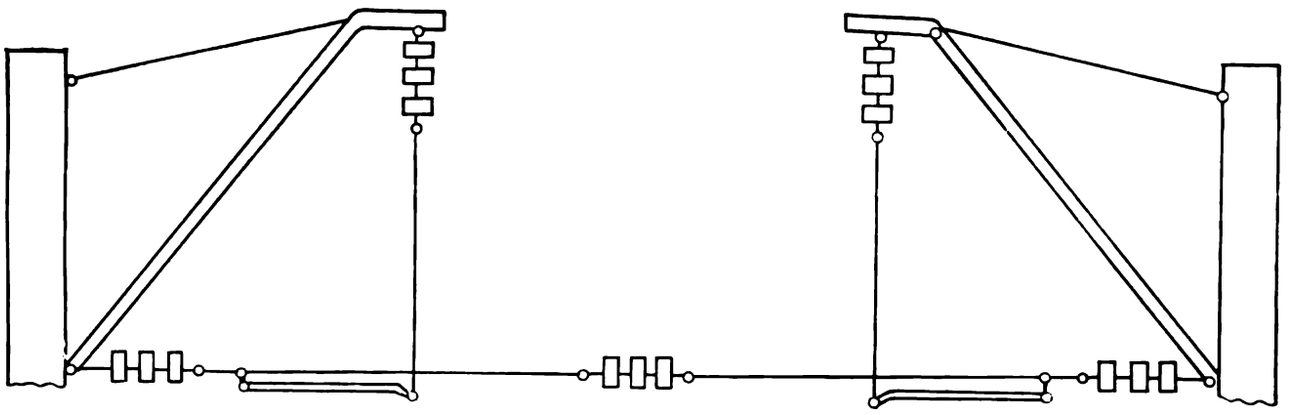

**3.63.** Transverse suspension without stick insulators, with earthed cantilevers and lower bracing rope

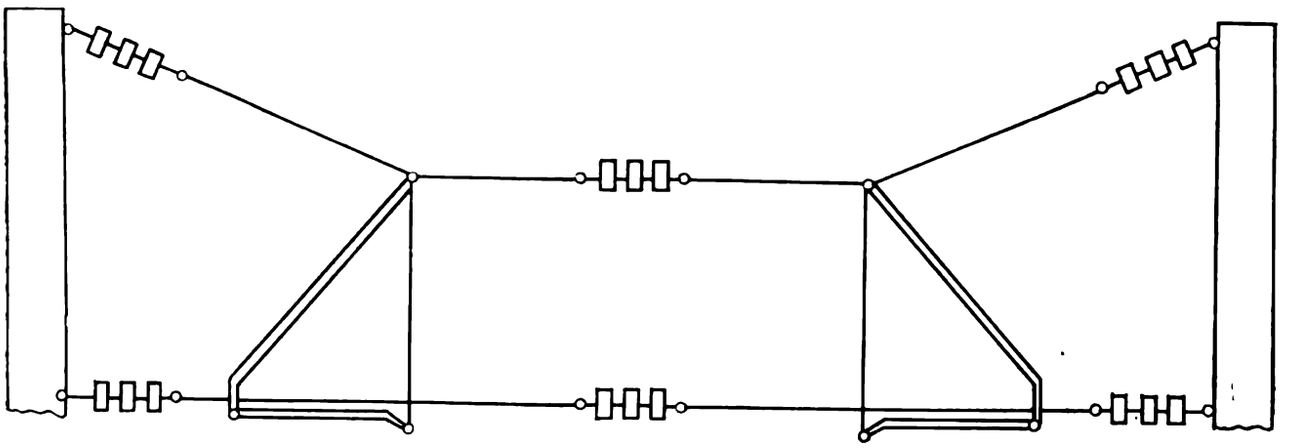

3.64. Flexible transverse suspension without stick insulators, with inclined bracing posts

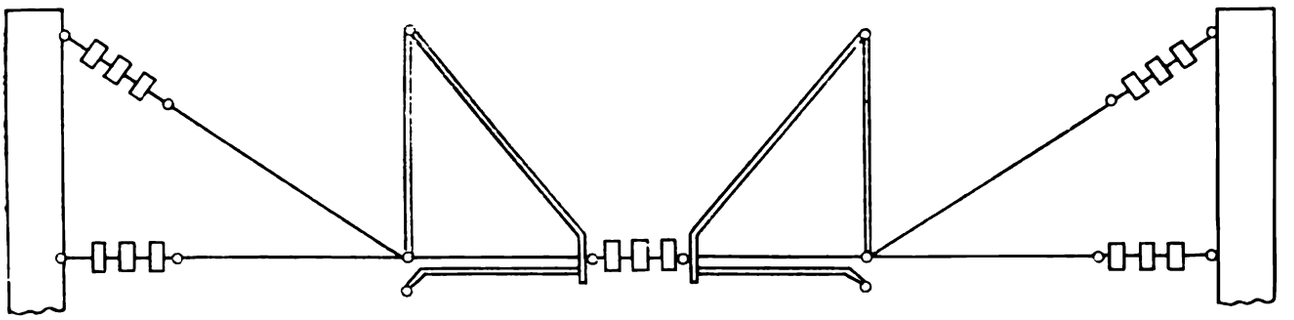

3.65. Transverse suspension without stick insulators allowing for reduction of pole height

of the bearer cable which is desirable with the compensated suspension and reduces the number of insulators required. A local mobility is to a large degree eliminated by the inclined bracing posts. It should be noted that flexible span-wire suspensions, without the top bracing cable have been used also without inclined bracing posts.

The disadvantage of the above-described design resides in a greater height of the poles. This can be avoided by using span-wire structure with catenary suspension and rigid posts (Fig. 3.65). The stability of the posts is ensured by inclined braces which are indispensable in this case.

There is another way of avoiding the use of stick insulators on the bracing: the brace pipe may be made of an insulating material. It goes without saying that the whole structure of the contact system should have no redundant constraints. The tensioning pulley should be installed on a single bearing of the 0000 or 2000 series,

rather than on two bearings since they adversely affect the performance of one another. The conical bearings of the 7000 series cannot be used altogether as they require adjustment.

Redundant constraints should not be used in the cantilever and its support insulators since they may cause overload and failure of these elements.

Therefore, a contact system reliably operating even at low temperatures may well be designed.

## 3.16. Conclusions and Recommendations

In multiple arm group, the mobility is equal to six, minus the number of arms if each arm imposes one restraint. For self-alignment, certain conditions of arms arrangement should be satisfied. In hydraulic actuator and helicopter mechanisms, redundant constraints are absent owing to a widespread use of spherical pairs and they appear only as a result of designer's errors. A helicopter rotor wobble plate mechanism may be substantially simplified by correctly choosing its structure (7 members instead of 13). There are known structures of gyration crushers for both primary and secondary crushing without redundant constraints, which have been tested during long years of operation. There are no redundant constraints in Hooke's joints which are correctly designed. Seven redundant constraints existed in a universal joint for rolling mills, and these constraints have been eliminated in a new design used in pilgrim mills. It is interesting to note that the Oldham clutch may be used as a Hooke's joint (Hooke's joint with a cube). Redundant constraints may be easily avoided in locomotive mechanisms (linkages) between parallel axles. In selecting the system, the equilibrium, number of joints, maximum load on the joint, and the sum of loads in all joints should be taken into account. Elimination of redundant constraints in locomotive current collectors makes it possible to reduce friction 3 to 4 times and to make it independent of the dimensional tolerances of the members (as shown in operation of an experimental batch). It has been established that there is a speed at which the contact pressure of the collector strip is constant (shown in the laboratory). The lift spring mechanism should be designed with the use of three points.

The spring stiffness depends on the second power of the transmission ratio in case where a transmission gearing is provided between the spring and the design point.

Chapter 4

# MECHANISMS WITH HIGHER PAIRS

## 4.1. Cam Mechanisms

The most commonly used is a design of a cam mechanism with a roller follower moving in its guideways either rectilinearly (Fig. 4.1) or circumferentially on a lever. In addition to the main mobility, the mechanism has one local mobility on account of the eventual slipping of the follower, i.e. when $w = 2$.

If the planar diagram of this mechanism is considered, by substituting $n = 3$, $p_l = 3$ and $p_h = 1$ in (1.5) we attain: $q_p = 2 - 3 \times 3 + 2 \times 3 + 1 = 0$, i.e. independently of the classes of the kinematic pairs, in a planar diagram a cam with a roller follower and force closure is devoid of redundant constraints.

With kinematic closure, irrespectively of whether it is done by a grooved cam (Fig. 4.2*a*) or a double mechanism (Fig. 4.2*b*), one high-class pair is added, so that $q_p = 1$.

In case of a groove cam machined with an end-mill cutter of the diameter equalling that of the follower roller, both profiles are machined in a single pass, and so the redundant constraint here is not very harmful. In case of a double mechanism, however, the

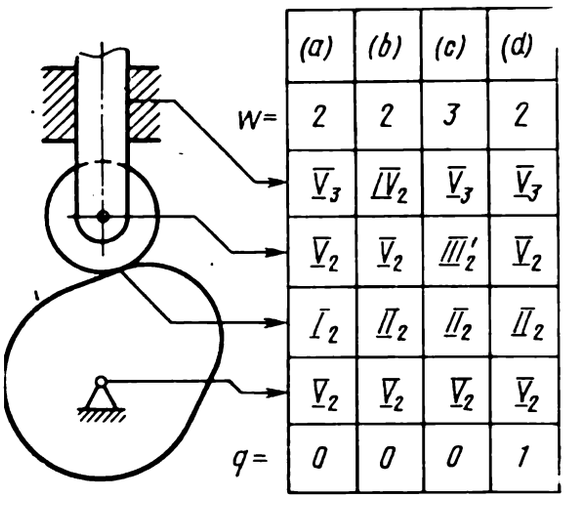


Fig. 4.1. Designs of cams with roller follower and forced closure (*a*)-(*c*) without redundant constraints; (*d*) with one redundant constraint

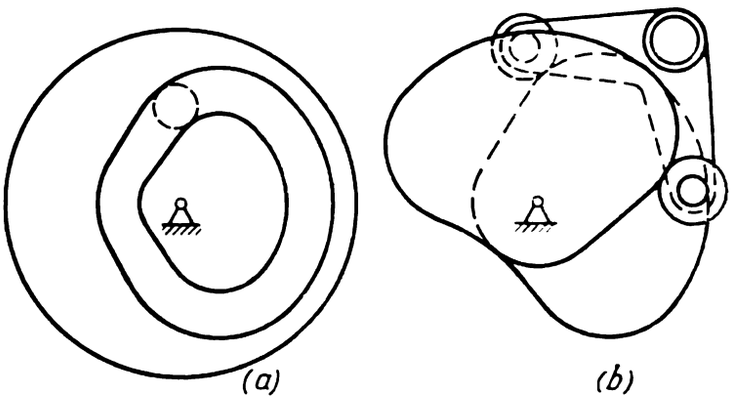


Fig. 4.2. Cams with kinematic closure (*a*) groove cam: (*b*) double cam

connection requires highly accurate manufacturing to avoid either jamming or knocking caused by excessive gaps. Thus, this redundant constraint is particularly undesirable, which is true of every double or twin mechanism.

To discuss actual mechanisms with force closure, let us substitute in (1.1) $w = 2$, $q = 0$ and $n = 3$ to obtain $0 = 2 - 6 \times 3 + 5p_{\mathrm{V}} + 4p_{\mathrm{IV}} + 3p_{\mathrm{III}} + 2p_{\mathrm{II}} + p_{\mathrm{I}}$. Then, $5p_{\mathrm{V}} + 4p_{\mathrm{IV}} + 3p_{\mathrm{III}} + 2p_{\mathrm{II}} + p_{\mathrm{I}} = 16$. As the mechanism has four kinematic pairs, $p_{\mathrm{V}} + p_{\mathrm{IV}} + p_{\mathrm{III}} + p_{\mathrm{II}} + p_{\mathrm{I}} = 4$.

These equations are satisfied with $p_{\mathrm{V}} = 3$, $p_{\mathrm{IV}} = p_{\mathrm{III}} = p_{\mathrm{II}} = 0$, and $p_{\mathrm{I}} = 1$ (cf. Fig. 4.1*b*). In this case a barrel-shaped follower roller is to be used to have a first-class kinematic pair (the point one). This design fits both disk (flat) and cylindrical cams with the follower moving either on a slider or on a pivoted lever.

The equations are also satisfied with $p_{\mathrm{V}} = 2$, $p_{\mathrm{IV}} = 1$, $p_{\mathrm{III}} = p_{\mathrm{I}} = 0$ and $p_{\mathrm{II}} = 1$ (cf. Fig. 4.1*b*). In this case a cylindrical follower roller is used. Besides, to have a fourth-class pair, the guideway of the follower is made cylindrical. This design can be recommended for great thrust angles. It is essential, though, that the rotation of the follower should be limited to a degree sufficient for attaining self-alignment. This design is employed in the mechanism of rheostat controller suggested by the author for suburban electric train and underground train motor coaches and has completely proved its worth. The rotation of the follower is limited by the slider or the follower encompassing the cam.

The pneumatic actuator of ПКГ-320 controller rated for 3 000 V and 1 500 V (Fig. 4.3) [54] rotates the camshaft of the controller in one direction only through a toothed gearing (the current being switched off by other device—the linear contactor). The cam (star-shaped) is welded to the actuator shaft, and the followers of the cam mechanism run on needle-roller bearings. The shaft bearings are mounted on a flange removable as a unit with the shaft and the star-shaped cam. The same flange supports the actuator.

ПКГ-756 rheostat controller is used in motor coaches of underground electric trains. Its shaft extends through the actuator (Fig. 4.4) to offer more reliable support to the shaft and to separate the low-voltage part of the apparatus from the high-voltage one. A slot is milled in the piston rod to accommodate the shaft, which has called for increasing the rod thickness (Figs. 4.3 and 4.4). To provide for inserting the rod through the cylinder, the piston disks are detachable. Besides, surfaces *1* and *2* (Fig. 4.4) had to be turned to a cylindrical surface with the axis offset from that of the cylin-

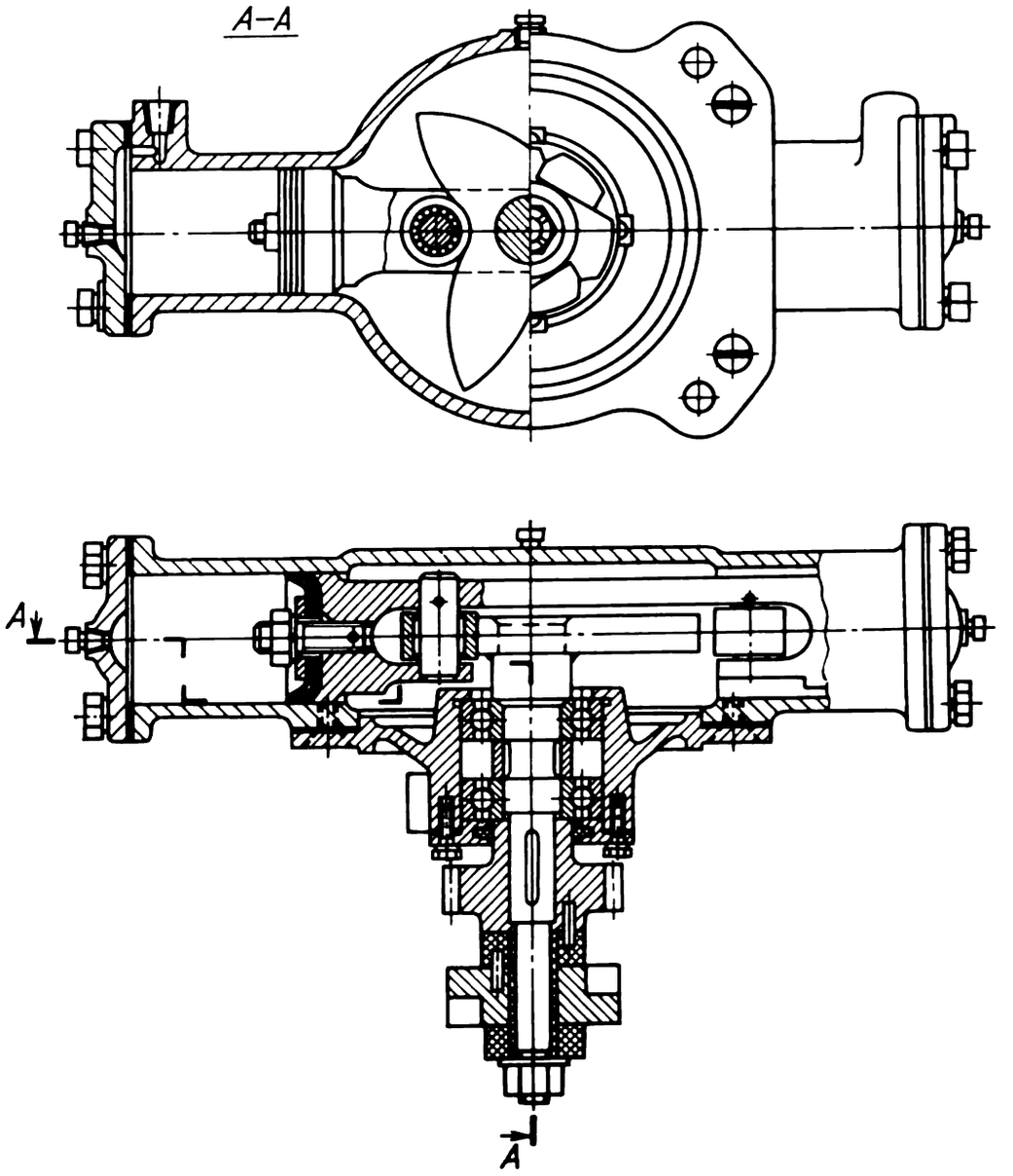


Fig. 4.3. Pneumatic cam actuator of ПКГ-320 controller for electric train

der, while the axis of surface *3* is aligned with the cylinder axis.

The design of Fig. 4.1*b* is quite suitable for a cylindrical cam. However, it would not fit a cam with a rotatable follower, for in this case the axis of the cylindrical pair is parallel with the engagement line of the cam and of the follower roller, and we get intolerable mobility of the follower along its axis of rotation instead of self-alignment.

A design free of redundant constraints can be obtained with a cylindrical follower roller by having a spherical kinematic pair (a spherical bearing) at the roller's axis of rotation (cf. Fig. 4.1*c*). The

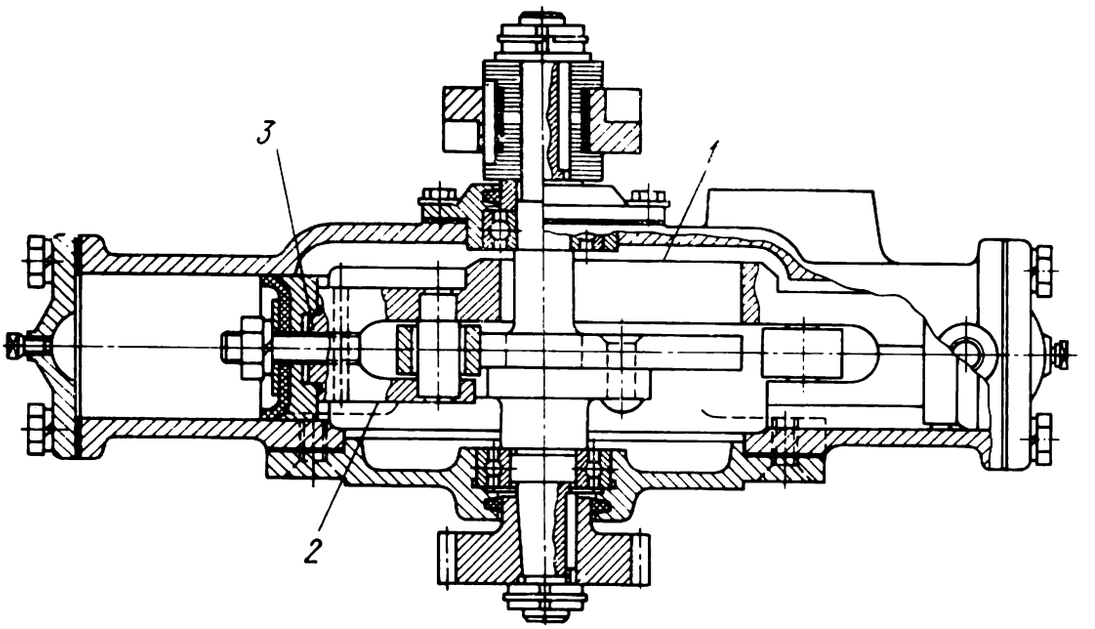


Fig. 4.4. Pneumatic cam actuator of ПКГ-756 controller (rated for 750 V) for motor coach of underground train

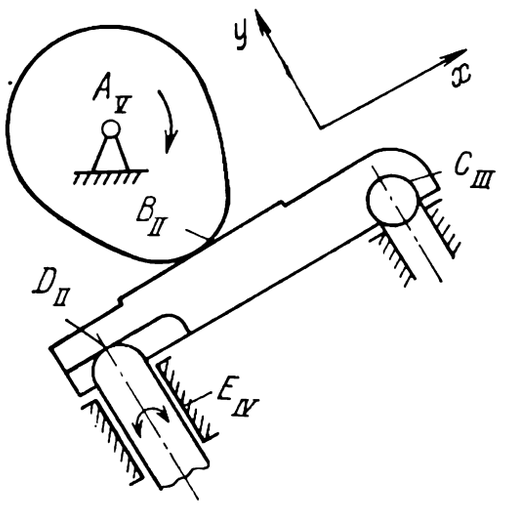


| | | | | |
|---|---|---|---|---|
| $w=2$ | 2 | 2 | | |
| $n=3$ | -18 | 12 | $ABC$ | |
| $p_V=1$ | 5 | -1 | | |
| $p_{IV}=1$ | 4 | -2 | | |
| $p_{III}=1$ | 3 | -3 | $ABDE$ | |
| $p_{II}=2$ | 4 | -8 | | |
| $K=2$ | 0 | 0 | | |

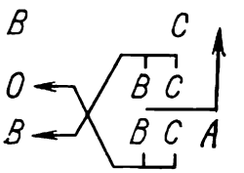


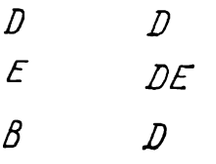


Fig. 4.5. Cam mechanism of LADA car engine

roller then acquires one additional local mobility—rotation about an axis perpendicular to the line of its engagement with the cam. This mobility is to be curbed within the limits sufficient for self-alignment, which presents no specific problem as the roller is usually accommodated in a slot of the slider of the follower.

From (1.1) with $w = 3$, $n = 3$ and $p_V = 2$ we have $p_{IV} = p_I = 0$; $p_{III} = 1$, $p_{II} = 1$ and $q = 3 - 6 \times 3 + 5 \times 2 + 3 + 2 = 0$.

The design fits both disk and cylindrical cams with the follower mounted either on a slider or on a pivoted lever.

If a cylindrical follower roller is used (a second-class line pair), and the rest of the pairs are fifth-class ones (cf. Fig. 4.1*d*), from (1.1) with $w = 2$, $n = 3$, $p_V = 3$ and $p_I = 1$ we have $q = 2 - 6 \times 3 + 5 \times 3 + 2 \times 1 = 1$.

The redundant constraint requires that several dimensions in this design should be observed with a high accuracy.

Redundant constraints are easily eliminated in mechanisms with a rotary (pivoted) follower (Fig. 4.5) by mounting the pivoted follower (the arm) on a spherical support $III_2'$. The other angular mobility of the arm is eliminated in this case by an annular pair $II_3$ connecting it to the valve tappet. This design for the flat follower of the "LADA" car engine is shown in Fig. 4.5, with the mobilities in the loop given at the bottom of the drawing.

## 4.2. Power Contacts of Electric Apparatus

Electric apparatus make wide use of line contacts—pairs $II_2$, for a planar contact has proved disappointing. Proper engagement of the jaws is a must in line contacts: if it is only a small portion of the theoretical length of a contact is actually working the load capacity is affected, and the contacts get burnt. The percentage of the working portion of a contact is subjected to quality control at acceptance of an apparatus. However, in operation this percentage deteriorates causing burnt jaws. Self-alignment may help ensure proper contact engagement. An example of a proper design are the contacts of the reverser of ЧС-2 electric locomotive where at the nominal current of 550 A the pressure of the pins upon the segments is but 2.2 to 2.5 kgf. For comparison, let us remember that in the ПР-156В reverser—without self-alignment—with the current of 400 A the pressure of the contact-making pins is 7 to 9 kgf, it is increased in service to 15-20 kgf, but the pins get burnt just the same.

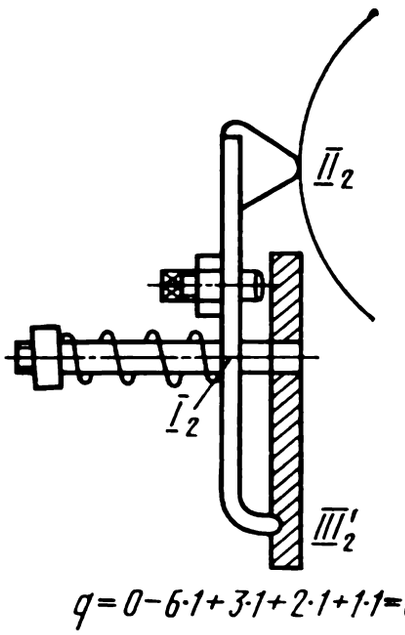


Fig. 4.6. Power contact pin without redundant constraints

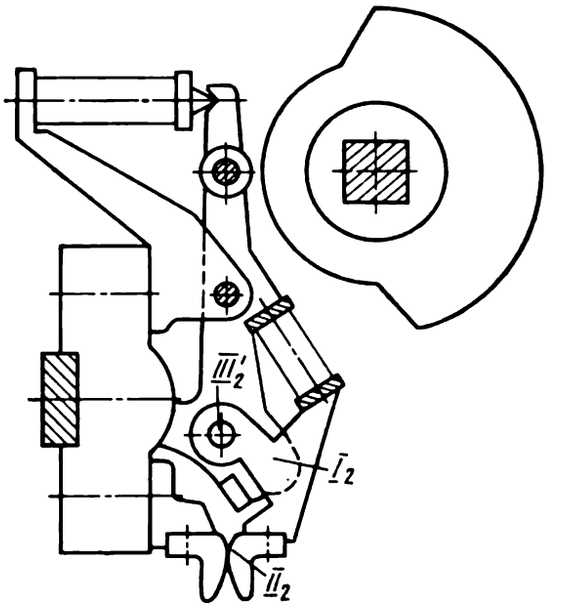


Fig. 4.7. Power contactor without redundant constraints

A contact pin devoid of redundant constraints is shown in Fig. 4.6. It forms a $II_2$ pair with the segment bolted to the drum, while a spherical pair $III_2'$ connects it to the insulated fixed member. The segment is urged by a spring whose spindle extends through a slot in the segment, defining with it a first-class pair $I_2$. The abutment bolt shown in Fig. 4.6 limits the "drop" of the pin when the segment of the drum moves from under the pin in a switching operation. For the pairs $I_2$ and $III_2$ not to be heated by current, a flexible shunt (not shown in Fig. 4.6) is connected in parallel with them.

From (1.1) $q = 0 - 6 \times 1 + 3 \times 1 + 2 \times 1 + 1 \times 1 = 0$, i.e. redundant constraints are none. It is essential in the fabrication of this structure that the pairs $I_2$ and $III_2$ should actually provide the necessary mobilities.

Redundant constraints may be likewise eliminated in power contactors. Fig. 4.7 shows a cam-actuated contactor in "on" position. The contactor of Fig. 4.7 makes by the action of the spring and breaks by the action of the cam (which is general practice nowadays). Redundant constraints may be eliminated by having a spherical pair $III_2'$ between the main arm and the movable contact holder. In this design the harmful angular mobilities have been eliminated by the holder abutting (pairs $I_2$) against the shoulders of the main arm. This design has been suggested by A. V. Padalko. The said

also applies to pneumatically and electromagnetically actuated contacts, for it is not the actuating mechanism which is considered, but solely the members under load in the "on" position.

## 4.3. Contact Devices in Control Circuitry (Low-Current)

Owing to low current values, control circuitry contacts are usually of the point or spot type—pairs $I_2$. To provide for their trouble-free operation (which is essential in such applications), reliable sliding (grinding-in) of the contacts and accurate contact-making effort should be ensured [31].

For accuracy of the contact-making effort, the spring is expected to be of small stiffness and, correspondingly, of a great extent of deformation. Leaf springs used with the contact pins of traction control apparatus and, particularly, blade contacts in radio devices would not meet this requirement, and their performance lacks reliability.

Proper (i.e. low) rigidity is afforded by helical springs, but when the contacts are numerous, accommodating the springs becomes a problem. This problem leads to that of loading several contacts by the same spring. Well and long known are bridge interlocks where a spring arranged at the centre of a straight bridge urges two contacts (No. 2 condition of Table 3.1 above). In this case the effort of the spring and the loads of the two contacts are directed parallel in one plane. To increase the number of contacts, parallel forces should be taken in space (No. 5 condition of Table 3.1) instead of arranging the contacts in a single plane. Then one spring could urge three contacts, and when the effort of its opposite end is also used, it could urge six contacts (Fig. 4.8).

This arrangement has been utilized in the multipath controller with 14 points of an electric motor coach.† Control circuit wires are connected to the segments mounted on discs *1* and *2* of fabric-based laminate. The segments are split with insulating inserts in accordance with the control circuitry. The disks are urged together by spring *3* (two such springs were in the prototype) providing the contact-making pressure. To preclude rotation, each disk is connected by an arm to the case of the apparatus, which provides for self-alignment of the disks. Movable contacts—three pairs—are mounted on disk *4* of fabric-based laminate carried by the controller shaft. To ensure uniform loading of contacts working on segments

of different radii, the central angles are correspondingly different. This structure has been reliably performing for a number of years.

The number of the contacts may be increased by replacing one of them by a lever with equal arms (a balance arm) engaging two

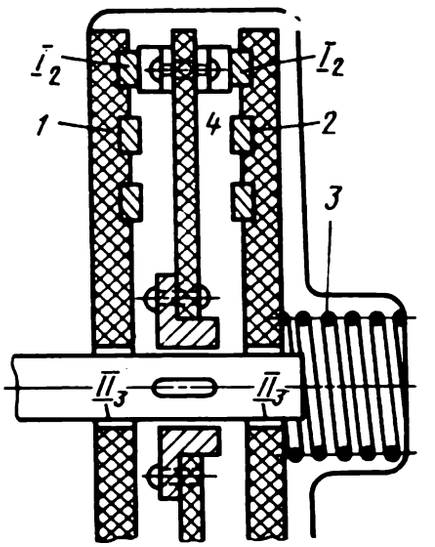


Fig. 4.8. Contact device where one spring urges six contacts in statically determinate fashion

segments. This device has been tested in an electric underground railway coach and proved reliable. If all the contacts are replaced by levers, twelve contacts may be actuated by a single spring, but this number is excessive since eight is the maximum number of contacts in practical applications.

The further path of stepping up the number of contacts urged by a single spring is to employ the general case of three-dimensional arrangement of forces (No. 7 condition of Table 3.1), with the efforts applied to the contacts extending in parallel planes and intersecting a line (cf. Fig. 3.3*b*). Thus, each end of the spring urges four contacts. This means that the segments should be arranged in practical cases on the surface of a cylinder.† The contact plate should be connected to the actuator by an annular pair $II_3$, with the axis of the latter being perpendicular to the cylinder axis. If both ends of the spring are utilized, it would urge eight contacts. An additional advantage of this design is its fitting both rotation and translation of the control member.

Finally, one end of a spring may urge six contacts (see Fig. 3.5*b*) by the general case of the arrangement of forces being used (No. 11 condition of Table 3.1). Unfortunately, in this case sliding (grinding-in) of the contacts is not provided, making it suitable only for applications when the fine surface state of the contacts is well ensured.

## 4.4. Gear Trains

In present-day toothed gearings the engagement factor is always in excess of a unity. This indicates that two teeth couples work simultaneously at the beginning and end of the line of contact (with $\varepsilon < 2$), their load being distributed in a statically indeterminate fashion, i.e. there is a redundant constraint, although not in a mechanism but in a kinematic pair where it is not harmful as a kinematic pair can be easily manufactured with adequate accuracy.

With an increased engagement factor gearings' operation is more quiet, and the teeth manufacturing accuracy requirements are less strict. The following explanation may be offered. When one pair of teeth works, any profile defect (e.g. a cavity) results in alteration of the law of the motion of the driven gear, accompanied by dynamic loads, noise, etc. When two pairs of teeth work simultaneously, an indentation in one of the profiles leads merely to redistribution of the loads among the teeth and would not practically affect the law of the motion of the driven gear. Therefore, the redundant constraint brought about by simultaneous work of two pairs of teeth will be disregarded in the following discussion, and we shall suppose that only one set works at a time.

A gearing with parallel axes (Fig. 4.9*a*), irrespective of the design of the kinematic pairs, has no redundant constraints according to formula (1.5) for a planar diagram. This can be easily ascertained by substituting $n = 2$, $w_p = 1$. $p_l = 2$ and $p_h = 1$ in (1.5): $q_p = 1 - 3 \times 2 + 2 \times 2 + 1 = 0$.

The same values of redundant constraints are obtained for a bevel gearing with intersecting axes, when determined from the formula for a spherical diagram.

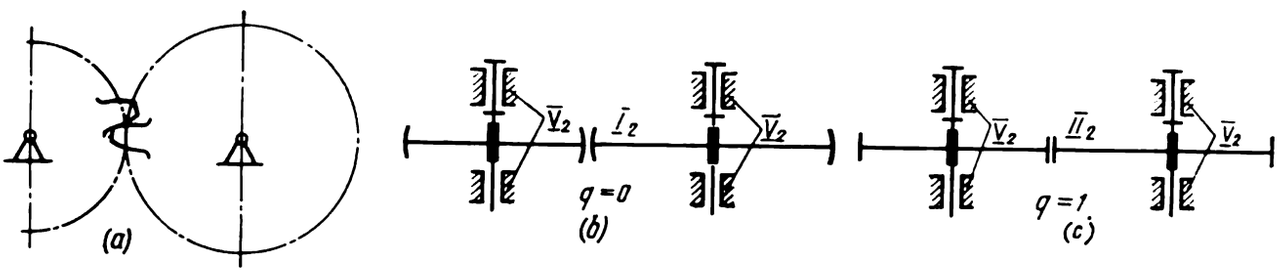


Fig. 4.9. Diagrams of spur gearing
(*a*) planar; (*b*) without redundant constraints; (*c*) with one redundant constraint

When actual mechanisms are considered with $w = 1$, $n = 2$, and $q = 0$, formula (1.1) yields:

$$0 = 1 - 6 \times 2 + 5p_V + 4p_{IV} + 3p_{III} + 2p_{II} + p_I,$$

whereby $5p_V + 4p_{IV} + 3p_{III} + 2p_{II} + p_I = 11$.

As the mechanism has three kinematic pairs, $p_V + p_{IV} + p_{III} + p_{II} + p_I = 3$.

The equations are satisfied with $p_V = 2$:

$p_{IV} + p_{III} + p_{II} = 0$ and $p_I = 1$ (Fig. 4.9*b*).

Therefore, a gearing without redundant constraints may be obtained by using teeth with a concentrated engagement spot (barrel-shaped), defining a first-class pair[1].

However, the efficiency of this solution is doubtful, as it replaces the line contact by a point one, with the pressure value being correspondingly higher. With a skewed barrel-shaped tooth the resultant of the circumferential force becomes sharply offset toward the face of the gear, which also steps up the engagement and bending strain. The contour curve of a barrel-shaped tooth will be assumed a circle (Fig. 4.10*a*), and its radius ρ will be found from the condition:

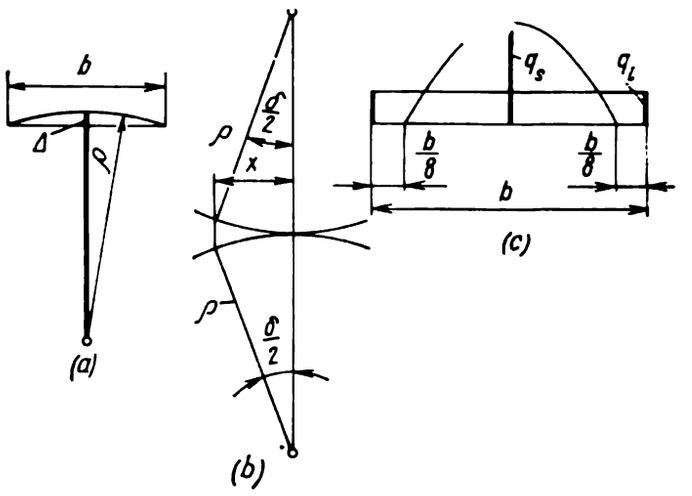


Fig. 4.10. Barrel-shaped tooth
(*a*) tooth line; (*b*) offsetting of engagement point with skewing; (*c*) adopted load curve

$$\frac{\Delta}{\frac{b}{2}} = \frac{\frac{b}{2}}{(2\rho - \Delta)}$$

or, neglecting the value of Δ in the denominator, we have

$$\rho = \frac{b^2}{8\Delta} \qquad (4.1)$$

[1]Such teeth will be shown in the drawings with a slightly convex shape of the rim (cf. Fig. 4.9*b*).

The service life of teeth is sharply reduced when the axes cross each other. The crossing may be caused by the effort developed by the teeth and bending the driving and driven shafts in opposite directions. The crossing angle is particularly pronounced in electric locomotive gear trains with plain bearings.

With the axes crossing at angle $\delta$, the offsetting of the resultant of the circumferential force (Fig. 4.10*b*) from the centre of a tooth equals

$$x = \rho \frac{\delta}{2} \text{ or } x = \frac{b^2\delta}{16\Delta} \tag{4.2}$$

i.e. the offsetting of the $x$ effort decreases with $\Delta$ increasing, but the thickness of the tooth is reduced to $S_0 - 2\Delta$.

Let us compare the maximum load $q_s$ lengthwise of a tooth with a concentration engagement spot with the load $q_l$ corresponding to a line contact. Fig. 4.10*c* shows the curves of the loads on the tooth. With a line contact of a self-aligning gear, the load curve will be a rectangle, and the tooth load

$$Q = q_l b \tag{4.3}$$

With a barrel-shaped tooth let us presume that the engagement spot clears the end faces by $\frac{b}{8}$, since a greater spot would not be practically attained. Let us further presume that the load curve would be parabolic. Then the load of the tooth will be described as the area of the parabola:

$$Q = \frac{2}{3} q_s \frac{3}{4} b = \frac{q_s b}{2} \tag{4.4}$$

By equalizing the load in (4.3) and (4.4) we obtain

$$q_s = 2\ q_l \tag{4.5}$$

This load corresponds to an instant when the spot works by its widest part. In other positions $q_s$ will be even greater. Thus, it is essential that with the axes skewing, uniform loading lengthwise of a tooth should be ensured with a line contact, with barrel-shaped teeth used only in cases where a line contact would not be attained.

Therefore, it is important to provide uniform loading lengthwise of a tooth with a line contact when the axes are skewed.

If spur gear teeth with a line contact are used, the engaging teeth define a second-class pair (cf. Fig. 4.9*c*) where $p_{\text{V}} = 2$, $p_{\text{IV}} = p_{\text{III}} = p_{\text{I}} = 0$ and $p_{\text{II}} = 1$.

In this case $q = 1$, which requires strict parallelism of the axes of the driving and driven gears. With their shafts skewing or deformed, the load lengthwise of a tooth becomes non-uniform.

A cylindrical pair $IV_2$ may not be used in the bearing, since it has a linear axial mobility in addition to the main angular one,

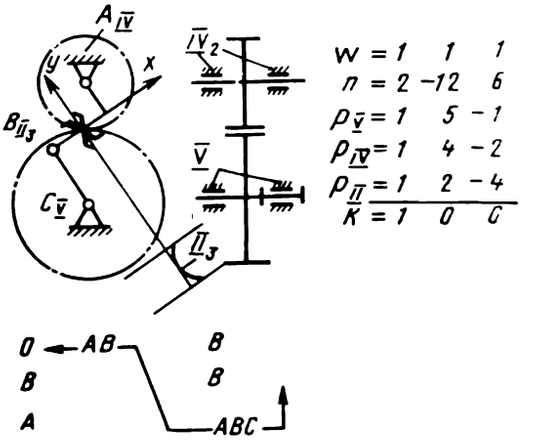


Fig. 4.11. Spur gearing with arch-shaped (curvilinear) tooth

whereas elimination of the redundant constraint requires angular mobility about an axis perpendicular to the line of the tooth. The redundant constraint is caused by moment $M_y$ transmitted between the teeth by the linear pair $II_2$ (cf. Table 1.1). It may be also eliminated by replacement of the pair $II_2$ by an annular pair $II_3$ which would transmit two forces along the two coordinate axes and would not transmit torques between the teeth. In this case the teeth would be arch-shaped (Fig. 4.11). The bearing assembly of the shaft of one gear should be a pair $V$, and that of the other gear a pair $IV_2$. The calculation of redundant constraints from structural formulas and mobilities in the loop are given in Fig. 4.11. This gearing would offer a high load capacity due to its low contact (Hertzian) stress.†

Arch-shaped teeth are used by Glisson Co. in bevel gears, offering an essential increase in load capacity. Gears of this type are widely used in automotive vehicles. However, the advantages offered by elimination of redundant constraints have not been exploited in full, as the axial force in bevel gears would not permit the corresponding mobility.

A common spur gearing with $V_2$ pairs has one redundant constraint which causes non-uniform loading lengthwise of a tooth with the shafts either skewing or deformed. To avoid this non-uniformity, one $V_2$ pair should be replaced by a $IV_3$ one—spherical-with-pin. However, this pair is structurally complicated. Hence, the required angular mobility is rather provided by mounting the housing of the reduction gear on a spherical support situated in the central

plane of the gears, internally of the greater gear†(Fig. 4.12). The reduction gear is suspended from two rods: the vertical one which transmits the torque (as usual) and the horizontal rod eliminating the excessive angular mobility.

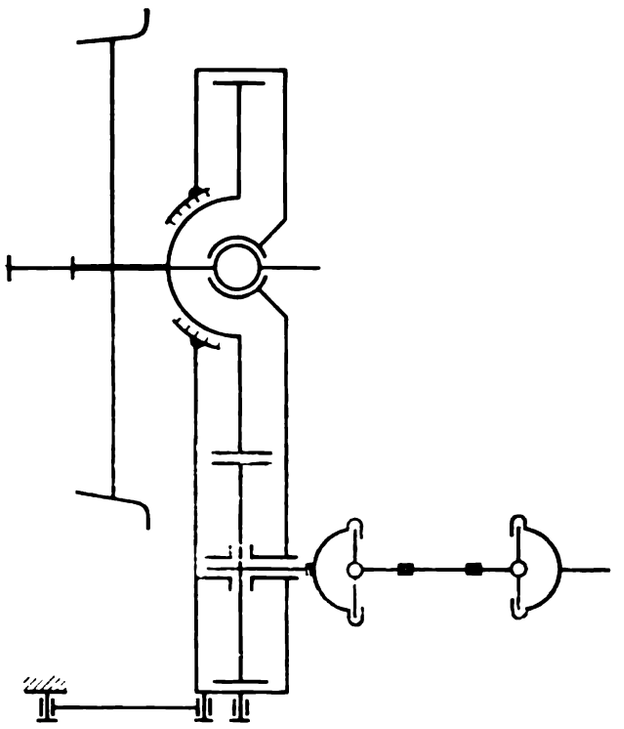

Fig. 4.12. Traction drive with gears which self-align owing to angular mobility of reduction gear suspended from wheel pair axle with the aid of spherical bearing

Another way to eliminate redundant constraints in a two-gear train with line contact of the teeth is to connect the toothed rim of one of the gears to the hub by a splined pair $IV_5$ so that the mobility would grow by a unity and equal two.

Then, by substituting $n = 3$, $w = 2$, $p_V = 2$, $p_{IV} = 1$ and $p_{II} = 1$ in (1.1) we obtain $q = 2 - 6 \times 3 + 5 \times 2 + 4 \times 1 + 2 \times 1 = 0$.

The second mobility is a local one: rotation of the toothed rim about the normal to the teeth profile. Experience has shown that this is harmless, being well damped by the friction between the teeth. Unfortunately, the friction in the toothed universal joint (i.e. in the splined pair) affects the uniform distribution of the load lengthwise of a tooth (Fig. 4.13).

If we assume the moment of friction in the toothed universal joint $M_M = 0.1\ M$ ($M$ being the torque transmitted by the joint), we can find the displacement $x$ of the circumferential force $Q$ from $Qx = M_M = 0.1\ Qr$, and $x = 0.1r$.

If we assume as the extreme case the distribution of the load applied to a tooth according to a triangle, the displacement will equal

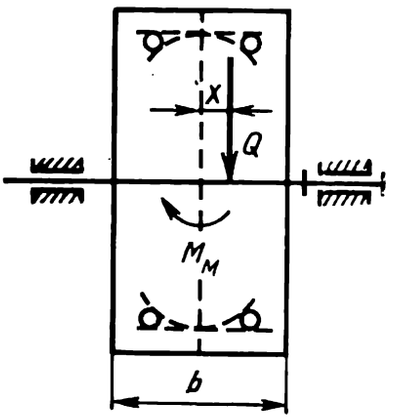


Fig. 4.13. Offsetting of circumferential force on account of friction in toothed universal joint

$b/6$. Substituting this into the formula for finding $x$ we obtain $b/6 > 0.1\,r$, so that

$$r < \frac{10}{6} b \qquad (4.6)$$

This condition is satisfied only when it is the smaller gear (or pinion) which is mounted on the toothed joint.

An advanced design of a splined pair was suggested by A. I. Belyaev†(Fig. 4.14*a*). The connection between the toothed rim and the hub in this design is effected with the barrel-shaped rollers of a spherical (self-aligning) roller bearing. The axial mobility is restrained by the rubber rings, one of them is mounted intermediate the second shoulder on the toothed rim and the nut securing the hub on the shaft, and the other one is received between the shoulders, through a steel washer. The antifriction bearing mounted at the end of the motor shaft supports the case of the reduction gear. The outcome of the testing of a diesel locomotive drive with this splined pair was positive: the drive was no longer noisy. Following the testing in a test rack, corresponding to 250 000 total kilometres logged by the diesel locomotive, the surface of the teeth became mirror-like. No wear was detected. The transmission of the old design tested concurrently with the new one was very noisy and showed significant wear.

Experiments with self-aligning gears in the side gearings of tractors have been conducted by tractor-making plants (Fig. 4.14*b*). Significant reduction of non-uniformity of the load lengthwise of a tooth has been attained notwithstanding the fact that the toothed rim of the bigger gear was mounted on the toothed joint.

With herringbone teeth and solid gears, redundant constraints would not be eliminated even with one of the gears having a spherical mounting (Fig. 4.15).

Let us discuss the mobilities in the loops of this mechanism.

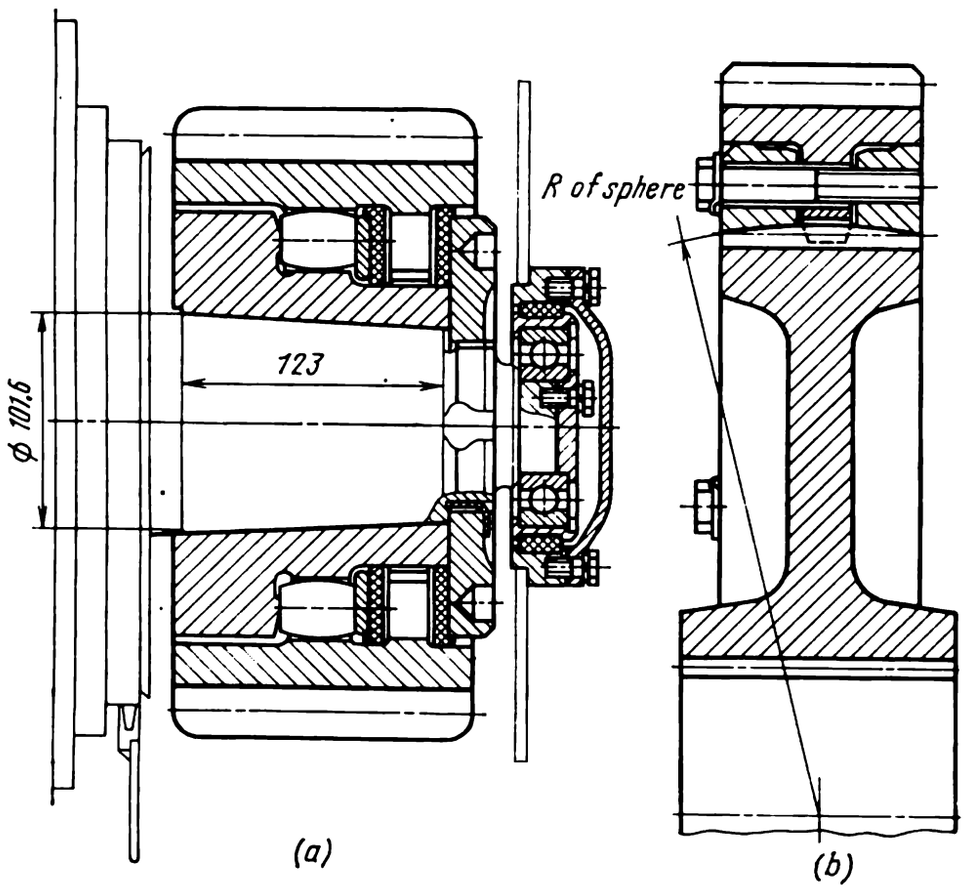


Fig. 4.14. Self-aligning gears
(*a*) by A. L. Belyaev; (*b*) produced by the Volgograd Tractor Factory

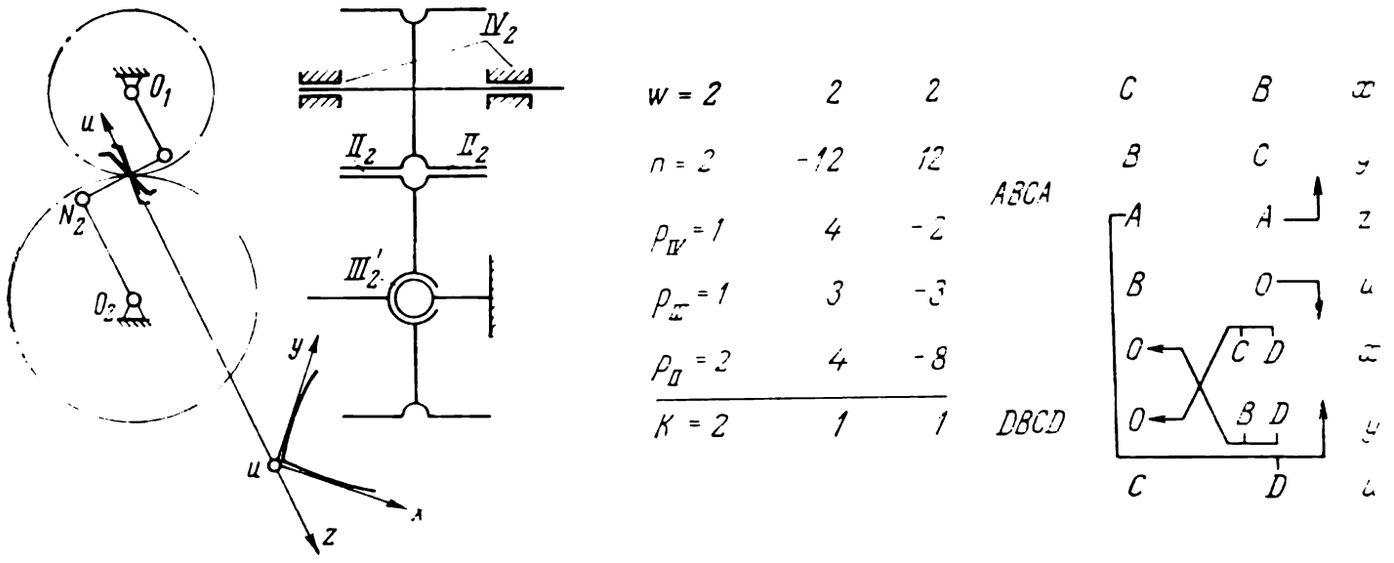


Fig. 4.15. Spur gearing with herringbone teeth and one of the gears on spherical bearing assembly

Axes $x$ and $y$ will be taken in the engagement plane, i.e. the plane tangent to the main cylinders, and will extend tangentially to the lines of the teeth.

Axis $u$ will extend perpendicularly to this plane, and axis $z$ will extend along the axes of the gears. There are two loops here, which we presume as $ABCA$ and $DBCD$.

Consider linear mobilities.

Along axis $x$—slipping along the line of the tooth of one half of the herringbone in pair $C$;

Along axis $y$—slipping along the line of the tooth of the other half in pair $B$;

Along axis $z$—lengthwise slipping in the fourth-class cylindrical pair $A$ of the first gear;

Along axis $u$—slipping of the teeth of both halves of the herringbone in pairs $B$ and $C$.

Altogether, we have five linear mobilities.

Consider angular mobilities.

Three angular mobilities of the spherical mounting $D$ of the second gear about the $x$, $y$ and $u$ axes in the $DBCD$ loop. In the same loop we have mobility of the spherical pair about axis $x$ and twirling of the teeth (relative to the normal) of the first herringbone half in pair $C$. The mobilities in pairs $B$ and $D$ about axis $y$ are similar.

Let us now discuss the distribution of the mobilities. Out of $f''_x = 2$ one mobility replaces the linear mobility along axis $y$. This is possible since there is a member—the second gear—of which line $O_2N_2$ is directed along axis $u$, i.e. along the third coordinate axis. Similarly, one of the angular mobilities about axis $y$ will replace the linear mobility along axis $x$. The angular mobility about axis $u$ is one for both loops. It would not be replaced, as the available angular mobilities are those about the $x$, $y$ and $z$ axes belonging to a plane perpendicular to axis $u$ and would not yield a component about this axis.

The lacking angular mobility imposes a redundant constraint causing a non-uniform distribution of the load lengthwise of the tooth. The angular mobilities are broken down as follows: the mobility about axis $z$ in pair $A$ is spent on the motion of the mechanism; the mobility about axis $y$ in pair $D$ jointly with the linear mobility in pair $A$ (shown with a brace) define a local mobility.

Thus, in the gearing under discussion $w = 2$ and $q = 1$.

The redundant constraint present should be more properly related to constraints in the kinematic pairs and not to those in the mechanism as a whole. Non-uniform distribution of the load lengthwise

of a tooth is caused by tolerances of the helix angles of the tooth, and these angles can be manufactured with sufficient precision. With the axes crossing, herringbone teeth engage at two points, and their load-bearing capacity is higher than that of either spur or helical teeth with their single engagement spot.

## 4.5. Mechanisms with Single Idler

The solution to the problem of selecting a rational structural diagram is the simplest in gearings with an idler (Fig. 4.16) which are being introduced nowadays in double-axle electric locomotive bogies with a single-motor drive; they are also widely used in planetary gearings. In a gearing of this kind it will suffice to mount the idler on a self-aligning bearing.†

As both theoretical studies and experience have proved, with skewing of any type, the idler would self-align by rotation about two coordinate axes and practically retain the line contact of the teeth. Although the idler would turn then about the normal to the tooth surface and form a gap at the sides, this gap has been found to be so small (less than one micron) with even the greatest degree of the skewing in comparison with the compression deformation of the teeth that for every practical purpose it may be considered nonexistent.

Let us discuss the mobilities in the loops of this mechanism (Fig. 4.17). It has two independent loops which for the purpose of our discussion will be those shown in the drawing. Let us select the following coordinate axes:

The $x_1$ and $x_2$ axes extending along the normals to the teeth surface;

the $y_1$ and $y_2$ axes along the tangents to the profiles;

the $z$ axis along the axis of the gears.

Considering the linear mobilities:

no mobilities along the normals: $f'_{x1}$ and $f'_{x2} = 0$;

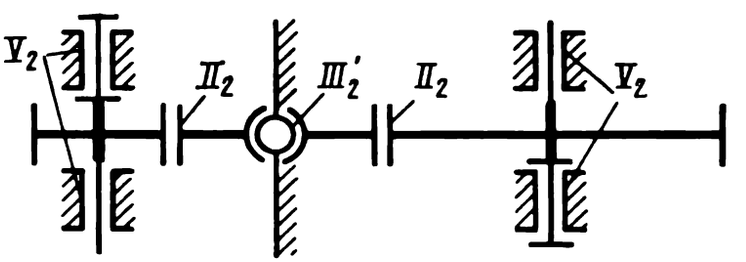


Fig. 4.16. Gearing with idler and line contact, free of redundant constraints

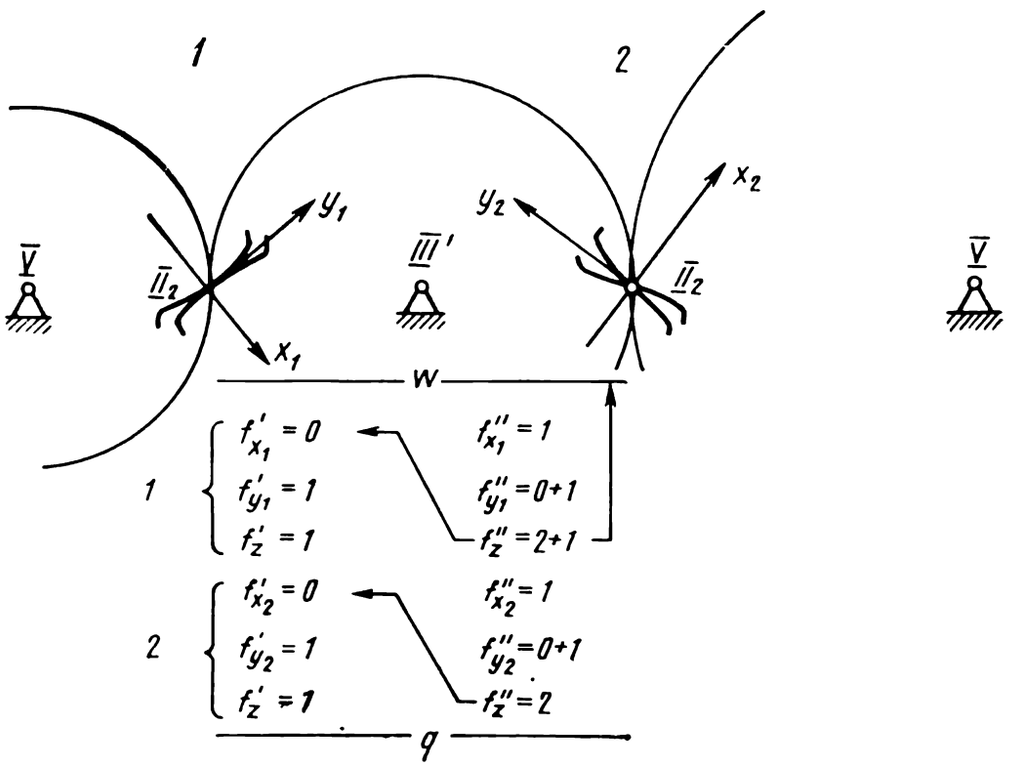


Fig. 4.17. Mobilities in loops of mechanism with idler

along the tangents—slipping of the teeth: $f'_{y1} = 1$ and $f'_{y2} = 1$;

along the $z$ axis in both loops—the longitudinal mobility in the meshing: $f'_z = 1$.

Considering the angular mobilities:

along the normal lines—twirling of the teeth: $f''_{x1} = 1$ and $f''_{x2} = 1$;

no mobility in pairs $II_2$ along the tangents. Thus, the mobilities of the spherical pair $III'$ would be spent on closing the loops, providing for self-alignment, with $f''_{y1} = 0 + 1 = 1$ and $f_{y2} = 0 + 1 = 1$.

Mobilities about $z$ axes—rotation in pairs $V$, rolling of the teeth in both meshing pairs $II_2$ and rotation in the pair $III'$ which we will relate to the first loop. Thus, for the first loop $f''_z = 2 + 1 = 3$ and for the second loop $f''_z = 2$.

Let us consider the distribution of the mobilities. In each loop one mobility $f''_z$ will be spent on replacing $f'_x$. This is possible due to the rotation of the driving and driven gears. One free mobility $f''_z$ remains in the first loop, which is the general mobility of the mechanism.

Let us now check the redundant constraints from (1.1) for a gearing with an idler; $q = 1 - 6 \times 3 + 5 \times 2 + 3 \times 1 + 2 \times 2 = 0$.

With an involute gear-tooth form system, even with the axes skewing, a line contact would be maintained with adequate accuracy.

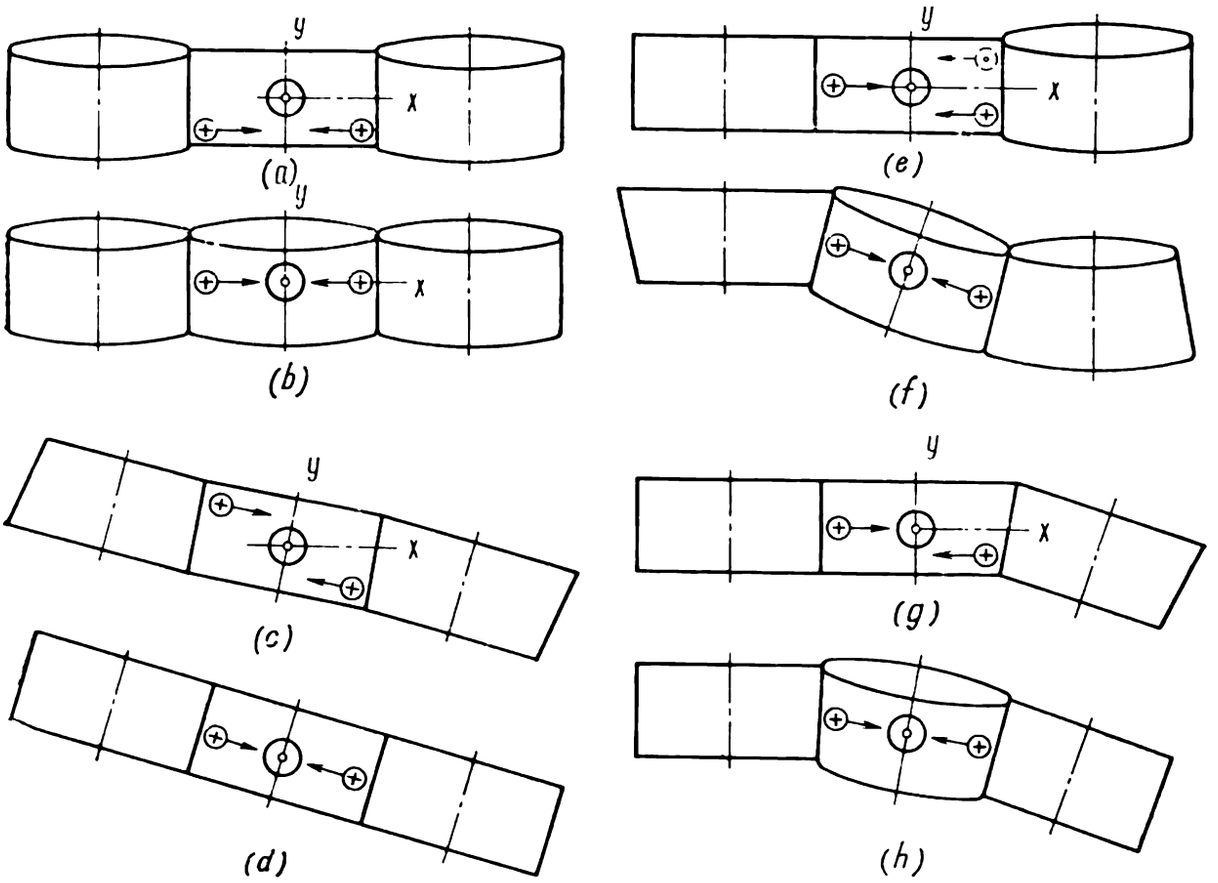


Fig. 4.18. Skewing of both axes in *yoz* plane prior to self-alignment (*a*) and upon self-alignment (*b*); of both axes in *xoy* plane prior to (*c*) and upon self-alignment (*d*); of one axis in *yoz* plane (crossing) prior to (*e*) and upon self-alignment (*f*); of one axis in *xoy* (non-parallelism) prior to (*g*) and upon self-alignment (*h*)

Let us assume the plane *xoy* of the axes to be horizontal (Fig. 4.18) and axis *z* which is parallel to the circumferential effort and perpendicular to the plane of the drawing to be vertical. Let us consider then the way the idler (Fig. 4.18*a* and *b*) is going to self-align. The forces acting upon the idler (at the bearing and the circumferential ones) are indicated with a point (the point of the arrow) or with a cross (the end of the arrow), and the radial forces applied to the teeth are indicated with arrows. The force at the bearing of the idler is twice the circumferential force. The axoidal surfaces of the gears would be cylinders, and the direction of the skewing is shown in the drawing by the shape of the end faces.

With both axes skewing in the *yoz* plane in the same direction, which is shown in Fig. 4.18*a* in an exaggerated manner, the radial forces would counterbalance and would not affect the displacement of the idler. The circumferential forces and the force at the bearing would create a moment rotating the idler about the *x* axis until the

three forces align along a single straight line and the axes of the three gears become parallel (Fig. 4.18*b*).

With both axes skewing in the *xoy* plane in the same direction (Fig. 4.18*c*), the circumferential forces join the reaction at the bearings by aligning along the same line and would not influence the displacement of the idler. The radial forces produce a moment rotating the idler around axis *z* until the forces align along a single straight line (Fig. 4.18*d*) practically at the centre of the tooth length.

Thus, with the parallelism of the axes of the driving and driven shafts retained, irrespectively of the direction and degree of their common deflection from the nominal position, the axis of the idler would extend parallel with them, irrespective of the direction of the torque being transmitted.

Line contact of the teeth with uniform distribution of the load is completely retained with the teeth skewing, e.g. on account of inaccurate positioning of the guides in the gear planer. With the parallelism broken on account of the skewing of one of the shafts in either direction, the line contact of the teeth would be likewise practically retained.

Let us consider the case of one axis skewing in the *yoz* plane (Fig. 4.18*e*). The direction of the skewing is reflected in the image of the end face of the axoidal cylinder. The radial forces create a moment rotating the idler about axis *z*, while the circumferential ones produce a moment rotating it about axis *x*. The moments set the idler to a position where the circumferential and radial forces and the reaction belong to a single plane (Fig. 4.18*f*). The forces existing between the skewed gear and the idler with the direction of the transmitted torque altering are shown with dash lines (cf. Fig. 4.18*e*). The radial forces retain their direction, but the sign of their arm alters, and the idler would self-align relative to axis *z* in the opposite direction. The circumferential forces alter their direction, and the sign of the arm of their application is also altered. Therefore, the idler would self-align relative to axis *x* in the same direction.

We have assumed above that the direction of the skewing is independent of the transmitted torque. This is true when the skewing is caused by manufacturing inaccuracies.

When the skewing is caused by either gaps or deformation of members, with the sign of the torque being transmitted reversing, the signs of the circumferential forces and the direction of the skewing in the *yoz* plane are likewise reversed. Therefore, the direction of the self-aligning of the idler about axis *z* would not change.

The case where one axis skews in the *xoy* plane is illustrated in Fig. 4.18*g* (with gross exaggeration). The radial and circumferential forces extend here similarly to the previously described case (Fig. 4.18*e*). The idler self-aligns in the same way, too (Fig. 4.18*h*). With the direction of the transmitted torque reversed, the direction of the skewing in the *xoy* plane would always remain the same. This is obvious in case of skewing caused by manufacturing inaccuracies, whereas as far as skewing on account of the gaps and deformations of members is concerned, it should be remembered that the skewing in the *xoy* plane is brought about by radial forces which do not alter their direction.

When the torque direction is reversed, the radial forces and their arms do not alter their signs, so that the direction of the rotation of the idler about axis $x$ is unaffected. The circumferential forces have their direction reversed, while their arms retain their sign, so that the rotation of the idler about axis $x$ would be reversed with the direction of the transmitted torque reversing.

Thus, in all cases of skewing of the axes the idler on a spherical support self-aligns, which ensures adequate engagement of the teeth with the resultant of the circumferential force extending practically centrally of the length of a tooth. Two pairs of teeth may work simultaneously, so that the overlap or engagement factor is retained. The above conclusions have been proved in an experimental test unit in the Baumann Higher Technical School.

Cylindrical teeth engaging with a side gap define a line kinematic pair $II_2$.This pair imposes two restraints: it restrains relative displacement along the normal and relative rotation about an axis perpendicular to the common normal and to the engagement line of the teeth. Four relative mobilities remain: two motions in the directions perpendicular to the common normal and rotations about the common normal and about the engagement line of the teeth.

The work of involute gearing is not affected by translatory motions, and so we are left with the task od determining the skewing angles only. The vector of the angular speed, as usual, will be directed along the axis of the relative rotation. With the skewing angles being small, the vectors of interest to us would define very small angles with a plane perpendicular to the axes — more often than not they are within 1° and only in exceptional cases (e.g., a unit for demonstrating the skewing pattern) they may be as great as 5°. Thus, we may assume with adequate accuracy that they extend in a plane perpendicular to the axes (Fig. 4.19). Therefore, angular speeds of rotation of the gears may be excluded from our

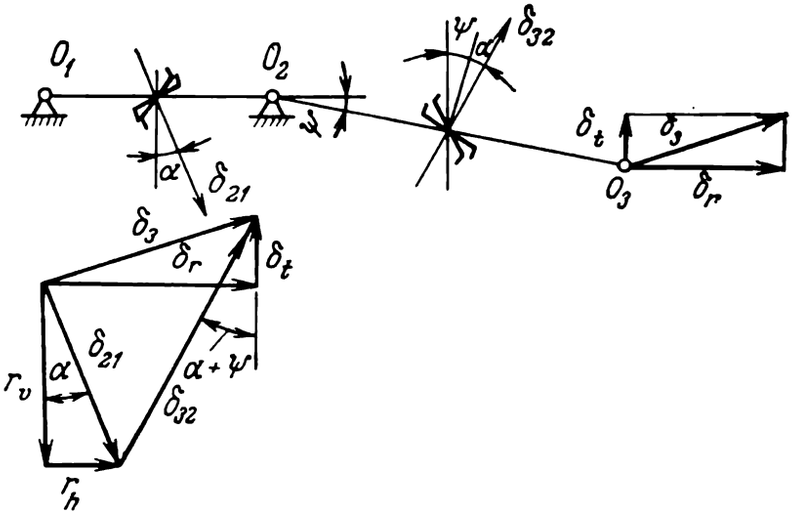


Fig. 4.19. Vectors of angular skewing in a gearing with idler

calculations. We are going to discuss but one mobility in the kinematic pairs defined by the meshing teeth—the relative rotation about the common normal to the profiles of the teeth.

The task has been thus reduced to solving a planar problem. The ratio of the angular speeds defined by a vector polygon is constant, yielding the same ratio of the angles. The skewing angle $\delta_3$ is the geometric sum of the angle $\delta_r$ of skewing about the radial axis and the angle $\delta_t$ of skewing about the tangential axis[1]:

$$\overline{\delta}_3 = \overline{\delta}_r + \overline{\delta}_t \tag{4.7}$$

On the other hand, the same angle is the sum total of the angles $\delta_{21}$ and $\delta_{32}$, i.e. of the angles of rotation of the second (idler) gear relative to the first gear and of the third gear relative to the second one. The vectors of the angles $\delta_{21}$ and $\delta_{32}$ are directed along the engagement lines. Therefore,

$$\overline{\delta}_3 = \overline{\delta}_{21} + \overline{\delta}_{32} \tag{4.8}$$

The corresponding polygon is shown in Fig. 4.19. By projecting the vector polygon upon the horizontal and vertical lines:

$$\delta_{21} \sin \alpha + \delta_{32} \sin (\alpha + \psi) = \delta_r \tag{4.9}$$

and

$$-\delta_{21} \cos \alpha + \delta_{32} \cos (\alpha + \psi) = \delta_t \tag{4.10}$$

By multiplying (4.9) by $\cos (\alpha + \psi)$ and (4.10) by $\sin (\alpha + \psi)$:

[1]The axes are taken relatively to the first gear.

$$\delta_{21} \sin \alpha \cos (\alpha + \psi) + \delta_{32} \sin (\alpha + \psi) \cos (\alpha + \psi)$$
$$= \delta_r \cos (\alpha + \psi)$$
$$-\delta_{21} \cos \alpha \sin (\alpha + \psi) + \delta_{32} \sin (\alpha + \psi) \cos (\alpha + \psi)$$
$$= \delta_t \sin (\alpha + \psi)$$

and by subtracting the last equation from the last-but-one:

$$\delta_{21} [\sin \alpha \cos (\alpha + \psi) + \cos \alpha \sin (\alpha + \psi)] = \delta_r \cos (\alpha + \psi) - \delta_t \sin (\alpha + \psi)$$

so that

$$\delta_{21} = \frac{\delta_r \cos (\alpha + \psi) - \delta_t \sin (\alpha + \psi)}{\sin (2\alpha + \psi)} \tag{4.11}$$

By multiplying (4.9) by $\cos \alpha$ and (4.10) by $\sin \alpha$

$$\delta_{21} \sin \alpha \cos \alpha + \delta_{32} \sin (\alpha + \psi) \cos \alpha = \delta_r \cos \alpha$$
$$- \delta_{21} \sin \alpha \cos \alpha + \delta_{32} \cos (\alpha + \psi) \sin \alpha = \delta_t \sin \alpha$$

By adding up the two last-mentioned equations:

$$\delta_{32} [\sin (\alpha + \psi) \cos \alpha + \cos (\alpha + \psi) \sin \alpha] = \delta_r \cos \alpha + \delta_t \sin \alpha$$

so that

$$\delta_{32} = \frac{\delta_r \cos \alpha + \delta_t \sin \alpha}{\sin (2\alpha + \psi)} \tag{4.12}$$

With the direction of the transmitted torque reversed, the sign of $\psi$ is reversed, so that expressions (4.11) and (4.12) take the following form:

$$\delta_{21} = \frac{\delta_r \cos (\alpha - \psi) - \delta_t \sin (\alpha - \psi)}{\sin (2\alpha - \psi)} \tag{4.13}$$

$$\delta_{32} = \frac{\delta_r \cos \alpha + \delta_t \sin \alpha}{\sin (2\alpha - \psi)} \tag{4.14}$$

With $\psi = 2\alpha$, $\delta_{21} = \delta_{32} = \infty$, so that there is no self-alignment [21].

Even with small values of $\psi$, self-alignment is adversely affected, as this angle increases the angles $\delta_{21}$ and $\delta_{32}$. It is solely with $\psi = 4\alpha$ that angles $\delta$ resume their values when $\psi = 0$. Thus, let us assume in the following discussion that $\psi = 0$, i.e. the line of the centres is straight. Then expressions (4.13) and (4.14) are transformed as

follows:

$$\delta_{21} = \frac{\delta_r}{2 \sin \alpha} - \frac{\delta_t}{2 \cos \alpha} \tag{4.15}$$

$$\delta_{32} = \frac{\delta_r}{2 \sin \alpha} + \frac{\delta_t}{2 \cos \alpha} \tag{4.16}$$

The angle $\delta_{21}$ is the full angle of rotation of the idler at self-alignment. It is the sum of the angle $r_h$ of rotation about the horizontal axis and the angle $r_v$ of rotation about the vertical axis:

$$r_h = \delta_{21} \sin \alpha \tag{4.17}$$

$$r_v = -\delta_{21} \cos \alpha \tag{4.18}$$

For the specific case where $\delta_t = 0$ (cf. Fig. 4.18*e*, *f*) from (4.15) and (4.16):

$$\delta_{21} = \delta_{32} = \frac{\delta_r}{2 \sin \alpha} \tag{4.19}$$

From (4.17) and (4.18):

$$r_h = \frac{\delta_r}{2} \tag{4.20}$$

i.e. with the axes projected onto a vertical plane, the idler axis divides in half the angle defined by the axes of the endmost gears:

$$r_v = \frac{\delta_r}{2 \operatorname{tg} \alpha} \tag{4.21}$$

For the specific case of $\delta_r = 0$ (cf. Fig. 4.18*g*, *h*), from (4.15) and (4.16):

$$-\delta_{21} = \delta_{32} = \frac{\delta_t}{2 \cos \alpha} \tag{4.22}$$

From (4.17) and (4.18):

$$r_h = \frac{\delta_t}{2} \operatorname{tg} \alpha \tag{4.23}$$

$$r_v = \frac{\delta_t}{2} \tag{4.24}$$

i.e. the axis of the idler divides in half the angle defined by the axes of the endmost gears, i.e. of the driving and driven ones.

In case of electric locomotive transmissions with plain bearings characterized by considerable gaps at the third gear (the hollow shaft), it would be logical to presume the skewing direction coinciding with the direction of the force between the teeth. In our representation, this means that $\delta_{32}$ is perpendicular to $\delta_3$.

Then,

$$\delta_t = -\delta_r \operatorname{tg} \alpha \tag{4.25}$$

By substitution in (4.15) and (4.16):

$$\delta_{21} = \frac{\delta_r}{\sin 2\alpha \cos \alpha} \tag{4.26}$$

$$\delta_{32} = \frac{\delta_r}{\operatorname{tg} 2\alpha \cos \alpha} \tag{4.27}$$

From (4.17) and (4.18)

$$r_h = \delta_r \frac{\operatorname{tg} \alpha}{\sin 2\alpha} \tag{4.28}$$

and

$$r_v = -\delta_r \frac{1}{\sin 2\alpha} \tag{4.29}$$

The engagement of the teeth should be calculated using the greater one of the angles $\delta_{21}$ or $\delta_{32}$ thus obtained (we will denote it below as $\delta$).

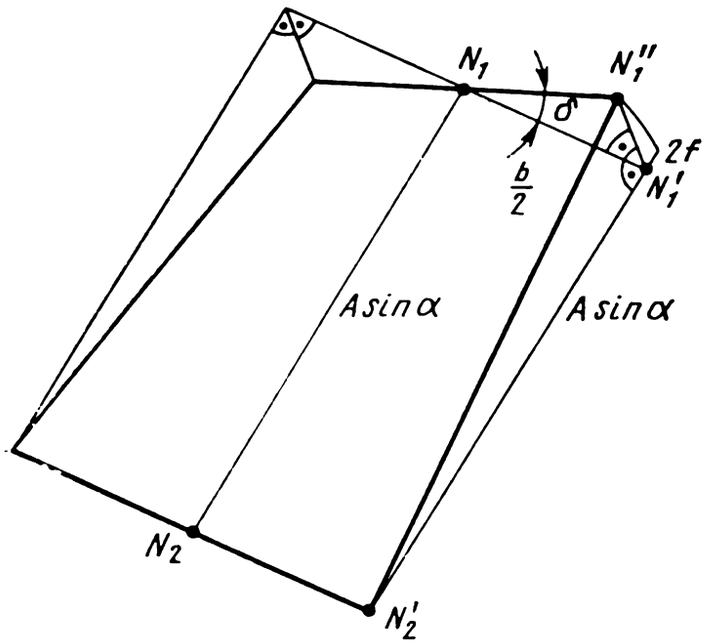


Fig. 4.20. Deformation of engagement plane with skewing at angle $\delta$ about the common normal

With the skewing angle $\delta$ about the common normal, two cylindrical teeth of the involute form work as barrel-shaped ones. Let us determine the arrow of their barrel shape. It is generally known that an involute engagement can be regarded as a strip of the length $A \sin \alpha$ running from one main cylinder onto the other one, with the engagement points $N_1$ and $N_2$ (Fig. 4.20). With the teeth skewing through an angle $\delta$, the strip becomes twisted (shown with bold lines), with its sidemost layers being extended from $N_1'N_2' = N_1N_2$

to $N_1''N_2''$. The elongation $2f = N_1''N_2'' - N_1'N_2'$ yields the gap between the teeth, and one half of this gap falls on the rise of the barrel shape of each tooth.

From the general relationships between the diameter of a circle $2(A \sin \alpha + 2f)$, the length of a semi-chord $N_1'N_1'' = \frac{b}{2}\delta$ and the rise $2f$ of the arch of this circle:

$$\frac{2f}{\frac{b}{2}\delta} = \frac{\frac{b}{2}\delta}{2(A \sin \alpha + 2f)}$$

By disregarding $2f$ (very small) in the denominator:

$$f = \frac{(b\delta)^2}{16A \sin \alpha} \tag{4.30}$$

By substituting $A = m\frac{z_1 + z_2}{2}$

$$f = \frac{(b\delta)^2}{8m(z_1 + z_2) \sin \alpha} \tag{4.31}$$

Let us consider the transformation of (4.31) for different cases of skewing. With the endmost axes crossing (cf. Fig. 4.18*e*, *f*), where $\delta_t = 0$, from (4.19):

$$\delta = \delta_{21} = \frac{\delta_r}{2 \sin \alpha}$$

Substituting this expression in (4.31):

$$f = \frac{(b\delta_r)^2}{32m(z_1 + z_2) \sin^3 \alpha} \tag{4.32}$$

With the axes skewing in their plane (Fig. 4.18*g*, *h*), and $\delta_r = 0$, from (4.22) $\delta = \delta_{32} = \frac{\delta t}{2\cos \alpha}$. Substituting in (4.31):

$$f = \frac{(b\delta_t)^2}{32m(z_1 + z_2) \sin \alpha \cos^2 \alpha} \tag{4.33}$$

With the force applied to the tooth of the third gear skewing in the plane, from (4.26) $\delta = \delta_{21} = \frac{\delta_r}{\sin 2\alpha \cos \alpha}$. By substituting in (4.31):

$$f = \frac{(b\delta_r)^2}{4m(z_1 + z_2) \sin^3 2\alpha \cos \alpha} \tag{4.34}$$

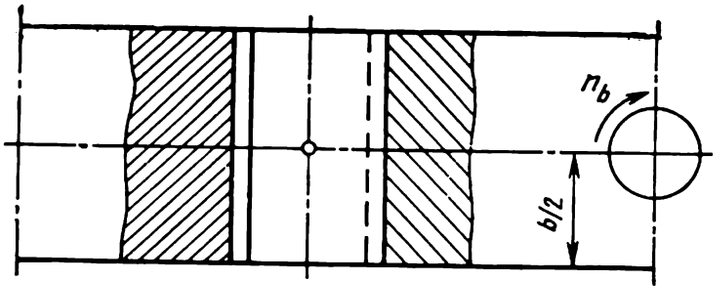


Fig. 4.21. Radial gaps with skewing idler

Let us calculate the rise of this barrel shape, using as an example the electric locomotive transmissions. Then, $z_1 = 29$, $z_2 = 43$; $m = 14$, $\alpha = 20°$ and $b = 140$ mm. The distance between the bearings of the hollow shaft (the shaft of the third gear) is 1 000 mm. The gap in the bearings (the standard one) is 3 mm. Assuming that one end of the hollow shaft abuts against the top of the bearing, while the other end against the bottom, $b\delta = 6.0 \frac{140}{1\,000} = 0.84$ mm. It is twice the value that had been taken in the exemplary calculation of the barrel-shaped tooth.

Assuming that the skewing is about the radial axis, from (4.32):

$$f = \frac{0.84^2}{32 \cdot 14\,(29+43)\sin^3 20°} = \frac{0.705}{32 \cdot 14 \cdot 72 \cdot 0.040} = 0.000\,546 \approx 0.5 \text{ micron}$$

Thus, even with the skewing as great as this, the line engagement is practically maintained. The rise is even smaller when the skewing is calculated about the tangential axis.

Then, from (4.33):

$$f = \frac{0.84^2}{4 \cdot 14 \cdot 72 \sin 20° \cos^2 20°} = 0.000\,072 \approx 0.07 \text{ micron}$$

If the skewing is taken in the plane of the force acting upon the tooth of the third gear, from (4.34):

$$f = \frac{0.84^2}{32 \cdot 14 \cdot 72 \sin^3 40° \cos 20°} = 0.000\,699 \approx 0.7 \text{ micron}$$

With the idler having rotated through $r_v$ (Fig. 4.21) at self-alignment, the radial gap is decreased by $r_v \frac{b}{2}$. By substituting $r_v$ from (4.18) and $\delta_{21}$ from (4.19) and disregarding the sign:

$$\frac{r_v b}{2} = \frac{b\delta_r}{4 \operatorname{tg} \alpha} \tag{4.35}$$

To determine the reduction of the gap along the normal, the above value has to be multiplied by 2 sin $\alpha$. Thus,

$$r_v b \sin \alpha = \frac{b\delta_r}{2} \cos \alpha \qquad (4.36)$$

$4f$ are to be subtracted from $r_v$, as two standard gaps, $2f$ each, are formed at the end face of the gear even if the standard or normal gaps are absent in the case of skewing.

For the example being discussed, from (4.35):

$$\frac{r_v b}{2} = \frac{b\delta_r}{4 \operatorname{tg} \alpha} = \frac{0.84}{4 \operatorname{tg} 29^\circ} = 0.578$$

and from (4.36):

$$r_v b \sin \alpha = \frac{b\delta_r}{2} \cos \alpha = \frac{0.84}{2} \cos 20^\circ = 0.394$$

By subtracting $4f = 0.002$ from 0.394, we have 0.392. The figures obtained prove that the required gaps are fairly small and would not limit the design engineer while designing the engagement.

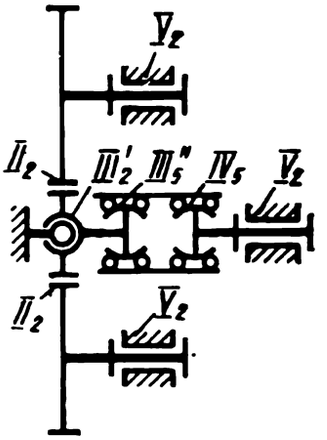


Fig. 4.22. Drive with driving intermediate gear

What is really essential is that these gaps should truly exist and not be consumed by manufacturing and assembling inaccuracies. It is also essential to ensure gaps between the idler and the casing of the reduction gear, sufficient for rotation through the angle $\delta_{21}$ at self-aligning. Unfortunately, the ability of the central gear to self-align with the line of the centres having no breaks is not retained when this gear is no longer the idler but the driving one (Fig. 4.22). In this case the normals to the surfaces of both working teeth are parallel (similar to the case when $\psi = 2\alpha$ in Fig. 4.19). To attain self-alignment, the line of the centres should include an angle $\psi$ not less than $2\alpha$.

Thus, in gearings with either an idler or a central gear used nowadays as traction transmissions of electric locomotives, same as in single-row planetary gearings, it is possible to attain line engage-

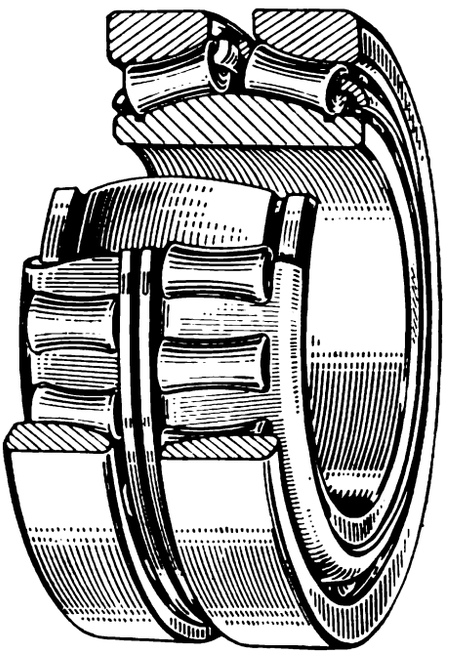

Fig. 4.23. Bearing with concave rollers and spherical surface of inner race

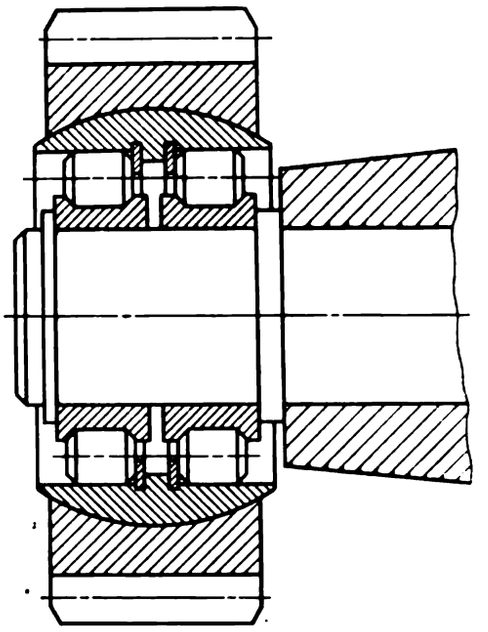

Fig. 4.24. Satellite (idler) gear with self-aligning bearing assembly, designed by D. I. Shatkus

ment with uniform distribution of the circumferential force lengthwise of a tooth. This is attained by making the idler (or satellite) self-aligning, by mounting it on a spherical bearing. With small skewing angles common-type spherical bearings may be used. With skewing angles in excess of 0.5°, friction resists self-alignment. Therefore, it is expedient to use bearings with concave rollers and the spherical surface on the inner race (Fig. 4.23), for in such bearings friction would not impair self-alignment of the idler.

Self-aligning idlers with line contact are of no use with skew and spiral-teeth gears. Barrel-shaped teeth should be used in such cases.

Bearings with cylindrical rollers can also be used as spherical bearings of self-aligning gears. Shown in Fig. 4.24 is D. I. Shatkus's bearing assembly for grain harvesters, with two roller bearings (Type 2000) having the common outer race with the spherical external surface. Two grooves are cut in the satellite gear to be mounted on this bearing for assembly purposes.

With spherical bearings, it is possible to use gears with the teeth of considerable lengths, so as to have smaller radial dimensions of reduction gears. Thus, E. L. Feldman has used gears with teeth 32.5 modulus long in a bucket-wheel excavator, and the whole reduction gear has been accommodated within the wheel.

When the transmission ratio is small, and the diameter of the satellite pinion is likewise small, the pinion may not be able to

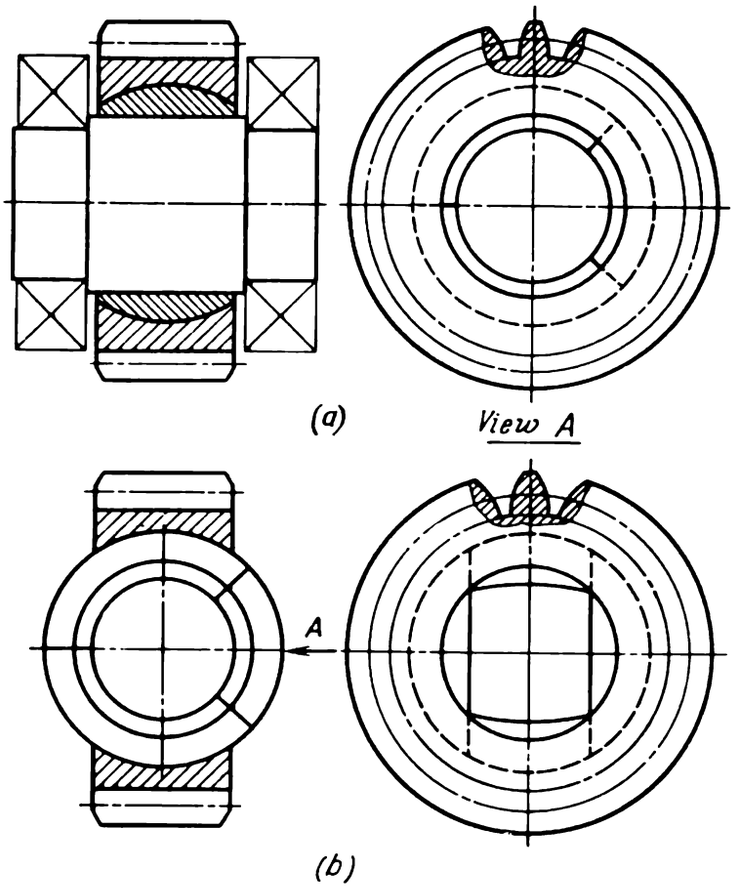


Fig. 4.25. Satellite (intermediate) gear with self-aligning bearing support, designed by V. N. Ermak

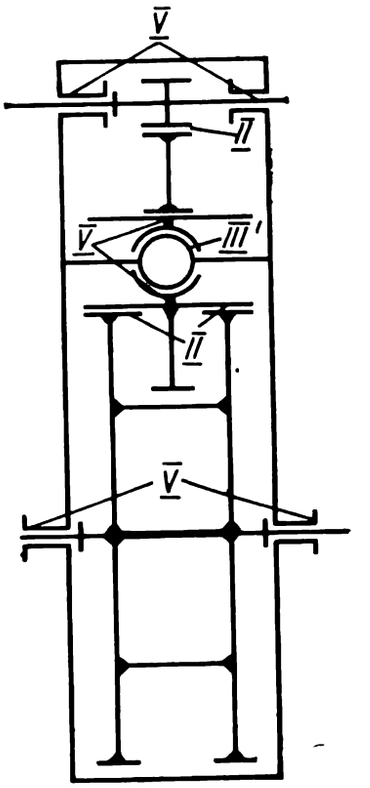


Fig. 4.26. Two-stage reduction gear with intermediate block of gears on a spherical bearing and with split low-speed stage

accommodate a spherical bearing of a sufficient capacity. To overcome this obstacle, V. N. Ermak has found a radical solution (Fig. 4.25*a*) by having the shaft of the satellite pinion supported by two bearings accommodated in the carrier, so that their diameter is not limited. The necessary angular mobilities are attained in this case by spherical connection of the toothed rim with the shaft. For assembly purposes, the sphere is made up of three segments with the central angles of 135°, 135° and 90°. The segments are turned through 90° to be inserted (Fig. 4.25*b*), and then the entire sphere is rotated into the normal position.

In a two-stage reduction gear, the block of the intermediate gears may not be mounted on a spherical bearing assembly for self-alignment purposes, lest the outward thrust forces which do not act along the same line (unlike the case with a single idler) would turn the block out, and the gears would disengage. To avoid this, the reduct-

ion gear should be symmetrical, with either the low-speed stage (Fig. 4.26) being split, or the high-speed one. The teeth of the split stage should be cut in a single pass, or else their precise matching should be ensured in some other way. Unfortunately, the strength of the shaft of the intermediate block limits the diameter of the gear of the low-speed stage and, hence, the transmission ratio. To avoid this, V. N. Ermak has suggested to split both stages, so that the spherical bearing of the intermediate block should be received between the gears. Then its dimensions are not limited, and the strength of the shaft of the intermediate block is not limited,either. It goes without saying that the requirement of precise matching or alignment of the teeth of the halves of the split stage is to be met.

## 4.6. Mechanisms with Two Intermediate Gears or Idlers

In planetary gearings, the driving and driven shafts are usually coaxial, which in most cases is the merit of such gearings. In some cases, e.g. in electric locomotives, the shafts are not coaxial, making it expedient to use a gearing with two intermediate gears (Fig. 4.27) which is equivalent to a planetary gearing with two satellite gears. In comparison with a two-side (double) transmission having the same number of gears, the said gearing has a small intermediate gear replacing the big gear stepping up the uncushioned weight of the wheel.

Furthermore, a transmission with two intermediate gears leaves a greater space for accommodation of the traction motor, which becomes of essential importance with the growth of the power ratings of electric locomotives. Quite naturally, uniform distribution of the forces among the two intermediate gears should be ensured. It should be remembered that reversing alters the ratio of the forces acting upon the intermediate gears, which complicates the task of equalizing the loads. The best solution is to level out the loads with the aid of an equalizing mechanism (cf. Fig. 4.27) providing for equality of the forces $Q$ transmitted by the teeth of these gears. Let us consider the forces acting upon the bearing supports of the intermediate gears:

$$R_1 = 2Q\sin(\beta - \alpha) \text{ and } R_2 = 2Q \sin(\beta + \alpha)$$

where $2\beta$ is the angle between the lines of the centres of the intermediate and driving gears and of the intermediate and driven gears.

The forces $R_1$ and $R_2$ are not equal. It should be pointed out that as the torque-transmitting direction is reversed (which may be either

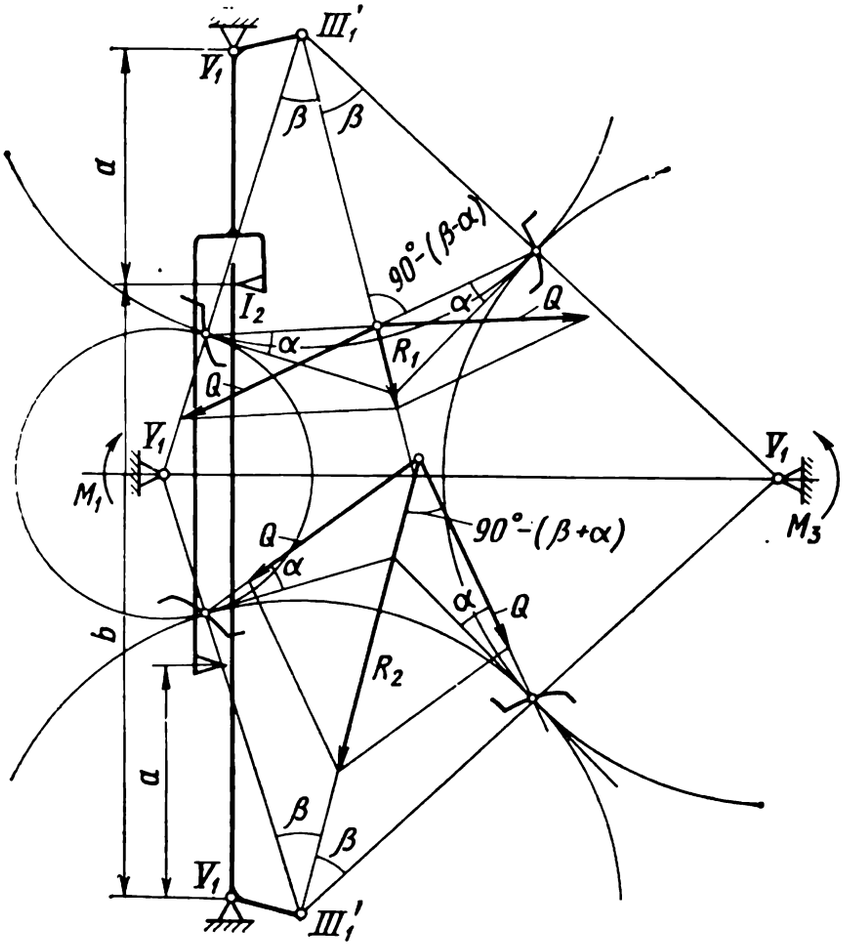


Fig. 4.27. Gearing with two intermediate gears and equalizing mecnanism

reversing of the locomotive or transition from traction to dynamic breaking), the forces $R_1$ and $R_2$ change places. Therefore, the transmission ratio of the equalizing mechanism is to be different for different directions of torque transmission. A mechanism of this kind is shown in Fig. 4.27. It has the following ratio of the arms of forces:

$$\frac{a}{b} = \frac{R_1}{R_2} = \frac{\sin(\beta - \alpha)}{\sin(\beta + \alpha)}$$

Self-alignment of the equalizing mechanism may be checked by counting the redundant constraints in (1.1) to make sure there are none: $q = 1 - 6 \times 6 + 5 \times 4 + 3 \times 2 + 2 \times 4 + 1 = 0$.

Gearings with two intermediate gears can also be used in applications where the rim of the larger gear has to have breaks in the succession of the teeth along the rim in which case the two intermediate gears ensure kinematic determinacy of the operation of the mechanism and do not reduce the forces. No equalizing mechanism may be incorporated, as this would affect the determinacy of the mot-

ion when one of the satellite gears or idlers meets the break between the teeth on the rim.

Gearings with two idlers may have any number of teeth, similar and non-similar idlers, with either normal or improved (corrugated) form of teeth and meshing. It is the spacing of the centres of the

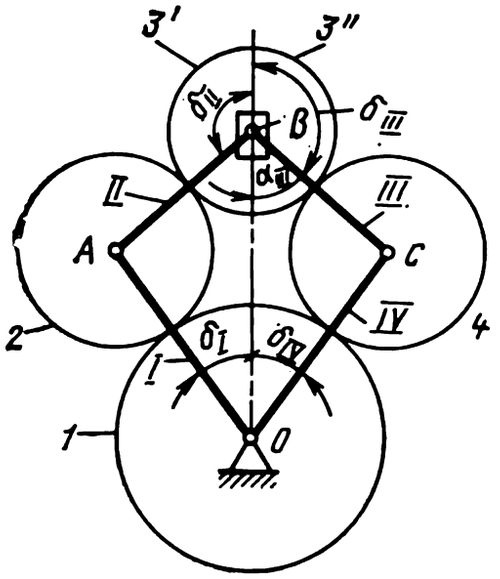


Fig. 4.28. Angles in gearing with two intermediate gears

satellite gears (or else the corresponding central angles) which are not to be selected at random and must be accurately calculated lest the assembling could become impossible. The determination of these parameters for the general case of non-similar intermediate gears is described below.

Let us consider two slider-and-crank mechanisms (Fig. 4.28) $OAB$ and $OCB$ with the slider moving vertically and pivots $O$, $A$, $B$ and $C$ at the centres of the gears. We have thus two planetary-pivotable mechanisms, one including the gears *1*, *2*, *3′* and the other including the gears *1*, *4* and *3″*. Let us assume that the common gear *1* of both mechanisms is stationary. With the slider moving, the gears 3′ and 3″ rotate in opposite directions.

Let us define the positions where the slider can be arrested and the gears 3′ and 3″ can be replaced by a single common gear. These would be the positions where the teeth of the gears 3′ and 3″ completely align, or else the sum of the angles of rotation of these gears $\delta_3' + \delta_3''$ equals an integer of the angular pitches of this gear, i.e. $k\,360°/z_3$, where $k$ is an integer.

Now we have an equation:

$$\delta_3' + \delta_3'' = k\frac{360°}{z_3} \qquad (4.37)$$

When defining the angles, we will take for the initial position of the mechanism the one where the pivots $O$, $A$, $B$ and $C$ all belong to a single vertical line, so that all the four meshing or engagement poles coincide, with the points $O$ and $B$ being below this single engagement pole, and points $A$ and $C$ being above it.

With identical intermediate gears, the initial position may be the other extreme one where the point $B$ is at the top and the engagement centres coincide in pairs.

Let us further assume that the positive direction of rotation of the crank in mechanism $OAB$ is counter-clockwise rotation, while that of mechanism $OCB$ is clockwise rotation. Let us denote the carriers of the planetary-pivotable mechanisms with Roman numerals. Their length will be found from the general theory of toothed gearings; thus, for carrier $I$ it will be:

$$l_{\mathrm{I}} = \frac{\cos \alpha}{\cos \alpha_w} m \frac{z_1 + z_2}{2} \tag{4.38}$$

Given the angle $\delta_1$, we shall find the angle of rotation of carrier II from triangle $OAB$:

$$\frac{\sin \delta_{\mathrm{II}}}{\sin \delta_{\mathrm{I}}} = \frac{l_{\mathrm{I}}}{l_{\mathrm{II}}} \tag{4.39}$$

The motion of the slider measured from point $O$:

$$S = l_{\mathrm{II}} \frac{\sin (\delta_{\mathrm{II}} - \delta_{\mathrm{I}})}{\sin \delta_{\mathrm{I}}} \tag{4.40}$$

The angles of rotation of carriers $III$ and $IV$ are found from triangle $OCB$:

$$\cos \delta_{\mathrm{III}} = -\frac{S^2 + l_{\mathrm{III}}^2 - l_{\mathrm{IV}}^2}{2 S l_{\mathrm{III}}} \tag{4.41}$$

$$\cos \delta_{\mathrm{IV}} = \frac{S^2 + l_{\mathrm{IV}}^2 - l_{\mathrm{III}}^2}{2 S l_{\mathrm{IV}}} \tag{4.42}$$

The checking formula is:

$$\frac{\sin \delta_{\mathrm{III}}}{\sin \delta_{\mathrm{IV}}} = \frac{l_{\mathrm{IV}}}{l_{\mathrm{III}}} \tag{4.43}$$

The angles of rotation of the gears can be found from the Willis formula where the angular velocity will be replaced by the angles of rotation proportional to them.

Thus, for the members *1*, *2* and *I*:

$$\frac{\delta_2 - \delta_{\mathrm{I}}}{\delta_1 - \delta_{\mathrm{I}}} = -\frac{z_1}{z_2}, \quad \text{but } \delta_1 = 0$$

Therefore,

$$\delta_2 = \delta_I \left(1 + \frac{z_1}{z_2}\right) \tag{4.44}$$

For the members *3'*, *2* and *II*:

$$\frac{\delta_3' - \delta_{II}}{\delta_2 - \delta_{II}} = -\frac{z_2}{z_3}$$

from which

$$\delta_3' = -\delta_2 \frac{z_2}{z_3} + \delta_{II}\left(1 + \frac{z_2}{z_3}\right) \tag{4.45}$$

Substituting $\delta_2$ from (4.44) into (4.45):

$$\delta_3' = -\delta_1 \frac{z_1 + z_2}{z_3} + \delta_{II} \frac{z_2 + z_3}{z_3} \tag{4.46}$$

Similarly:

$$\delta_3'' = -\delta_{IV} \frac{z_1 + z_4}{z_3} + \delta_{III} \frac{z_4 + z_3}{z_3} \tag{4.47}$$

By giving various values of $\delta_1$, angles $\delta_3'$ and $\delta_3''$ may be found from (4.39), (4.41), (4.42), (4.46) and (4.47), and the value of the angle $\delta_1$ satisfying (4.37) can be found by trial and error.

Naturally, care should be taken that the following conditions should be also met (cf. Fig. 4.28):

$$S > \frac{D_{e1} + D_{e3}}{2} \tag{4.48}$$

$$AC > \frac{D_{e2} + D_{e4}}{2} \tag{4.49}$$

where $D_{e1}$, $D_{e2}$, $D_{e3}$ and $D_{e4}$ are the external diameters of the gears.

The task is much simpler when the two intermediate gears are identical, i.e. when $z_2 = z_4$. In this case, because of the symmetry of the mechanism $\delta_3' = \delta_3''$, and from (4.37):

$$\delta_3' = \delta_3'' = k \frac{180°}{z_3} \tag{4.50}$$

The angle $\delta_{II}$ can be determined from (4.39), and the angle $\delta_3'$ can be found from (4.46), and then the value $\delta_1$ is selected to satisfy equation (4.50).

The conditions of assembling a gearing with two idlers, the kinematics and possible errors have been investigated by V.N. Ermak [12].†

## 4.7. Gearing in Load Handling Machines

An interesting case is presented by the crowding gear of excavators. The rack-and-pinion mechanism incorporated in this gear of big machines rapidly wears out on account of high thrust values. To reduce these values, in gantry cranes (in the outreach varying mechanism) a twin rack-and-pinion mechanism is used with an equalizing lever between the racks, although the two racks and equalizing levers significantly increase the weight. One rack may suffice, however (Fig. 4.29), engaged with two pinions, providing an equalizing mechanism to ensure uniform distribution of the efforts among the pinions, based on equalizing the axial effort of helical gears. The thrust pinions should be straight-tooth ones. All the large gears should have the same direction of the helix (e.g. the r.h. direction), while the driving and intermediate gears should have the opposite direction of the helix. The drive effort may be taken either off the central intermediate gear or from the sidemost one.

The mechanism can also serve for driving several thrust gears, with the leverage becoming more complicated. With two gears, it may have two levers connected by a rod. By selecting properly the helix angle, the axial effort transmitted by the mechanism can be limited, while the arrangement of the arm may ensure that the rod works in tension.

The mechanism becomes considerably simpler when the drive makes use of bevel gears (cf. Fig. 4.29*b*). It may do without a leverage altogether, as the equalizing is attained by the axial displacement of the block of the driving bevel gears. The provision for such displacement should be made, though, either by mounting a corres-

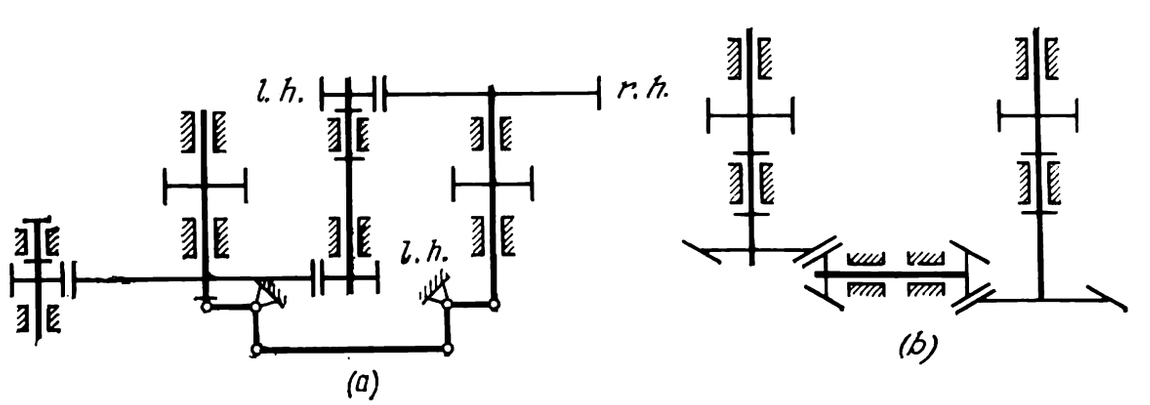


Fig. 4.29. Mechanisms for equalizing the loads of two thrust gears
(*a*) using axial effort of skew gears; (*b*) using axial effort of bevel gears

ponding coupling on the driving shaft, or else, which is even better, by using a spur gearing so that friction would not distort the forces. It is worth mentioning that equalizing mechanisms based on the axial efforts of bevel gears have convincingly proved their merits in aircraft reduction gears.

The above mechanisms can be used in cases where the torque derived from a single prime mover is to be transmitted through either two or more gears, e.g. in crane slewing mechanisms or in transmissions of electric locomotives. The last stage of the slewing mechanism is designed as a gearing where the great gear is either internal or external. In large machines, the efforts in this mechanism are huge, the load applied to a running centimetre of the length of a tooth being very high. The huge efforts cause skewing of the gears, so that the wear of their teeth is drastically accelerated. The skewing is particularly pronounced with the gear being mounted in a cantilever fashion, and with internal meshing this fashion of mounting is practically inavoidable. In crane mechanisms the skewing is exceptionally great, being caused not only by the efforts applied to the teeth, but also by external forces which are of a significantly higher value, e.g. the efforts of the ropes in the winches. The situation with a slewing mechanism is even worse as the casing of the reduction gear is specifically deformed by the external gear with its cantilever mounting. Therefore, the performance may be essentially enhanced by making the gear self-aligning to ensure line engagement with uniform distribution of the load lengthwise of the tooth. The best solution is to use an arch-shaped tooth, although the impossibility of employing it with internal meshing and the lack of big tooth-cutting machines curbs down its broad application.

With machines of the highest duties, it is expedient to employ a mechanism with two intermediate gears and an equalizing device (cf. Fig. 4.27 and refer to p. 304), with the intermediate gears or idlers mounted on spherical bearings. To make self-alignment possible, the break angle of the line of the centres should not equal $2\alpha$. In case of a crowding gear the equalizing mechanism is significantly simplified owing to the effort being transmitted practically in one direction only. With the power being divided into two paths, the load on a running centimetre of a tooth is reduced by one half, and, which is even more important, uniform distribution of the load lengthwise of the tooth is provided. The entire mechanism becomes simpler, less costly and more compact than its counterpart with two racks and an equalizing lever between them (to say nothing of the line contact of the teeth not being ensured).

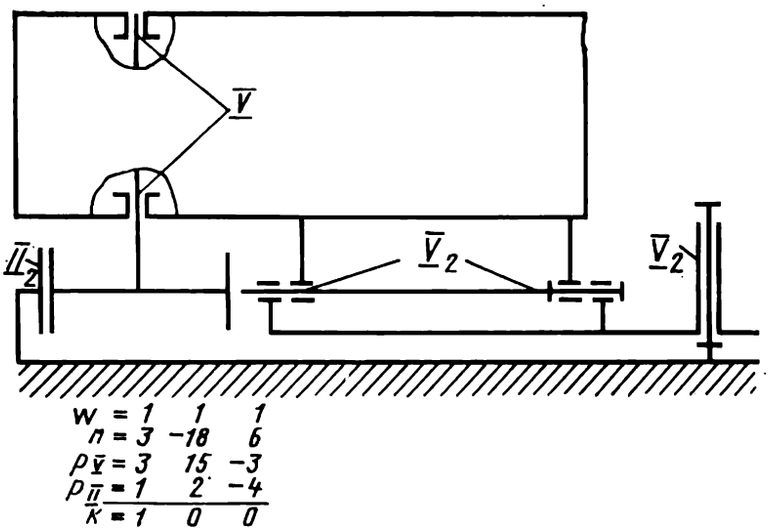


Fig. 4.30. Last drive stage of crane slewing mechanism (self-alignment attained by mobility of engine block and reduction gear about horizontal axis passing through central plane of the gear)

In comparatively smaller machines a gearing with one idler may be recommended. The mechanism becomes simpler, but the running load of the teeth grows. In machines of a contemporary design the drive is usually electric, and the motor and reduction gear are structurally united in a single module—a geared motor. Then the double universal joint of Fig. 4.12 is no longer needed. The geared motor is preferably connected with the framework of the excavator by a horizontal pivot whose axis intersects the line of a tooth at the centre. This design of a slewing mechanism with internal engagement is shown in Fig. 4.30. The distance between the centres is adjustable here by adding or removing spacers in this pivotal joint.

The assembling of the horizontal pivot may be complicated if it is situated under the platform. The remedy may be to replace the rotary pair by a spherical one $III_4'$ and two land ones $I_4$ which impose the same five restraints. A design of this kind for a slewing gear with internal meshing is shown in Fig. 4.31.

The entire mounting of the geared motor may be placed at the top (Fig. 4.32) by employing the instant rotation centre (axis) $P$ which replaces the horizontal pivot and is located at the point of intersection of the arms $III_4'$ $III_4'$ and $V_2V_2$. In this case, however, the arm $V_2V_2$ should be a rigid frame connected by rotary pairs both to the platform and the geared motor. If compared with the КБ 100.1 crane where the mounting is effected with a pivot and a rod, the proposed mechanism has a single extra joint, but self-alignment and line engagement of the teeth are ensured.

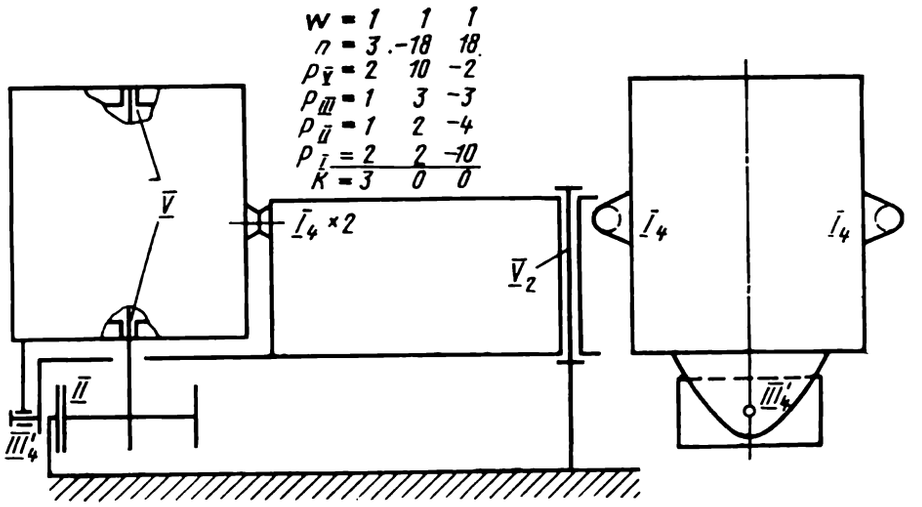


Fig. 4.31. Last stage of crane slewing mechanism drive (self-alignment attained by mobility about a horizontal axis, provided by one spherical pair and two point pairs)

In mechanisms with a planetary reduction gear self-alignment of the gear of the last stage can be attained by utilizing the mobility of the planetary gearing. In the КБ 100.1 crane, for instance, the gear is supported by two ball bearings mounted internally of the gear. To

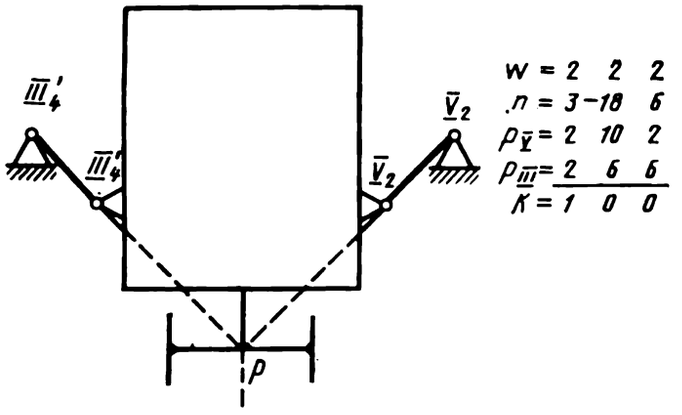


Fig. 4.32. Last stage of crane slewing gear drive (self-alignment attained by suspending the motor and reduction gear unit on two arms)

eliminate the redundant constraints, they should be replaced by a single spherical roller bearing arranged at the central plane of the gear (Fig. 4.33). The satellite gears should be likewise supported by spherical bearings. As the mechanism is a three-stage one, it would be expedient to include a spherical bearing between the first and second connecting members, to bring down the number of local mobilities. One local mobility would remain, however: rotation of the last stage gear about an axis perpendicular to the plane of the drawing. It is harmless, for experience proves that mobilities of this kind are well damped by the friction in the teeth and would never cause resonance vibration.

The next, and more simple, solution is to mount the gear on a toothed universal joint with limiter rings $IV_5$ (Fig. 4.34). The remaining local mobility is the same as in the design of Fig. 4.33 and is

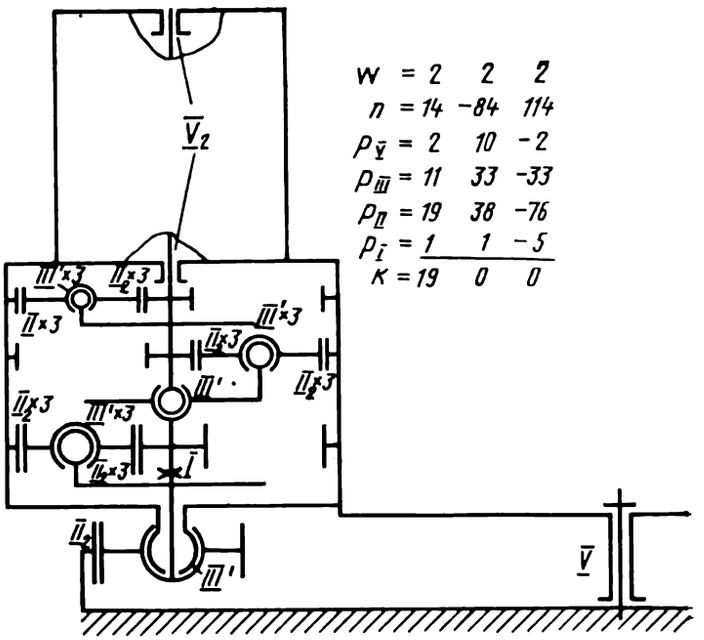


Fig. 4.33. Last stage of crane slewing gear drive (self-alignment attained owing to mobilities of planetary reduction gear with spherical pairs)

harmless. It may happen in this case that the diameter of the gear has to be increased to accommodate the universal joint, which, in its turn, would require a greater transmission ratio of the reduction gear.

Finally, redundant constraints may be avoided by using a gear with barrel-shaped teeth (Fig. 4.35). Then, however, the engagement of the teeth changes from line to point, and the contact stresses

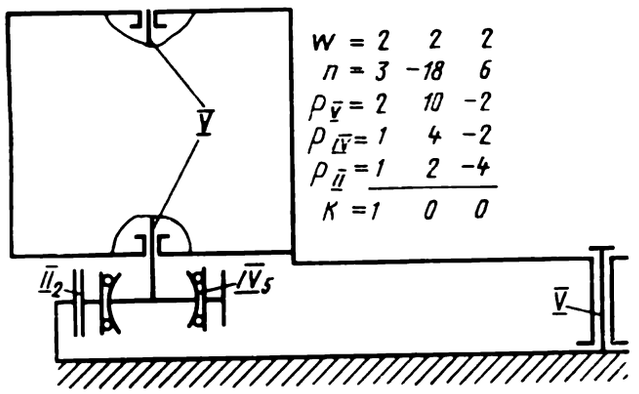


Fig. 4.34. Last stage of crane slewing gear drive (self-alignment attained by mounting the gear on a toothed universal joint)

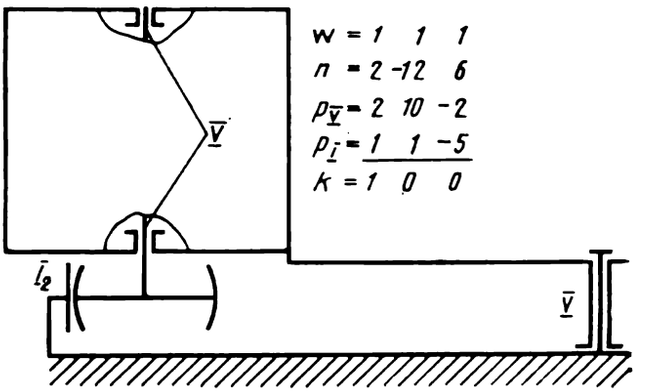


Fig. 4.35. Last stage of crane slewing mechanism drive (redundant constraint eliminated by using barrel-shaped tooth)

would grow. Thus, although this structure of a reduction gear is the simplest, it may be recommended solely for machines with lighter duties.

## 4.8. Classification of Traction Drives

The higher speeds of our days have called for new designs of traction drives. However, the terminology still in use for description of these new drives is sometimes obsolete, incidental and altogether incorrect. Thus, in the expression "frame-support suspension" the word "support" is devoid of meaning and merely obscures the issue. The expression "independent suspension" is even worse, for it contradicts its commonly accepted meaning in the domain of automotive vehicles where independently suspended wheels are not connected by an axle and may oscillate on their suspension springs truly independently.

A.A. Shatsillo [51] has classified traction drives into four groups. Unfortunately, the numbering of the groups is conventional and would not reflect the essence of the drives. The terminology that is suggested below corresponds to the physical essence of every case under consideration, care being taken of adequate brevity, too. A traction drive includes a motor, a reduction gear and a transmission mechanism (universal joints, Alstom mechanisms and others—see Section 3.9 above). Thus, it is logical that the first part of a term should refer to the type of suspension of the motor, the other part, to that of the reduction gear, and the third part should concern the transmission mechanism. If in the motor suspension all the six restraints are transmitted to the frame, it is logical to call this suspension the frame type. We understand here under "a restraint" the limited displacement: either linear along a given coordinate axis or rotational about a given coordinate axis, as it is understood in the theory of mechanisms.

When, in the suspension of a motor, five restraints are transmitted to the axle and only one is transmitted to the frame (the tram type), i.e. the axle dominates, this suspension should be called the axle type. The same terminology is suggested for the suspension of the reduction gear.

Thus, it is suggested to call the drives with the axle suspension of both the motor and reduction gear "the axle drives"; those with the frame suspension of the motor and the axle suspension of the reduction gear "the frame-axle drives"; and those with the frame suspension of both the motor and reduction gear "the frame drives".

The suggested terminology obviates the need to explain the location of the transmission mechanism, as with the frame-axle suspension it is to be between the motor and the reduction gear, whereas with the frame suspension its place is between the reduction gear and the axle.

Let us now deal with the third part of a term—the classification of the transmission mechanism. The frame-axle drives generally differ in the length of the universal joint or cardan shaft which may be short, with both joints arranged between the motor and the reduction gear (Д and ЭР motor coaches), or else medium-long with one joint received within the motor armature (ЧС-2, ЧС-3 and ЧС-4 electric locomotives), or long with one joint arranged beyond the motor (designs of Brown-Bovery, Secheron, ЧС-1).

In the frame drives a cardan shaft transmission has been employed only in the Jackman drive where it is situated between the wheels

*Table 4.1*

| Drive System | Shatsillo's Group | Arrangement | Suggested Term |
|---|---|---|---|
| Tram | — | Axle suspension of motor and reduction gear | Axle |
| Д and ЭР motor coaches | II | Frame suspension of motor, axle suspension of reduction gear, short cardan shaft | Frame-axle with short cardan shaft |
| ЧС-2 to ЧС-4 electric locomotives | II | Frame suspension of motor, axle suspension of reduction gear, medium-long cardan shaft | Frame-axle with medium-long cardan shaft |
| Brown-Bovery, Secheron, ЧС-1 electric locomotives | II | Frame suspension of motor, axle suspension of reduction gear, long cardan shaft | Frame-axle with long cardan shaft |
| Jackman | III | Frame suspension of both motor and reduction gear with idler and cardan-joint transmission | Frame with idler and cardan-joint transmission |
| Alstom | IV | Frame suspension of both motor and reduction gear with twin articulated Alstom transmission | Frame with Alstom transmission |

(medium-long cardan shaft). Ganz drives with the external reduction gear—both with the short cardan shaft and with the hollow axle accommodating the long cardan shaft inside—have not been widely used. Therefore, it would be improper to classify the frame drives by the length of the cardan shaft. It is logical to classify the third part of the term according to the system of the transmission mechanism, or, even better, by its kinematics (when it is possible).

The suggested terminology enables one to make required refinements by appropriate additions, e.g. "with idler", "with bevel gearing and vertical motor", etc. To make this terminology better understood, it is applied in Table 4.1 to commonly known drive types.

## 4.9. Rational Designs of Traction Reduction Gears

The use of self-aligning idlers, i.e. intermediate gears on spherical bearing supports (see, for example, the design described on p. 299) makes it possible to have line contact of the teeth even with the gears skewing to a considerable degree. This, in turn, enables us to use wider gears (i.e. longer teeth), with the increased load-carrying capacity and durability of the transmission.

However, the power ratings of axles have been steadily growing: while in the advent of electric traction the power per single axle was 300-400 kW, now it is usually 700-800 kW. This calls for finding new ways of stepping up the load-carrying capacity of toothed gearings. It is commonly known, for example, that planetary gearings are capable of transmitting a load which is several times that of gearings with stationary axes of the same dimensions. This is explained by the fact that the load is transmitted via several satellite gears.

A planetary gearing is hardly incorporable in an electric locomotive as it would require co-axiality of the driving and driven shafts. To provide for this, the armature shaft has to be hollow and arranged coaxially with the axis of the wheel pair. In operation, such a motor would call for repeated detachment of the wheel pair for maintenance and repairs (e.g. replacement of the armature bearings). This shortcoming is non-existent in gearings with intermediate gears, while parallel transmission of power via two, three or even four intermediate gears would permit increasing the load-carrying capacity.

With alternating current, drive systems where a single motor drives two or three axles found use, because one motor is lighter, less costly

in manufacture and maintenance, of a higher efficiency and requires smaller space than two motors of half the power rating. Direct-current systems required several motors in an electric locomotive, as the travelling speeds were selected by combinations of their switching. It is not so with alternating-current drives where the speed is con-

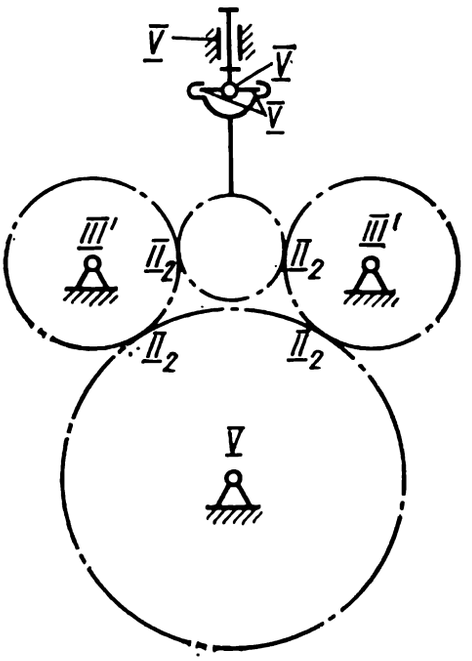


Fig. 4.36. Individual drive with two idlers and floating pinion

trolled with a staged transformer. Therefore, we are going to discuss several cases: one motor per axle (individual drive), one motor per two axles, one motor per three axles and two motors per three axles.

The number of gears and the circumferential forces will be compared with an individual drive with a single-path transmission.

**Individual drive** (one motor per axle). In case of two intermediate gears, an equalizing mechanism would be required to balance the circumferential forces transmitted by these gears (cf. Fig. 4.27).

Equalizing, however, may be attained by using another principle (Fig. 4.36), i.e. by having a floating pinion connected to the armature through a single universal joint. (In Fig. 4.36 and in subsequent drawings the pinion shaft is conventionally turned through 90° to belong to the plane of the drawing.) Furthermore, the dimensions of the intermediate gears should be such that their centres and that of the pinion belong to a single straight line. The teeth number of the intermediate gear (the idler) is found from the expression

$$z_i = \frac{z_g + z_p}{z_g - z_p}(z_p + 3)$$

The arrangement of the cardan shaft is similar to the mechanism of ЧС-1, ЧС-2, ЧС-3 and ЧС-4 electric locomotives, the difference

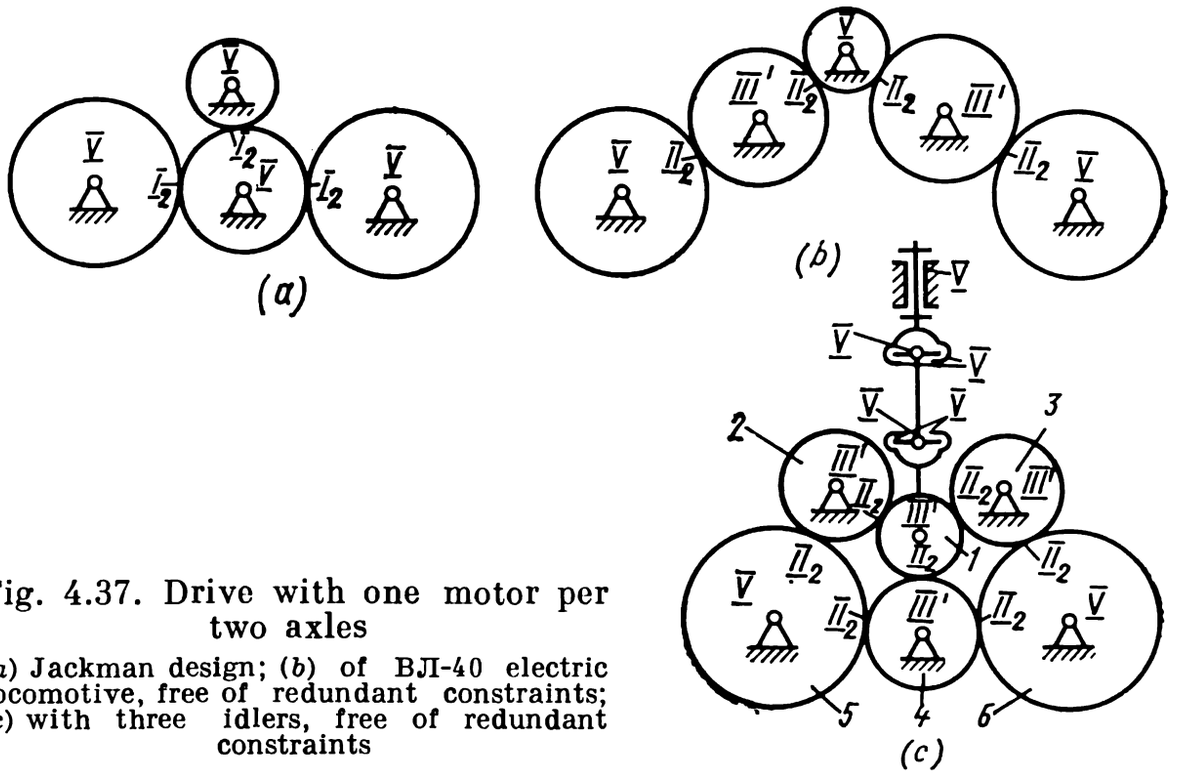


Fig. 4.37. Drive with one motor per two axles

(*a*) Jackman design; (*b*) of ВЛ-40 electric locomotive, free of redundant constraints; (*c*) with three idlers, free of redundant constraints

being in the single universal joint instead of two and in the addition of two idlers. The mechanism has one extra mobility: displacement of the pinion between the idlers within the radial gaps. One should not worry about it as the friction between the teeth precludes oscillation. The circumferential force is one half of that of a drive with a single-path transmission.

However, the dimensions of the bottom idler make this design practical only when the armature axis is somewhat above that of the wheel. To eliminate this drawback, V.N. Ermak has suggested to provide the floating pinion with two abutments working alternatingly depending on the direction of the torque being transmitted.

**Drive with one motor per two axles.** An example is the Jackman drive (Fig. 4.37*a*) used by Gemont, France, in high-speed locomotives. The idler here is not self-aligning, so that barrel-shaped teeth with point engagement had to be used, although this affected the load capacity. The load applied to the pinion tooth is twice that of a single-path transmission, while the load of other teeth is as in a one-side transmission.

Fig. 4.37*b* illustrates the drive of ВЛ-40 electric locomotive, incorporating self-aligning idlers. This enables one to use very long teeth with line engagement and thus to have a great load capacity. The load of each tooth here is equal to that in a one-side transmission and is one half of that of the Jackman drive. The load applied to the

tooth may be reduced even further by having three idlers positioned at similar angles about the driving pinion (Fig. 4.37*c*)†, the latter being the floating one and connected to the armature shaft through a double universal joint. The height of the motor shaft is selected by using the idlers with different teeth numbers.

Naturally, for the idlers to mesh with the pinion and the gear (and not to creep upon their teeth), the numbers of their teeth are to be selected by appropriate calculation (refer to Section 4.6 above).

In this mechanism there is one extra mobility, although it is harmless as friction between the teeth precludes the appearance of an oscillation process. The teeth load is 1.5 times less here than with a one-side transmission and is one third of that of the Jackman drive. The load of the teeth of the bottom idler meshing with the driven gears is even less (one half).

**Drive with one motor per three axles.** With the motor arranged above the central axle (Fig. 4.38*a*), the latter has to be driven through an idler, otherwise a high-power motor would not be accommodated. Each end axle is driven through three idlers. Out of these, two should be mounted on rotary pairs (*V*) and five on spherical pairs (*III'*). The engagement of all the teeth is the line one, so the teeth may be very long. The load of one tooth equals that of the single-path transmission, and the total number of gears is 11, approaching that of a double-side gearing. However, one motor is used here instead of three, the work of the teeth is not affected by skewing, and the gears are smaller than those in a one-side transmission.

With the motor situated between the axles (Fig. 4.38*b*), its pinion should be floating and connected to the armature shaft through a single universal joint. The three idlers on spherical bearings should be uniformly spaced about the motor pinion, one of them driving the endmost axle and the other two driving the central one. The other endmost axle is driven from the central axle through an idler on a spherical bearing.

Same as in the design of Fig. 4.37*c* the height of the motor is changed by varying the dimensions of the idlers. The teeth load equals that of a one-side transmission of an individual drive. The number of gears is eight, i.e. close to that of a one-side gearing. Besides, in this design there is but one motor per three axles, and the work of the teeth is unaffected by skewing.

Therefore, there are all reasons to believe that both designs with the three axles driven from a single motor are promising. In the last-described design the torques transmitted to the three axles are the same. However, with the uneven wear of the wheel tyres and resulting

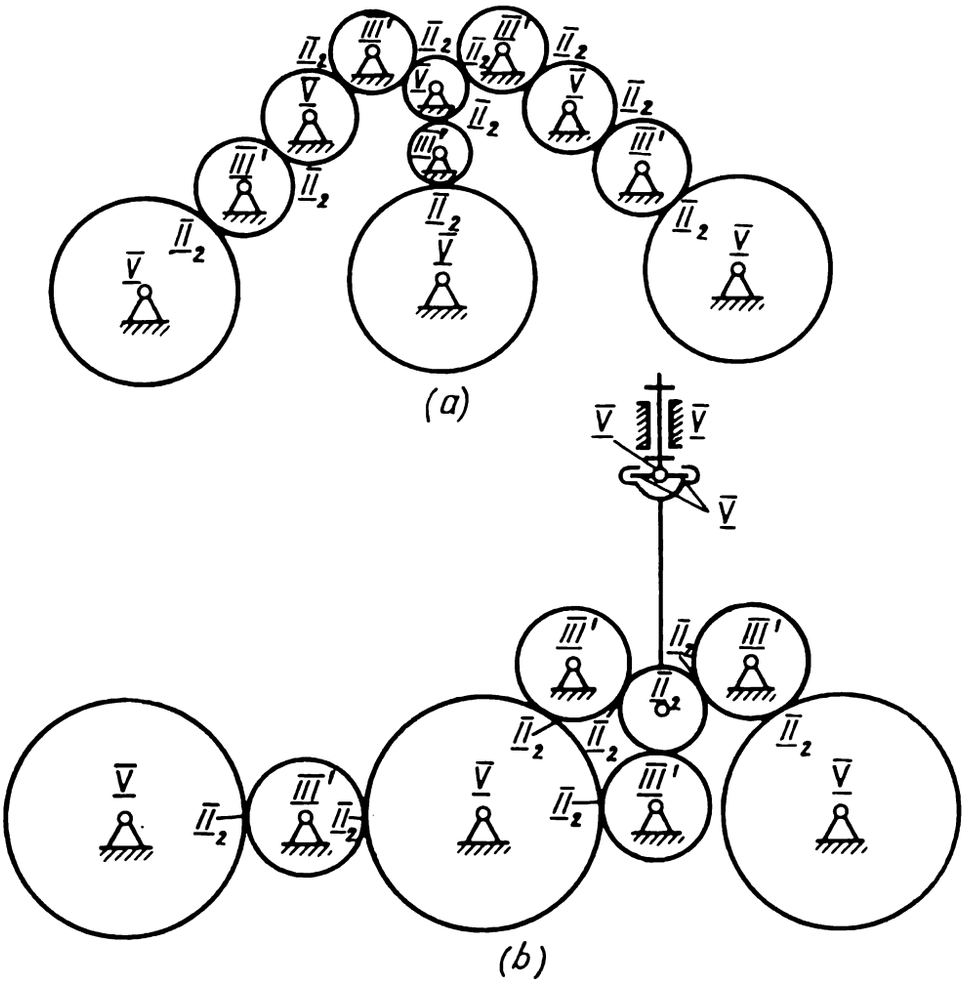


Fig. 4.38. Drive with one motor per three axles
(*a*) with motor overlying the central axle; (*b*) with motor between the axles and three idlers

slipping, the torques at the axles would differ. So that it would not affect the drive operation, firstly, the motor pinion may be provided with abutments limiting its displacement. The abutments are preferably in the form of cylinders of a radius equalling that of the polloid circle, mounted on the motor pinion and onto the three idlers surrounding it. Secondly, the bottom idler may engage both greater gears (Fig. 4.37*c*), although in this case the motor pinion has to be connected to the armature not by a single universal joint, but by a double one. Thirdly, the bottom idler may mesh with the second large gear with a lateral gap, so that this meshing would not oppose self-alignment in normal operation and would be engaged in operation only when slipping occurs.

**Drive with two motors per three axles.** A three-axle bogie may require two motors when a single motor of the required power would

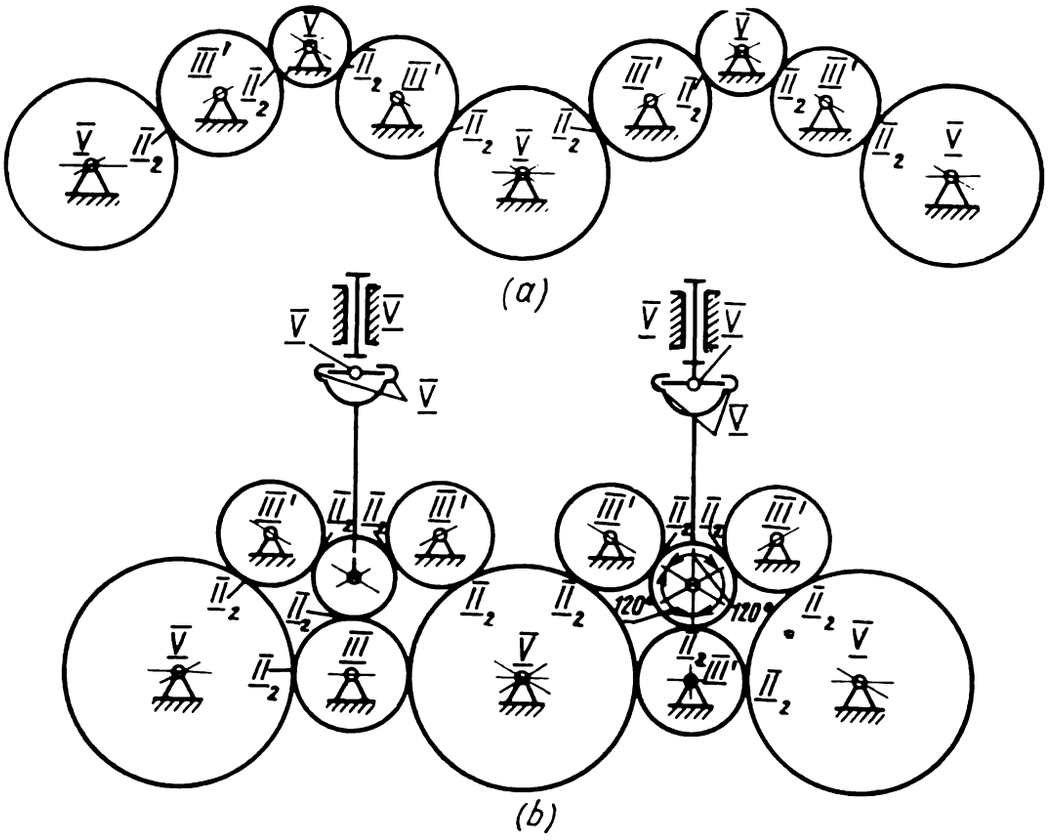


Fig. 4.39. **Drive** with two motors per three axles
(*a*) with big bogie wheelbase; (*b*) with three idlers

not be accommodated. With two motors, the centre of the bogie is cleared to accommodate the king pin, which simplifies the structure of the bogie. Moreover, the conditions of arranging the gearings are better.

With a big wheelbase of the bogie, the drive of Fig. 4.39*a* may be recommended. The shafts of the motor pinions are journalled in rotary pairs, while the idlers are supported by spherical bearings. The teeth load in the transmissions to the endmost axles equals that of a one-side gearing, while the load in the transmission to the central axle is twice as small, i.e. it is the same as in a double-side gearing. The number of the gears should be nine.

A small wheelbase requires the drive of Fig. 4.39*b*. The motor pinions here are floating and connected to the armature shafts through single universal joints, each motor pinion being engaged by three idlers on spherical bearings. Two idlers mesh with each one of the large gears. For the performance of the drive not to be affected by slipping, the same remedies may be recommended as in the case of a single motor per three axles.

The teeth load of each gear is equal here, being one half of that of a one-side transmission. The gear number is 11, i.e. it is even less than with a double-side transmission, while the gear dimensions are considerably smaller. Besides, the work of the teeth is unaffected by skewing, which makes the last-described design particularly attractive.

## 4.10. High-Speed Traction Drive

When a train travels at a high speed, the vertical acceleration of a wheel pair may be very high. In winter, with the frozen upper structure of the track, it may be as high as 50 g. Thus, it is of essential importance to design the drive so that this acceleration should not cause additional dynamic loading of the gears and the motor armature, i.e. appropriate mobility should be afforded. Let us make use of the theorem of additional tangential accelerations and construct its proof. Assuming that point $A$ of a mechanism moving at speed $v_A$ acquires an additional tangential acceleration $a_{Aa}$. Then, in $dt$ time the point $A$ will have the speed $v_A + dv_A$. Correspondingly another point $B$ of the same mechanism will travel at $v_B + dv_B$. Then

$$\frac{v_B+dv_B}{v_A+dv_A}=\frac{v_B}{v_A}, \quad \text{or} \quad \frac{v_B+dv_B}{v_B}=\frac{v_A+dv_A}{v_A}$$

Taking the ratios of the differences of the preceding and successive members of the proportion to the respective successive members:

$$\frac{dv_B}{v_B}=\frac{dv_A}{v_A} \quad \text{or} \quad \frac{dv_B}{dv_A}=\frac{v_B}{v_A}$$

By multiplying the numerator and denominator of the l.h. expression by $dt$

$$\frac{dv_B}{dt}\frac{dt}{dv_A}=\frac{v_B}{v_A} \quad \text{or} \quad \frac{a_{Bd}}{a_{Aa}}=\frac{v_B}{v_A}$$

i.e. the additional tangential accelerations of the points of a mechanism are proportional to their absolute velocities.

Since within an infinitesimal period of time the displacement of a point is proportional to its speed, it may be presumed that the additional tangential accelerations of the mechanism points are proportional to their absolute displacements. In case of a traction-drive this means that vertical translational displacements of a wheel pair (owing to the play of the suspension springs) would not cause

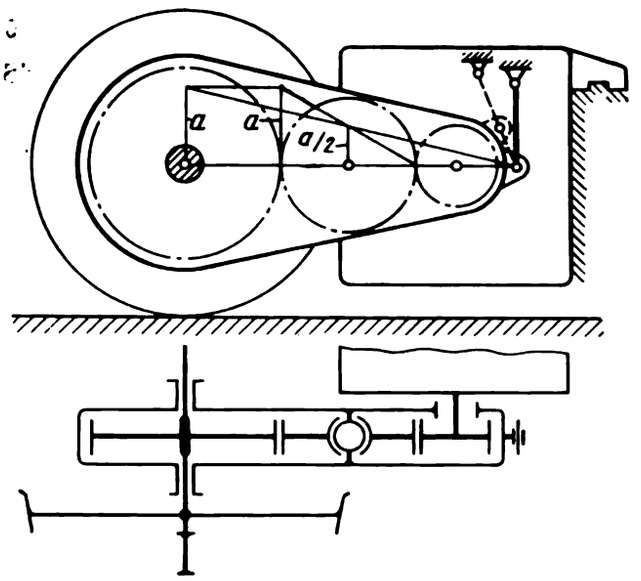


Fig. 4.40. High-speed drive with straight line of centres

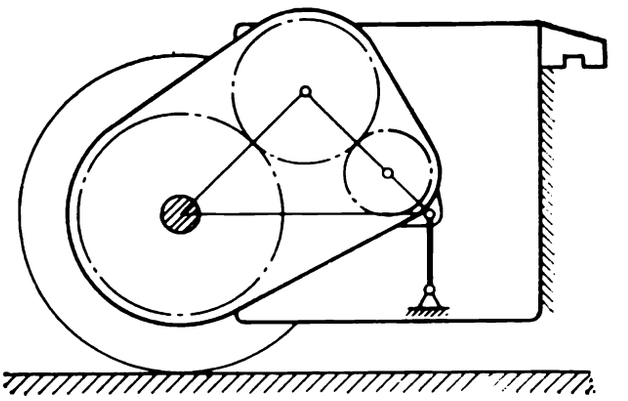

Fig. 4.41. High-speed drive with broken line of centres

an additional rotation of the motor armature. This condition is broken in case of an axle suspension (tram type) of the motor, poor dynamics of this suspension is commonly known. With the frame-axle suspension (the frame suspension of the motor and the axle suspension of the reduction gear), the satisfaction of the above condition depends on the direction of the rod from which the reduction gear is suspended. If the rod is horizontal, the condition is satisfied, although the universal joint in this case should afford the complete play of the suspension springs, which is a rather awkward task. With the rod either vertical or inclined the condition of fine dynamics would not be satisfied. With the frame suspension and any transmission (Siemens-Schukkert, Bukhli, Oerlikon, Ganz, Skoda, Kravchenko, Alstom), or else with a double universal joint (Jackman) connected to the wheel pair axle, the condition is satisfied completely. The condition may be satisfied in a drive with an idler without any universal joint† (Fig. 4.40), provided the spacing of the axis of the idler from the suspension point and from the wheel pair axis is the same. Velocity triangles which are also the triangles of additional tangential accelerations are shown in Fig. 4.40.

The acceleration of the centre of the idler is $\frac{a}{2}$, its left-hand side being accelerated at $a$, while the acceleration of the right-hand side is zero, as required. Appropriate mobility should be provided at the point where the armature shaft extends through the wall of the reduction gear casing, afforded by the design of the sealing device.

The line of the centres in this transmission may be either straight, as in Fig. 4.40, or broken, as in Fig. 4.41. The break angle, however, should not equal $2\alpha$ lest the idler mounted on the spherical bearing would fail to self-align. It is also necessary that the spacing of the idler axis from the suspension point and from the wheel pair axis should be equal.

## 4.11. Mechanisms with Bevel Gears

Bevel gears are not the first choice in a machinery design on account of their more complicated manufacture and more demanding performance, as compared with cylindrical gears. However, in cases where their use is unavoidable, it is possible at least to avoid redundant constraints.

With this aim, in a two-satellite design the circumferential forces may be balanced by employing the equality of the axial efforts of the satellites, proportional to the circumferential forces (Fig. 4.42). The satellites should be connected by a common shaft having axial mobility in the bearings of the carrier. Same as with cylindrical gears, two solutions are possible. The satellite gears may be made self-aligning on spherical bearings $III'_2$ (Fig. 4.42*a*), with the centre of the sphere belonging to the line interconnecting the points of application of the circumferential forces of the bevel gears. These points are offset from the centres of teeth in the direction opposite

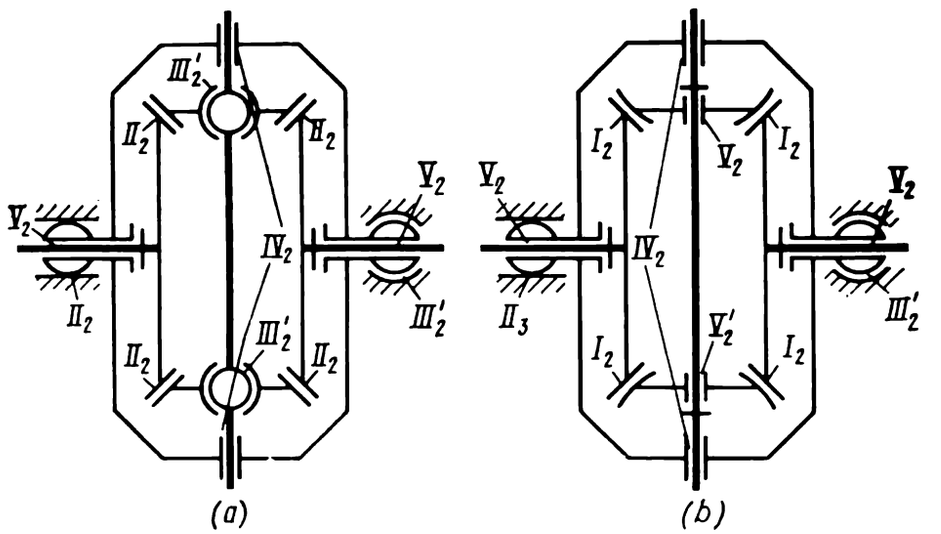


Fig. 4.42. Two-satellite symmetrical differential gear
(*a*) with line engagement; (*b*) with point engagement

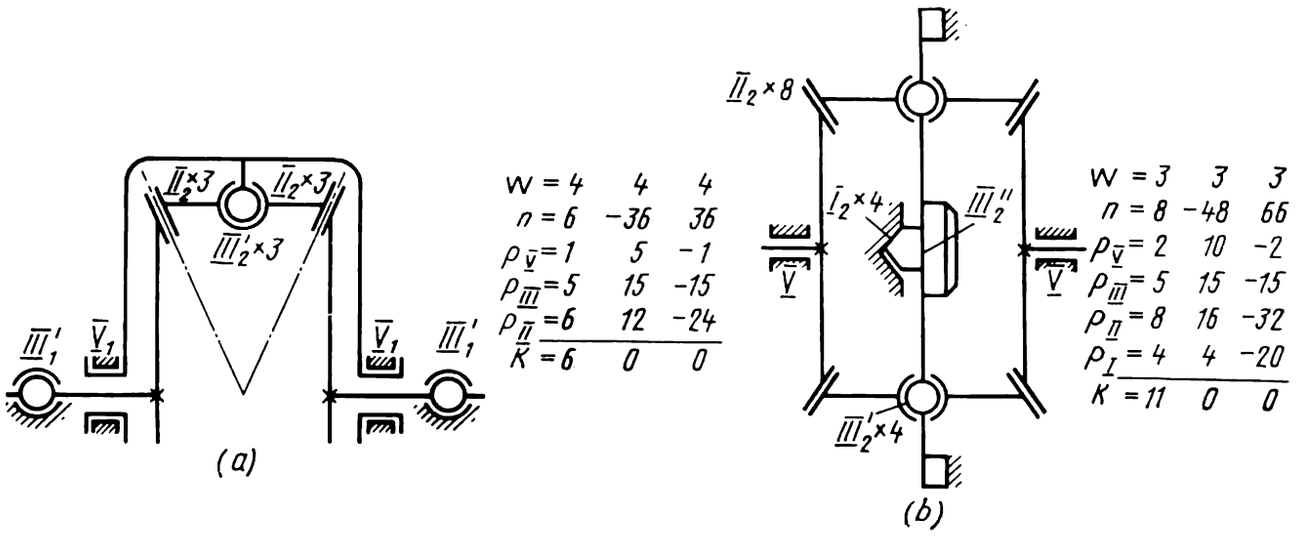


Fig. 4.43. Car differential gear with bevel satellites
(*a*) with three satellite gears; (*b*) with four satellite gears

to the apex of the cone, by the value

$$\frac{b}{6}\frac{r'-r''}{r'+r''}$$

where $r'$ is the maximum radius of the axoid cone, $r''$ is the smallest radius of the axoid cone. The teeth in this case should have line engagement $II_2$. Alternatively, the satellites may be mounted on rotary pairs $V_2$ (Fig. 4.42*b*), but then the teeth should be barrel-shaped, with point contact $I_2$ which brings down the load-carrying capacity. In both cases the mechanism is free of redundant constraints. It is expedient to use a mechanism of this kind in the differential gears of compact cars and motorcycles. To minimize friction in the equalizing mechanism, the shaft should be rotatable, connected to one of the satellite gears.

Let us now consider a differential gear with three satellites (Fig. 4.43*a*). To have the circumferential forces uniformly distributed among the satellite gears, the half-axle gears should be floating using either the mobility of spherical supports $III_1'$ or flexibility of the half-axles. It is true that having only one half-axle gear floating would be sufficient, but for symmetry sake both are made floating. Then to two general mobilities of the differential gear are added two local mobilities: the motion of the half-axle gears vertically and horizontally. Thus, $w = 4$.

The levelling-out of the circumferential forces in a four-satellite construction has been attained in the Thorntton Power Lock differential gear shown in Fig. 4.43*b* with the carrier conventionally

shown stationary. The spiders have been replaced in this design by perpendicular shafts urged against one another by a planar pair $III_2''$ and against the carrier by inclined pairs $I_2$. The equality of the forces in pairs $I_2$ of one axle yields the equality of the torques transmitted by the satellite gears carried by one axle. The equality of

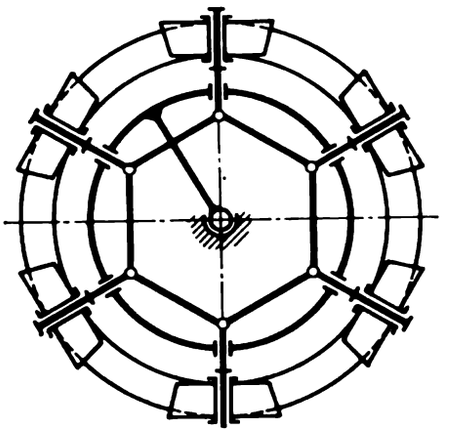

Fig. 4.44. Planetary differential gear with multiple bevel satellites

the action and reaction in pair $III_2''$ yields the equality of the torques transmitted by the pairs of the satellite gears on two axles.

With the satellite number in excess of three, an equalizing mechanism is required to level out the circumferential forces. Equalizing mechanisms are particularly simple when the axes of the satellite gears are perpendicular to those of the main members, the mechanisms being articulated polyhedrons interconnecting the axles of the satellite gears to make their axial forces even (Fig. 4.44). However, as axial displacement of bevel gears breaks the alignment of the apices of their cones, equalizing mechanisms of this kind are suitable only for gears with point engagement.

By employing the above general patterns, rational designs (free of redundant constraints) may be developed for other similar planetary mechanisms.

To avoid redundant constraints in double differential gears (in the turn mechanisms of crawler vehicles) is particularly difficult, as their every satellite made up of two gears engages four other gears. For this purpose the mechanism should include numerous floating members and toothed universal joints which could not be practically accommodated. Therefore, double differential gears would not perform well enough. If other shortcomings are taken into account (poor road-holding capacity of the vehicles) these gears are not advisable for use.

## 4.12. Cylindrical-Bevel Reduction Gear

Self-alignment of a gear may be also attained in a two-stage reduction gear made up of a bevel gearing and a cylindrical gearing† (Fig. 4.45). Same as in a gearing with an idler, the intermediate gear block made up here of the greater bevel gear and the cylindrical pinion should be mounted on a spherical support *III'*. The driving bevel gear and the driven cylindrical one are to be supported by rotary pairs *V*. The mechanism should be designed to assure line engagement—class $II_2$ pairs—of the gear teeth.

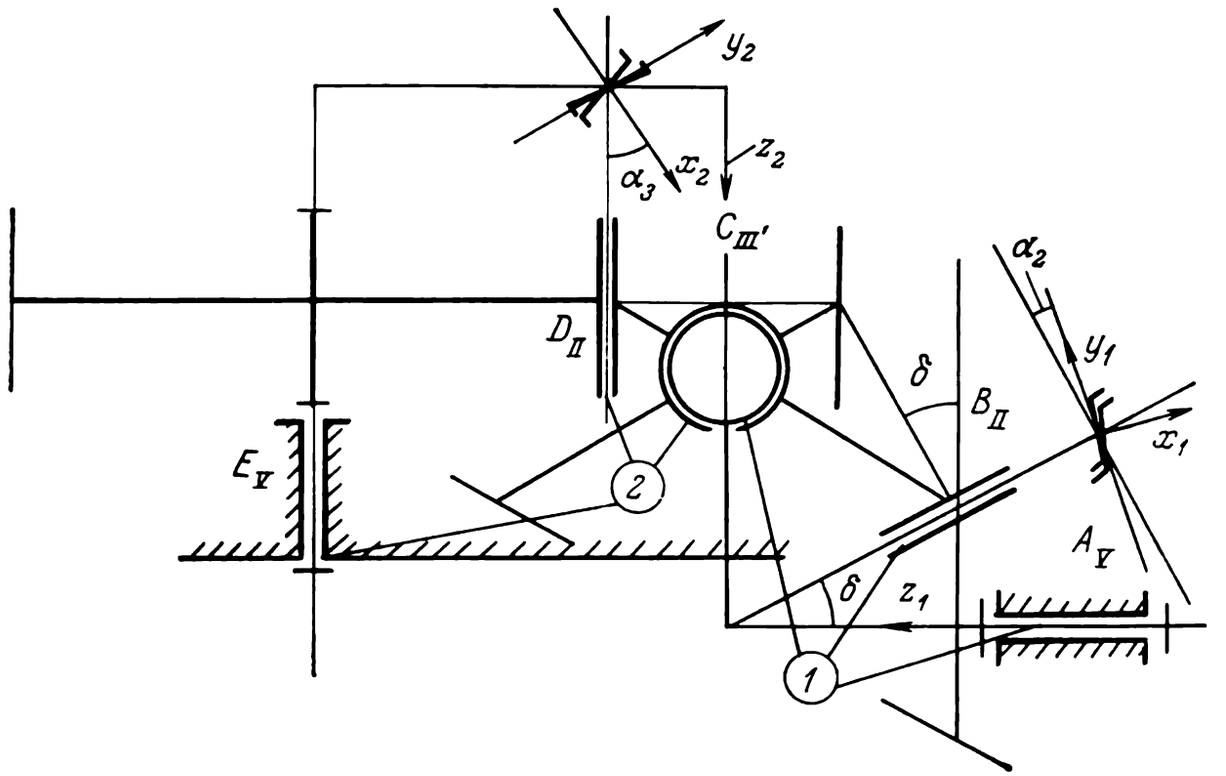


| | | | | | |
|---|---|---|---|---|---|
| $w=1$ | 1 | 1 | | 0 | B $x_1$ |
| $n=3$ | -18 | 12 | $\dot{A}\dot{B}C$ | B | C $y_1$ |
| $p_V=2$ | 10 | -2 | | B | A B $z_1$ |
| $p_{III}=1$ | 3 | -3 | | 0 | D $x_2$ |
| $p_{II}=2$ | 4 | -8 | $C\dot{D}\dot{E}$ | D | C $y_2$ |
| $K=2$ | 0 | 0 | | D | C D E $z_2$ |

Fig. 4.45. Cylindrical-bevel reduction gear

Calculation by (1.1) shows that redundant constraints are absent.

Let us consider the mobilities in the loops. The first loop—the fixed member, pair $V$, small bevel gear, pair $II_2$, great bevel gear,

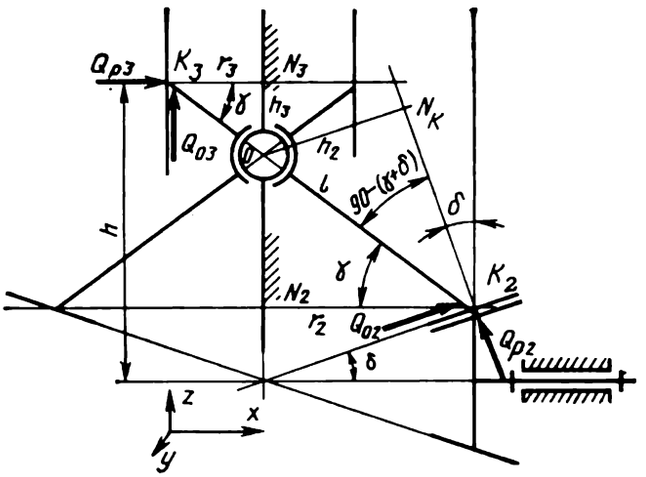


Fig. 4.46. Equilibrium of the floating member

pair $III'$, fixed member. The second loop—the fixed member, pair $V$, great cylindrical gear, pair $II_2$, pinion, pair $III'$, fixed member. The coordinate axes are shown in Fig. 4.45, with $x$ axes in both engagements extending normally to the teeth profiles, $y$ axes extending tangentially and $z$ axes extending along the axes of rotation of the gears.

The pair $III'$ belongs to both loops. Let us take its three angular mobilities about axes $y_1$, $y_2$ and $z_2$, which is permissible as the axes do not belong to one plane. Naturally, should they belong to a single plane, self-alignment would be absent. The distribution of the mobilities is shown in Fig. 4.45. The diagram shows that the mechanism has neither harmful local mobilities nor redundant constraints. Let us discuss the equilibrium of the floating member made up of the second and third gears (Fig. 4.46), since this equilibrium is the prerequisite of self-alignment. In most cases it is attained automatically, but in the presently described one certain conditions have to be observed, which we are going to define below.

Let us consider the tangential forces $Q_{t2}$ and $Q_{t3}$ and the outward thrust ones $Q_{p2}$ and $Q_{p3}$ separately. If the meshing angles in the two engagements are presumed different, $Q_{p2} = Q_{t2} \operatorname{tg} \alpha_2$ and $Q_{p3} = Q_{t3} \operatorname{tg} \alpha_3$, so that

$$\frac{Q_{p2}}{Q_{p3}} = \frac{Q_{t2}}{Q_{t3}} \frac{\operatorname{tg} \alpha_2}{\operatorname{tg} \alpha_3} \tag{4.51}$$

The equilibrium equations are thus reduced to the equations of the moments about three axes which meet at point $O$ (cf. Fig. 4.46).

In this drawing the coordinate axes extend differently from Fig. 4.45, namely, $x$ axis extends along the axis of the smaller bevel gear, $z$ axis extends along the axis of the great gear, and $y$ axis extends perpendicularly to the former two.

$$\text{From } \sum M_x = 0: \quad \frac{ON_3}{ON_2} = \frac{Q_{t2}}{Q_{t3}}$$

$$\text{From } \sum M_z = 0: \quad \frac{K_3N_3}{K_2N_2} = \frac{Q_{t2}}{Q_{t3}} = \frac{r_3}{r_2} \tag{4.52}$$

so that

$$\frac{ON_3}{ON_2} = \frac{K_3N_3}{K_2N_2}$$

which means that triangles $ON_2K_2$ and $ON_3K_3$ are similar, so that $K_2OK_3$ is a straight line.

Thus, the spherical support should belong to a line connecting the centres of the teeth of both engagements.

$$\text{From } \sum M_y = 0: \quad \frac{h_3}{h_2} = \frac{Q_{p2}}{Q_{p3}}$$

By substituting $\frac{Q_{p2}}{Q_{p3}}$ from (4.51) and $\frac{r_3}{r_2} = \frac{Q_{t2}}{Q_{t3}}$ from (4.52): $\frac{h_3}{h_2} = \frac{r_3 \operatorname{tg} \alpha_2}{r_2 \operatorname{tg} \alpha_3}$

From Fig. 4.46, it is obvious that $h_3 = r_3 \operatorname{tg} \gamma$ and $h_2 = \frac{r_2}{\cos \gamma} \times \sin [90° - (\gamma + \delta)] = r_2 \frac{\cos(\gamma+\delta)}{\cos\gamma}$.

By substituting these values in the expression for $\frac{h_3}{h_2}$ and by reducing by $r_2$ and $r_3$:

$$\frac{\operatorname{tg} \gamma \cos \gamma}{\cos (\gamma+\delta)} = \frac{\operatorname{tg} \alpha_2}{\operatorname{tg} \alpha_3}$$

or

$$\frac{\sin \gamma}{\cos (\gamma+\delta)} = \frac{\operatorname{tg} \alpha_2}{\operatorname{tg} \alpha_3} \tag{4.53}$$

In the specific case when $\alpha_2 = \alpha_3$, $\cos (90° - \gamma) = \cos (\gamma + \delta)$. As the cosines are equal, $90° - \gamma = \gamma + \delta$,

$$\gamma = 45° - \frac{\delta}{2} \tag{4.54}$$

In general, from (4.53)

$$\frac{\cos\gamma\cos\delta-\sin\gamma\sin\delta}{\sin\gamma}=\operatorname{ctg}\gamma\cos\delta-\sin\delta=\frac{\operatorname{tg}\alpha_3}{\operatorname{tg}\alpha_2}$$

or

$$\operatorname{ctg}\gamma=\frac{\operatorname{tg}\alpha_3}{\operatorname{tg}\alpha_2\cos\delta}+\operatorname{tg}\delta$$

and

$$\operatorname{tg}\gamma=\frac{1}{\frac{\operatorname{tg}\alpha_3}{\operatorname{tg}\alpha_2}\frac{1}{\cos\delta}+\operatorname{tg}\delta}=\frac{1}{\left(\frac{\operatorname{tg}\alpha_3}{\operatorname{tg}\alpha_2}\frac{1}{\sin\delta}+1\right)\operatorname{tg}\delta} \tag{4.55}$$

The distance between the central plane of the cylindrical gears and the axis of the driving gear

$$h=(r_2+r_3)\operatorname{tg}\gamma+r_1 \tag{4.56}$$

The described reduction gear may have spiral teeth instead of straight ones, provided the equilibrium of the floating block relative to $y$ axis is maintained.

It is necessary that the forces directed along the generatrices should be balanced separately, i.e.

$$Q_{02}=Q_{t2}\operatorname{tg}\beta_2 \quad \text{and} \quad Q_{03}=Q_{t3}\operatorname{tg}\beta_3 \tag{4.57}$$

and the outward thrust forces $Q_{p2}$ and $Q_{p3}$ should be likewise separately balanced.

This is necessary because with the direction of the torque reversed, the directions of the forces $Q_{02}$ and $Q_{03}$ alter, while the directions of the forces $Q_{p2}$ and $Q_{p3}$ are retained.

Equation (4.53) remains valid for the outward thrust forces.

For the forces directed along the generatrices $\Sigma M_y = 0$. Then $Q_{03}K_3N_3 = Q_{02}K_2N_k$. By substituting the values of $Q_{02}$ and $Q_{03}$ from (4.57) and also

$$K_3N_3=r_3 \quad \text{and} \quad K_2N_k=r_2\frac{\cos[90^\circ-(\gamma+\delta)]}{\cos\gamma}=r_2\frac{\sin(\gamma+\delta)}{\cos\gamma}$$

we obtain

$$Q_{t3}\operatorname{tg}\beta_3 r_3=Q_{t2}\operatorname{tg}\beta_2 r_2\frac{\sin(\gamma+\delta)}{\cos\gamma}$$

But $Q_{t3}r_3 = Q_{t2}r_2$, and therefore

$$\frac{\operatorname{tg}\beta_3}{\operatorname{tg}\beta_2}=\frac{\sin(\gamma+\delta)}{\cos\gamma} \tag{4.58}$$

## 4.13. Mechanisms of Friction Variable-Speed Drives

At present, there is a great number of systems [16] of friction variable-speed drives. Let us discuss the technique of eliminating redundant constraints, taking as an example a multidisc variable-speed drive—one of the best types (Fig. 4.47).

A major shortcoming of friction gearing is the big load on the bearings: $N = \frac{Q_c}{f}$ (where $Q_c$ is the circumferential force and $f$ is the coefficient of friction), which is $\frac{1}{f}$ times greater than in toothed gearings where the load of the bearings approximately equals $Q_c$. In multidisc variable-speed drives this shortcoming is obviated by the normal forces being closed within the disc stack and not transmitted to the bearings. There is yet another way to reduce the load on the bearings: by using the centrifugal forces of the satellite gears, which is possible in planetary-friction variable-speed drives. Let us consider a friction drive with tapering discs, line contact (pair $II_2$) and the bias produced by extension at assembling (Fig. 4.48*a*). The transmission ratio is controlled here by varying the distance between the centres. In this drive $w = 2$, with the second mobility being that of slipping, as friction is not considered a restraint in kinematic pairs. From (1.1) $q = 2 - 6 \cdot 2 + 5 \cdot 2 + 2 \cdot 1 = 2$. The first redundant constraint is caused by the line contact, which produces uneven distribution of the load along this contact and is removed by using point contact—a pair $I_2$.

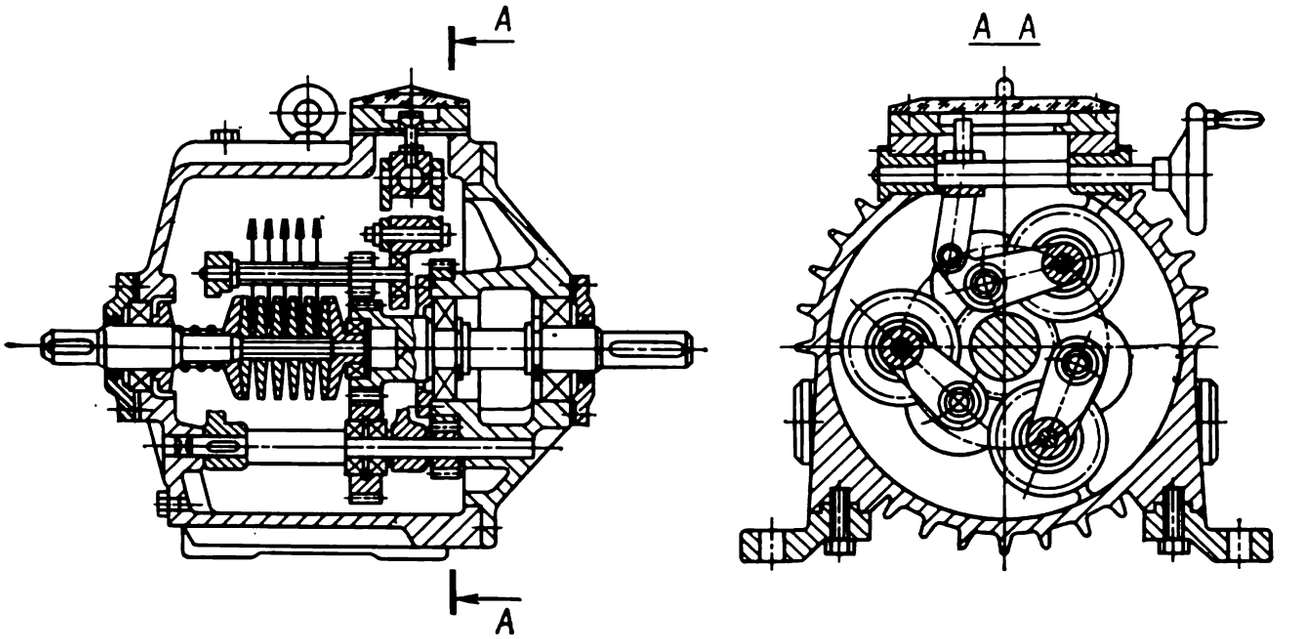


Fig. 4.47. Multidisc variable-speed drive

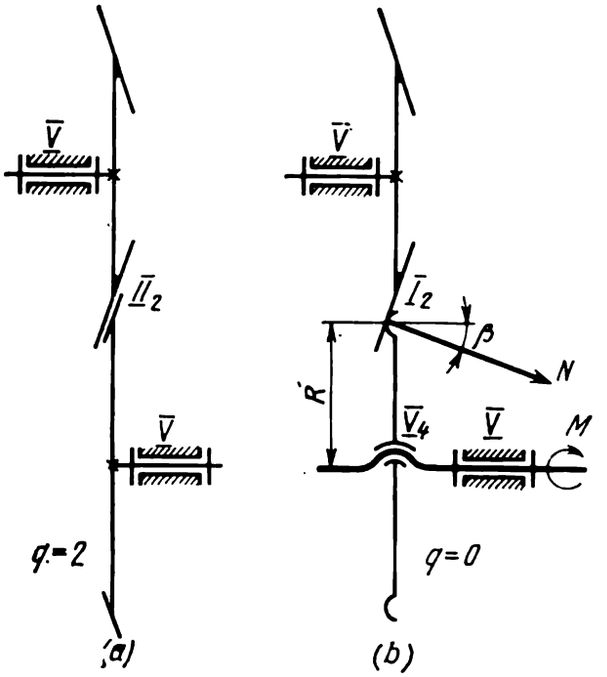


Fig. 4.48. Friction drive with tapered discs

(*a*) with two redundant constraints and manual adjustment of pressure; (*b*) free of redundant constraints, with self-adjustment of pressure

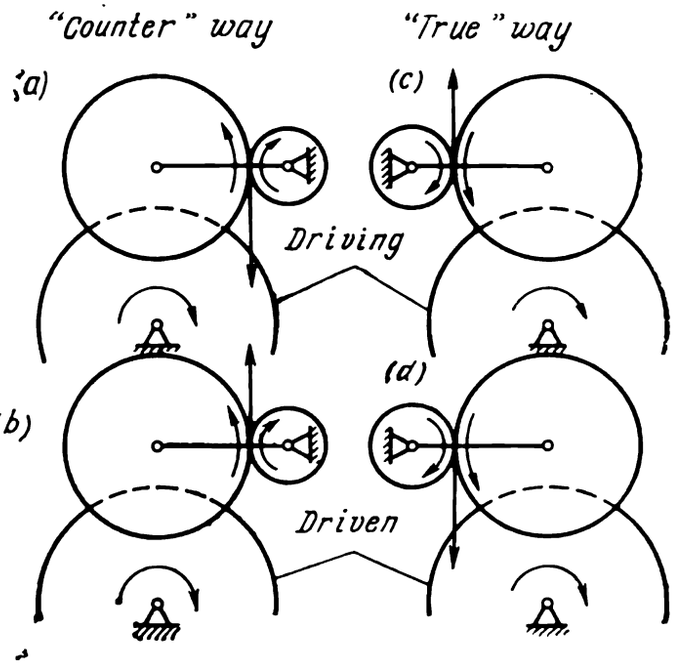


Fig. 4.49. Direction of circumferential force acting upon the gear of the side block of discs

The second redundant constraint is the statically indeterminate dependence of the pressure $N$ on the deformation of the members, removable by self-adjustment. This is attained by connecting one of the friction wheels with the shaft by a screw pair $V_4$ (Fig. 4.48*b*), with the axial effort of the screw $N \cos \beta$ being used to provide this pressure $N$. Let us denote the radius of the disc as $R$, the screw radius as $r$, the helix angle as $\alpha$, the pitch of the screw as $S = 2\pi r \operatorname{tg} \alpha$. The torque transmitted by friction is $M = fNR$; the torque transmitted by the screw is $M = Nr \cos \beta \operatorname{tg} \alpha$. We have not provided here for the friction in the thread, for the direction of the motion in the screw pair will vary in operation, i.e. the torque will vary from $Nr \cos \beta \operatorname{tg} (\alpha + \varphi)$ to $Nr \cos \beta \operatorname{tg} (\alpha - \varphi)$, $\varphi$ being the angle of friction, with the mean value $M = Nr \cos \beta \operatorname{tg} \alpha$. By equating these torques:

$$fNR = Nr \cos \beta \operatorname{tg} \alpha, \quad \text{but} \quad r \operatorname{tg} \alpha = \frac{S}{2\pi}$$

therefore

$$\frac{R}{\cos \beta} = \frac{S}{2\pi f} = \text{constant}$$

In a multidisc variable-speed drive $\beta$ is constant, so that $R$ is constant, i.e. the device adjusting the pressure should be mounted

on a shouldered disc the radius of which does not vary, be it the driving or driven disc.

In designs where the angle is variable, the disc supporting the pressure-adjusting device should have a profile $\frac{R}{\cos\beta}=$ constant.

A specific kind of redundant constraints may take place in multi-disc variable-speed drives. By their principle of operation, such drives are multipath ones. If the transmission ratio is different in different paths on account of manufacturing and assembly inaccuracies, slipping becomes unavoidable with the resulting increased wear and affected efficiency factor. Thus, a mechanism should be designed for the transmission ratios in different paths to self-equalize, and this can be attained by equalizing the efforts and torques being transmitted. Let us consider the forces acting upon the gear of a peripheral stack of discs (Fig. 4.49) where angular velocities are indicated with arrows. The angular velocity of the central gear opposes the angular velocity of the central stack of the discs.

Let us take the case where this central stack includes a device for adjusting the pressure and the discs are provided with shoulders. The side stacks should have tapering discs. In the designs *a* and *d* the force acting upon the side gear pulls the disc stack in, whereas in the designs *b* and *c* it pushes them out. When the side stack in the design *a* lowers beneath the other ones, its angular velocity will tend to increase, with the transmitted torque and pulling-in force also increasing. Hence, the stack will tend to descend still lower, and the performance will be unstable. When the side stack lowers in the design *b*, its angular speed will also increase, with the transmitted torque and the pushing-out force increasing, too, the latter tending to raise the stack and restore the equilibrium, i.e. the performance will be stable. Similarly, we may find that the design *c* is characterized by unstability, while the design *d* yields stable performance.

To summarize what has been said above, we may conclude that when the central stack has shouldered discs, the carriers of the side stacks should be arranged in the "true" way relative to that central stack to assure stable performance.

With the discs of the side stacks shouldered, stable performance is assured when their carriers are arranged in the "counter" way.

To level out the adjustment forces, the member controlling the transmission ratio should be floating. The simplest solution is to mount it on an Oldham coupling. This design has been suggested by Ja. Ja. Gaipel and the Author (Fig. 4.50) and provides adjustment at permanent power rating, with the torque of the motor being con-

stant and the torque applied to the driven shaft increasing when the speed decreases, which is optimal. Experiments conducted by Ja.Ja. Gaipel showed that, owing to self-alignment, the efficiency

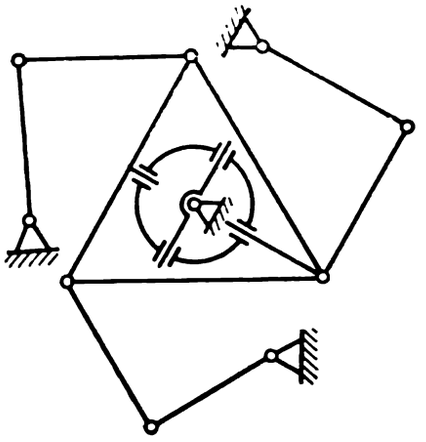

Fig. 4.50. Equalizing mechanism for multidisc variable-speed drive

factor at full load increases by 5 to 10 per cent, while the friction losses are reduced by one half. To attain this, however, the weight of the peripheral stacks has to be counterbalanced, which has been done by incorporating a spring.

## 4.14. Automotive Transmission (Gearbox)

Self-aligning gearwheels* at every gearshift are possible by using arch-shaped teeth which offer both a high load capacity and noiseless running. Such a transmission with five forward gears or stages, one overdriving, and a single reverse gear is shown in Fig. 4.51. All the gearwheels here are constant-mesh ones, their engagement being effected by clutches.

The axial mobility required to eliminate redundant constraints associated with arch-shaped teeth may be allotted solely to the countershaft supports by a $IV_1$ pair. As neither the drive shaft nor the output one may be axially movable, the other axial mobility can be provided through the connection of the driven gearwheels with the output shaft, by mounting the gearwheels on cylindrical pairs $IV_1$ and engaging them by cylindrical clutches $III_5''$ providing axial mobility. In Fig. 4.51 the second gear is engaged. The calculation of redundant constraints from structural formulas is given at the bottom of the drawing.

*In this and following Section, the term "gearwheel" will be used to distinguish it from "gear" as implying a transmission stage or ratio. *Translator's note.*

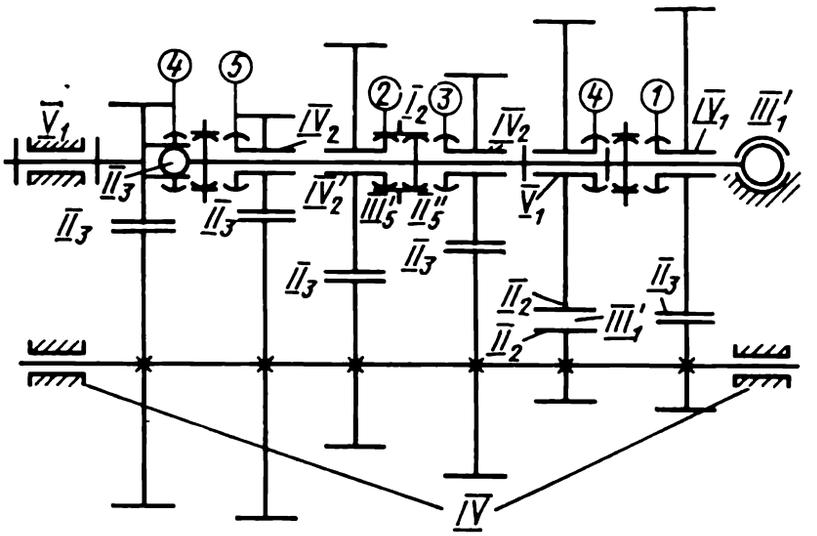


| 2nd Forward | | | | Reverse | | | |
|---|---|---|---|---|---|---|---|
| $W = 1$ | 1 | 1 | | $W = 1$ | 1 | 1 | |
| $n = 5$ | −30 | 30 | | $n = 6$ | −36 | 36 | |
| $p_V = 1$ | 5 | −1 | | $p_V = 2$ | 10 | −2 | |
| $p_{IV} = 2$ | 8 | −4 | | $p_{IV} = 1$ | 4 | −2 | |
| $p_{III} = 3$ | 9 | −9 | | $p_{III} = 4$ | 12 | −12 | |
| $p_{II} = 3$ | 6 | −12 | | $p_{II} = 4$ | 8 | −16 | |
| $p_I = 1$ | 1 | −5 | | $p_I = 1$ | 1 | −5 | |
| $K = 5$ | 0 | 0 | | $K = 6$ | 0 | 0 | |

Fig. 4.51. Car transmission with self-aligning gear and arch-shaped teeth

For reverse gear, straight-tooth gearwheels are to be used, with the idler (not shown in Fig. 4.51) mounted on a spherical pair $III_1'$. No axial mobility is required here, so that the reverse gearwheel is to be connected with the output shaft by a rotary pair $V_1$. The calculation of redundant constraints from structural formulas for the reverse gear is given in Fig. 4.51 at the bottom.

## 4.15. Multishift Transmissions with Return Stages

Owing to the small number of the gearwheels, transmissions of this kind are particularly suitable for heavy-duty wheeled and crawler vehicles. It is relatively easy to make these transmissions self-aligning by using the clutches as toothed universal joints, as it can be readily illustrated by an eight-gear transmission (Fig. 4.52). In the standard design, each gearwheel used to be supported by two bearings mounted in intermediate partitions, with eight such partitions in an eight-gear transmission. The partitions boosted both

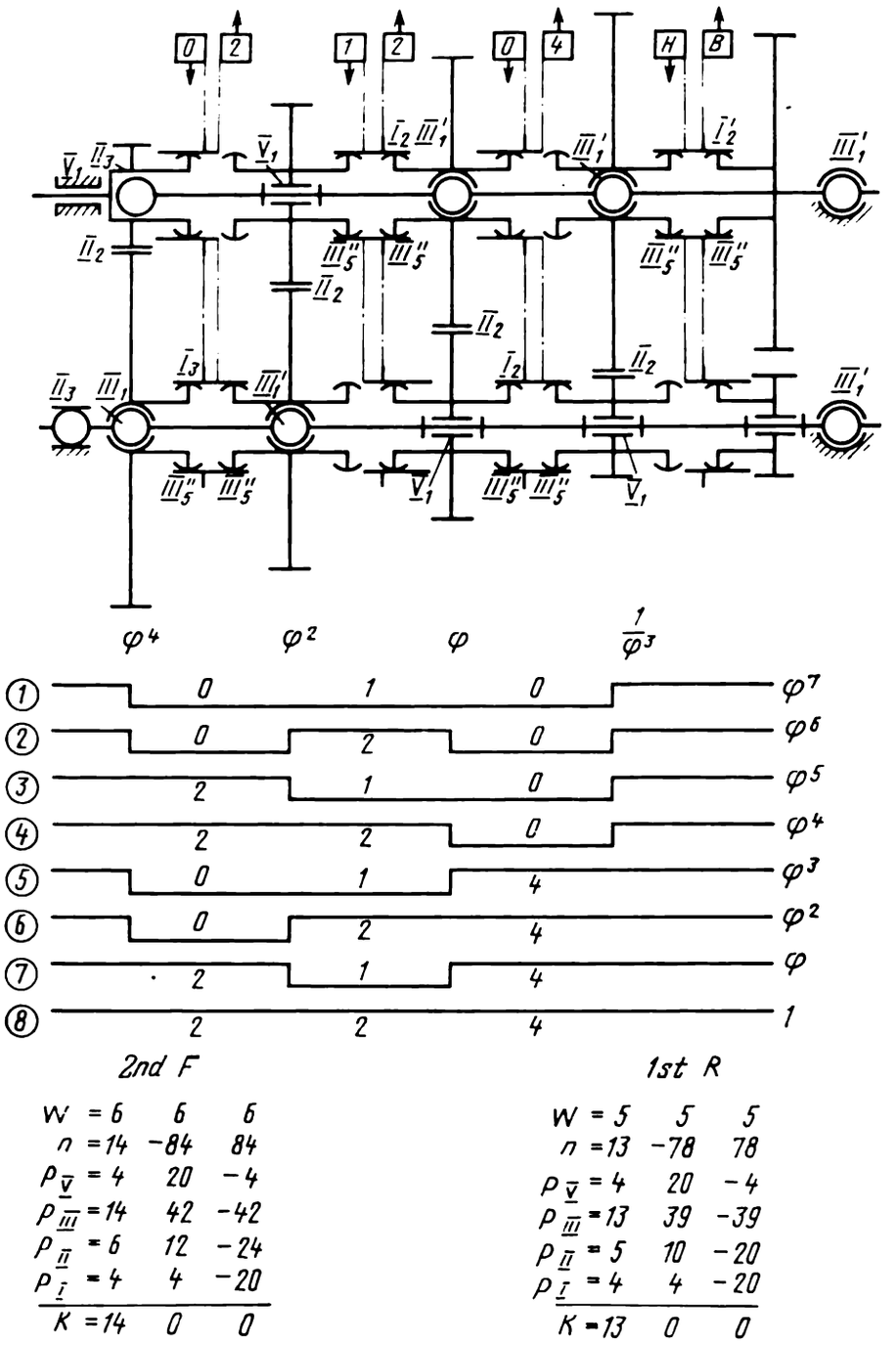


Fig. 4.52. Transmission with return stages with straight teeth (*B* stands for forward, *F*, and *H* for reverse, *R*)

the manufacturing cost of the transmission and its weight. This can be avoided and redundant constraints can be eliminated by mounting the idler gearwheels on the output shaft and countershaft of sufficiently large diameters (Fig. 4.52).

For self-alignment sake, the idler of the reverse gear (not shown in Fig. 4.52) is supported by a spherical bearing. In each meshing pair one gearwheel is likewise mounted on a spherical bearing, this

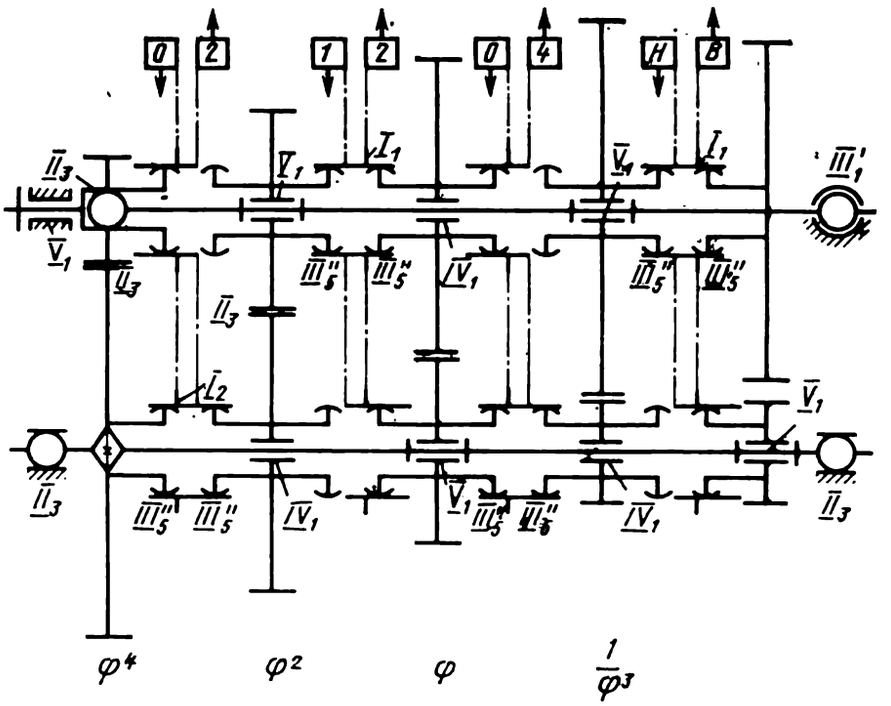


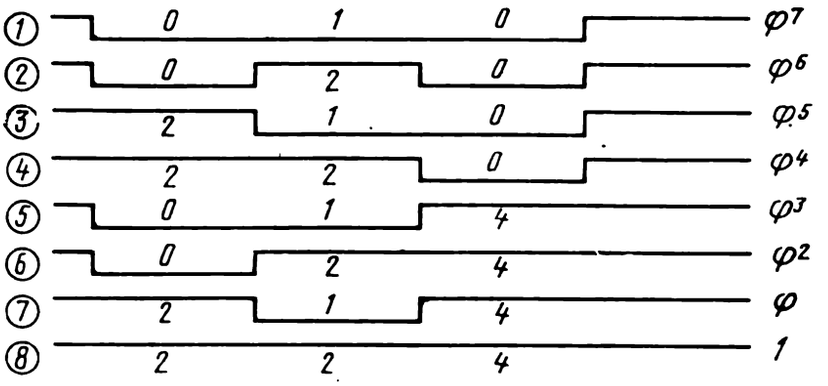


| | 2nd F | | | 1st R | | |
|---|---|---|---|---|---|---|
| W | 1 | 1 | 1 | 3 | 3 | 3 |
| n | 13 | −78 | 84 | 12 | −72 | 78 |
| $p_{\bar{V}}$ | 4 | 20 | −4 | 3 | 15 | −3 |
| $p_{\bar{IV}}$ | 3 | 12 | −6 | 2 | 8 | −4 |
| $p_{\bar{III}}$ | 9 | 27 | −27 | 10 | 30 | −30 |
| $p_{\bar{II}}$ | 7 | 14 | −28 | 6 | 12 | −24 |
| $p_{\bar{I}}$ | 4 | 4 | −20 | 4 | 4 | −20 |
| K | 14 | 0 | 0 | 13 | 0 | 0 |

Fig. 4.53. Transmission with return stages with arch-shaped teeth

being the larger gearwheel to accommodate a bearing of a sufficient load capacity. Each gearwheel retains then one local mobility, but experience has shown that it is harmless.

Let us denote the denominator of the geometric progression of the gears as φ, with the transmission ratios of every pair of gearwheels shown under it.

In the transmission being discussed the clutches of the output shaft and those of the countershaft are engaged or disengaged simultaneously (they are joined in the drawing of Fig. 4.52 with dash-and-dot lines).

The Nos. of the states of the clutches are shown in squares in Fig. 4.52. The numbering is done so that the sum of the Nos. of the engaged clutches should yield the No. of the engaged gear [30]. Short arrows accompanying these Nos. point either up or down, to indicate that the power is transmitted at this portion via either the output shaft or the countershaft, respectively.

The power path is shown as a broken line under the diagram of the mechanism in Fig. 4.52, with gear Nos. (in circles) given to the left of each line, the transmission ratios to the right of the lines and the Nos. of the engaged clutches adjoining the lines (directly below the respective clutches). Top, at the right, is the calculation of redundant constraints for the 2nd forward gear (the one with the most intricate path). The mobility is made up of the main one and local mobilities of the countershaft and of the four gearwheels mounted on the spherical bearings. Below is given the calculation for the 1st reverse gear, where the mobility includes the main one and the local mobilities: the axial mobility of the countershaft and the three angular mobilities of two gearwheels mounted on spherical bearings. One of these gearwheels, the second one on the countershaft, retains two local mobilities as its teeth transmit no torque.

Another version of this transmission has gearwheels with arch-

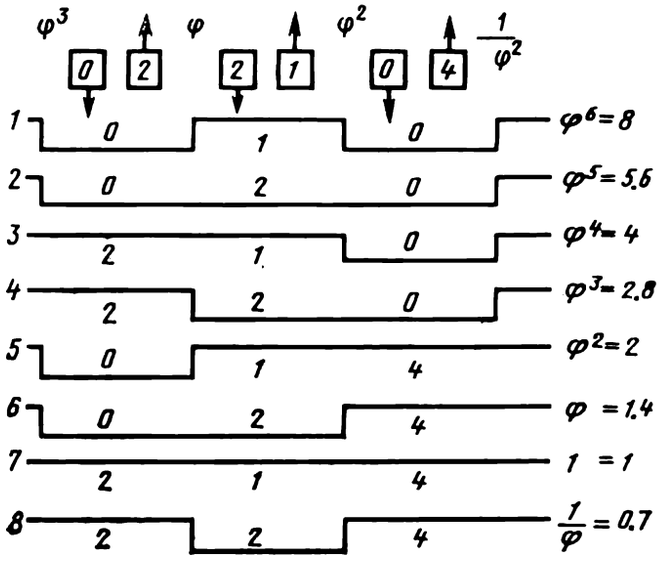


Fig. 4.54. Engagement pattern with one overdrive gear

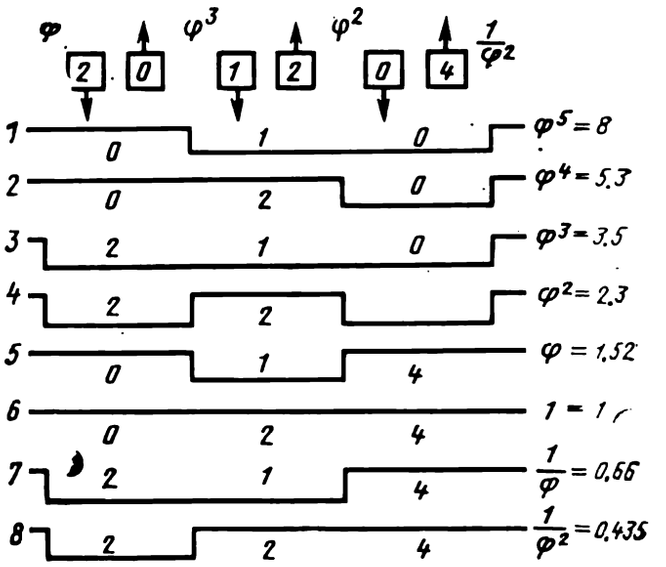


Fig. 4.55. Engagement pattern with two overdrive gears

shaped teeth, except the reverse gear unit where straight-teeth gearwheels and the idler on the spherical bearing remain (Fig. 4.53). This version is devoid of gearwheels on spherical bearings whose accommodation might be complicated in transmissions with overdrive gears and has no local angular mobilities associated with such gearwheels. In this version one gearwheel of each meshing pair should have an axial mobility, i.e. it has to be mounted on a kinematic pair $IV_1$.

The calculation of redundant constraints for the 2nd forward gear and 1st reverse gear is given at the bottom of Fig. 4.53. In the latter case $w = 3$: the main mobility and two axial mobilities of the two gearwheels on $IV_1$ bearings. These mobilities have to be introduced into the structural formulas, since we do not consider the meshing of these gearwheels which eliminate the local mobilities.

The transmissions under discussion may have overdrive gears: either one (Fig. 4.54) or two (Fig. 4.55). The symbols in these drawings are the same as in Figs. 4.52 and 4.53. In addition, the numeric values of the transmission ratio are given at the right for the case when the ratio is 8:1 in direct drive.

## 4.16. Self-Alignment in Traction Gearings

An electric locomotive gearing with $m = 10$ mm is practically at the crest of its endurance when it transmits the power as high as 800 kW.

Let us compare an electric locomotive gearing with a similar gearing in ships. The second-stage toothed gearing of turbine-plant motorships of the "Leninski Komsomol" type runs for a number of years without repairs and with no visible wear. With its parameters of $m = 7$ mm and the angular speed nearly that of its electric locomotive counterpart it transmits 10 000 kW.

The comparison makes it obvious that the traction gearing has huge unused reserves, and its poor performance is brought about by its improper design.

Let us discuss the factors adding up to this improperness. The first is the skewing axes of the driving and driven shafts, so that not the entire width of the gear is engaged in operation, and even the part which does work is loaded unevenly, which significantly curtails the service life. The skewing is caused by the wear of the motor and axle bearings, which is particularly great with one-side transmission and with axle (tram-type) suspension of the motor. The second cause of the skewing is deformation of the traction drive which cannot be

done symmetrical as the centre of the locomotive is occupied by the traction motor. Neither can its rigidity be enhanced as it is limited by the weight of the drive and the permissible load of the axle. The third cause of the skewing is the tolerances for the dimensions of the drive components. Thus, the reduction gear of the ЧС-2 locomotive has eleven connections affecting the non-parallelism of the axes of the gears. The admissible misalignment of the axes must be within 1 micron, whereas in the reduction gear of the ЧС-2 the working deformation of the teeth in one hour of running at full current is 0.02 mm, and the displacement of the tooth due to skewing, naturally, should be much less of this deformation.

And still, in the frame-axle suspension (frame suspension of the motor and axle suspension of the reduction gear) the partial elimination of the first factor—the skewing—significantly enhances the performance of the gears, as compared with freight electric locomotives. The reason, of course, is not that the locomotive is a "passenger" one (as its traction motor power is not below that of a "freight" locomotive), but the better design of the drive.

The parallelism of axes is best assured by using self-aligning gears. Their incorporation in grain harvesters has increased the service life fourfold, and now they are used in every grain harvester manufactured in the USSR.

Adequate performance can be attained in single-stage gearings even in the cases of skewing by using arch-shaped involute-form gear teeth. Gears with such teeth are unaffected by skewing.

Gearings of this type have bright prospects of use in locomotives.

The second factor is the jolts at rail joints, which are transmitted to the gearing and wear it out. Besides, the armature of the traction motor is drastically damaged. The harm caused by the jolts may be eliminated by designing the traction drive so that the play of the suspension springs should not cause additional rotation of the armature. In other words, the traction drive should transmit to the wheel pair either the torque or only the horizontal force (the force applied to the tooth), while either vertical or inclined direction of the force is not to be tolerated. There is no need to prove here these two requirements. They are satisfied in drives with the hollow shaft and in Jackman drive with a double universal joint on the wheel pair axle. They are also met in a high-speed drive of the frame-axle type, with the reduction gear suspension including a horizontal rod (as suggested by I.V. Biryukov). The harmful influence of the jolts can be minimized, if not completely eliminated, by mounting either

springs or rubber cushions inside the bigger gear, or a torsion-spring shaft inside the armature.

Conditions very close to those required were provided in the quite ancient ПВ Model of an electric locomotive. It had a gearing with the hollow shaft and, for fine adjustment of the gears to assure adequate teeth engagement, the gears were mounted on the shaft with

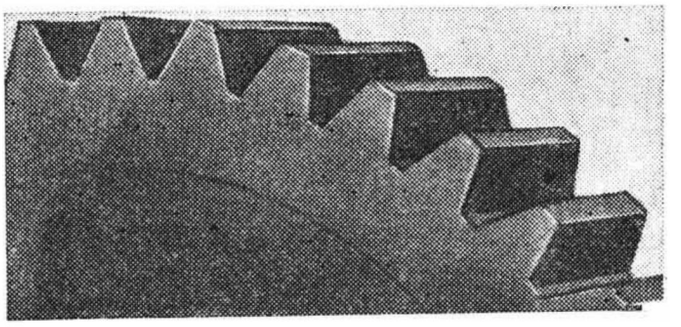

Fig. 4.56. Toothed wheel of ПВ electric locomotive that has logged 900 000 km

the aid of friction connections clamped upon the completion of the adjustment. The torque was transmitted from the bigger gear to the wheel pair through helical springs preventing the transmission of jolts on rail joints. Thus, the gearings of the ПВ locomotive could be expected to perform nicely. True enough, the gears bore no traces of wear and destruction, although the locomotive had logged as many as 900 000 km (Fig. 4.56).

It is worth reminding that gears made at that time for locomotives with tram-type suspension were completely destroyed after 200 000 km of running. This observation is just another substantiation of the statement that elimination of the two above factors of improper design enables us to have a traction toothed gearing proof against untimely wear and destruction.

## 4.17. Conclusions and Suggestions

In cam mechanisms self-alignment may give uniform distribution of the load along the line of contact, with the corresponding increase of the load capacity and durability.

In case of a pivoted follower, self-alignment is attained by mounting it on a spherical support, the second mobility may be used for eliminating the rudandant constraint in the connection between the follower and the driven member.

With a slide follower, self-alignment is provided for by using the slider of the cylindrical type ($IV_2$) under the condition that the pressure angle is not zero, or else by mounting the follower roller on a spherical bearing, which, however, yields one local mobility.

In power contact pins, self-alignment is capable of reducing the required contact pressure several times.

In "bridge banking" employed in control circuitry, one spring urges two contacts. By making the banks self-aligning, a single spring may uniformly urge three, four and even five contacts, and when both ends of a spring are used, it may urge as many as eight contacts, while providing for slipping essential for stable performance of the contacts (owing to self-cleaning).

In toothed gearings self-alignment allows for stepping up the load-transmitting capacity several times over.

Self-alignment may be attained by using an arch-shaped tooth in combination with axial mobility of one of the gears (single-stage gearings), by employing spherical bearings ($III'_1$) (idler gears and multistage reduction gears) and barrel-shaped teeth ($I_2$), although the latter have the drawback of a lower load capacity as the maximum load lengthwise of the teeth being twice that under a line contact with the same torque transmitted.

A reduction gear with two idlers requires an equalizing mechanism whose transmission ratio should be different for the two directions of torque transmission.

Reduction gearings with bevel gears (automotive differential gears) can have the load of the satellite gears levelled out: with two satellite gears by a floating axle balancing their axial forces; with three satellites by one of the main members floating; with four satellites by a wedge mechanism balancing the torques transmitted by either satellite pair; with multiple satellites by an articulated polyhedron balancing their axial forces.

Self-alignment of a reduction gear made up of a cylindrical and a bevel gearing is provided for by mounting the block of the intermediate gears onto a spherical bearing, with the following conditions satisfied:

the bearing should belong to a straight line connecting the centres of the teeth in both engagements and defining with the axis of the pinion an angle of $45° - \frac{\delta}{2}$;

the helix angle in both engagements should be determined from the condition of equilibrium of the intermediate gear block;

the axes of the driving, intermediate and driven shafts should belong to the same plane.

In an automotive transmission, arch-shaped teeth ($II_3$) should be used for self-alignment, with axial mobility provided by the gear-engaging clutch ($III''_5$).

In a transmission with return stages, it is expedient that the output shaft and countershaft should be used as the gearwheel axles. Straight teeth ($II_2$) may be employed, with the greater gearwheels of each gear mounted on spherical supports ($III_1'$). Alternatively, arch-shaped teeth may be used, with all the gearwheels mounted on rotary ($V_1$) and cylindrical ($IV_1$) pairs, and axial mobility provided in the gear-engaging clutch ($III_5''$).

In case of friction variable-speed drives, stability of self-alignment should be checked and ascertained while designing. This is capable of stepping up the efficiency factor by as many as 10 per cent, with the losses reduced to one half and the durability and working temperature enhanced correspondingly.

# Chapter 5

# PLANETARY MECHANISMS

## 5.1. Mobilities in Single-Row Mechanisms

In self-aligning mechanisms tolerances bring about additional movements which have to be provided for by affording corresponding mobilities. Let us discuss the influence of deviations of dimensions (tolerances) on the performance of a single-row mechanism[1]. To do this, we shall take a substituting mechanism with lower pairs. We already know that an involute toothed gearing may be replaced by a four-member linkage $ON_1'N_2'C$ (Fig. 5.1) where the pivots $O$ and $C$ belong to the axes of the gears, while the pivots $N_1'$ and $N_2'$ are situated at the points of tangency of the line of meshing with the generating circles. Therefore,

$$ON_1' = r_{01} = r_1 \cos \alpha; \quad CN_2' = r_{02} = r_2 \cos \alpha$$
$$N_1'P_{12} = r_1 \sin \alpha; \quad N_2'P_{12} = r_2 \sin \alpha$$
$$N_1'N_2' = (r_1 + r_2) \sin \alpha$$

Similarly, $N_c'N_3' = (r_3 - r_2) \sin \alpha$.

But in a single-row mechanism $r_3 = r_1 + 2r_2$, or $r_3 - r_2 = r_1 + r_2$. Thus, $N_1'N_2' = N_c'N_3'$.

As the tolerances are small, we will presume that the dimensions of the substituting mechanism are constant. Let us now consider how a deviation of the dimension of the carrier $OC$ influences the performance of a single-row mechanism. Supposing that the carrier is stationary and the centre of the satellite gear moves radially at a velocity $v_c$ (exclusively within the tolerances), we see that the centre $P$ of instantaneous rotation of the satellite gear is at the point of intersection of the normal $CP$ to the path of the point $C$ with the normal $N_c'N_3'P$ to the path of the point $N_c'$.

If the meshing or engagement angles of the gear pairs *1* and *2*, *2* and *3* are equal, $PN_2'$ aligns with an extension of the connecting-rod $N_1'N_2'$, and the velocity $v_{N2}$ of the point $N_2'$ is perpendicular to the

[1]In similarity to single-row bearings, the term "single-row" mechanism, as used here, implies that all the gears involved are in one plane.—*Translator's note.*

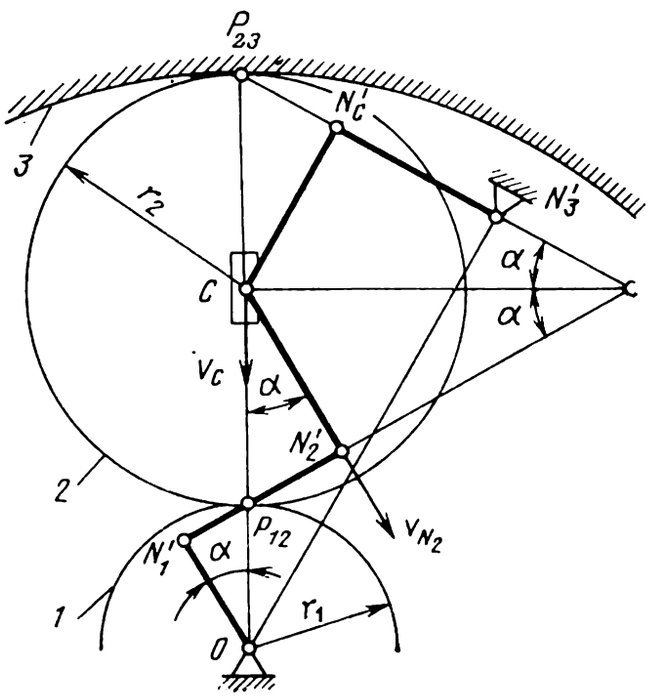


Fig. 5.1. Radial displacement of satellite gear

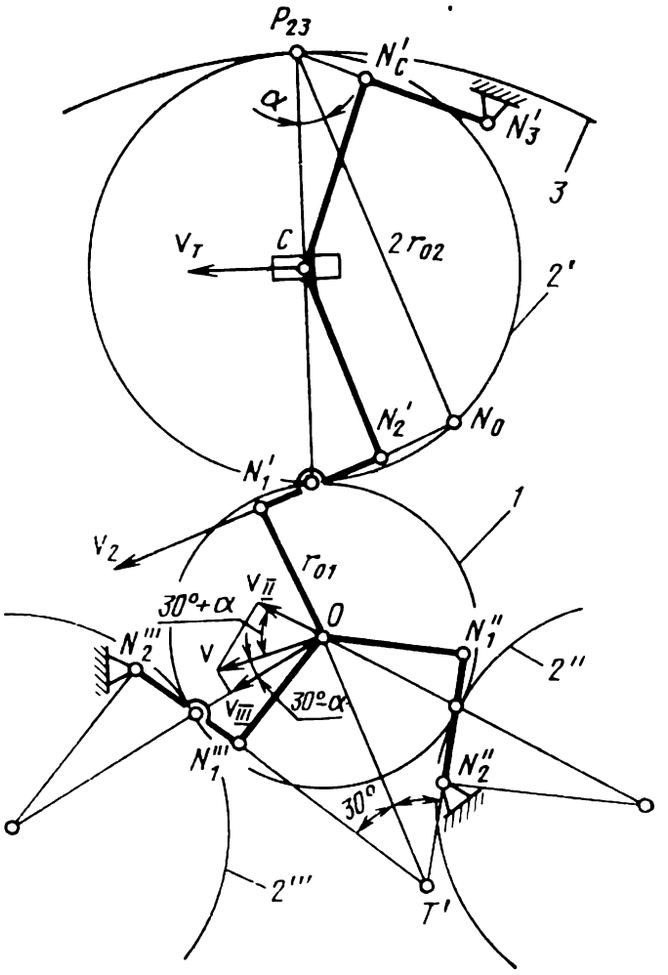


Fig. 5.2. Tangential displacement of satellite gear

connecting-rod $N_1'N_2'$. Thus, neither point $N_1'$, nor the gear *1* would move. Consequently, a tolerance for the radius of the carrier would not influence the performance of the mechanism. This tolerance has to be selected by the radial and lateral gaps of the teeth of the gears *1* and *2*, *2* and *3*, so that the engagement factor should not be less than 1, i.e. the tolerance for the radius of the carrier may be relatively big.

To determine the influence of the tolerance upon the central angle between the satellite gears and upon the performance of the mechanism, let us consider a mechanism with a stationary carrier (Fig. 5.2) where the centre of one satellite gear moves tangentially at a velocity $v_T$. The supporting gear with the fixed point $N_3'$ and satellites with the fixed points $N_2''$ and $N_2'''$ will likewise be stationary. Let us assume that the central gear *1* is floating, so that in the diagram it is connected with three arms $N_1'N_2'$, $N_1''N_2''$ and $N_1''' N_2'''$.

Let us determine the influence of the displacement of the satellite gear on the displacement of the central or sun gear. The centre of instantaneous rotation of the satellite gear is the pole $P_{2\,3}$ of its meshing with the supporting gear. The velocity $v_2$ of the point $N_1'$

equals that of the point $N_0$. Thus,

$$\frac{v_2}{v_T} = \frac{P_{2\,3}N_0}{P_{2\,3}C} = \frac{2r_{02}}{r_2} = 2\cos\alpha$$

The instantaneous centre of rotation of the central gear is the point $T'$ of intersection of extensions of the connecting-rods $N_1''N_2''$ and $N_1'''N_2'''$. Then

$$OT' = \frac{ON_1''}{\sin 30^\circ} = 2r_0$$

We can determine the velocity $v$ of the centre $O$ from the proportion:

$$\frac{v}{v_2} = \frac{OT'}{N_1'T'} = \frac{2r_{01}}{3r_{01}} = \frac{2}{3}$$

Let us multiply the equation obtained by $\frac{v_2}{v_T} = 2\cos\alpha$:

$$v = \frac{4}{3} v_T \cos\alpha$$

This expression multiplied by $\Delta t$ time interval gives:

$$v\Delta t = \frac{4}{3} v_T \Delta t \cos\alpha$$

But $v\,\Delta t = E_{ce}$—the displacement of the centre of the gear *1*, while $v_T\,\Delta t = e$—the tangential displacement of the satellite gear. Therefore,

$$E_{ce} = \frac{4}{3} e\cos\alpha \qquad (5.1)$$

with $\alpha = 20^\circ$,

$$E_{ce} \approx \frac{5}{4} e \qquad (5.2)$$

The above expressions do not include the radii of the gears, which means that $E_{ce}$ is independent of the transmission ratio of the assembly.

Besides, the above expression of $E_{ce}$ equally fits the case where the internally meshing gear *3* is floating. With the mechanism operating, the tangential displacement of the satellite gear through the value $e$ results in the centre of the floating gear *1* (or *3*) describing a circle of the radius $E_{ce}$, making one full revolution per revolution of the carrier. Therefore, its centrifugal force $mE_{ce}\omega^2_{cr}$ is small, as $\omega_{cr}$ is small.

If the carrier is made with an eccentricity $E$ (Fig. 5.3), the centres of the three satellite gears will become displaced in parallel by this

eccentricity value. For the position shown in Fig. 5.3, the tangential displacement of the upper satellite gear will equal $E_4(E)$, and each of the two lateral satellite gears will be displaced by $\frac{E_4}{2}$.

The displacement of the centre of gear *1* caused by the tangential displacement of the upper satellite gear equals (4/3) $E_4 \cos \alpha$ and

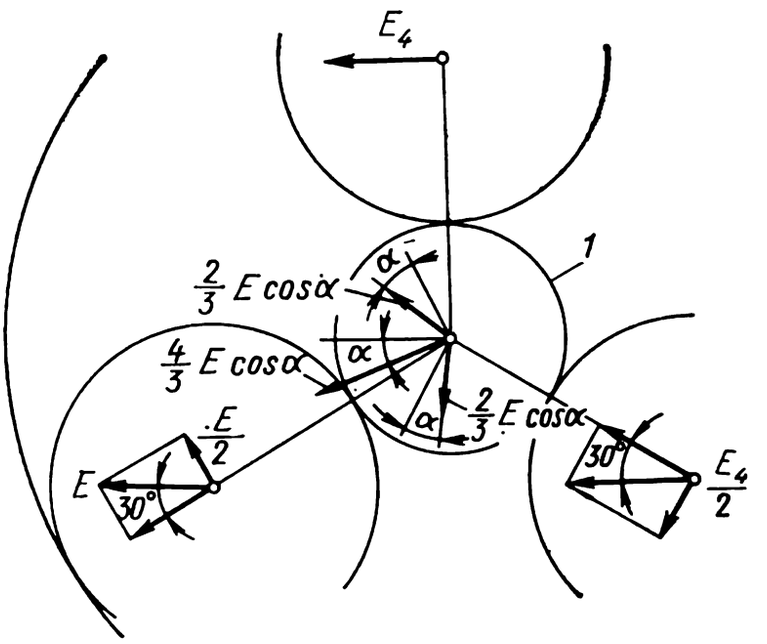


Fig. 5.3. Carrier displacement

defines an angle $\alpha$ with the direction of the eccentricity.

The displacement of gear *1* caused by the tangential displacement by each of the lower satellite gears equals (2/3) $E_4 \cos \alpha$ and its direction defines with the first-mentioned displacement 60° angles. We may calculate the total displacement of gear *1* as a geometric sum of the two displacements, i.e. $E_{c4} = \frac{4}{3} E_4 \cos \alpha + 2 \frac{2}{3} E_4 \times \cos \alpha \cos 60°$:
hence,

$$E_{c4} = 2E_4 \cos \alpha \tag{5.3}$$

The same conclusion may be drawn with the aid of velocity polyhedrons (the plan views of rotated velocities) shown in Fig. 5.4*a* and *b*. The points $N_3'$, $N_3''$ and $N_3'''$ of the supporting gear are stationary. The carrier translates to the left, so that the velocities of centres $C'$, $C''$ and $C'''$ are equal and indicated by the straight line segment *pc* (cf. Fig. 5.4*a*). We shall find the velocities of the points $N_c'$, $N_c''$ and $N_c'''$ by drawing lines parallel to the members, with the points $n_c'$, $n_c''$ and $n_c'''$ belonging to a circle of the diameter *pc*, as the angle

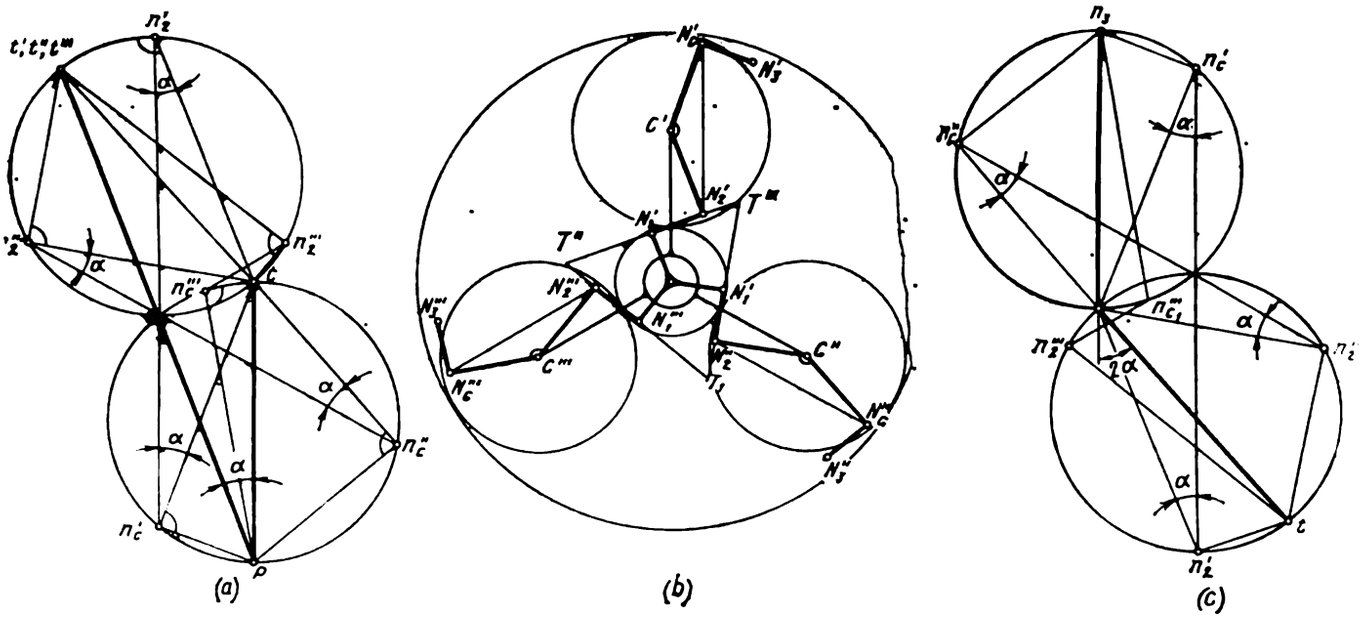


Fig. 5.4. Single-row planetary gearing with three satellites
(*a*) velocity polyhedron with carrier being displaced; (*b*) mechanism pattern; (*c*) velocity polyhedron with ring gear being displaced

resting on the diameter is the right one, and the velocities are parallel in pairs. The velocities of the points $N_2'$, $N_2''$ and $N_2'''$ will be likewise found by drawing lines parallel to the members—the sides of the isosceles triangles $C'N_c'N_2'$, $C''N_5''N_2''$ and $C'''N_c'''N_2'''$. Therefore, $cn_2' = cn_c'$ and defines with them an angle equalling $180° - 2\alpha$. The same is true of the segments $cn_2''$ and $cn_c''$; $cn_2'''$ and $cn_c'''$.

The points $n_2'$, $n_2''$ and $n_2'''$ also belong to the circumference of the diameter $pc$, in similarity with the points $n_c'$, $n_c''$ and $n_c'''$. The floating gear *1* is suspended from the three arms $N_1'N_2'$, $N_1''N_2''$ and $N_1'''N_2'''$, so that the calculation of the velocity of this member should begin with determining the velocities of the specific points $T'$, $T''$ and $T'''$ of intersection of the arms.

Owing to the members being perpendicular in pairs and their corresponding parallel velocity segments being also perpendicular in pairs, the representations of the specific points will belong to the end of the diameter $c$ ($t'$, $t''$ and $t'''$) and will coincide. As these points are the points of the gear *1*, whose velocities are equal to one another, the gear *1* should move through a translatory motion, its velocity being represented by the segment $pt$. From the isosceles triangle $pct$ (cf. Fig. 5.4*a*):

$$\frac{pt'}{pc} = 2\cos\alpha = \frac{E_{c4}}{E_4}$$

i.e. the same expression (5.3) is obtained. The centre of the floating gear will move along a circle of the radius $E_{c4}$, caused by the eccentricity of the carrier, making one full revolution per revolution of the carrier. This radius related to the skewing angle and the rise of the barrel shape of the teeth should be used as a base for determining the tolerance for the eccentricity of the carrier. The above-drawn relationship simplifies the discussion of the case of a floating carrier.

When the central gear displaces radially by a value $E_1$, the displacement of the floating carrier will be:

$$E_{cr1} = \frac{E_1}{2 \cos \alpha}$$

If the first central gear is carried by a shaft with the eccentricity $E_1$, the floating carrier should describe a circle of a radius $E_{cr}$, making one revolution per revolution of the first central gear. The centrifugal force acting upon the carrier is:

$$\omega_1^2 m_{cr} E_{cr1} = \omega_1^2 \frac{m_{cr} E_1}{2 \cos \alpha}$$

As $\omega_1$ is of a relatively high value, the centrifugal force could be considerable. To reduce it, the value of tolerable eccentricity of the central gear should be kept small (with the carrier floating).

The case of an eccentricity $E_3$ (runout) of the ring gear may be likewise considered with aid of a velocity polyhedron (cf. Fig. 5.4*b*, *c*). Let us assume that the carrier is stationary. Then the points $C'$, $C''$ and $C'''$ will coincide with the pole $p$. Taking that the ring gear moves horizontally, the velocities of the points $N_3'$, $N_3''$ and $N_3'''$ will be equal and represented by a segment $pn_3$. Same as in Fig. 5.4*a*, we shall find points $n_c'$, $n_c''$ and $n_c'''$ by drawing lines parallel to the members. The points will belong to a circle of the diameter $pn_3$. Similarly, we shall find points $n_2'$, $n_2''$ and $n_2'''$ by drawing lines parallel to the members—the sides of the rigid isosceles triangles. They will belong to the circumference of the circle of the diameter $pt = pn_3$.

All the three specific points coincide at point $t$ at the end of the diameter $pt$. Therefore, the floating gear *1* moves through a translatory motion, the velocities of all its points being represented by the segment $pt$. Hence, the eccentricity $E_3$ would cause a displacement of the centre of the gear *1*, equal to it. The direction of this displacement defines an angle $180° - 2\alpha$ with the direction of $E_3$.

To investigate the influence of a runout (eccentricity) of a satellite gear upon the performance of the mechanism, let us consider a

gearing with a stationary carrier and a floating central gear (Fig. 5.5). The centre of the satellite gear (of the idler) would move here along a circle of a radius equalling its eccentricity, $E_2$. Let us devide the displacement of the satellite gear into the radial and tangential

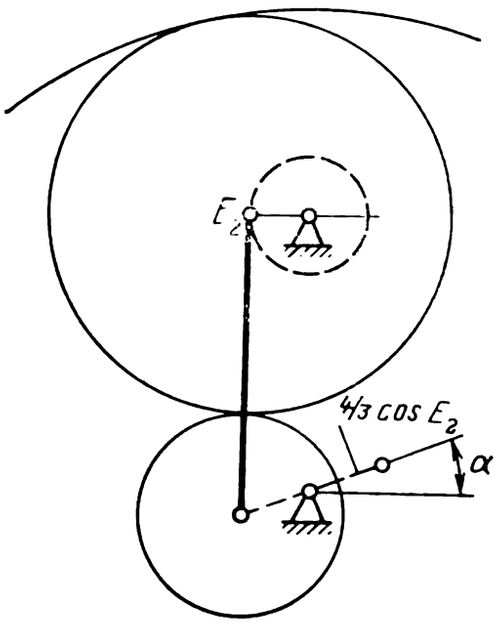


Fig. 5.5. Displacement of floating gear, caused by satellite gear eccentricity

ones. The first one will not influence the position of the central gear, whereas the other varies in accordance with the harmonic law, being as it is the projection of a point uniformly moving along a circle. The tangential displacement of the satellite gear will cause a proportional displacement of the floating central gear. Thus, the centre of the floating gear will move rectilinearly in accordance with a harmonic law with the amplitude $\frac{4}{3} E_2 \cos \alpha$. The direction of this motion will define an angle $\alpha$ with the direction of the tangential displacement, its full period corresponding to one full res volution of the satellite gear. Should all the three satellite gear- have eccentricities, the displacements of the central gear, caused by them, will be expressed as their geometric sum. For the most adverse case this sum will equal:

$$A_c = \frac{4}{3} E_2 \cos \alpha + 2 \frac{4}{3} E_2 \cos \alpha \cos 60° = \frac{8}{3} E_2 \cos \alpha \qquad (5.4)$$

i.e. the amplitude will only double, not treble.

The maximum inertia force of the central gear is

$$\omega_2^2 m_1 \frac{8}{3} E_2 \cos \alpha$$

If it is the carrier that floats, it would move along the same line with the same full period, but the amplitude would be 2 cos $\alpha$ times smaller [cf. (5.3)], i.e. the amplitude would be $\frac{4}{3} E_2$.

The maximum inertia force of the carrier is then

$$\omega_2^2 m_{cr} \frac{4}{3} E_2$$

There remains in the planetary mechanism the harmonic oscillation of the floating member, caused by the eccentricity of the satellite gear. Its amplitude in the case of the floating central gear is still (8/3) $E_2 \cos \alpha$, and with the floating carrier it is (4/3) $E_2$.

However, the straight line along which this oscillation occurs would not remain stationary and would rotate together with the carrier. The period of this oscillation, i.e. the interval between two extreme positions corresponds to the time of one full revolution of the satellite gear about the carrier.

The influence of the runout of the satellite gears onto the performance of the mechanism can be either avoided or at least minimized by proper setting of the directions of the eccentricities of the satellite gears while assembling the unit, so that their action upon the mechanism should counterbalance one another. To do this, the directions of the eccentricities (the runout directions) of the satellite or planet gears are indexed in assembling fan-wise, with satellite gears being selected for assembling in one reduction gear having the same degree of eccentricity.

Expressions (5.1)-(5.4) are preferably united in Table 5.1 where the argument (the kind of tolerance) can be used to find easily its influence upon the eccentricity of the floating gear or the floating carrier.

The most adverse is the case where the mentioned defects sum up to influence the total skewing of the floating member.

With the floating central gear, its eccentricity is made up of its own eccentricity $E_1$, that of the supporting gear, $E_3$, caused by the tangential displacement $E_{ce} = (4/3)\, e \cos \alpha$ of the satellite gear, caused, in its turn, by the eccentricity $E_{c4} = 2\, E_4 \cos \alpha$ of the carrier and of the lateral displacement caused by the eccentricity of all the three satellite gears, i.e. $A_c = (8/3)\, E_2 \cos \alpha$.

As all the abovementioned eccentricities are random (not correlated) ones, square addition is preferably used. Thus, the complete displacement $E_c^2 = E_{c1}^2 + E_{c3}^2 + E_{ce}^3 + E_{c4}^2 + A_{c2}^2$, or else

$$E_c^2 = E_1^2 + E_3^2 + \left(\frac{4}{3} e \cos \alpha\right)^2 + (2E_4 \cos \alpha)^2 + \left(\frac{8}{3} E_2 \cos \alpha\right)^2 \quad (5.5)$$

*Table 5.1*

| Argument | Eccentricity | |
|---|---|---|
| | of floating gear | of floating carrier |
| $e$ | $E_{ce}=\frac{4}{3}e\cos\alpha$ | $E_{cre}=\frac{2}{3}e$ |
| $E_1$ | $E_{c1}=E_1$ | $E_{cr1}=\frac{E_1}{2\cos\alpha}$ |
| $E_2$ | $A_{c2}=\frac{8}{3}E_2\cos\alpha$ | $A_{cr2}=\frac{4}{3}E_2$ |
| $E_3$ | $E_{c3}=E_3$ | $E_{cr3}=\frac{E_3}{2\cos\alpha}$ |
| $E_4$ | $E_{c4}=2E_4\cos\alpha$ | $E_{cr4}=E_4$ |

The above expression is true both for the case of a small floating central pinion and with a central internal (ring) gear. With the floating carrier, its displacement is $2\cos\alpha$ times smaller, i.e.

$$E_{cr}^2=\frac{E_1^2+E_3^2}{(2\cos\alpha)^2}+\left(\frac{2}{3}e\right)^2+E_4^2+\left(\frac{4}{3}E_2\right)^2 \qquad (5.6)$$

A displacement of a floating member causes its skewing. The most adverse case is the one where the displacements in the assemblies supporting the floating member are directed opposingly. Assuming these displacements equal, we find that the skewing angle equals $\delta = 2E/l$, where $l$ is the length of the floating member.

Skewing of the axes causes gaps at the sides of the meshing teeth, so that their performance becomes similar to that of barrel-shaped ones. In practice, however, the rise of this barrel shape is infinitesimal; nevertheless, its value should be checked from (4.31):

$$f=\frac{(b\delta)^2}{32m\,(z_1+z_2)\sin^3\alpha}$$

where $b$ is the length of the tooth.

The value of this rise can be used to set the tolerances of the parts of the mechanism. Quite obviously, these tolerances would be much greater than those associated with a statically indeterminate mechanism.

**Example.** For the case of a floating central gear $m = 3$; $z_1 = 20$; $z_2 = 40$; $\alpha = 20°$; $e = 0.2$ mm; $b = 25$ mm; $l = 100$ mm; $E_1 = E_2 = E_3 = E_4 = 0.05$ mm.

Then, from (5.5):

$$E_c^2 = E_1^2 + E_3^2 + \left(\frac{4}{3} e \sin\alpha\right)^2 + (2E_4 \cos\alpha)^2 + \left(\frac{8}{3} E_2 \cos\alpha\right)^2$$

$$E_c^2 = 2 \times 0.05^2 + \left(\frac{4}{3} 0.2 \sin 20°\right)^2 + (2 \times 0.05 \cos 20°)^2 + \left(\frac{8}{3} 0.05 \cos 20°\right)^2$$

$$E_c^2 = 2 \times 0.05^2 + 0.251^2 + 0.094^2 + 0.125^2$$

$$E_c^2 = 0.303 \text{ mm}$$

$$\delta = \frac{2E}{l} = \frac{2 \times 0.303}{100} = 0.00606$$

$$f = \frac{(25 \times 0.00606)^2}{32 \times 3 \times 60 \sin^3 20°} = 0.0000998 \text{ mm} \approx 0.1 \text{ micron}$$

i.e. notwithstanding the given big tolerances, with the spherical bearings of the satellite gears the rise of the barrel shape has proved to be infinitesimal, which means that the engagement of the teeth is practically along a line.

## 5.2. Friction in Connection Mechanisms

The self-aligning member is connected to the driving shaft by a mobile joint (a toothed universal joint, a slider coupling, a Hooke's joint). The friction in this mobile joint, however, distorts the balance of forces acting upon the satellite gears (Fig. 5.6).

Let us denote: $Q_0$—mean circumferential force; $Q_1$, $Q_2$ and $Q_3$—normal forces transmitted by the satellite gears; $F$—the force of friction in the mobile joint; $\beta$—angle defined by this force with $Q_1$.

Then,

$$Q_1 + Q_2 + Q_3 = \frac{3Q_0}{\cos\alpha}$$

By projecting these forces onto the direction $Q_1$:

$$-Q_1 + \frac{Q_2 + Q_3}{2} + F\cos\beta = 0$$

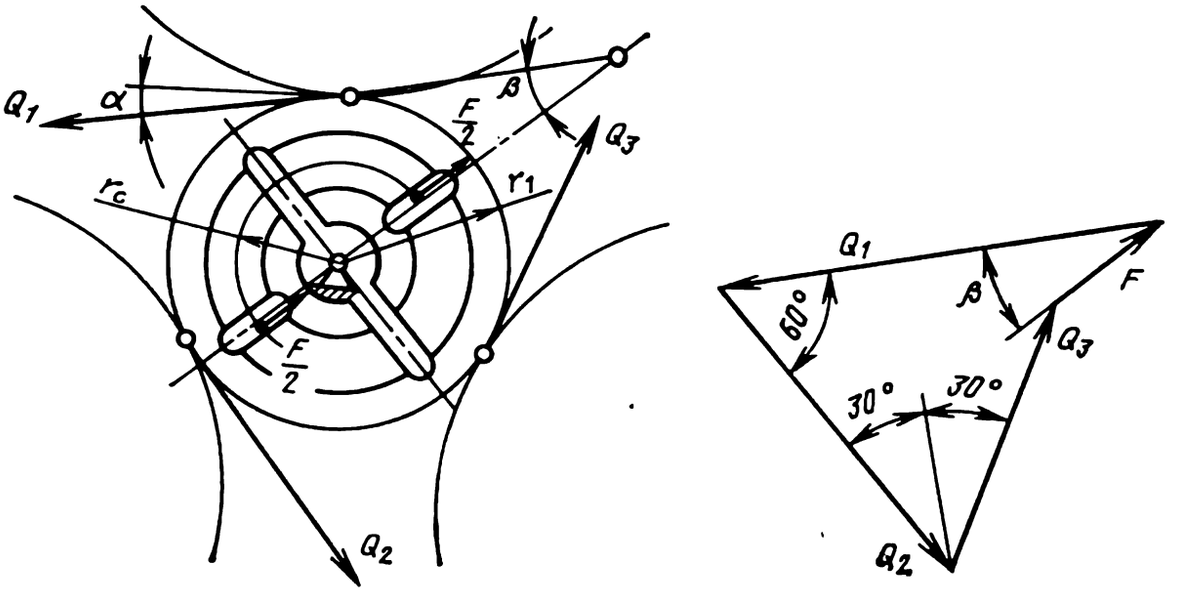


Fig. 5.6. Influence of friction on forces transmitted by satellite gears

Let us multiply the latter expression by two and subtract it from the first one:

$$3Q_1 - 2F\cos\beta = \frac{3Q_0}{\cos\alpha}$$

Thus,

$$Q_1 = \frac{Q_0}{\cos\alpha} + \frac{2}{3}F\cos\beta$$

Let us consider the variation of the forces transmitted by the satellite gears in a single-row planetary gearing with the floating central (sun) gear on account of the friction in the connection mechanism. With the carrier eccentricity $E_4$, the floating gear displaces through $E_{c4} = 2E_4\cos\alpha$ in the direction defining the angle $\alpha$ with the direction of $E_4$. With the carrier rotating, the centre of the floating gear moves along a circle of the radius $E_{c4}$ with the same period, i.e. the position of the central gear relative to the carrier would not vary. Thus, $\beta$ = const, and the forces $Q_1$, $Q_2$ and $Q_3$ would also be constant, although, naturally, not equal to one another. The picture would be exactly the same when the satellite gear displaces tangentially.

Let us consider the eccentricity $E_3$ of the supporting gear which may be particularly big, for it is influenced by the accuracy of several connections. The eccentricity $E_3$ causes displacement of the centre of the floating gear through $E_{c3} = E_3$ in a direction at an angle $2\alpha$, after which the centre remains stationary. Therefore, $\beta$ would equal the angle of rotation of the carrier, and the forces

$Q_1$, $Q_2$ and $Q_3$ would vary in accordance with first-order sine curves relatively displaced, naturally, through 120°.

Similarly, the eccentricity of the floating gear would cause variation of the forces $Q_1$, $Q_2$ and $Q_3$ according to sine curves, with the period equalling one full revolution of the gear relative to the carrier.

With $\beta = 0$,

$$Q_1' = \frac{Q_0}{\cos \alpha} + \frac{2}{3} F$$

With $\beta = 180°$,

$$Q_1'' = \frac{Q_0}{\cos \alpha} - \frac{2}{3} F$$

Let us determine the coefficient of the rising of the forces, i.e. the ratio of the maximum force to the mean one:

$$\Omega = \frac{Q_1'}{Q_0} \cos \alpha$$

or

$$\Omega = 1 + \frac{2}{3} \frac{F}{Q_0} \cos \alpha \qquad (5.7)$$

In a slider coupling (cf. Fig. 5.6):

$$F = 3Q_0 \frac{r_1}{r_c} f$$

where $r_c$ is the mean radius of the coupling.

By substituting this expression in (5.7):

$$\Omega = 1 + 2 \frac{r_1}{r_c} f \cos \alpha$$

With $f = 0.1$, presuming $\frac{r_1}{r_c} \cos \alpha = 1$, we have $\Omega = 1.2$.

If one remembers that in the absence of an equalizing mechanism the forces are considered acting upon but two satellite gears out of the three, it is clear that a slider coupling provides practically no equalizing action, and thus it should not be used. An exception is the case where the sliders are replaced in the coupling by rollers on antifriction bearings. Mechanisms of this kind have been suggested by Yu. A. Grin, and they are used in planetary gearings having two internal gears (cf. Fig. 5.24 below).

A toothed universal joint imposes three restraints, transmitting forces along two axes and a torque about the third one, i.e. it is a third-class kinematic pair $III_5''$. However, if limiting rings are

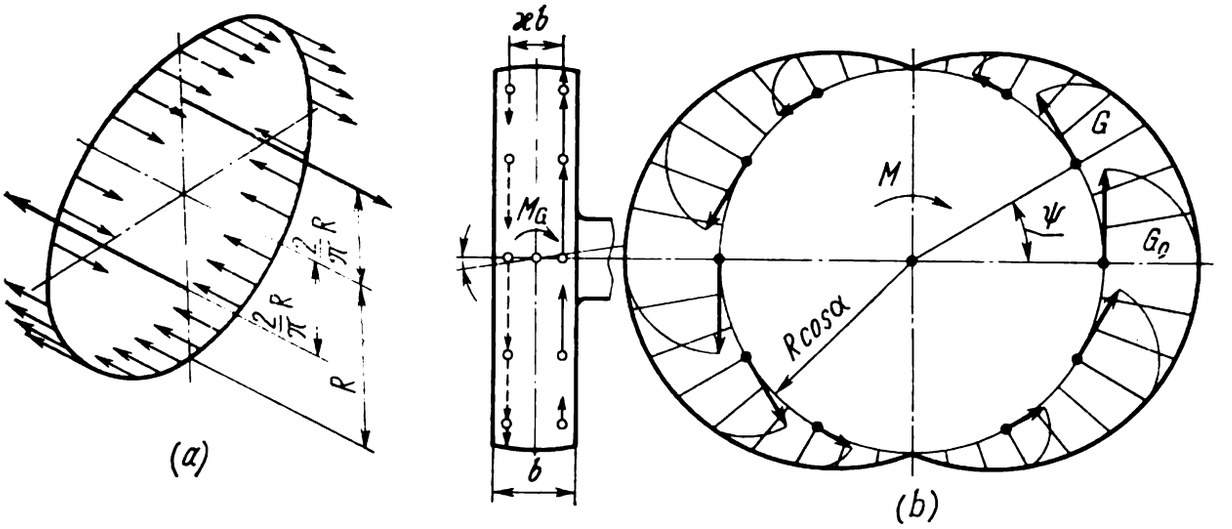


Fig. 5.7. Forces acting in toothed universal joint

mounted in the joint, it becomes capable of transmitting a force also along the third axis. Thus, a toothed universal joint with limiting rings will be considered a $IV_5$ fourth-class pair.

When the shafts define an angle $\delta$, the force transmitted by each tooth of the joint fails to pass through the centre of a tooth and is offset sideways (Fig. 5.7*a*). The offsetting is in opposite directions at the two halves of the base cylinder.

If the tooth is a cylindrical one, the planes including the forces being transmitted align with the end face ones (when deformation of the teeth is not taken into account). If the tooth is a barrel-shaped one, the planes will be spaced by $\varkappa b$ (Fig. 5.7*b*) where $\varkappa < 1$ and depends on the rise of the barrel shape and the angle between the shafts. However, $\frac{\varkappa b}{2} = x$ should not be found from (4.2), as this expression has been derived for the case of barrel-shaped teeth on both meshing gears, whereas in a toothed universal joint only one gear has barrel-shaped teeth. Therefore, the value of $x$ would be twice as great, i.e. $x = \frac{\varkappa b}{2} = \frac{b^2\delta}{8\Delta}$.

This arrangement of the forces produces a torque $M_G$ acting upon the toothed joint and depending on its geometry. Let us call this torque or moment the geometric one. To determine it, let us switch from discrete distribution of the forces transmitted by the teeth to conditional continuous distribution over the base circle of the toothed universal joint, of a radius $R\cos\alpha$ [9]. Assuming (as it is usually done) that the effort is distributed about the circumference of the coupling by the cosine law $G = G_0\cos\psi$, where $G$ is the transmitted force per 1 mm of the base circle of the coupling; $G_0$ is its maximum

value, $\psi$ is the angle between $G$ and $G_0$, we shall determine $G$ by finding the torque $M$ transmitted by the coupling. The force with an angle $d\psi$ is $GR \cos \alpha \, d\psi$; the torque with the angle $d\psi$ is

$$dM = G (R \cos \alpha)^2 \, d\psi = G_0 \cos \psi R^2 \cos^2 \alpha \, d\psi$$

Then,

$$M = G_0 R^2 \cos^2 \alpha \, 2 \int_{-\frac{\pi}{2}}^{+\frac{\pi}{2}} \cos \psi \, d\psi = 4 G_0 R^2 \cos^2 \alpha$$

$$G_0 = \frac{M}{4R^2 \cos^2 \alpha}; \quad G = \frac{M \cos \psi}{4R^2 \cos^2 \alpha}$$

Let us now determine the torque $M_G$: the force with the angle $d\psi$ is

$$GR \cos \alpha \, d\psi = \frac{M \cos \psi \, d\psi}{4R \cos \alpha}$$

its projection onto a vertical line is

$$\frac{M \cos^2 \psi \, d\psi}{4R \cos \alpha}$$

and the torque is

$$dM_G = x \frac{M \cos^2 \psi \, d\psi}{4R \cos \alpha}$$

By substituting $x = \frac{b^2 \delta}{8\Delta}$ and integrating the expression upon the substitution,

$$M_G = M \frac{b^2 \delta}{32 R \Delta \cos \alpha} 2 \int_{-\frac{\pi}{2}}^{+\frac{\pi}{2}} \cos^2 \psi \, d\psi$$

but

$$\int_{-\frac{\pi}{2}}^{+\frac{\pi}{2}} \cos^2 \psi \, d\psi = \int_{-\frac{\pi}{2}}^{+\frac{\pi}{2}} \frac{1 + \cos 2\psi}{2} \cdot \frac{d(2\psi)}{2} = \pi/2$$

Substituting this into the expression of $M_G$, we obtain:

$$M_G = M \frac{\pi}{32} \frac{b^2 \delta}{R \Delta \cos \alpha} \tag{5.8}$$

i.e. the torque $M_G$ depends on the ratio of the square length of a tooth to the radius of the coupling, $\frac{b^2}{R}$, and on the angle $\delta$ between the shafts.

The moment of friction $M_F$ in the universal joint can be found in a similar way. The force with the angle $d\psi$ equals

$$GR\cos\alpha\, d\psi = \frac{M\cos\psi\, d\psi}{4R\cos\alpha}$$

the friction force is

$$f\frac{M\cos\psi\, d\psi}{4R\cos\alpha}$$

and with the friction acting at the pitch circle, its moment at the arm $R\cos\psi$ is

$$dM_F = \frac{Mf\cos\psi\, d\psi}{4R\cos\alpha} R\cos\psi$$

Thus,

$$M_F = \frac{M}{4}\frac{f}{\cos\alpha} 2\int_{\frac{-\pi}{2}}^{\frac{+\pi}{2}} \cos^2\psi\, d\psi = \frac{M}{2}\frac{f}{\cos\alpha}\frac{\pi}{2}$$

or

$$M_F = \frac{\pi}{4}\frac{fM}{\cos\alpha} \tag{5.9}$$

i.e. the moment of friction is dependent neither on the radius $R$ of the coupling, nor on the length $b$ of the tooth, nor on the angle $\delta$ between the shafts.

The moments $M_G$ and $M_F$ act at right angles, so that the resultant moment is

$$M_M = \sqrt{M_G^2 + M_F^2} = \sqrt{\left(M\frac{\pi}{32}\frac{b^2\delta}{R\Delta\cos\alpha}\right)^2 + \left(\frac{\pi}{4}\frac{fM}{\cos\alpha}\right)^2}$$

or

$$M_M = \frac{\pi}{4}\frac{M}{\cos\alpha}\sqrt{\left(\frac{b^2\delta}{8R\Delta}\right)^2 + f^2} \tag{5.10}$$

To illustrate: if $f = 0.1$, $\frac{b}{R} = \frac{1}{5}$, $\frac{b}{\Delta} = 100$, $\delta = 1\frac{1^\circ}{2}$ and $\alpha = 20^\circ$, then $M_M \approx 0.1M$.

Let us substitute $M = 3Q_0 r$ in (5.10) to find the force $F$ of friction reduced to the centre of the floating member, by dividing $M_M$ by the length $l$ of the universal joint:

$$F = \frac{3}{4} \frac{\pi Q_0}{\cos \alpha} \frac{r}{l} \sqrt{\left(\frac{b^2 \delta}{8R\Delta}\right)^2 + f^2}$$

By substituting this in (5.7):

$$\Omega = 1 + \frac{\pi}{2} \frac{r}{l} \sqrt{\left(\frac{b^2 \delta}{8R\Delta}\right)^2 + f^2} \qquad (5.11)$$

To reduce the coefficient of the rising of the forces, the length $l$ of the universal joint has to be increased (which, unfortunately, increases the overall dimensions), while $r$ should be as small as possible. Thus, the best solution is to have the small central or sun pinion as the floating member, whereas having the big supporting gear floating is the worst solution, with the floating carrier in-between. Let us calculate the coefficient of the rising of the forces.

For approximate calculation, let us take $M_M = 0.1M$. Then,

$$F = \frac{M_M}{l} = \frac{0.1M}{l} = \frac{0.1 \times 3Q_0 r}{l} \qquad (5.12)$$

By substituting this expression in (5.7):

$$\Omega = 1 + 0.2 \frac{r}{l} \cos \alpha \qquad (5.13)$$

This formula should be regarded as an approximation. More accurate value of $\Omega$ can be obtained from (5.11). To illustrate: with the small central pinion floating, let us take $\frac{r}{l} = \frac{7}{10}$ and $\alpha = 20°$.

From (5.13): $\Omega = 1 + 0.2 \frac{7}{10} \cos 20° = 1.13$, i.e. the value of $\Omega$ rises by 13%. To reduce it, the length of the universal joint shaft has to be increased.

If the supporting internal gear (ring gear) is floating, we should take $\frac{r}{l} = \frac{28}{7} = 4$; then from (5.13): $\Omega = 1 + 0.2 \times 4 \cos 20° = 1.75$, i.e. the value of $\Omega$ rises by 75%. Therefore, this arrangement is capable of compensating only for the eccentricity of the supporting ring gear, as this compensation takes place but once at the very start, and the friction in this case does not influence the distribution of the forces. The construction fails to compensate for manufacturing inaccuracies of other members, as these members cause oscillation of the supporting ring gear, and the friction in the toothed universal

joint is at its fullest. However, we have not taken into account the resilience of the ring gear, which somewhat levels out the loads.

Let us discuss efforts associated with a gimbal joint (Fig. 5.8). The effort applied to the stud of the gimbal is $\frac{3Q_0r}{2R}$.

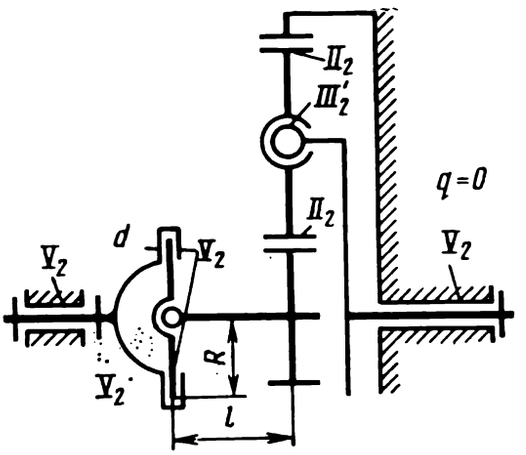


Fig. 5.8. Gimbal mechanism

The moment produced by friction in the gimbal (provided two studs are engaged) equals

$$2\frac{3Q_0r}{2R}\frac{\pi}{2}f\frac{d_g}{2}$$

The friction here (with allowance) is taken from the formula for a new journal, with the reduced friction coefficient $\frac{\pi}{2}f$.

The reduced force of friction:

$$F=\frac{3\pi Q_0rd_gf}{4Rl}$$

By substituting this in (5.7):

$$\Omega=1+\frac{\pi}{2}\frac{r}{l}\frac{d_g}{R}f\cos\alpha$$

To illustrate: with $\frac{r}{l}=0.7$ (as above), $f=0.1$ and $\frac{d_g}{R}=\frac{1}{5}$, we have from the last expression:

$$\Omega=1+\frac{\pi}{2}0.7\,\frac{1}{5}0.1\cos 20^\circ=1.021$$

This design is not practical solely due to designing difficulties involved.

To reduce friction, pivotal or articulated connecting mechanisms are used. Their structure is the simplest with the supporting member floating.

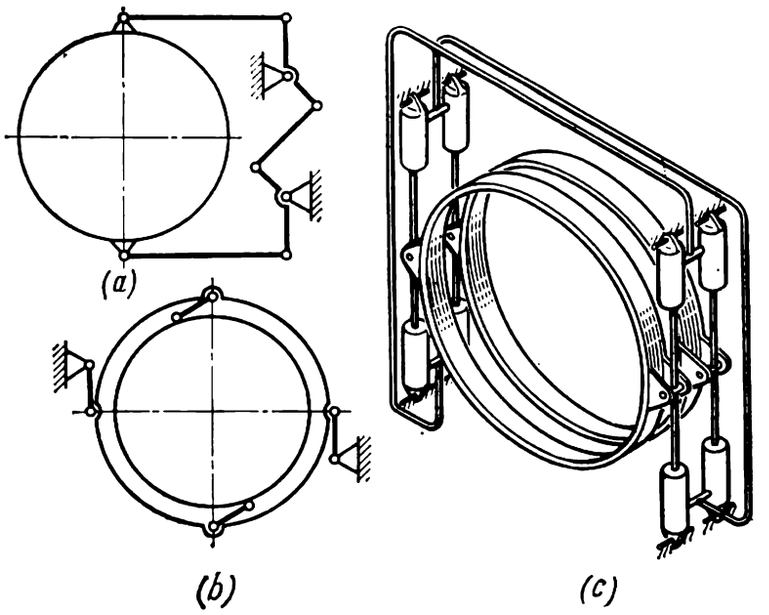


Fig. 5.9. Articulated connection mechanisms

Fig. 5.9*a* illustrates a linkage suggested by G.A. Anopov and A.F. Krainev for motor-drums; Fig. 5.9*b* shows a more compact design, not unlike the Alstom mechanism, used in locomotives.

Hydraulic connecting mechanisms are also used, which also level out the loads of two ring gears (Fig. 5.9*c*). The cylinders are pivotally mounted on the housing, so that their supply conduits should be flexible. The piston rods of the cylinders are likewise pivotally interconnected at their point of connection to the ring gear. Only one hydraulic system is active in the transmission of the torque (with one restraint imposed), levelling out the forces in the four cylinders, with no pressure present in the other system.

The construction should provide means preventing oil spills.

The influence of friction in connecting mechanisms may be eliminated by having all the three major members—the sun gear, the carrier and the ring gear—floating.

Let us consider a single-row mechanism with the sun gear floating on a double-toothed universal joint, with the eccentricity of this gear equalling $E_1$ (Fig. 5.10*a*). The floating gear will position itself centrally between the three satellite gears and will rotate about its geometric centre, while the universal joint shaft will describe a conical surface. The mechanism will perform as if its central gear were ideal: the driving universal-joint shaft and the central gear will rotate as a unity, and no friction will develop in the universal joint. The eccentricity, though, will cause a centrifugal force; thus,

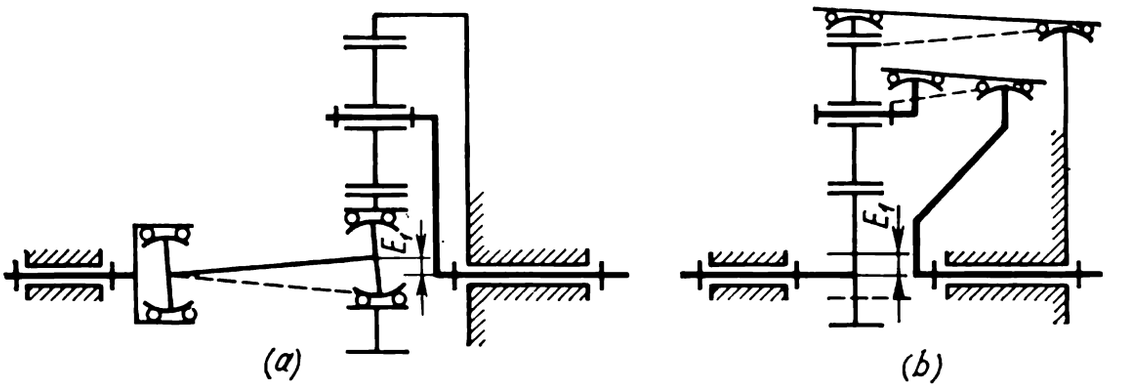


Fig. 5.10. Movement of the connection mechanism in the presence of eccentricity
(*a*) of floating member; (*b*) of member other than floating

care should be taken that it is small enough. The double universal joint will also do away with the skewing of the central gear.

The performance of a mechanism where the central gear has an eccentricity, while either the carrier or the ring gear is floating, will be quite different (Fig. 5.10*b*). In this case the universal joint shafts of either the carrier or the ring gear will likewise describe conical surfaces per one revolution of the central gear. This period, however, will not coincide with the time of full revolution of the floating member. Thus, the carrier, the universal joint shaft and the driven shaft will not rotate as a unity, and the friction in the connection mechanism will influence the performance.

In general, each floating member compensates for its deficiencies with no friction, while compensating for deficiencies of other members with friction developed in the connection mechanism. Quite naturally, with the three members floating, local mobilities will be present, but experience has shown that no oscillatory processes take place in such mechanisms owing to their adequate damping by the friction between the teeth [17].

The performance of the equalizing mechanism may be influenced not only by friction, but by inertia force as well [56].

The degree of uniformity of the distribution of the load among the satellite gears can also be affected by the weight of the floating member. Let us see how the distribution is influenced by the dimensions of the mechanism, which are proportional to the modulus $m$.

The weight of a toothed wheel, usually assumed proportional to the volume of the pitch cylinder, is:

$$G = \gamma V = \gamma \frac{\pi d^2}{4} b = \gamma \frac{\pi}{4} (mz)^2 \psi_m m = \frac{\pi}{4} \gamma z^2 \psi_m m^3$$

i.e. it is proportional to cubed modulus. This could have been also derived directly from the law of similitude, even without resorting to the above assumption.

Let us consider two mechanisms "*a*" and "*b*" whose parameters will be denoted by the respective subscripts. Then,

$$\frac{G_a}{G_b} = \frac{m_a^3}{m_b^3} \tag{5.14}$$

The circumferential forces will be found from the bending strength analysis [2]:

$$m = \sqrt[3]{\frac{2y_F kM}{z\psi_m [\sigma]_b}}$$

where $y_F$ is the strength factor of the tooth;

$k$ is the load factor;

$M = Q\frac{d}{2}$ is the torque being transmitted;

$\psi_m = \frac{b}{m}$ is the factor of the length of the tooth;

$[\sigma]_b$ is the bending stress.

By substituting $M$ and $d = mz$,

$$m = \sqrt{\frac{y_F kQ}{\psi_m [\sigma]_b}}$$

For mechanisms "*a*" and "*b*":

$$m_a = \sqrt{\frac{y_F kQ_a}{\psi_m [\sigma]_b}} \text{ and } m_b = \sqrt{\frac{y_F kQ_b}{\psi_m [\sigma]_b}}$$

so that

$$\frac{m_a}{m_b} = \sqrt{\frac{Q_a}{Q_b}} \text{ or } \frac{Q_a}{Q_b} = \frac{m_a^2}{m_b^2} \tag{5.15}$$

i.e. the relationship is not the cubic one as in 5.14, but a square one.

From the same source [2]:

$$\sigma_s = z_N z_M z_E \sqrt{\frac{q}{d_1} \times \frac{u \pm 1}{u}}$$

where $\sigma_s$ is the contact stress.

$z_N$, $z_M$, $z_E$ are coefficients providing for the shape of the engaging surfaces, the mechanical properties of the gear materials and the end-face engagement factor:

$$u = \frac{z_2}{z_1}; \quad q = \frac{Q}{b}; \quad d_1 = mz_1 \text{ and } \psi_m = \frac{b}{m}$$

By substituting these values:

$$\sigma_s = z_N z_M z_E \sqrt{\frac{Q}{\psi_m m^2 z_1} \frac{u \pm 1}{u}}$$

so that

$$m = z_N z_M z_E \sqrt{\frac{u \pm 1}{\psi_m z_2}} \sqrt{Q}/\sigma_b$$

and

$$\frac{m_a}{m_b} = \sqrt{\frac{Q_a}{Q_b}}, \text{ or } \frac{Q_a}{Q_b} = \frac{m_a^2}{m_b^2}$$

i.e. we have the same expression (5.15).

To evaluate the influence of the weight upon the distribution of the load among the satellite gears, let us find the ratio $G$:$Q$ through dividing (5.14) by (5.15).

In this way we find that

$$\frac{G_a}{Q_a} : \frac{G_b}{Q_b} = \frac{m_a}{m_b}$$

i.e. the larger is the modulus (the size of the reduction gear), the greater is the degree to which the weight of the floating member distorts the distribution of the load among the satellite gears. Thus, with big values of the modulus, it is essential that the weight of the floating member should be as small as possible; in other words, in such cases it is particularly important that the sun pinion should be the floating member, and not the ring gear or the carrier. The said is just as true of a mechanism with a horizontal shaft and three intermediate or idler gears.

In mechanisms with vertical shafts the weight of the floating member has no influence on load distribution among the satellite gears.

In planetary mechanisms, the engagement or meshing angle should be selected of a greater value in multisatellite gearings than in simpler gearings.

When the engagement angle is selected for a gearing, it is commonly accepted that the drawback of a greater angle is the greater outward thrust forces, which is absolutely true of simple gearings. However, the situation in planetary mechanisms with several satellite gears and in mechanisms with several idlers is quite different, because here the forces acting upon the central or sun gear, which in most cases is floating, are counterbalanced and not transmitted to the bearings. The same is true of outward thrust forces acting

upon an internal ring gear, which are not transmitted to the bearings, either. In single-row mechanisms the outward thrust forces acting upon either a satellite gear or an idler are balanced if the engagement angles with the sun and ring gears are the same. Thus, in single-row mechanisms the outward thrust forces acting upon the gears are counterbalanced and do not load the bearings.

If the angle of engagement of the satellite gear with the ring gear is greater than that in the engagement with the sun gear, the difference between the outward thrust forces can be utilized to compensate, either partly or in full, for the centrifugal inertia force of the satellite gear.

Inertia forces are also capable of influencing the performance of an equalizing or balancing mechanism [17], in addition to the influence of friction.

## 5.3. Desings of Single-Row Planetary Mechanisms

Multisatellite modifications of planetary gearings are superior to gearings with stationary shafts in that their dimensions and weight are smaller. Thus, with the transmitted torques and transverse dimensions being the same (i.e. the sum of the diameters of the gears of a single-stage toothed gearing being equal to the ring gear diameter of a planetary one), with three satellite gears and transmission ratios $u = 3$ to 7, the circumferential forces in the planetary gearing are one fourth to one sixth of those of the simple gearing $\left(\text{in general, they are smaller } \frac{1}{3}\frac{u-1}{u+1} \text{ times}\right)$. However, this is true solely when uniform distribution of the circumferential forces among the satellite gears is assured.

In a single-row planetary mechanism without a floating member and three satellite gears with fifth-class bearings (Fig. 5.11*c*) there are eight redundant constraints [33] of which two—the most harmful ones, detected with aid of expression (1.5) for a planar design—cause non-uniform distribution of the circumferential force among the satellites, while the six remaining ones cause uneven loading lengthwise of the teeth in the six engagements. Such a great number of redundant constraints calls for highly accurate manufacturing of such mechanisms.

Non-uniform load distribution among the satellite gears is easily eliminated by providing a floating member, whereas uneven load distribution lengthwise of the teeth is eliminated by providing

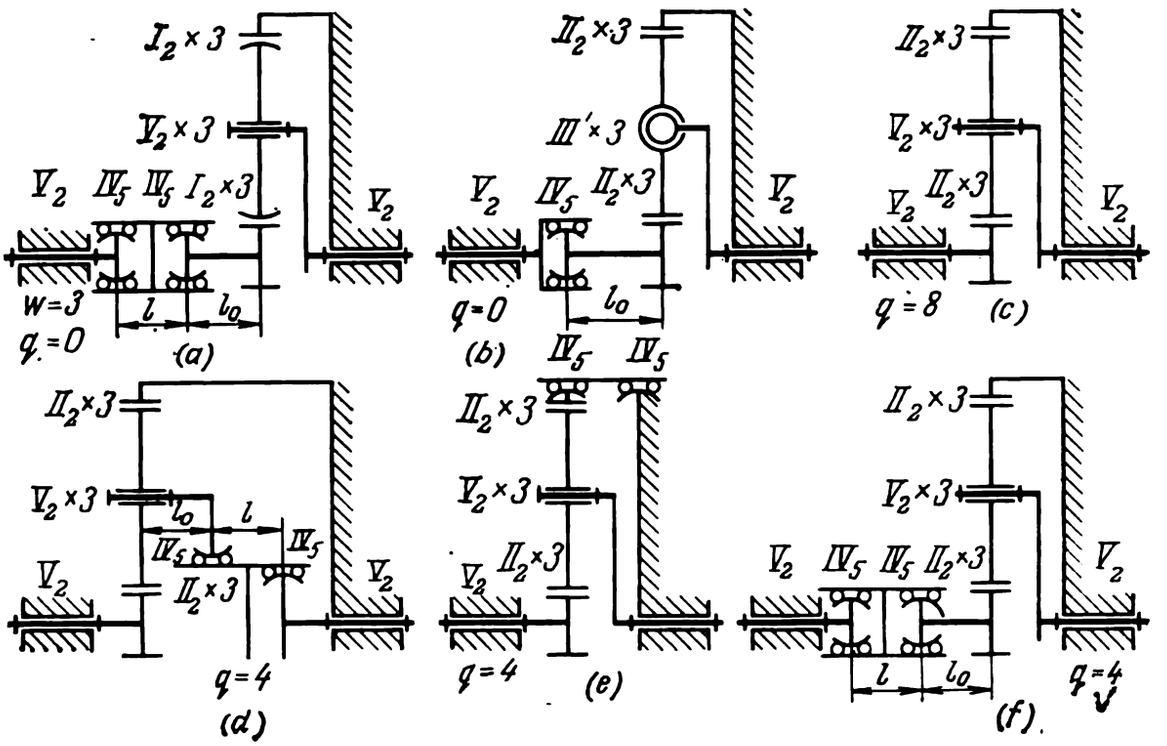


Fig. 5.11. Single-row planetary reduction gears

*a*) with point engagement (free of redundant constraints); (*b*) with one floating member and satellite gears on spherical bearings (free of redundant constraints); (c) nonself-aligning, with eight redundant constraints; (*d*), (*e*) and (*f*) suggested by V. N. Kudryavtsev, with one floating member and four redundant constraints

additional angular mobilities. Those are preferably provided by mounting the satellite gears on spherical *III'* pairs (Fig. 5.11*b*).

It will suffice to mount the floating member on a single toothed universal joint $IV_5$. This design has been tested and proved fully adequate in a mill for rolling ribbed tubing. D.I. Shatkus [50, 60] has used it in the chassis of a grain harvester where it has tripled the durability (Figs. 4.24, 5.12). Thus, a single-row planetary mechanism with satellite gears on spherical bearings can be convincingly recommended for any practical application. Unfortunately, with small transmission ratios (i.e. with small diameters of the satellite gears) the satellite gear fails to accommodate a spherical bearing of adequate capacity. The field of applications of this design can be, however, significantly broadened by using the very satellite gear as the outer race of the spherical bearing (by grinding there the inner spherical surface), i.e. by employing the "satellite-bearing" design, as suggested by G.A. Snesarev. This calls for elaborating a standard for satellite gears of this kind and for arranging their production, and this would be fully justified by the significant increase of the load capacity, which is an ever-important factor. Another way to broaden the field of application is using V.N. Ermak's

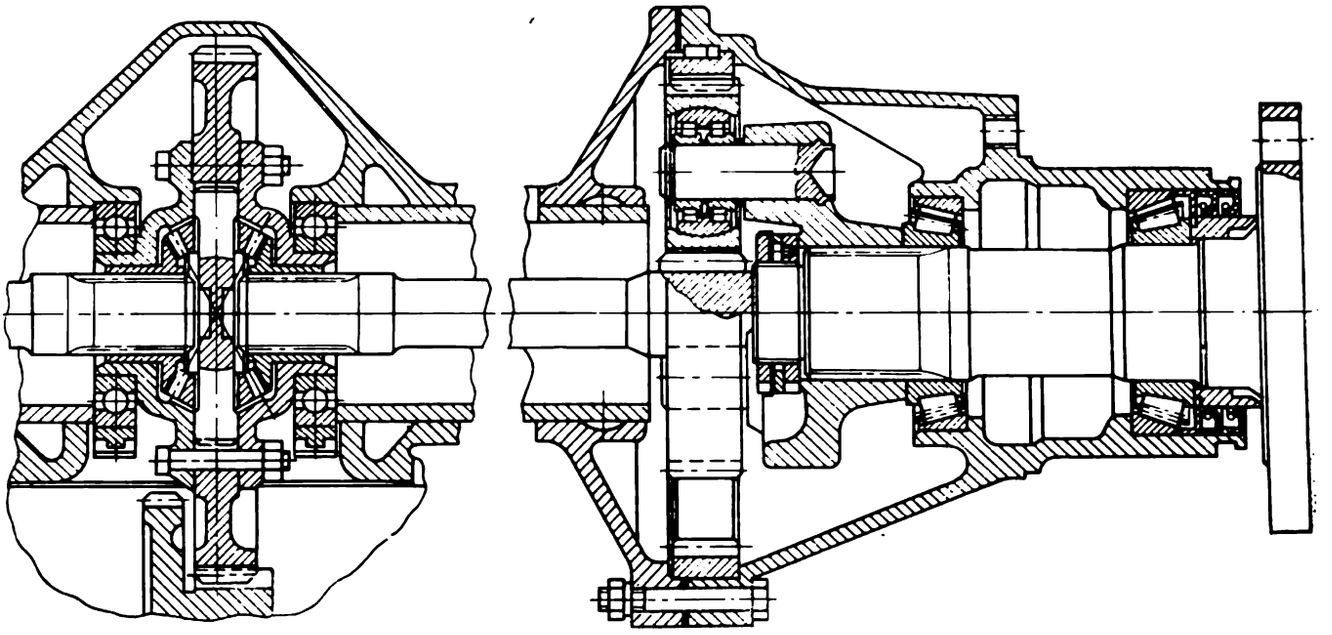

Fig. 5.12. Shatkus's reduction gear for grain harvester, with floating sun gear and satellite gears on spherical bearings (free of redundant constraints)

self-aligning bearing assembly (cf. Fig. 4.25); the third way is to use multi-row satellite gears (cf. Fig. 5.18), or else to use designs developed for electric motor-wheels.

Let us now consider mechanisms to be employed when there is absolutely no way to accommodate a spherical bearing in the satellite gear, i.e. when the satellite gears simply have to be mounted on fifth-class pairs. By using barrel-shaped teeth with point engagement ($I_2$ pairs) and one floating member (cf. Fig. 5.11*a*) redundant constraints can be avoided. It is better to use a double universal joint to minimize the skewing of the shafts, as the barrel-shaped teeth are highly susceptible to it, since the skewing displaces the point of engagement axially. The two local mobilities in this case would not be harmful. Unfortunately, point engagement results in a higher contact stress, as compared with line engagement, which means that the latter should be preferably used. V.N. Kudryavtsev has attained this by using a single floating member on a double universal joint. The floating member may be the central or sun gear (Fig. 5.11*f*), the ring gear (Fig. 5.11*e*) or the carrier (Fig. 5.11*d*). The three versions are not equivalent since friction in the toothed universal joint affects the load distribution among the satellites differently. The best choice is the mechanism of Fig. 5.11*f*, although its axial dimension is substantial, and the worst choice is that of Fig. 5 11*e*, as having the biggest ratio of the floating member radius to the universal joint length.

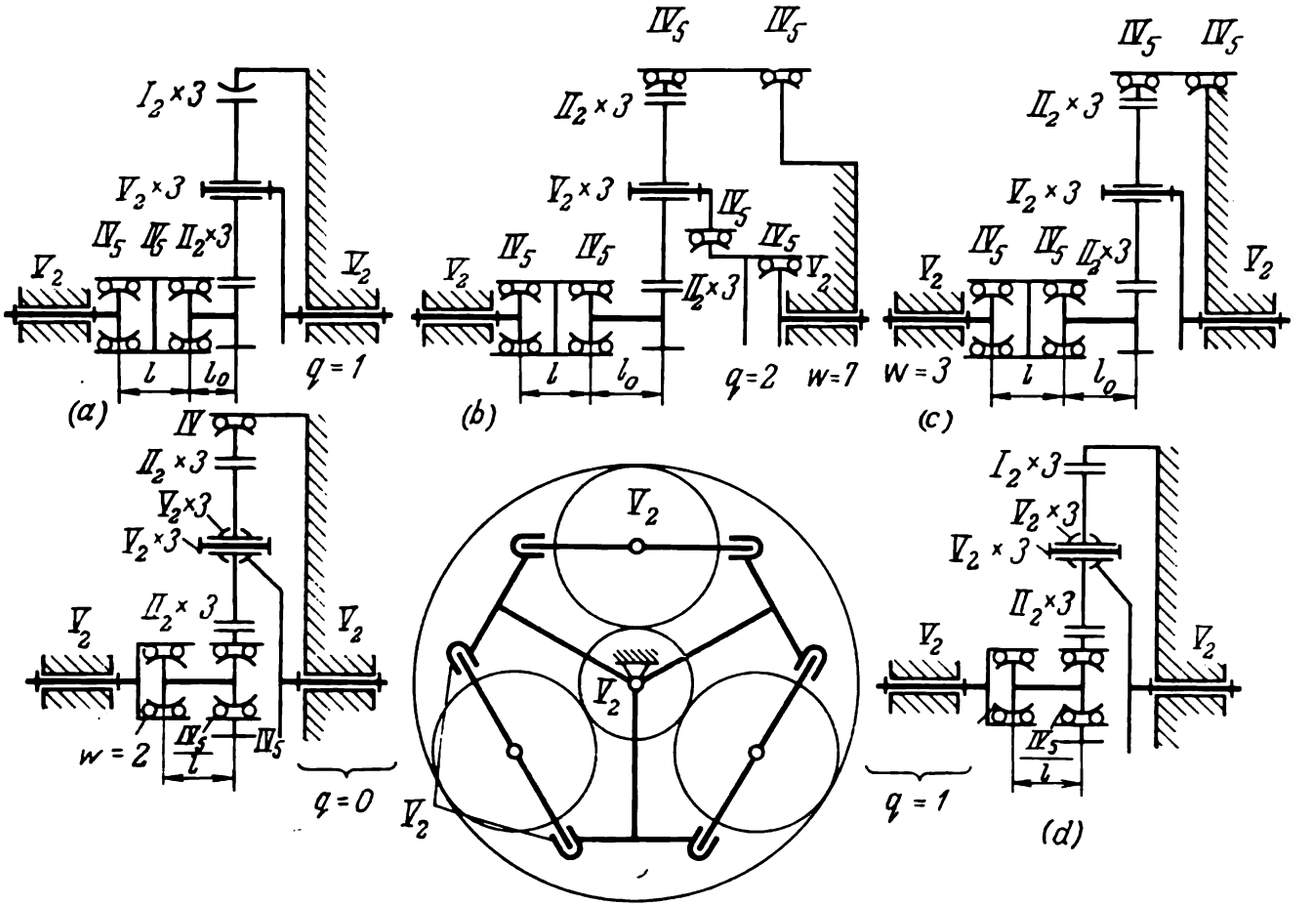


Fig. 5.13. Single-row planetary reduction gears

(*a*) with two floating members on double universal joints (two redundant constraints); (*b*) with three floating members on double universal joints (two redundant constraints); (*c*) Schuster s gears with one floating member on double universal joints and barrel-shaped teeth of ring gear (one redundant constraint); (*e*) with satellite gears on rocking frames and one floating member on double universal joint (one redundant constraint); (*d*) with satellite gears on rocking frames, with one floating member on double universal joint and self-aligning ring gear (no redundant constraints)

The incorporation of a second universal joint yields two angular mobilities (mobilities of the first universal joint are spent on the floating of the sun gear and produce no angular mobilities), whereas six such mobilities are required by the six engagements. Hence, this design lacks four mobilities, i.e. it has four redundant constraints per six engagements. This can be also ascertained from (1.1).

In the design of Fig. 5.11*d*, the axial dimension can be reduced by arranging the intermediate hollow shaft of the double universal joint so that it will encompass the carrier, with corresponding windows provided for the satellite gears. Two more redundant constraints may be eliminated by mounting the ring gear, too, on a toothed universal joint. This would leave two redundant constraints per six engagements. Schtekicht has used a double universal joint (Fig. 5.13*c*) for this purpose, with two local mobilities introduced:

displacement of the central gear and ring gear vertically and their displacement horizontally.

It has been proved above (cf. Fig. 5.4*c*) that any displacement of the ring gear causes displacement of the central or sun gear to the same extent, defining with the first-mentioned displacement an angle equalling $2\alpha$. This angle, however, is of no account when the mobility is determined. Experience has shown that the abovementioned local mobilities are harmless. They are even useful, for in the case of the floating members being eccentric, they would self-center, causing no movement of the rest of the members (cf. Fig. 5.10). For these reasons Schtekicht's mechanism is widely used abroad.

When three members are made floating, the number of redundant constraints is not decreased (cf. Fig. 5.13*b*, where the members are mounted on double universal joints). The explanation is that only two relative angular mobilities are possible between the central gear and the three satellite gears mounted on rotational $V_2$ pairs (apart from the rotation of the mechanism), whereas three such mobilities are required by three engagements. Similarly, one redundant constraint and two local mobilities take place between the ring gear and the satellite gears. Thus, the two angular mobilities of the third floating member would not eliminate redundant constraints and local mobilities would remain. Altogether, the mechanism has six local mobilities and one general mobility. However, in the mechanism (Fig. 5.13*b*), should the three floating members be eccentric, they would self-center causing no movement of the other members of the mechanism. The eventual eccentricity of the three satellite gears remains, though, which may cause additional movement of the entire mechanism. Therefore, it is hardly expedient to have three members of the mechanism floating.

Thus, it is impossible to eliminate redundant constraints by virtue of angular mobility of the major members in the presence of three satellite gears, for two redundant constraints will remain. They can be eliminated by mounting the satellite gears on rocking frames, as suggested by V.M. Yastrebov and F.I. Plekhanov (Fig. 5.13*d*). The pivots of the frames may be very simple, for the relative motion in them is minimal. Now, if one member is mounted on a double universal joint, one redundant constraint is left per six engagements. If the central or sun gear is set on a double universal joint, while the ring gear is mounted on a single one (Fig. 5.13*e*), the redundant constraints are completely avoided. One local mobility appears, though, but it is harmless.

There is one more way of reducing the amount of redundant con-

straints, suggested by A.E. Schuster (Fig. 5.13*c*). In this case line engagement should be between the sun gear and the satellite gears ($II_2$ pair), while point engagement should take place between the satellite gears and the ring gear (pair $I_2$) by having the ring gear with barrel-shaped teeth. The point engagement here is not hazardous, as a convex profile works with the concave one, and the contact pressure values will not be great. A shortcoming of this design is the difficulty of manufacturing a ring gear with barrel-shaped teeth.

There is known a design with the shafts of the satellite gears floating in radial slots. This yields one angular mobility to each satellite gear, similarly to the design with the rocking frame, with one more linear mobility remaining in the radial direction. The satellite is urged toward the ring gear by the centrifugal force, so that this design is suitable in applications only where the centrifugal forces are not excessively high, i.e. either in the last reduction stage (of slow action), or else in case of idle gears.

With a herringbone tooth, it is far more difficult to have a planetary gearing free of redundant constraints, than with straight teeth, since every engagement of the herringbone teeth imposes as many as four restraints. On the other hand, the herringbone tooth allows for having high load capacities with small dimensions.

The Schtekicht's gearing shown in Fig. 5.14*a*, is widely used abroad. It has floating sun gears and ring gears, so that two local mobilities are added to the general mobility—the rotation of the reduction gear.

Let us regard the engagement of herringbone teeth as two second-class pairs. It has been demonstrated above (cf. Fig. 5.4*c*) that any displacement of the ring gear causes displacement of the sun gear of the same extent, at an angle $180° - 2\alpha$ (the angle being of no account for the purpose of determining the mobility). With two floating main members, each mounted on a double universal joint (the toothed universal joint in the design under discussion), this unit of two floating gears has two local group mobilities—in the vertical and horizontal directions, and altogether $w = 3$.

It should be pointed out that the experience of operating Schtekicht's reduction gears has proved these mobilities harmless, with no oscillation processes and shocks detected. It appears that they are well damped by friction in the teeth.

From (1.1): $q = w - 6n + 5p_{\mathrm{V}} + 4p_{\mathrm{IV}} + 3p_{\mathrm{III}} + 2p_{\mathrm{II}} + p_{\mathrm{I}}$, i.e. $q = 3 - 6 \times 11 + 5 \times 2 + 4 \times 8 + 3 \times 1 + 2 \times 12 = 6$.

Let us discuss the harm brought about by these redundant constraints. The torque of the sun gear or pinion is equally divided

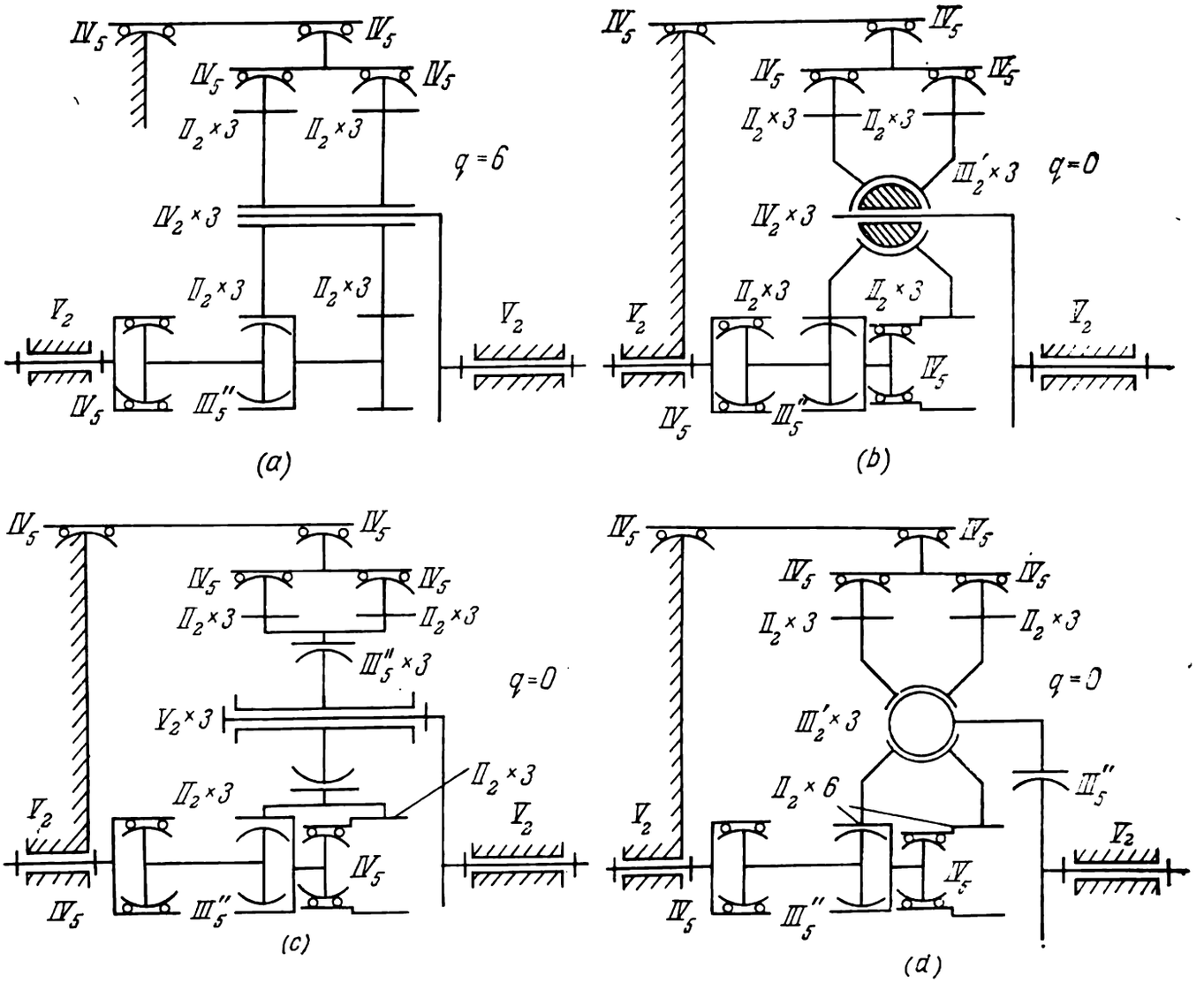


Fig. 5.14. Planetary reduction gears with herringbone teeth
(*a*) Schtekicht's with six redundant constraints; (*b*), (c) and (*d*) without redundant constraints, due to two mobilities at the bearing of each satellite gear and universal joint between the halves of sun gear

among the herringbone halves, owing to the equality of the forces in these engagements. This distribution is due to the axial mobility of the third-class pair in the toothed universal joint.

In each herringbone half the circumferential force is equally distributed among the satellite gears owing to the floating of the respective end of the sun gear. Thus, all the six forces in the six engagements of the sun gear with the three satellite gears are levelled out. The forces in the meshing of the satellite gears with the ring gear are likewise levelled out due to the latter's axial mobility. Thus, the forces in every engagement are levelled out.

To assure uniform distribution of the force lengthwise of the teeth, one angular mobility is required for each simple engagement

(or two for a herringbone engagement), i.e. 12 angular mobilities are required altogether. The Schtekicht's reduction gear being discussed has but six angular mobilities: four in the two toothed universal joints of the ring gears (fourth-class pairs) and two in the second universal joint of the sun gear. Thus, six angular mobilities are lacking. They are the very redundant constraints found from (1.1) above, and they will cause (on account of manufacturing inac-

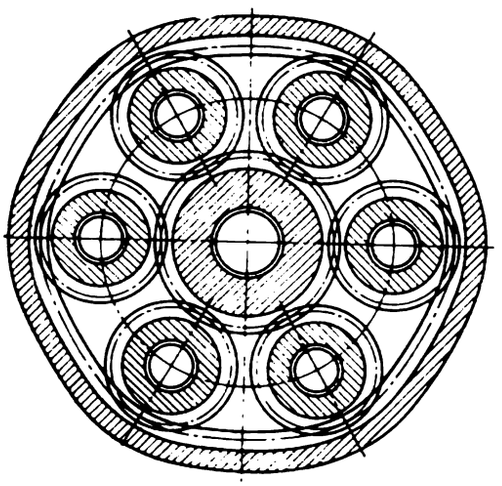

Fig. 5.15. Resilient ring gear in Schtekicht's reduction gears

curacies) non-uniform loading lengthwise of the teeth. To eliminate them, corresponding angular mobilities have to be added. V.G. Frolov has avoided two of the redundant constraints by mounting a universal joint between the gears of the central member. Toothed universal joints are incorporated in the designs shown in Fig. 5.14*b*, *c*, and *d* ($IV_5$ pairs). Third-class pairs should be provided at the shafts of the satellite gears to add more angular mobilities. They are spherical pairs in Fig. 5.14*b*, with the intermediate block being connected to the carrier by a fourth-class cylindrical pair, so as not to lose the axial mobility required.

The mobilities in this design are different from those in Fig. 5.14*a*. In addition to the group linear mobilities of the sun gear with the ring gears in the vertical and horizontal directions, there are also two more angular mobilities. The sun gear may have instantaneous angular mobility about the vertical axis, with corresponding displacement of the satellite gears and ring gears, the spherical bearings of the satellite gears not opposing such displacement (unlike the cylindrical ones of Fig. 5.14*a*). Neither should the double toothed universal joints of the sun gear nor of the ring gears oppose this displacement. Similar group angular mobility takes place about the transverse axis, too. The blocks have a local mobility—rotation about their own axes, i.e. in the entire mechanism $w = 8$.

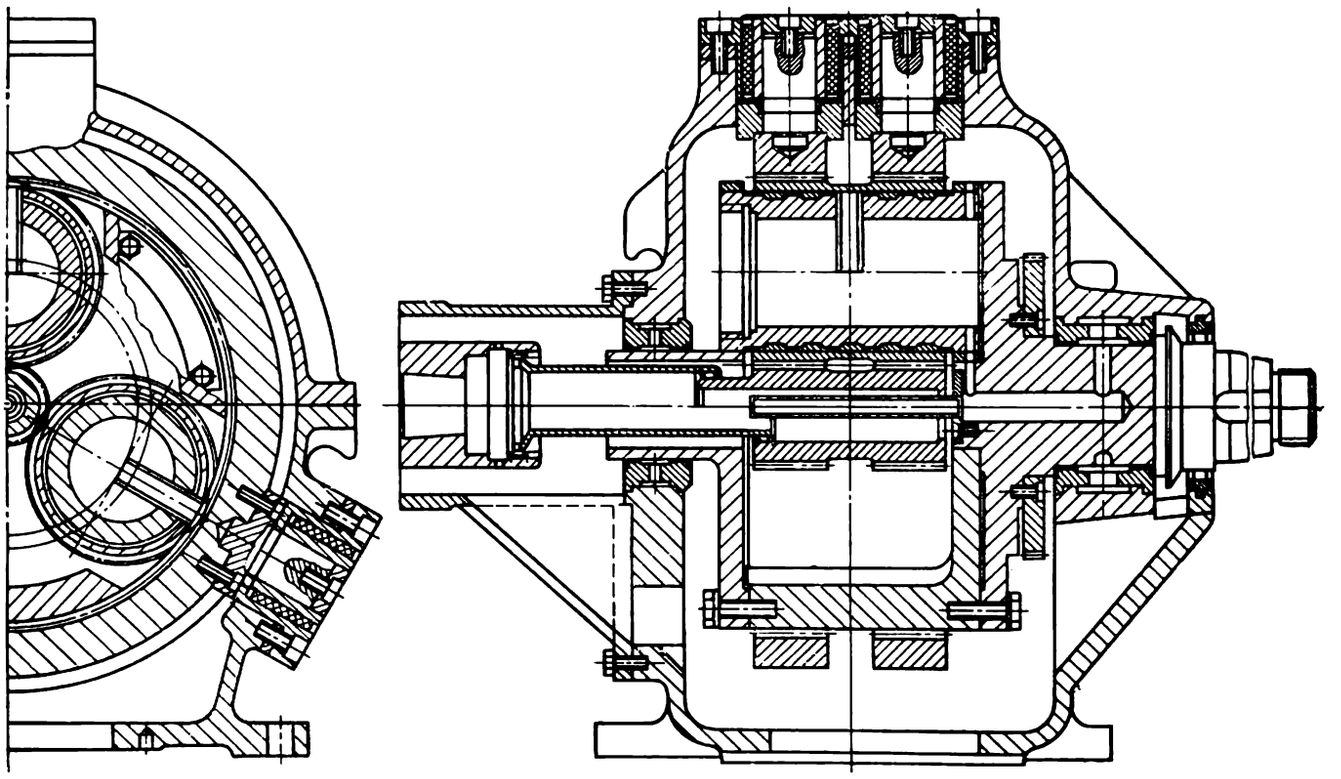

Fig. 5.16. Resilient bearing units of ring gears in Skoda reduction gear

In Fig. 5.14*c* the satellite gear is connected with the intermediate sleeve by a third-class toothed universal joint yielding two angular mobilities and the necessary axial one. In Fig. 5.14*d* the satellite gear is connected to the carrier by a third-class spherical pair. To retain the axial mobilities of all the three satellite gears, the carrier is connected with its shaft by a third-class toothed universal joint. The designs of Fig. 5.14*c*, *d* have no blocks, so that $w = 5$.

When a universal toothed joint transmits a torque to a helical gear, it is expected to transmit also an axial force. To attain this, the universal joint should have likewise helical teeth, with the axial pitch of its helix equalling that of the gear it drives.

Resilience is in some cases employed in mechanisms with redundant constraints to minimize the latter's influence. Thus, Schtekicht has used resilience of the ring gear in a gearing with six satellite gears (Fig. 5.15). Another example of this approach is one of Skoda designs where the internal gears are connected with the housing through rubber bushes (Fig. 5.16).

## 5.4. Tolerances in Single-Row Mechanisms

The USSR State Standard 1643-72 stipulates the values of the minimum displacement $A_H$ of the initial contour and of tolerances $T_H$ for its displacement, providing not only for a guaranteed lateral gap $j_n$, but also for possible inaccuracies in manufacture and assembling, caused by deviations of the inter-axial spacing $f_a$, runout $F_r$ of ring gears, deviations $F_\beta$ of the direction of the teeth, non-parallelism $f_x$ and skewing $f_y$ of the shafts, deviations $f_{pb}$ of the main pitch in both gears of a pair.

Apart from these inaccuracies provided for in standard tolerances for toothed gearings, planetary mechanisms are associated with specific inaccuracies arising from the presence of the carrier and several satellite gears. They call for a specific approach to the selection of the displacement coefficients and geometric computation of the gearings.

**Single-row planetary mechanism without floating members.** Specific inaccuracies associated with a multisatellite planetary mechanism are the eccentricity $E_4$ of the carrier and the tangential displacement $e$ defined by the tolerance on the angle between the satellite gears. To compensate for these inaccuracies, it is necessary to reduce the nominal thickness of the teeth of gears.

Let us determine the additional coefficient $\Delta x$ of displacement of the initial contour, providing for tangential displacement of the centre of a satellite gear from the "ideal" position by a value $E_{\tau 2}$. As the directions of $e$ and $E_4$ are independent of each other,

$$E_{\tau 2} = \sqrt{e^2 + E_4^2} \tag{5.16}$$

At any given moment of time, the sun gears in a multisatellite mechanism may be considered fixed relative to one another. The displacement of the centre of a satellite gear through $E_{\tau 2}$ causes overlapping of the profiles of the teeth. To make assembling possible, the thickness of the teeth along the arc of the pitch circle should be reduced by a value

$$j_w = 2E_{\tau 2} \tag{5.17}$$

The lateral gap along the engagement normal:

$$j_n = j_w \cos \alpha_w \tag{5.18}$$

The additional displacement coefficient, providing for $j_n$:

$$\Delta x' = \frac{j_n}{2m \sin \alpha} \tag{5.19}$$

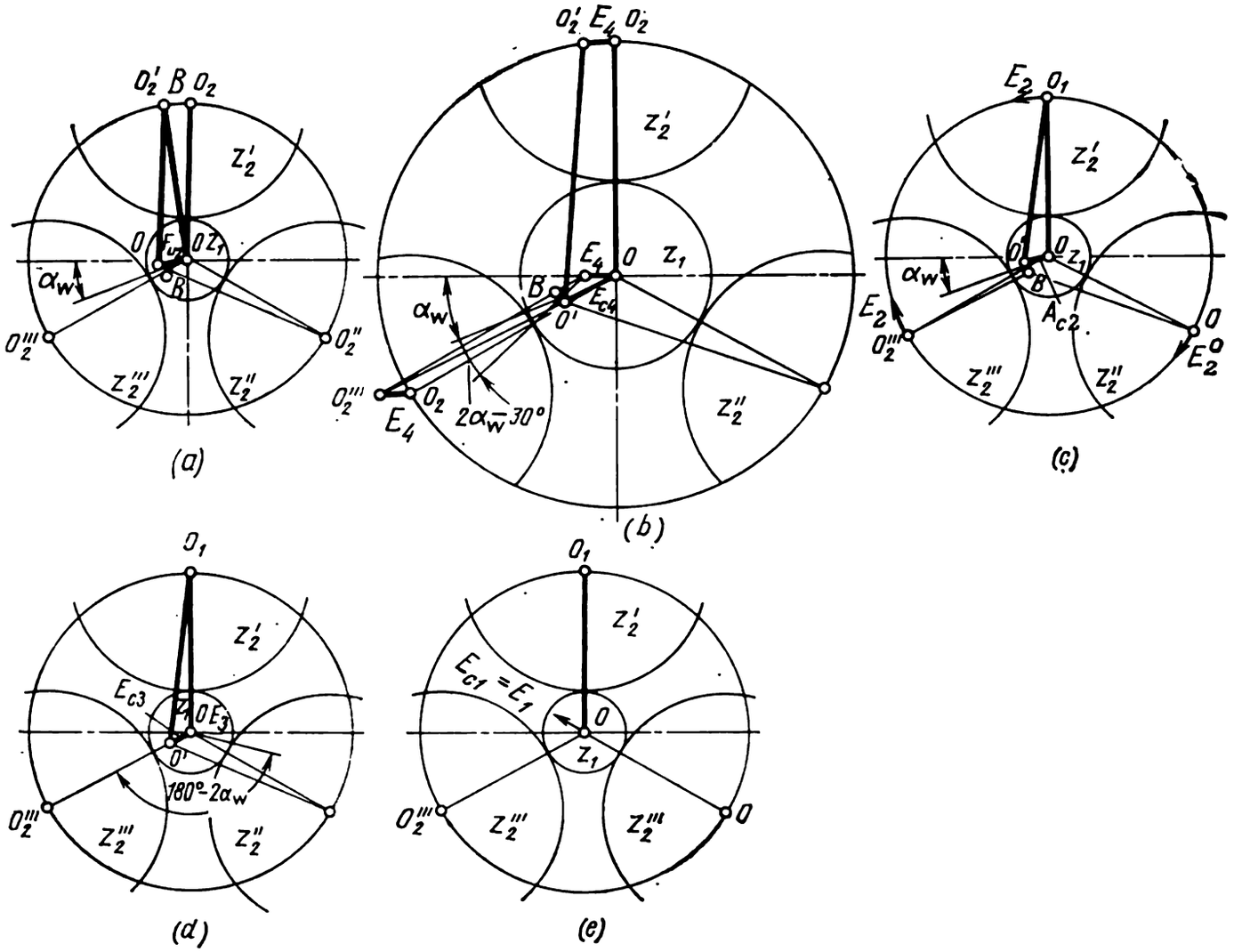


Fig. 5.17. Displacement of floating gear tolerances for dimensions of members (*a*) due to tangential displacement $e$ of satellite gear; (*b*) due to eccentricity $E_4$ of carrier; (*c*) due to eccentricity $E_2$ of satellites; (*d*) due to eccentricity $E_3$ of ring gear; (*e*) due to eccentricity $E_1$ of sun gear

The additional displacement coefficient may be related both to the sun gear $z_1$ and the satellite gear $z_2$. However, with the transmission ratio of the mechanism $u > 3$ and with the sun gear $z_1$ having a small number of teeth, a reduction of the displacement coefficient $x_1$ may cause intolerable undercutting of the teeth of the sun gear $z_1$. In this case it is rational to compensate for irregularities by reducing the displacement coefficient of the satellite gear, as it will be done below, i.e. to take $\Delta x'_2 = \Delta x'$.

The displacement coefficient of the satellite gear:

$$x'_2 = x_2 - \Delta x'_2 \qquad (5.20)$$

When testing the geometric parameters of the quality of the engagements, the possibility of the direction of the eccentricity $E_4$

of the carrier aligning with the line of the centres should be also taken into account.

**Planetary mechanism with a floating member.** Let us consider the influence of each tolerance associated with a planetary mechanism upon the displacement of the floating member $z_1$ in relation to the geometric parameters of the gears.

Tolerance for central angle between the satellites causes (Fig. 5.17*a*) displacement of the floating member $z_1$, determined from (5.1)

$$E_{ce} = \frac{4}{3} e \cos \alpha_w$$

The distance $a_w$ between the axes in the engagement $z_1 z_2'''$ is thus reduced to a value $a_w''' = O_2'''O' \approx O_2B$. Then,

$$a_{w12}''' = a_w - E_{ce} \cos (30° - \alpha_w) \tag{5.21}$$

The engagement angle decreases to a value

$$\alpha_{w12}''' = \arccos \left[ \frac{m (z_1 + z_2)}{2a_{w12}'''} \cos \alpha \right] \tag{5.22}$$

For the movement of the floating member not to cause jamming of the mechanism, the thickness of the teeth has to be reduced in comparison with its theoretical value. Thus, with the ideal arrangement of the centres of the gears there appears a certain lateral gap which should ensure that, with the distance between the axes equalling $a_{w12}'''$, there is no gap in the engagement $z_1 z_2'''$. The additional displacement coefficient $\Delta x_{2(e)}$ compensating for the reduction of the distance between the axes:

$$\Delta x_2 = x_1 + x_2 - \frac{(\text{inv}\, \alpha_{w12}''' - \text{inv}\, \alpha)(z_1 + z_2)}{2 \operatorname{tg} \alpha} \tag{5.23}$$

Eccentricity $E_4$ of the carrier causes (Fig. 5.17*b*) displacement of the floating gear $z_1$ through a distance $E_{c4} = 2E_4 \cos \alpha_w$. This alters all the distances between the axes. The engagement $z_1 z_2'''$ calls for the maximum additional displacement coefficient to compensate for the variation of the distance between the axes.

From Fig. 5.17*b*, the distance between the axes in this engagement:

$$a_{w12}''' = O_2'B = a_w - E_4 \cos (2\alpha_w - 30°) \tag{5.24}$$

We may find the angle $\alpha_{w12}'''$ from (5.22) and the additional displacement coefficient $\Delta x_{2(E_4)}$ from (5.23).

Eccentricity $E_2$ of satellite gears in the most adverse case would cause displacement of the floating member $z_1$ through a value

$$A_{c2} = \frac{8}{3} E_2 \cos \alpha_w$$

When determining the altered distances between the axes, let us take into account solely the displacement $A_{c2}$ of the floating member, as the runout $E_2$ of ring gears is stipulated by the Standard.

From Fig. 5.17*c*:

$$a'''_{w12} = a_w - A_{c2} \cos (30° - \alpha_w) \tag{5.25}$$

Now, $\alpha'''_{w12}$ and $\Delta x_{2(E_2)}$ can be found, respectively, from (5.22) and (5.23).

Eccentricity $E_3$ of ring gear $z_3$ causes displacement of the floating member $z_1$ through

$$E_{c3} = E_3 \tag{5.26}$$

The runout $E_3$ of the ring gear is stipulated by the Standard. In the most adverse case, the minimum distance between the axes with the floating member $z_1$ having been displaced through $E_{c3}$ (Fig. 5.17*d*) equals

$$O''_2 O' = a'''_{w12} = a_w = E_{c3} \tag{5.27}$$

The engagement angle $\alpha'''_{w12}$ and the additional displacement coefficient $\Delta x_{2(E_3)}$ compensating for the displacement of $z_1$ will be found, respectively, from (5.22) and (5.23).

The eccentricity $E_1$ of the sun gear $z_1$ is also stipulated by the Standard.

As the abovediscussed irregularities are random and uncorrelated values, the total additional displacement coefficient can be found from square addition:

$$\Delta x''_2 = \sqrt{\Delta x^2_{2(e)} + \Delta x^2_{2(E_1)} + \Delta x^2_{2(E_2)} + \Delta x^2_{2(E_3)}} \tag{5.28}$$

The displacement coefficient of the satellite gear:

$$x''_2 = x_2 - \Delta x''_2 \tag{5.29}$$

The minimum distance between the axes of the externally meshing pair $a_{w12\min}$ can be found from the value of $x''_2$ thus obtained, using the known relationships (5.19) and (5.20).

The overlap coefficient $\varepsilon_2$ should be checked by the maximum value $a_{w12\max}$ that the distance between the axes may attain on account of the floating.

## 5.5. Multirow Single-Stage Reduction Gear with Straight Teeth†

When a satellite gear of a single-row mechanism fails to accommodate a spherical bearing of an adequate load capacity, each satellite may be split into several parts, e.g. into three parts (Fig. 5.18), with each part supported by its own bearing. In this way the mechanism becomes the multirow one (the mechanism of Fig. 5.18 is a three-row one, with the load capacity of the bearings of the satellite gear having tripled). To ensure uniform distribution of the load among the rows (to retain static determinability), the sun pinion likewise has to be split, with its components interconnected by toothed universal joints with helical teeth. The torques transmitted by the toothed universal joints would be then $M$, $2M$, $3M$, and so on.

The design calculation of the toothed universal joints should be based on the equality of the axial forces, i.e.

$$Q_0 = M\frac{\operatorname{tg}\beta_1}{R_1} = 2M\frac{\operatorname{tg}\beta_2}{R_2} = 3M\frac{\operatorname{tg}\beta_3}{R_3} \qquad (5.30)$$

From practical considerations, it is expedient that the radii $R_1$ and $R_2$ of the universal joints arranged within the sun pinions should be equal, while the radius $R_3$ of the universal joint connected with the driving shaft and transmitting the greatest torque should be somewhat greater. Thus, if $R_3 = 2R_1 = 2R_2$ and $\beta_3 = 45°$, we have $\beta_1 = 56.3°$ and $\beta_2 = 36.9°$, which is quite acceptable from the designer's point of view.

For the axial forces of the endmost members of the driving system not to be transmitted to its bearings, it is reasonable to interconnect

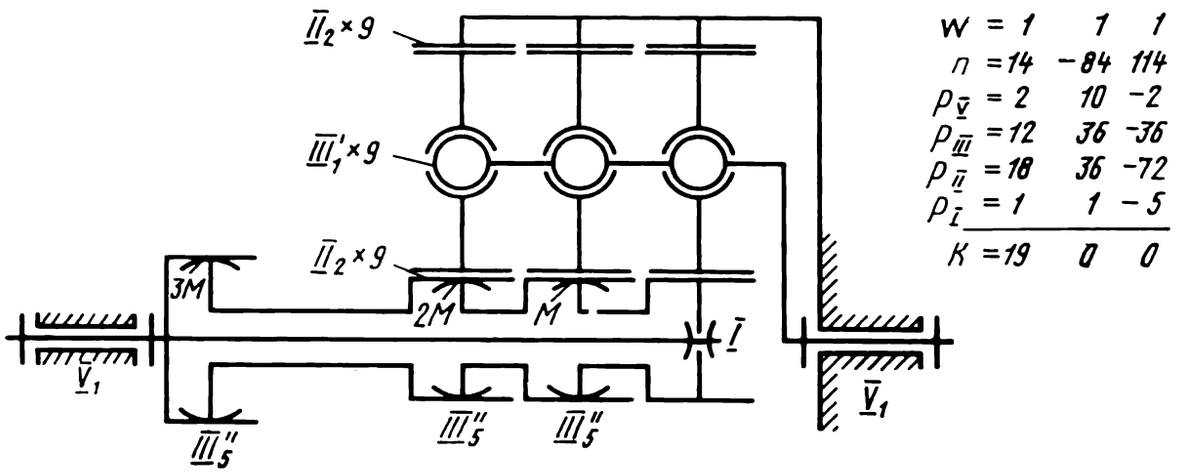


Fig. 5.18. Multirow single-stage reduction gear with straight teeth

these members by a rod with either a single $I_2$ pair or two $III_4'$ pairs at the ends. In the latter case a local mobility—a harmless one—occurs, i.e. rotation of the rod about its axis. The mechanism is free of redundant constraints, which can be seen from the Table accompanying Fig. 5.18.

## 5.6. Multisatellite Mechanisms

Multisatellite planetary gearings enable to achieve substantial reduction of the dimensions and weight of a mechanism, particularly, when the number of the satellite gears is big. However, the said is true only under the condition that the load is evenly distributed among the satellite gears, which is attained by incorporating an equalizing mechanism. The correctness of the equalizing mechanism design can be checked by counting the redundant contraints. The equalizing mechanism must be statically determinate. Expression (1.5) may be used for planar mechanisms.

The simplest equalizing mechanism is one with two satellite gears (Fig. 5.19*a*), with the carrier made floating and connected to the driven shaft by two arms which must be parallel with the line connecting the centres of the satellite gears. This should be ensured because a radial displacement of the centre of a satellite gear does not influence the movement of other members, whereas a tangential displacement does. This is the displacement that should be afforded by the equalizing mechanism.

With two satellites, the equalizing mechanism may be mounted neither on the sun pinion nor on the supporting or ring gear, otherwise the abovementioned direction of the arms would not be attained.

In this mechanism $w = 2$. The second mobility has been brought about by the rotation of the carrier about the pairs $III_4'$, $III_4'$. This mobility is harmful and should be eliminated by corresponding abutments. With $n = 7$, $p_V = 4$, $p_{III} = 4$ and $p_{II} = 4$, $q = 2 - 6 \times 7 + 5 \times 4 + 3 \times 4 + 2 \times 4 = 0$.

With the two satellite gears mounted on spherical bearings, the equalizing mechanism can be even simpler (Fig. 5.19*b*). The carrier is then connected to the driven shaft by a rotary pair $V_2$ whose axis is parallel with the line of the centres of the satellite gears. In this mechanism: $w = 1$, $n = 5$, $p_V = 3$, $p_{III} = 2$ and $p_{II} = 4$, so that $q = 1 - 6 \times 5 + 5 \times 3 + 3 \times 2 + 2 \times 4 = 0$.

It may be of interest to compare this mechanism with the one illustrated in Fig. 5.19*a*: it has five members (Fig. 5.19*b*) and nine

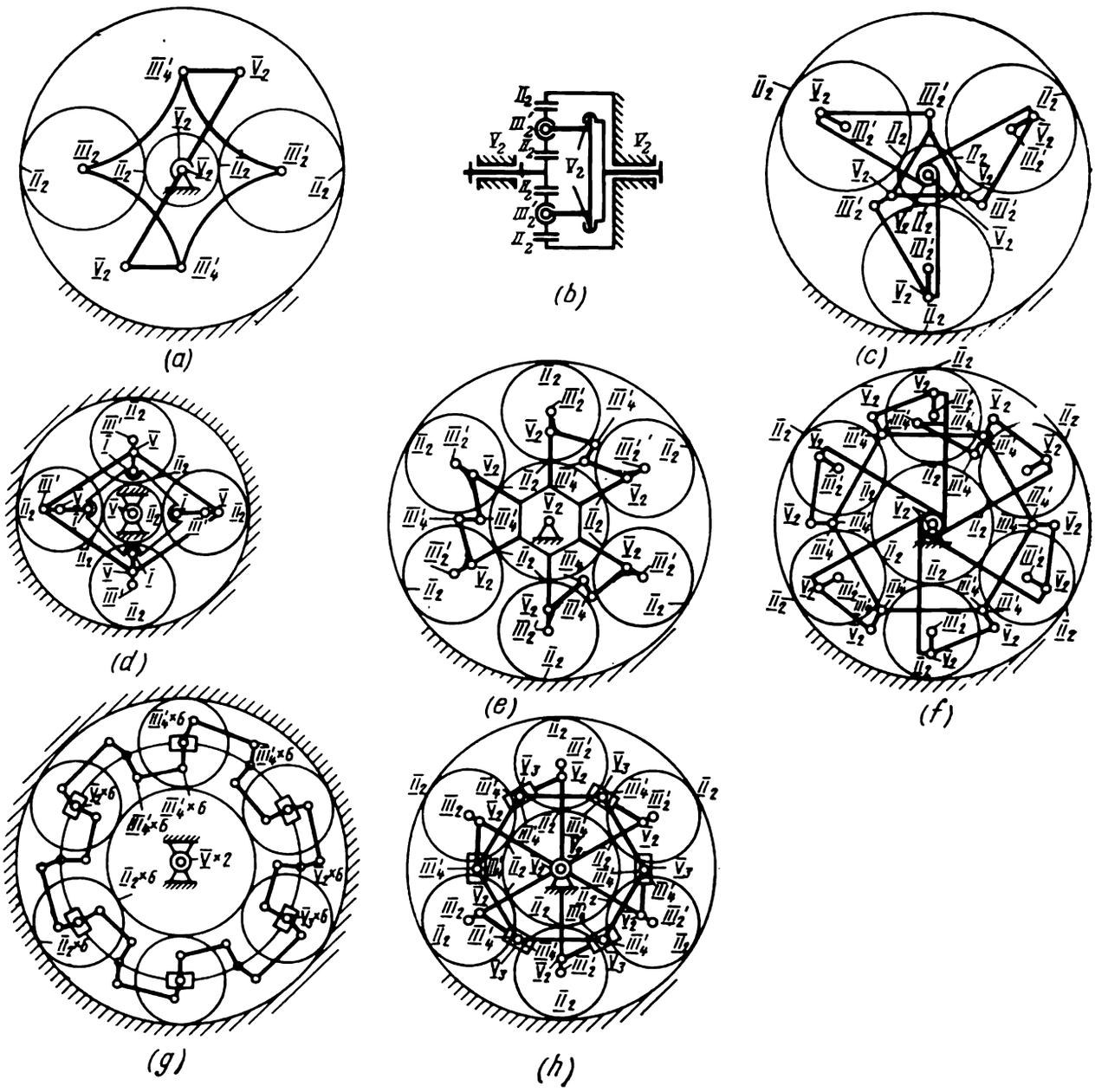


Fig. 5.19. Equalizing mechanisms of multisatellite reduction gears
(*a*), (*b*) with two satellite gears; (*c*) with three satellite gears; (*d*) with four satellite gears — Simmering design; (*e*) with six satellite gears and floating member; (*f*) without floating member, with any number of satellite gears; (*g*) Arnaudov's design; (*h*) with translatory pairs

pairs against the seven members and twelve pairs of the mechanism of Fig. 5.19*a*.

With three satellites, the design with a floating member becomes simpler. However, one can come across a design (Fig. 5.19*c*) where each satellite gear is carried by an angular lever connected to the carrier by a rotary $V_2$ pair, with the other ends of the levers being interconnected via arms $III_2'V_2$ by a floating member conventionally

shown as a triangle. This arrangement levels out the efforts applied to the arms (approximately) and, consequently, equalizes the loads on the satellite gears. To avoid a local mobility, possibly harmful, one of the arms is rigidly connected to the floating member.

In this mechanism $n = 11$, $p_V = 7$, $p_{III} = 6$, $p_{II} = 6$ and $w = 1$, $q = 1 - 6 \times 11 + 5 \times 7 + 3 \times 6 + 2 \times 6 = 0$.

An interesting mechanism with three satellite gears has been proposed by G. A. Anopov and A. F. Krainev.†

The angular levers may be interconnected, instead of the arms, by a stud-and-slot connection [57]. An equalizing mechanism with angular levers can be also used in a design with two satellite gears, with the angular levers interconnected by toothed segments [58]. They can be also interconnected by a counter-parallel crank mechanism.

An equalizing mechanism for four satellite gears used by the Simmering firm of Austria is shown in Fig. 5.19*d* (where the carrier is shown as a rhomb). The floating member is acted upon by four forces, and thus it is essential that these forces should not intersect at one point, or condition (No. 6) of Table 3.1 is not satisfied. Therefore the general case of the arrangement of the forces in a plane is applied: with two forces acting in a horizontal direction and two forces acting in a vertical direction (for the position of the mechanism illustrated in Fig. 5.19*d*). Two satellites bear upon levers of the first order (the top and bottom ones), while the other two bear upon levers of the second order, so that the moments they transmit upon the floating member are directed oppositely and thus counterbalanced.

To avoid a harmful mobility, the floating member has to be connected to the carrier by a planar $III_2''$ pair; alternatively, out of the four pairs connecting the carrier with the arms three pairs should be of the second and one of the first class.

In the mechanism $w = 1$, $n = 11$, $p_V = 6$, $p_{III} = 5$, $p_{II} = 8$ and $p_I = 4$. Then, from (1.1) $q = 1 - 6 \times 11 + 5 \times 6 + 3 \times 5 + 2 \times 8 + 4 \times 1 = 0$.

In real-life mechanisms of this type, however, all the four pairs on the floating member are second-class ones, so that $q = 1$, but this has proved to be not critical owing to the substantial axial gaps in the pairs of the floating member.

If the number of the satellite gears is more than three, a single floating member is incapable of levelling out the loads, so that mechanisms equalizing the loads of adjacent satellites have to be used.

An arrangement of this kind for six satellite gears is shown in Fig. 5.19*e*. Its mobilities are: the main motion, the rotation of the three arms $III'_4III'_4$ about their axes, the three mobilities of the floating member (the movement axially of the mechanism and two rotations about axes perpendicular to the axis of the mechanism), i.e. $w = 7$, $n = 17$, $p_V = 7$, $p_{III} = 12$ and $p_{II} = 12$. Thus, $q = 7 - 6 \times 17 + 5 \times 7 + 3 \times 12 + 2 \times 12 = 0$.

A similar arrangement with two auxiliary equalizing mechanisms can be used with five satellite gears, or else with one auxiliary mechanism with four satellite gears. One of the central members is still the floating one, in either case. When the number of the satellite gears is in excess of six, the mechanism cannot be employed.

A common equalizing mechanism without a floating member can be used with any number of satellite gears (Fig. 5.19*f*), provided its polyhedron is an articulated one, with the three members at each corner connected by two $III'_4$ pairs. To reduce friction, rotary pairs alone are used, with no translatory pairs whatsoever. With six satellites, $w = 8$ (the main motion plus the rotation of the seven arms about their axes), i.e. $n = 27$, $p_V = 14$, $p_{III} = 20$, $p_{II} = 12$. Thus, $q = 8 - 6 \times 27 + 5 \times 14 + 3 \times 20 + 2 \times 12 = 0$.

When the mechanism is intended to transmit a torque in one direction only, with the short rods connected to the polyhedron working in extension, the mechanism may be simplified. In this case the polyhedron is suspended from the rods and requires no guiding mechanism. Thus, we can omit one arm, two $III'_4$ pairs and the local mobility of the arm. One mobility—rotation of the polyhedron about the axis of the mechanism—is added, but it will not affect the performance of mechanism, as the polyhedron is centered by the rods. In this case: $w = 8$, $n = 26$, $p_V = 14$, $p_{III} = 18$ and $p_{II} = 12$, so that $q = 8 - 6 \times 26 + 5 \times 14 + 3 \times 18 + 2 \times 12 = 0$.

An even more complicated mechanism has been suggested by K. Arnaudov (Fig. 5.19*g*), in which the shafts of the satellite gears are connected with the carrier with the aid of tangentially movable $V_3$ sliders. The circumferential efforts are equalized by a system of equal-arm levers of which one half has their pivot axes $V_2$ on the sliders, while the other half has their pivot axes $V_2$ on the carrier. The levers are interconnected by $III'_4$-$III'_4$ rods. The mechanism displays a group mobility—the rotation of all the levers in one direction, e.g. counterclockwise. Admittedly harmless, it may result in clatter in the mechanism. With six satellite gears, in the mechanism $w = 14$ (the main motion plus the group mobility plus rotation of the 12 rods about their axes), $n = 38$, $p_V = 20$, $p_{III} = 30$, $p_{II} =$

$= 12$. Thus, $q = 14 - 6 \times 38 + 5 \times 20 + 3 \times 30 + 2 \times 12 = 0$.

It should be pointed out that the mechanism with six satellite gears illustrated in Fig. 5.19*e* is significantly simpler than those of Fig. 5.19*f* and g. It has 17 members and 19 rotary pairs against the 27-26 members and 34-32 pairs of the mechanism of Fig. 5.19*f*, or

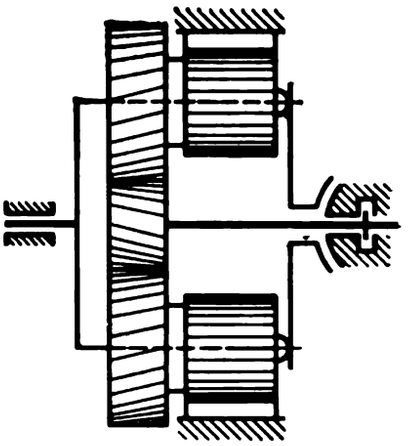

Fig. 5.20. Equalizing mechanism with helical-teeth gears, utilizing the axial effort of satellite gears

else against the 38 members and 50 pairs of Arnaudov's design (Fig. 5.19*g*).

By using translatory pairs, the number of the members may be reduced still further (Fig. 5.19*h*).

To reduce friction to the minimum, the dimensions should be so selected that the motion of the slider in operation of the mechanism should be minimized, with the centre of the slider belonging to a straight line interconnecting the centres of rotation of the levers of the adjacent satellite gears. In this mechanism $w = 7$ (the main motion and local mobilities of the six arms), $n = 25$, $p_V = 13$, $p_{III} = 18$ and $p_{II} = 12$. Then, $q = 7 - 6 \times 25 + 5 \times 13 + 3 \times 18 + 2 \times 12 = 0$.

Mechanisms with double-row satellite gears and helical gear teeth (Fig. 5.20) may utilize the axial effort to equalize the load. The equalizing member is supported by a spherical bearing and is restrained by a plane to which the axial efforts are transmitted. This mechanism is operable only with three satellite gears and a single direction of rotation, which is its shortcoming. Moreover, it is more complicated than a mechanism with a single floating member, so that the prospects of its application are dubious.

## 5.7. Single-Row Planetary Mechanism with Six Self-Aligning Satellite Gears†

There are known single-row mechanisms with three self-aligning satellite gears. However, in high-duty gearings used as reduction gears, as reversing mechanisms, or else as the elements of either multiple or closed planetary gearings the three satellite gears would not suffice, and their number has to be stepped up. Mechanisms of this kind are required in marine plants, in aircraft (e.g. helicopters) and other fields, but one should remember that the greater is the number of the satellite gears, the smaller is the attainable transmission ratio. With six satellite gears it is about 3.7 : 1, so that a further increase of the number of the satellite gears may be called for in exceptional cases.

With six satellite gears, one may use equalizing mechanisms levelling out the circumferential forces of all the satellite gears. However, such mechanisms become highly complicated, with the number of their members being as great as 27 or even 38 (Fig. 5.19*g*). Fig. 5.21 illustrates a mechanism where the same problem is solved in a far simpler manner. In the mechanism the sun gear *1* and the low-speed shaft *7* are supported by bearings which are fifth-class rotary kinematic pairs. The satellite gears *2* and *4* are connected with the carriers *3* and *5* by *III′* class spherical bearings.

Owing to the spherical bearings, line engagement of the satellite gear teeth with the sun gear and fixed ring gear is ensured. Each carrier has three satellite gears spaced through 120°, with both

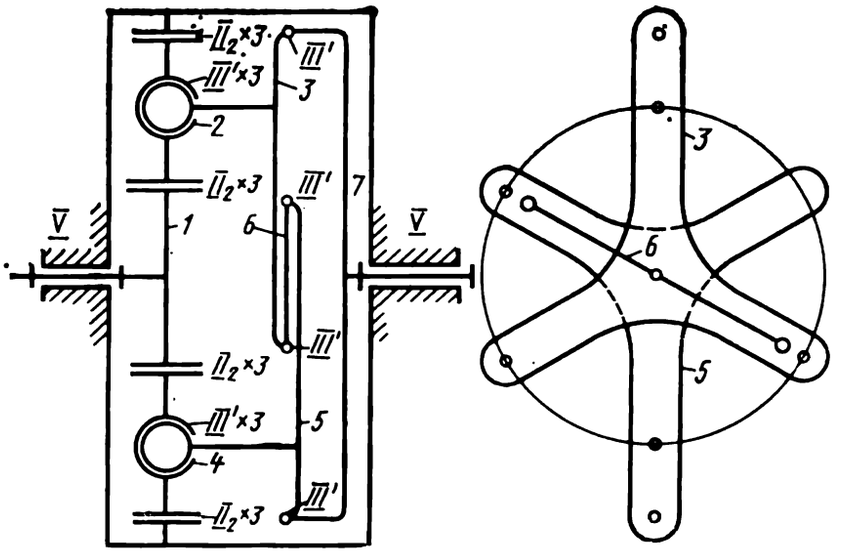


Fig. 5.21. Single-row planetary mechanism with six self-aligning satellite gears

carriers floating to provide for even distribution of the load among the three satellite gears of each carrier. Each carrier is connected to the low-speed shaft *7* by one spherical joint of the *III'* class, and rotations about the two perpendicular axes of this joint afford the floating of the carrier and uniform distribution of the circumferential force among its satellites. Rod *6*, interconnecting carriers *3* and *5* and providing for uniform distribution of the torque of the low-speed shaft among the two carriers, cancels rotation about *z* axis that is parallel to the axis of rotation of the mechanism. The rod *6* may be connected to the carriers *3* and *5* at points belonging to the axes of the satellite gears, or else other points may be selected, provided the equality of the arms of the force acting along this rod is maintained, which is essential for having the equality of the torques transmitted by the carriers.

In this mechanism the mobility equals 2: the main mobility and a local one—rotation of the rod *6* about its axis. Redundant constraints calculated either from (1.1) or from (1.2) are absent (cf. Table below, left in Fig. 5.22), but the number of the loops $k = p - n = 13$.

This great number of the loops complicates the investigation of the mechanism as far as the checkup of mobilities in the loops is concerned. The number of the loops, though, can be significantly reduced by substituting a kinematic connection of a corresponding mobility for a group of kinematic pairs. It may be useful to remind that when the kinematic pairs are connected in series, their mobilities add up, whereas when the pairs are connected in parallel, it is the restraints they impose which are added up. To simplify the picture even further, let us presume that the sun gear *1* is fixed by being fast with the fixed member, which would not affect the amount of redundant constraints.

Let us consider the kinematic connection between the carrier and the fixed member, defined by the sun gear and the ring gear. Two pairs $II_2$ connected in parallel are included between the satellite gear and the fixed member, i.e. $2 + 2 = 4$ restraints or $6 - 4 = 2$ mobilities (linear ones). A spherical pair *III'* is between the satellite gear and the carrier, whose mobility equals three and which is included in series with the connection between the satellite gear and the fixed member. As there is one satellite gear in the design the mobility between the carrier and the fixed member is $2 + 3 = 5$, with the number of restraints being $6 - 5 = 1$. The three satellites which are connected in parallel impose $3 \times 1 = 3$ restraints.

Therefore, the kinematic connection between the carrier with

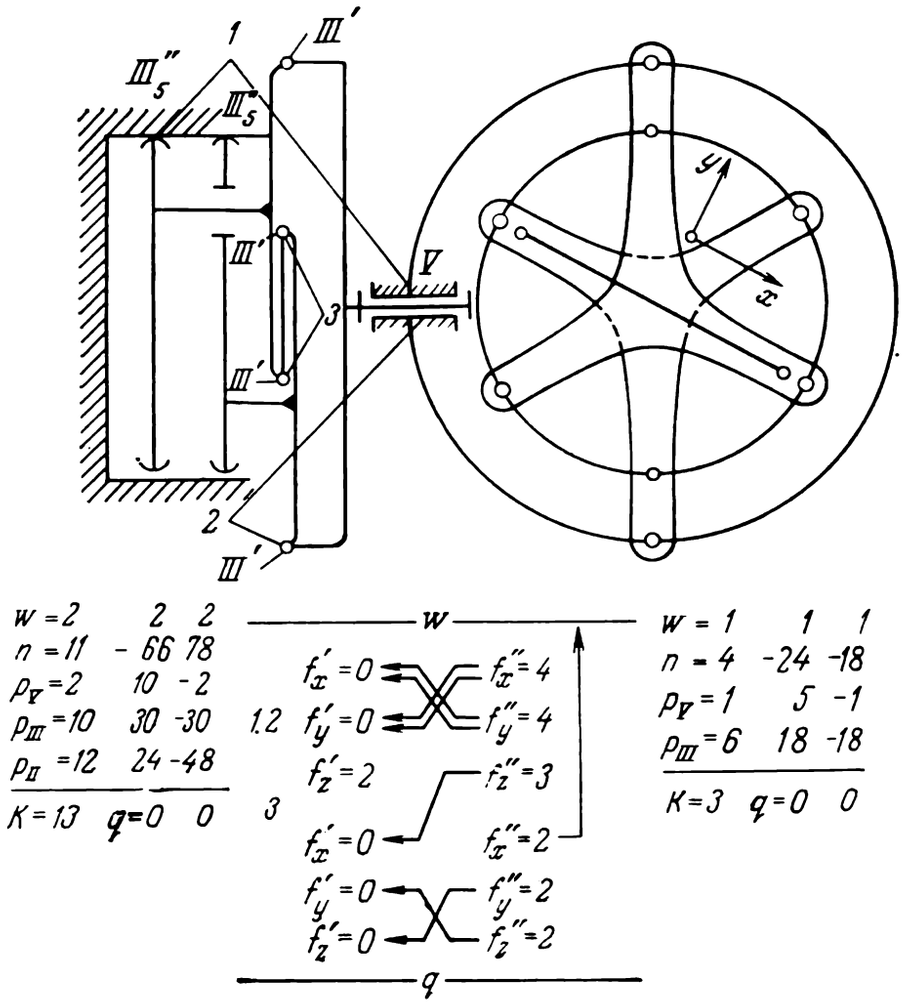


Fig. 5.22. Mobilities in the loop for mechanism shown in Fig. 5.21

three satellites on spherical bearing supports and the fixed member may be regarded as a toothed universal $III''_5$ joint. A mechanism with such connections is shown in Fig. 5.22. It has but one local mobility—rotation of the rod *6* about its axis, as the main mobility equals zero. From (1.1) or (1.2) we can find that $q = 0$. The number of the loops now is $k = p - n = 3$.

Let us draw the coordinate axes: $x$ axis along the connection rod, $y$ axis perpendicularly to it in the end plane, and $z$ axis axially of the mechanism.

Now considering the loops: the first loop—the fixed member, *V* class pair, the driven shaft, *III'* pair, the carrier, $III''_5$ pair, the fixed member; the second loop—the same, but through the other carrier; the third loop—the driven shaft, *III'* pair, the carrier, *III'* pair, the rod, *III'* pair, the carrier, *III'* pair, the driven shaft.

The mobilities of the first and second loops will be considered concurrently. Linear mobilities $f'_x$ and $f'_y$ are absent in all the three

loops. Linear mobility $f'_z$ exists in the $III''_5$ pairs in the first and second loops. Thus, in the two loops $f'_z = 2$. Mobilities $f''_x$ are afforded by the pairs $III''_5$ and $III'$ in the first loop, same as in the second one. Thus, in the two loops $f''_x = 4$. Similarly, $f''_y = 4$. Mobilities $f''_z$ are afforded in the first and second loops by their one $V$ pair and two $III'$ pairs; thus, $f''_z = 3$.

The mobilities in both spherical pairs at the ends of the connection rod *6* will be referred to the third loop. Thus, $f''_x = f''_y = f''_z = 2$.

Let us consider the distribution of the mobilities. In the 1st and 2nd loops two angular mobilities $f''_x$ are spent to substitute for $f'_y$. This is possible owing to the presence of the members (the carriers) directed along $z$ axis, as the satellite gears and the equalizing mechanism are situated in different planes perpendicular to the axis of rotation, which arrangement is a must for the equalizing mechanism. The two other angular mobilities $f''_x$ will be spent on closing the loop. The distribution of the angular mobilities $f''_y$ is exactly the same. In the 3rd loop one angular mobility $f''_x$ is spent on closing the loop, while the other one remains as a local mobility—rotation of the connecting rod about its axis. One angular mobility $f''_y$ will replace $f'_z$, as there is a member (the rod itself) directed along $x$ axis. The other mobility is left for closing the loop. Similarly, one angular mobility $f''_z$ will replace $f'_y$, and the other will be spent on closing the loop. The closing of the 3rd loop along $x$ axis will be achieved owing to the angular mobility $f''_z$ remaining free in the 1st and 2nd loops, as there is a member (the driven shaft) extending along $y$ axis.

The above investigation proves the absence of local mobilities not accounted for, which could have led to an error in determining the number of redundant constraints from (1.1) and (1.2). The calculation is given in Table at the bottom of Fig. 5.22.

## 5.8. Positive Planetary Gearings for Big Transmission Ratios

We will call "positive" the mechanisms with the positive transmission ratio of the mechanism in the reduced state, i.e. in the state where its carrier is arrested. Positive planetary mechanisms are used in applications with a big transmission ratio, when the efficiency factor is of little essence. There is one ingenious design suggested by V. N. Kudryavtsev.

In his mechanism with two internal meshings (Fig. 5.23) the driving shaft and the double satellite gear are mounted each on two spherical roller bearings. To avoid redundant constraints, the teeth

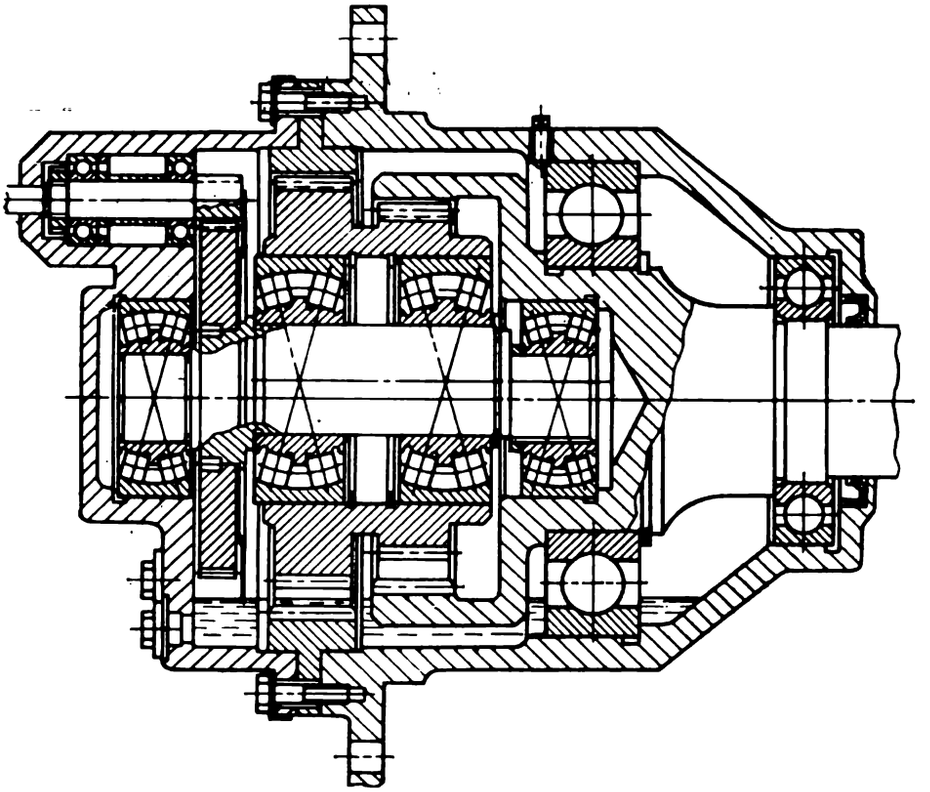

**Fig. 5.23.** Planetary reduction gear for large transmission ratios designed by V. N. Kudryavtsev

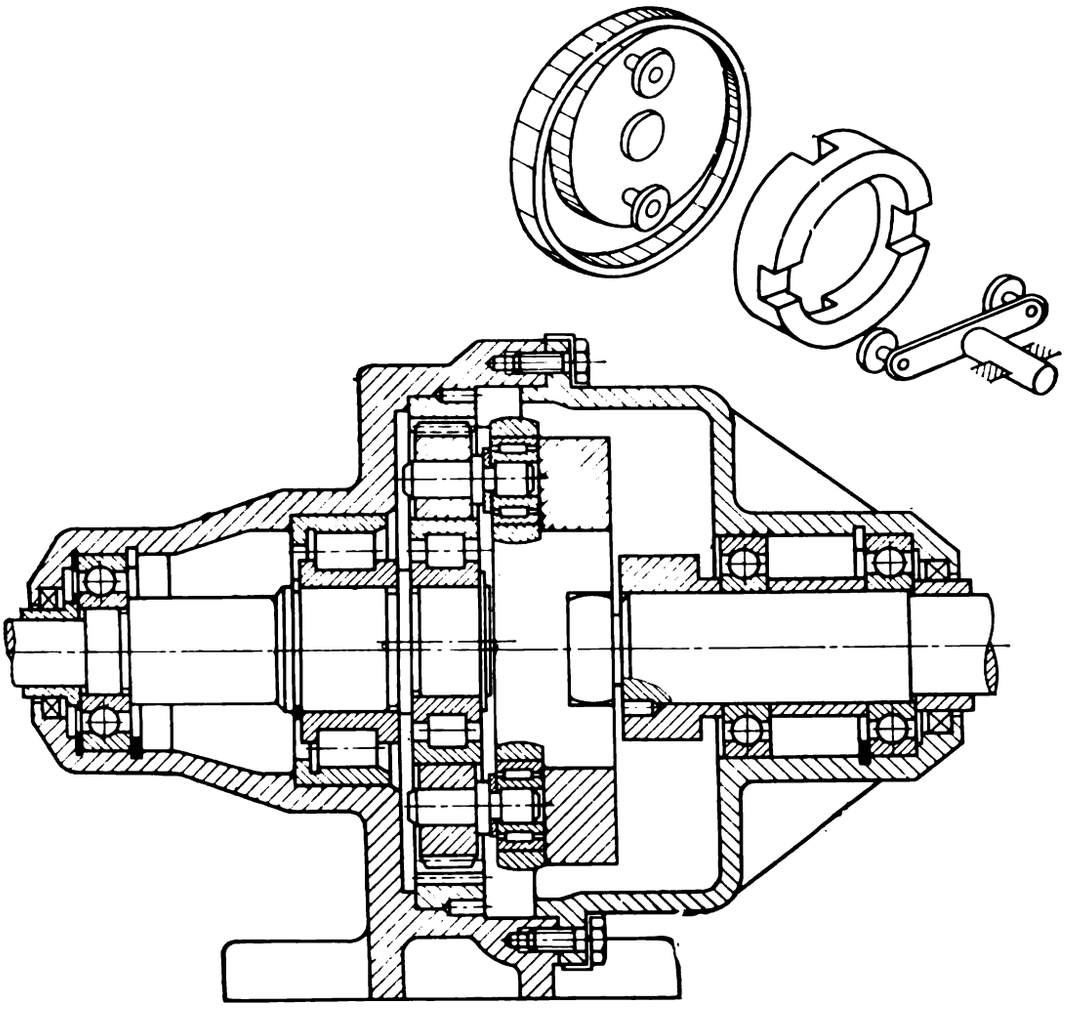

**Fig. 5.24.** Planetary reduction gear for large transmission ratios designed by Yu. A. Grin

have to be barrel-shaped. The planetary gearing is associated with a plain cylindrical gearing, which, of course, is not obligatory.

In another design of the mechanism with one internal meshing and a small difference between the numbers of the teeth, Yu. A. Grin has incorporated a slider coupling with the translatory pairs on rollers journalled on needle-roller bearings (Fig. 5.24). The slider coupling is intended to transmit torque between the satellite gear and the driven shaft, and the losses in this gearing are small. The rollers have barrel-shaped rims ($I_2$ pair). If the teeth are made barrel-shaped, too, the gearing would have no redundant constraints. A mechanism with a parallel multistud crank is sometimes used for the same purpose, although it has a great number of redundant constraints and, therefore, is ill-advisable.

## 5.9. Flat Planetary Mechanism with Self-Aligning Satellite Gear

The efficiency factor of a positive planetary mechanism with two internal meshings can be stepped up by arranging the four gears in a single plane (Fig. 5.25). The satellite gear is preferably mounted

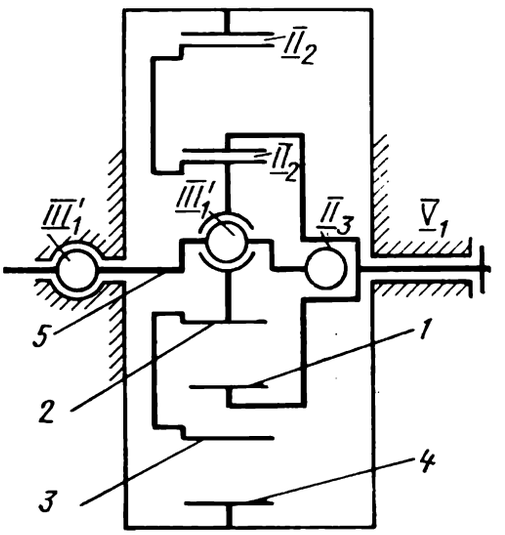


Fig. 5.25. Planar planetary reduction gear with self-aligning satellite gear

on a spherical bearing $III_1'$ to provide for self-alignment and line engagement of the teeth in both meshings. The mechanism has been suggested by Wildhaber. Self-alignment is quite attainable here, for both gears *2* and *3* of the satellite unit are externally toothed, so that the normals to the working profiles of the teeth, about which self-alignment should take place, are not parallel but define an angle $180° - 2\alpha$, which is required for self-alignment. From (1.1): $q =$

$= w - 6n + 5p_V + 4p_{IV} + 3p_{III} + 2p_{II} + p_I = 1 - 6 \times 3 + 5 \times 1 + 3 \times 2 + 2 \times 3 = 0$. The teeth of the mechanism are in line engagement ($II_2$ pair), which is its serious advantage over other positive mechanisms with their point engagement of the teeth. Thus, a flat planetary reduction gear offers a greater load capacity and longer life.

## 5.10. Mechanism with Free Carrier

In such a mechanism (Fig. 5.26) the idle carrier, as the name implies, rotates freely and transmits no torques.

The rotation of the carrier can be used, however, when two coaxial driven shafts rotatable at predetermined angular speeds are required, e.g. in a drive of a tower clock where the carrier may rotate the minutes' hand, and the driven gear may rotate the hours' one. The teeth numbers in that case may be, as follows: $z_1 = 12$, $z_5 = 36$, $z_3 = 33$ and $z_2 = z_4 = 11$. A single-gear satellite is employed here, which is advisable for all gearings with a free carrier to avoid emergencies caused by improper assembling (the engagement of wrong teeth).

When considering redundant constraints two problems are to be solved:

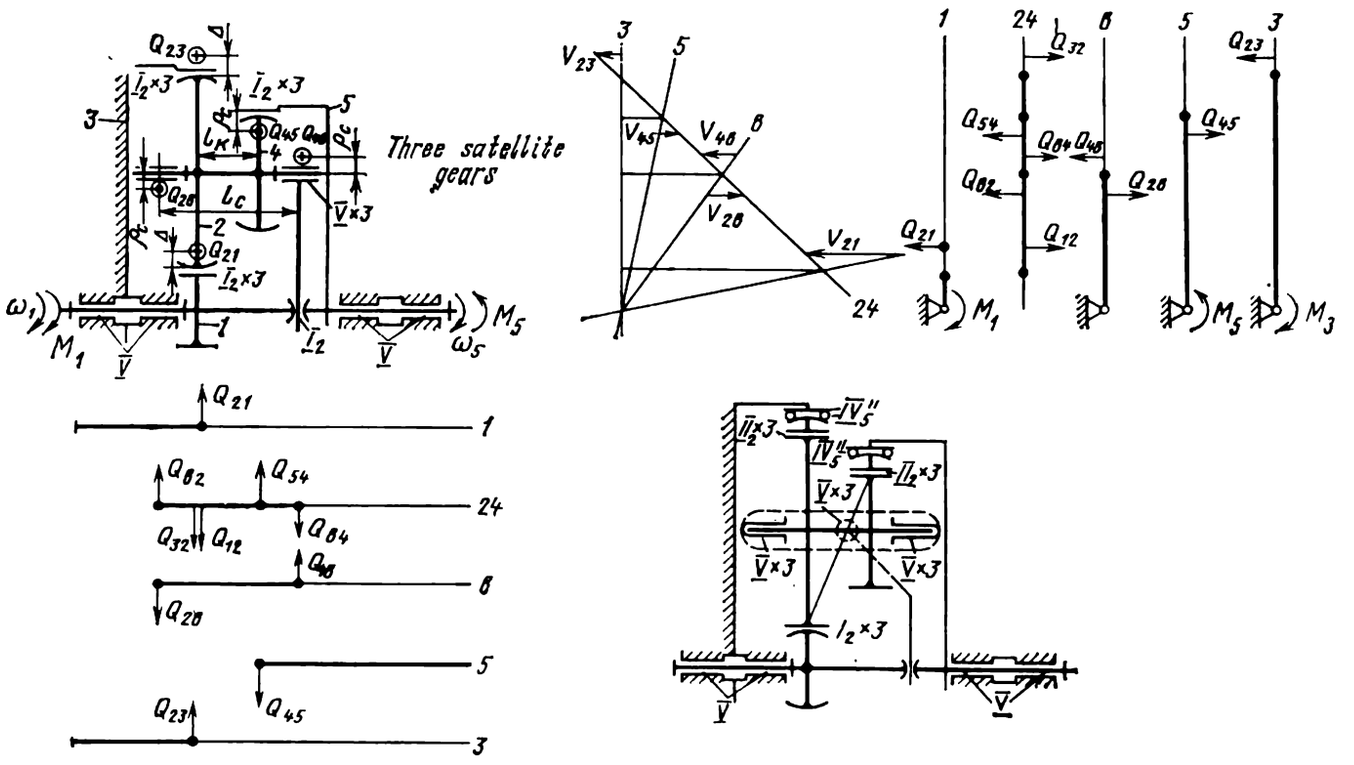


Fig. 5.26. Mechanism with free carrier

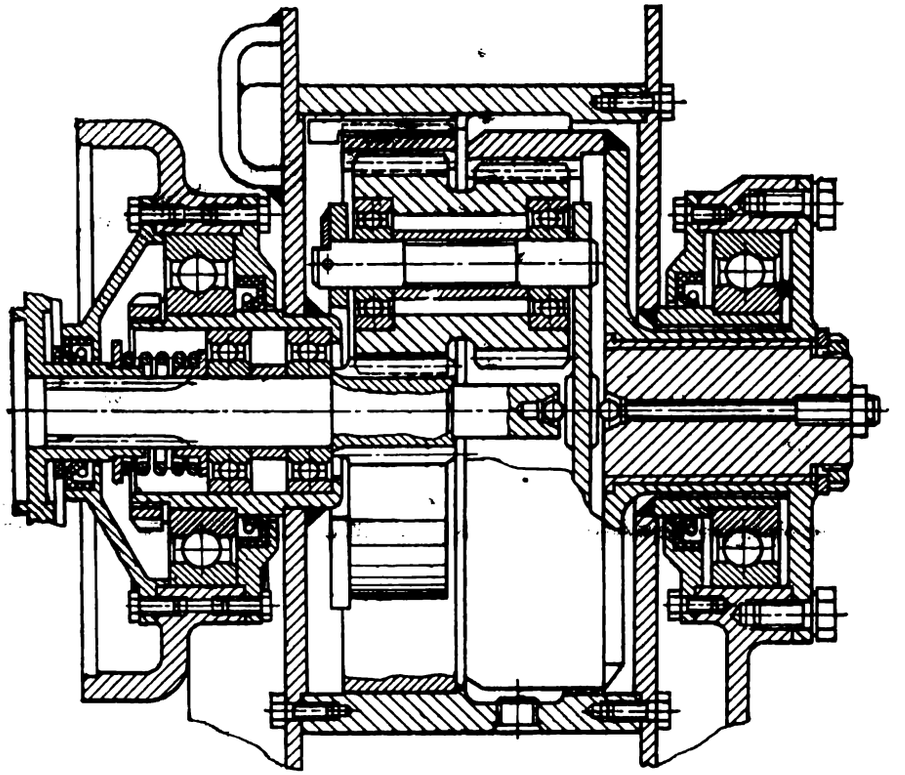

Fig. 5.27. Reduction gear of design shown in Fig. 5.26, manufactured by the Kovrov Excavator Works (USSR)

— even distribution of the load between the satellite gears is to be ensured;

— redundant constraints in the meshings have to be avoided.

The first problem has been solved by the Author by using a carrier completely devoid of bearings and merely retained against axial displacement by a first-class pair. This general design has been industrially implemented (Figs. 5.27, 5.28). In the design of Fig. 5.27 axial retaining is done by a steel ball abutting against a plane, while in that of Fig. 5.28 the first-class pair is quite ingenious, with the carrier being connected to the high-speed shaft by two ball-bearings set with a big radial gap affording the necessary mobility (designed by V. M. Yastrebov). Another way to solve the first-mentioned problem is to set two ring gears (one will not suffice) on toothed universal joints. This structure is shown in Fig. 5.29. However, friction in the toothed universal joints affects the load distribution among the satellite gears in this gearing, to say nothing of this design being more complicated than the one of Fig. 5.28, with 13 toothed rims against 9, and 12 bearings against 10.

The second problem—prevention of redundant constraints in the meshings of free carrier mechanisms—can be solved completely by

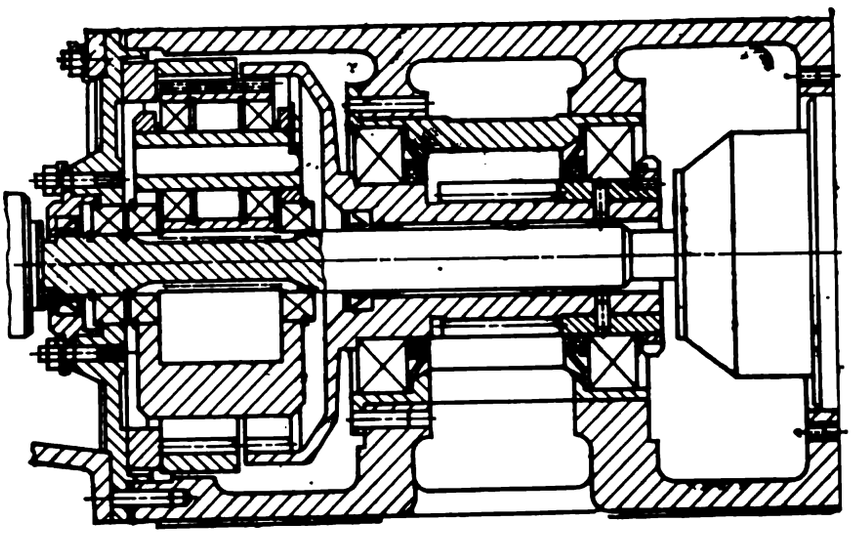

Fig. 5.28. Reduction gear of design shown in Fig. 5.26 (V. M, Yastrebov's version)

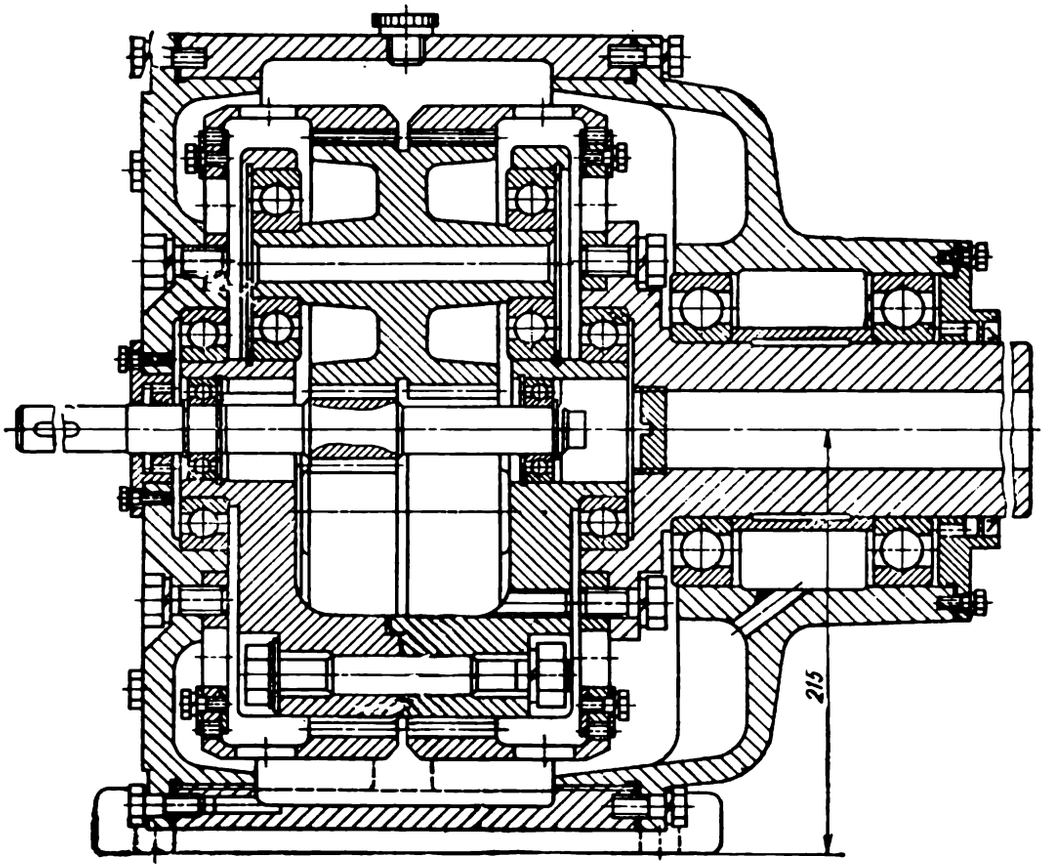


Fig. 5.29. Reduction gear with free carrier

having point engagement of the teeth ($I_2$ pairs). Barrel-shaped teeth of the satellite gears ensure this.

For the mechanism of Fig. 5.26, from the structural formula: $q = 1 - 6 \times 6 + 5 \times 5 + 1 \times 10 = 0$.

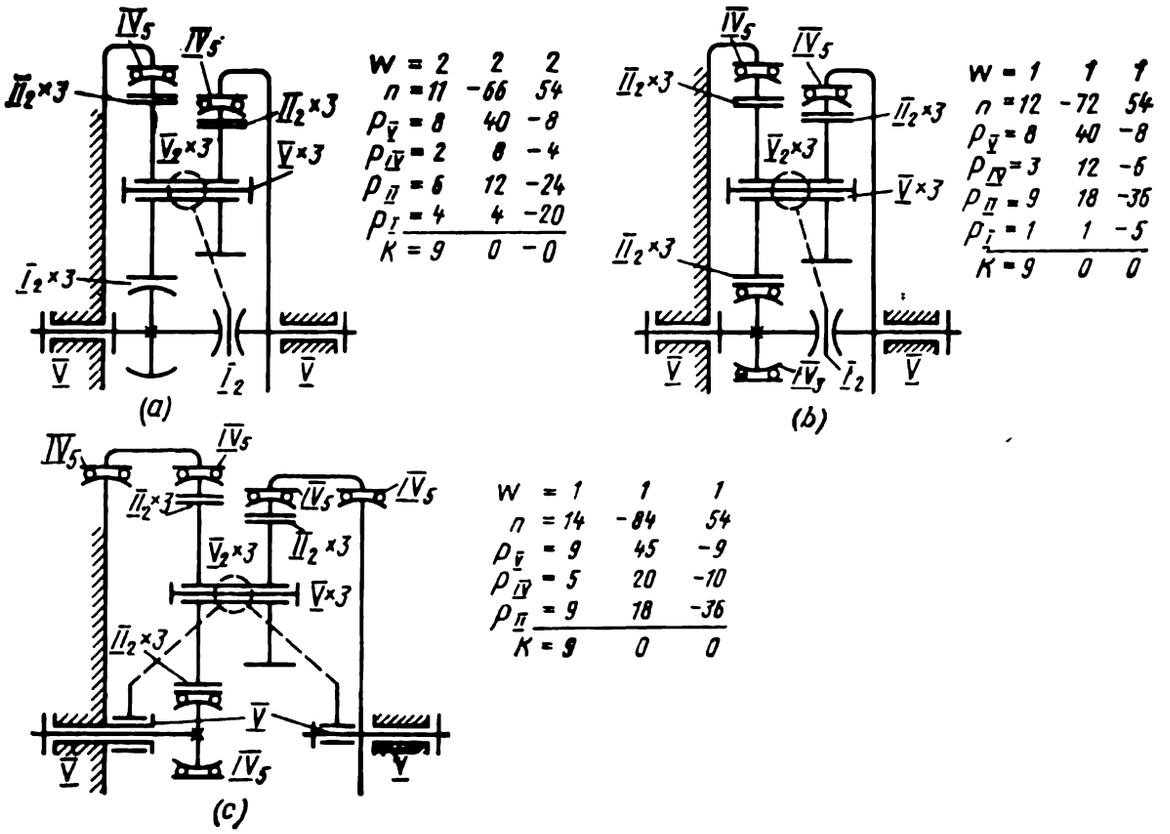


Fig. 5.30. Reduction gear with free carrier, ring gear on toothed universal joints and satellite gears on rocking frames

For the mechanism of Fig. 5.29, if all the engagements are point ones: $q = 1 - 6 \times 8 + 5 \times 6 + 4 \times 2 + 1 \times 9 = 0$.

Redundant constraints are avoided with a far greater difficulty when all the meshings have line engagement ($II_2$ pairs).

Let us consider a case where line engagement is used in the meshings with the ring gears, while the sun gear where the forces (with the same modulus) are far less, has line engagement. The amount of the redundant constraints can be additionally reduced by having two toothed universal joints $IV_5''$ supporting the ring gears. In the structure of Fig. 5.29 each ring gear will be then mounted on one universal joint, so that from (1.1): $q = 1 - 6 \times 8 + 5 \times 5 + 4 \times 2 + 2 \times 6 + 1 \times 4 = 2$.

Redundant constraints can be completely eliminated by mounting the satellite gears on rocking frames (Fig. 5.30*a*), although this would add three angular mobilities, whereas only two are required. One of them would remain a local one (harmless), and $w = 2$. Table in Fig. 5.30*a* gives the calculation of redundant constraints. Point engagement of the teeth may be avoided, too, by mounting the sun gear on a toothed universal $IV_5$ joint (Fig. 5.30*b*). Instead of having

the floating carrier, the ring gears may be mounted on double universal joints $IV_5$, $IV_5$ (Fig. 5.30*c*).

For comparison sake, let us count the redundant constraints of the obsolete design with no floating members and line engagement

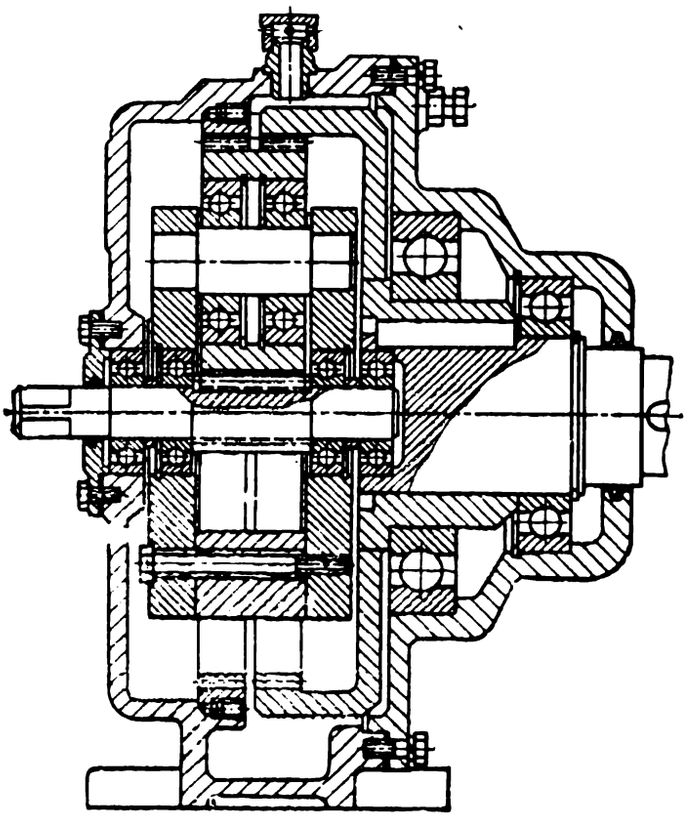

Fig. 5.31. Obsolete design of free carrier reduction gear, with redundant constraints

of the teeth (Fig. 5.31) from (1.1): $q = 1 - 6 \times 6 + 5 \times 6 + 2 \times 9 = 13$ out of which four would produce uneven load distribution between the satellite gears, while the remaining nine would yield uneven distribution of the load lengthwise of the teeth in nine meshings.

## 5.11. Multiple and Closed Planetary Mechanisms

We have already seen that a single-row planetary mechanism can be made statically determinate by mounting the satellite gears with cylindrical teeth on spherical bearings and by having one of the main members floating by being connected to the respective shaft by a universal joint (1st pattern).

Another solution to the problem is using barrel-shaped teeth ($I_2$ pairs) which are conventionally shown in the accompanying drawings with rounded toothed rims. Satellites in such designs (2nd pattern) are supported by rotary pairs $V_2$. In engagements with internal

gears, as D. M. Lukichev has suggested, the manufacture can be facilitated by having barrel-shaped tooth on the external gear, and the internal gear with cylindrical teeth. Designs of this very kind will be discussed below.

The first pattern is preferable. Even in cases of skewing shafts, it is capable of retaining line engagement of the teeth and central

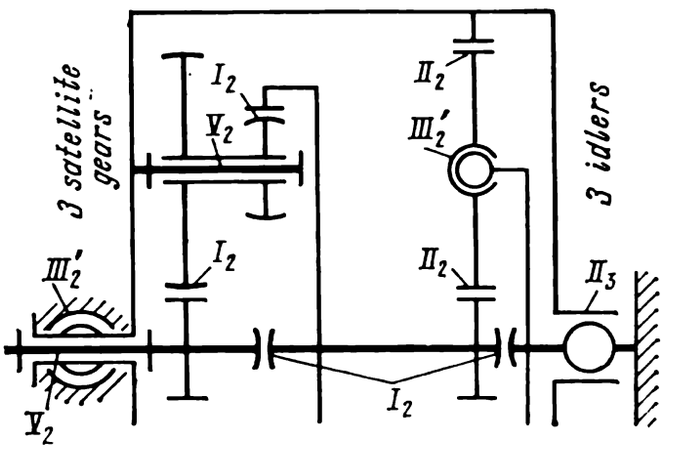


Fig. 5.32. Closed-design planetary mechanism

application of the circumferential force. However, it is operable with single-row satellite gears exclusively. Should a satellite be made of two gears (Fig. 5.32), the design is inoperable, as the outward thrust forces would make the teeth disengage. It is for this reason that the satellite of Fig. 5.32 conforms to the second pattern, while the idler which transmits considerably greater forces conforms to the first one. When the direction of the transmitted torque does not change, the moment produced by the thrust forces can be count-

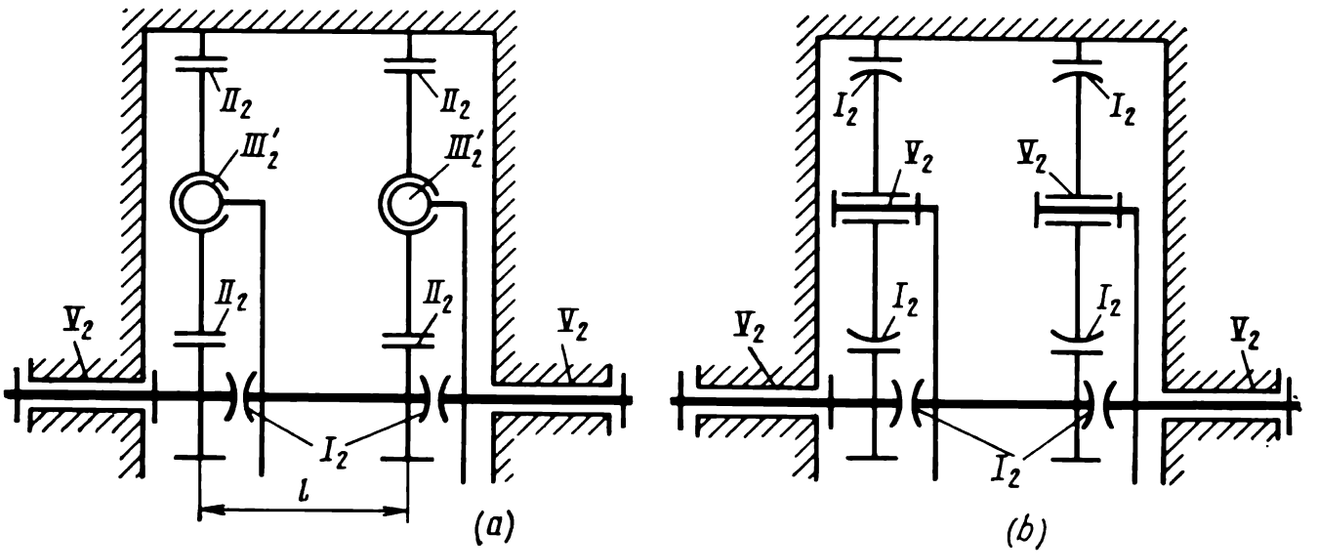


**Fig. 5.33. Planetary mechanism made of two single-row mechanisms**
**(*a*) with cylindrical teeth; (*b*) with barrel-shaped teeth**

erbalanced by a moment of axial forces by selecting the direction and helix angle of the teeth accordingly. This case, however, is exceptional, and barrel-shaped teeth have to be used with double-row satellites.

The universal joint, as structurally simple as it is (when it is a double toothed one), complicates the structure of a single-row mechanism, to say nothing of its friction significantly influencing load distribution among the satellite gears. To avoid this, the Author has suggested to use in double and closed planetary mechanisms a floating transmitting member between the first and second units (Figs. 5.32 and 5.33) bearing by one its end on three gears of one unit and levelling out their circumferential forces, while bearing by its other end upon three gears of the other unit and equalizing their circumferential forces, too [33, 35]. Thus, a single transmitting member is capable of equalizing the forces in two units.

With irregular angular spacing of the satellite gears on account of manufacturing inaccuracies, same as with non-concentric mounting of the gears of the floating member, the latter would skew. Hence, the length of this floating member (the spacing of the planes of the gears) should be as great as possible to minimize this skewing. The floating transmitting member should be retained in the axial direction by abutments regarded in the structural formula as $I_2$ pairs. The abutments may be quite simple, as axial forces in this mechanism are practically non-existent. The mechanism illustrated in Fig. 5.33*a* has been already industrially implemented, its production versions being shown in Figs. 5.34*a* and 5.35. In the design of Fig. 5.35 the satellite gears are mounted on two bearings, so that their load is unevenly distributed lengthwise of the teeth. The structure of Fig. 5.34*b* warrants a comparison with an older one which had two double universal joints and four satellite gears in the lower-speed stage. The new structure has the number of the toothed rims reduced from 19 to 10, and that of antifriction bearings from 17 to 10. The major merit of this design is the uniform distribution of the load both along the teeth and among the satellite gears, owing to elimination of the influence of friction in the universal joints. The Lectra Haul Company of the USA has employed the design of Fig. 5.34*b* in the reduction gear of the highest (known) duty in their 180-ton dump truck. Unfortunately, the satellite gears of the first stage alone are mounted there on spherical bearings.

The Kiev Research Institute for Reduction Gears (USSR) has used satellite gears on spherical bearings in the second stage of the MIIa2-80 gear motor [53]. Satellite gears of the first stage have been

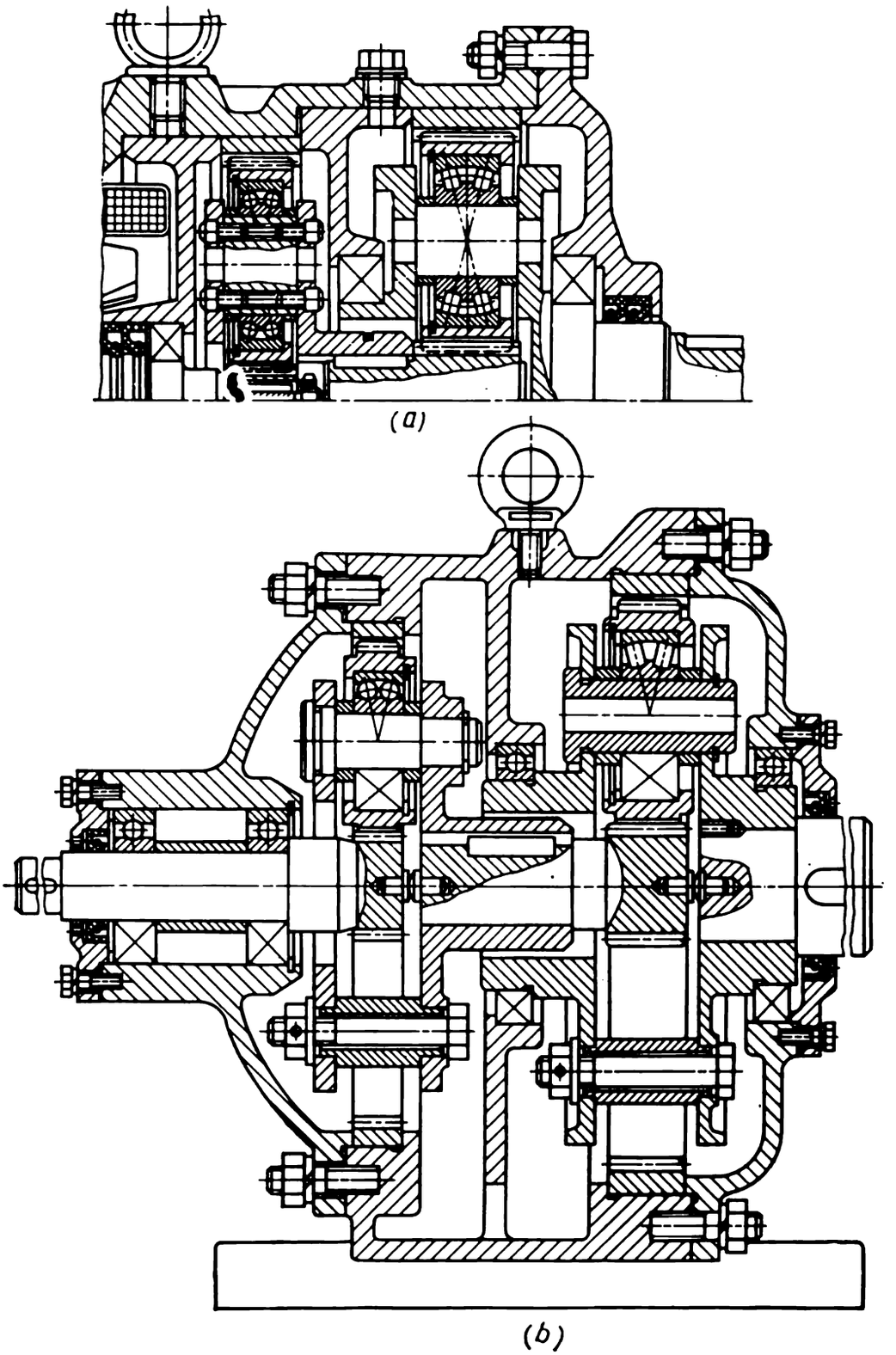


Fig. 5.34. Structures of reduction gear of 5.33, *a*
(*a*) by Odessa Politechnical Institute; (*b*) by N. L. Reshetov

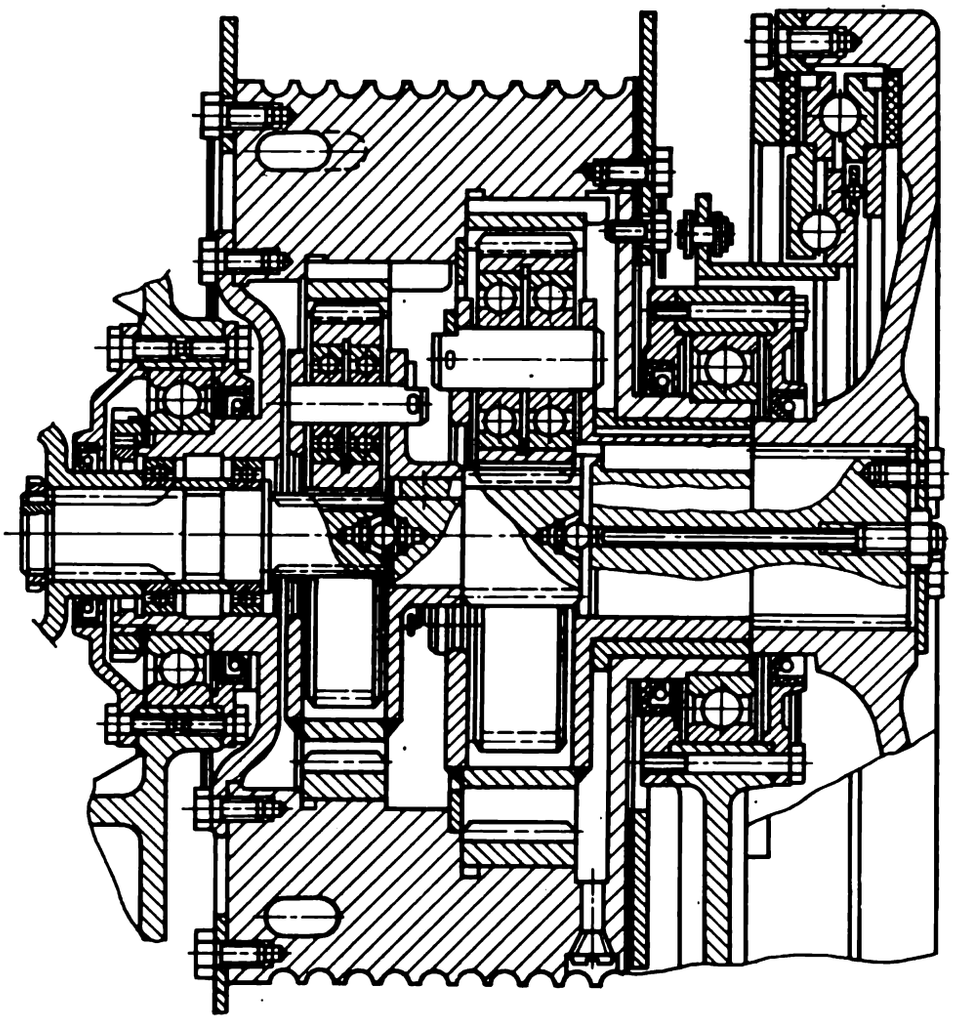

Fig. 5.35. Structure of reduction gear of 5.33, *b*, manufactured by the Kovrov Excavator Works (USSR)

left without self-alignment, as their performance proved satisfactory as it was.

Z. E. Garbuzov of the Research Institute for Earth-Moving Machines (USSR) has produced a tractor with wheels 2 metres in diameter and completely self-aligning gears, which has successfully passed the field tests.

A four-stage reduction gear—be it of a closed structure or of a simple multiple one (Fig. 5.36*a*)—requires two floating transmitting members: between the first and second units and between the third and fourth ones. The transmitting member between the second and third units should be supported on bearings, as the efforts in these units are already equalized by the floating members. The bearings may be stationary, although supporting this transmitting member by floating parts with the aid of spherical pairs $III_2'$ is preferable. This would offer a very inexpensive structure where neither of the

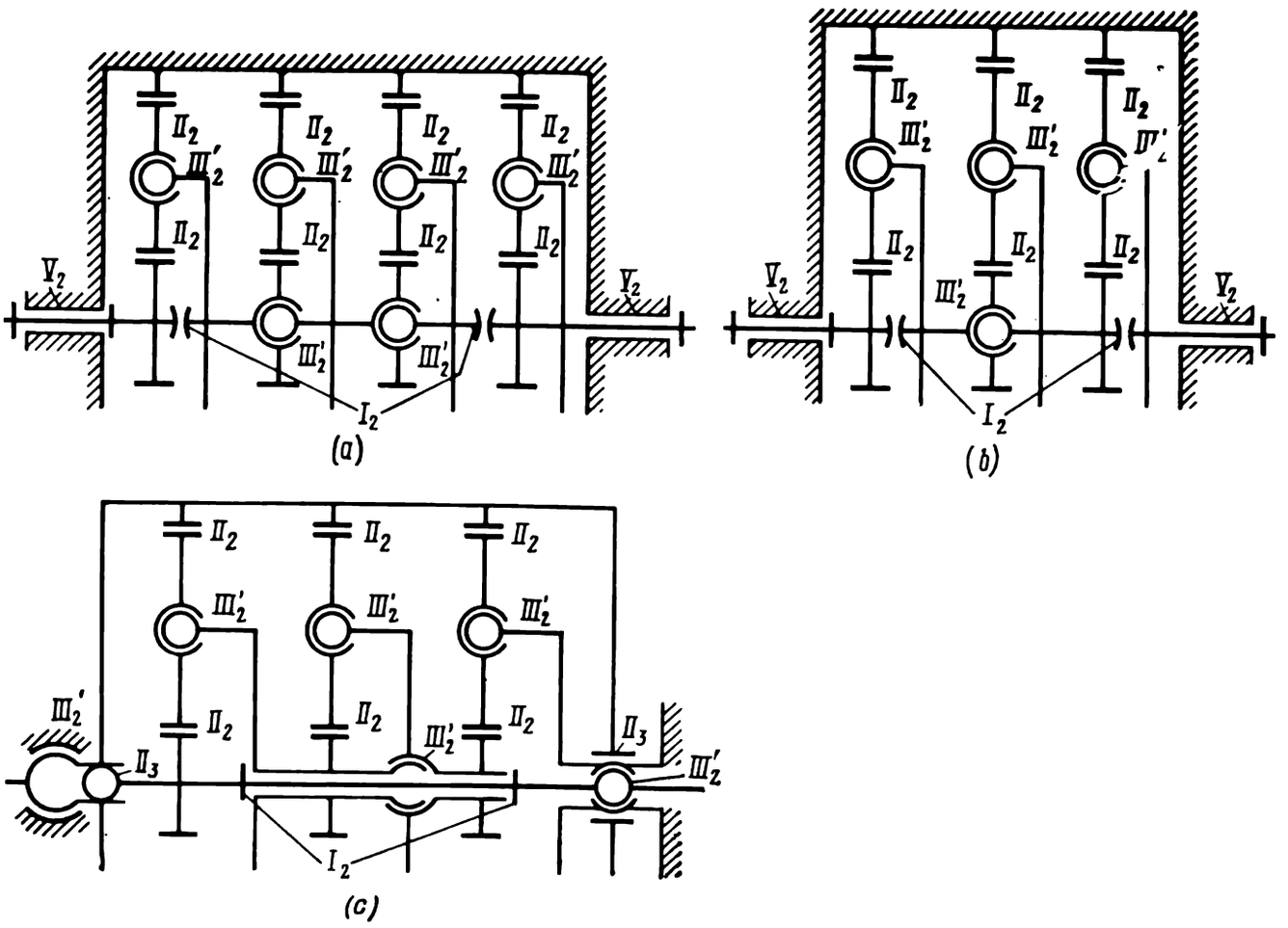


Fig. 5.36. Complex planetary mechanisms

(*a*) four-stage; (*b*) three-stage (triple) with floating members connected in the plane of central unit; (*c*) closed, with a connection of floating members axially offset from central unit plane

intermediate members has stationary bearings, and the boring of the reduction gear housing is therefore significantly simplified. It is true, however, that the high-speed stages of a four-stage mechanism are preferably plain gearings. Thus, the design being discussed is warranted in exceptional cases and is explained here to illustrate the approach to selection of the floating members.

A three-stage (triple) mechanism calls theoretically for one and a half floating transmitting members. Thus, two floating members can be used, with the extra mobilities eliminated by interconnecting these members by a spherical kinematic pair (Fig. 5.36*b*). A similar design for a closed planetary mechanism is shown in Fig. 5.36*c*.

The connections of the floating members can be either arranged in the central plane of the gears (cf. Fig. 5.36*b*) or offset axially (cf. Fig. 5.36*c*). Although the first-mentioned design has smaller angles of skewing with the same tolerances, it is less structurally

simple and might be altogether infeasible with a small diameter of the sun gear.

The correctness of the suggested designs (cf. Fig. 5.32 and 5.36) may be checked by calculating the redundant constraints from (1.1). All the designs have self-aligning satellite gears on spherical $III_2'$

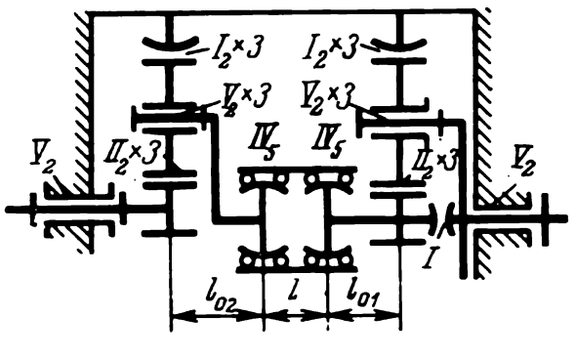


Fig. 5.37. Reduction gear with cylindrical teeth of sun and satellite gears and barrel-shaped teeth of ring gears

pairs with cylindrical teeth affording line engagement ($II_2$ pair). Alternatively, satellite on rotary pairs $V_2$ with barrel-shaped teeth yielding point engagement ($I_2$ pair) may be used, as the number of imposed restraints is the same in both cases. For comparison sake, both versions of the general design are shown in Fig. 5.33*a* and *b*. However, the two versions are not equivalent. As it has been already mentioned, the version with barrel-shaped teeth has greater contact strains and, hence, a lower load capacity; therefore, it should be used when the satellite gear fails to accommodate a spherical bearing of an adequate capacity. Even in such cases cylindrical teeth are preferred, although the elimination of redundant constraints would call for mounting the satellite gears on rocking frames, and the sun and ring gears on double toothed universal joints. This, naturally, would complicate the structure, to say nothing of the friction in the toothed universal joints affecting the uniformity of the satellite gear loading.

An in-between design has been suggested by A. E. Schuster (Fig. 5.37) [15]. He has used cylindrical teeth on the sun gears and satellites and barrel-shaped teeth on the ring gears where the influence of the barrel shape is not so adverse, owing to the internal meshing and the convex tooth engaging the concave one. The design has but two redundant constraints. Its drawback is the difficulty of making barrel-shaped teeth on ring gears. Small values of $l_{01}$ and $l_{02}$ are essential for this design, lest friction could annihilate the advantage of having the double universal joint on the intermediate shaft.

Each of the designs dealt with in the present Section has three satellite gears in every row. If a greater number of satellite gears is

called for, the mechanisms are operable solely with equalizing mechanism designs with a floating carrier.

For particularly great torques, a split low-speed stage may be recommended, with the high-speed stage employed as the equalizing mechanism (Fig. 5.38). Each row here has three satellite gears.

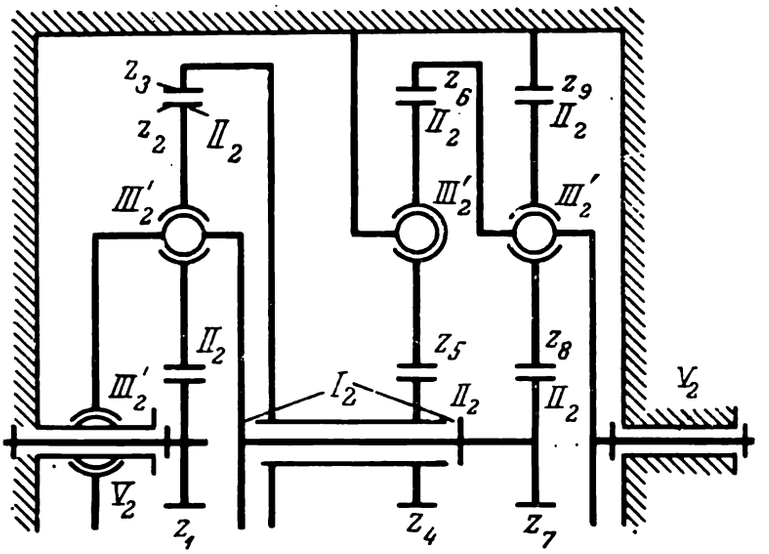


Fig. 5.38. Reduction gear with split second stage for very high torques

The levelling out of the circumferential forces of the satellite gears $z_2$ and idlers $z_5$ is effected by the floating member made up of the gears $z_3 z_4$.

The circumferential forces of the satellites $z_8$ are equalized by the floating gear $z_7$. Redundant constraints of this mechanism from (1.1): $q = 1 - 6 \times 13 + 5 \times 2 + 3 \times 10 + 2 \times 18 + 1 = 0$.

The transmission ratio (the deduction is omitted):

$$u = \frac{\omega_1}{\omega_6} = 1 + \frac{z_3}{z_1} + \frac{z_9}{z_7} + \frac{z_3 z_6}{z_1 z_4} + \frac{z_3 z_9}{z_1 z_7}$$

## 5.12. Reduction Gears of Wheel Motors

The most suitable for high power values are reduction gears made up of single-row mechanisms not possessing redundant constraints, while retaining line engagement of the teeth. This engagement offers higher load capacity and durability than point engagement of barrel-shaped teeth; thus, there are no reasons to discuss reduction gears of other designs. If self-alignment is not made use of, mechanisms of this kind would have 16 redundant constraints.

There are two known structures made up of single-row mechanisms (Figs. 5.39 and 5.40) [7, 27]. The kinematic diagram of both structures is the same: the first stage is a planetary one, the sun pinion is

the driving member, the driven members are the carrier connected to the sun gear of the second stage and the ring gear connected to the vehicle wheel. The second stage is a plane gearing with three idlers. The sun gears of both stages in both designs are floating, so

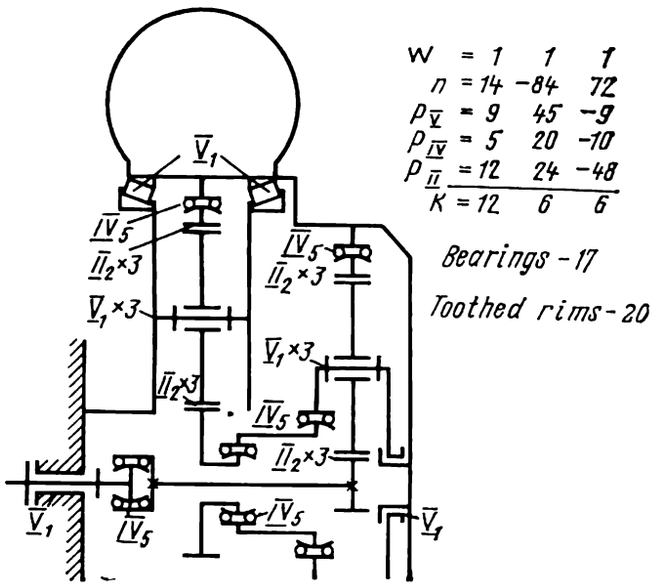


Fig. 5.39. Motor-wheel reduction gear by VNIIStroidormash

that uniform distribution of the load among the satellite gears and among the idlers is provided for.

To check the mechanism for the presence of redundant constraints, Malyshev's and Ozol's formulas will be used, the calculations by these formulas being illustrated in Tables accompanying the diagrams of the mechanisms (cf. Fig. 5.39).

There are six redundant constraints in Fig. 5.39 and eight in Fig. 5.40. They are caused by the satellite gears and idlers being mounted on two bearings, so that the gears and idlers would not self-align and would not provide for uniform distribution of the load along the teeth. The non-uniformity is somewhat decreased by the toothed universal joints, each affording two angular mobilities. However, each sun gear has three engagements, so that three angular mobilities are required for self-alignment, while the universal joint yields but two such mobilities. Thus, the member on the toothed universal joint retains one redundant constraint per three engagements. This is true of both ring gears and the second-stage sun gear of the design in Fig. 5.39; and of the first-stage sun gear and second-stage ring gear of that in Fig. 5.40.

The work conditions are the poorest for those members which are not associated with toothed universal joints and have one redundant constraint per each engagement. This applies to the first-stage sun

gear in Fig. 5.39 and to the first-stage ring gear and second-stage sun gear in Fig. 5.40.

Angular mobilities can be provided only by those toothed universal joints which are the closest to the sun gear, while the rest of them can only provide for its linear self-alignment (floating) and uniform distribution of the load among the satellite gears. Therefore, it

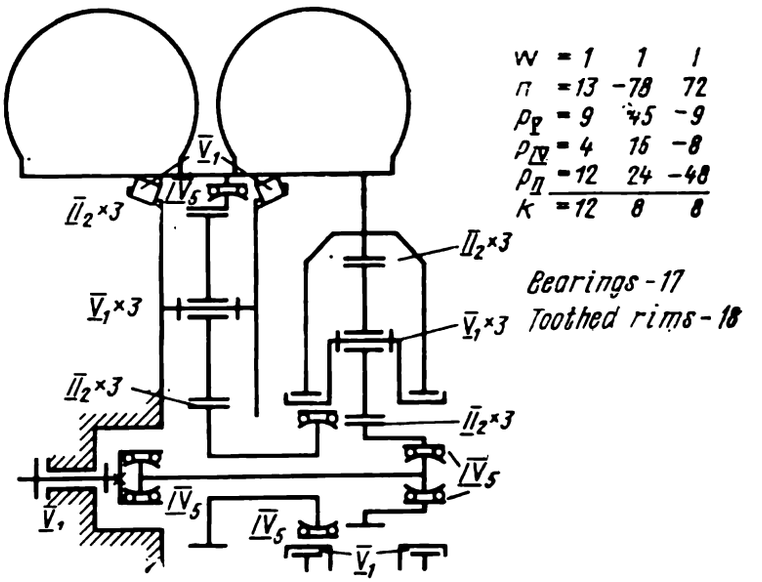


Fig. 5.40. Motor-wheel reduction gear by Belorussian Auto Works

is expedient to mount the second universal joint on the connecting member in the design of Fig. 5.40, in similarity with that of Fig. 5.39.

The toothed universal joint in front of the first-stage sun gear is axially offset in Fig. 5.40, so that friction in the universal joints affects the uniformity of load distribution along the teeth. Thus, it is further expedient to arrange this universal joint in the central plane of the gears of the first stage and to mount the first-stage ring gear on another toothed universal joint (as in Fig. 5.39). With all this done, the number of redundant constraints would be reduced to 4 per 12 engagements. To eliminate the redundant constraints completely, the satellite gears and idlers have to be mounted on spherical bearings (Fig. 5.41). This would additionally simplify the structure, as the amount of antifriction bearings is reduced from 17 to 11.

In this case the number of the toothed universal joints is reduced from 20 (Fig. 5.39) or 18 (Fig. 5.40) to 12 (Fig. 5.41). However, the major advantages of the last-discussed design are the increased durability and load capacity and its noiseless operation (which has been proved by test-bed trials).

When a wheel-carried motor is designed in accordance with Fig. 5.41, difficulties can be encountered in accommodating the

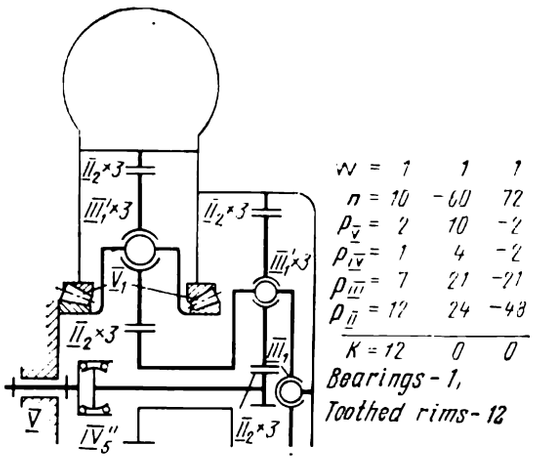


Fig. 5.41. Reduction gear made of single-row mechanisms, free of redundant constraints

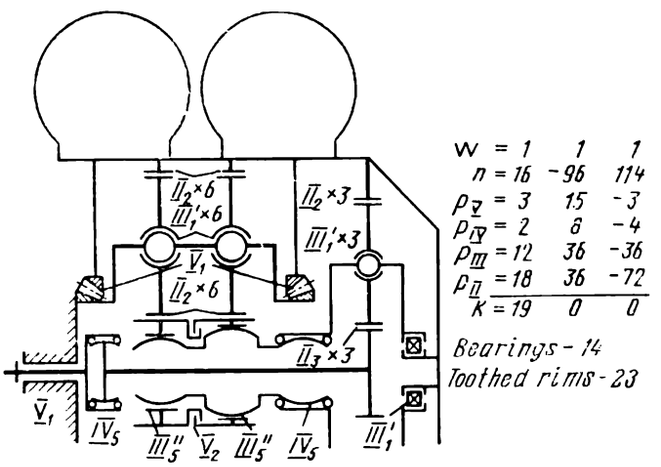


Fig. 5.42. Reduction gear with split second stage and equalizing mechanism on toothed universal joints (designed by V. V. Panarin)

roller bearings inside the idle axles. They may be overcome by using gears split into two halves, each supported by its own roller bearing and provided with an appropriate equalizing mechanism. There may be several versions of split gear designs.

1. There has been developed a draft design of a wheel-carried motor for a 180-ton dump truck (Fig. 5.42). In this reduction gear the two sun gears of the second stage are floating, therefore the mobilities of the $III_1'$ pair turned to be insufficient, and the toothed universal joint $IV_5$ had to be introduced.

The equalizing mechanism is in the form of two universal joints $III_5''$ with helical teeth whose axial forces acting upon the sun gears are equal and directed in opposition, assuring the equality of the transmitted torques.

With forward running, the axial forces between the sun gears are transmitted by the gears being urged toward each other, while in the reverse, the forces are transmitted through the $V_2$ pair which should be of the breech-block type for assembly purposes.

Quite naturally, the mechanism with split gears is more complicated, with its 14 bearings (which is still three bearings short of the mechanisms of Figs. 5.39 and 5.40) and 23 toothed rims.

2. The wheel motor (Fig. 5.42) can be further simplified by eliminating the toothed universal joint $IV_5$, but stepping up the mobility of the bearing support of the carrier by making it a pair $I_1$ (instead of the pair $III_1'$), as shown in Fig. 5.43. This can be done by using a spherical bearing with the outer race movable in both radial direc-

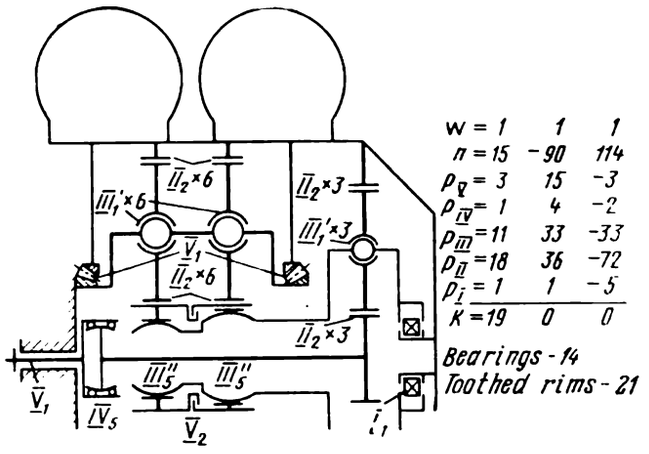


Fig. 5.43. Reduction gear with additional mobilities of intermediate member, doing away with one toothed universal joint

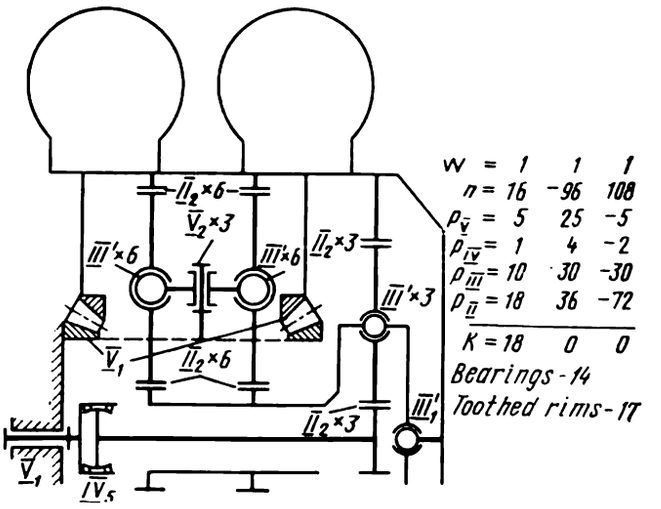


Fig. 5.44. Reduction gear with shafts of idlers serving as equalizing mechanism, suggested by A. I. Zvyagintsev et al.

tions (owing to a radial gap). The number of the bearings remains 14, but the number of the toothed rims, reduced by two, is 21.

3. In general, toothed universal joints complicate the design of a wheel-carried motor, their friction affecting the even distribution of load between the satellite gears and idlers. Thus, a preferred solution would be to do away with these universal joints by using other devices for torque equalization: e.g. by connecting the shafts of the second-stage idlers to the fixed member by radially* directed rotary pairs $V_2$ (Fig. 5.44). This reduction gear has 14 antifriction bearings and 17 toothed rims.

To save space in the axial direction, it is possible to replace the radial joint by providing the shaft of the idlers with pointed ends (Fig. 5.45) and thus to attain uniform distribution of the torques between the idler halves by equalizing the axial forces.

The designs of Figs. 5.44 and 5.45 are also suitable for a satellite gear shaft if the gear would not accommodate a single spherical bearing of adequate capacity.

4. The ring gear of the first stage may be connected not with the vehicle wheel, but with one of the sun gears of the second stage. As the carrier and ring gear of the first stage rotate in opposite directions, the two halves of the second stage have to be different: one remaining a plain gearing with idlers and the other being a planetary gearing (Fig. 5.46).

*As suggested by V. M. Yastrebov, F. I. Plekhanov and A. I. Zvyagintsev.

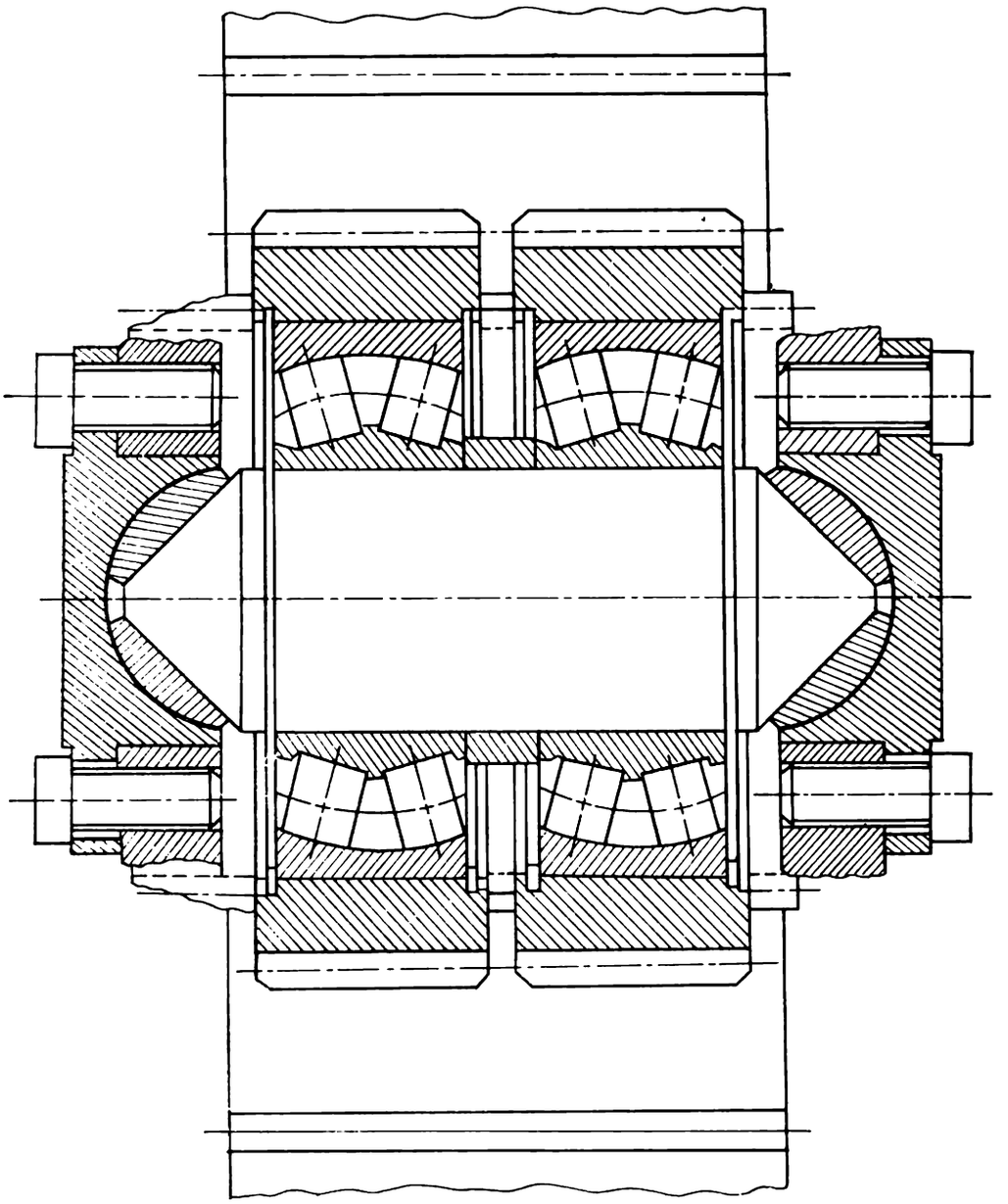

Fig. 5.45. Self-aligning gear with wedge-type equalizing mechanism

To ensure equality of the circumferential efforts and bearing loads of the second stage, the sun gears of this stage may have different diameters. To secure the ring gear of the first stage axially, it has to be connected with the carrier by a $I_1$ pair. It may be a spherical bearing with a radial gap of the outer race. This mechanism is simpler than the previously described one: it has 15 bearings and 15 toothed rims. With the same number of the teeth, its transmission ratio is nearly twice as great, defined by the following expression:

$$\frac{\omega_1}{\omega_9} = -\frac{z_3}{z_1} - \frac{z_9}{z_7} - \frac{z_7 z_8}{z_1 z_4} - \frac{z_3 z_9}{z_1 z_7}$$

Its sole disadvantage is certain complexity of designing the second stage.

5. The first-stage carrier is split (Fig. 5.47)† and includes two discs, i.e. the disc *3* connected to the sun gear *2* and the disc *4* connected

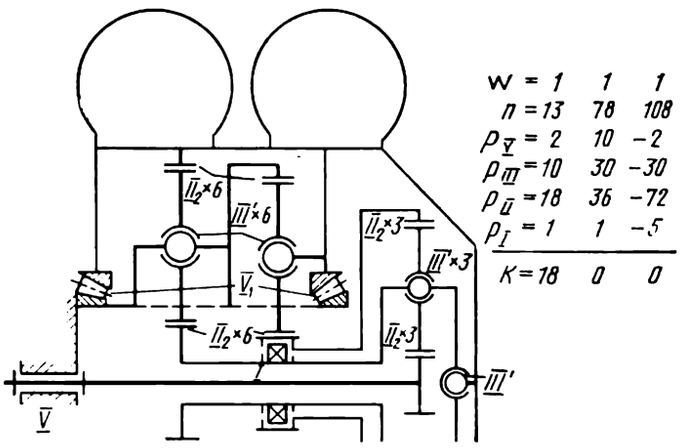


Fig. 5.46. Reduction gear with different designs in the two rows of the second stage

to the sun gear *1* of the second stage. The discs are relatively centered by a rotary sliding-contact pair $V_2$. This is quite permissible, as their relative motion is minimal. The shafts of the first-stage satellite

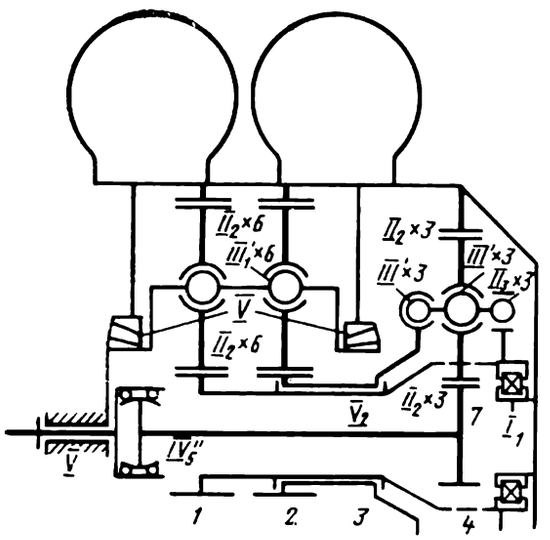


| | | | |
|---|---|---|---|
| $w$ = 4 | 4 | 4 |
| $n$ = 17 | -102 | 126 |
| $\rho_V$ = 3 | 15 | -3 |
| $\rho_{IV}$ = 1 | 4 | -2 |
| $\rho_{III}$ = 12 | 36 | -36 |
| $\rho_{II}$ = 21 | 42 | -84 |
| $\rho_I$ = 1 | 1 | -5 |
| $K$ = 21 | 0 | 0 |

Bearings - 14
Toothed rims - 17

Fig. 5.47. Reduction gear with the first-stage satellite shafts acting as equalizing levers

gears are connected to the discs with the aid of spherical bearings one of which $III'$ has no axial mobility, while the other one $II_3$ is axially movable. Alternatively, it may have no axial mobility, but then the discs have to be centered not by a rotary pair $V_2$, but by a ring or annular one $II_3$. The satellite shafts now would serve as levers levelling out the torques acting upon the sun gears of the second stage. Some skewing of the satellite gears would not affect the performance of the teeth, as the satellite gears are mounted on spherical bearings. The skewing of these shafts would not influence the performance of the bearings, either, if, as V. N. Ermak has suggested, the spherical antifriction bearings are mounted between the shaft and the discs, while a plain bearing is mounted between the shaft and the satellite gear. This design also solves the problem of accommodating antifriction bearings of a high capacity to support the self-aligning satellite gear (cf. Fig. 4.25).

Another way to avoid the influence of a skewing shaft upon the performance of the bearings is to mount the satellite gear onto a bearing with concave rollers, where the inner race has a spherical working surface. Then the skewing of this race (i.e. of the shaft) would not affect the work of the bearing. Bearings of this kind are manufactured in the USA by Link Belt and Bentam Companies (cf. Fig. 4.23).

To attain uniform load distribution among the idlers. both sun gears *1* and *2* of the second stage are floating. To avoid a harmful local mobility, one of the discs is connected to the reduction gear housing by a spherical bearing $I_1$ with an increased radial gap ($I_1$ pair) between the outer race and the carrier disc *6*. To equalize the load of the satellite gears, the first-stage sun gear is likewise floating: it is connected to the electric motor shaft by a toothed universal joint $IV_5''$ with limiting rings.

6. The reduction gear may be even simpler by using two satellite gears in the first stage, each having its own carrier (Fig. 5.48). The two carriers are to be connected by a rotary pair $V_2$, which is structurally simple if the pair is made up of two bearings arranged at two sides of the plane of the first-stage gears.

The first stage here has two satellite gears instead of the traditional three, so that the sun gear has one local mobility, although the latter is not harmful, as the friction in the teeth adequately precludes any oscillation process by damping. The mobility of the mechanism is thus $w = 2$.

Two satellite gears are quite sufficient to transmit the torque,

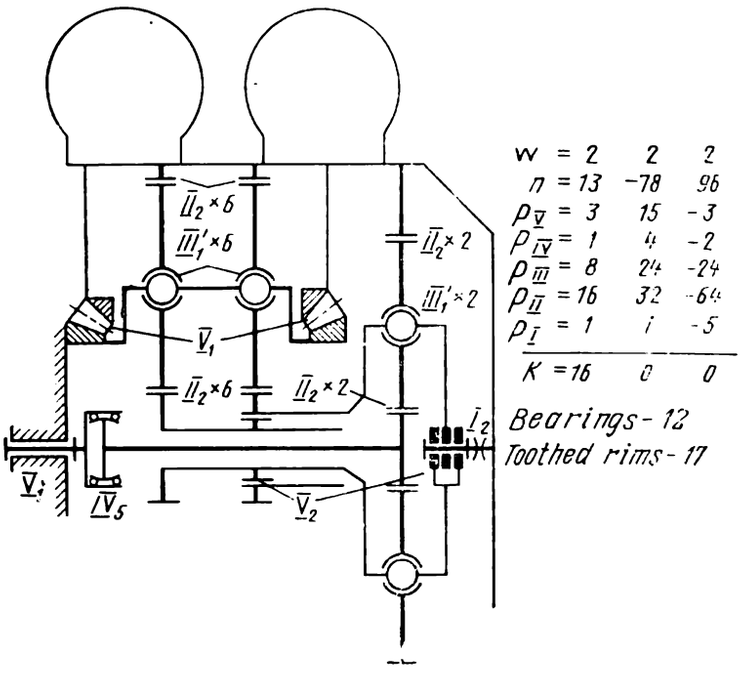


Fig. 5.48. Reduction gear with two carriers in the first stage (one satellite on each carrier)

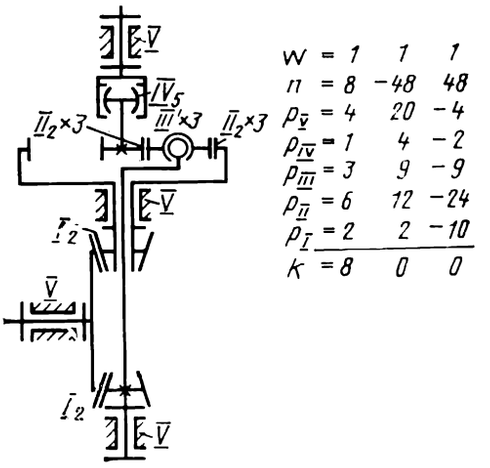


Fig. 5.49. Wheel motor reduction gear with bevel gears

with one satellite gear of the first stage conveying the power stream to three idlers of the second stage.

If the transmission ratio of the first stage is presumed to be 6 : 1 (which is quite close to the real situation), one satellite gear would suffice even for six idlers of the second stage (with the dimensions being the same).

Notwithstanding the split second stage, this reduction gear has 13 bearings and 16 toothed rims.

7. There are designs of motor-wheels where the motor axis is perpendicular to that of the wheel, so that bevel gearing is necessary. To reduce the load of the teeth, it is useful to have two small pinions meshing with one big bevel gear and rotating in opposite directions (Fig. 5.49). It is expedient that the bevel gears be with circular teeth and point engagement ($I_2$ pair), such as teeth cut in machine-tools manufactured by Gleason or Oerlikon.

A single-row planetary mechanism is used in the design of Fig. 5.49 to drive the bevel gears, its carrier being connected to one of the gears, while its ring gear is connected to the other one. As compared with the traditional design—the one with the stationary ring gear—the transmission ratio has been doubled, which is a serious advantage, as it enables one to simplify the reduction gear.

To avoid redundant constraints in a design with three satellite gears, the latter are to be mounted on spherical bearing, and the sun gear should be floating on a single toothed universal joint.

## 5.13. Method of Structural Groups for Investigating Self-Alignment of Planetary Mechanisms

As it has been already explained above, structures of mechanisms can be investigated with the aid of known Malyshev's and Ozol's structural formulas for determining the number of redundant constraints:

$$q = w - 6n + 5p_V + 4p_{IV} + 3p_{III} + 2p_{II} + p_I,$$

$$q = w + 6k - f$$

where $w$ is the mobility of the mechanism; $n$ is the number of its movable members; $k$ is the number of independent loops in the mechanism; $f = p_V + 2p_{IV} + 3p_{III} + 4p_{II} + 5p_I$ is the sum of the mobilities of the kinematic pairs, respectively, of the fifth, fourth, third, second and first classes.

The drawback of these formulas is that each equation has two unknown values, i.e. the number $q$ of redundant constraints and the mobility $w$ of the mechanism.

The method of mobilities in a loop is free from this drawback and presents a nice tool for solving the problem in mechanisms with a relatively small number of the loops. With a great number of the loops the task is significantly complicated at the stage of distributing the mobilities among the loops, and thus it is important to minimize the number of the loops. This Section suggests that this should be done by selecting structural groups from a mechanism for preliminary investigation, and then by investigating the rest of the mechanism. In a planetary mechanism, this group is preferably a single-row block of the members (Fig. 5.50*a*) including the sun gear, the ring gear and the three satellite gears with their bearings. The bearings of the central members, i.e. of the sun gear, the carrier and the ring gear are not included in the group. In blocks of this kind, the satellite gears may be mounted either on $V$-class bearings or $III'$-class spherical bearings. The calculation by structural formulas for the block with the satellite gears with V-class bearings is shown in Fig. 5.50*b*, and for that with the satellite gears on $III'$-class bearings is given in Fig. 5.50*c*. The number of the loops is calculated from formula $k = p - n$. For both designs $k = 4$. Redundant constraints are

calculated from Malyshev's formula $q = w - 6n + 5p_V + 4p_{IV} + 3p_{III} + 2p_{II} + p_I$ (second column) and from Ozol's formula $q = w + 6k - f$ (third column). Mobilities in the loops are investigated in Fig. 5.50*d* and *e*. The names of the loops are written down in first column; second column contains the alphabetic symbols of kinematic pairs yielding linear mobilities along the respective coordinate axes; third column contains the alphabetic symbols of kinematic pairs yielding angular mobilities about the respective axes; fourth column names the axes shown in Fig. 5.50*a*. Constraints are indicated with downward arrows ↓, while mobilities are shown as upward arrows ↑. Usually, it takes two pairs to have a local mobility, with the mobility of one pair being spent on closing the loops (for assembling), while the mobility of the other pair remaining the local one. The two pairs in the diagram are connected with a brace, with the arrow indicating the local mobility leading from this brace.

The analysis of distribution of the mobilities in Fig. 5.50*d* has shown two angular redundant constraints about the $x_1$ and $x_3$ axes, one angular mobility about the $z$ axis (rotation of the mechanism), two axial mobilities of the sun and ring gears along the $z$ axis and radial movements of the sun gear with the ring gears along the $x_1$ and $x_2$ axes. There are no redundant constraints in Fig. 5.50*e*. There remain: two linear mobilities along the $z$ axis, radial joint mobilities of the sun ring gears along the $x_2$ and $x_1$ axes and angular mobility about the $z$ axis (rotation of the mechanism). Besides, four angular mobilities of the sun and ring gears about the $y_3$, $y_2$ and $y_1$ axes are added. The parameters of these blocks are written in Fig. 5.50*b* and *c*.

To look into radial mobilities (Fig. 5.51), let us consider velocities with the carrier being immobile and the ring gear moving radially at a velocity shown as line segment *pc* in Fig. 5.52. The points $C'_{II}$, $C''_{II}$ and $C'''_{II}$ of the ring gear move at the same speed. The velocities of the points of the satellite gears, coinciding with the above points and shown as segments $pc'_c$, $pc''_c$ and $pc'''_c$ are directed perpendicularly to the radii $B'_V C'_{II}$, $B''_V C''_{II}$ and $B'''_V C'''_{II}$.

The velocity triangles are closed by lines $cc'_c$, $cc''_c$ and $cc'''_c$ illustrating the sliding velocities of the teeth, directed tangentially to their profiles.

The velocity of the point $A'_{II}$ of the satellite gear is equal to and opposes the velocity of the point $C'_{II}$ (owing to the radii being equal). Therefore, $pa'_c = pc'_c$; $pa''_c = pc''_c$ and $pa'''_c = pc'''_c$.

The velocities of the points $A'_{II}$, $A''_{II}$ and $A'''_{II}$ of the sun gear can

be found by drawing from points $a'_c$, $a''_c$ and $a'''_c$ the directions of the velocities of the sliding of the teeth, parallel to the tangents to their profiles. These straight lines intersect at one point $a_{sg}$, which means that the motion of the sun gear will be translatory and shown as segment $pa_{sg}$.

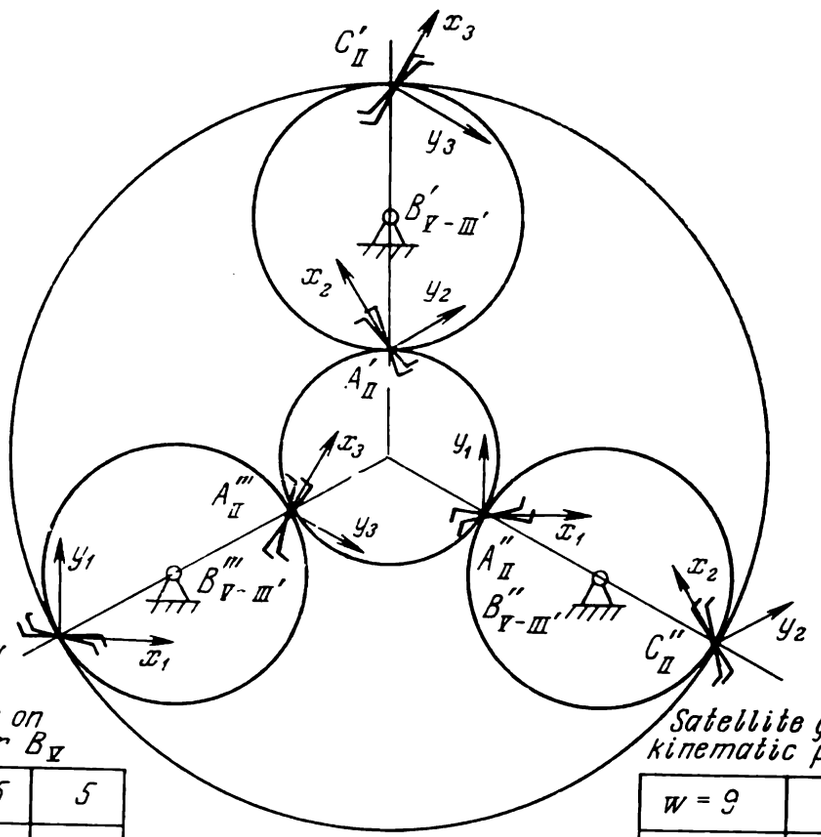


(a)

Satellite gears on kinematic pair $B_V$

| $w=5$ | 5 | 5 |
|---|---|---|
| $n=5$ | -30 | 24 |
| $p_V=3$ | 15 | -3 |
| $p_{II}=6$ | 12 | -24 |
| $K=4$ | 2 | 2 |

Satellite gears on kinematic pair $B_{III'}$

| $w=9$ | 9 | 9 |
|---|---|---|
| $n=5$ | 30 | 24 |
| $p_{III}=3$ | 9 | -9 |
| $p_{II}=6$ | 12 | -24 |
| $K=4$ | 0 | 0 |

| | |
|---|---|
| Radial displacements of sun gear with ring gear | $f'_x=1$, $f'_y=1$ |
| Axial displacement, separately, of sun gear and ring gear | $f'_z=2$, $f''_z=1$ |
| Rotation of mechanism | $f_\Sigma=5$ |
| Redundant constraints | $q''_x=1$, $q''_y=1$ |
| | $K=4$ |

(b)

| | |
|---|---|
| Radial displacements of sun gear with ring gear | $f'_x=1$, $f'_y=1$ |
| Axial displacement, separately, of sun gear and ring gear | $f'_z=2$, $f''_z=1$ |
| Rotation of mechanism | $f_\Sigma=9$ |
| Rotation of sun and ring gears | $f''_x=2$, $f''_y=2$ |
| | $K=4$ |

(c)

Let us find the value and direction of this velocity. Denoting: the angle $pa_{sg}a'_s = x$;

from triangle $pcc'_s$: $pc'_s = pc \cdot \operatorname{tg} \alpha_w = pa'_s$;

from triangle $pcc''_s$: $pc''_s = pc \dfrac{\sin(60° - \alpha_w)}{\sin(90° + \alpha_w)} = pa''_s$;

from triangle $pa_{sg}a'_s$: $pa_{sg} = pa'_s \dfrac{\sin(90° + \alpha_w)}{\sin x}$

$= pc \dfrac{\operatorname{tg}\alpha_w \sin(90° + \alpha_w)}{\sin x} = -pc \dfrac{\sin\alpha_w}{\sin x}$;

from triangle $pa_{sg}a''_s$: $pa_{sg} = pa''_s \dfrac{\sin(90° - \alpha_w)}{\sin(60° - x)}$

$= pc \dfrac{\sin(90° - \alpha_w)\sin(60° - \alpha_w)}{\sin(60° - x)\sin(90° + \alpha_w)} = -pc \dfrac{\sin(60° - \alpha_w)}{\sin(60° - x)}$

Thus, $pa_{sg} = -pc \dfrac{\sin(60° - \alpha_w)}{\sin(60° - x)} = -pc \dfrac{\sin\alpha_w}{\sin x}$

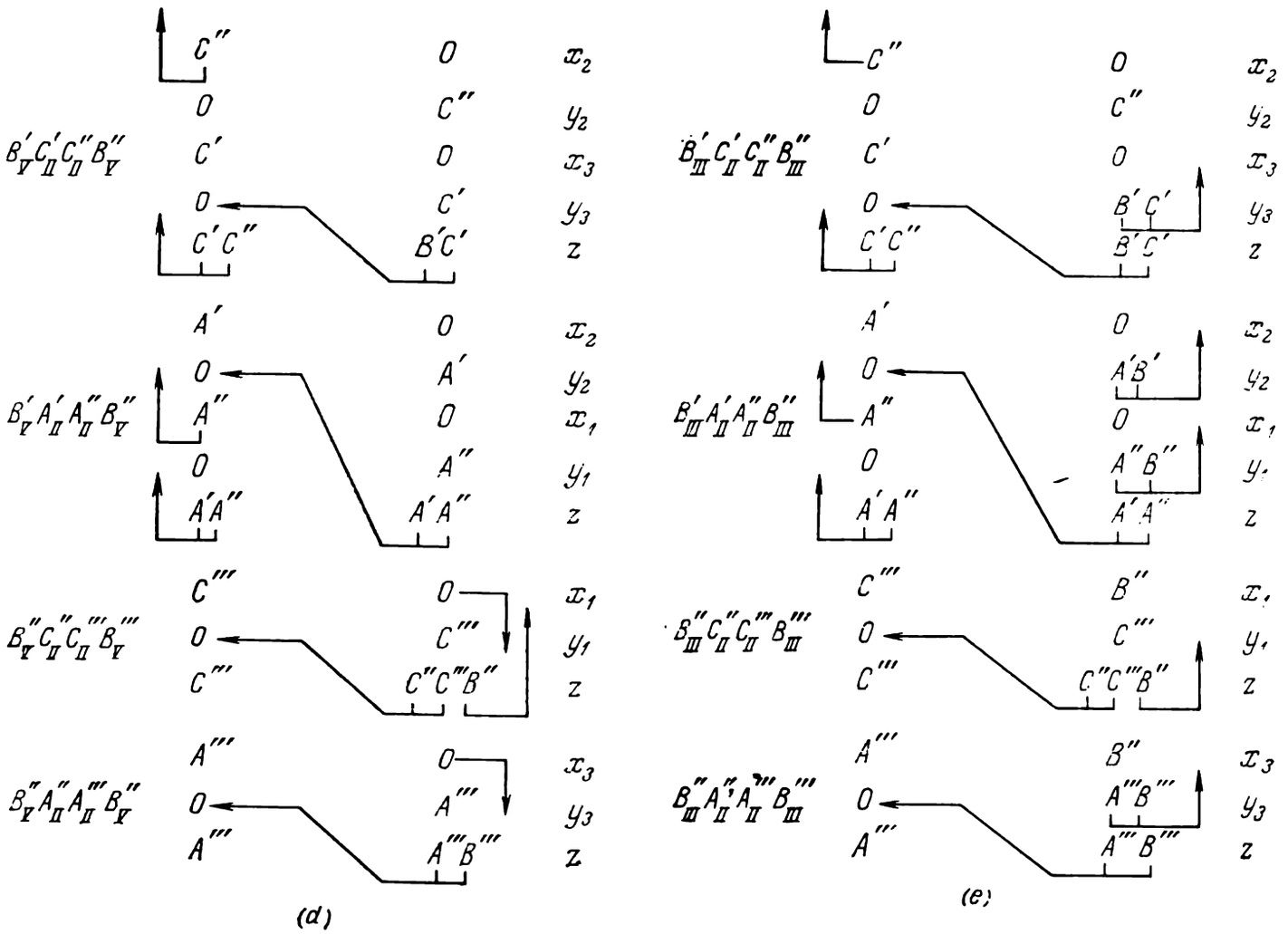


Fig. 5.50. Single-row structural group (structural block)
(*a*) diagram; (*b*), (*c*) mobility Tables; (*d*), (*e*) mobility diagrams; (*b*) and (*c*) for satellites on rotary pairs; (*c*) and (*e*) for satellites on spherical pairs

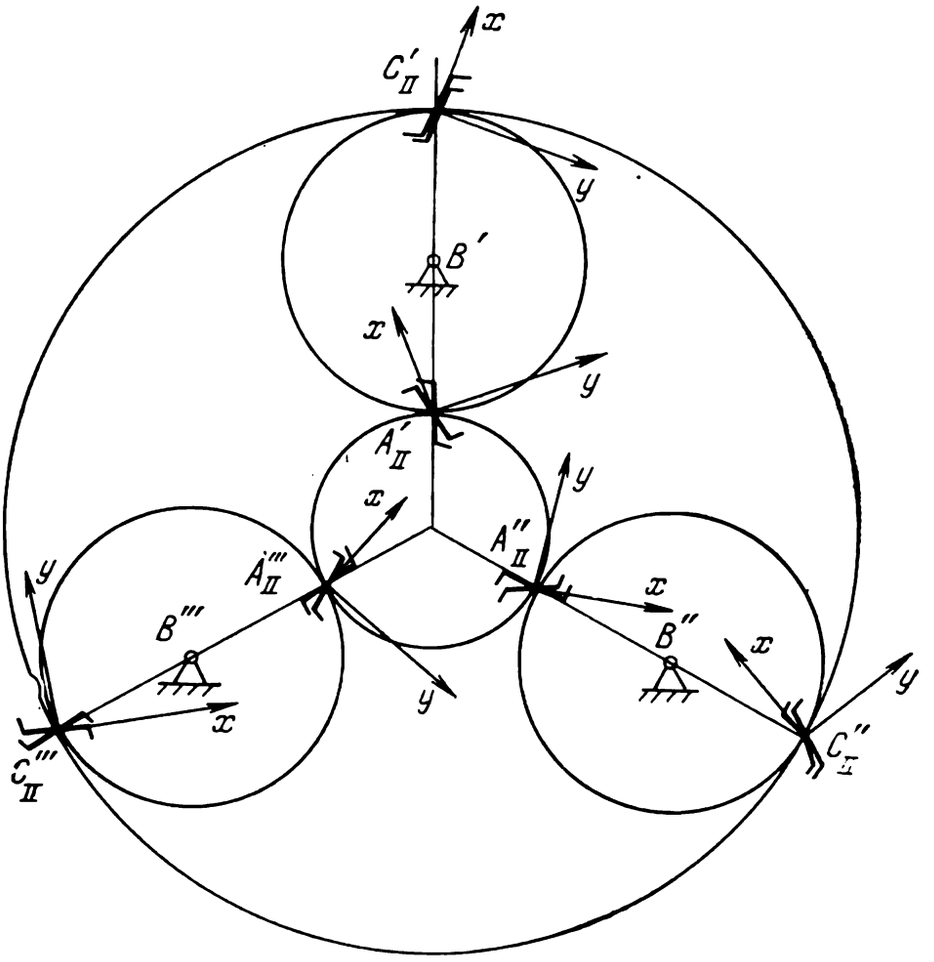


Fig. 5.51. Single-row structural block with accurate representation of pressure angles

or $\sin \alpha_w \sin (60° - x) = \sin x \cdot \sin (60° - \alpha_w)$
and $\sin \alpha_w \sin 60° \cos x - \sin x \sin 60° \cos \alpha_w$
$- \sin \alpha_w \sin 60° \cos x = \sin x \sin 60° \cos \alpha_w$
By reducing by $\sin 60°$ and by dividing by $\cos x \cos \alpha_w$:

$$\operatorname{tg} \alpha_w = \operatorname{tg} x, \quad \text{so that} \quad \boxed{x = \alpha_w.}$$

From the expression for $pa_{sg}$ we have, neglecting the algebraic sign: $\boxed{pa_{sg} = pc,}$ i.e. with the ring gear moving radially, the sun gear will move at the same velocity in a direction defining an angle $2\alpha_w$ with the direction opposite to the direction of the motion of the ring gear.

Thus, one radial mobility $f'_y = 1$ has been explained. Another angular mobility $f'_x = 1$ can be deciphered in the same manner. Furthermore, from the diagram of the distribution of the mobilities in the loops, Fig. 5.50*d*, we find $f'_z = 2$, $f''_z = 1$ and two redundant constraints $q''_x = 1$ and $q''_y = 1$, i.e. in the block under consideration

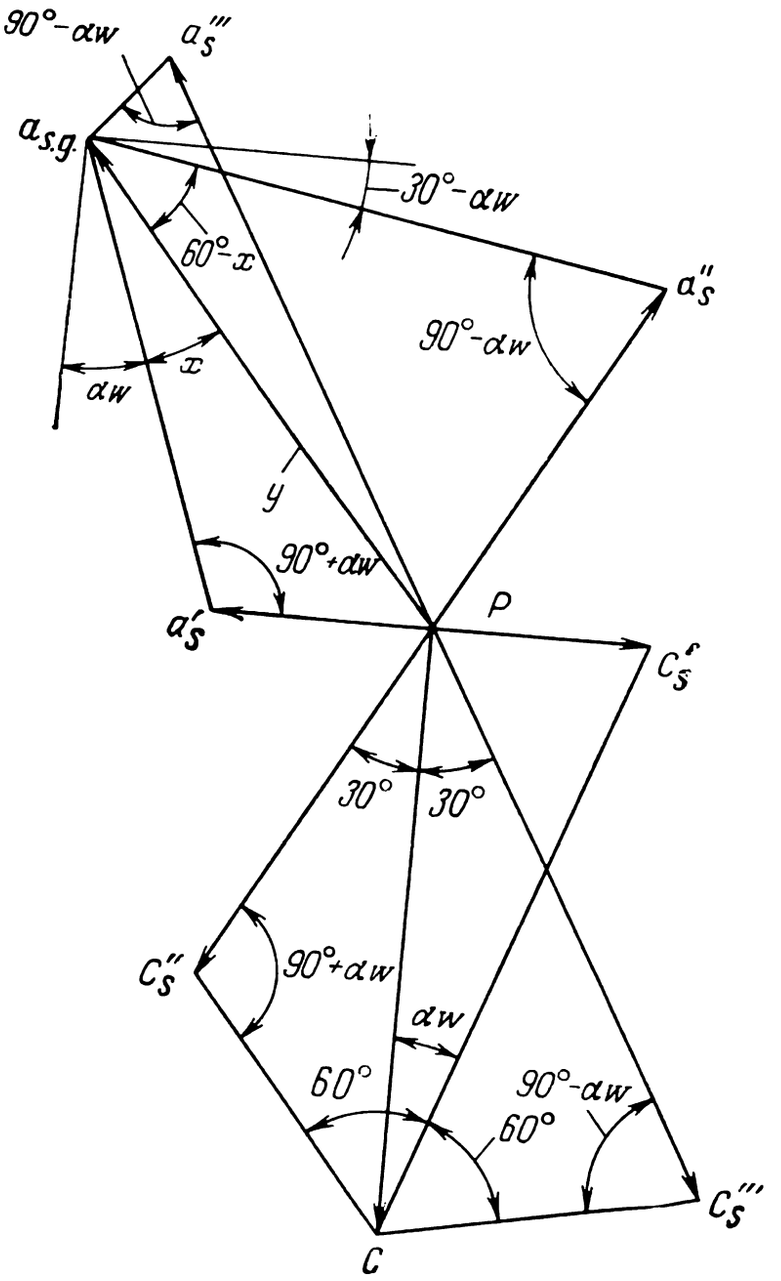


Fig. 5.52. Polyhedrons of linear mobilities for mechanism of Fig. 5.51

there are five mobilities and two redundant constraints. With incorrect designing, redundant constraints can be added to these two redundant constraints, whereas the latter can be eliminated exclusively within the very block and not outside it.

The above considerations concerning mobilities $f_x$ and $f'_y$ are exactly the same in the case of a single-row block with satellite gears on spherical bearings.

To look into angular mobilities of a single-row block with spherical bearings of the satellite gears, let us consider this block with the sun gear and the carrier fixed. Presuming that the ring gear has

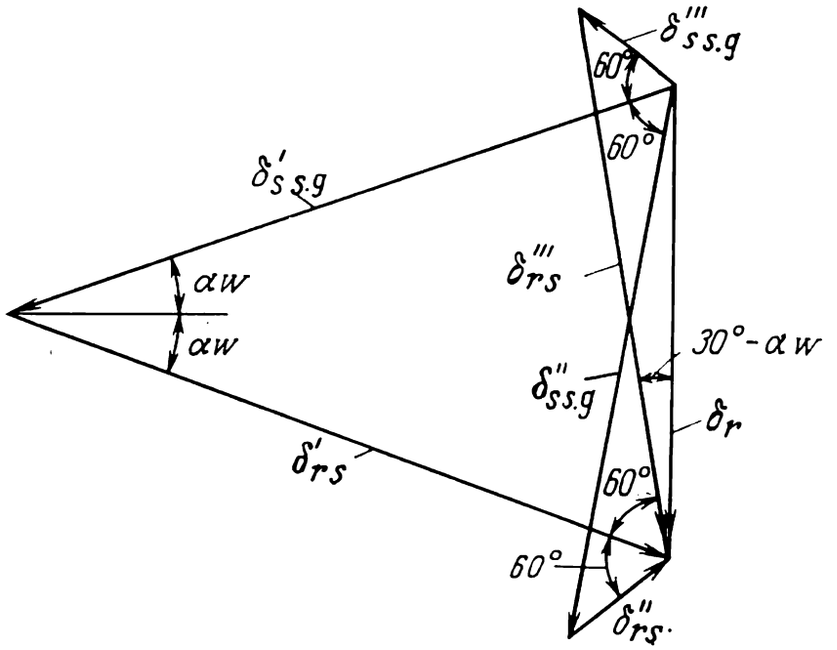


Fig. 5.53. Polyhedrons of angular mobilities for mechanism of Fig. 5.51 with satellites on spherical bearings

rotated through $\delta_r$, let us find the angle of rotation of the first satellite gear $\delta'_{ss.g}$ (Fig. 5.53) whose vector will be directed along the normal to the teeth profiles at point $A'_{II}$. The triangle in Fig. 5.53 will be closed by vector $\delta'_{rs}$ directed along the normal to the point $C'_{II}$ of the engagement of the teeth profiles. Similar triangles will be formed of vectors $\delta''_{ss.g}$, $\delta''_{rs}$ and $\delta_r$ for the second satellite gear and of vectors $\delta'''_{ss.g}$, $\delta'''_{rs}$ and $\delta_r$ for the third satellite gear. Thus, the satellite gears have rotated through angles $\delta'_{ss.g}$, $\delta''_{ss.g}$ and $\delta'''_{ss.g}$ with the sun gear being immobile.

A similar situation takes place with the ring gear being immobile and the sun gear having skewed, which indicates that the two cases of skewing are independent. Relating this to the axes $x$ and $y$ of the ring and sun gears, we have $f''_x = 2$ and $f''_y = 2$. All the mobilities of the single-row blocks are registered in Fig. 5.50*b* and *c*.

Let us explain the subsequent notation. The blocks will be denoted by small letters, with the same letters denoting mobilities in the loops in the diagram of mobilities. The loops will be denoted by their component outer pairs and structural blocks. Figs. 5.54 and 5.55 present diagrams of single-row planetary mechanisms, with the structural formula being expressed in their upper tables without the use of structural blocks, so that $k = 6$; while in the lower tables, with structural blocks, $k = 2$, i.e. with subtraction of the number of the loops in the structural blocks. To account for mobilities in the

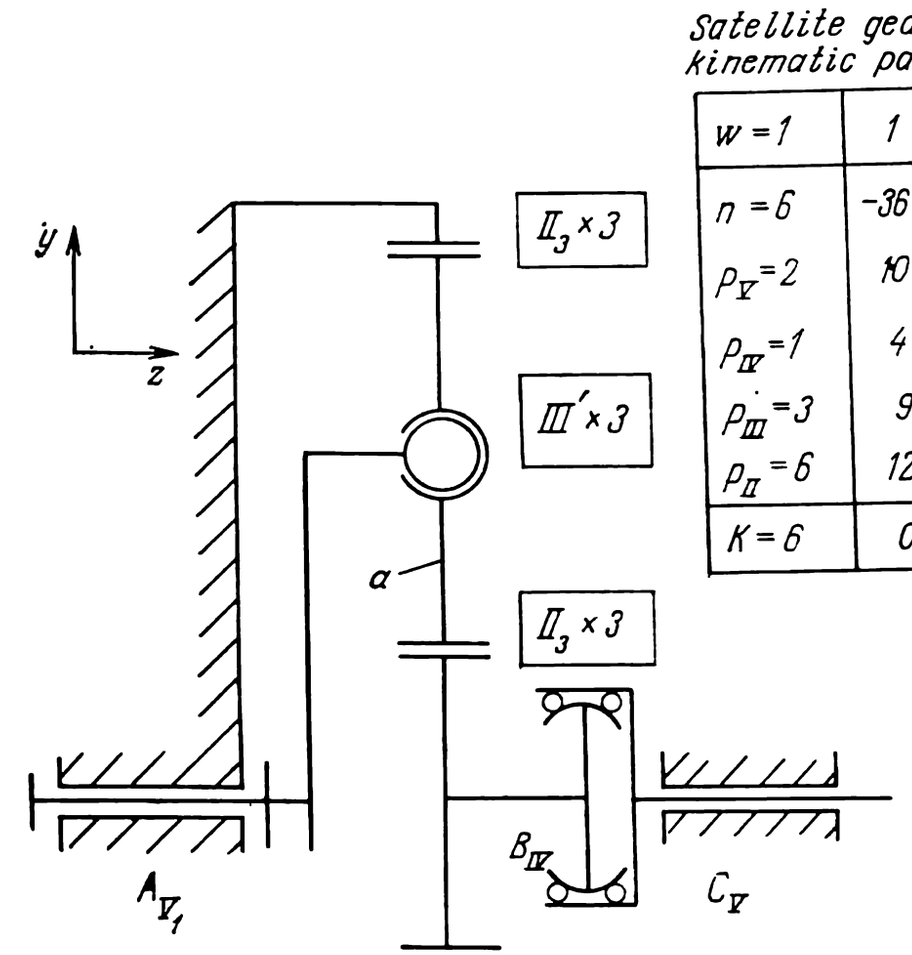


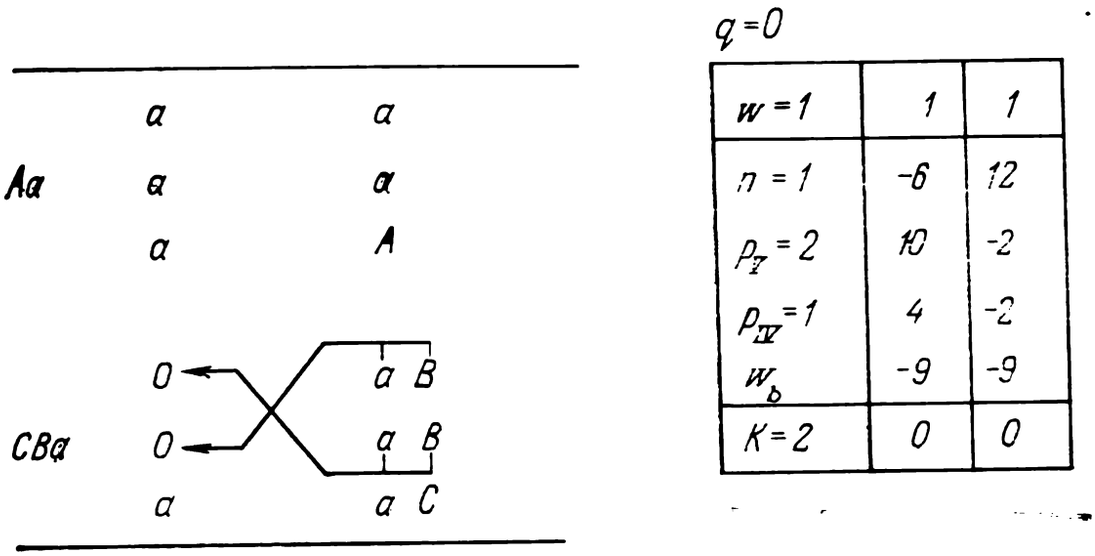


Fig. 5.54. Investigation of structure of single-row mechanism with satellites on spherical bearings: top—without using structural blocks; bottom—using structural groups

blocks, $w_{bl}$ is written down in the lower table with a minus sign. The number of the members in this table is found as the difference between the total number of the members and the number of the

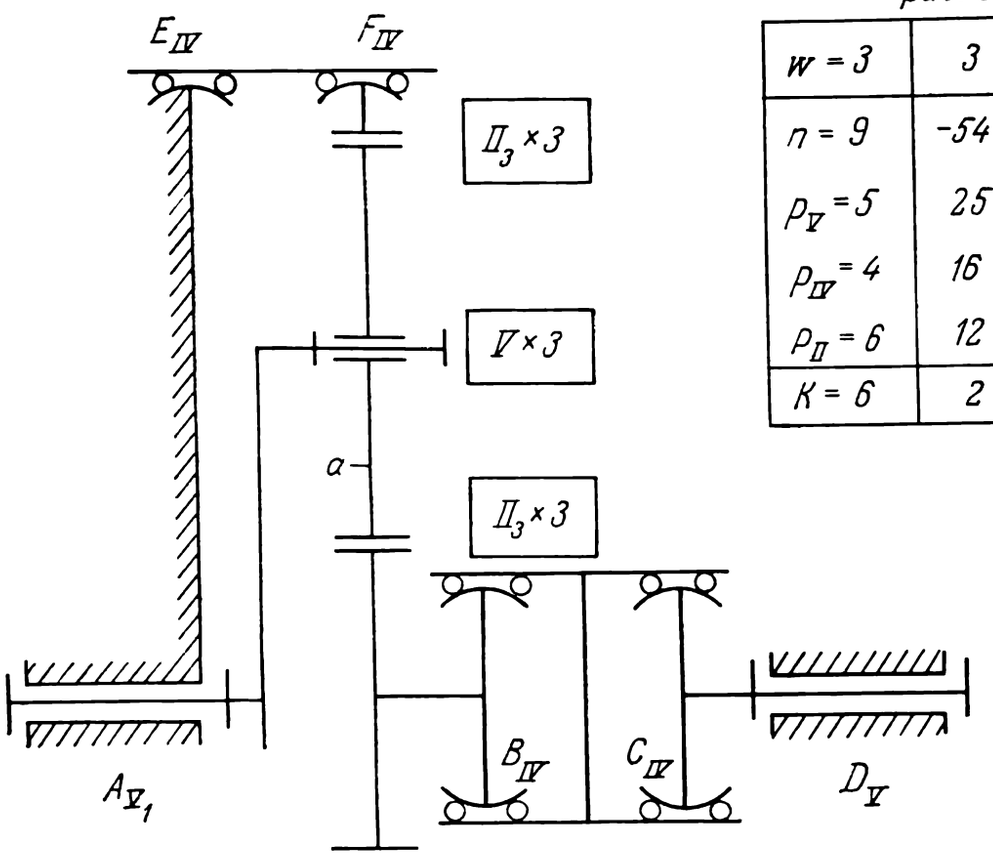


*Satellites on kinematic pairs $B_V$*

| $w = 3$ | 3 | 3 |
|---|---|---|
| $n = 9$ | -54 | 36 |
| $p_V = 5$ | 25 | -5 |
| $p_{IV} = 4$ | 16 | -8 |
| $p_{II} = 6$ | 12 | -24 |
| $K = 6$ | 2 | 2 |

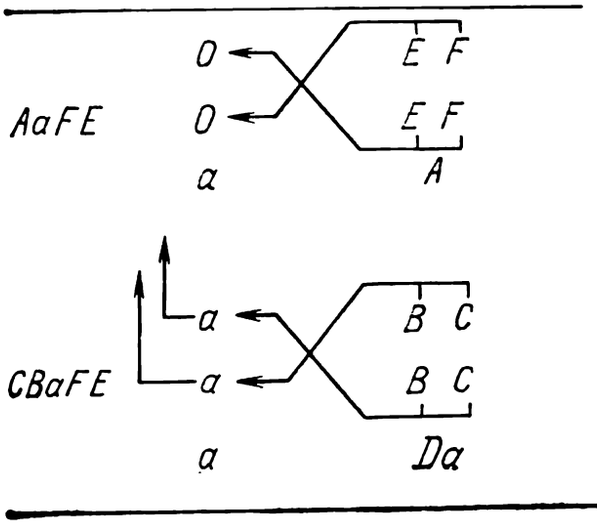


*q = 2 in block*

| $w = 3$ | 3 | 3 |
|---|---|---|
| $n = 4$ | -24 | 12 |
| $p_V = 2$ | 10 | -2 |
| $p_{IV} = 4$ | 16 | -8 |
| $w_b$ | -5 | -5 |
| $K = 2$ | 0 | 0 |

**Fig. 5.55. Investigation of structure of single-row mechanism with satellites on rotary bearings: top—without using structural blocks; bottom—using structural blocks**

members in the structural blocks. so that it can equal either zero or a negative figure. The structural analysis in case of the two loops thus obtained proves to be far simpler than that of six loops.

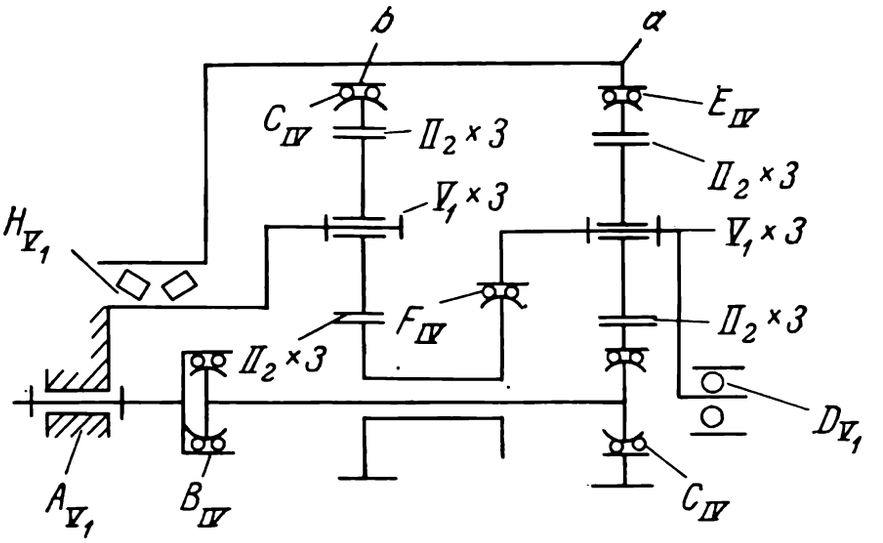


| | | |
|---|---|---|
| ABCaD | 0 | B C |
| | 0 | B C |
| | a | A |
| DaEH | a | E |
| | a | E |
| | a | a |
| EaFbG | 0 | F |
| | 0 | F |
| | b | b |
| DaFbGH | b | G |
| | b | G |
| | b | DH |

*Satellites on kinematic pairs $B_V$*

*Without using struct. groups*

| | | |
|---|---|---|
| $w = 1$ | 1 | 1 |
| $n = 14$ | -84 | 72 |
| $p_V = 9$ | 45 | -9 |
| $p_{IV} = 5$ | 20 | -10 |
| $p_{II} = 12$ | 24 | -48 |
| $K = 12$ | 6 | 6 |

*q = 4 in two struct. groups*

*Using struct. groups*

| | | |
|---|---|---|
| $w = 1$ | 1 | 1 |
| $n = 4$ | -24 | 24 |
| $p_V = 3$ | 15 | -3 |
| $p_{IV} = 5$ | 20 | -10 |
| $w_{str.\,gr.}$ | -10 | -10 |
| $K = 4$ | 2 | 2 |

**Fig. 5.56.** Investigation of structure of double-stage planetary reduction gear

In the design of Fig. 5.54 redundant constraints are absent, while in that of Fig. 5.55 redundant constraints $q = 2$ are only in the block, while the mechanism itself has two local mobilities.

Fig. 5.56 shows a diagram of a double-row planetary reduction

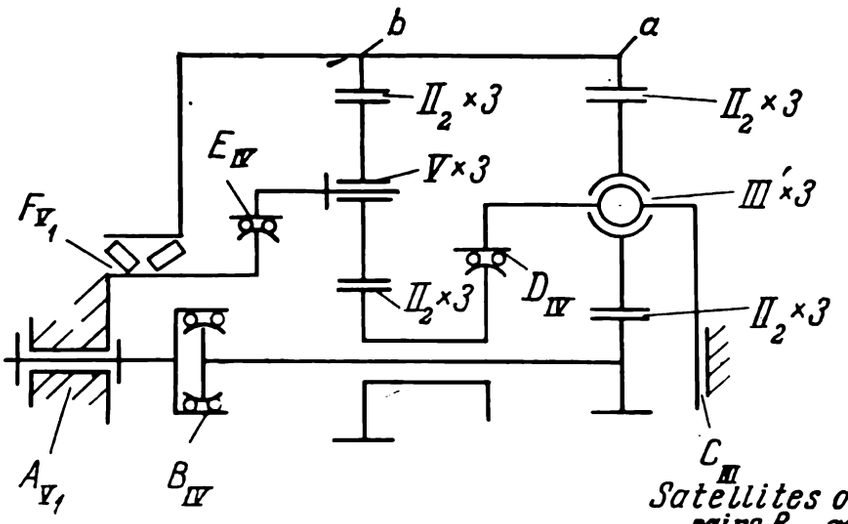


| | | |
|---|---|---|
| ÀḂaC | 0 → a B<br>θ → a B<br>a → A | |
| CaF | C → a<br>C → a<br>a → C | |
| aḊb | a → D<br>a → D<br>b → a | |
| ĖbF | b → E<br>b → E<br>b → bF | |

*Satellites on kinematic pairs $B_{III}$ and $B_V$*

*Without using struct. groups*

| $w = 1$ | 1 | |
|---|---|---|
| $n = 12$ | 72 | 72 |
| $p_V = 5$ | 25 | -5 |
| $p_{IV} = 3$ | 12 | -6 |
| $p_{III} = 4$ | 12 | -12 |
| $p_{II} = 12$ | 24 | -48 |
| $K = 12$ | 2 | 2 |

*q=2 in struct. group „b"*

*Using struct. groups*

| $w = 1$ | 1 | 1 |
|---|---|---|
| $n = 2$ | 12 | 24 |
| $p_V = 2$ | 10 | -2 |
| $p_{IV} = 3$ | 12 | -6 |
| $p_{III} = 1$ | 3 | -3 |
| $w_{str.\ gr.}$ | -14 | -14 |
| $K = 4$ | 0 | 0 |

Fig. 5.57. Investigation of the structure of reduction gear of wheel motor of Lectra Haul 180-ton dump truck

gear. The satellite gears of the first and second stages are mounted on kinematic pairs $V_1$. Without the use of structural blocks, twelve loops would have to be analyzed (top tabl)e, whereas by employing

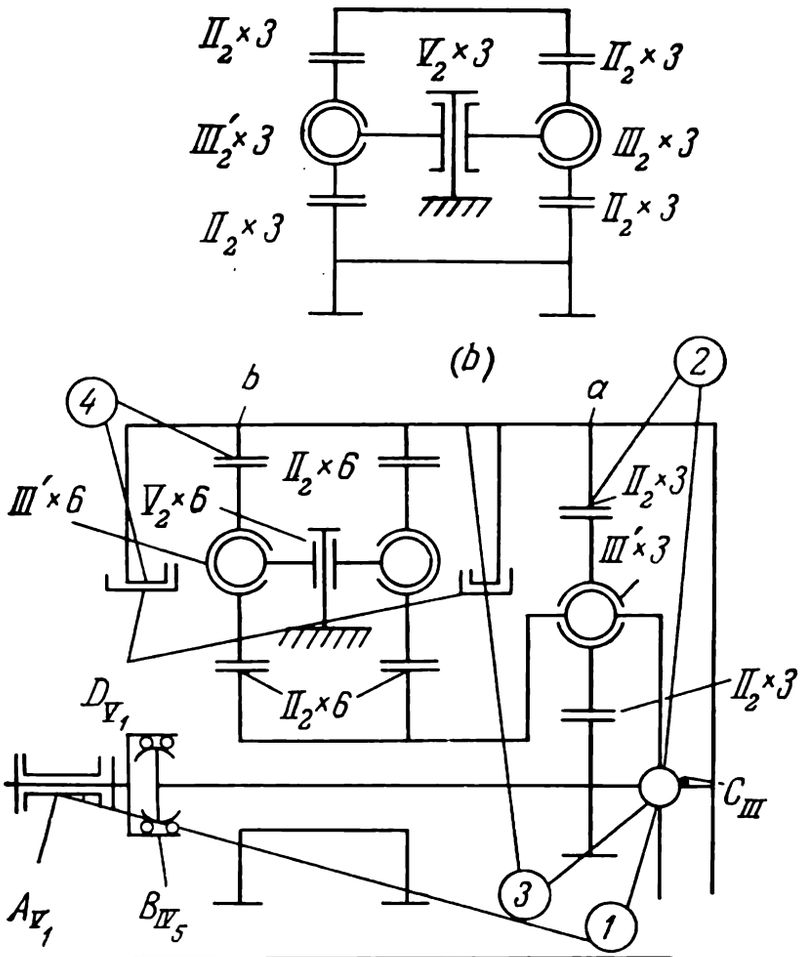


| | | |
|---|---|---|
| ① ABaC | 0 ← Ba<br>0 ← Ba<br>a A | |
| ② Ca | a a<br>a a<br>a a | |
| ③ Cab | 0 ← Cb<br>0 ← Cb<br>b C | |
| ④ Db | b b<br>b b<br>b bD | |

(a)

*Structural block-satellites on two kinematic pairs $B_{III}$*

| $w = 9$ | 9 | 9 |
|---|---|---|
| $n = 11$ | -66 | 60 |
| $p_V = 3$ | 15 | -3 |
| $p_{III} = 6$ | 18 | -18 |
| $p_{II} = 12$ | 24 | -48 |
| $K = 10$ | 0 | 0 |

*Without using struct. groups*

| $w = 1$ | 1 | 1 |
|---|---|---|
| $n = 16$ | -96 | 108 |
| $p_V = 5$ | 25 | -5 |
| $p_{IV} = 1$ | 4 | -2 |
| $p_{III} = 10$ | 30 | -30 |
| $p_{II} = 18$ | 36 | -72 |
| $K = 18$ | 0 | 0 |

*Using struct. groups*

| $w = 1$ | 1 | 1 |
|---|---|---|
| $n = 0$ | 0 | 24 |
| $p_V = 2$ | 10 | -2 |
| $p_{IV} = 1$ | 4 | -2 |
| $p_{III} = 1$ | 3 | -3 |
| str. gr. | 18 | -18 |
| $K = 4$ | 0 | 0 |

Fig. 5.58. Investigation of the structure of reduction gear of Fig. 5.44

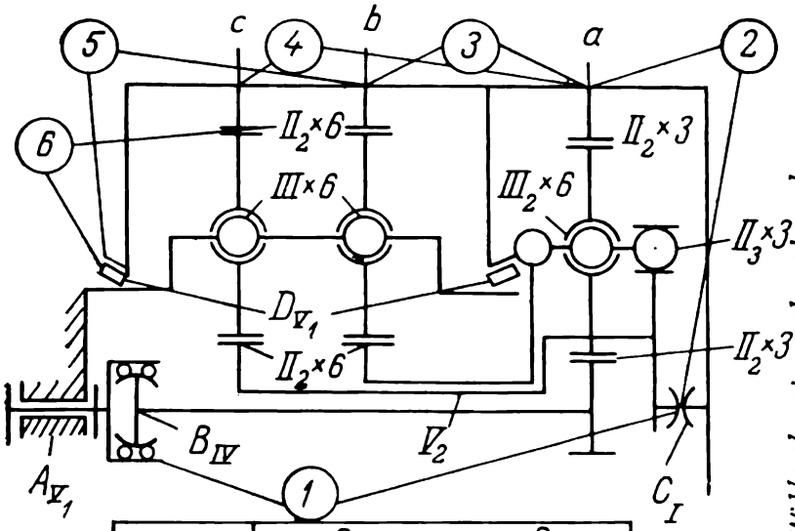


| | | |
|---|---|---|
| ① ABaC | 0 0 a | Ba Ba A |
| ② Ca | C C a | C C aaaC |
| ③ ab | a a b | b b a |
| ④ ab | 0 0 b | a c a c a |
| ⑤ bD | b b b | b b b |
| ⑥ cD | c c c | c c cD |

(a)

| Using structural groups | | |
|---|---|---|
| w = 4 | 4 | 4 |
| n = 17 | 102 | 126 |
| $p_V = 3$ | 15 | -3 |
| $p_{IV} = 1$ | 4 | -2 |
| $p_{III} = 12$ | 36 | -36 |
| $p_{II} = 21$ | 42 | -84 |
| $p_I = 1$ | 1 | -5 |
| K = 21 | 0 | 0 |

| Without using structural groups | | |
|---|---|---|
| w = 4 | 4 | 4 |
| n = -2 | 12 | 36 |
| $p_V = 2$ | 10 | -2 |
| $p_{IV} = 1$ | 4 | -2 |
| $p_I = 1$ | -1 | -5 |
| str. gr. | -31 | -31 |
| k = 6 | 0 | 0 |

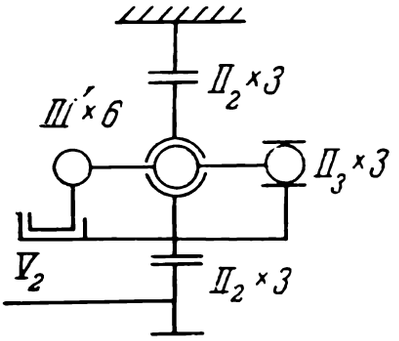


| | | |
|---|---|---|
| $f'_x = 1$ | $f''_x = 2$ | |
| $f'_y = 1$ | $f''_y = 2$ | |
| $f'_z = 2$ | $f''_z = 5$ | |

(b)

| Structural block | | |
|---|---|---|
| w = 13 | 13 | 13 |
| n = 9 | -54 | 42 |
| $p_V = 1$ | 5 | -1 |
| $p_{III} = 6$ | 18 | -18 |
| $p_{II_2} = 6$ | 12 | -24 |
| $p_{III_3} = 3$ | 6 | -12 |
| K = 7 | 0 | 0 |

Fig. 5.59. Investigation of the structure of reduction gear of Fig. 5.47

the structural block with the satellite gears on kinematic pairs $B_V$ for both stages only four loops are left. The design has four redundant constraints in the two structural blocks, and two of them have been detected by analyzing the mobilities in the four loops.

Fig. 5.57 presents a diagram of a double-row planetary reduction gear with the first-stage satellite gears on spherical bearings. Here, too, $K = 12$. By employing structural groups with satellite gears on kinematic pairs $B_{\text{V}}$ and $B'_{\text{III}}$ (Fig. 5.50*b* and *c*), the number of loops is reduced to four, with the redundant constraints in block "δ" ($q = 2$).

Let us discuss a planetary mechanism with a split second stage and idlers on equalizing levers (Fig. 5.58*a*). Here, the block shown in Fig. 5.50*c* can be used for the first stage, and the structural group of Fig. 5.58*b* is separated for the second stage, where the number of the movable members $n = 11$, the number of the loops $K = 10$ and the mobility number $w = 9$ (the mobilities are the same as in the block of Fig. 5.50*c*).

The use of structural blocks has enabled us to analyze four loops instead of eighteen in the table of Fig. 5.58*a*.

A structural block for the design of Fig. 5.59*a* can be similarly separated but for the first stage only. The mobility number for this block $w = 13$. All the mobilities of the previous block have remained, plus three local mobilities of the rotation of the shafts of the satellite gears about the *z* axes, and two general mobilities instead of one, as the mechanism is of the differential-gear type.

Arabic numerals are used in Figs. 5.58 and 5.59 to denote the loops in the planetary mechanism diagrams. In the mobility diagrams the loops are denoted by the same Arabic numerals; additionally, there are given alphabetic symbols of the kinematic pairs and structural groups included in the loops.

## 5.14. Strain Wave Gearings

Operation of a strain wave gearing (speed-changer) (Fig. 5.60) is based on deformation of the driven toothed wheel made in the form of a bell-shaped flexible shell. The deformation is produced by rollers (two or three) rotating on the carrier serving as the driving member—the wave generator. The number of teeth of the driven toothed wheel does not equal that of the fixed gear, which fact causes rotation of the driven member.

A multitude of teeth works simultaneously in strain wave gearings, so that the engagement factor is very high, which is the reason for the high load capacity of such gearings. The redundant constraints caused by the high engagement factor are harmless, as they act exclusively within the kinematic pair, and not within the entire

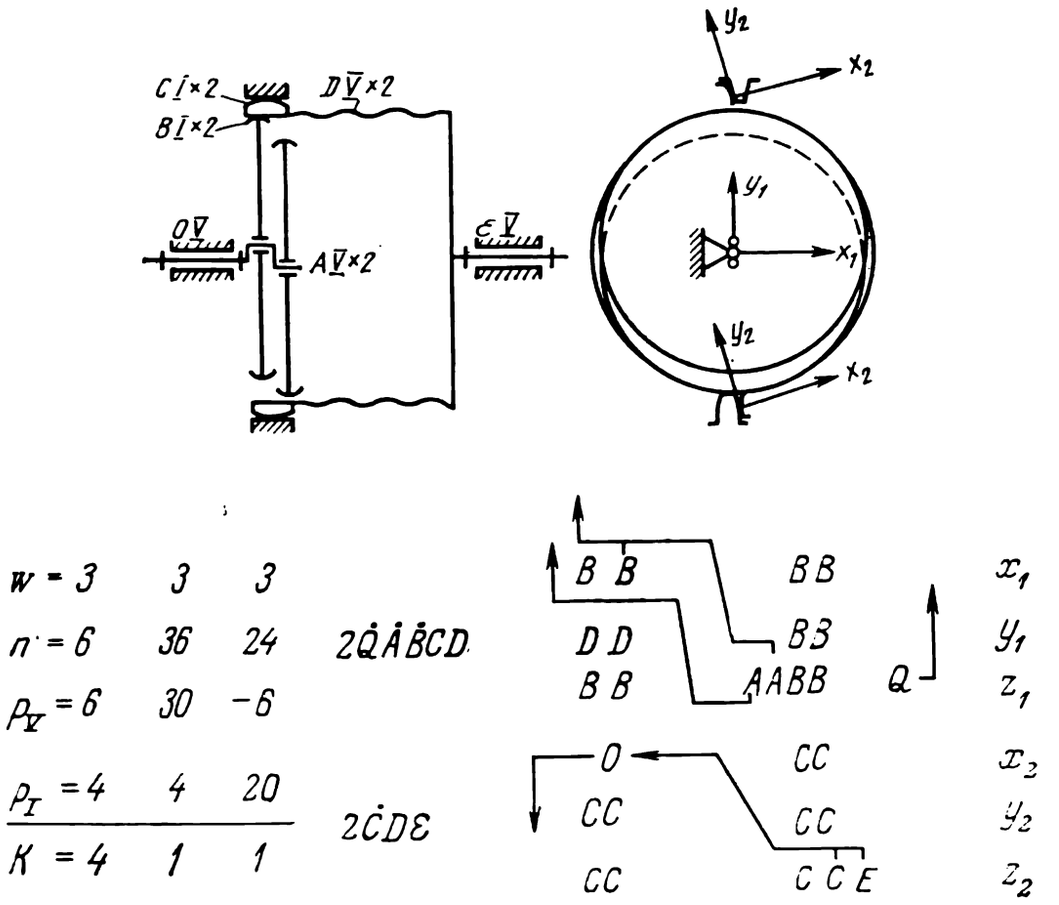


Fig. 5.60. Strain wave gearing with one redundant constraint

mechanism. Thus, we will not determine them and will assume that $\varepsilon = 1$.

The deformation of the flexible shell may take place in two areas, *viz.* at the cylindrical part or at the bottom of the bell. The shell is expected to transmit the driving torque, as well as the torques flexing the teeth, so that it cannot be too thin. It should merely flex under the pressure of the roller, not engage the teeth. Thus, point contact alone—$I_2$ pair—is possible in the engagement. The engagement between the roller and the shell will be likewise of the point kind—$I_2$ pair. The contact stress is not high, as the contact takes place between the concave and convex surfaces.

Sagging of the cylindrical part of the shell against each roller yields one mobility. Hence, we shall consider the corresponding portion of the shell a fifth-class pair and symbolize it with a sinuous line. When counting the members, the portion of the flexible toothed rim opposing each roller has to be regarded a separate member. The bottom of the bell is either flexible or rigid. With a rigid bottom, the corresponding mobility is absent, and the carrier has to be made

floating for even distribution of the load among the teeth. A flexible bottom is to be considered a sheet $III_4''$ pair, and there is no need for the carrier to float. Neither should the carrier be a floating one when the shell is tubular and connected to the bottom by a spline $IV_5$ pair.

Let us analyze a strain wave gearing with a rigid bottom, two rollers and no floating members (see Fig. 5.60).

The mobility is made up of the main one and the slipping of the two rollers, i.e. $w = 3$.

Calculation from either (1.1) or (1.2) (see bottom, left, in Fig. 5.60) gives $q = 1$, i.e. uniform loading of the teeth urged by different rollers cannot be assured. Let us prove it by considering mobilities in the loops. The coordinate axes in this case and in the following discussion of two-roller strain wave gearings will be as follows: $z$ axis—along the axis of rotation; $y_1$ axis—along the normal to the rollers; $x_1$ axis—tangentially of the rollers; $y_2$—tangentially of the teeth; $x_2$—along the normals to the teeth.

Counting the loops from (1.3): $k = p - n = 10 - 6 = 4$. The first loop will have the following members: the fixed member, the carrier, the first roller, a portion of the toothed rim, the driven shaft, the fixed member, and kinematic pairs $OABDE$. The second loop will be similar, but through the second roller. For simplicity sake, let us consider the mobilities of these loops jointly (bottom, right in Fig. 5.60). Here, mobilities $f_y' = 2$ are due to the sagging of the cylindrical part of the shell ($V$ pairs). The third loop will comprise the following members: the fixed member, the tooth urged by the first roller, the driven shaft, the fixed member, and kinematic pairs $CDE$. The fourth loop will be similar, but with the tooth urged by the second roller.

Let us consider jointly the mobilities in the third and fourth loops. One linear mobility along $x_2$ axis is replaced by angular mobility about $z$ axis, as there is the $CE$ member directed along $y_2$ axis. As there is no similar mobility, a redundant constraint evolves. Mobilities $f_z''$ will be spent on the main mobility of the mechanism and slipping of the rollers. The redundant constraint has to be eliminated by a floating member. Therefore, let us consider a similar mechanism, but with a floating carrier connected with the driving shaft by a universal joint—a gimbal (Fig. 5.61).

The coordinate axes and loops will be the same as in Fig. 5.60. The one formerly lacking mobility $f_{x2}'$ is now replaced by $f_z''$ (cf. Fig. 5.60), since there is the member $EG$ directed along the $y_1$ axis.

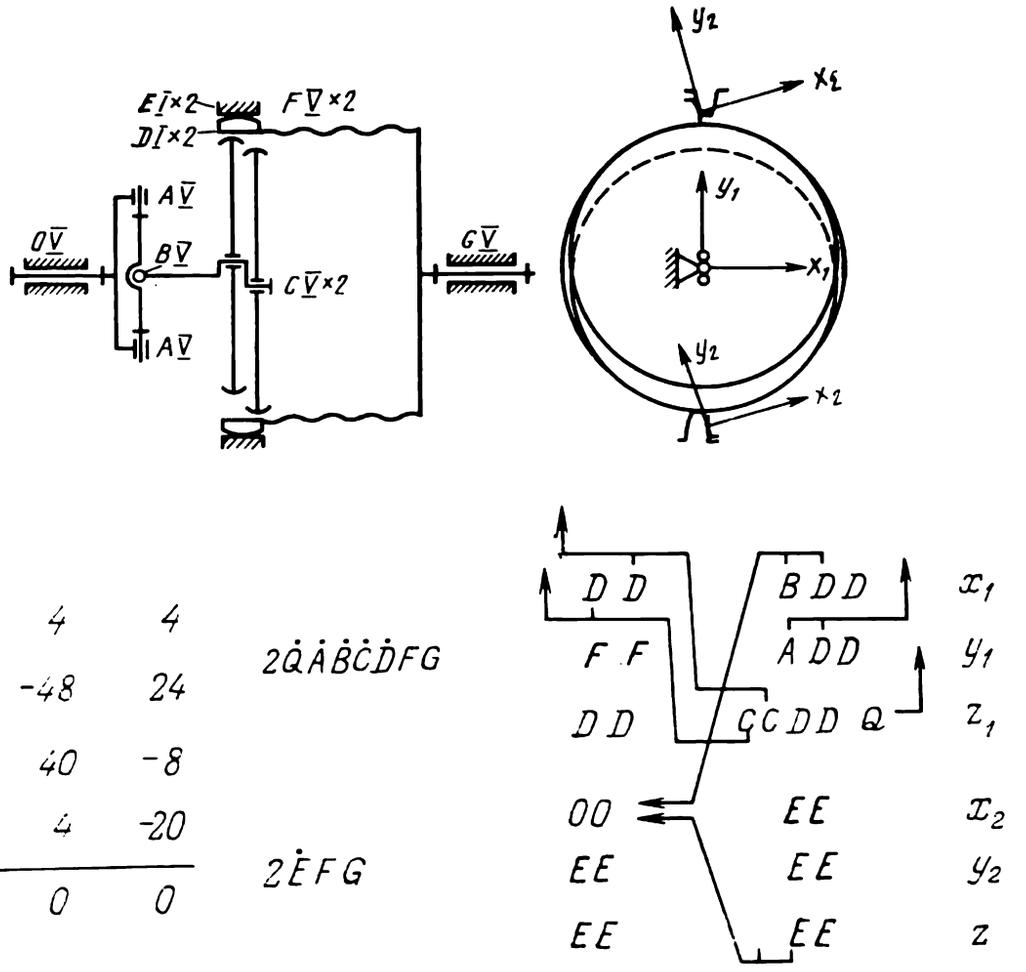


Fig. 5.61. Strain wave gearing with universal joint having harmful mobility

Self-aligning takes place in the following way: the shaft $BC$ turns about the pivot $B$, with one roller pressing the bell-shaped shell to deform it in the pair $F$, while the other roller lowers the shell, and the other pair $F$ is deformed (the shell slants under the pressure). The tooth at the first roller (owing to the wedge shape) is urged, while the tooth at the other roller is relieved, so that the loads of the teeth are levelled out. In other words, the self-aligning is due to the misalignment of the $x_1$ and $x_2$ axes and to the angle they define. In the designs of Figs 5.62, 5.64 and 5.65 the load of the teeth is equalized in a similar way.

Redundant constraints are thus absent, while angular mobilities $f''_z$ are the same as in Fig. 5.60.

There has appeared a new angular mobility $f''_{y1}$ in the pair $A$. It permits rotation of the shaft $BC$ about the vertical pivot of the gimbal joint, displacement of the rollers tangentially (along $x_1$ axis) and eventual jamming of the rollers. Hence, this mobility is

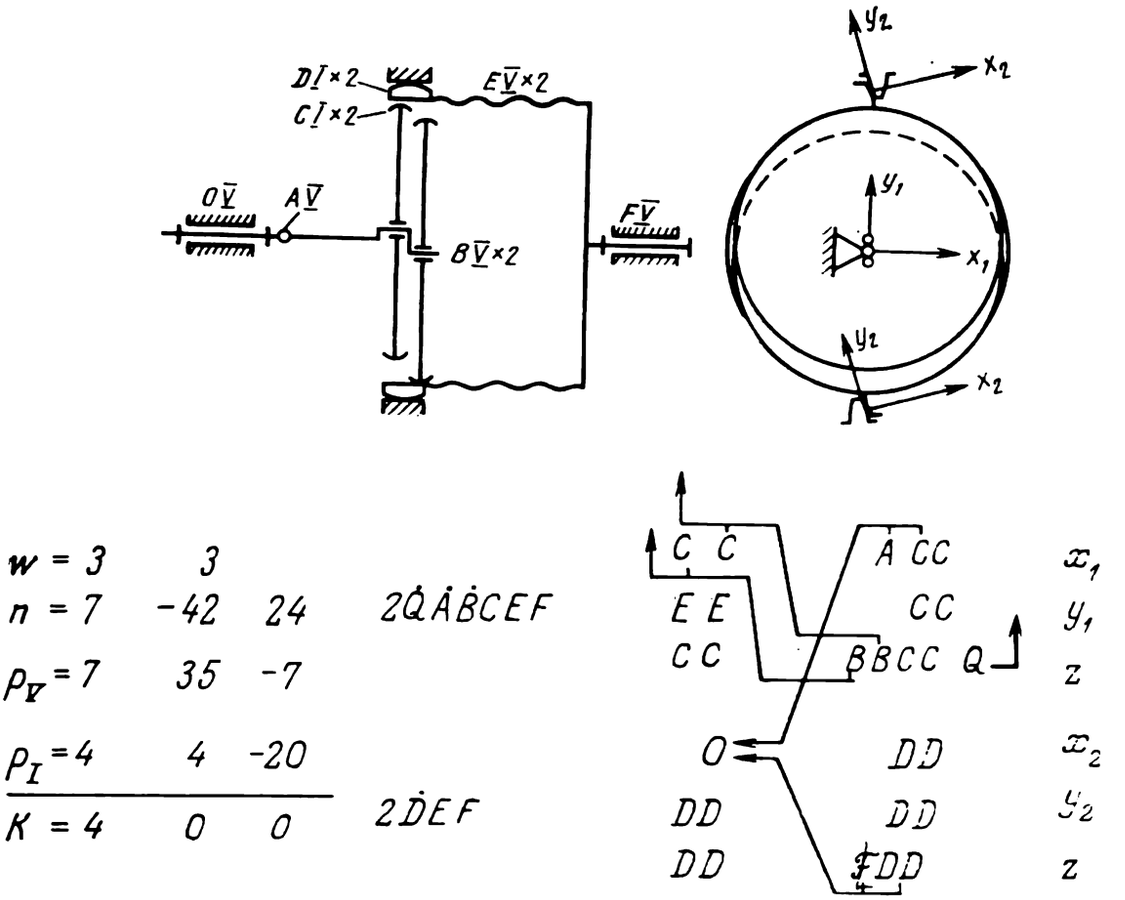


Fig. 5.62. Strain wave gearing with one transverse pivot (recommended)

harmful. It could be eliminated by using a gearing with three rollers, but the transmission ratio would then be brought down, which in most cases is undesirable. Alternatively, the mobility can be avoided by having two rollers and eliminating in the gimbal joint the pivot in the plane of the axes of the rollers (Fig. 5.62). This design, as far as the mobilities and the redundant constraints are concerned, is adequate and can be recommended for practical utilization.

A strain wave gearing with a flexible bottom and two rollers is shown in Fig. 5.63. The analysis of the mobilities in the loops shows that it has no redundant constraints and has five mobilities. When the mobilities are counted by the structural formulas, the ring connecting the cylindrical and flat parts of the shell should be considered as a separate member. Apart from the three mobilities present in the formerly discussed designs of strain wave gearings, the gearing with the flexible bottom has two additional ones: $f'_z$ due to the flexing of the bottom of the shell in the pair $E$ (the sufficient rigidity makes this sagging very small, and the mobility is harmless), and $f''_{x1}$ which is the angular mobility of the ring connecting the cylindrical and flat parts of the shell. Owing to the sufficient rigidity of the

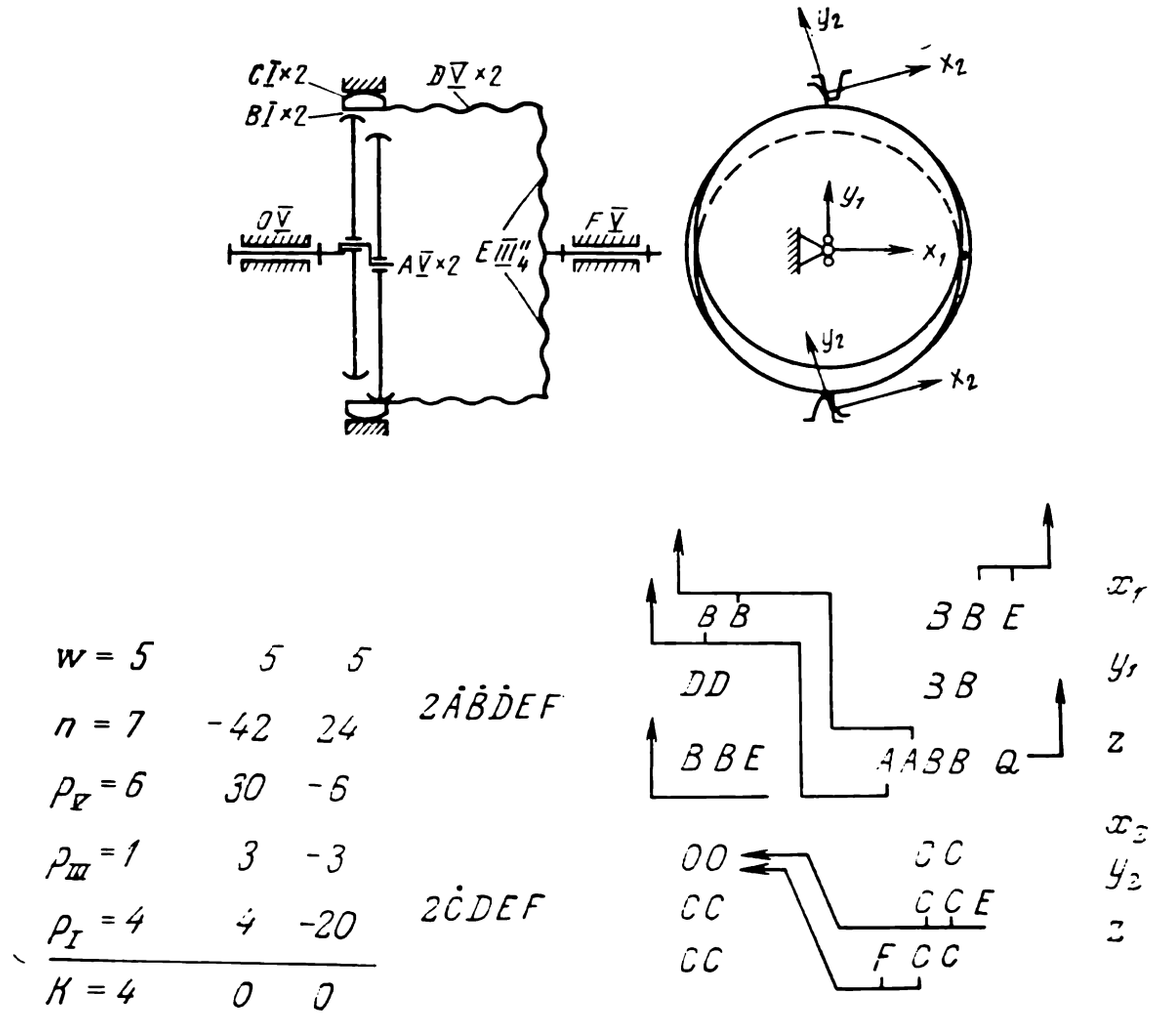


Fig. 5.63. Strain wave gearing with flexible bottom (recommended)

shell, this angular deformation is also very small and harmless. The simplicity makes this design attractive. A similar design is obtained by having a cylindrical shell connected to the rigid bottom by a $IV_5$ pair. This eliminates the linear mobility along $z$ axis. This design can be likewise recommended for practical implementation.

With two rollers, their arrangement in one plane with the toothed rim is not feasible. Thus, the shell is loaded by undesirable bending moments which can be avoided by having a wave generator with three rollers (Fig. 5.64) where the two rollers on the same shaft may be regarded as a single split roller. With no floating members, this design would have two redundant constraints: $q = 2$, with the second redundant constraint leading to non-uniform distribution of the load between the two halves of the split roller. It can be eliminated by adding the second joint $BV$ with the axis parallel to that of $AV$. There are five loops. The three loops $OABCDFG$ and the two loops $EFG$ are analyzed jointly.

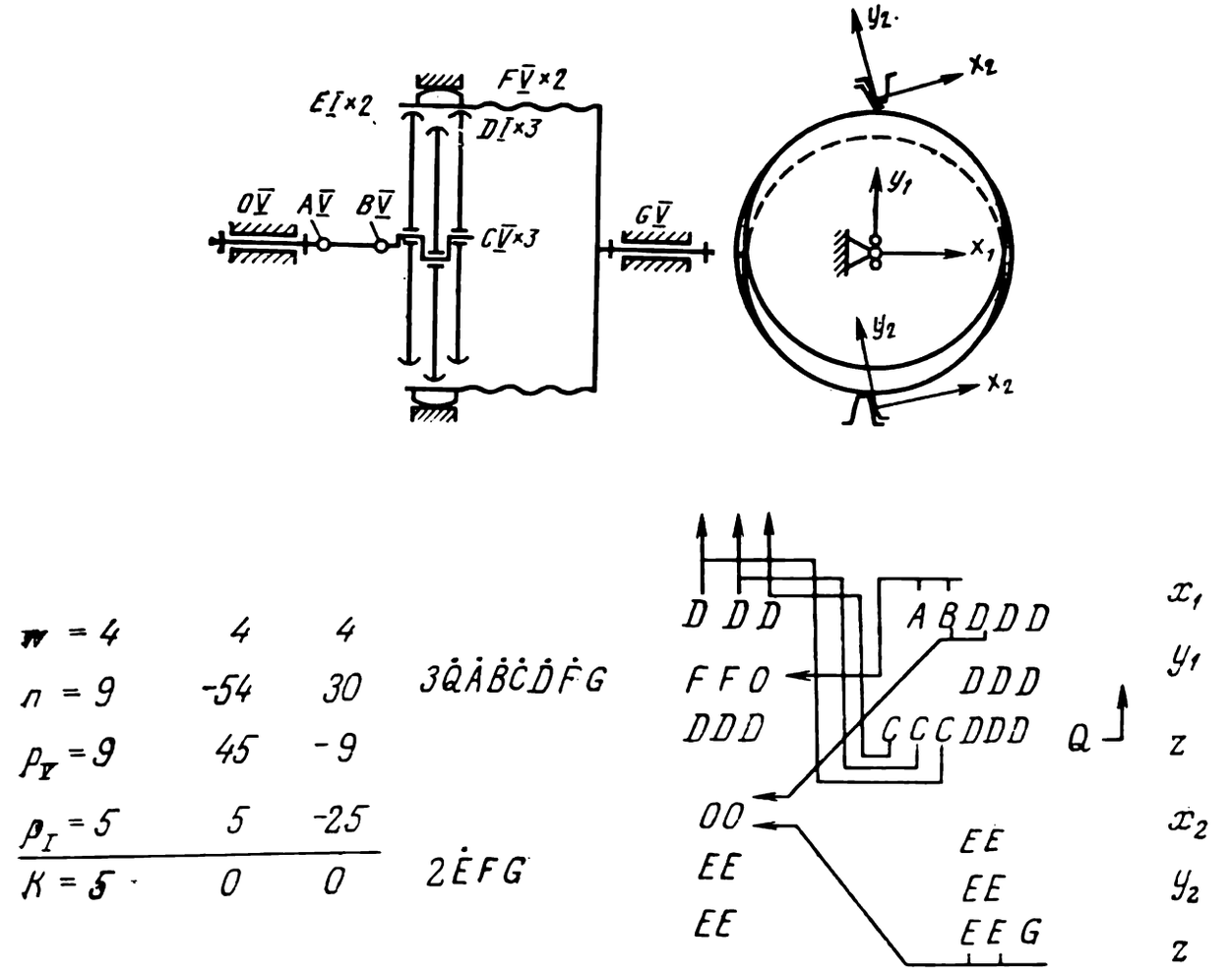


Fig. 5.64. Three-roller gearing where undesirable bending of shell is eliminated

Unwanted flexing of the shell may be avoided in a different way—by using a cam-type wave generator (Fig. 5.65) in the form of an oval-shaped cam with a groove, with an array of balls interposed between the groove and the shell (only two balls are shown in Fig. 5.65). Small rollers are sometimes used instead of balls, but this results in redundant constraints and should be avoided. Let us investigate a mechanism with two balls only, as redundant constraints caused by the balls in excess of two are harmless, so that their determination is not necessary. Because of slipping, each ball has four local mobilities: slipping along the groove and rotations about the three axes, so that $w = 9$. With a cam-type wave generator devoid of floating members, there is one redundant constraint $q = 1$. The latter causes non-uniform distribution of the load among the teeth (same as in the wave generator with rollers). This can be

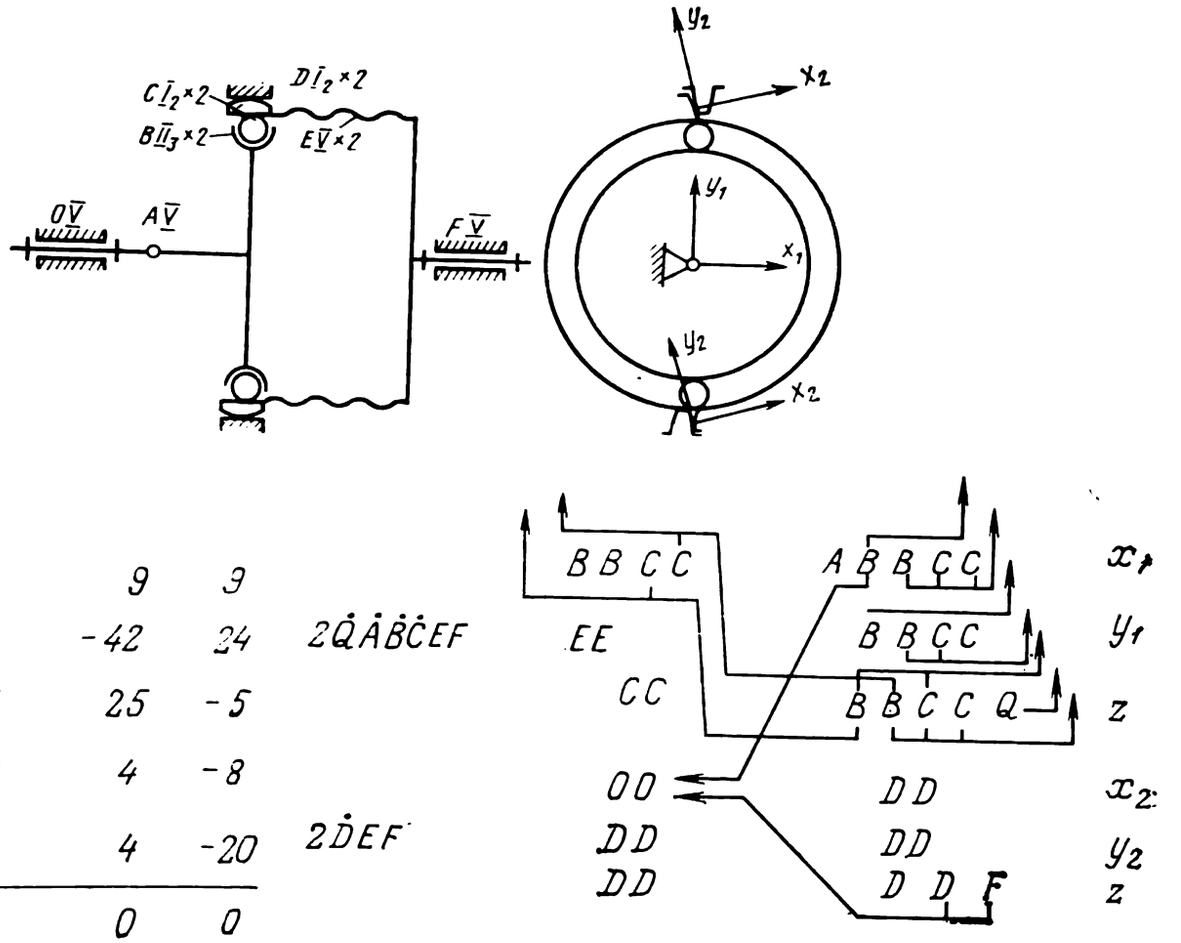


Fig. 5.65. Gearing with cam wave generator and one transverse pivot (recommended)

avoided in three ways:

(1) by using a floating cam connected to its shaft by the $AV$ joint perpendicular to the axis of rotation (cf. Fig. 5.65);

(2) by using the shell with a flexible bottom;

(3) by connecting the cylindrical part of the shell to the bottom by a toothed joint $IV_5$.

There are other designs of strain wave gearings, e.g. those with an external wave generator proposed by V. B. Tarabarin and G. A. Tirmofeev†, so that the space saved inside the shell can be utilized for accommodating other members. There are also hermetically sealed gearings, harmonic speed-changers with high transmission ratios, etc. Elimination of redundant constraints in such designs is simila, to what has been already discussed above.

## 5.15. Conclusions and Suggestions

The moment of friction in a toothed universal joint is dependent neither on its radius, nor on the length of the teeth, nor on the angle $\delta$ defined by the shafts.

The geometric moment is proportional to the square length $b$ of the tooth, to the angle $\delta$ between the shafts and inversely proportional to the radius $R$ of the coupling and the rise $\Delta$ of the point.

With some approximation, the full moment in a toothed joint can be assumed equalling one tenth of the torque being transmitted.

The reduced force of friction in a connecting mechanism is proportional to the ratio of the radius of the floating member (gear) to the length of the universal joint.

Short shafts of universal joints should be avoided, as the friction in such joints is great. The friction is the smallest with the floating sun gear, and the greatest with the floating ring gear and of the in-between value with the floating carrier.

The bigger the modulus of a tooth, the more the mass of a member distorts the distribution of forces.

When a satellite gear fails to accommodate a spherical bearing, Ermak's design can be used. Split satellite gears with an equalizing mechanism may be used, too. The equalizing mechanism may be in the form of helical spline joints. The shaft of a satellite gear may serve as the equalizing mechanism, when connected to the carrier either pivotally, or with the aid of pointed ends. An equalizing mechanism is imperative with the number of the satellite gears in excess of three. With six satellite gears its structure may be particularly simple.

In a planetary reduction gear with a high transmission ratio (the positive one), all the gears are preferably arranged in one plane, with the satellite gears mounted on spherical bearings.

Mechanisms with a free carrier should have this carrier floating, its axial displacement alone being limited.

Multiple and closed planetary mechanisms may do without toothed joints and their inherent friction by having the floating connecting member.

In electric wheel-carried motors, the second stage has to be split to accommodate spherical bearings. The first stage may serve as the equalizing mechanism. The first stage may have two satellite gears and two carriers connected each with the respective sun gear of the second stage. The first-stage carrier may be in the form of two discs connected each with the respective sun gear of the second stage, the

shafts of the satellite gears of the first stage serving as equalizing levers.

In strain wave speed changers with a wave generator either of the two-roller or the cam type, the wave generator should be floating about an axis perpendicular to the axes of the rollers. In case of a wave generator with three rollers, it should float about two parallel axes that are perpendicular to the axes of the rollers.

Chapter 6

# LOAD HANDLING MECHANISMS

## 6.1. Rope Drum Drive

A noteworthy type of the rope drum drive is used in modern lifting cranes, comprising a reduction gear (Fig. 6.1). The output shaft of the reduction gear is supported by two bearings. Owing to a large length, the drum cannot be installed to cover the whole span as it is the case with the rope guide pulleys in lifts. Therefore, one more bearing should be provided. The shaft is thus installed in three bearings. In order to avoid a statically indeterminate system, the reduction gear should be coupled to the drum by means of a Hooke's joint (generally, a toothed joint). To relieve the toothed clutch from the radial forces (which are very large), a spherical coupling is provided, which is generally made in the form of a spherical roller bearing (Fig. 6.1*b*). To minimize friction, it is necessary for the toothed clutch to be in one and the same plane with the centre of the bearing sphere. Unfortunately, this is not realized in the mechanism shown in Fig. 6.1*a*, where the plane of the jaw clutch is axially offset.

Another way of correcting the structural system is to install one bearing in the reduction gearing casing, rather than two. In such a case only a seal is installed at the point where the shaft extends through the casing of the reduction gear, and the bearing is dispensed with. The shaft is thus journalled in two supports: the external support and that disposed within the casing of the reduction gear. The design is used in the escalator drives and proved completely expedient.

The third way resides in making the reduction gear (with two bearings) self-aligning. The outside support should be in the form of the spherical support $III'_2$, and the reduction gear should be connected to a fixed member by means of a toothed Hooke's joint $III''_5$. In practice, it is better to use only two teeth disposed in one and same horizontal plane, rather than the toothed Hooke's joint. This design is preferable where the motor is made integral with the reduction gear. In other applications, changes in the design of a coupling clutch between the motor and reduction gear may prove necessary.

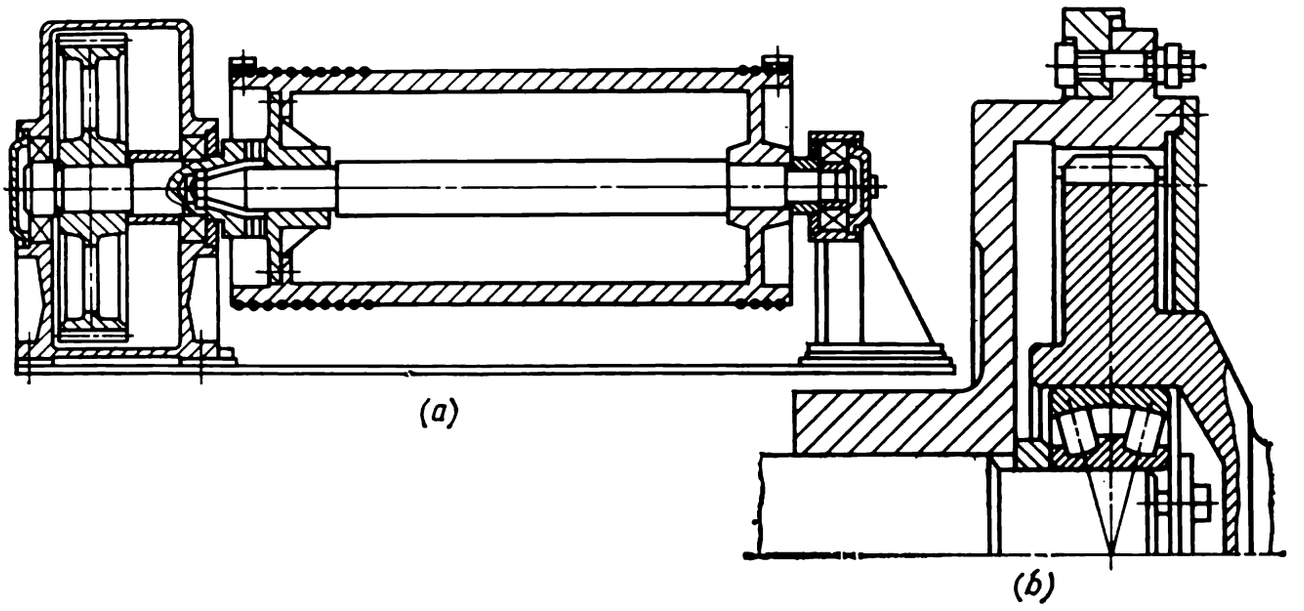


Fig. 6.1. Rope drum drives

An interesting design of a drum is used in winches of the tower crane КБ-100.1 (Fig. 6.2). Here the reduction gear is coupled to the drum by means of the rotational pair $V$ and is fixed to the crane plat-

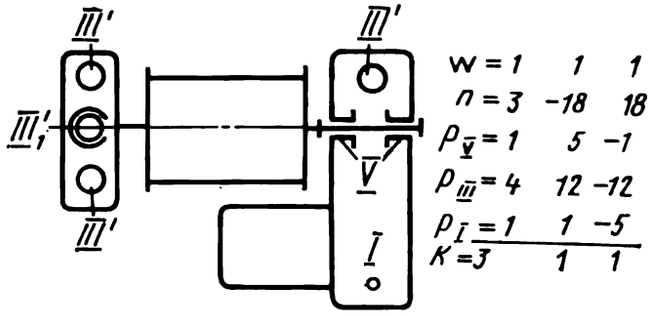


Fig. 6.2. Block diagram of a winch

form by means of the pairs $III'$ and $I$. An outside bearing is connected to the drum by the spherical pair $III'$ and attached to the platform by the supports $III'$ and $III'$. A redundant constraint is formed in these supports—a strain along the line $III'III'$, but this strain is not dangerous owing to large plays.

The redundant constraint is determined by formula (1.1) in the right-hand part of Fig. 6.2.

The supports $I$ and $III'$ shown in Fig. 6.3 represent kinematic couplings formed by the spherical pair $III'_2$ and the planar pair $III''_2$ for the pair $I$ (Fig. 6.3*a*) or rotation pair $V_2$ for the pair $III'$ (Fig. 6.3*b*). The planar pair $III''_2$ differs from the rotational pair $V_2$ only by the diameter of the bore in a support foot. Intermediate members—spherical bushings in both supports—have local mobility (rotation about their axes).

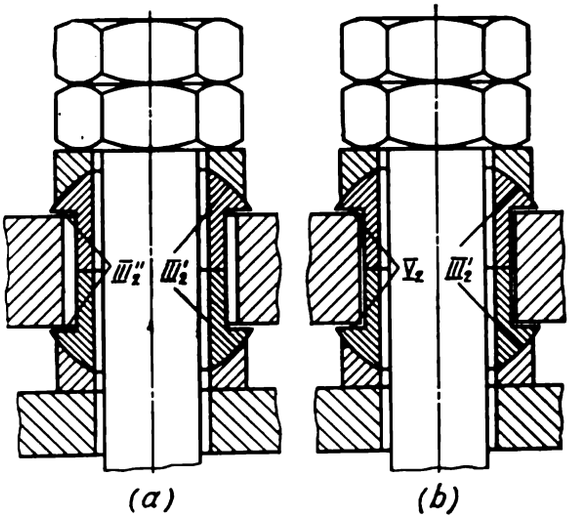


Fig. 6.3. Supports of the winch of Fig. 6.2
(*a*) with one restraint; (*b*) with three restraints

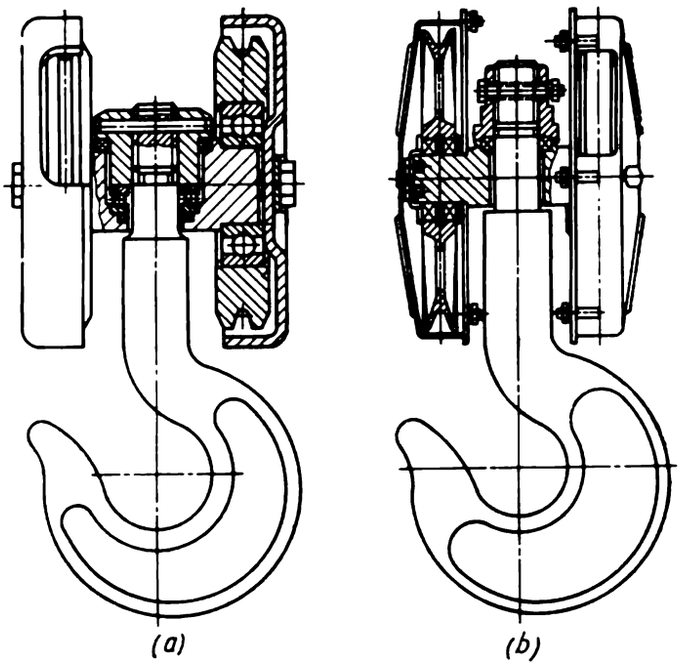


Fig. 6.4. Hook suspension
(*a*) correct design without redundant constraints; (*b*) improper design with five redundant constraints

With a misalignment of the supports $III_1'$ and $V$ of the drum (due to tolerances) in operation of the winch the reduction gear is displaced in the support $I$ (see Fig. 6.2). In operation, the displacements of up to 2.5 mm are permitted, otherwise the winch is rejected.

## 6.2. Pulleys

A pulley in load handling devices does not require such accuracy of rotation as, e.g. a work-table in a revolving machine tool where oscillations measured by microns are already important for the accuracy of a product. Moments causing a skewing of the bearing and axial forces cannot be too large since substantial deviation of the bearing from the plane of the pulley rotation is not permitted to avoid rapid wear of the rope. Such moments are absent altogether in movable pulleys owing to self-alignment.

In addition, bearings 0000 which are used for this application adequately transmit axial forces. There is enough room for the bearing inside the pulley. The pulley is therefore preferably supported by a single rolling-contact bearing: a single-row ball bearing 0000 or a roller bearing with short cylindrical rollers 92 000 (or a bearing of a similar type).

The correct design is shown in Fig. 6.4*a*. There are no redundant constraints in this design. Unfortunately, generally a design involv-

ing the pulley support with two rolling-contact bearings is used (Fig. 6.4*b*). There are five redundant constraints here, and the influence of these constraints on the operation of the bearings is strongly pronounced, especially owing to a close position of the bearings (influence of tolerances).

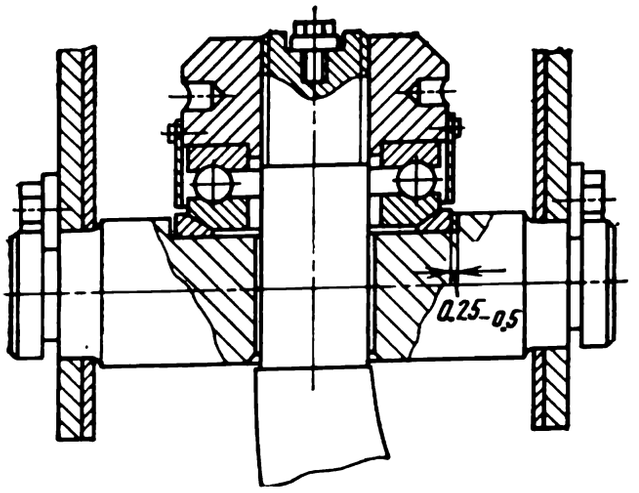


Fig. 6.5. Improper design of the hook journal with a harmful mobility

A change for a single-bearing support would make it possible to save a large number of bearings and reduce the axial size.

With the use of supports in the form of sliding-contact bearings, pulleys have always been supported by a single bushing, and the accuracy of rotation was quite adequate. Therefore, in changing for rolling-contact bearings which are much more accurate the use of the design with two support bearings can only be explained by the tradition of journalling a shaft in two bearings.

In designing a hook suspension, one should not complicate it with unnecessary mobilities. An example of such an improper design is given in Fig. 6.5 where a hook is supported by means of a thrust ball bearing 18 000 having a spherical pad ring. The spherical pad ring is superfluous in this application, since both angular mobilities about horizontal axes are achieved by the self-alignment of the pulley itself.

## 6.3. Grabs

There are double-jaw (Fig. 6.6) and multiple-jaw grabs (Fig. 6.7). The former are used for light-weight materials with limited particle size and the latter for heavy-weight materials in the form of large-size lumps. Two-rope grabs are most widely used. Lifting is effected by winding-up both ropes, and unwinding both ropes results in

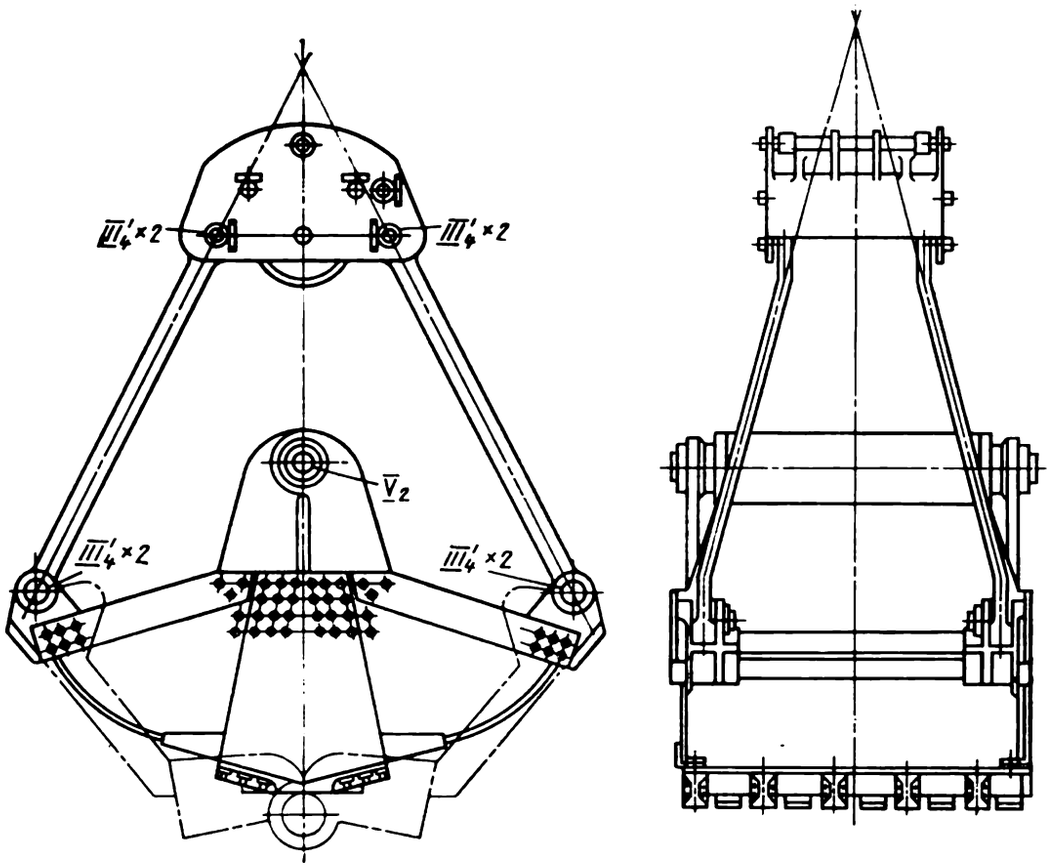


Fig. 6.6. Double-jaw grab

lowering. The grab is opened or closed by winding-up one rope or by winding both ropes at different speeds.

In the double-jaw grab (see Fig. 6.6) the jaws are coupled by means of a pivotal joint which is to be regarded as the rotational pair $V_2$ since otherwise the teeth would not close-up. To this pivotal joint is attached a lower shackle of a control pulley block. The jaws are suspended to an upper shackle by means of four inclined rods having pivotal joints which are to be regarded as the spherical pairs $III_4'$. The position of these rods is very critical. They must not intersect one another at one point because then the condition No. 6 of Table 3.1 would not be fulfilled: maximum three arms can extend through one point. Otherwise the mechanism would have a redundant constraint. This may be seen by check strains in assembling with such an arrangement. After the installation of three rods (assuming the upper shackle stationary), the system formed by the rods and jaws can only rotate about the intersection point, and the distance between the points of fixing the fourth rod cannot be changed as necessary for its installation. The redundant constraint would require fitting the length of the fourth rod. During a repair the rods may be confused, and then $4! = 24$ combinations must be tried

which is clearly impossible. The main disadvantage resides in an improper loading of the members of the grab in operation. Therefore, the redundant constraint is inadmissible in such an application. To eliminate the redundant constraint one must make it certain that the

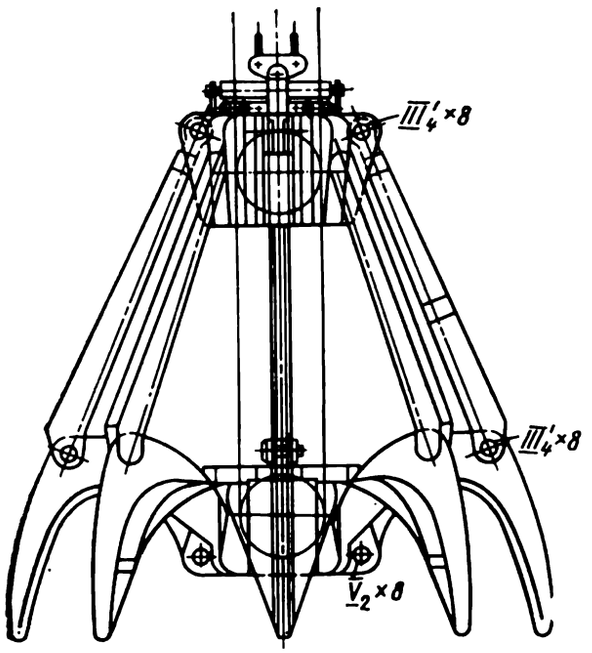


Fig. 6.7. Multiple-jaw grab

points of intersection of the rod axes in both projections in Fig. 6.6 should be at possibly different levels. Let us check-up this mechanism (Fig. 6.6) using the structural formula (1.1). Let us find the mobilities by assuming the upper shackle of the pulley block to be a fixed member. The mobilities include opening, four local mobilities of rotation of the four rods, and two oscillations in two planes: in total $w = 7$. Then $q = 7 - 6 \times 6 + 5 \times 1 + 3 \times 8 = 0$. In case the rods intersect one another at one point, a rotation about the vertical axis is added, and $w = 8$. Then $q = 8 - 6 \times 6 + 5 \times 1 + + 3 \times 8 = 1$.

The multiple-jaw grab is designed properly. However the jaws should be coupled to the lower shackle of the pulley block by means of the rotational pairs $V_2$, and the rods should be made with spherical supports $III'_4$ (due to plays). With eight jaws, assuming the upper shackle of the pulley block to be a fixed member, there are the following mobilities: opening, eight local mobilities of the eight rods, and five mobilities of the lower shackle of the pulley block—two linear along horizontal axes, two angular about the same axes, and one angular about a vertical axis extending through the point of inter-

section of the rods, that is in total $w = 14$. Then, according to formula (1.1), $q = 14 - 6 \times 17 + 5 \times 8 + 3 \times 16 = 14 - 102 + + 40 + 48 = 0$.

## 6.4. Crane Carriages

Loading bridges, movable conveyors, gantry, portal and building cranes move along tracks by means of carriages. With a low lifting capacity, the carriages are made for a single rail (Fig. 6.8) and for a large lifting capacity they are made for two (Fig. 6.9) and even four rails.

Let us consider a support of one leg of a crane. We find the restraint between the wheel and rail. The contact between the cylindrical surface of the wheel and the rail is the first class pair owing to a small size of the rail width compared to the crane dimensions. Consequently, if the flanges do not work owing to plays, the coupling belongs to the first class, and in case the flange is effective the coupling belongs to the second class (one more restraint is added). The pairs are denoted accordingly in Figs. 6.8 and 6.9. The coupling of the single-rail carriage to the crane leg or to a balance beam should have two angular mobilities: one about the vertical axis for inscribing into curves and one about the transverse axis for equalizing loads on wheels. The mobility about the longitudinal axis should not exist for the single-rail carriage (so that the carriage should not tilt). For two-rail carriages this mobility is also necessary for equalizing the load on both rails.

The mechanism has the following mobilities: the main mobility (movement of the carriage), slippage of the wheels (or axles) equal to their number, and three angular mobilities of the crane leg (one of them together with the carriage for the single-rail carriages). The restraints imposed on the crane by other carriages are not considered here, so that the leg has three mobilities.

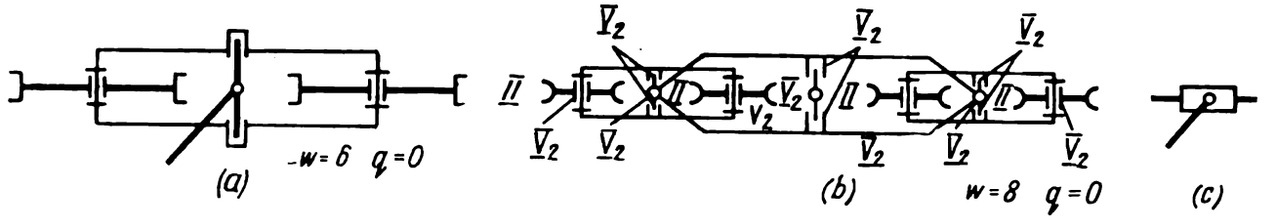


Fig. 6.8. Single-rail crane carriages
(*a*) two-wheel; (*b*) four-wheel; (*c*) conventional symbol

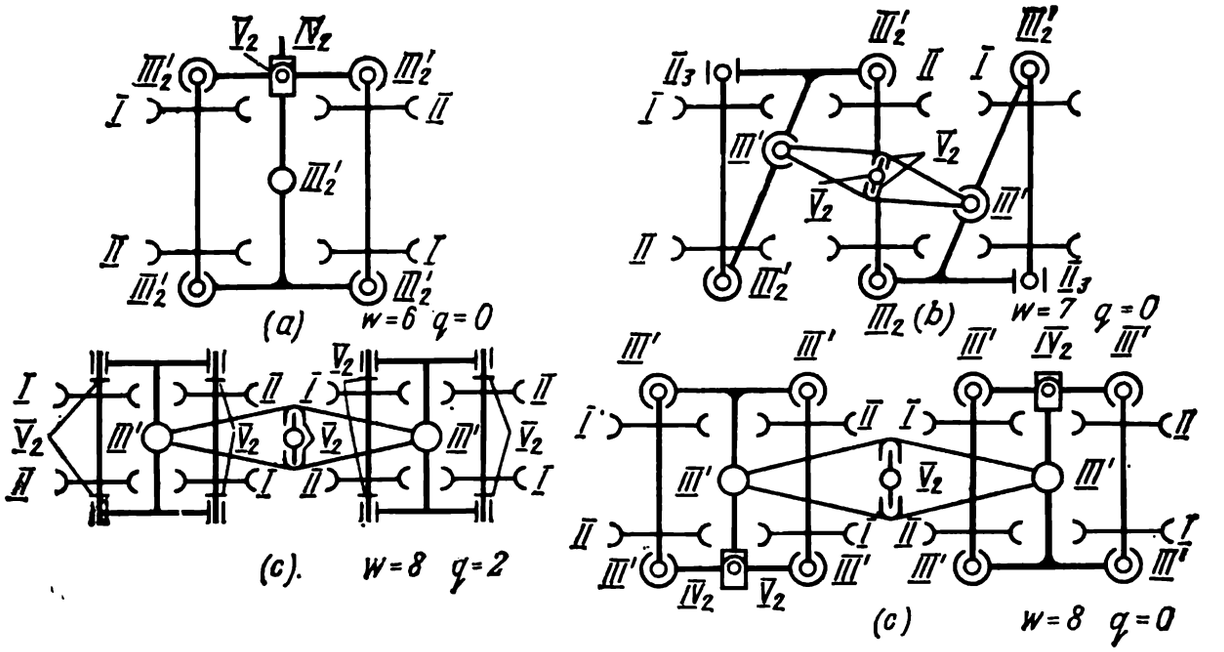


Fig. 6.9. Two-rail crane carriages
(*a*) four-wheel; (*b*) six-wheel; (*c*) eight-wheel with two redundant constraints; (*d*) eight wheel without redundant constraints

For a two-rail four-wheel carriage there is one redundant constraint due to the support at four points. It is eliminated in the design shown in Fig. 6.9*a*. Here the carriage body consists of two members coupled to one another by means of the pairs $IV_2$ and $V_2$. The additional advantage resides in that neither of the carriage beams is subjected to torsion.

With six wheels, they may be combined into two three-wheel carriages (Fig. 6.9*b*). A very simple structure is obtained (compare the number of members with other designs). The disadvantage of this design is that one of the beams extends over the wheel, and the whole structure is too high so that it cannot be used for electric locomotives. The use of internal frames eliminates this disadvantage and makes it possible to obtain a very compact design.

With eight wheels, they are combined into two four-wheel carriages (Fig. 6.9*c* and *d*). With integral bodies of the carriages (Fig. 6.9*c*) there are two redundant constraints. In order to eliminate them, the use should be made of composite carriages (Fig. 6.9*a*), as shown in the design of Fig. 6.9*d*. With a larger number of wheels, the design without redundant constraints may be obtained in a similar manner.

The above-described mechanisms guide the crane leg along the line running parallel with the rails, that is in a planar system the same restraints are imposed as those imposed by a slide. Therefore,

they will further be denoted as a slide in the planar system. The slide belongs to the fourth class for a single-rail carriage and to the fifth class for the two-rail carriage.

## 6.5. Loading Bridges and Movable Conveyors

The span is as large as up to 200 m in the loading bridges. With such sizes it is almost impossible to manufacture the crane with a required accuracy. This makes it necessary to eliminate redundant constraints.

In the conventional design, one pillar of the loading bridge is made in the form of a latticed truss (Fig. 6.10*a*, left) and the other pillar is made with pivotal joints (Fig. 6.10*a*, right). Although this mechanism inscribes into a varying width track, it has two redundant constraints. One of them causes torsion of the bridge girder and non-uniform loading of the carriages, and the other results in non-uniform distribution of load in the pairs $V_2V_2$ coupling the pillar legs to the bridge. These constraints are very easily eliminated (Fig. 6.10*b*). For that purpose, the flexible pillar is to be made in the form of a triangular truss and coupled to the bridge by means of the spherical pair *III'*.

At present the use is also made of inclinable bridges which may incline at an angle of up to 10-15° with respect to the direction perpendicular to the rails. This is important in case one installation is simultaneously serviced by two cranes. In inclinable loading bridges the rigid support is coupled to the bridge by means of a turntable $V_2$. The design shown in Fig. 6.10*b* is suitable for such loading bridges,

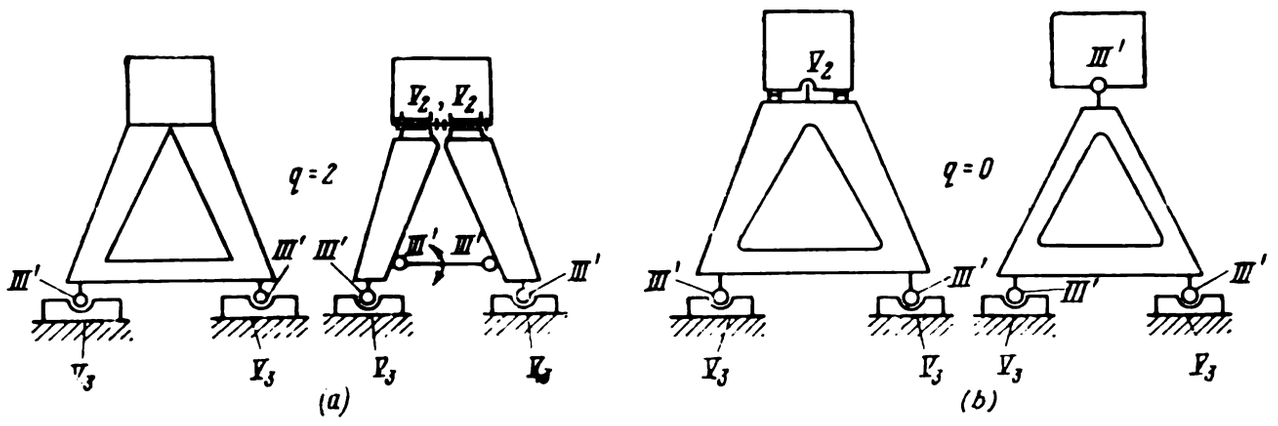


Fig. 6.10. Pillars of loading bridges:
(*a*) without inclined installation with two redundant constraints; (*b*) for an inclined installation of the loading bridge with a turntable

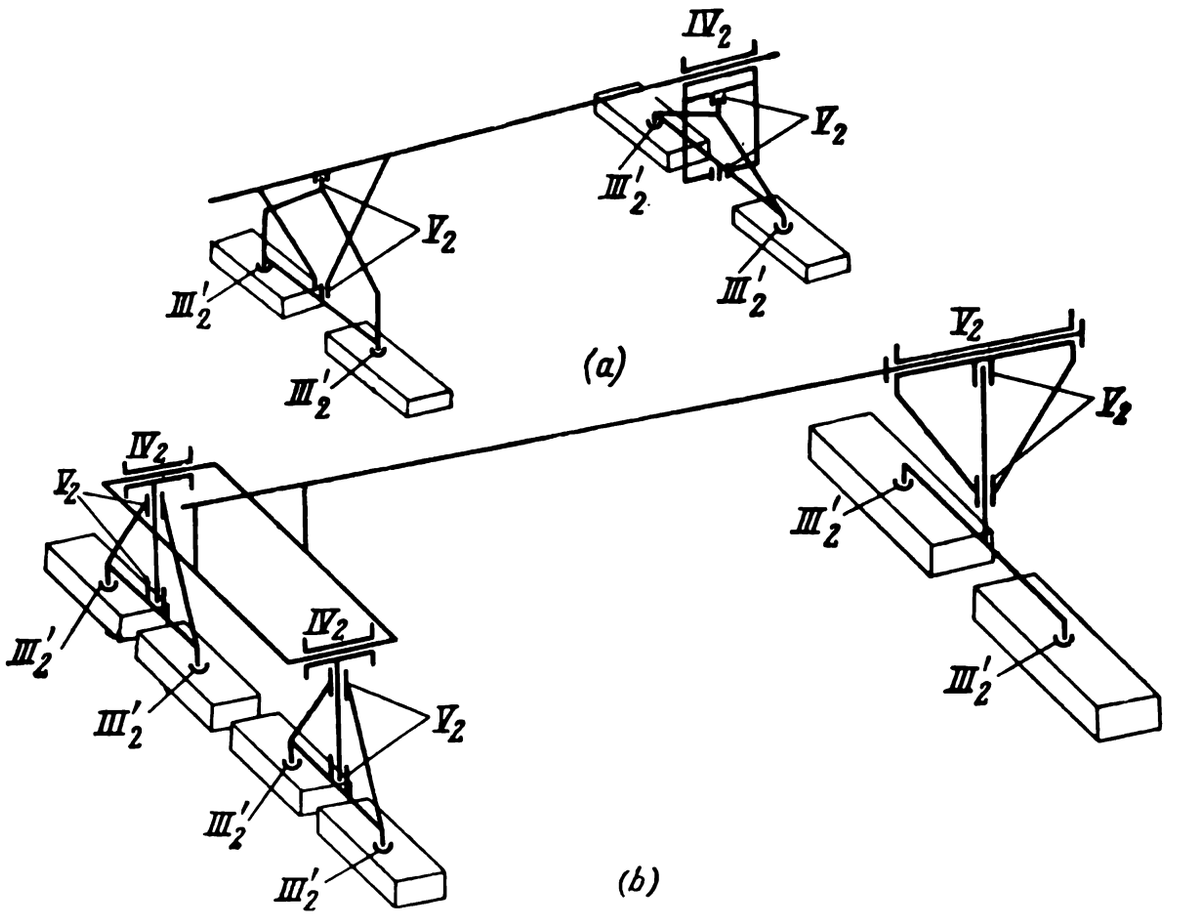


Fig. 6.11. Support and undercarriage part of loading bridges with a new design of the rotational pair
(*a*) with four carriages; (*b*) with six carriages

and its structure was calculated taking into account the turntable (mobility $w = 2$). The turntable exhibits a strong friction and is expensive in the manufacture (it requires turning large-diameter workpieces) so that a different design is used for movable conveyors (Fig. 6.11*a*), wherein the rotational pair is made in the form of largely spaced (in height) bearings. Structurally, the truss of the rigid pillar and the truss of the intermediate balance beam are installed in one another which is disadvantageous as it hampers the disassembly.

A similar design for a movable large-capacity conveyor with the bridge supported by six carriages is shown in Fig. 6.11*b*.

With a change in the track width, the flexible support (see Fig. 6.10*a* and *b*) is caused to incline. This design proved expedient in loading bridges where a change in the track width is small. For a conveyor, where a change in the track width is much greater, this design is unsuitable. Instead, one of the pillars is coupled to the bridge by means of the cylindrical pair $IV_2$.

## 6.6. Travelling Cranes

Statically determinate mechanisms have found application in new travelling cranes. In such cranes, the crane rails are largely spaced at a distance equal to the crane span and are coupled to different walls of a building. Non-uniform settlement of the building results in a distortion of the crane track in both plan and vertical elevation. In statically indeterminate cranes this causes a rapid wear of the undercarriage of the travelling crane, especially of the wheel flanges.

G. P. Popov, V. A. Ivanov et al. have proposed a travelling crane† (Fig. 6.12*a*) in which all redundant constraints are eliminated. The bridge consists of two members, each comprising a main beam and an end beam rigidly connected to one another. The bridge members are interconnected by the pairs $II_3$ made in the form of a wheel in a trough, and the wheels are coupled to the bridge by means of the rotational pairs $V_2$. One of the wheels should be made wider so as to obtain the first class pair. The reduction of the redundant constraints has prolonged the life of the wheels from 2-3 months to several years.

In this design all wheels may be made identical without rim widening, but in such a case one wheel should be supported by a cylindrical pair (with the axial play). The wheels may be made identical using another method (Fig. 6.12*b*). For that purpose, the main and

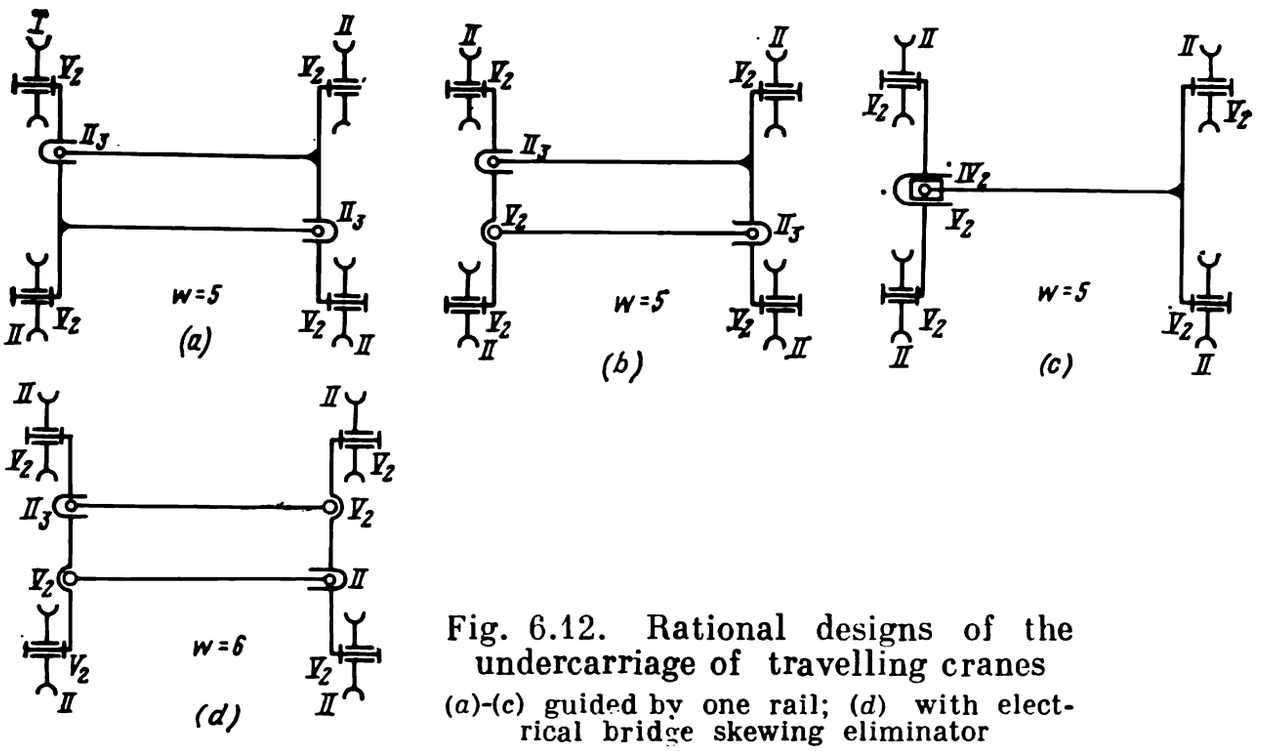


Fig. 6.12. Rational designs of the undercarriage of travelling cranes
(*a*)-(*c*) guided by one rail; (*d*) with electrical bridge skewing eliminator

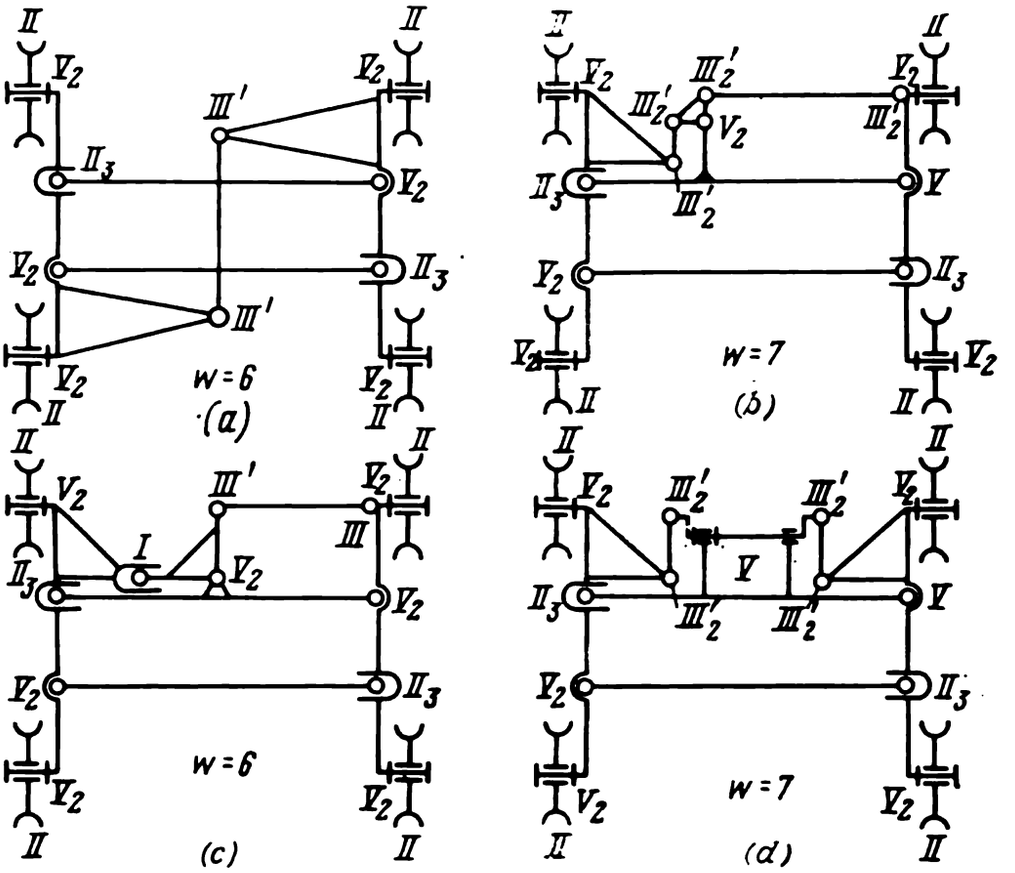


Fig. 6.13. Rational designs of the undercarriage of travelling cranes guided by two rails

end beams of the bridge in one half of the bridge should be interconnected by means of the rotational pair $V_2$.

This design proves simpler in the single-beam bridge (Fig. 6.12*c*). In this case the main beam should be coupled rigidly to one end beam and through the rotational pair $V_2$ and the cylindrical pair $IV_2$ to the other end beam.

Only one rail guides the crane in the above three systems: the right-hand rail in Fig. 6.12*a*, which is disadvantageous though not very critical since this rail can be fixed stronger in the horizontal direction. The elimination of this disadvantage results in a more complicated design of the crane. The bridge may be articulated (Fig. 6.12*d*) by providing couplings of the main and end beams of the bridge in the form of two rotational pairs $V_2$ and two pairs $II_3$. The bridge carriages should have independent drive, which is advantageous for large-span cranes. Here it is necessary to eliminate a redundant constraint—skewing of the bridge—which must be made electrically, that is the contacts controlling drive motors should be actuated upon skewing.

In bridges guided by two rails, the mechanism eliminating the skewing should comply with two requirements:

—it should not hamper a change in the track width, which is achieved by means of a longitudinal rod $III_2'III_2'$ (Fig. 6.13*a*, *b*), the left-hand rod $III_2'III_2'$ in Fig. 6.13*d* inclinable upon a change in the width, or by means of a link (Fig. 6.13*c*) which is conventionally shown as the pair *I*; in practice it should be made in the form of a number of series connected lower pairs;

—the end beams (bridge carriages) should rotate with respect to the main beams in opposite directions through equal angles which is achieved by using an antiparallelogram mechanism (see Fig. 6.13*a*). This mechanism can, however, find application only in exceptional cases owing to a large length of the levers equal to one half of the span. In Fig. 6.13*b* this is achieved by means of two rods $III_2'III_2'$ and $III_2'III_2'$ and two angle levers, and in Fig. 6.13*c* by means of the rod $III_2'III_2'$ and two angle levers interconnected by the link *I*.

In Fig. 6.13*d* the end beams are interconnected by a two-crank shaft extending in parallel with the main beams and coupled to the end beams by means of three-dimensional four-joint mechanisms. This shaft should be checked not only for strength but also for torsion angle, especially with a large span.

The guidance of the bridge by one rail has found widespread use in the loading bridges and in bridges of movable conveyors so that there are all grounds to believe that it is quite suitable for travelling cranes as well.

## 6.7. Undercarriage of Building Cranes

Mechanisms of the undercarriage of tower cranes should especially be made statically determinate as the rails for them (as for all building cranes) are installed temporarily. In addition, each rail is placed on its own sleepers. The crane speeds are much lower than those of trains. Therefore the accuracy of installation of the rails for such cranes is much lower than that for railway tracks. It is inexpedient to improve this accuracy as this would result in higher cost of construction operations. On the contrary, in order to lower the construction cost and to speed up the construction, it is desirable to lower the requirements to the accuracy of installation of the rails, and this is made possible by using cranes with self-aligning mechanisms. Such cranes generally move on two-wheel carriages (see Fig. 6.8*a*). Two joints should be provided between the crane truss and the

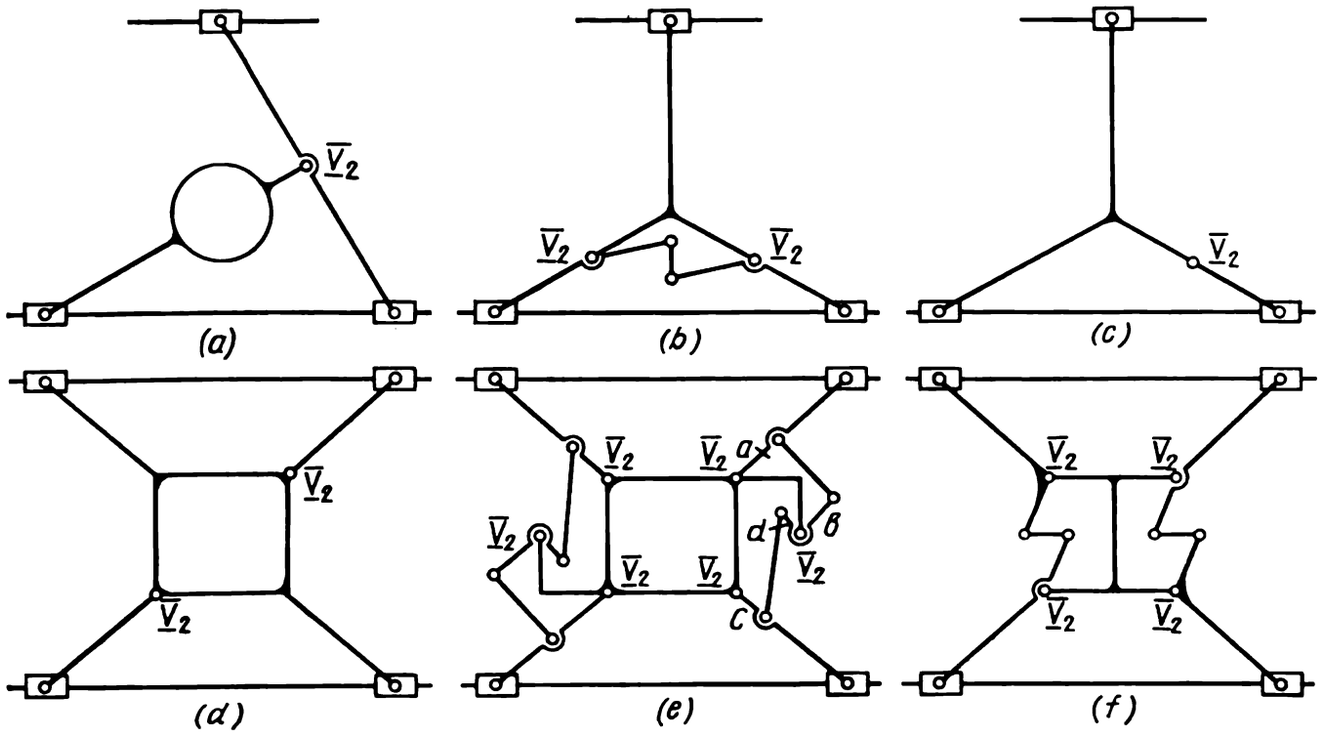


Fig. 6.14. Designs of couplings of crane carriages
(*a*)-(*c*) with three carriages; (*d*)-(*f*) with four carriages

wheels: a vertical one for rotation of the carriage in accordance with the profile of the track in plan, and a horizontal one for equalizing loads on the wheels.

In case the crane is supported by three such carriages, its weight is distributed in a statically determinate manner among six wheels. Of course, it does not mean that the distribution is uniform since there are also tilting forces (weight of the load and wind pressure), apart from the crane weight. However, this crane will not follow the profile of the track in plan. Thus, such a crane cannot travel (without failure) along a varying width track. It is especially difficult to fit the rails for this crane on curved portions of the track. Therefore, it is used only for straight tracks. This disadvantage can be eliminated by interconnecting two carriages installed on different rails by means of a truss. The crane should be supported by means of a third carriage and by the middle of the truss (Fig. 6.14*a*). The centre of the crane should be twice as close to the point of coupling with the truss than to the coupling with the carriage. The coupling of the truss with the crane should necessarily be made by means of the rotational pair $V_2$, that is on two largely spaced bearings. This crane can move also along a varying width track and along

curved portions. The wind force is uniformly distributed among the three carriages.

The same problem is solved from the structural point of view in the design shown in Fig. 6.14*b*. Here one leg is made integral with the crane, and two other legs are coupled to the crane by means of the rotational pairs $V_2$ made in the same manner as in Fig. 6.14*a*. In addition, the legs are interconnected by means of a pivotal mechanism which enables their rotation only through equal angles in opposite directions. Unfortunately, the carriages installed on rotatable legs do not participate in the transmission of the wind load. This force is transmitted only by one carriage and to one rail only (to the upper rail in Fig. 6.14*b*). Therefore, such a design can have but a very limited application (e.g. for cranes installed in closed rooms).

The same problem is solved in a much simpler manner in Fig. 6.14*c*. where the wind load is also applied to one carriage only. Compared to the design of Fig. 6.14*b* in this case the adaptability of the crane to a change in the track width is somewhat worse.

With four wheels, one redundant constraint is inevitable owing to the transmission of vertical forces to four points, which causes a statically indeterminate distribution of forces among the wheels.

The absence of adaptability to the profile of the track in plan may be eliminated. Generally the legs are coupled to the crane by means of the vertical joints $V_2$. For transportation, the legs are folded. In the operating position the legs are secured by means of rods, and they become integral with the crane. In order to eliminate the redundant constraints in the horizontal plane, it is necessary to secure only two legs disposed opposite to one another (Fig. 6.14*d*), and the other two legs should remain free on rotational pairs. This crane can work with varying width of the track as well. Unfortunately, only two carriages (those on the secured legs) participate in the transmission of the horizontal force, that is this design has the disadvantage of the design shown in Fig. 6.14*b*. This disadvantage may be eliminated if all four legs remain rotating in the joints $V_2$ (Fig. 6.14*c*). To avoid redundant mobilities, two adjacent legs should be interconnected by articulated mechanisms enabling their rotation only through equal angles in opposite directions. For that purpose, the following condition should be met:

$$\frac{a}{b}=\frac{c}{d}$$

The mechanism proves to be lightweight and inexpensive since a change in the track width is small, hence, the dimensions of the levers $b$ and $d$ are also small. The legs should be coupled to the carriages installed on different rails. The legs cannot be coupled to carriages installed on the same rail since in this case the carriages will

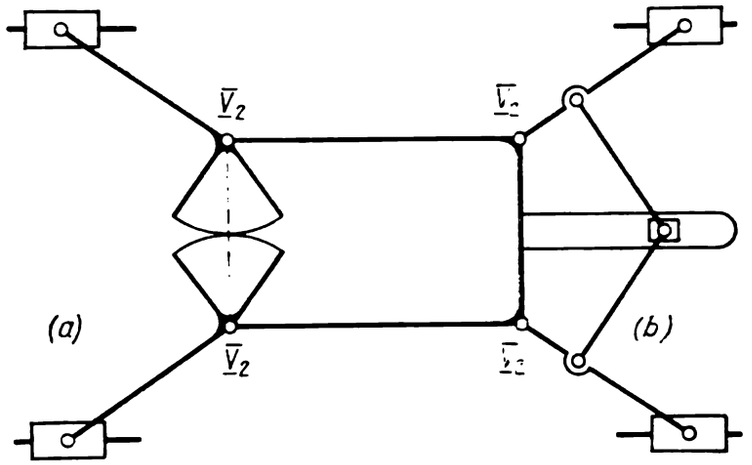


Fig. 6.15. Patented designs of four-carriage cranes
(*a*) with toothed sectors; (*b*) with crank-and-slide mechanism

not be able to transmit wind forces (the disadvantage of the design shown in Fig. 6.14*b*). In addition, the redundant constraints would not be eliminated, and a local harmful mobility (crane movement transversely of the rails) would appear.

Instead of the coupling mechanism (Fig. 6.14*e*), a mechanism of an antiparallel crank may be used (Fig. 6.14*f*). The latter mechanism is simpler, but forces in it and size of the members are greater compared to those in the former mechanism.

The legs may be interconnected by means of toothed sectors (Fig. 6.15*a*) as well as by a twin crank-and-slide mechanism (Fig. 6.15*b*).

## 6.8. Cranes with Folding Boom (Portal Cranes)

The cranes with folding boom are installed on gantries. Railway tracks extend inside the gantry. Such cranes are generally used in ports for unloading ships. The folding boom is necessary for passing clear between masts of ship. The length of the free end of the rope is reduced to a large extent in such cranes so that swinging of the load is reduced which is very important for high productivity.

Cranes with rigid members interconnected by means of joints (Fig. 6.16*a*) and flexible guy and boom (Fig. 6.17) are used. The latter cranes enable large variations of the boom range, but the

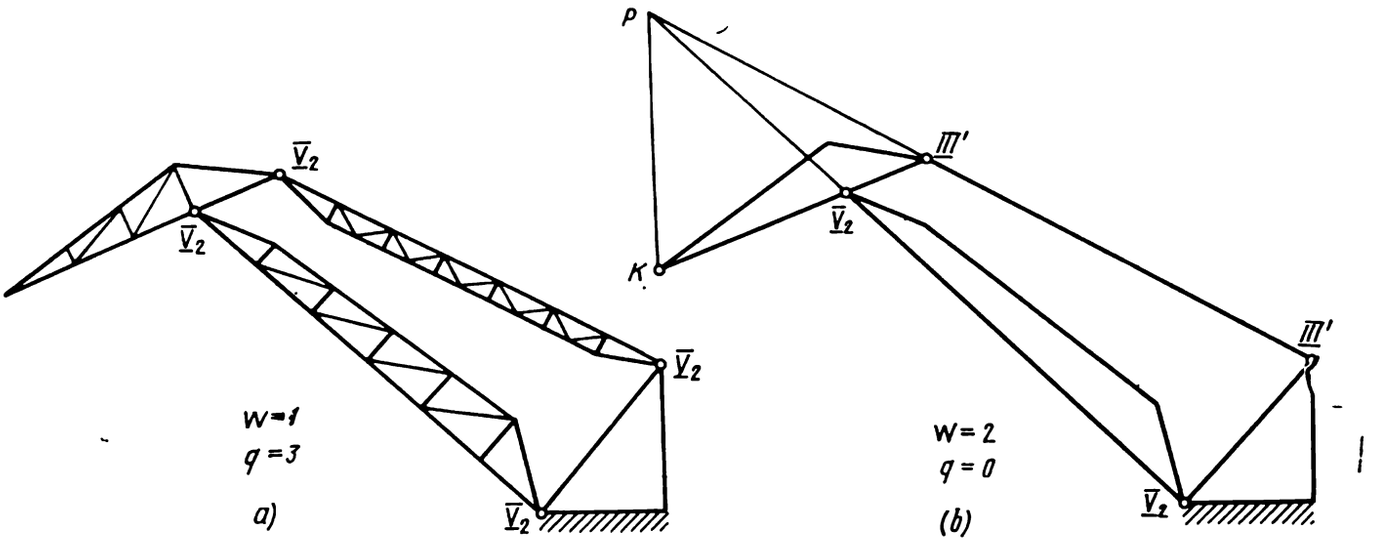


Fig. 6.16. Crane with rigid members
(*a*) old design; (*b*) new design without redundant constraints

boom is subjected to torsion during turning. In addition, a throw-back of the jib may occur in case of load drop.

In the earliest designs of cranes with folding boom all three movable members—boom, jib and guy (Fig. 6.16*a*) were made in the form of rigid trusses. They were interconnected by means of the rotational pairs $V_2$. This mechanism had three redundant constraints which required an exact parallelism of all joints and their position in one and the same plane. It is very difficult to comply with these requirements with a long boom range.

The redundant constraints may be eliminated in case the guy is made in the form of a rod coupled to the jib and fixed member by means of the joints *III'* (Fig. 6.16*b*). These joints may also be made as the rotational joints $III'_4$ with a play. With a large length of the guy they function as spherical joints. This design was recently used by the firm Demag for large lifting capacity cranes. Its disadvantage is that the boom is subjected to the action of torque during turning similarly to the case of the flexible guy. Consequently, the boom in this crane is made integral, box-shaped so as to improve the torsional strength.

The transmission of torque by the boom may be avoided (Fig. 6.18) by making the guy rigid in the form of a triangular truss and by coupling it to the jib by means of the spherical pair *III'* and to the fixed member by means of the rotational pair $V_2$ (struts of the trusses of the jib and brace are not shown in Fig. 6.18 for the sake of clarity, and only chords are shown).

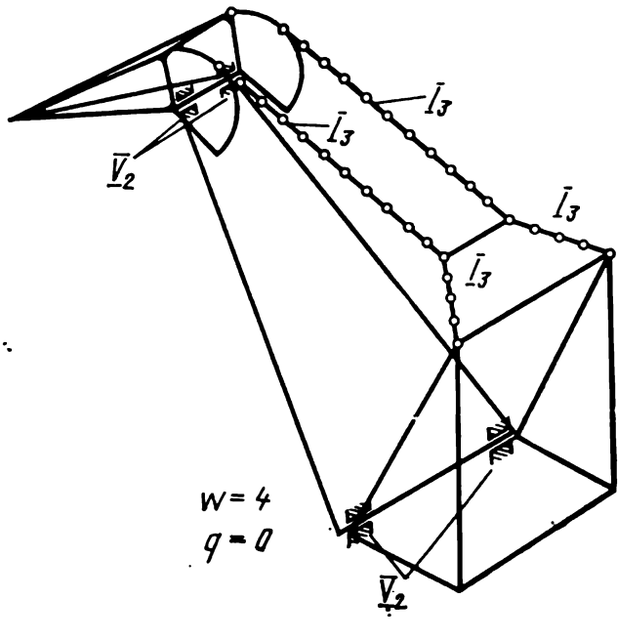


Fig. 6.17. Crane with flexible guy ropes

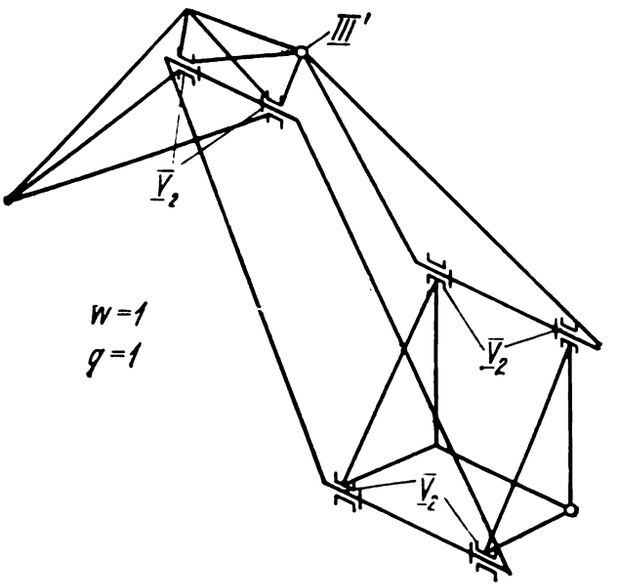


Fig. 6.18. Crane with the boom that does not transmit torque

The boom should be made in the form of a planar quadrangular truss and coupled to the jib and fixed member by means of the rotational pairs $V_2$. Such a truss has a very small torsional rigidity about the longitudinal axis so that it cannot practically transmit torque about this axis.

In accordance with formula (1.1), $q = 1$ in this mechanism, but this constraint is harmless since it only causes a torsional deformation of the boom for which the boom is very resilient as shown above.

Generally the rod of the mechanism of boom lift in folding boom cranes is connected to an intermediate point of the boom, which results in its bending. In order to eliminate the bending moment which cannot be resisted by the planar truss, it is advisable to couple the joint of the lift rod to the truss by means of three tensioned rods. Two rods should be coupled to two upper corners of the truss and one rod to the middle of the lower cross-bar. Four rods cannot be used since this would result in a very torsionally rigid frame, and the redundant constraint would become harmful.

The design of the mechanism shown in Fig. 6.19 makes it possible to eliminate completely both redundant constraints and torsion. Here the boom is made in the form of a triangular truss which is coupled to the jib by means of the spherical joint $III'_2$ and rod $III'III'$. The guy consists of a triangular frame $III'V_2$.

For choosing the dimensions of the crane members, the use is made of the method for designing mechanisms using three points (Fig. 6.20).

The preset values are: the boom length $l_y$, the jib dimensions $l_x$ and $a$, the height of the pulley centre $h$, and three values of the boom

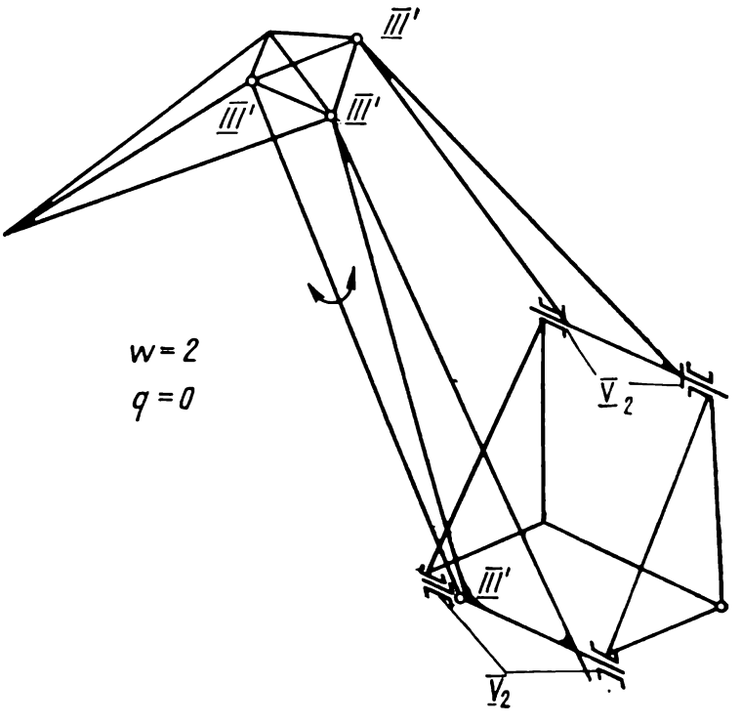


Fig. 6.19. Crane without redundant constraints

range $l_1$, $l_2$, $l_3$ at design points. The unknown values are: the length of the guy $l_g$ and coordinates of the point $O$—$x_0$ and $y_0$.

For graphical design, the crane mechanism is drawn in three positions. The point $O$ is found as the centre of a circle drawn through points $A_1$, $A_2$ and $A_3$. The plotting is made as follows. Marks are traced with a radius close to $l_0$ from centres $A_1$, $A_2$ and $A_3$. A curvilinear triangle is thus obtained. It is easy to see that the centre $O$ is disposed on the side of the "base" of this triangle. With this in view, it is not difficult to change the tracing radius so as to obtain another triangle disposed on the other side of the point $O$. Then the point $O$ can be found at the point of intersection of three straight lines interconnecting similar vertexes of the curvilinear triangles.

For the analytical solution, let us determine an auxiliary angle $\alpha_1$ and an auxiliary line length $u_1$:

$$\operatorname{tg} \alpha_1 = \frac{h}{l_1} \tag{6.1}$$

$$u_1 = \frac{l_1}{\cos \alpha_1} \tag{6.2}$$

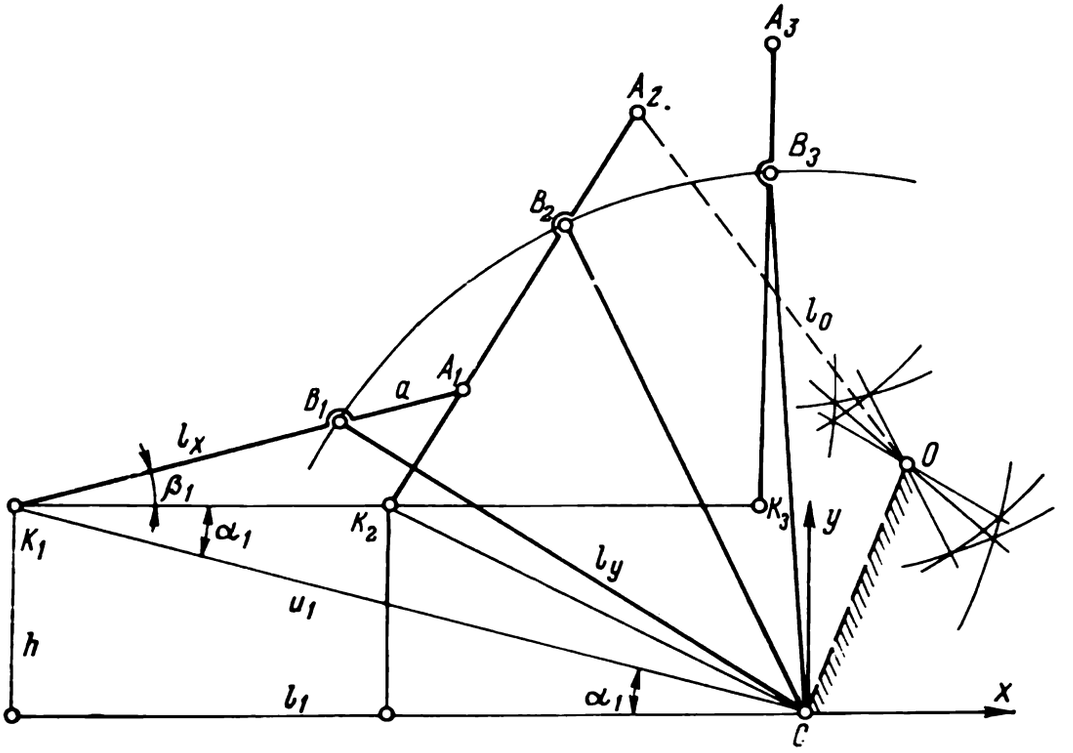


Fig. 6.20. Plotting of dimensions of an articulated crane with preset dimensions of boom and jib

From the triangle $CB_1K_1$ we obtain

$$\cos(\alpha_1+\beta_1)=\frac{u_y^2-(l_y^2-l_x^2)}{2l_xu_1} \tag{6.3}$$

From this expression we can find $\beta$.

Let us determine the coordinates of the point $A_1$:

$$x_1=(l_x+a)\cos\beta_1-l_1 \tag{6.4}$$

$$y_1=(l_x+a)\sin\beta_1+h \tag{6.5}$$

Coordinates $x_2$, $y_2$ and $x_3$, $y_3$ can be found using absolutely the same formulae. By formula for the distances between the points $A_1$, $A_2$, $A_3$ and $O$

$$\left.\begin{aligned}(x_1-x_0)^2+(y_1-y_0)^2&=l_0^2\\(x_2-x_0)^2+(y_2-y_0)^2&=l_0^2\\(x_3-x_0)^2+(y_3-y_0)^2&=l_0^2\end{aligned}\right\} \tag{6.6}$$

By transformation, we obtain

$$\begin{aligned}x_1^2-2x_1x_0+x_0^2+y_1^2-2y_1y_0+y_0^2&=l_0^2\\x_2^2-2x_2x_0+x_0^2+y_2^2-2y_2y_0+y_0^2&=l_0^2\\x_3^2-2x_3x_0+x_0^2+y_3^2-2y_3y_0+y_0^2&=l_0^2\end{aligned}$$

By subtracting the first equation from the second and third equations, we have

$$(x_2^2 - x_1^2) - 2x_0 (x_2 - x_1) + (y_2^2 - y_1^2) - 2y_0 (y_2 - y_1) = 0$$
$$(x_3^2 - x_1^2) - 2x_0 (x_3 - x_1) + (y_3^2 - y_1^2) - 2y_0 (y_3 - y_1) = 0$$

or

$$2 (x_2 - x_1) x_0 + 2 (y_2 - y_1) y_0 = (x_2^2 - x_1^2) + (y_2^2 - y_1^2) \quad (6.7)$$

$$2 (x_3 - x_1) x_0 + 2 (y_3 - y_1) y_0 = (x_3^2 - x_1^2) + (y_3^2 - y_1^2) \quad (6.8)$$

Thus, a system of two linear equations with the unknowns $x_0$ and $y_0$ is obtained. After solving it, we can find the guy length $l_0$ by one of the formulae (6.6), the other equations being used for checking.

The crane dimensions can also be designed based on different conditions. Coordinates of the point $O$ may be preset, and coordinates of the point $A$ and the length $l_0$ may be found (see Fig. 6.20). In such a case the principle of the reversal of motion should be applied. The mechanism is again drawn in three positions. In one of the positions (the second one in Fig. 6.21) the jib $K_2B_2$ is fixed, and the boom is rotated about it. For that purpose, a circle of a radius $B_2C_2$ is drawn from the point $B_2$. Points $C_1$ and $C_3$ are found by tracing from the point $K_2$ with radii $K_1C_2$ and $K_3C_2$. For plotting the positions $O_1$ and $O_3$ in Fig. 6.21, let us show the position of a straight line which passes horizontally through the point $C$ in the crane (see Fig. 6.20). This line will extend as the tangent line to a circle of a radius $h$ having its centre at $K_2$. Further it is feasible to construct an equilateral triangle $C_2O_2E_2$ at $C_2$ with $C_2O_2 = C_2E_2$ (so as to be able to transfer it by tracing with two radii, rather than three) and to construct equal triangles $C_1O_1E_1$ and $C_3O_3E_3$. The point $A_2$ is found as the centre of a circle drawn through the points $O_1$, $O_2$ and $O_3$. It may be outside the straight line $K_2B_2$ since a more general case is considered.

After the determination of dimensions, the mechanism should be drawn in several positions so as to find the deviation from the straight line.

It should be borne in mind that with the maximum boom range the jib may be thrown back in such a mechanism. Such positions should not be permitted.

In cranes having flexible guys (see Fig. 6.17), for the convenience of the structural arrangement with the jib truss, the scrolls are gener-

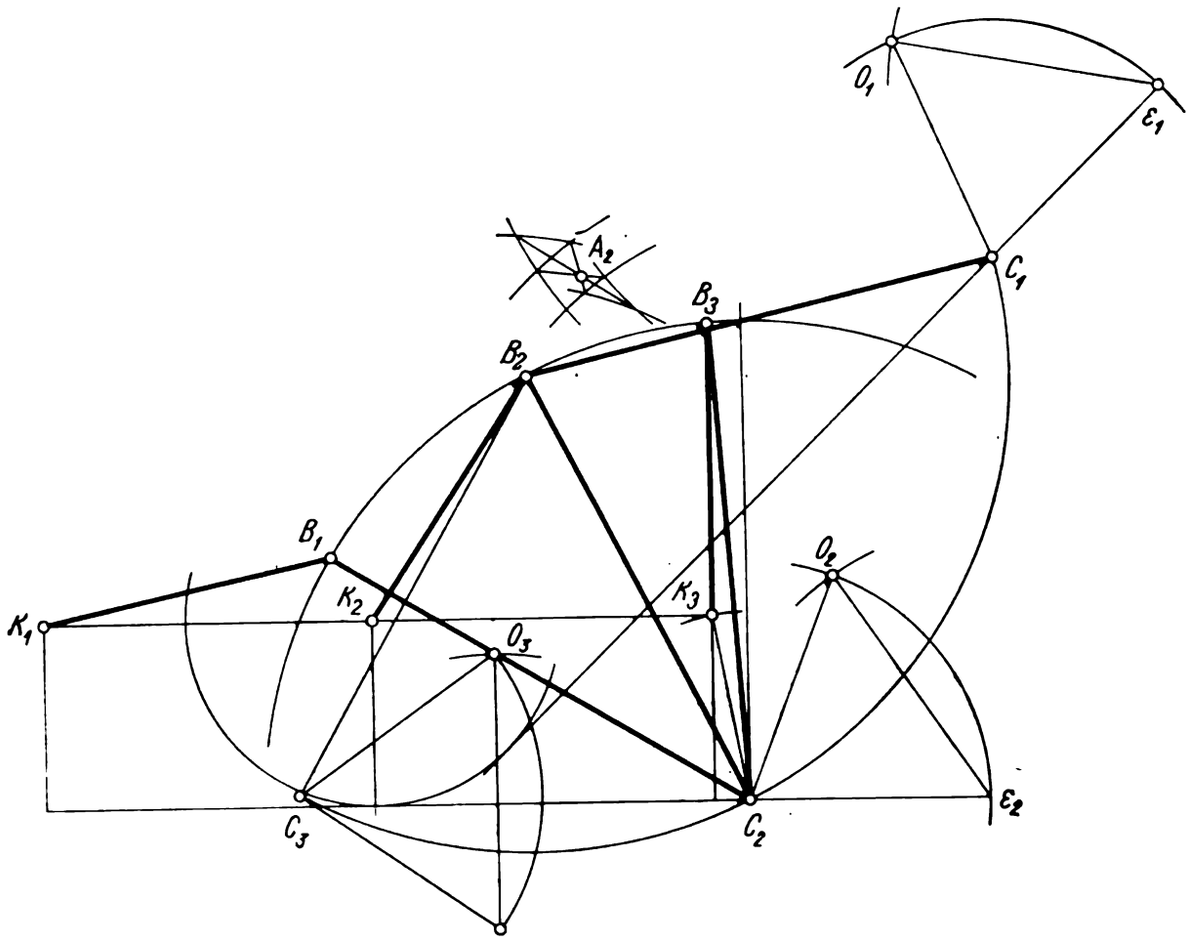


Fig. 6.21. Plotting of dimensions of an articulated crane with preset dimensions of the boom and fixed member

ally made twin. In order to obtain uniform distribution of load among the scrolls, an equalizing device is used, and for that purpose the ropes are interconnected by means of a cross-bar and their ends are spaced apart. Unequal length of the ropes is avoided by longitudinal shifting of the cross-bar. Checking the mechanism, it must be borne in mind that the cross-bar has three local mobilities: rotation about its axis and movements of its ends (independent) in the direction perpendicular to the plane of the ropes. The ropes do not hamper these mobilities: the first mobility is not hampered because theoretically the ropes extend through the axis of the cross-bar, and the second and third mobilities are not hampered because they are in one and the same plane, which corresponds to the dead centre of the mechanism at which an additional mobility of the mechanism appears. Taking into account the main mobility, the mobility of the mechanism is $w = 4$ (the turntable is regarded as a fixed member).

## 6.9. Elevators (Lifts)

Generally elevators have winches with a rope-guide pulley for three or four ropes. The rope pulley is narrow so that it is always overhung. Therefore, a lightweight structure is obtained with two supports of the pulley shaft in the casing of a reduction gear. A globoidal worm gearing which is generally used in lift winches comprises a system with redundant constraints, and the ways for eliminating such constraints have not so far been found. The problem of distribution of the load among ropes also remains unsolved. A suspension in the form of an equalizing linkage is installed on the lift car for equalizing the load in ropes. The ropes are connected to a counterweight by means of springs, that is the system remains statically indeterminate, though unequality of forces is partly compensated for by the springs.

If one of the ropes is deeper (or higher) in the pulley groove compared to other ropes, its travel is shorter than that of the other ropes owing to a smaller length of the circumference. Therefore, the tensions in the rope in the upmost and lowermost positions of the lift car are different, and the rope slips. Then this groove wears out more rapidly compared to the others, and the pulley is to be replaced.

As the groove dimensions always vary (within tolerances), the cause of non-uniform wear is inherent in the design of the mechanism. This disadvantage can be readily eliminated. For that purpose, a second suspension should be provided on the counterweight, rather than springs. Here the local mobilities are not harmful as they are eliminated by the friction between the ropes and the pulley.

For the suspensions to function about their middle position, where their friction is at minimum, stops should be provided for the levers which should cause slack or slip of the rope at the end of travel (once for a cycle).

Lift suspensions serve to equalize loads on lift ropes. Most widely used suspensions are shown in Fig. 6.22. Fig. 6.22*a* and *c* shows suspensions for three ropes, and Fig. 6.22*b* and *e* shows suspensions for four ropes. The worst design is shown in Fig. 6.22*e* as the system of four parallel forces acting on one body is statically indeterminate. Consequently this design does not result in equalizing loads in the ropes. The ropes are calculated based on the condition that one of them can withstand the full load of the lift car and with a multiple strength margin at that. Hence, the reliability of the ropes is very high. Unfortunately, the joint connected to the lift car in such suspensions transmits the full load and has no redundancy. In case

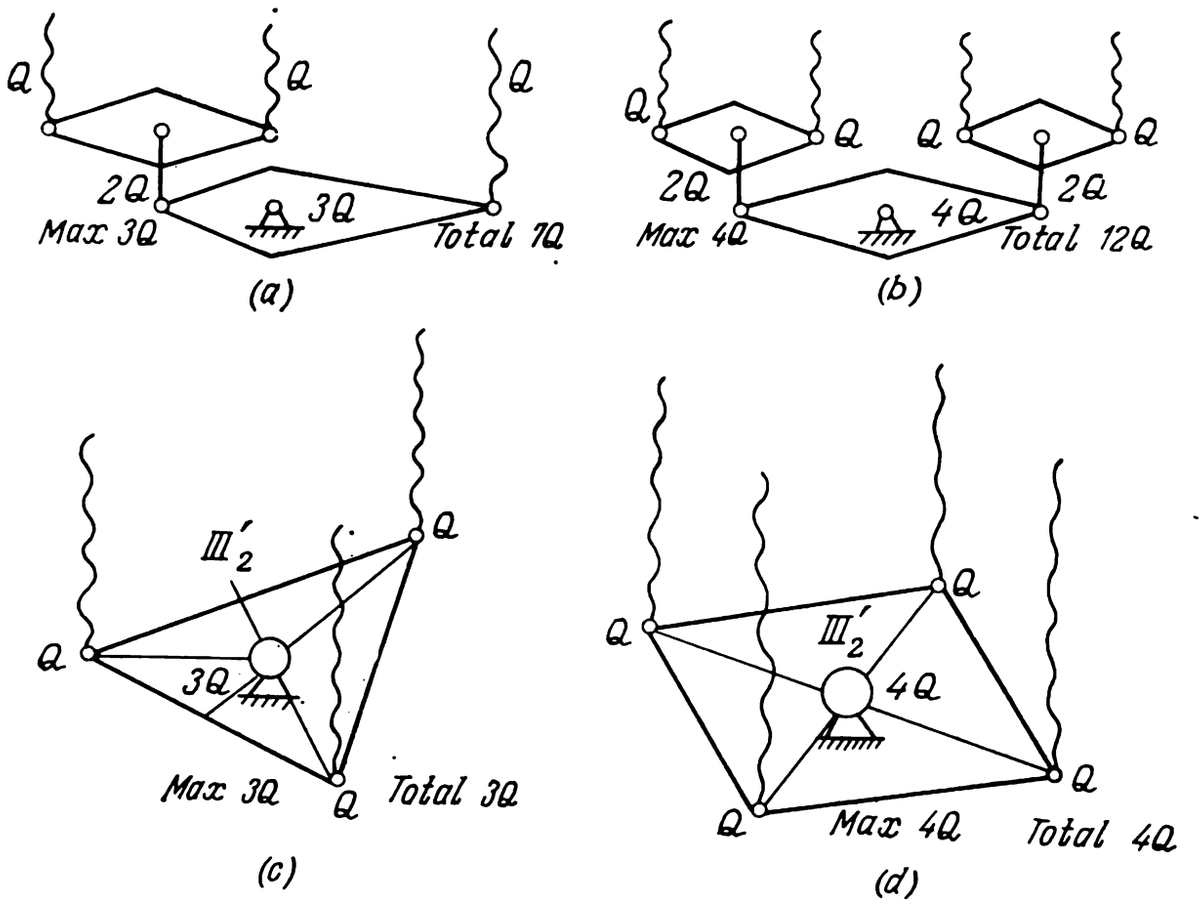


Fig. 6.22. Dangerous suspensions of lifts with transmission of the whole load to one bolt (stub shaft)

(*a*) and (*c*) for all ropes; (*b*) and (*d*) for four ropes; (*a*) and (*b*) with joints $V_2$; (c) and (*d*) with joints $III_2'$

of failure of the joint the lift car would fall. In order to avoid accidents, while eliminating friction in the linkage, an individual counterweight may be used for each rope. Fig. 6.23*a* shows a suspension for three ropes. Here only one rope extends in the central position, and its counterweight is symmetrical. Two other ropes are offset from the central position by the amount of $y$ (Fig. 6.23*b*). Their counterweights are asymmetrical. For that purpose, the upper weight should be shortened to a length $x$.

Let us denote the number of long weights as $i$ and, assuming their masses to be proportional to their lengths, the lengths can be written instead of the weights. The moments with respect to the middle of the counterweight will be as follows:

moment of the shortened weight $x\,\frac{b-x}{2}$

moment of the rope load $(bi + x)\,y$

By equalizing these moments, we have

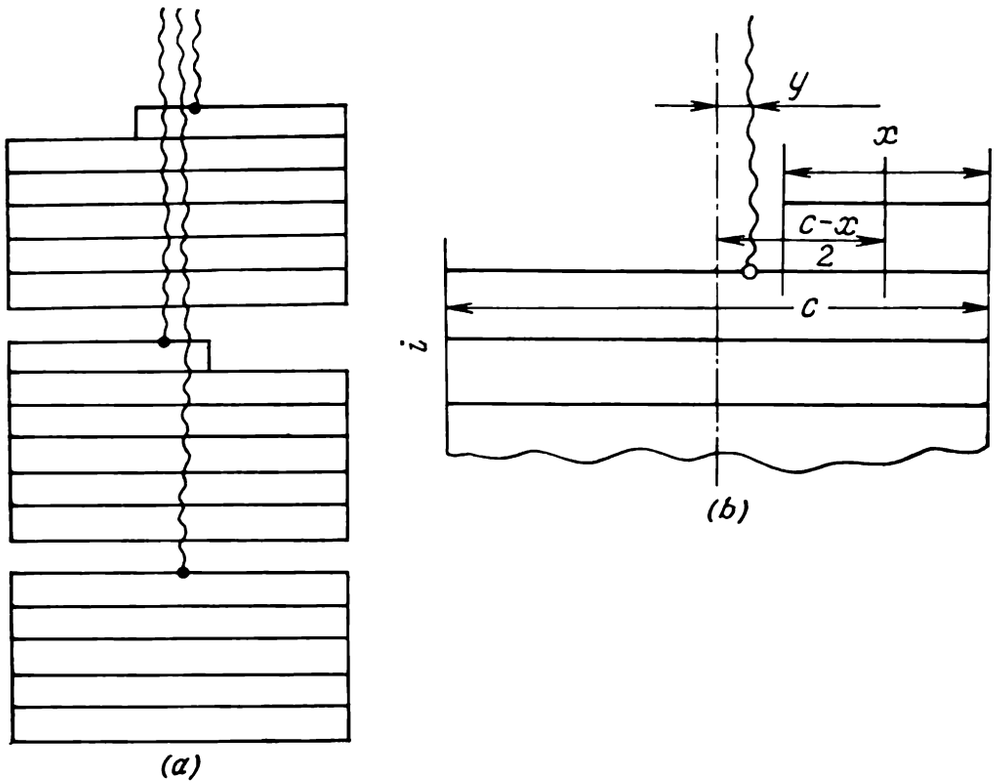


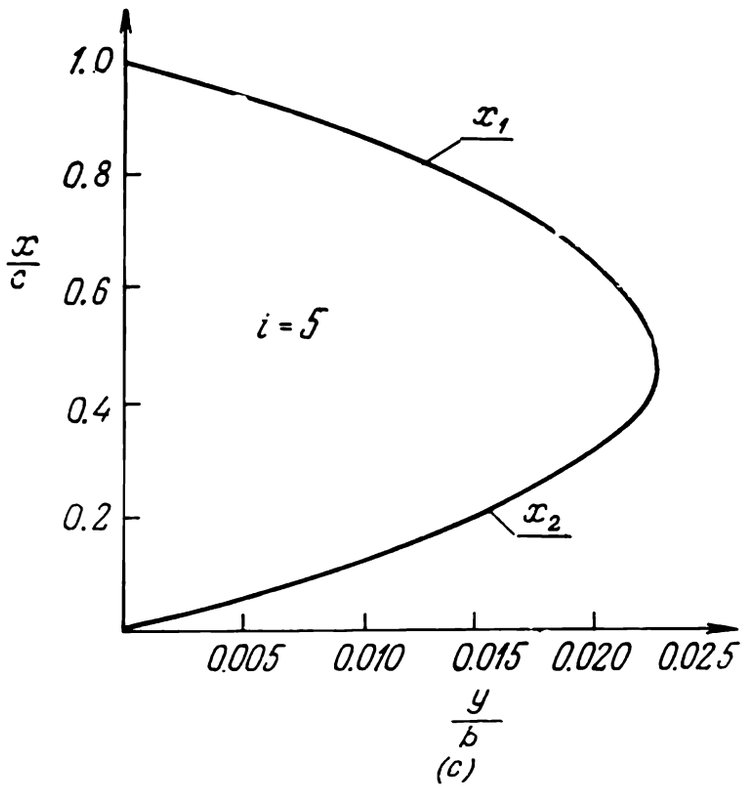


**Fig. 6.23. Suspension with individual counterweights for each rope**

$$x\,\frac{b-x}{2}=(bi+x)\,y$$

or $x^2+(2y-b)\,x+2biy=0$
hence

$$\frac{x}{b}=\left(0.5-\frac{y}{b}\right)\pm\sqrt{\left(0.5-\frac{y}{b}\right)^2-2i\,\frac{y}{b}} \qquad (6.9)$$

The chart showing this function is given in Fig. 6.23*c*. The vertex of the parabola is of major importance as it gives the maximum possible value of $\frac{y}{b}$ and a corresponding value of $\frac{x}{b}$. At this point both solutions of the equation are identical. Hence, the expression under the root should be equal to zero

$$\left(0.5-\frac{y}{b}\right)^2-2i\,\frac{y}{b}=0$$

$$\frac{1}{4}-\frac{y}{b}+\left(\frac{y}{b}\right)^2-2i\,\frac{y}{b}=0$$

or

$$\left(\frac{y}{b}\right)^2-(1+2i)\,\frac{y}{b}+\frac{1}{4}=0$$

hence,

$$\frac{y}{b}=\frac{1+2i}{2}-\sqrt{\left(\frac{1+2i^2}{2}\right)-\frac{1}{4}}=\frac{1+2i}{2}-\frac{1+2i}{2}\sqrt{1-\frac{1}{4\left(\frac{1+2i}{2}\right)^2}}$$

The minus sign is used here because the plus would result in a senseless solution.

The root is transformed using the approximate formula for small values:

$$\sqrt{1-\frac{1}{4\left(\frac{1+2i}{2}\right)^2}}=1-\frac{1}{8\left(\frac{1+2i}{2}\right)^2}$$

and after substitution, obtain:

$$\frac{y}{b}=\frac{1+2i}{2}-\frac{1+2i}{2}+\frac{1}{8\left(\frac{1+2i}{2}\right)^2}$$

$$\text{hence, } \frac{y}{b}=\frac{1}{4\,(1+2i)} \qquad (6.10)$$

$$\text{Accordingly } \frac{x}{b}=0.5-\frac{y}{b} \qquad (6.11)$$

$$\text{with } i=5 \qquad \frac{y}{b}=\frac{1}{4(1+2.5)}=0.0228$$

$$\text{and } \frac{x}{b}=0.4772$$

In case the resultant maximum value of $\frac{y}{b}$ proves inadequate, two shortened weights should be used for each counterweight. This system offers a guarantee against the lift car fall. It does not have a joint without doubling. In addition, even in the case of a rope breakage at the upper or middle conterweight, the counterweight would not fall but lie down on the lower counterweight. The same effect is obtained for the lower counterweight by providing an appropriate protective bracket.

**Combination designs.** The number of counterweights may be reduced and they can be made symmetrical. For that purpose, one counterweight should be installed for each pair of ropes interconnected by means of an equiarm balance beam (Fig. 6.24). With an odd number of ropes (Fig. 6.24*a*), one of the ropes is connected to an individual counterweight which is twice as light as the counterweights of the pairs of ropes. With an even number of ropes (Fig. 6.24*b*) all ropes are coupled pairwise.

**Suspension linkages.** For a reliable operation of a suspension, all its members should be coupled to the lift car (or counterweight) by means of at least two joints. One lever is coupled to the lift car in each joint. The discussion of designs of reliable suspensions begins with these two levers. One rope can be connected to one arm of each lever (Fig. 6.25*a*). The other ends of the levers, which are to be made in the form of angle levers, may be interconnected. This is the design of a suspension for a lift having two ropes. This design is applicable to a larger number of ropes as well, e.g. to a four-rope lift as shown in Fig. 6.25*b*. In this design, one more angle lever is added per rope. The design is also suitable for an odd number of ropes. In Fig. 6.25*b* the ratio of lever arms is equal to 3. Maximum force is $3Q$ and the total force is $18Q$. In case of equiarm levers, we have $Q$ and $6Q$, respectively, that is the design is the best one in all characteristics.

With three ropes (Fig. 6.26), the other ends of straight levers should be coupled to the third rope by means of a floating lever. This is a planar mechanism so that it is convenient to install it on the counterweight. Long levers may be used in this design which is favourable to reduce friction. The mechanism has 5 members and is more complicated compared to that shown in Fig. 6.22*a*; but, this

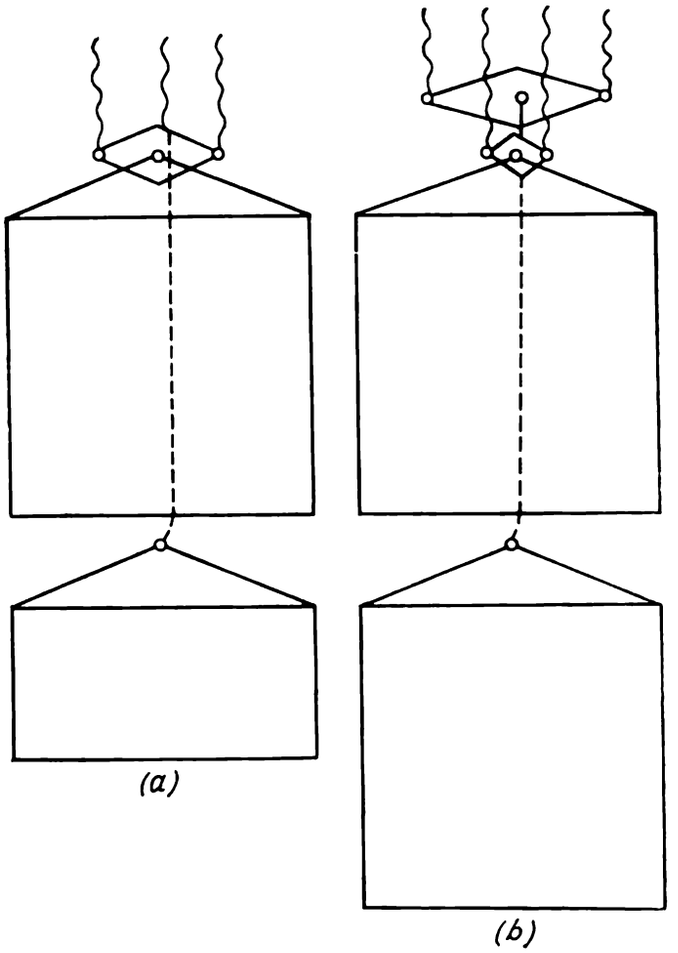


Fig. 6.24. Combination suspension with several counterweights and equalizing levers
(*a*) for three ropes; (*b*) for four ropes

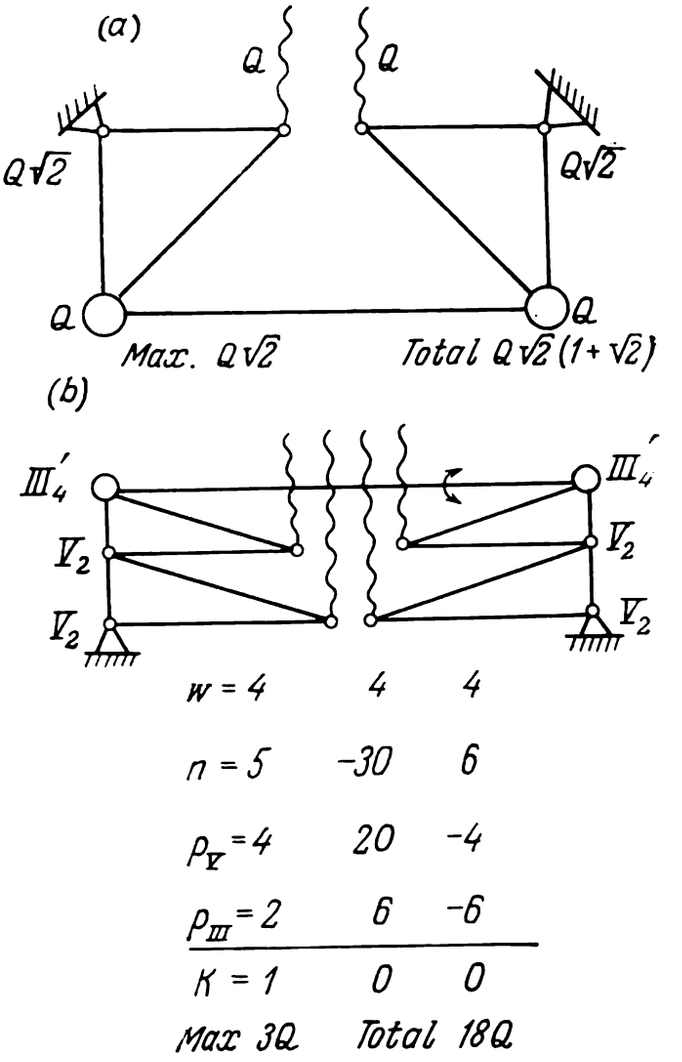


Fig. 6.25. Suspensions with angle levers
(*a*) for two ropes; (*b*) for four ropes

mechanism ensures a greater reliability, and the maximum load in the joint is one and a half $Q$ compared to $3Q$.

The full load on all joints is also a very informative characteristic of the mechanism. In Fig. 6.26 this load is $5Q$ compared to $7Q$ in Fig. 6.22*a*. The calculation of the number of redundant constraints is given in Fig. 6.26 in the table. Calculation data are given in the first column. The second column contains calculation using the Malyshev formula

$$q = w - 6n + 5p_V + 4p_{IV} + 3p_{III} + 2p_{II} + p_I$$

and the third column contains calculation using the Ozol formula

$$q = w + 6k - f$$

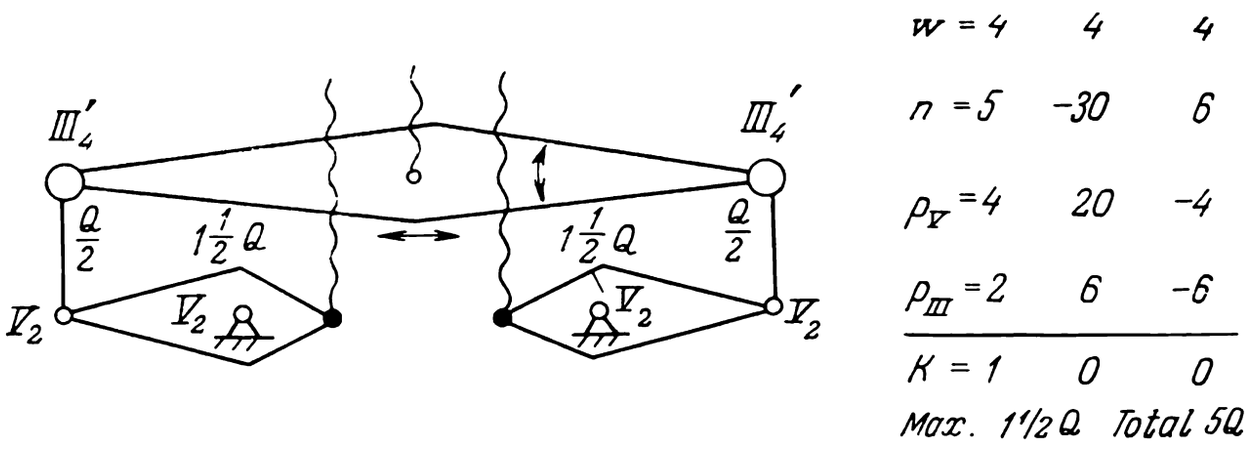


Fig. 6.26. Suspension for three ropes

The mobility $w$ consists of a sum of local mobilities and an equalizing mobility which is equal to the number of ropes minus unity. The ropes are not considered here, and an equalizing mobility is introduced to take into account the constraints imposed by the ropes. Owing to this, the number of loops in the calculation is strongly reduced, which is very important to simplify the calculation.

Local mobilities are shown by arrows in Fig. 6.26. They are mobilities of the floating lever along axis $x$ and rotation about axis $y$.

The suspension design for four ropes may be obtained by two methods. Still another, short balance beam may be provided on the floating lever as shown in Fig. 6.27*a*. There are 6 members compared to 5 in Fig. 6.22*b*, but the maximum load on the joint is $2Q$ compared to $4Q$ and the full load is $10Q$ compared to $12Q$ in Fig. 6.22*b*.

Another method of equalizing loads in two ropes is the use of the mobility of the floating lever about the second horizontal axis (see Fig. 6.27*b*). Here the ropes are disposed in two planes at the vertexes of a square. The mechanism has 5 members, but two rotational pairs $V_2$ had to be replaced by the spherical pairs $III'_2$. The loads in the joint are the same as in Fig. 6.27*a*, and the full load is $8Q$.

To obtain an additional mobility with five ropes, the mobility about the second horizontal axis should also be used, but this time for two members, rather than for one. For symmetry, it is better to use levers connected to the lift car and the levers are preferably made triangular as shown in Fig. 6.28. The number of members here is 5. The ropes are arranged at the vertexes and at the centre of gravity of the square. In this case four pairs $V_2$ should be replaced by the spherical pairs $III'_2$. Maximum load in this design is $2.5Q$, and the full load is $7Q$. The spherical joints coupling the triangular levers to the lift car should be spaced at 1/5 of the height from the

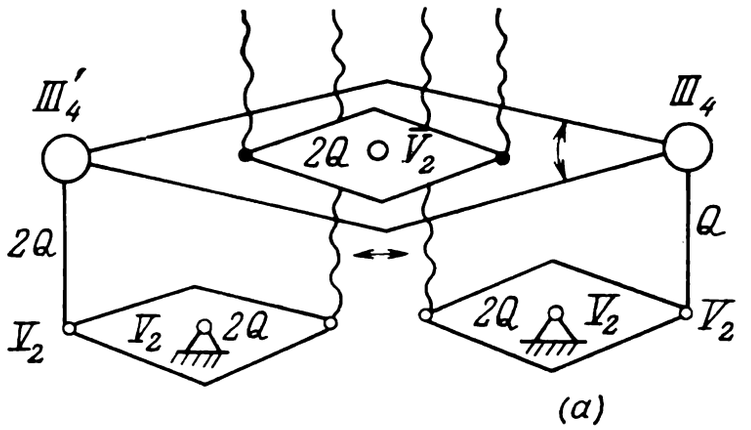


| | | |
|---|---|---|
| $w = 5$ | 5 | 5 |
| $n = 6$ | -36 | 6 |
| $p_V = 5$ | 25 | -5 |
| $p_{III} = 2$ | 6 | -6 |
| $K = 1$ | 0 | 0 |

Max. 2Q Total 10Q

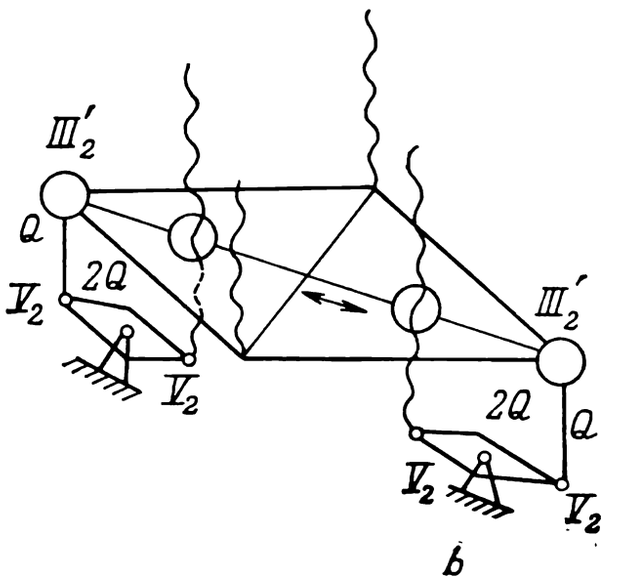


| | | |
|---|---|---|
| $w = 4$ | 4 | 4 |
| $n = 5$ | 30 | 6 |
| $p_V = 4$ | 20 | -4 |
| $p_{III} = 2$ | 6 | -6 |
| $K = 1$ | 0 | 0 |

Max. 2Q Total 8Q

Fig. 6.27. Suspension for four ropes
(*a*) planar suspension; (*b*) three-dimensional suspension

base (the arm ratio is 1 : 4). The diagram showing the mobility in the loop of this mechanism is given in the right-hand part of Fig. 6.28. The equalizing mobilities are denoted by $y$, local mobilities—rocking of the members—by $k$. The type and number of mobilities can be seen in the diagram.

With six ropes, mobilities about the second horizontal axis for three members should be used to increase the number of the equalizing mobilities (Fig. 6.29). In addition to the triangular members (the arm ratio 1 : 2), these members will include a floating lever $CD$. In this design, all six rotational pairs are to be replaced by the spherical pairs. The ropes extend in two parallel planes, three ropes in each plane. The designer is free in the choice of the ropes spacing, which represents the advantage of the system. Maximum load here

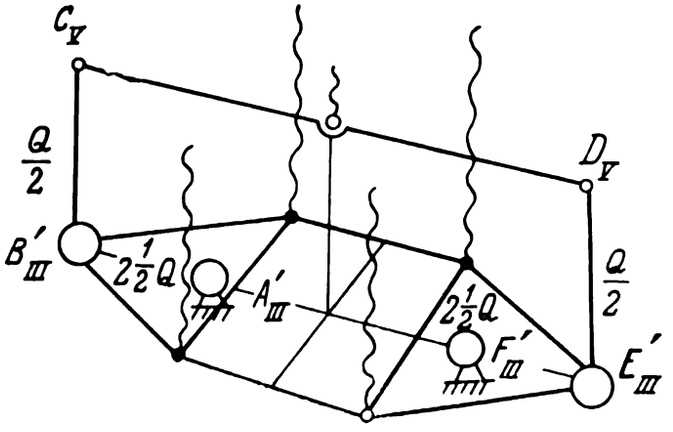


| | | | |
|---|---|---|---|
| $w = 8$ | 8 | 8 |
| $n = 5$ | 30 | 6 |
| $p_V = 2$ | 10 | -2 |
| $p_{III} = 4$ | 12 | -12 |
| $K = 1$ | 0 | 0 |

Max. 2½Q Total 7Q

ABCDEF

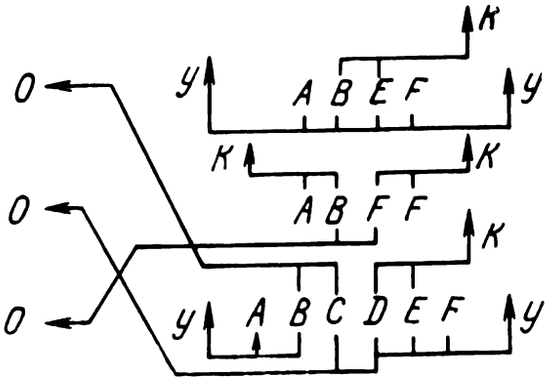


Fig. 6.28. Suspension for five ropes—three-dimensional

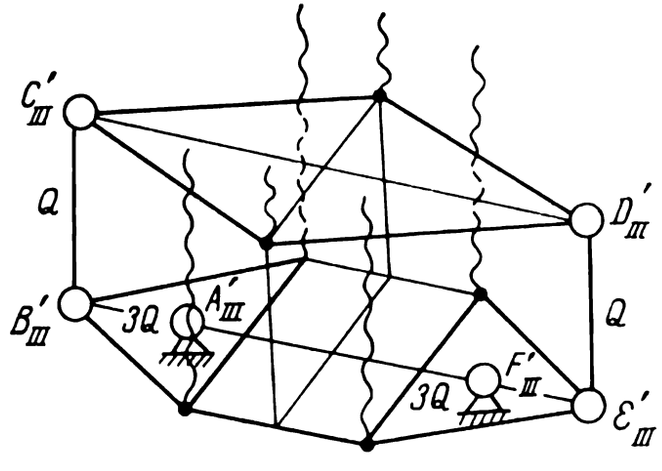


| | | | |
|---|---|---|---|
| $w = 12$ | 12 | 12 |
| $n = 5$ | -30 | 6 |
| $p_{III} = 6$ | 18 | -18 |
| $K = 1$ | 0 | 0 |

Max. 3Q Total 10Q

ABCDEF

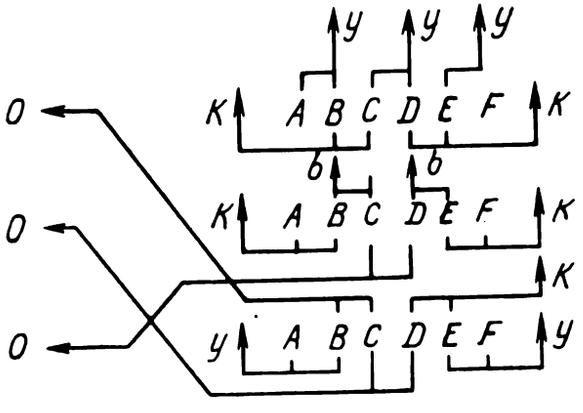


Fig. 6.29. Suspension for six ropes—three-dimensional

is $3Q$ and the full load is $10Q$. The diagram of mobilities in the loop is shown in the right-hand part of Fig. 6.29. Two members $BC$ and $DE$ with the spherical pairs can rotate about their axes. This mobility is denoted as $b$. It is interesting to compare the mechanism of

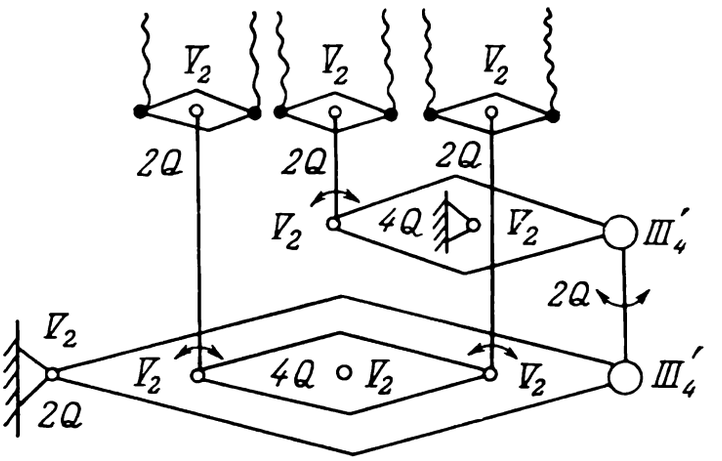


| | | | |
|---|---|---|---|
| $w = 9$ | 9 | 9 |
| $n = 10$ | -60 | 6 |
| $p_V = 9$ | 45 | -9 |
| $p_{III} = 2$ | 6 | -6 |
| $K = 1$ | 0 | 0 |
| Max. $4Q$ | Total $26Q$ | |

Fig. 6.30. Suspension for six ropes—planar

Fig. 6.29 with a similar mechanism shown in Fig. 6.30. The upper balance beams are conventionally shown as turned through 90°. Local mobilities in this figure are shown by arrows. The ropes also extend in two parallel planes. The design is much more complicated as it has 10 members compared to 5 in Fig. 6.29. Maximum load here is $4Q$ compared to $3Q$, and the full load is $26Q$ compared to $10Q$. The friction is also respectively greater. The simplicity of the design shown in Fig. 6.29 is due to the use of the spherical pairs, each having three mobilities, rather than one as is the case with the rotational pairs.

A suspension coupled to the lift car by means of three joints may be designed to improve the reliability. Such a suspension for four ropes is shown in Fig. 6.31. Here there are three levers coupled to the lift car, with the arm ratio 1 : 3. This design has one member more compared to that shown in Fig. 6.27*a* and two members more

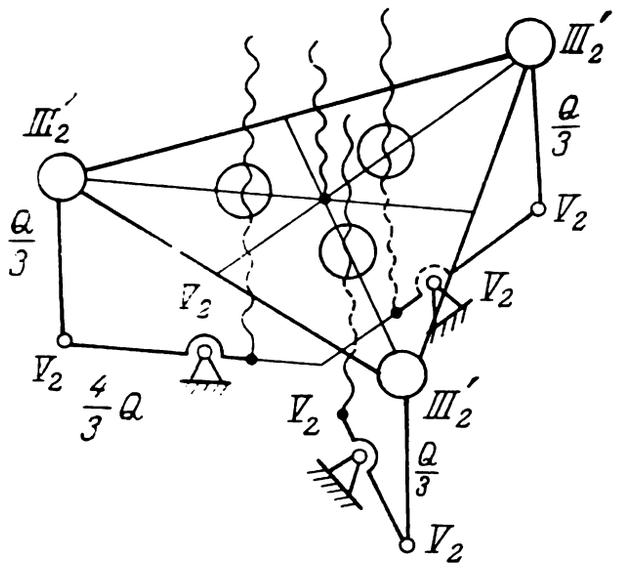


| | | |
|---|---|---|
| $W = 3$ | 3 | 3 |
| $n = 7$ | −42 | 12 |
| $p_V = 6$ | 30 | −6 |
| $p_{III} = 3$ | 9 | −9 |
| $K = 2$ | 0 | 0 |

Max. 4/3 Q Total 6Q

Fig. 6.31. Suspension for four ropes with a triple linkage

compared to Fig. 6.27*b*. Maximum load is, however, 4/3Q compared to $2Q$, and the full load is $6Q$ compared to $10Q$ in Fig. 6.27*a*. Moreover, the reliability is higher: there are three joints instead of two. The only disadvantage is that the suspension is a three-dimensional structure, and it cannot be installed on the counterweight.

The number of joints coupled to the lift car can be made still greater and the load thereon may be reduced by using a suspension proposed for vertical-lift bridges (Fig. 6.73*c*).

The lift car safety device stopping the car in the case of rope breakage is a very important mechanism. An instant-action wedge safety device is a statically indeterminate system. Simultaneous actuation of safety devices on two tracks is achieved by adjustment. With a poor adjustment only one safety device may operate which can cause skewing of the car. Jaw-type sliding-action safety devices are free from this disadvantage. The design of the mechanism ensures identical pressure of the jaws on both tracks.

The car platform is a very vital mechanism of the lift, controlling the platform contact. In case of failure of this mechanism the lift can depart with open doors of the car which can cause an accident with lethal consequences. It is especially dangerous in case there are children without adult persons in the car (small mass of children hampers operation of the movable car platform). Therefore, it is very important for the platform to function with a low friction which should not depend on incidental factors, that is the mechanism must have no redundant constraints.

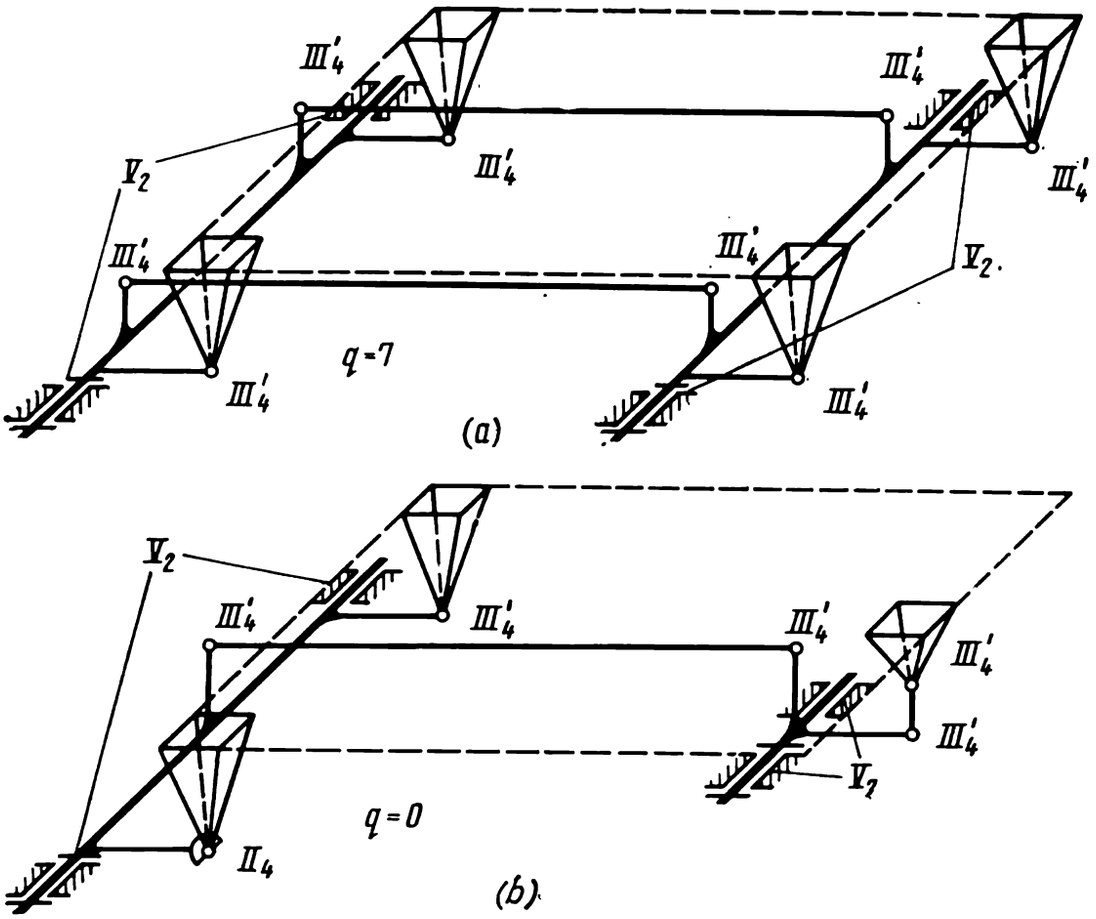


Fig. 6.32. Designs of the movable lift car platform
(*a*) improper design with seven redundant constraints; (*b*) correct design without redundant constraints

There are seven redundant constraints in the design of a passenger lift of 350 kg capacity (Fig. 6.32*a*). An exact equality of lengths of connecting rods should be maintained (an improper design is a twin mechanism), and an accurate position of the joints coupling the platform to the cranks is required: the position of the first joint may not be accurate, the position of the second joint requires an exact spacing from the first joint, the position of the third joint requires an exact spacing from the second and first joints (diagonal line), the position of the fourth joint requires an exact spacing from the third and first joints and an exact vertical installation.

In the correct design without redundant constraints (Fig. 6.32*b*) the shafts are interconnected by means of a unitary parallel crank mechanism. The platform is supported at three points (one by the joint $III'_4$, another by the joint $II_4$ with an axial displacement, and the third one by the rod $III'_4III'_4$). No special accuracy is required, and the only condition is for the platform not to interfere with the lift car walls.

The winch frame is supported by the ceiling through rubber pads (for sound insulation), the height of the pads being adjusted by screws. Six supports are generally used so that a statically indeterminate system is obtained, which obviously offers difficulties in setting-up the frame. It is very easy to avoid such difficulties. Three supports and three screws should be used, with a respective enlargement of these elements.

In the real structure, the counterweight is guided by means of six shoes—three for each track. This design is characterized by a large number of redundant constraints. The alignment of three shoes of one track along a straight line requires an especially high accuracy. The number of shoes of the counterweight ought to be reduced to three: two shoes on one track (at the top and bottom ends of the frame) and one on the other track (in the middle of the frame). The other three shoes may be provided for safety by mounting them with a large clearance. In such a case no accurate setting of the shoes is required.

The lift car is generally guided by means of four shoes. Long shoes must be made owing to a possibility of an off-centre loading in case of passengers standing on one side of the car, which caused larger loads applied to the tracks. These shoes should be couples to the frame by means of two joints: a vertical and a horizontal joint in the track plane. There is no horizontal joint with the axis

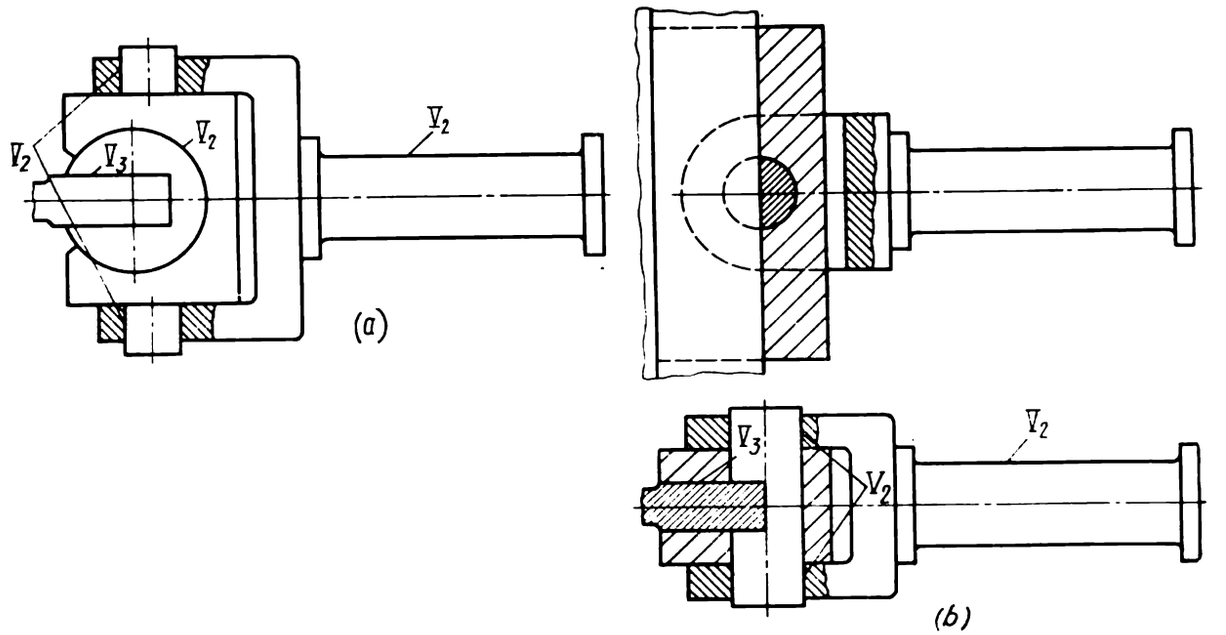


Fig 6.33. Rational designs of guide shoes of the lift car

perpendicular to the track plane in this design though such a joint is necessary because respective misalignments are the largest ones, and it is very frequently that the shoe works by one edge only. The guide shoe having both horizontal and vertical joints is shown in Fig. 6.33*a*. The parts necessary for the disassembly are not shown in the figure. For the simplicity, the joint with the vertical axis may be sacrificed (Fig. 6.33*b*). Here the problem may be structurally solved by using an axle with a half-diameter flat in the middle part.

The use of three shoes is certainly most preferred, but then the design of the middle shoe differs from the two others, and a door should be provided in the car wall for servicing the shoe.

## 6.10. Roller Supports of Rotary Kilns and Transfer Drums

Apart from bearings, rollers (wheels) may serve as supports for rotary motion (Figs. 6.34 and 6.35). If the roller has a small axial length, especially with a barrel-shaped rim, its contact with the drum should be regarded as the first class pair $I_2$. Then five rollers are needed to obtain five restraints. In the lower elevation of Fig. 6.34

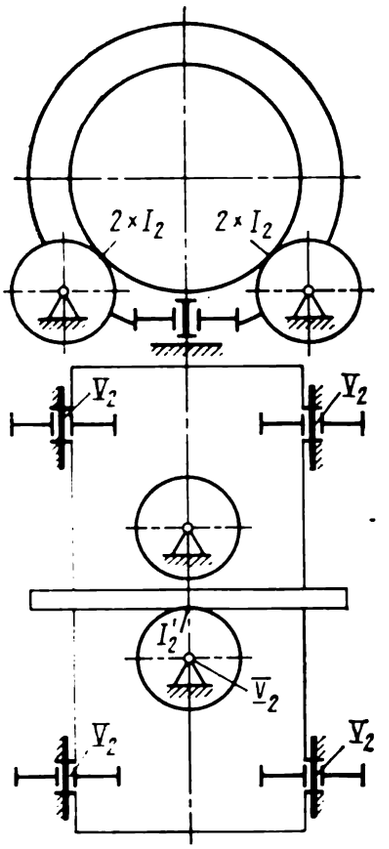


Fig. 6.34. Roller support with five short rollers

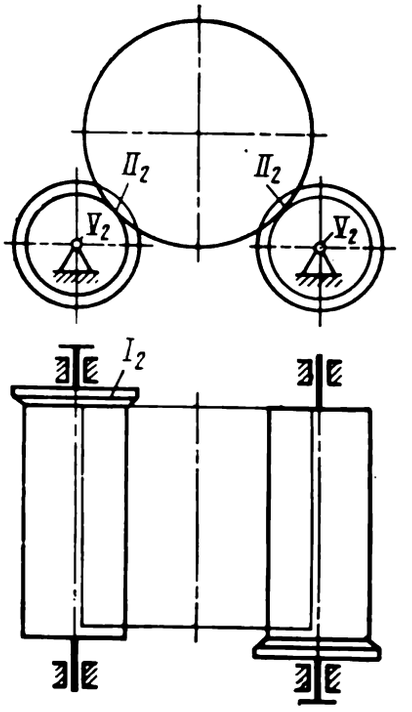


Fig. 6.35. Roller support with two long flanged rollers

the drum is shown with a thin line so as not to shade the rollers. In case the axis of rotation is horizontal, a sixth roller is required (which is shown with a play) so as to prevent the drum from slipping. This roller is unnecessary with an inclined axis. Generally four rollers work over the cylindrical surface and one over the end wall. This distribution of rollers is not, however, necessary. More than one (but maximum three) rollers may be used over the end wall, the remaining rollers working over the cylindrical surface.

With a large radial force, it is preferred to use the design with four rollers working over the cylindrical surface, and with a large axial force the design with three rollers working over the end wall. The above numbers of rollers are justified for the case of a force closure of a loop, that is with an inclined axis of rotation. If a constant direction of load on the roller is not ensured, additional rollers should be installed for kinematic closure of the loop. Unfortunately, each new roller gives a redundant constraint. Therefore, in making a design one should try to minimize the number of additional rollers.

With a large length of a roller (see Fig. 6.35) it should be regarded as the second class pair $II_2$. To obtain five restraints, either a roller with a vertical axis may be used (see Fig. 6.34), or a flange may be provided on one of the rollers (see Fig. 6.35). In case both rollers are flanged, the axial play may be adjusted by axially displacing one of the rollers.

It is obvious that the roller surface should not necessarily be cylindrical all way round, and in the majority of cases only a part of the surface may be made cylindrical so that the roller is made in the form of a railway half-wheel. It is certain that two wheels are better made flangeless, and the flanges should be made on wheels of different rollers.

With a large mass of a drum supported by four rollers it is advisable to make the rollers with a larger generatrix length, and the contact is regarded as the pair $II_2$. Two ways are open here for obtaining self-alignment. Each pair of rollers (Fig. 6.36*a*) may be installed on a common swinging frame which is supported by the spherical pair $III'_2$, and the frame is prevented from "tilting" by connecting it to a fixed member by means of the arm $III'_4III'_4$. This arm transmits only incidental forces so that the load on it is very small.

The mobility of the mechanism consists of the main mobility, slippage of the four load-bearing rollers and one thrust roller, and rotation of two arms about their axes. In total, $w = 8$. The self-alignment in this mechanism is the same as in the transmission with an intermediate gear on the spherical support (see Section 4.5).

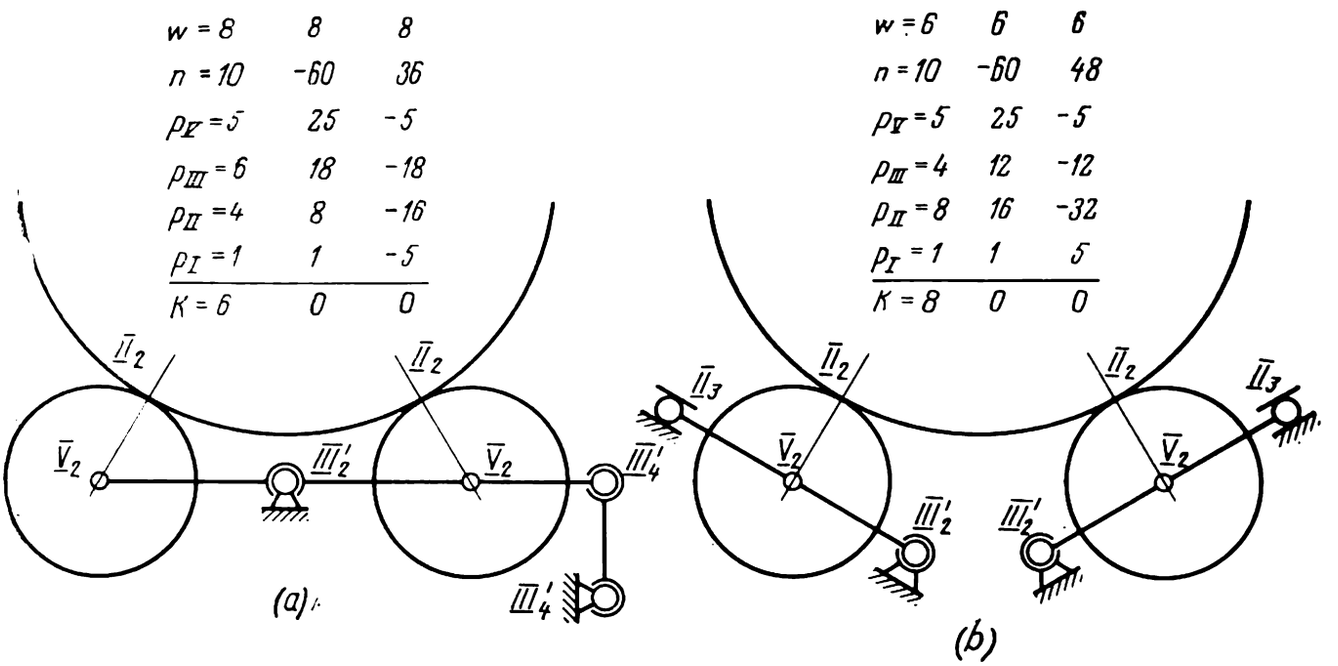


Fig. 6.36. Pair of rollers of a four-roller support
(*a*) rollers interconnected by a common frame; (*b*) independently installed rollers

The design of Fig. 6.36*a* is the most simple, but it is deficient in that the movable frame transmits a very large bending moment in the section over the spherical pair $III'_2$.

Another way for obtaining self-alignment is to impart to each roller an angular mobility about an axis extending perpendicularly to the line of contact and in parallel to a tangent plane (Fig. 6.36*b*). The design is more complicated in this case, but it is free from the disadvantage of the former design.†

At present rotary kilns 180-200 m long, 7 m in diameter and of a mass up to 6 000 tons are designed. They must be supported by 14 rollers with a generatrix length of 700 to 800 mm, and the load on each roller as great as 500 tons.

Statically indeterminate kilns are deformed during rotation, which causes a premature failure of lining and results in enormous cost of repair.

It should be reminded that with four supporting rollers load is distributed in a statically determinate manner between them. With a greater number of rollers, four groups should be provided, and load should be uniformly distributed within each group by means of equalizing mechanisms.

Let us discuss a mechanical equalizing device for a group of four rollers. When the load on the roller is 500 tons and the distance between the rollers is up to 30 m, it is not possible to use balance

beams, as is the case with locomotives. In order to reduce forces in the equalizing mechanism, it is preferably coupled to the roller frames by means of linkage transmissions (Fig. 6.37). In this manner a force of 25 tons may be obtained rather than 500 tons, that is there is the same order of force as in locomotives.

The mobility of the linkage consists of rotation of the roller, lifting and self-alignment along the line of contact, that is $w = 3$.

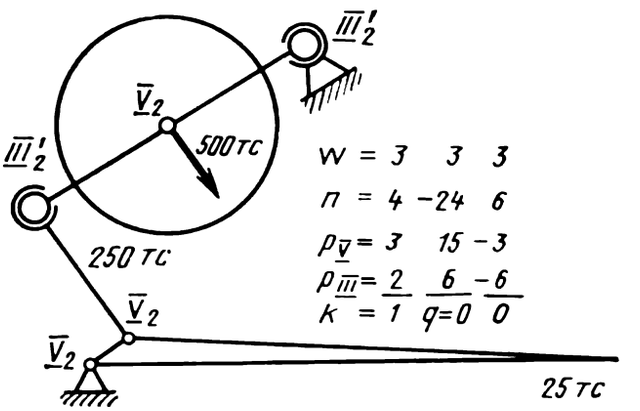


Fig. 6.37. Linkage coupling the roller to the equalizing mechanism

The classes of pairs necessary to eliminate redundant constraints are shown in Fig. 6.37.

An equalizing linkage for four rollers is shown in Fig. 6.38*a*, *b*, *c*, *d* (four modifications). The total number of rollers of the kiln here is $4 \times 4 = 16$. The condition for the modification *a* is that horizontal tilting forces should not act on the roller foundation. For that purpose, forces are transmitted by means of two rods with equal loads: one rod is tensioned and the other (tubular) rod is compressed.

In case this condition is not fulfilled, the mechanism proves much simpler (Fig. 6.38*b*) and there is no compressed rod.

In case the equalizing mechanism is made in the form of struts (Fig. 6.38*c*), it is somewhat more complicated compared to that shown in Fig. 6.38*b*, and forces are greater. Therefore, it is advisable to use it only for applications where the load on each bearing is equalized individually.

The equalizing mechanism may be substantially simplified if the transmission levers (see Fig. 6.37) are alternately made in the form of levers of the first and second order (Fig. 6.38*d*). This design is preferred only in case where the load is individually equalized for each bearing. Then, the vertical rods of bearings of one roller are arranged close to one another so that quadrangular intermediate members are compactly arranged.

In order to use the structural formula for the planar design in Fig. 6.38, the angle levers are turned through 90° and brought into

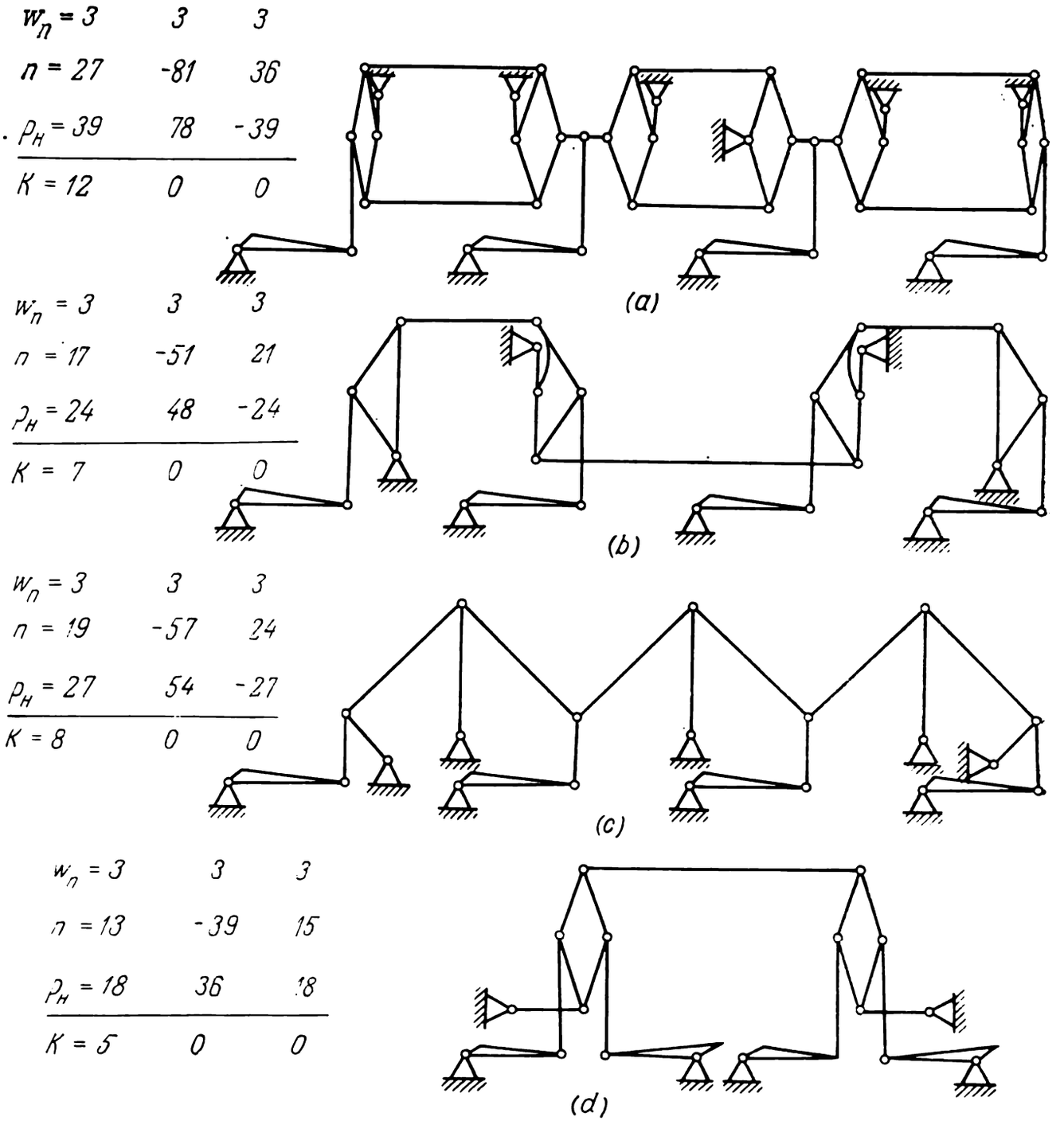


Fig. 6.38. Equalizing mechanisms
(*a*) linkage with elimination of forces tilting the foundation; (*b*) linkage with tilting forces; (*c*) strut-type; (*d*) with transmission levers of the first and second order (alternating)

the plane of the drawing. The mobility of the equalizing mechanism between the four rollers is $w = 4 - 1 = 3$. There are no redundant constraints in all four designs *a*, *b*, *c* and *d*. In choosing the design, it should be borne in mind that the horizontal force is transmitted only to the supports of the end rollers. In addition, the value of

this force should be taken into account, which is about 8 tons with the dimensions shown in Fig. 6.38 and with a load on the roller of 500 tons, and also that this force is applied at a very low level in the design of Fig. 6.38*b* and *d* so that the moment tilting the end support is very small.

The equalizing device may also be made in the form of a hydraulic device. For that purpose, one hydraulic cylinder is installed under each roller; the cylinders of one group of rollers (four groups in total) should be interconnected by a common pipeline (one restraint). Losses in the pipelines will certainly influence the distribution of load among the rollers. The way of reducing such losses will be discussed below.

Let us denote: $Q$ is the load on the roller; $V$ is the roller velocity along the normal line (piston speed), $D$ is the cylinder diameter, $p$ is the pressure, $l$ is the length of the pipeline (reduced for taking into account resistances in bends, L- and T-pieces), $d$ is the diameter of the pipeline, $\lambda$ is the coefficient of losses in the pipeline (for turbulent flow, for laminar flow the problem is discussed in [42]), $\gamma$ is the density of working fluid, $v$ is the velocity of flow in the pipeline. Then

$$Q = \frac{\pi D^2}{4} p$$

From this formula

$$D^2 = \frac{4Q}{\pi p}$$

Pressure loss in the pipeline is

$$\Delta p = \gamma \lambda \frac{l}{d} \frac{v^2}{2g}$$

By substitution of the value of $v$ from the continuity equation $\frac{v}{V} = \left(\frac{D}{d}\right)^2$, we obtain

$$\Delta p = \frac{\lambda}{2g} \gamma \frac{l}{d^5} V^2 D^4$$

By substitution here of the above value of $D$ and determining $\frac{\Delta p}{p}$, we obtain

$$\frac{\Delta p}{p} = \frac{8\lambda}{\pi^2 g} l V^2 Q^2 \frac{\gamma}{d^5 p^3} \qquad (6.12)$$

This relationship characterizes non-uniformity of load distribution among rollers and depends on the value of the fraction $\frac{\gamma}{d^5 p^3}$. The

diameter of the pipeline has the greatest influence namely as $d^5$ (by increasing the diameter twice, the losses may be reduced by 32 times!); the pressure is of a slightly smaller importance, it influences as $p^3$.

A noteworthy method for affecting the density $\gamma$ has been discovered by prof. G. V. Raevsky. He replaced water with air at 5 kgf/cm$^2$, then $\gamma = \gamma_0 p$, wherein $\gamma_0$ is the air density at atmospheric pressure, $\gamma_0 = \frac{1}{770}$. In this case the fraction $\frac{\gamma}{d^5 p^3} = \frac{\gamma_0}{d^5 p^2}$,

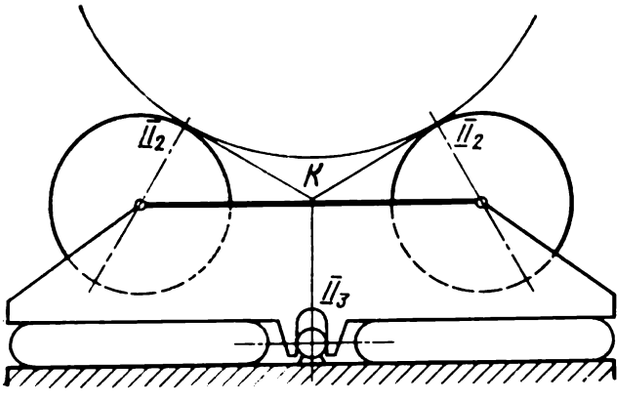


| | On i load-bearing rollers | |
|---|---|---|
| $w = 2 + i$ | $2 + i$ | $2 + i$ |
| $n = 2 + \frac{3}{2} i$ | $-12 - 9i$ | $24 + i$ |
| $p_{I} = 1 + i$ | $5 + 5i$ | $-1 - i$ |
| $p_{II} = \frac{3}{2} i$ | $3i$ | $-6i$ |
| $p_{I} = 5$ | $5$ | $-25$ |
| $K = 4 + i$ | $0$ | $0$ |

Fig. 6.39. Support of a pair of rollers with common frame and two air pads

that is the chosen pressure has a smaller influence as it appears in the second, rather than in the third power, in the formula. At the same time, $\gamma = \frac{1}{770} \cdot 5 = \frac{1}{154}$, that is the advantage of the use of air compared to water is represented by the factor of 154. To avoid leakage and friction in piston rings, rubber pads can be used to replace hydraulic cylinders in this design. Thus, the design of supports of rotary kilns in the form of air pads has been developed, which proved very good. Therefore, we will discuss below the designs of supports for rotary kilns with an equalizing mechanism based on air pads.

In such cases both the design with a common frame for a pair of rollers (Fig. 6.39) and the design with individual frames may be used. With a common frame, the self-alignment is achieved in the

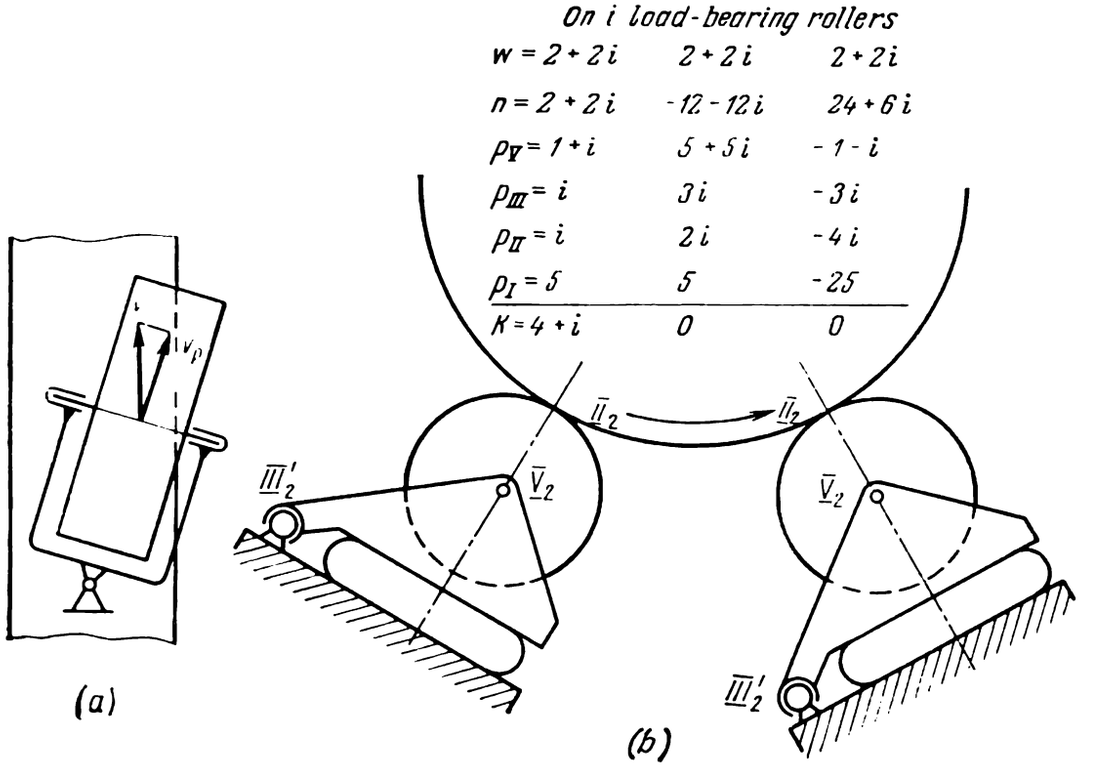


Fig. 6.40. Individual supports of a pair of rollers
(*a*) view of the roller from bottom; (*b*) cross-sectional view

same manner as for the case of the intermediate gear on the spherical support (see Fig. 4.16). The frame is supported by two pads connected to different groups of pipelines so as to avoid tilting. The frame is coupled to a fixed member by means of the pair $II_3$, rather than to $III'_2$ (see Fig. 6.36*a*). This makes it possible to eliminate a large bending moment at this point. More exactly, the pair $II_3$ should be replaced by a kinematic coupling of the pairs $III'_2$ and $IV_2$ owing to large forces.

The position of the pair $II_3$ should comply with the following two requirements:

for durable operation the pads should be only compressed without shear. For that purpose, the pair $II_3$ should be disposed in the middle plane of the pads;

friction of the rollers should not tilt the frame. For that purpose, the pair $II_3$ should be disposed at a point of intersection of common tangent lines of the drum and rollers.

The first condition is more important. The friction of rollers in case rolling-contact bearings are used is small so that tilting is readily avoided by feeding different pressures into the right-hand and left-hand pads. In addition, the pads can be installed with different

lengths of arms taking into account the constant direction of the kiln rotation. Redundant constraints for this system may be determined by the structural formula (1.1) for the whole kiln with $i$ load-bearing rollers.

The mobility consists of the main mobility and slip of the thrust roller and of the $i$ load-bearing rollers, that is $w = 2 + i$. The numbers of movable members and fifth and second class pairs are shown in Fig. 6.39. The number of the first class pairs is one contact of the thrust roller and four groups of the pads united into four systems. There are no redundant constraints.

With the rollers installed on individual frames, the frame may be coupled to a fixed member by means of the spherical pair $III_2'$ (Fig. 6.40*a*). It is only necessary that the frame should be arranged in the direction of rotation. The speeds of the yoke $v$ and roller $v_p$ for this design are given in Fig. 6.40*a* showing the bottom view of the drum. The axial component of the friction force will align the roller. This design of rollers has been long used in furniture legs. In this design aligning is added to the mobility of each roller through slippage.

A pair of load-bearing rollers with an equalizing device based on air pads is shown in Fig. 6.40*b*. The spherical pairs $III_2'$ are arranged in the middle plane of the air pads so as to provide best conditions for their operation. The second condition becomes senseless in this case since with such a mechanism the kiln can only rotate in one direction. There are no redundant constraints as calculated in the table of the figure.

This design is deficient in that deformations of the pads during lifting of the roller are different; each deformation is proportional to the distance to the spherical pair $III_2'$, and varies very strongly. This will, of course, affect the service life of the pads.

This disadvantage is eliminated in the design of Fig. 6.41. The spherical pair is replaced here by three arms having spherical heads which impose the same number of restraints. In the projection to a transverse plane the arms extend in parallel so that during lifting the frame performs a linear movement, and deformations of all pads are identical. In the projection to a horizontal plane or a plane extending in parallel with the air pad, the arms intersect one another at centres of instant rotation $P_1$ and $P_2$ so as to ensure alignment of the rollers. The arms enable rotation of the frame also about the axis running in parallel with the air pad which is necessary to obtain a constant load along the roller contact line.

Each load-bearing roller here has the following mobilities: slippa-

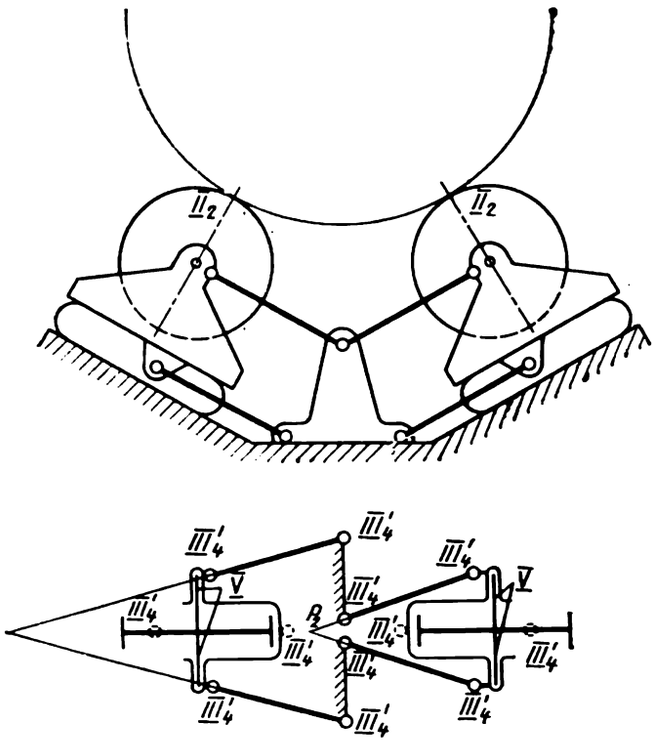

| | | |
|---|---|---|
| $w = 2 + 5i$ | $2 + 5i$ | $2 + 5i$ |
| $n = 2 + 5i$ | $-12 - 30i$ | $24 + 18i$ |
| $p_V = 1 + i$ | $5 + 5i$ | $-1 - i$ |
| $p_{III} = 6i$ | $18i$ | $-18i$ |
| $p_{II} = i$ | $2i$ | $-4i$ |
| $p_I = 5$ | $5$ | $25i$ |
| $K = 4 + 3i$ | $0$ | $0$ |

Fig. 6.41. Rollers supported with uniform deformation of air pads

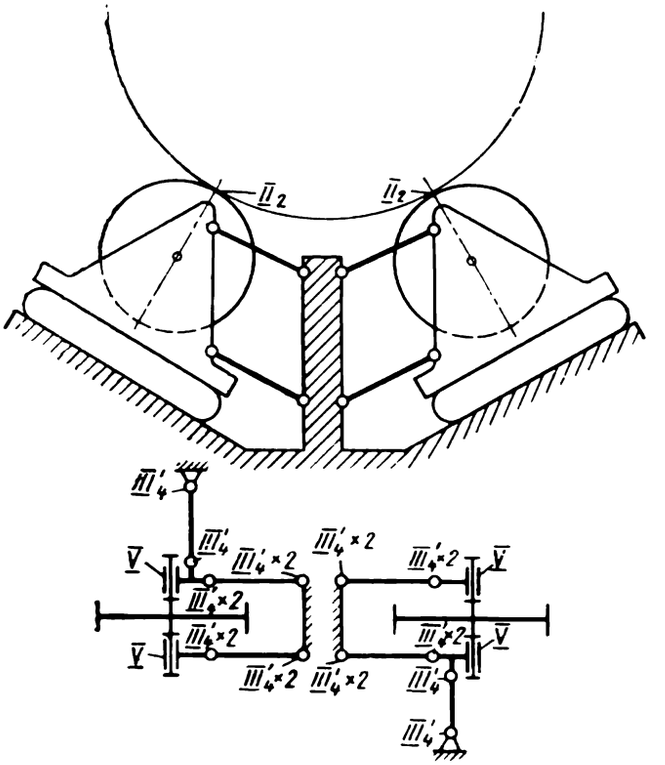

| | | |
|---|---|---|
| $w = 2 + 6i$ | $2 + 6i$ | $2 + 6i$ |
| $n = 2 + 8i$ | $-12 - 48i$ | $24 + 30i$ |
| $p_V = 1 + 2i$ | $5 + 10i$ | $-1 - 2i$ |
| $p_{III} = 10i$ | $30i$ | $-30i$ |
| $p_{II} = i$ | $2i$ | $-4i$ |
| $p_I = 5$ | $5$ | $-25$ |
| $K = 4 + 5i$ | $0$ | $0$ |

Fig. 6.42. Rollers supported by four-row conical bearings

ge, alignment, and rotation of the three arms, that is 5. In total, taking into account the main mobility and slippage of the thrust roller, $w = 2 + 5i$.

The number of the first class pairs is again five: the contact of the thrust roller and four restraints provided by the four groups of air pads.

There are no redundant constraints as calculated in Fig. 6.41.

This design is intended for one direction of rotation. But the support ends of the arms may be arranged along one straight line. Then a mere re-arrangement of the arms enables the change for the reversed

rotation of the kiln. This is the advantage of this design, because it enables the use of both sides of teeth of the drive after their wear.

Owing to enormous loads in rotary kilns, rollers cannot be journalled in spherical bearings (bearings of appropriate size are not commercially available). Thus, the rollers are journalled in conical four-row bearings (type 77 000) each forming the fifth class pair. Consequently redundant constraints remain in the coupling between the roller and its frame, which may be avoided by dispensing with the roller frame and by supporting each roller by means of its individual system of air pads (Fig. 6.42). It is obvious that the pads should be arranged symmetrically with respect to the middle plane of the bearing. Then each bearing should be coupled by means of two parallel arms. Now the roller moves along the line and it cannot align itself. Therefore the roller should be fixed with one more, axial, arm.

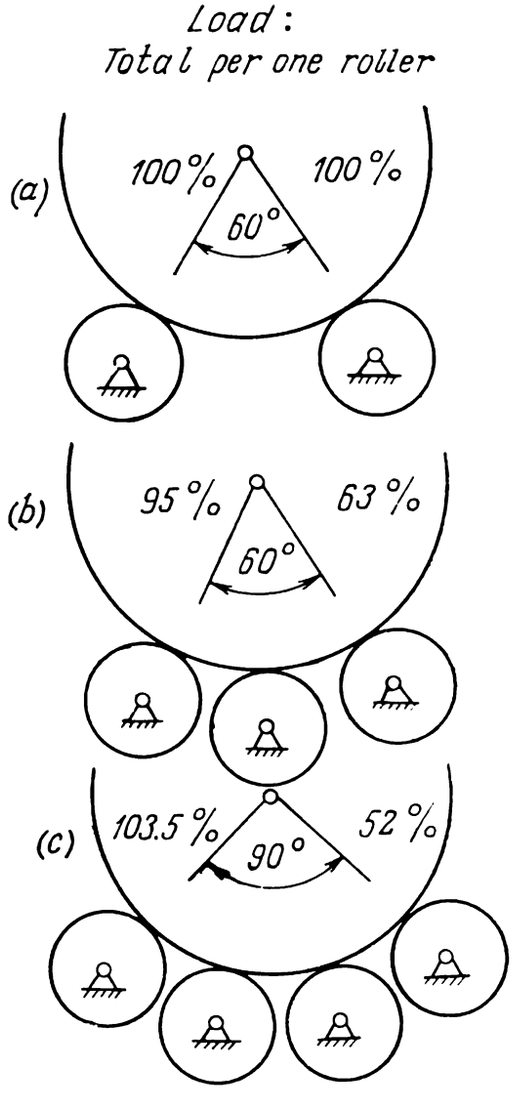


Fig. 6.43. Roller supports
(a) two rollers; (b) three rollers; (c) four rollers

At present two rollers are installed in each yoke. For rigid supports this was due to difficulties in ensuring uniform distribution of the load among several rollers. With the advent of the air pads these difficulties were eliminated. With two rollers a bearing of the largest possible diameter is to be used, and its rating life proves inadequate. The bearings frequently fail. Therefore, with several rollers the life of the bearings may be substantially prolonged (Fig. 6.43). The full load will not change substantially. Assuming this load corresponding to 100% for two rollers with the angle of camber 60°, the load will be 95% for three rollers with the same angle of camber and 103.5% for four rollers with the angle of camber 90°. The full load increase is 3.5%, and the load on each roller is only 52% of the load on one roller in the two-roller system.

## 6.11. Choice of Design of Shoe Brakes

*Simple Brakes*

Redundant constraints are especially harmful in brakes. They produce unequal load on the brake pads (ferrodo) resulting in non-uniform wear and scorching. Their main disadvantage resides in that the redundant constraints affect the braking moment.

In case of a strong engagement of the portion of ferrodo which is close to the axis of rotation of the shoe (short arm length), a strong pressure force and a large braking moment appear, and the wheel may get jammed. On the contrary, if the portion away from the axis of rotation of the shoe is pressed stronger, the braking moment is inadequately weak.

The braking moments on the right-hand and left-hand wheels may, therefore, differ from one another. This may result in skidding of vehicle and cause a serious accident. Consequently the brakes must be adjusted. Expensive stands are used for this purpose at automobile service centres. This problem is solved at the Belorussian Automobile Works by turning the shoe pads assembled with the axle.

Besides large consumption of ferrodo, this measure cannot improve the situation even if the shoes are replaced during repair since it is not possible to turn the shoes under garage conditions.

Absence of redundant constraints is a necessary condition for good functioning of a brake which will not require frequent adjustment, but it is not a sufficient condition. A favourable application of forces is also necessary which would ensure uniform distribution of load between the shoe and drum and uniform wear of ferrodo; this can be determined by making analysis of forces. Let us take as an example the brake of the rear wheel of Moskvich and Lada cars (Fig. 6.44). There are no redundant constraints; this can be checked-up using structural formulae (table of Fig. 6.44) and mobilities in the loop (the diagram in the same figure). The shoe is subjected to the action of horizontal forces from piston $T$ and a reaction at point $C_1$, $T_2$ or $T_1$. The reaction from the drum $Q_r$ or $Q_f$ should also be horizontal as per the equilibrium conditions and be tangent to the friction circle of a radius $\rho$

$$\rho = \frac{4}{\pi} fR$$

where $R$ is the radius of the drum; $f$ is the coefficient of friction.

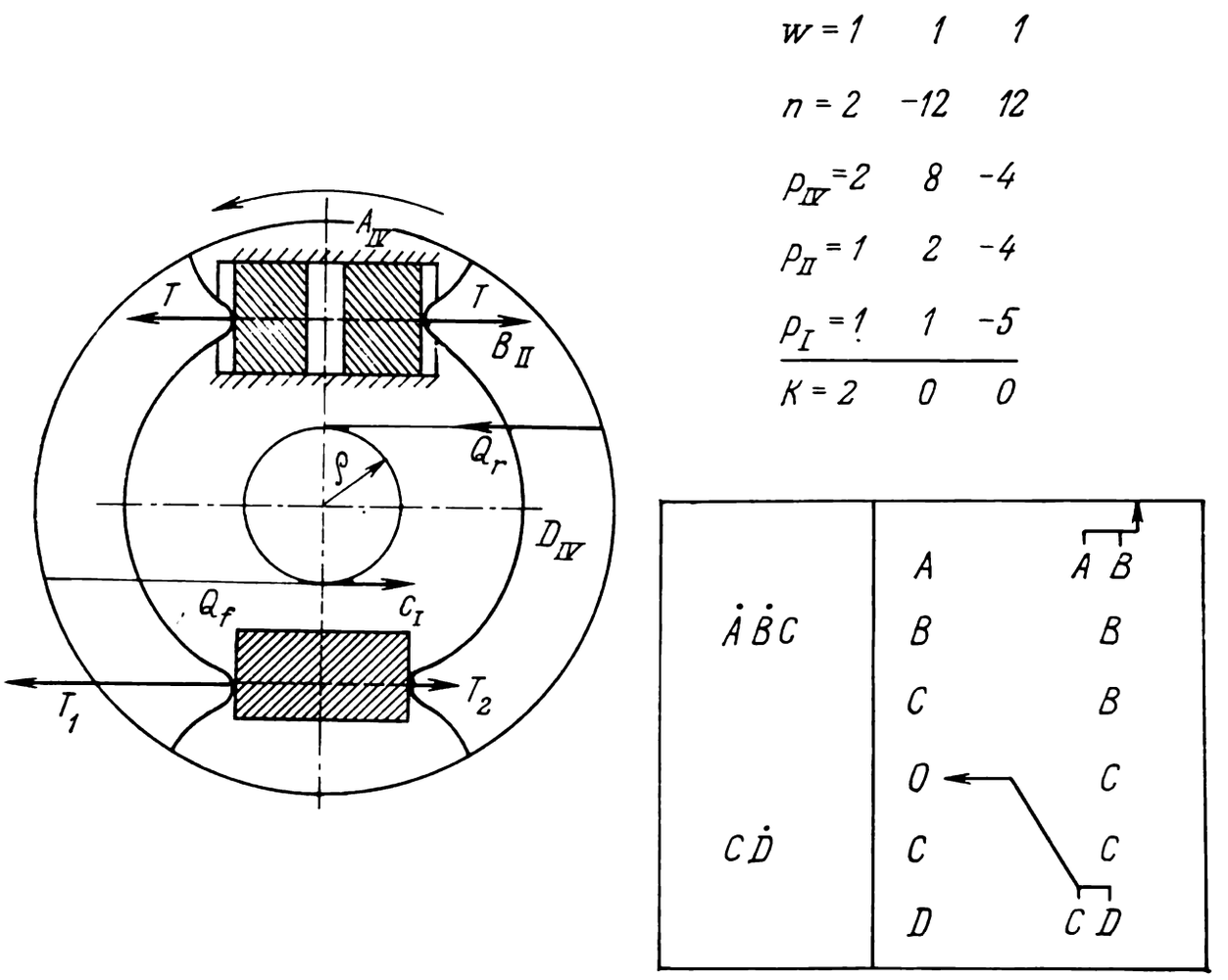


Fig. 6.44. Self-aligning brake of Moskvich and Lada cars with non-uniform shoe load

These forces can be found from the condition of equilibrium of the shoes. The resultant system of forces is very disadvantageous: forces $Q_f$ and $Q_r$ are very different, they are offset from the middle of the shoes and this produces non-uniform load on ferrodo.

To equalize the forces $Q_f$ and $Q_r$, a stepped hydraulic cylinder should be used (as it is done in certain vehicles) (see Fig. 6.45). Another method of equalizing forces is shown in Figs. 6.52 and 6.53.

For uniform wear of the shoes, the forces $Q_f$ and $Q_r$ should pass through the middle of the shoes $P_f$ and $P_r$ and be tangent to the friction circle, that is the line of action of the force pressing the shoe is preset. Use will be made of this condition in further discussion. The condition can be met by making the support surfaces of the shoes inclined (Fig. 6.45).

The inclination (direction of forces $T_1$ and $T_2$) can be determined from the condition that the forces $T_f$, $Q_f$ and $T_1$ acting on the front

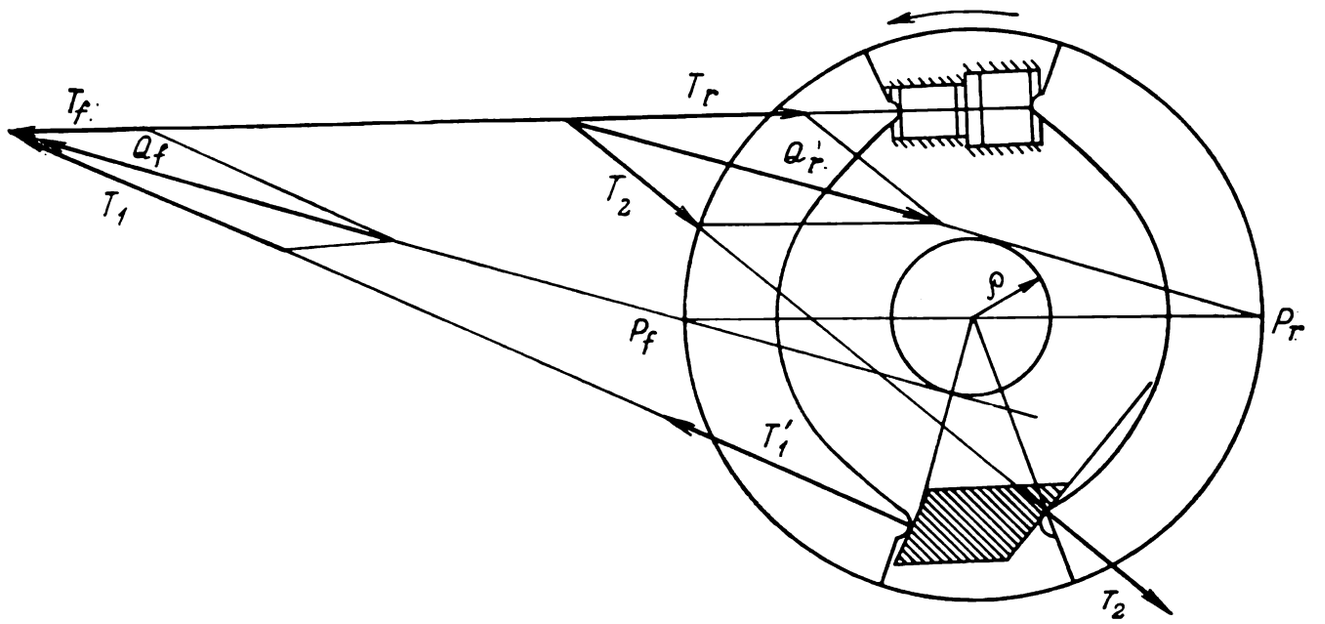


Fig. 6.45. Self-aligning brake with uniform shoe load

shoe and the forces $T_r$, $Q_r$ and $T_2$ should intersect at one point. Different inclinations are obtained for the support surface of the front and rear shoes.

Figure 6.46 shows a brake of a dumper truck 549 Belaz of 75 tons capacity with a hydraulic actuator. It has 6 redundant constraints—three for each shoe. To eliminate the redundant constraints, the shoes should be connected to the housing through the arm $III_2'V_2$, rather than the rotational pair $V_2$, as shown in Fig. 6.47. The direc-

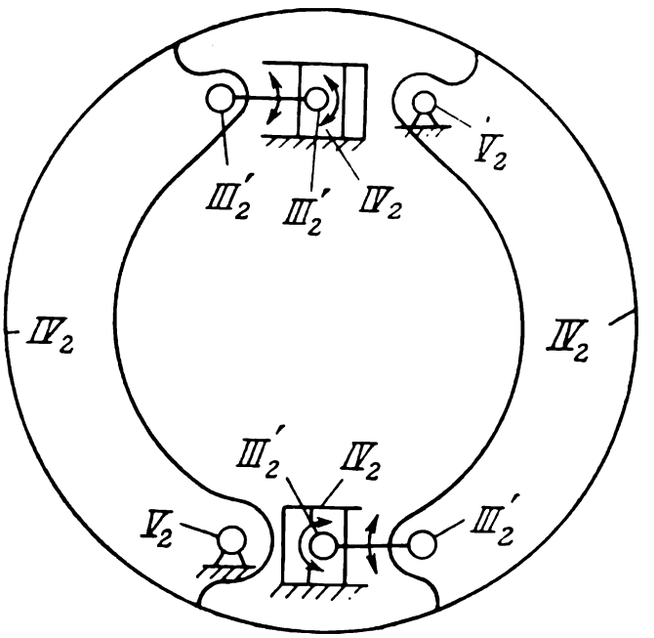


| | | | |
|---|---|---|---|
| $W = 4$ | 4 | 4 |
| $n = 6$ | -36 | 24 |
| $p_V = 2$ | 10 | -2 |
| $p_{IV} = 4$ | 16 | -8 |
| $p_{III} = 4$ | 12 | -12 |
| $K = 4$ | 6 | 6 |

Fig. 6.46. Brake of Belaz dump trucks with six redundant constraints

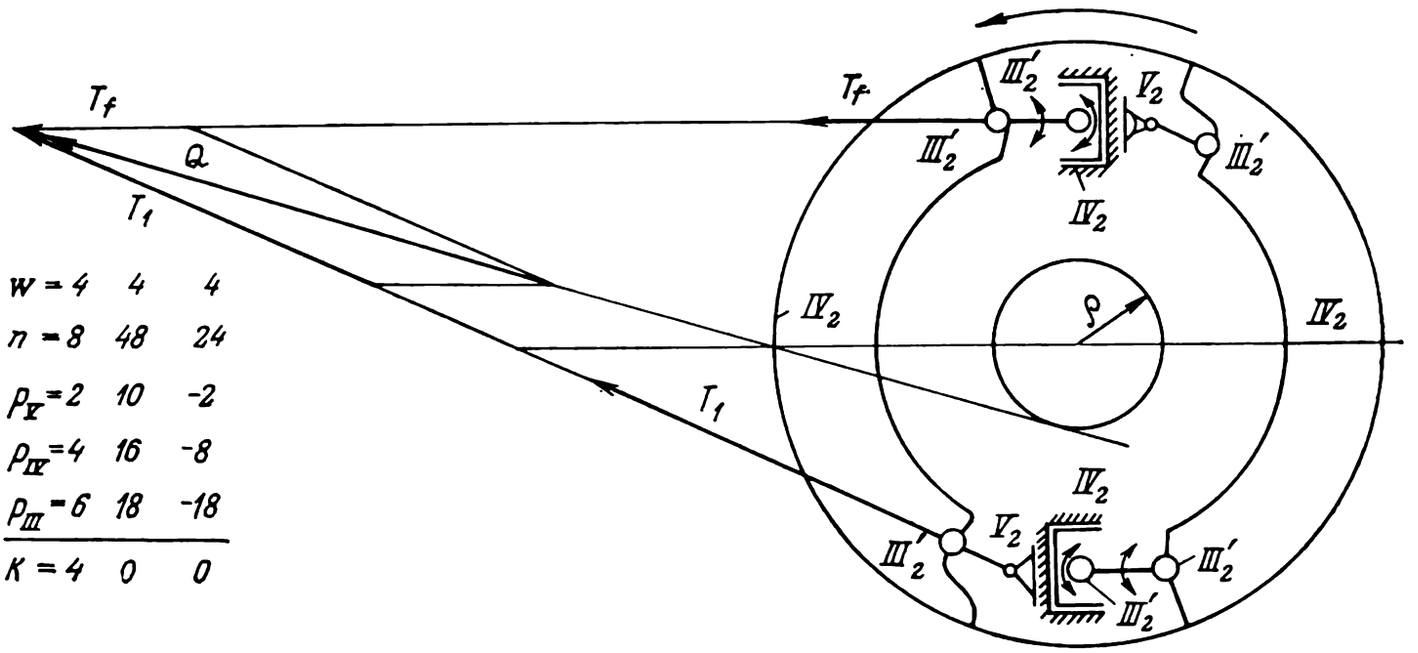


Fig. 6.47. Self-aligning brake for dump trucks

tion of the arm can be found from the condition that the forces $Q_f$, $T_f$ and $T_1$ should intersect at one point. In this case the line of action of the take-up force remains the same, that is it passes through the middle of the shoe and is tangent to the friction circle of radius ρ, which is indispensable. The hydraulic cylinder and the force $T_f$ are horizontal, but this is not necessary. The inclination of the cylinder and arm may be changed, but all the three forces should intersect at one point as shown in Fig. 6.48.

Figure 6.49 shows a brake of dumper trucks 540A of 27 tons capacity and 548 of 40 tons capacity manufactured at the Belorussian Automobile Works. Similar brakes were used in AMO-3, Mercedes Benz and Я-5 automobiles. The brake has four mobilities in the loops, which are considered pairwise, and are shown at the bottom of the Figure. The drum is regarded as a fixed member. There are two mobilities in the mechanism: the slippage of rollers. There are 9 redundant constraints.

One mobility $f_x'$ lacks in two loops $ABCD$. This causes different pressure in the front and rear shoes. Sometimes these loops lack two mobilities $f_y''$. These are conventional redundant constraints for cams with line contact. They may be readily eliminated by using grooved rollers and convex cams or convex rollers and grooved cams. Two $f_y'$ lack in the loops $DE$. These are most harmful redundant constraints since they affect the braking moment. Also lacking are two $f_x''$ and two $f_y''$—corresponding redundant constraints will cause non-uniform wear of the lining.

Let us see how the redundant constraints can be eliminated (Fig. 6.49). The lacking mobilities $f'_y$, $f''_x$ and $f''_y$ may be obtained by coupling the shoe to the lever by means of the joint $III'_2$ (Fig. 6.50). The mobility $f'_y$ is here replaced by the mobility $f''_z$ given by this joint. This is generally done in crane brakes, the pair $V_2$ is used rather than $III'_2$, that is angular redundant constraints remain.

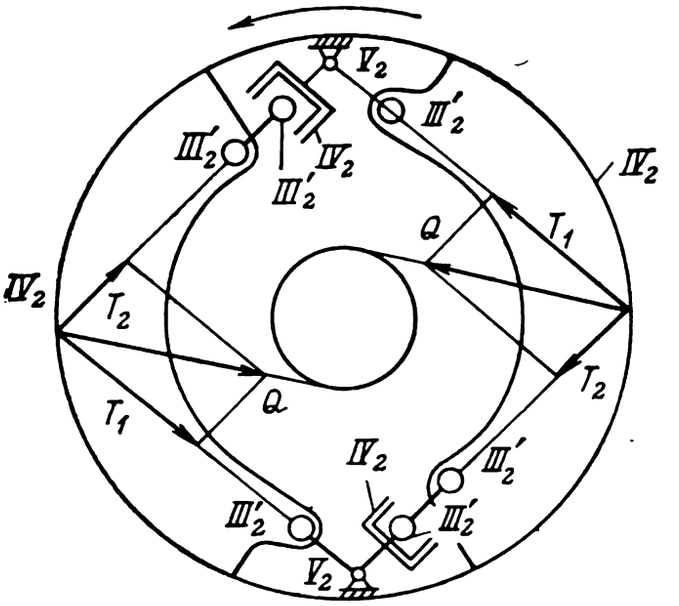


**Fig. 6.48. Self-aligning brake for dump cars with uniform shoe load**

In railway brakes, the majority of joints may be regarded as $III'_4$ owing to large plays. Therefore, there are no redundant constraints in such brakes.

To obtain the mobility $f'_y$ in vehicle brakes, the shoe should be installed on arms $III'_4$ $III'_4$ as shown in Fig. 6.51. The linear mobility $f'_y$ is replaced by the mobility $f''_z$ and the rotation of the arm. At the same time, the spherical joints of the arm give the mobilities $f''_x$ and $f''_y$. The lacking mobility $f'_x$ (Fig. 6.49) may be obtained by coupling the cam with the braking shaft by means of the translatory pair $V_3$ as shown in Fig. 6.51. Redundant constraints at the cam may be readily eliminated by using either a grooved roller with the pair $II_3$ and a convex cam or a convex roller and a grooved cam. A mechanism very similar to the brake of the ГАЗ automobile is thus obtained, but the arms are coupled to the housing at different points, rather than at one point (to ensure uniform wear of the shoes). The angle of inclination of the arm $\beta_r$ is determined by the common print of intersection of forces $T$, $Q_r$ and $T_1$ acting on the rear shoe. The forces acting on the front shoe are not shown in Fig. 6.51. This angle may be found analytically. The lengths $a$, $b$ and $c$ are given in the drawing. The angle of inclination of the force $T$ is the angle of pres-

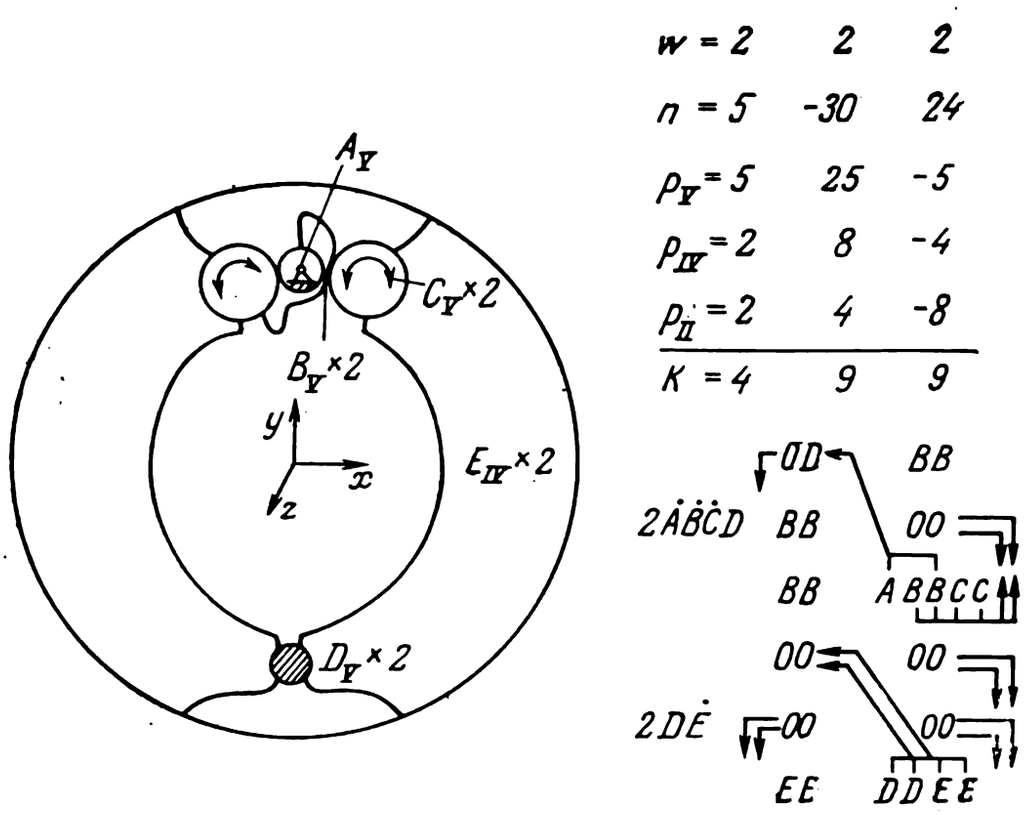


Fig. 6.49. Truck brake with nine redundant constraints

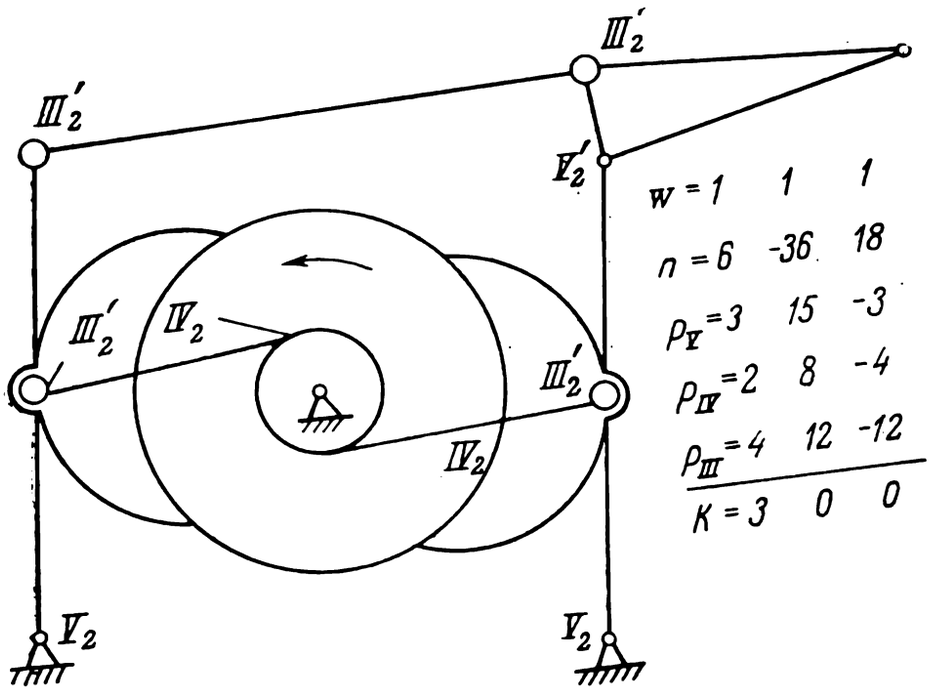


Fig. 6.50. Self-aligning truck crane brake

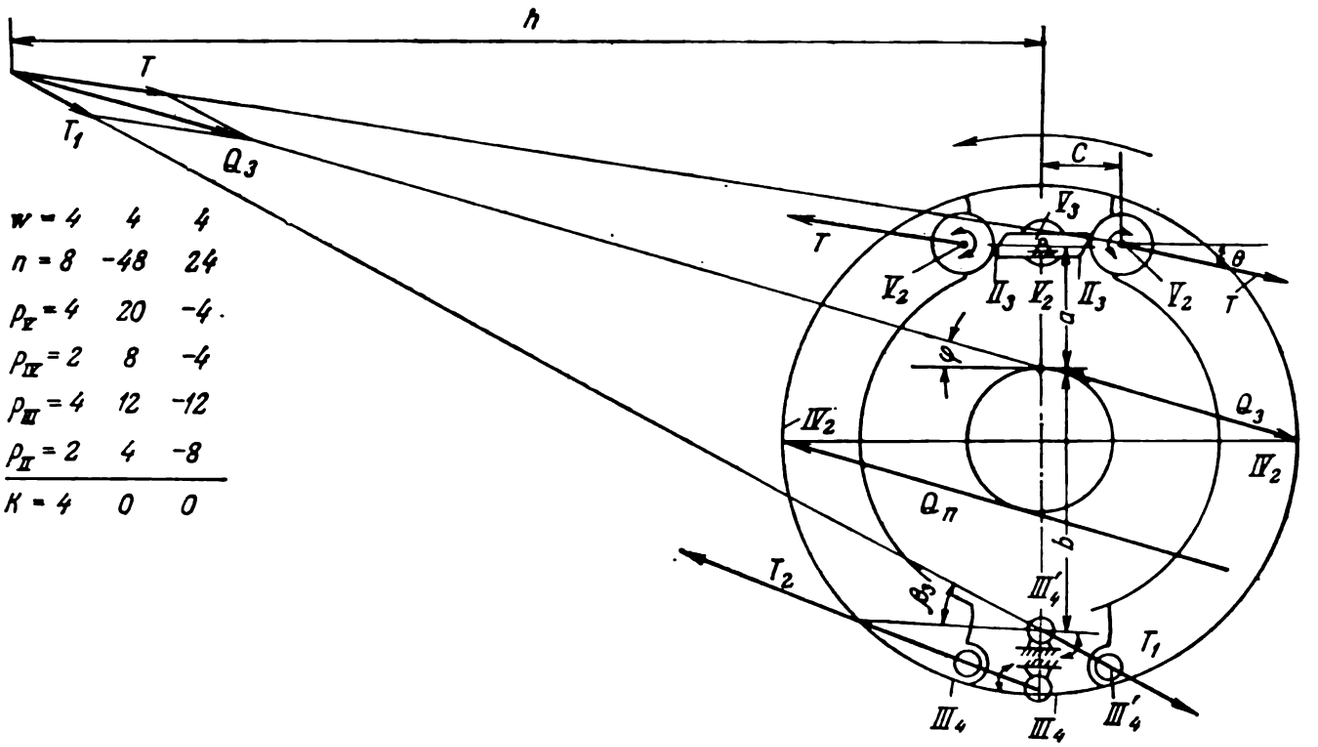


Fig. 6.51. Self-aligning motor vehicle brake with uniform though unbalanced shoe load. (Here, $Q_3$ stands for $Q_r$, $\beta_3$ for $\beta_r$, and $Q_n$ for $Q_f$)

sure of the cam θ. The angle of inclination of the force $Q_r$ is the reduced angle of friction φ

$$\operatorname{tg}\varphi = \frac{\rho}{R} = \frac{4}{\pi} f$$

The angle of inclination of the force $T_1$ (arm) is the unknown angle $\beta_r$. From the right-angle triangles, shown in Fig. 6.51 we find

$$a = h \operatorname{tg}\varphi - (h + c) \operatorname{tg}\theta = h \operatorname{tg}\varphi - h \operatorname{tg}\theta - c \operatorname{tg}\theta$$

$$a + b = h \operatorname{tg}\beta_r - (h + c) \operatorname{tg}\theta$$

By subtracting, obtain $\beta = h \operatorname{tg}\beta_r - h \operatorname{tg}\varphi$, hence

$$h = \frac{b}{\operatorname{tg}\beta_r - \operatorname{tg}\varphi}$$

Substitution in the first equation gives:

$$a = b \frac{\operatorname{tg}\varphi - \operatorname{tg}\theta}{\operatorname{tg}\beta_r - \operatorname{tg}\varphi} - c \operatorname{tg}\theta$$

$$a + c \operatorname{tg}\theta = b \frac{\operatorname{tg}\varphi - \operatorname{tg}\theta}{\operatorname{tg}\beta_r - \operatorname{tg}\varphi}$$

$$\operatorname{tg}\beta_r - \operatorname{tg}\varphi = b\frac{\operatorname{tg}\varphi - \operatorname{tg}\theta}{a + c\operatorname{tg}\theta}$$

$$\operatorname{tg}\beta_r = b\frac{\operatorname{tg}\varphi - \operatorname{tg}\theta}{a + c\operatorname{tg}\theta} + \operatorname{tg}\varphi = \operatorname{tg}\varphi\left(b\frac{1 - \dfrac{\operatorname{tg}\theta}{\operatorname{tg}\varphi}}{a + c\operatorname{tg}\theta} + 1\right)$$

The last transformation is made for making use of slide rule. This formula may be used also for finding the angle of inclination of the arm for the front shoe, with the only difference that for it $c < 0$ and the values $a$ and $b$ will be different. This formula may also be used for finding $\beta$ in Figs. 6.45 and 6.47 by substituting $\theta = 0$. It is preferred to use this formula when the point of intersection of forces lies very far from the centre of the drum.

Figure 6.51 shows a brake cam rotating clockwise. It is disadvantageous to use the cam rotating counterclockwise because the angles of inclination of the arms $\beta$ attain large values.

The mechanism shown in Fig. 6.51 has a disadvantage—forces $Q_f$ and $Q_r$ pressing the shoes differ. Correspondingly, their rates of wear differ. They may be equalized if a rotational equalizing mobility is imparted to the cam, rather than the translatory mobility (Fig. 6.52). For this purpose, the cam should be connected to the brake shaft by means of a joint. Three varying forces act on the equalizing cam: forces due to shoe rollers $T_f$ and $T_r$ and due to the drive pin $T$. By choosing the arm lengths one can obtain a desired ratio of forces $T_f$ and $T_r$ and equalize the forces $Q_f$ and $Q_r$, and hence the wear of the shoes.

In Figure 6.51 the forces pressing the shoes $Q_f$ and $Q_r$ were different. They can be equalized by using an articulated mechanism shown in Fig. 6.53. Owing to the inclination of the correcting rod $III_2'V_2$

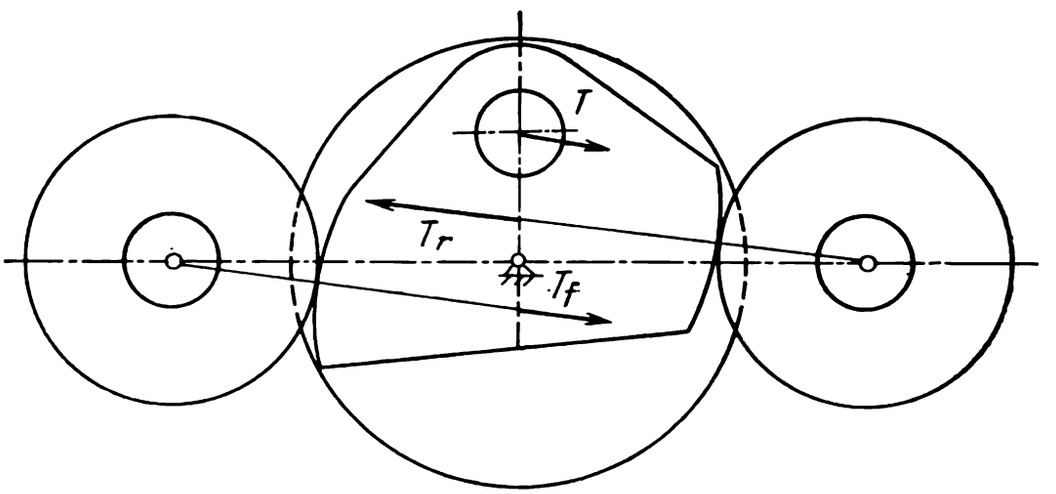


Fig. 6.52. Cam mechanism for ensuring equal shoe loads

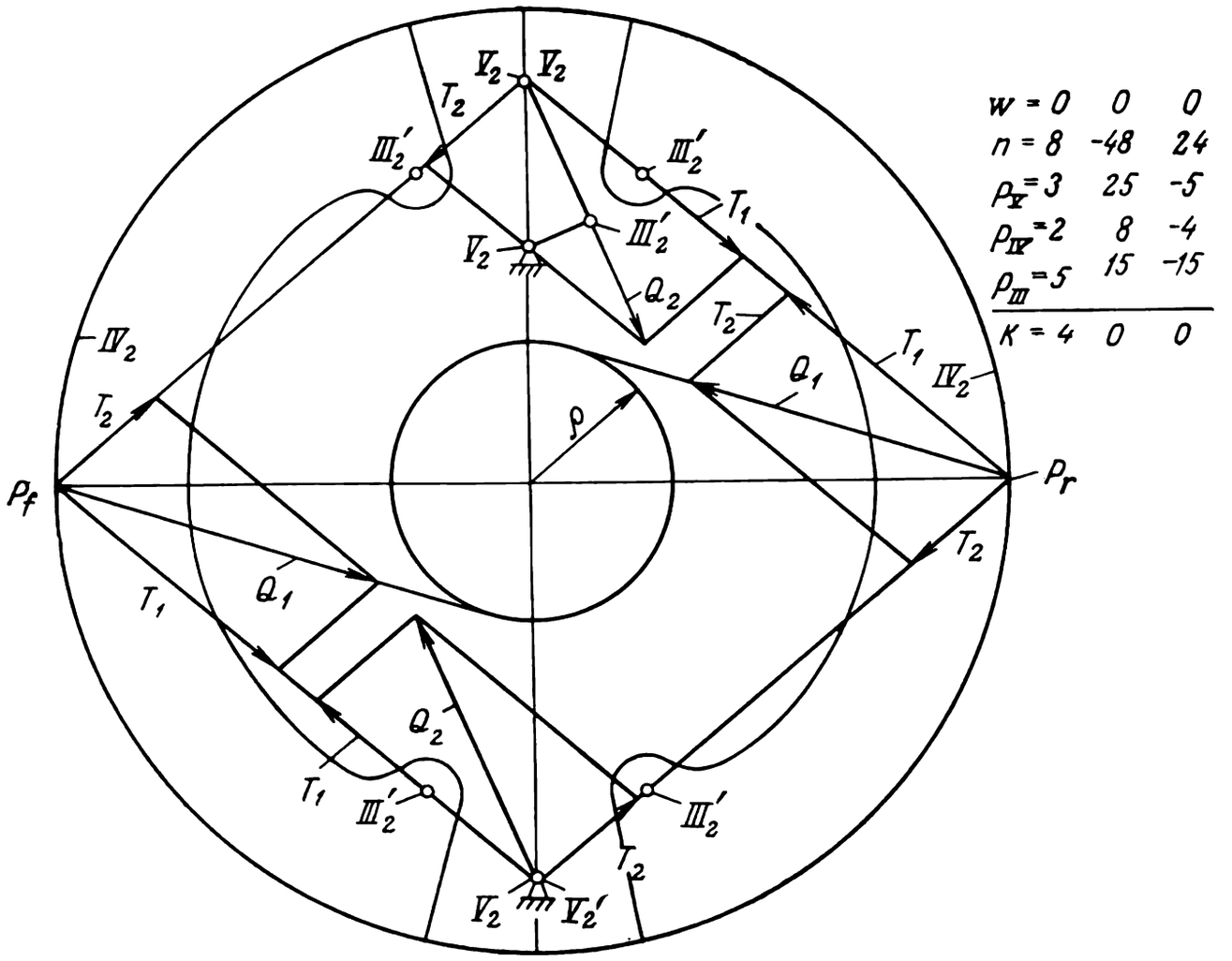


Fig. 6.53. Leverage for ensuring equal shoe loads

in this mechanism, the force $T_1$ transmitted to the rear shoe is greater than the force $T_2$ transmitted to the front shoe. By choosing this inclination, the ratio of the forces $T_1$ and $T_2$ may be adjusted, i.e. equal pressure forces for the shoes may be obtained. In Figure 6.53 the points $P_f$ and $P_r$ are taken on the periphery of the drum, but this is not necessary. It is important that they should lie on the lines of action of the pressure forces $Q$, i.e. on the straight lines tangent to the friction circles and passing through the middle of the shoes.

### *Self-Boosting Brakes*

The friction force of one shoe may be used for increasing the pressure at the other shoe in shoe brakes. This makes it possible to reduce the pressure work by 50%, though the equality of pressure forces is disturbed. Therefore, in designing the brakes it is preferred either

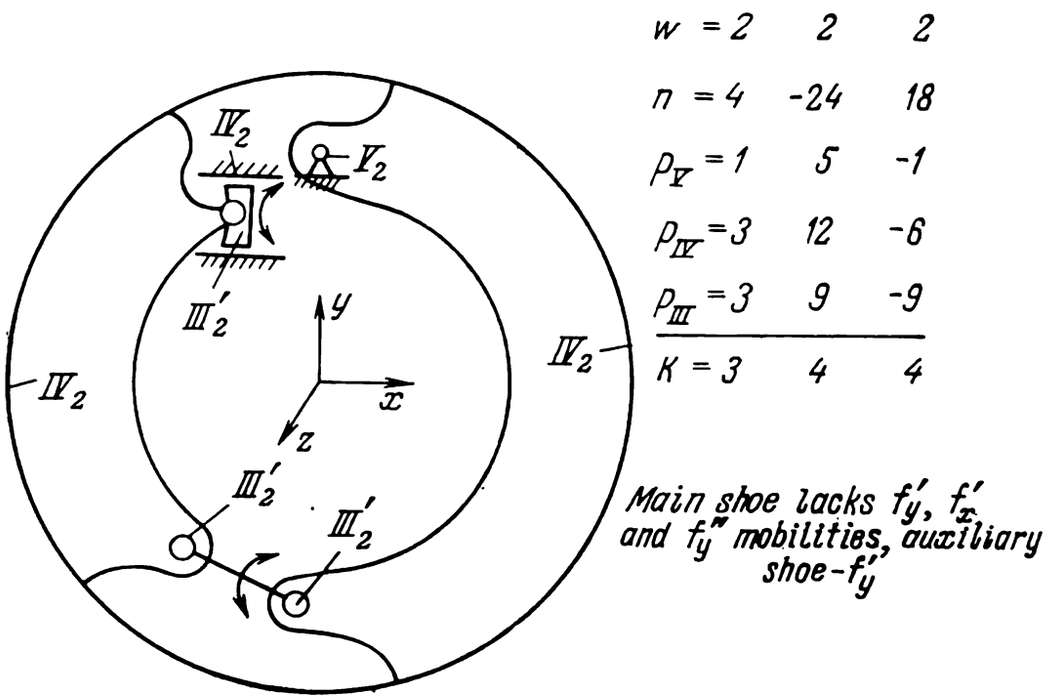


Fig. 6.54. Self-boosting aircraft brake with four redundant constraints

to envisage overturning the shoes or interchanging them, or to engage them at different angles so as to equalize specific pressures. This is known as self-boosting. The terms self-braking and servo-braking will not be used as inadequate.

Figure 6.54 shows a unidirectional aircraft brake. There are four redundant constraints which resulted in very bad operation. The main shoe lacks the mobilities $f_x'$, $f_x''$ and $f_y''$ as those shown in Figs. 6.46 and 6.49. In order to obtain these mobilities, the main shoe should be installed on the arm $III_2'V_2$ as shown in Fig. 6.55. The auxiliary shoe lacks the mobility $f_y'$. In order to obtain this mobility, the shoe should be connected to the piston by means of arm $III_2'V_2$.

In choosing the direction of the arm one should bear in mind that the direction of the force $T_2$ and arm $III_2'III_2'$ interconnecting the shoes cannot be changed as in Fig. 6.51. This direction must, therefore, be regarded as a preset direction. The uniform loading condition for the auxiliary shoe may be met only by choosing the angle of inclination of the hydraulic cylinder and force $T_1$ and for the main shoe by the angle of inclination of the support arm $V_2III_2'$. The lines of action of the forces pressing the shoes $Q_1$ and $Q_2$ should be regarded as preset lines.

The directions and values of the forces for auxiliary and main shoes are found respectively from the conditions of intersection of forces $T_1$, $Q_1$ and $T_2$ and forces $T_2$, $Q_2$ and $T_3$ at one point.

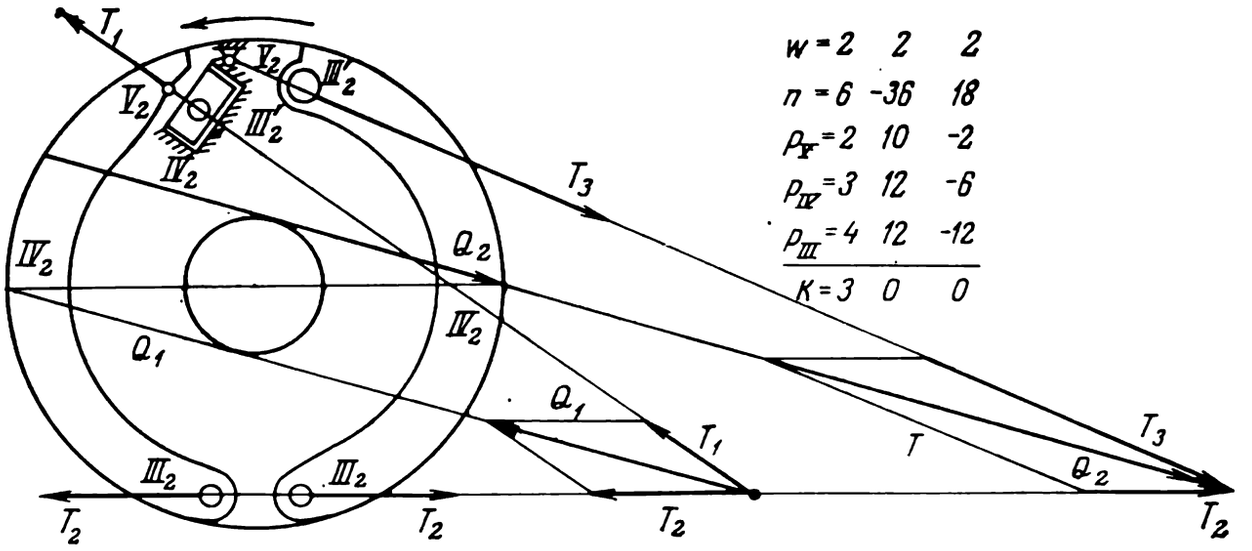


Fig. 6.55. Self-aligning aircraft brake

The brake with a mechanical drive for bi-directional rotation is shown in Fig. 6.56. The shoe stops are made in the form of pins with washers received in recesses of the shoes. This coupling is the pair $II_3$ for the main shoe which rests against the pin during braking. This coupling is the pair $I_2$ for the auxiliary shoe in which a gap remains between the pin and recess during braking. Other kinematic pairs for a rational design are shown in Fig. 6.56. On changing the direction of rotation, the main and auxiliary shoes exchange the functions. The selection of direction of arms and the study of forces made for the rotational direction shown by arrow are similar to those made in Fig. 6.55.

The forces $T_1$ produced by the actuator on shoes should be equal so that the operation of the brake remains unchanged on changing the direction of rotation. A triangular floating lever $V_2$, $I_2$, $I_2$ is used for equalizing these forces (Fig. 6.56). Another appropriate mechanism may also be used.

Four forces act on the main shoe: $T_1$ from the actuator, $T_2$ from the auxiliary shoe, minus $Q_2$ from the drum, and the unknown force $T_3$ from the stop pin. To keep the shoe in equilibrium it is necessary that the resultant force of the forces $T_2$ and $-Q_2$ should be equal, opposite to, and act along the same straight line with the resultant of the forces $T_1$ and $T_3$. This straight line passes through the point of intersection of the forces $T_2$ and $-Q_2$ and forces $T_1$ and $T_3$; this is shown by thin line in Fig. 6.56. The direction of the force $T_3$, hence the direction of the recess in the shoe can be readily determined.

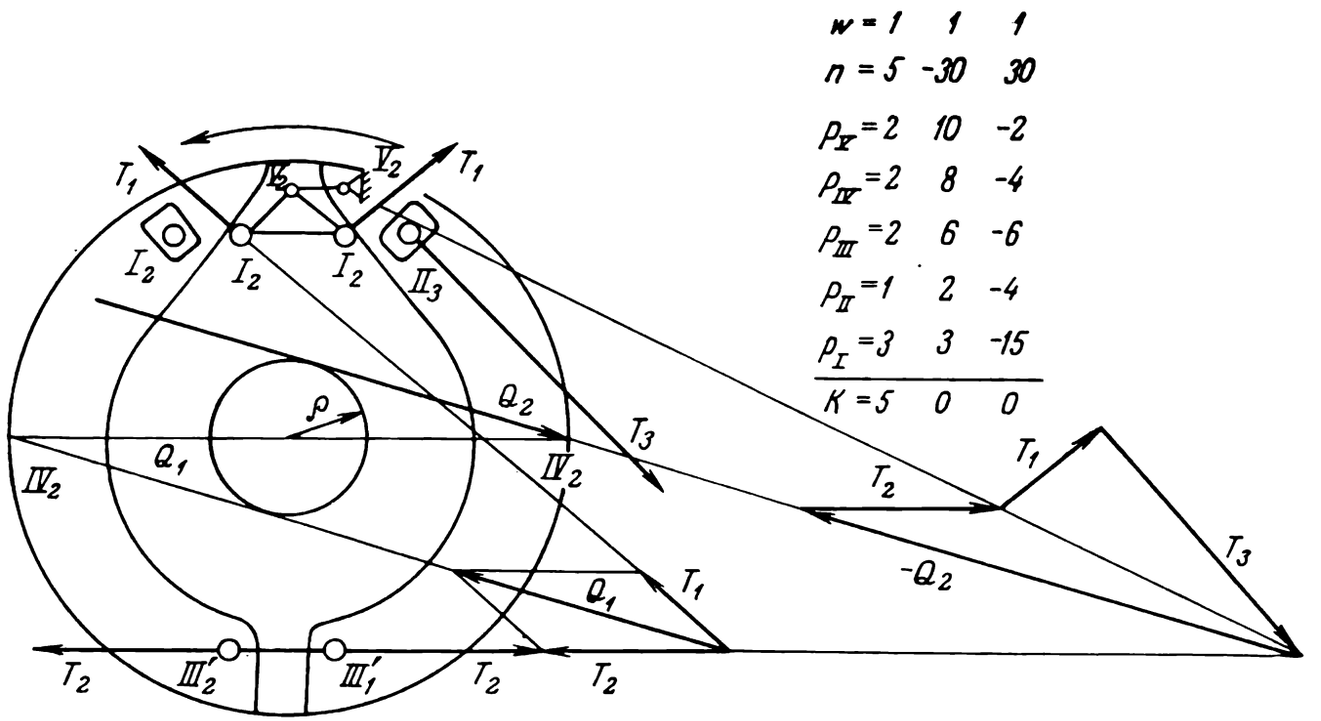


Fig. 6.56. Self-aligning self-boosting bi-directional brake with uniform shoe load

A bi-directional hydraulically actuated brake is shown in Fig. 6.57. For reverse movement, the main and auxiliary shoes are reversed. Two hydraulic actuators are therefore generally provided in a common cylinder, one of the actuators being active for each rotational direction; this is the disadvantage of the design.

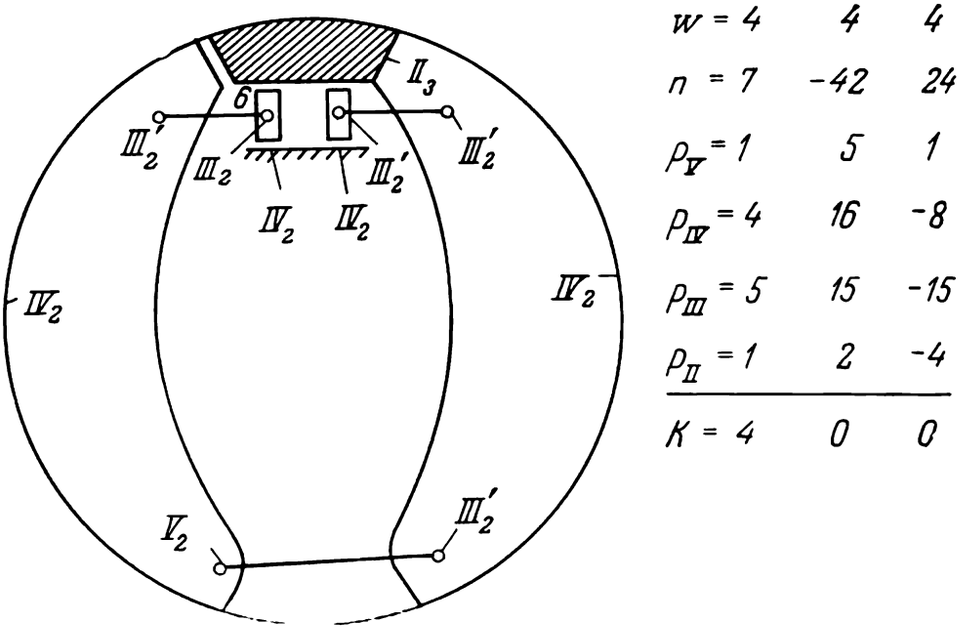


Fig. 6.57. Self-aligning self-boosting bi-directional hydraulically actuated brake

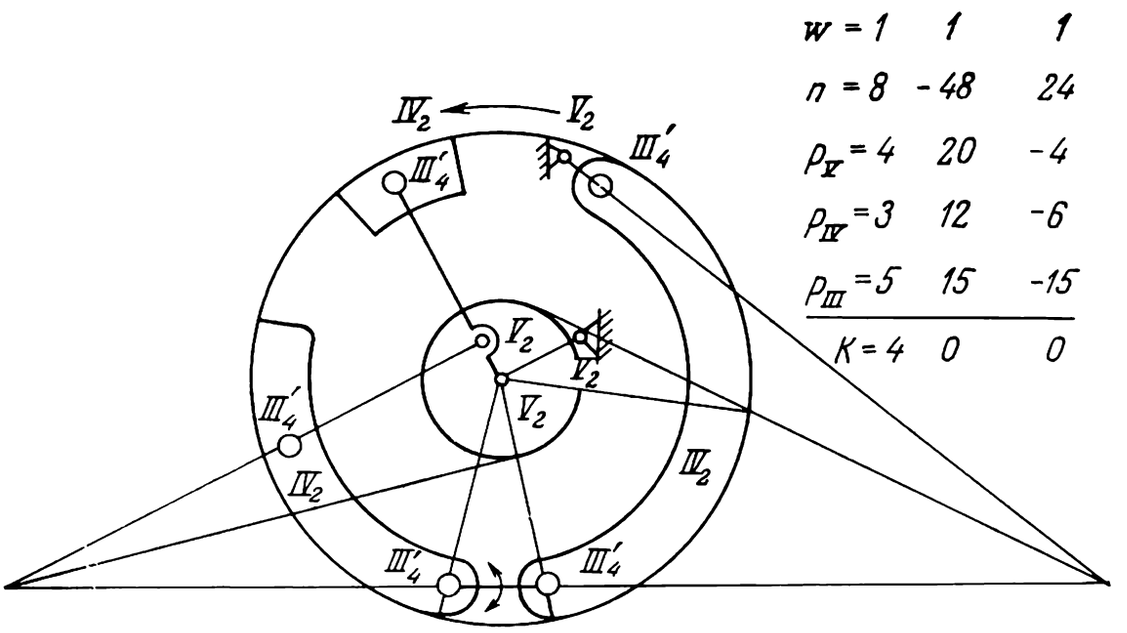


Fig. 6.58. Unidirectional self-aligning brake with enhanced self-boosting

The classes of the kinematic pairs for $q = 0$ are shown in Fig. 6.57. This design does not comply with the requirements for exerting uniform pressure on the shoes. To meet the requirements, two hydraulic cylinders should be used instead of one, having inclined them as shown in Fig. 6.55.

The self-boosting effect in the designs shown in Figs. 6.54, 6.55, 6.56 and 6.57 is insignificant. This is due to the fact that the second shoe is pressed by the friction force of the first. Much greater effect may be obtained by providing a boosting lever $V_2$, $V_2$, $III'_4$ between the shoes (Fig. 6.58). In this case the first shoe should be given a greater circumferential displacement (for a stronger pressure of the second shoe). Therefore, the centre $V_2$ of the boosting lever should coincide with the centre of the drum. This is not always possible because the axle of the wheel generally passes through this point. The mechanism shown in Fig. 6.59 is free from this disadvantage. Here the centre $III'_4$ of the first shoe moves along a circle with its centre lying at the centre of the drum (approximately) by means of two levers $III'_4V_2$ and $III'_4V_2$ and a triangular connecting rod $III'_4$, $III'_4$, $III'_4$. The lever lengths are selected in such a manner that the curve drawn by the connecting rod should be as close to a circle as possible. One of the levers (the right hand lever in Fig. 6.59) is made as a curved lever and it presses the second shoe by means of short arm $V_2III'_4$. The third (left) shoe is pressed by the right shoe by means of long rod

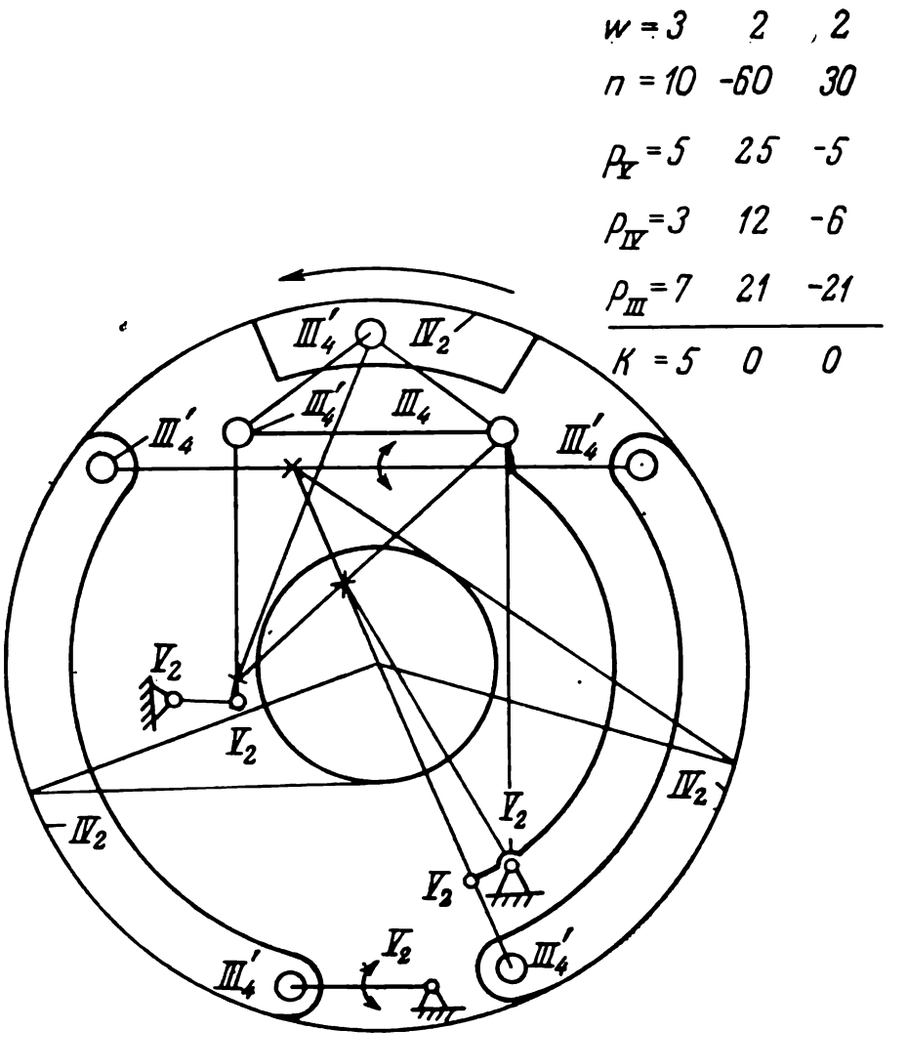


Fig. 6.59. Unidirectional self-aligning brake with enhanced self-boosting and relieved central portion, 1st version

$III'_4III_4$. In this design, the short lever $V_2V_2$ and the brake shaft extend close to the centre of the drum.

This disadvantage is eliminated in Fig. 6.60. Here the first shoe is provided with a roller which is pressed by a cam by means of a parallel crank mechanism $V_2III'_4V_2III'_4$ and two angle arms. The cam should have the circumferential profile concentrical with that of the drum. It is a complicated mechanism (13 members) but, owing to greater self-boosting, it makes it possible to get rid of a pneumatic actuator and eventual booster, and the system as a whole may prove much simpler.

The mechanisms shown in Figs. 6.58, 6.59 and 6.60 are not suitable for reverse movement. This disadvantage is eliminated in Fig. 6.61. A long transmission lever $III'_4V_2V_2$ has at its lower end two sli-

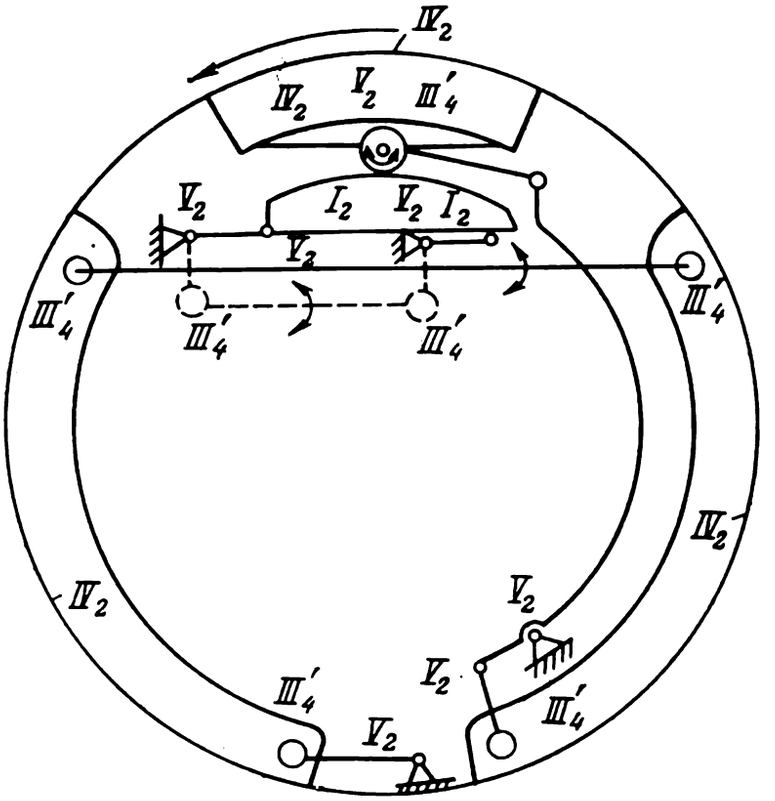


| $w = 3$ | 3 | 3 | 1 | 1 | 2 | 2 |
|---|---|---|---|---|---|---|
| $n = 13$ | -78 | 42 | -39 | 21 | -39 | 21 |
| $p_V = 8$ | 40 | -8 | 16 | -8 | 24 | 0 |
| $p_{IV} = 3$ | 12 | -6 | 6 | -3 | 6 | -3 |
| $p_{III} = 7$ | 21 | -21 | 14 | -7 | 7 | -14 |
| $p_I = 2$ | 2 | -10 | 2 | -4 | 0 | -6 |
| $K = 7$ | 0 | 0 | 0 | 0 | 0 | 0 |

Fig. 6.60. Unidirectional self-aligning brake with enhanced self-boosting and relieved central portion, 2nd version

de blocks which cause the second and third shoes to move apart during braking. The upper ends of these shoes are secured by means of the arms $III'_4$, $V_2$. It must be remembered that the upper slide block functions with its one end and the lower slide block has two effective ends $III'_2I_2$ because, in addition to the horizontal force moving the shoes apart, this slide block should also transmit a vertical force produced by the reaction due to the pressure on the first shoe.

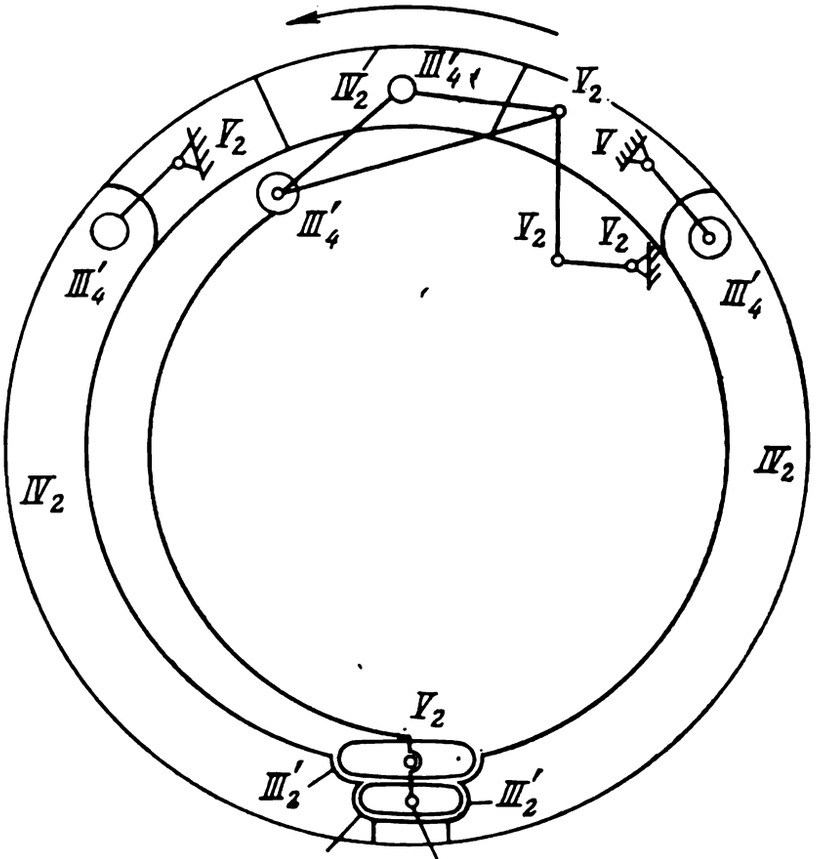


| | | | |
|---|---|---|---|
| $w = 0$ | 0 | 0 | |
| $n = 11$ | -66 | 36 | |
| $p_V = 7$ | 35 | -7 | |
| $p_{IV} = 3$ | 12 | -6 | |
| $p_{III} = 6$ | 18 | -18 | |
| $p_I = 1$ | 1 | 5 | |
| $\Sigma = 6$ | 0 | 0 | |

Fig. 6.61. Bi-directional self-aligning brake with enhanced self-boosting and relieved central portion

*Railway Brakes*

For efficient braking, the pressure of the shoes should correspond to the actual load on the wheel pair. This load varies. The front-end pairs are loaded and the rear-end pairs are relieved during braking owing to the action of the tilting moment. In addition, the loads on the wheel pair with loaded and empty car are different.

In order to eliminate the effect of the tilting moment, the brake levers should be inclined towards the centre as shown in Fig. 6.62*a* which illustrates the front-end pair. Then

$$Pl = N_f a - F_f b = N_f (a - fb)$$

Hence $N_f = \frac{Pl}{a - fb}$.

Similarly, obtain for the shoes of the rear-end wheel pair:

$$N_r = \frac{Pl}{a + fb}$$

By choosing the value of $b$ one can obtain a desired ratio of pressure forces at the shoes of the front and rear axles.

In multiple-axle rolling stock different inclinations of brake levers are taken for different wheel pairs.

In order to eliminate the effect of the loaded and empty car, the brake shoes are arranged above the wheel centre as shown in Fig. 6.62*b*. When the springs sag the shoes down, the clearance decreases, and the protrusion of the piston rod of the brake cylinder also decreases. For the Westinghouse brake, pressure in the brake cylinder increases as required. Certainly this effect cannot be obtained on applying Matrosov or Kazantsev brakes.

## 6.12. Bridges

Additional stresses appear in statically indeterminate structures of bridges due to unequal settlements of pier foundations and non-uniform heating of elements of trusses. These structures should, therefore, be permanently monitored and controlled. Consequently, it is very important to make bridges statically determinate. The bridge structure may be regarded as a mechanism with zero mobility. This enables the theory of self-alignment and redundant constraints to be applied to bridge structures. The ways of creating statically determinate structure of bridges will be discussed below. The plane diagram and a respective structural formula (1.2) will be used.

**Beam bridges.** There are no redundant constraints in a continuous beam only in case of two end supports and without intermediate piers. In case of intermediate piers the number of redundant constraints is equal to the number of intermediate piers.

It is inexpedient to cut beams at each intermediate pier as they would have a large bending moment. The design should eliminate

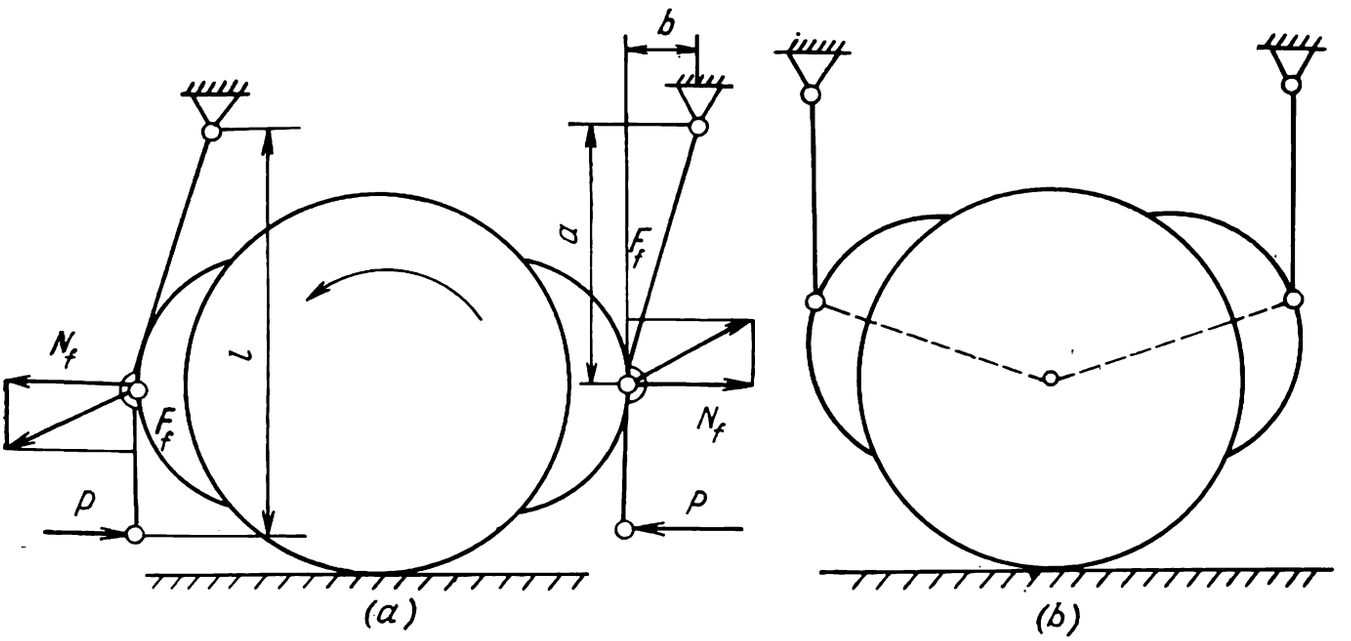


Fig. 6.62. Rail vehicle brakes:
(*a*) pressure adjusted upon redistribution of momentum forces at braking; (*b*) pressure adjusted upon car load varying

redundant constraints without increasing the design bending moment (Figs. 6.63 and 6.64). In the Herber design, joints are provided at those points at which the bending moment for a continuous beam passes through zero point. Here the number of joints is equal to the number of intermediate piers which is what is needed to eliminate the redundant constraints.

Fig. 6.63*a* and *b* show the Herber design for a three-span bridge and Fig. 6.63*c*, *d* and *e* show the designs for a five-span bridge. Ma-

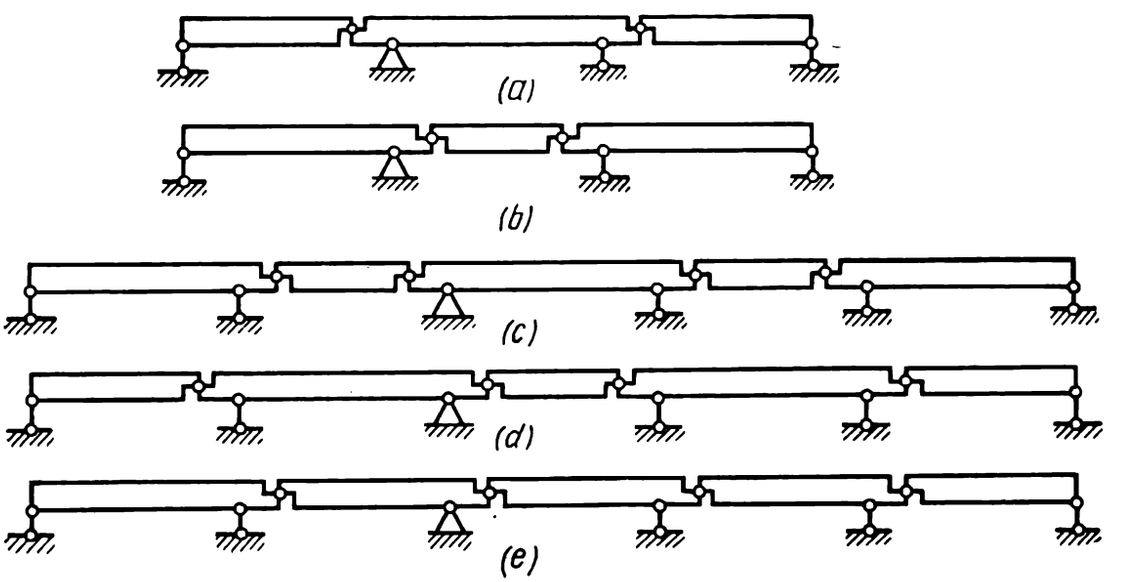


Fig. 6.63. Herber bridges

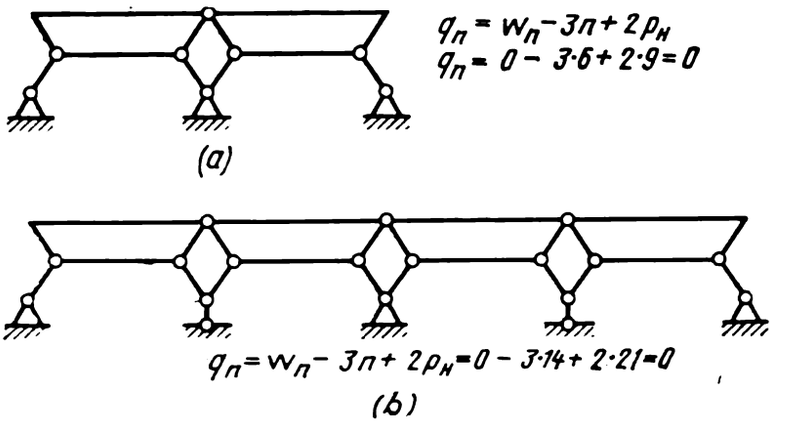


Fig. 6.64. Wichert bridges

ximum length, hence the mass of the beam for the three-span bridge in the design *b* is less than in the design *a*.

The difference is especially large in case the end spans are shorter than the middle span. Consequently, if the beams are to be transported in full length, the design *b* has a certain advantage. Comparing the designs *c*, *d* and *e* in the similar way it can be concluded that the designs *c* and *d* are of equal value, and the design *e* is more advantageous, especially with short end spans.

In the Wichert bridges, the cut beam is simply supported, but this is done at intermediate points by means of inclined struts, rather than at the ends (Fig. 6.54*a* and *b*). Owing to the inclined position of the struts, the arm lengths of forces transmitted by the struts decrease, and hence the design bending moment. The length of the Wichert beam is small compared to the Herber beam; this is important for transportation. The required height of the piers is decreased owing to inclined struts.

Fig. 6.64*a* shows the Wichert design for a two-span bridge and Fig. 6.64*b* for a four-span bridge.

Generally this design, similarly to the Herber design, may be applied to any number of spans.

The Wichert design may be regarded as an intermediate modification between beam and arch structures.

**Arch bridges.** First arch bridges were made with arches without joints and with restrained heels (Fig. 6.65*a*). In a plane system such an arch has three redundant constraints. To reduce the number of constraints, double-joint arches were used (Fig. 6.65*b*) with heel joints. One redundant constraint remains in this case.

The redundant constraints are completely eliminated in a three-joint arch (Fig. 6.65*c*) where the third joint is installed in the key.

The disadvantage of arch bridges resides in the horizontal thrust increasing the load on the foundation.

It is inexpedient to install a horizontal tie rod along the bottom because this reduces the clearance for navigation. Therefore, a design with two half-arches (made of concrete) with a top tie rod (made

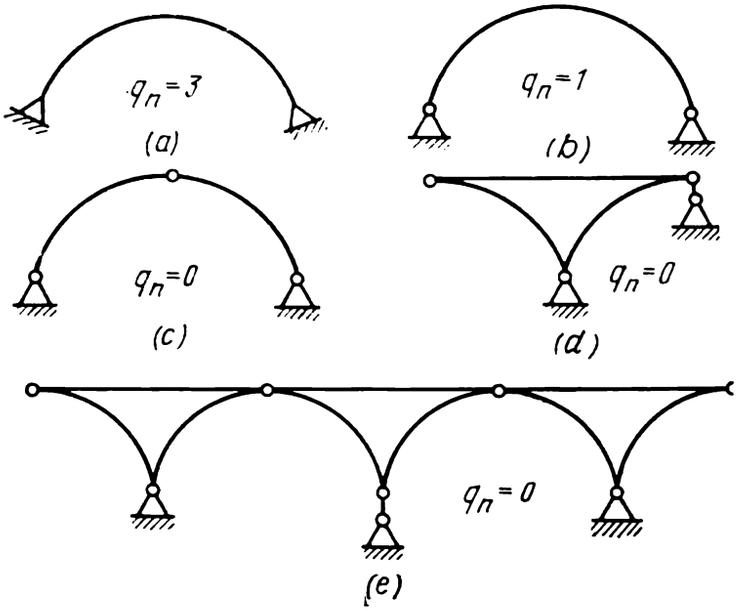


Fig. 6.65. Arch bridges

of steel bars) was suggested (Fig. 6.65*e*). Multiple-span arch bridges are constructed with such elements: Fig. 6.65*f* shows a four-span bridge with two intermediate spans twice as long as the end spans.

**Suspension bridges.** Elements of the span structure in the suspension bridges are tensioned so that they have a small mass. The elements which work in compression (which are to be designed for pitch stability and therefore are very heavy) are only pylons. Their weight causes no load in the span structure and does not affect design bending moments. The span structure is, therefore, very light, and suspension bridges may span over very large distances. Another advantage of the suspension bridges is the convenience of installation by suspending the elements of the span structure on the cables that have been tensioned.

For the sake of simplicity, only one span of the bridge will be discussed below using the plane diagram.

Two types of suspension bridges are used: those with straight cables fanning from the point of attachment to the pylon (Fig. 6.66*a* and *b*) — the so called guy-rope bridges, and bridges with catenary ropes extending between two pylons along a string polygon close to a catenary line (see Fig. 6.68*a* and *b*) — suspension cable or chain bridges.

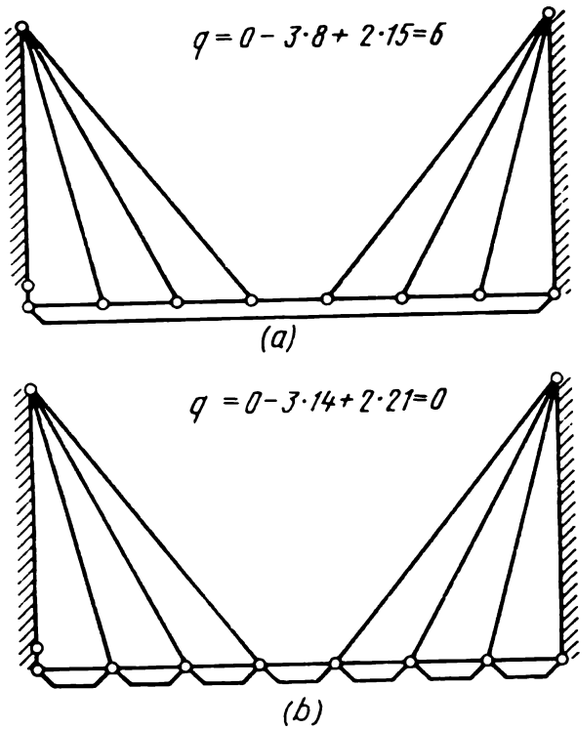


Fig. 6.66. Guy-rope bridges:
(*a*) improper design with redundant constraints; (*b*) correct design

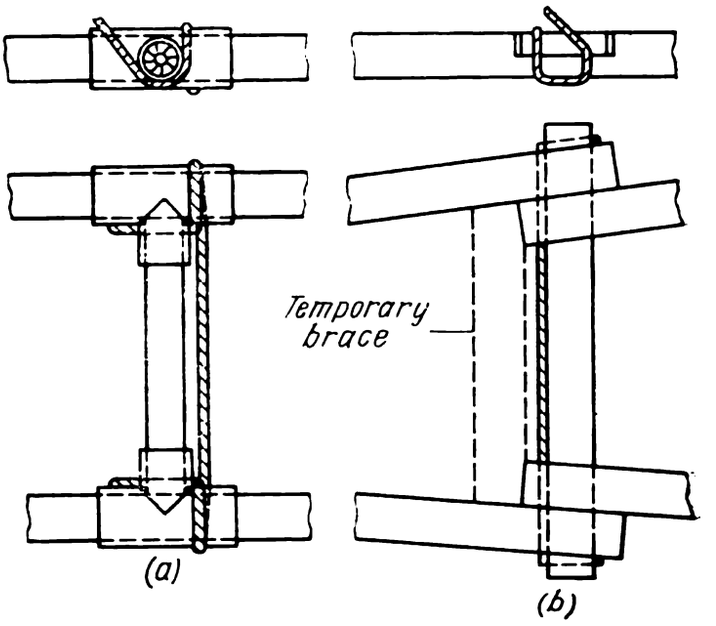


Fig. 6.67. Wooden structures for short-span pedestrian bridges:
(*a*) with welded tubular H-pieces; (*b*) with "jointer" joints

With straight cables and with the span structure made in the form of a rigid beam (Fig. 6.66*a*) the number of redundant constraints calculated by the structural formula is equal to the number of cables. This resulted in that many bridges built with this system proved unfit for use, and they had to be re-built. The redundant constrains may be eliminated by providing joints in the span beam (Fig. 6.66*b*). Here each joint eliminates one redundant constraint so that the number of joints should be equal to the number of cables. With proper execution, such a joint designed for a very small angle of rotation will not interfere with traffic movement (this is not an expansion joint). In addition, the joints reduce the design moments of the span beam so as to reduce the beam mass.

Pedestrian short-span bridges are preferably made from logs using written-off crane cables as guy ropes (Fig. 6.67*a* and *b*). The logs may be interconnected by means of *H*-pieces welded of pipes (Fig. 6.67*a*) or by simple "jointer" joints for very small spans (Fig. 6.67*b*).

In chain-type suspension bridges, in case a rigid span bridge is used (Fig. 6.68*a*). there is one redundant constraint. The distribution of load between the suspension system and the beam is statically

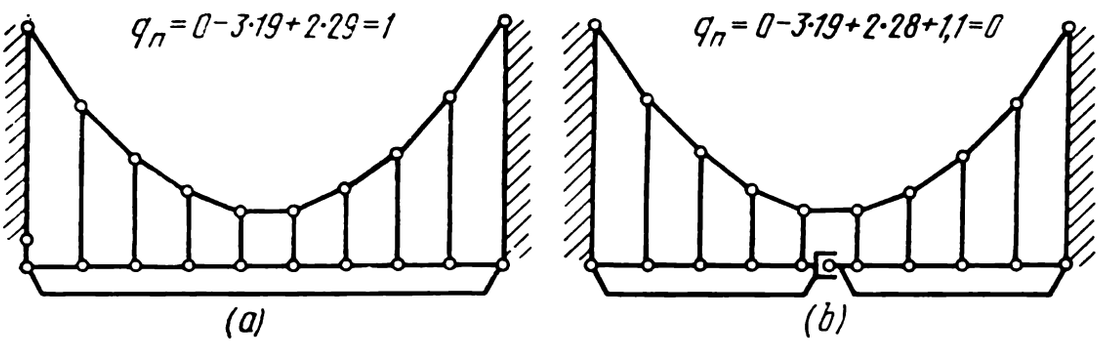


Fig. 6.68. Chain suspension bridges

indeterminate. To avoid this, the span beam is made of two parts connected by means of a joint (Schwartz bridges) which gives angular and linear mobilities as an expansion joint (Fig. 6.68*b*).

The disadvantage of this design is that in case of thermal deformations of the load-bearing cable bending occurs in one hinge — over the beam point which may lead to fatigue phenomena. This effect may be reduced by using an even number of rods supporting the span structure. In this case bending is distributed between two joints (Fig. 6.68*b*). With large spans (which may be even more than one kilometre) and with non-uniform load the moment bending the span beams is very large, which will appreciably increase the weight of the beam, of course. This can be avoided by providing additional joints (Fig. 6.69*a* and *b*).

If joints are provided under all vertical rods, harmful mobilities appear, the number of the mobilities being equal to the number of the vertical rods less one. This design is used in small pedestrian bridges where it is practically impossible to make the lower chord rigid. This can be avoided if each vertical rod is replaced by two inclined rods (Fig. 6.69*b*). This design was used in the bridge across

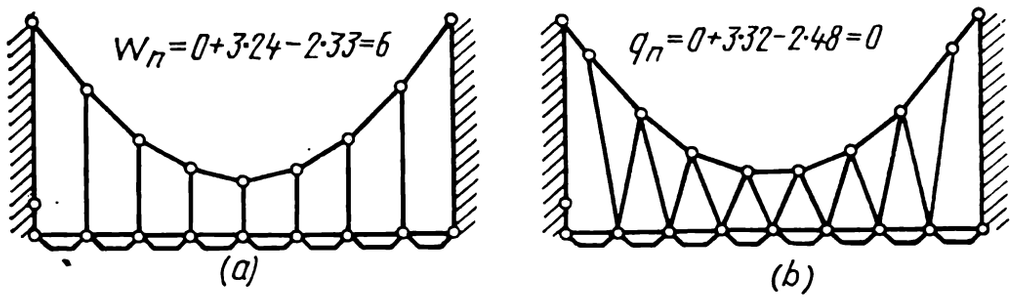


Fig. 6.69. Chain suspension bridges:
(*a*) with harmful mobilities (the number of vertical rods less one); (*b*) proper design with two rods per each intermediate joint

the Bosphorus in Istanbul. However this bridge does not have joints in the span structure. The rods cannot certainly transmit compression forces. The design diagram should, therefore, be calculated so that all rods are always loaded with tension forces only.

A very large number of joints are used in the span beam shown in Fig. 6.69*b*. This complicates the structure and does not enable the strength and rigidity of the beam to be fully utilized.

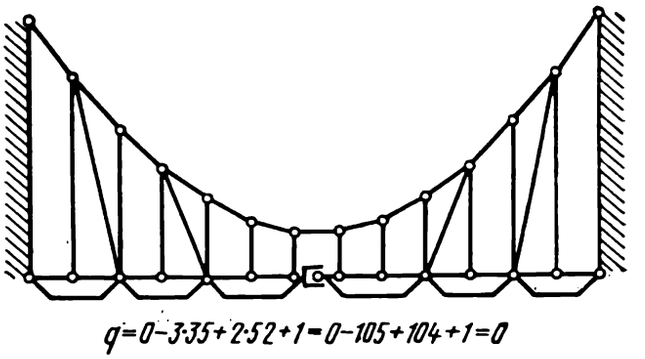


Fig. 6.70. Chain suspension bridge with joints at every other vertical rod

It is obviously expedient to install joints only under a part of the vertical rods, e. g. under every second rod, rather than under all rods, as shown in Fig. 6.70 (or under every third rod, and the like). One rod should be installed on each joint. The arrangement of the rods should be chosen based on the condition of best distribution of forces.

A design with several chains for one side of the bridge (three in Fig. 6.71*a*) may be used, one rigid member of the span structure of the beam being suspended to each chain by means of vertical rods.

Each group consisting of the chain, vertical rods (independent of their number), and the span structure member has two mobilities in the plane. To eliminate these mobilities, a joint may be installed (end groups in Fig. 6.71*a*), or it may be connected to other members through an arm and a higher pair (the middle group in Fig. 6.71*a*).

The use of two chains (on one side) with different deflections, each chain supporting all members of the span structure, is useless (Fig. 6.71*b*). The calculation in accordance with the structural formula (1.2) shows that the number of harmful mobilities does not decrease, only a redundant constraint appears.

The upper chord of suspension bridges is made of chains or cables (the latter for large-span bridges). The chain chord is made of several plates connected by joints so that it is statically indeterminate. This requires that the lengths of elements of chain links be maintained with sufficient accuracy. With the cable design of the upper chord the load is distributed among many cables, and in each cable

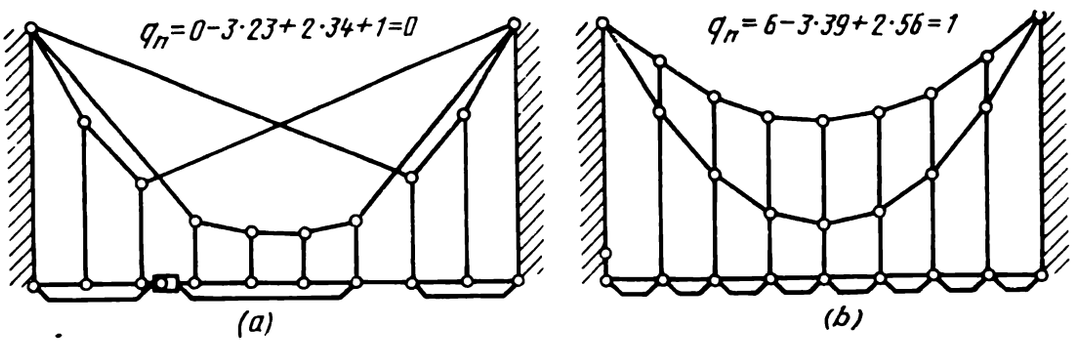


Fig. 6.71. Chain suspension bridge:
(*a*) with three chains, one rigid member of the span structure being suspended to each chain by means of vertical rods; (*b*) with two chains with different deflections (improper design which does not reduce the number of harmful mobilities)

the load is distributed among individual wires. Therefore, it is necessary that the cable attachment design should ensure uniform distribution of the load.

**Drawbridges.** These may be of the following types: traversing bridges in which the span structure receives a translatory motion in the horizontal or almost horizontal direction;

swing bridges in which the span structure rotates about a vertical axis;

bascule bridges in which the span structure rotates about a horizontal axis;

traversing and bascule bridges in which the span structure rotates about a horizontal axis receiving a motion in the horizontal direction;

vertical-lift bridges in which the span structure performs a translatory vertical movement [11].

**Swing bridges.** In conventional designs a horizontal electric motor is used with a system of spur gearings and bevel gearing connected to a drive pinion of the last stage. Technically it is difficult to make use of the bevel gearing and the last gearing stage because of the large size of the pinion. The bevel gearing may be avoided by using a vertical shaft motor (flange motor) and by making the axles of all intermediate gears vertical.

The last stage may be made in the form of a pin gearing so as to avoid the use of a large-size gear cutting machine. Drilling of holes for pins as well as indexing can be performed on the same vertical turning and boring mill. The involute pinion may be made in accordance with the approximate theory by R.V. Beschastnov [3] and by using standard gear cutting tools. To obtain a proper contact line of teeth, the method described in Section 4.4 should be used.

**Bascule and traversing-and-bascule bridges.** It is a common practice in such bridges to support each shaft by means of two self-aligning bearings that do not give redundant constraints.

The bridge is opened by means of drive pinions meshing with a toothed sector secured in the tail portion of the trusses. Generally two trusses are used. For uniform distribution of the load between the toothed sectors, a differential gearing is provided in the drive which is normally made in the form of a bevel gearing.

The loads on the toothed sectors may be easily equalized (compared to the differential gearing) by using axial forces of spiral gears (as it is done in herringbone gearings). For this purpose, the last shaft of the "common" drive should be made with an axial mobility, and gears should be installed on it: one gear should be with the right-hand spiral and the other with the left-hand spiral.

**Vertical-lift bridges.** It is not possible to guide the translatory moving span structure by means of a slide since such slide would have large dimensions. Therefore many types of mechanisms are used: rope, roller, and the like, and it is crucial to match the constraints which they impose on the span structure. The ropes connected to balance beams which equalize their loads will be referred to as rope group. Each group imposes one linear vertical restraint. For a statically determinate structure (absence of redundant constraints) there can be maximum three groups—three parallel forces. The three groups of ropes fix the span structure in the vertical direction, about the transverse axis and about the longitudinal axis, that is they ensure the horizontal position of the plane extending through the upper (or lower) chords of the trusses. Unfortunately, the bridge structure requires four groups of ropes arranged at the corners of the trusses (in the plan view); this group proves superfluous and gives a redundant constraint.

Drives with rope drive pulleys or drives with drive drums are used in bridges. In the former case the pulleys are formed by the blocks supporting the suspension ropes on which counterweights (generally two) are suspended to balance the span structure. Two pulleys installed in one tower are rotated by one electric motor connected to a common mechanical drive. The drive of pulleys of the second tower is coupled to the drive of the first tower by means of an "electrical shaft" coupling. Therefore, all the four pulleys, and the four groups of ropes receive the same displacement. One redundant constraint exists, but this is not harmful as it is caused only by friction force; self-equalization will take place owing to inevitable slippage.

In rope drive drums, the drive is effected by means of special

working ropes secured in the drums. Therefore, there can be no equalization, and an adjustment is necessary. The redundant constraint may be eliminated by installing one differential gearing in the drive; this complicates the design. The second differential gearing is only

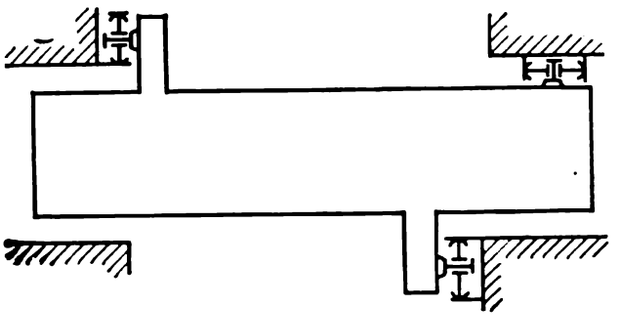

Fig. 6.72. Guide rollers of a vertical-lift bridge

expedient in case the angular constraint about the longitudinal axis is to be transmitted to guide rollers.

Earlier it has been mentioned that the ropes impose three restraints on the span structure, whereas six restraints are necessary. Assuming that each roller is the pair $I_2$, that is it imposes one restraint, three guide rollers are necessary (Fig. 6.72).

In actual structures one can find 12 rollers arranged in two horizontal planes (one above the other): in the plane of the upper chord of the trusses and in the plane of the lower chord. Compared to the discussed designs, the design-diagram shown in Fig. 6.72 is simpler by nine rollers and ensures better operation of the drive due to the absence of strains and overloads caused by redundant constraints.

In vertical-lift bridges, the counterweights are suspended using a large number of ropes. The number of ropes is up to 80 or more. An equalizing mechanism is necessary to achieve uniform distribution of load. Wide use is made of the mechanism having equiarm levers. Figure 6.73*a* shows such a mechanism for eight ropes. With the increase in the number of ropes the loads on joints in such mechanism increase tremendously (shown in the figure), with an increase in dimensions and moments bending the levers, and also in the overall height of the mechanism. Therefore, such a mechanism can hardly be used when the number of ropes is more than eight.

Theoretically it is possible to install an individual counterweight on each rope. The advantage of this design is that the friction in the equalizing mechanism does not interfere with the distribution of loads among the ropes. Its disadvantage is that the counterweights are in the form of thin slabs, which makes the structure very expensive.

It is preferred to use an intermediate variant (Fig. 6.73*b*). In this case the ropes are connected pairwise by means of balance beams, an

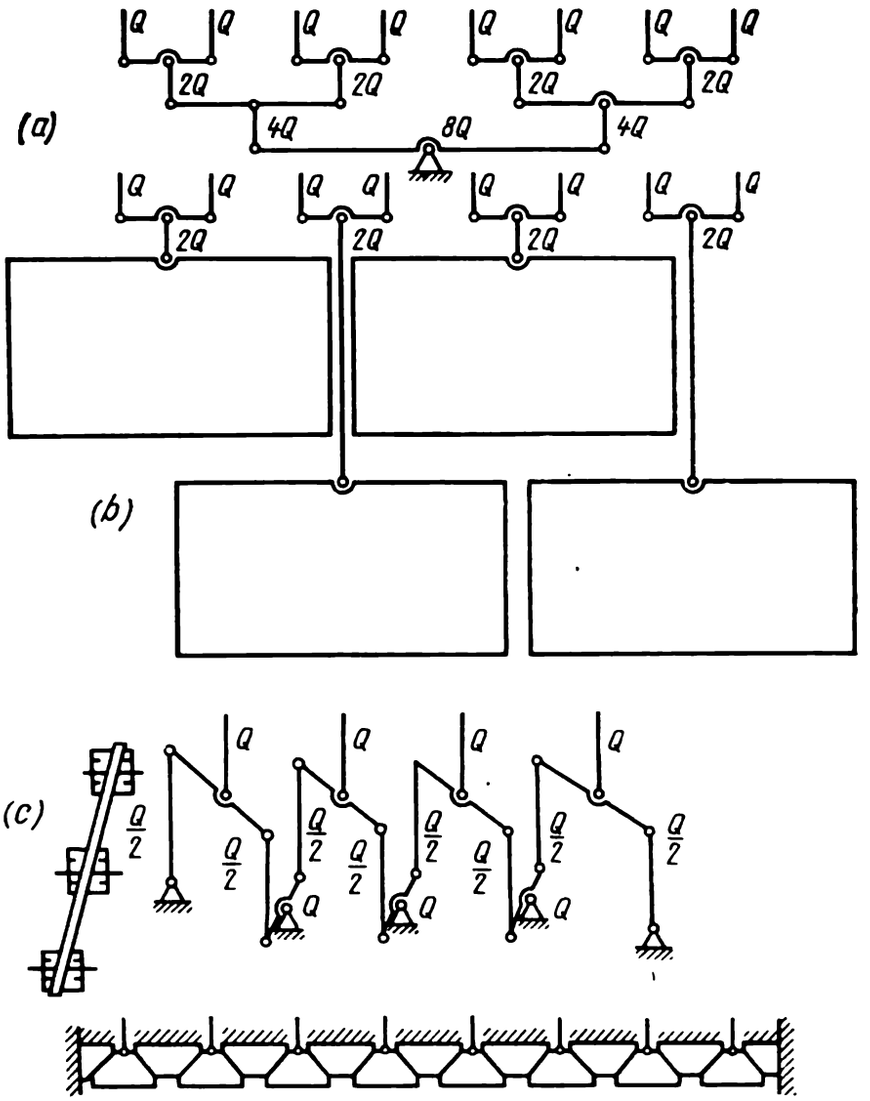


Fig. 6.73. Equalizing mechanisms for cables of vertical-lift bridges:
(*a*) conventional linkage; (*b*) combination mechanism; (c) with inclined equally loaded levers; (*d*, *bottom*) wedge-type

individual counterweight being used for each pair of ropes. The counterweights are arranged in a staggered fashion so that the arrangement is quite adequate from the structural point of view.

A single common counterweight can be used (Fig. 6.73*c*), but in this case the balance beams should be installed both on the ropes and on the counterweight hinge-joints, the counterweight being conventionally shown in the form of a fixed member in the figure. The balance beams are inclined (as shown in the left-hand part of Fig. 6.73*c*), but they are all identical and have low loads: only $Q$ and $\frac{Q}{2}$, rather than $8Q$ as shown in Fig. 6.73*a*. They can be easily manufactured (using welding techniques). Their overall height is small, and the sum

of loads on the joints is much less compared to the design shown in Fig. 6.73*a*.

It is interesting to compare the three designs of the equalizing mechanisms shown in Fig. 6.73*a*, *b* and *c*. They will be compared as regards the maximum load at the joint. In addition, we may determine total load acting on the joints which is an essential characteristic of the mechanism.

In Fig. 6.73*a* the number of rows of the levers $x$ can be found from equation $2^x = i$,

wherefrom $x = \lg_2 i$;

maximum load $= iQ$;

full load $= 2xiQ$.

In Fig. 6.73*b*, the number of rows of the levers is 2, the number of the levers $= \frac{i}{2}$,

maximum load $= 2Q$;

the number of rods $= \frac{i}{2}$;

full load $= 3iQ$;

the number of joints = number of members $= i$.

In Fig. 6.73*c*,

the number of rows of the levers is 2,

the number of levers $= 2i-1$,

the number of rods $= 2i$;

maximum load $= (4i-1)\,Q$;

the number of members $= 4i-1$.

The comparison shows that by maximum load, the design of Fig. 6.73*a* is the worst, the designs *b* and *c* differ slightly : $2Q$ and $Q$. The design *b* is the best from the point of view of the full load — $3iQ$. The design *c* is worse—$(4i-1)\,Q$. Finally, the design *b* is the best as regards the number of members.

Finally, a wedge-type equalizing mechanism may be used (Fig. 6.73*d*). The ropes (8 ropes) are attached to working wedges. Intermediate wedges are placed in between the working wedges; they are supported by the counterweight and can move in the horizontal direction. The disadvantage of this mechanism is large friction.

## 6.13. Bogies for Rolling Stock

Bogies with a rigid frame are widely used in electric and diesel locomotives, as well as in both motor and trailing coaches.

Bogies without a rigid frame having several members movably connected to one another are generally used in freight cars. Normal-

ly they are made in the form of two longitudinal girders connected to the wheel pairs by means of bushings and one transverse king-bolt girder supported by the longitudinal girders by means of springs.

The internal redundant constraints in the articulated bogies are eliminated or at least their number is reduced.

Let us asssume that $x$ axis passes along the bogie, $y$ axis is vertical, and $z$ axis runs parallel to the axis of the wheel rotation.

There are three kinematic pairs operating in parallel between the wheel pair and the rails. A kinematic coupling is thus obtained in which the restraint is equal to the sum of restraints (classes of kinematic pairs).

To simplify calculation, the kinematic coupling between the rails and the wheel pair will be discussed. The wheel with a non-engaged flange is regarded as the first class pair which imposes one linear restraint along $y$ axis.

The wheel with engaged flange imposes one linear restraint along $y$ axis and one linear restraint along $z$ axis.

In total there are three restraints, that is the coupling is of the class $III_5''$. Linear constraints are imposed along $y$ and $z$ axes, and an angular constraint along $x$ axis, and the following mobilities are left: a linear mobility along $x$ axis and angular mobilities about $y$ and $z$ axes. Therefore the kinematic coupling "rails-wheel pair" may be regarded as a spline-type kinematic pair with longitudinal axis.

The mobilities of the articulated bogies may be divided into operational mobilities, mobilities associated with vibrations of the springs, and specifically bogie-induced mobilities.

The operational mobilities include:

$f_x'$ — slippage of wheel pairs (skidding or slippage) designated as $Sl$ in the diagrams of mobilities;

$f_z''$ — rolling of wheel pairs designated as $Rl$.

The mobilities associated with oscillations of the king-bolt girder on springs include:

$f_y'$ — jumping — $j$;

$f_x''$ — swinging — $s$;

$f_z''$ — galloping — $g$.

The specific bogie-induced mobilities include:

$f_\varphi''$ — skewing, i.e. change in angles in the rotational plane—$Sk$.

Generally the king-bolt girder lies above the axles of the wheel pairs by a value $h$ (Figs. 6.74, 6.76). Therefore, both longitudinal girders can rotate together about the axes connecting the bushing bearings (rocker arms). They are interconnected by the king-bolt girder (connecting rod). Resetting to the neutral position takes place due

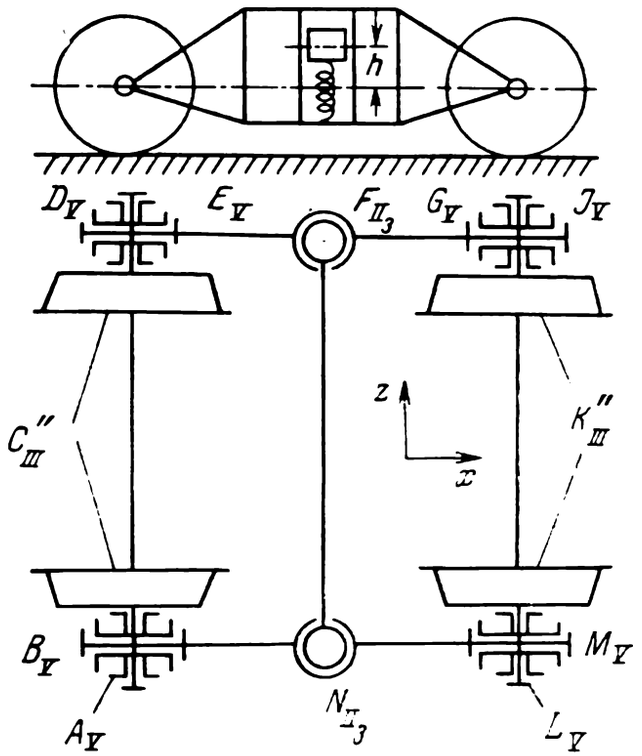


| $w=7$ | 7 | 7 | 5 | 5 | 2 | 2 |
|---|---|---|---|---|---|---|
| $n=9$ | .54 | 18 | -27 | 9 | -27 | 9 |
| | | | 8 | -4 | 12 | 3 |
| $p_V=8$ | 40 | -8 | 12 | -0 | 8 | -4 |
| $p_{III}=2$ | 6 | -6 | 2 | -4 | 4 | -2 |
| $p_{II}=2$ | 4 | -8 | 2 | -4 | 2 | -4 |
| $K=3$ | 3 | 3 | 2 | 2 | 1 | 1 |

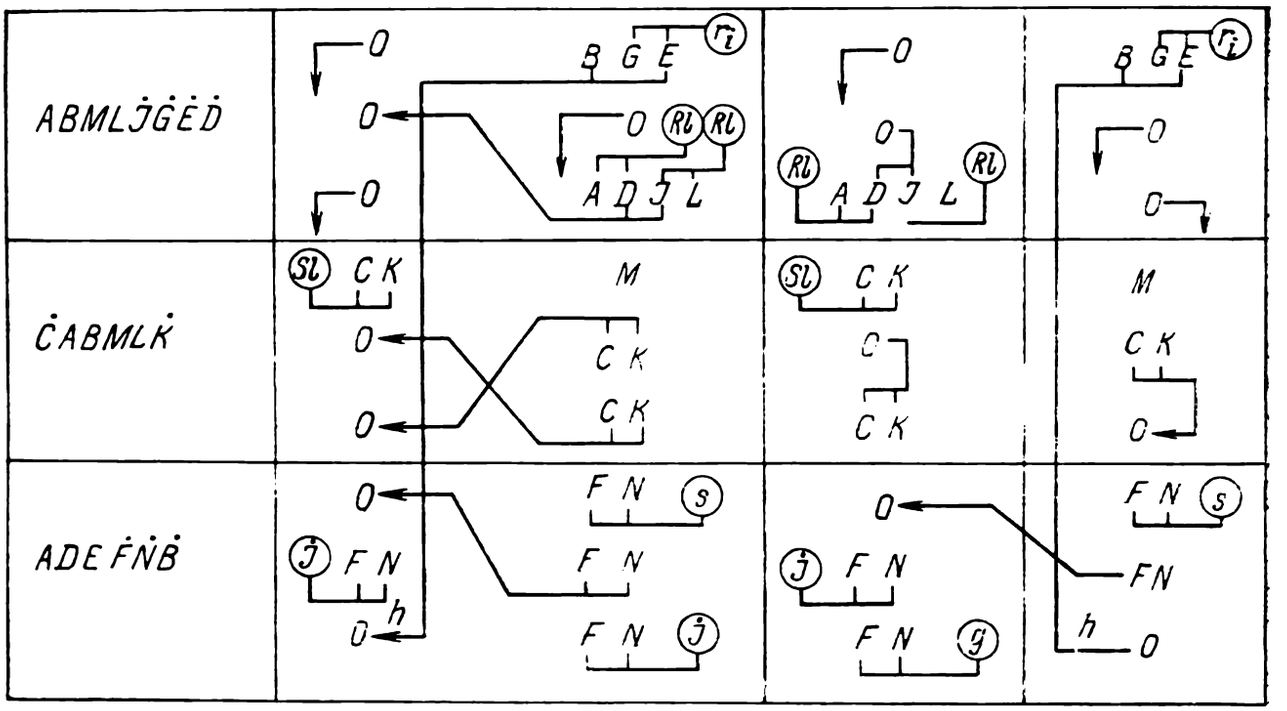


Fig. 6.74

to asymmetrical deformations of the springs. Hence $f''_x$—rotation of the longitudinal girders designated as $r$. In case $h = 0$ individual rotations of the longitudinal girders about $x$-axis are possible which are designated as $r_i$. The mobilities such as "slippage", "rolling", "jumping", and "galloping" are plane mobilities, and the mobilities

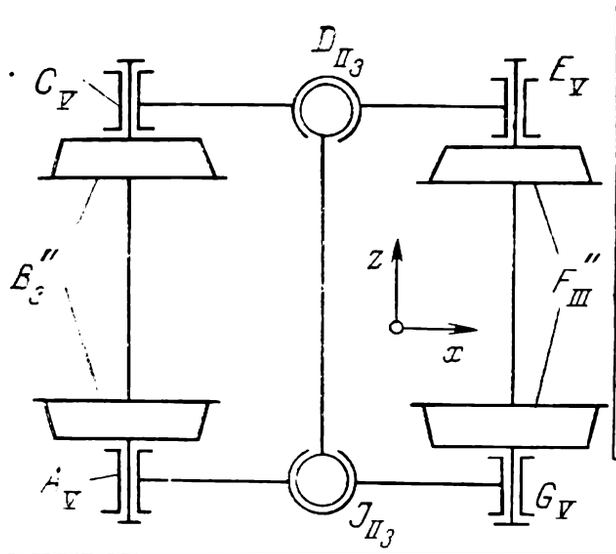


| $w=6$ | 6 | 6 | 1 | 1 | 5 | 5 |
|---|---|---|---|---|---|---|
| $n=5$ | -30 | 18 | -15 | 9 | -15 | 9 |
| $p_V=4$ | 30 | -4 | 12 | 0 | 8 | -4 |
| $p_{III}=2$ | 6 | -6 | 2 | -4 | 4 | -2 |
| $p_{II}=2$ | 4 | -8 | 4 | -2 | 0 | -8 |
| $K=3$ | 6 | 6 | 4 | 4 | 2 | 2 |

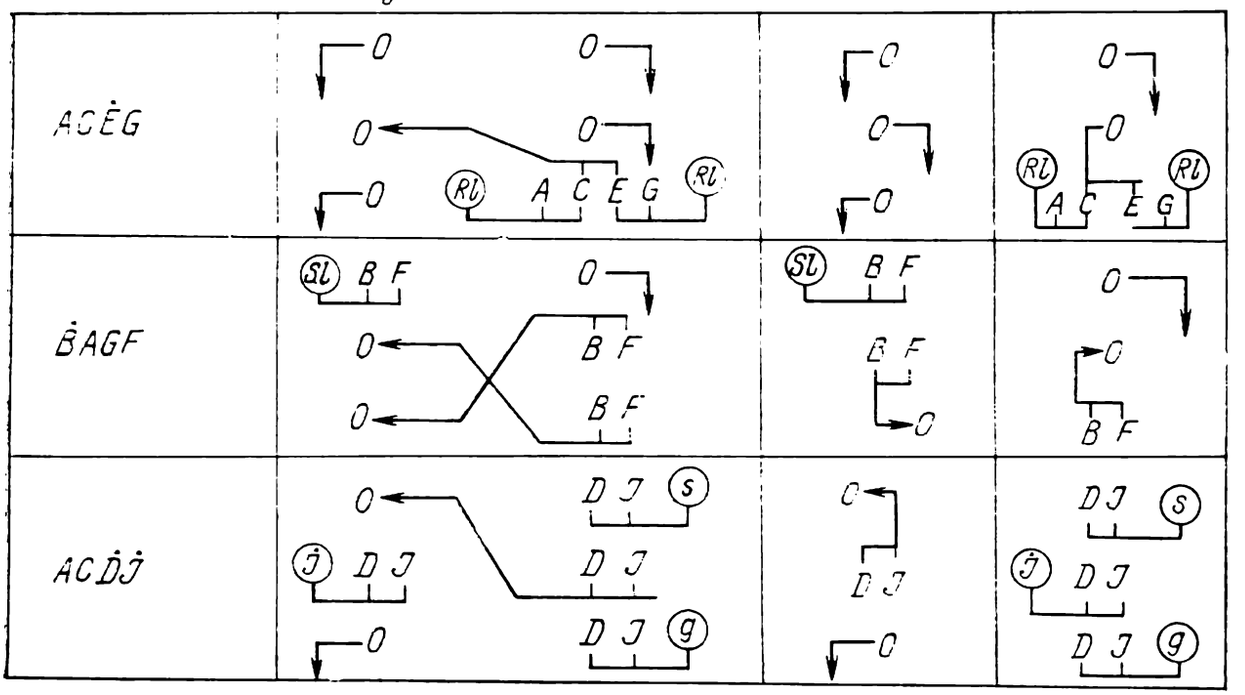


Fig. 6.75

such as "skewing" and "rotation of longitudinal girders" are non-planar mobilities.

Among such bogies, the Diamond-type freight bogie is widely known. It has no springs for primary suspension. Therefore, the mobility ensuring uniform distribution of load among its four wheels (external statical determinacy) is necessary here. For this reason it has large unsprung weight and this makes this bogie unsuitable for high speeds.

There are Diamond-type freight bogies with sliding-contact bearings. They use self-aligning bushing liners which move about the longitudinal axis (Fig. 6.74). The coupling of the longitudinal gir-

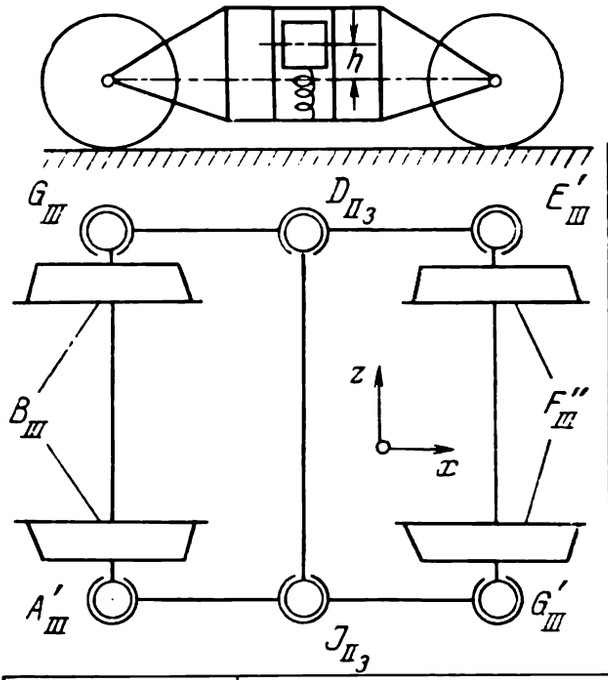


| $w = 8$ | 8 | 8 | 5 | 5 | 3 | 3 |
|---|---|---|---|---|---|---|
| $n = 5$ | -30 | 18 | -15 | 9 | -15 | 9 |
| | | | 8 | -4 | 4 | -8 |
| $p_{III} = 6$ | 18 | -18 | 2 | -4 | 4 | -2 |
| $p_{III} = 2$ | 4 | -8 | 2 | -4 | 2 | -4 |
| $K = 3$ | 0 | 0 | 2 | 2 | -2 | -2 |

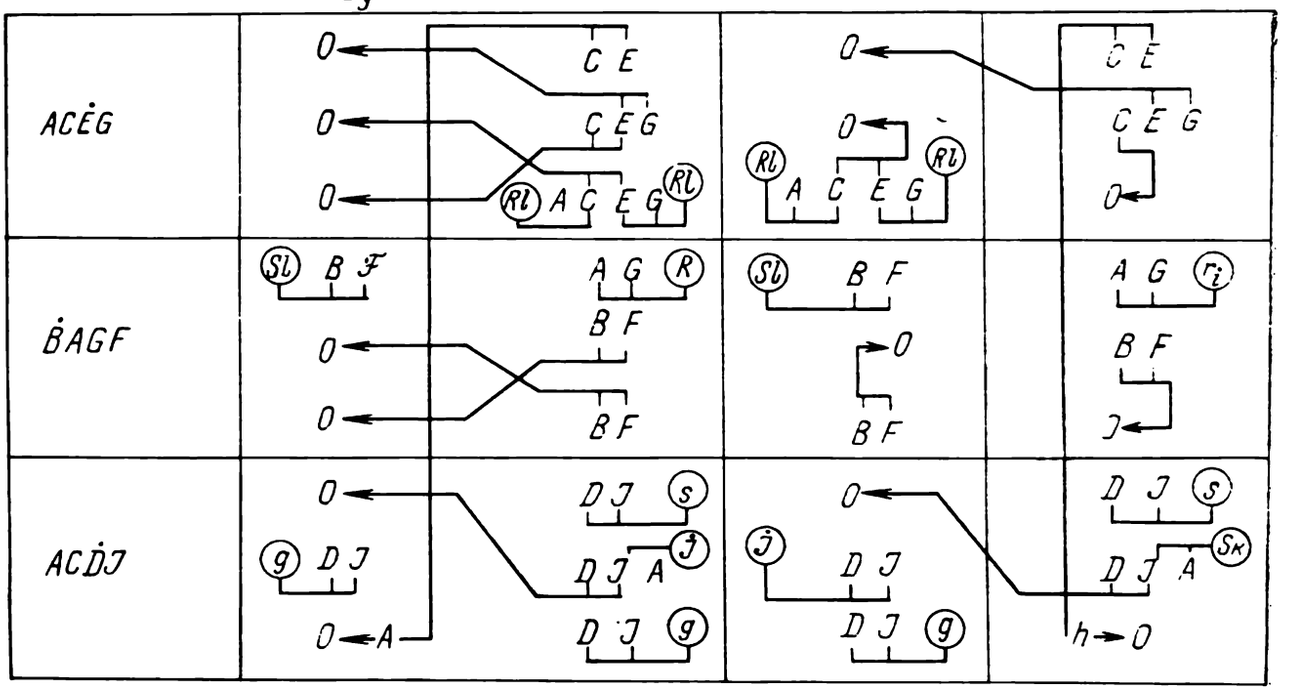


Fig. 6.76

der to the king-bolt girder is regarded as the kinematic pair $II_3$— a ring pair of the type of "sphere-in-the-tube" owing to the play.

This bogie has the following mobilities: *s*, *r*, *r*, *j*, *s*, *g*, *r*.

Tables for calculation with use of structural formulae and distribution of mobilities in loops are given in the figure. General constraints and mobilities (planar and non-planar) (according to Kachalova) are also given.

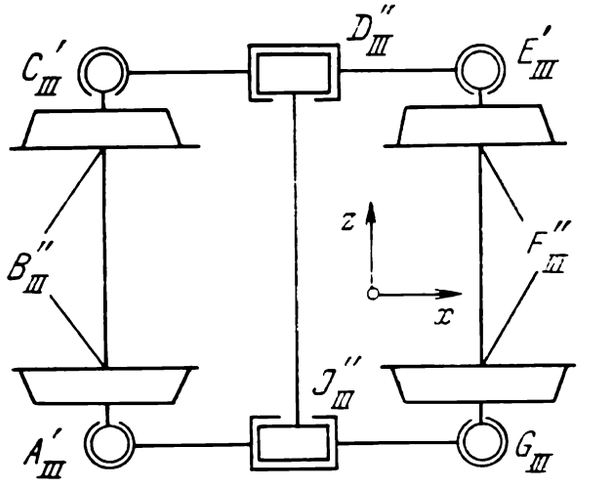


| $w=$ | 7 | 7 | 5 | 5 | 2 | 2 |
|---|---|---|---|---|---|---|
| $n=5$ | -30 | 18 | -15 | 9 | -15 | 9 |
| $p'_{III}=4$ | 12 | -12 | 8 | -4 | 4 | -8 |
| $p''_{III}=4$ | 12 | -12 | 4 | -8 | 8 | -4 |
| $K=3$ | 1 | 1 | 2 | 2 | -1 | -1 |

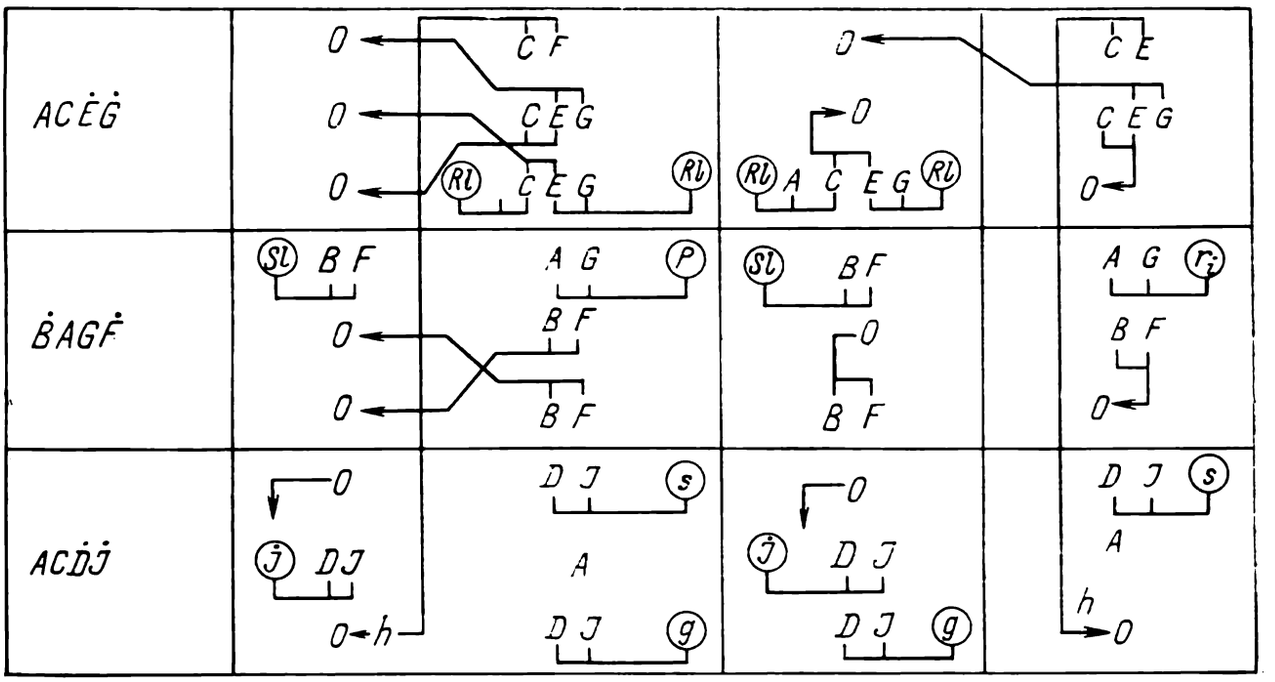


Fig. 6.77

A vertical plane, i.e. the plane of rotation of wheels may be taken. In this case, the mechanism is multiplanar, and its study is more complicated (see Figs. 6.74, 6.76 and 6.77). Therefore, it is preferred to take a horizontal plane in which the bogie moves (see Figs. 6.75, 6.78 and 6.79).

The attention is drawn to the fact that the planar mobilities in this case include $f'_x$, $f''_y$ and $f'_z$ and non-planar mobilities include $f''_x$, $f'_y$ and $f''_z$. They are given in Fig. 6.79. The mobility is designated with the same letter as in the above list of mobilities, but in a circle. Three linear redundant constraints along the transverse $z$-axis exist here.

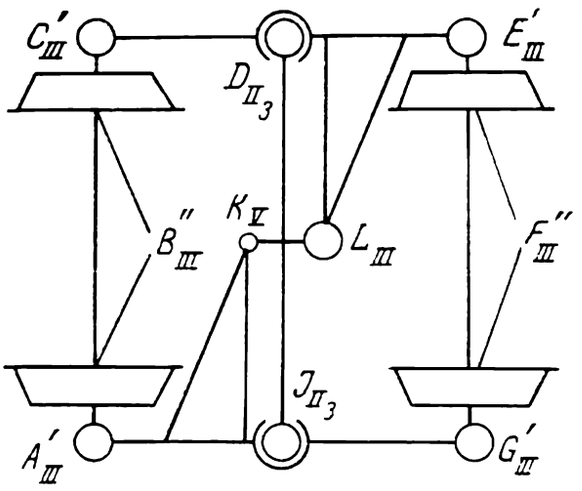


| $w=7$ | 7 | 7 | 1 | 1 | 6 | 6 |
|---|---|---|---|---|---|---|
| $n=6$ | -36 | 24 | -18 | 13 | -18 | 12 |
| $p_V=1$ | 5 | -1 | 2 | -1 | 3 | -0 |
| $p'_{III}=5$ | 15 | -15 | 10 | -5 | 5 | -10 |
| $p''_{II}=2$ | 6 | -6 | 2 | -4 | 4 | -2 |
| $p_{II}=2$ | 4 | -8 | 4 | -2 | 0 | -6 |
| $K=4$ | 1 | 1 | 1 | 1 | 0 | 0 |

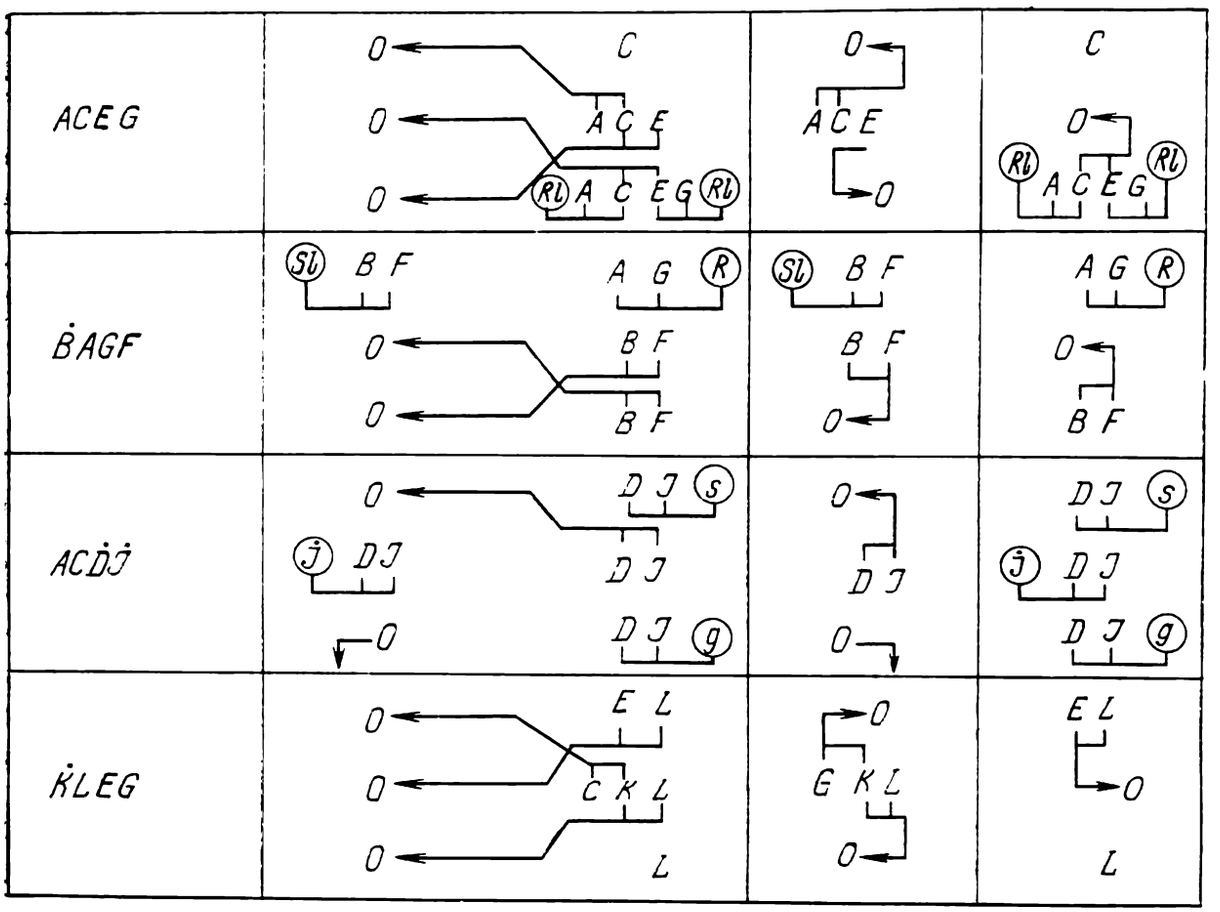


Fig. 6.78

These redundant constraints should be considered as associated with the design of the bogie bushings. In the Diamond bogie the bearing is installed in the bushing housing and transmits a vertical force through a slide block whose upper surface is cylindrical (for self-alignment of the bearing) with axis perpendicular to the axis of the

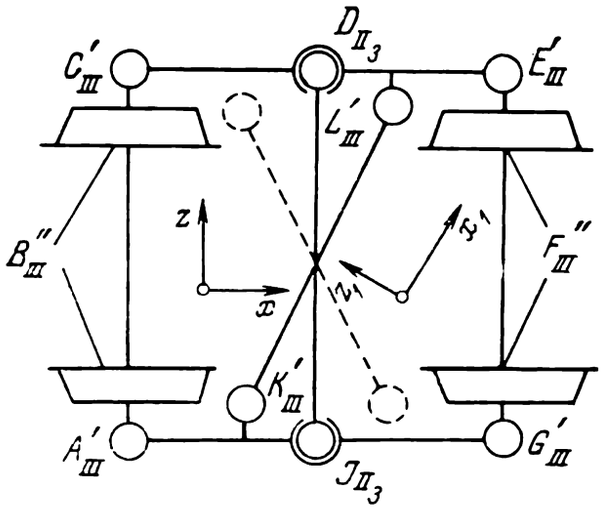


| $w=9$ | 9 | 9 | 1 | 1 | 8 | 8 |
|---|---|---|---|---|---|---|
| $n=6$ | -36 | 24 | -18 | 12 | -18 | 12 |
| $p'_{III}=6$ | 18 | -18 | 12 | -6 | 6 | -12 |
| $p''_{III}=2$ | 6 | -6 | 2 | -4 | 4 | -2 |
| $p_{K_3}=2$ | 4 | -8 | 4 | -2 | 0 | -6 |
| $K=4$ | 1 | 1 | 1 | 1 | 0 | 0 |

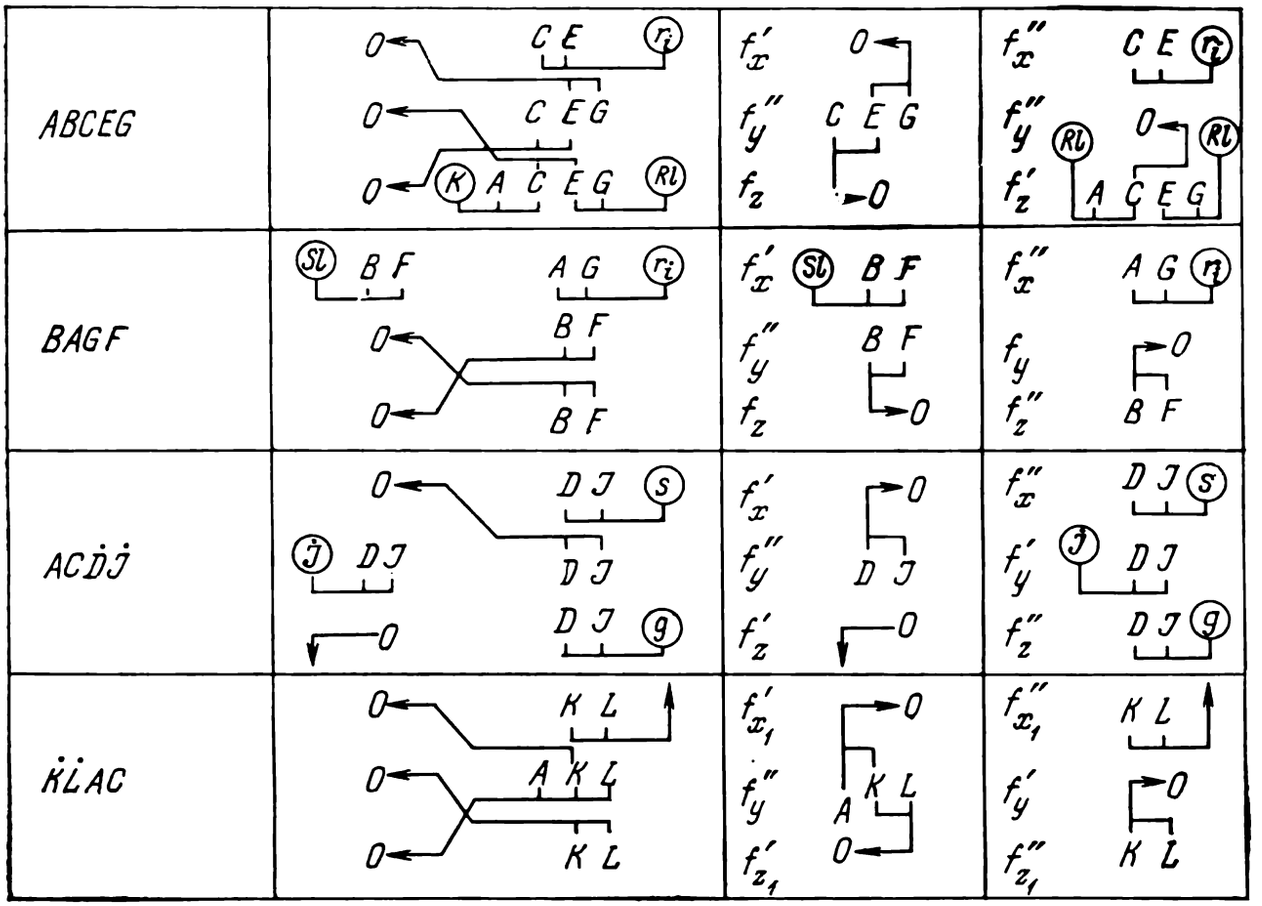


Fig. 6.79

wheel pair. It is these Diamond bogies with sliding-contact bearings that have found widespread use, and they are taken here to evaluate this design.

Despite the disadvantage, i.e. large unsprung weight, these bogies have proved under heavy-duty conditions of operation of freight cars. They are certainly unsuitable for high speeds.

In a freight-car bogie with roller bearings, two bearings with straight rollers of the series 2000 are generally used in each bushing. The bushing should therefore be regarded as the fifth-class pair (Fig. 6.75). In this case the mobility "R" is eliminated, but the number of redundant constraints increases to 6. The skewing of the frame is eliminated by the moments bending the axle journals. Thus, breakage of axle journals in such bogies is not infrequently reported.

An attempt to eliminate these redundant constraints was made at a research institute of the Ministry of Railways (USSR) by installing in each bushing one spherical roller bearing of the 3000 series (Fig. 6.76). The redundant constraints were eliminated, but the number of mobilities increased to 8. The *Sk* mobilities—skewing of the frame—were added even compared to Fig. 6.74. This mobility proved harmful. The bogie movement became unsmooth, and the design had to be abandoned.

To eliminate the harmful mobility—skewing of the bogie—the longitudinal girders should be connected to the king-bolt girder by means of the third-class pair $III_5''$, rather than with ring pairs $II_3$ (Fig. 6.77). These are vertically positioned spline-type pairs. It is convenient from the design point of view to make one member of the pair in the form of a parallelepiped of small height, the angular mobilities are obtained owing to plays.

Another method of eliminating mobilities of skewing is shown in Fig. 6.78. The longitudinal frames are provided with triangular projections and coupled to a longitudinal rod $K_V L'_{III}$.

The third method consists in using an inclined rod $K'_{III}L'_{III}$ as shown in Fig. 6.79. It is preferred to use two such rods without calculating them for buckling (the second rod is shown with dotted line in Fig. 6.79). Only one rod will work in tension, the other will not work in compression as it is not designed to withstand buckling. Hence there will be no redundant constraints.

The weakest point in the frames of coach bogies is the joint of longitudinal and transverse girders (Fig. 6.80).

Special attention should be paid to horizontal forces distorting the frame and causing moments about the vertical axis in the joints of longitudinal and transverse girders. This moment is practically transmitted only by the horizontal plates which should be made considerably thicker, making the frame heavier.

The vertical plates of the transverse girder which can adequately transmit the moment about the vertical axis do not participate in the operation of the joint owing to the deflection of the vertical plates of the longitudinal girder.

The design of the frame having the transverse girder in the form of a circular pipe cut in the longitudinal girder which was used in the electric locomotive "Ф" cannot also be considered good. The longitudinal girder is appreciably weakened in this design, and therefore the cross-sectional area of the transverse girder has to be reduced.

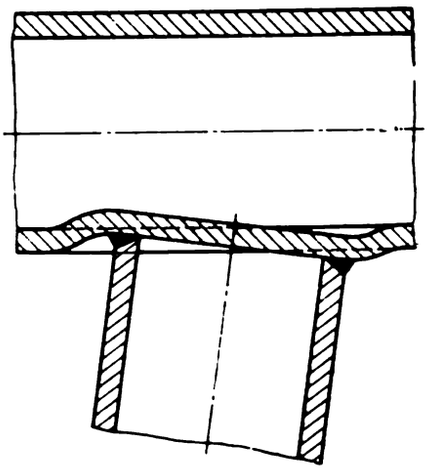

Fig. 6.80. Diagram of deformations in the coupling of tubular girders (longitudinal and transverse girders)

I-beams could have transmitted to the joint the same moment which they transmit to the full section. Open sections are, however, bad for torsion. This was confirmed in the plate frames which proved inadequate.

The coupling (joint) of the girders is also loaded with a moment about the transverse axis caused by the weight of the overhanging motor, which impairs the functioning of the coupling.

A reliable and durable structure may be obtained by eliminating moments transmitted through couplings of the girders. For that purpose, a joint (or a flexible coupling) should be used, and the moment should be transmitted through other members which are more suitable for the purpose, e.g. diagonal braces. Joints for eliminating loading moments are used in the aviation industry for joining the blade of the main rotor of helicopter to the hub (Fig. 3.13).

The statically indeterminate structure is generally regarded to be more advantageous. This is based on the concept that a beam on two supports is bent by larger moment compared to the beam with restrained ends. This comparison is not correct since the former beam does not develop a moment in the restraint, and the latter develops a moment which damages the bogie frames.

If a statically determinate beam has its supports loaded with moments, correct selection of the points of location of the joints may even give a smaller value of the bending moment compared to a statically indeterminate beam. The bending moment can be reduced or elimi-

nated altogether at a desired point. This should be done in the designs of the bogie frames.

Let us find the number of redundant constraints in a bogie having a rigid frame. There is one external redundant constraint in the bogie as the number of wheels is four. There are six internal redundant constraints in each loop. There are six such constraints in an open H-shaped frame for one loop, and 18 redundant constraints in a closed H-shaped frame for three loops.

**Comparison of beams and trusses.** The use of a truss to replace the beam may appreciably increase the bogie mass. Let us compare them when loaded with vertical forces. Let us take a beam of tubular rectangular cross-section which is most frequently used. Horizontal plates are completely loaded in the beam, and the vertical plates are utilized three times worse.

In a truss, the chords are loaded completely. In addition, the depth of the truss may be much greater than the depth of the beam, therefore the truss is much advantageous compared to the beam.

The diagonal struts which relieve the coupling of the longitudinal and transverse girders from the moment about the vertical axis are used for a long time in Pullmann, Fette and other bogies; they have proved very good.

The truss is preferably used also for transmitting vertical forces. According to the recommendations of V.A. Rakov, the frame of the traction motor should be used as truss member. This steel-cast frame represents a ring of about 800 mm in diameter and cross-sectional area of 550 × 50 mm (for ДК-106Б motor) which is a rather sturdy member compared to a longitudinal beam of 280 × 260 mm section.

The frame of the traction motor was used as a load-bearing structure in the Ford, Jacquemain and other electric locomotive bogies. I.V. Astakhov and A.I. Kravchenko also proposed to use the truss in the design of bogies. A truss was used by Jacquemain and A.A. Shatsillo for the transmission of traction forces (ВЛ-40 No. 002).

Articulated bogies are also used in coaches of the Stockholm underground railway (Fig. 6.81). The springs over the bushings and the cradle-type suspension are not shown in the figure. The bogie frame has two T-shaped half-frames interconnected by joints. Therefore, the frame can bend relative to the axis passing through the centres of the joints (shown with dotted line in Fig. 6.81), this enables a statically determinate distribution of load among four wheels. This is an advantage of the bogie, though not very significant, as springs provide for uniform distribution, although incomplete. Even if the joints are regarded as the spherical pairs $III'$, they give a redundant

constraint—strain along the dotted line, that is they impose six restraints, whereas five restraints are needed for the rotational mobility.

This redundant constraint is taken into account, and the coupling between the half-frames will in the further discussion be regarded as the fifth-class rotational pair. Then there are three independent loops

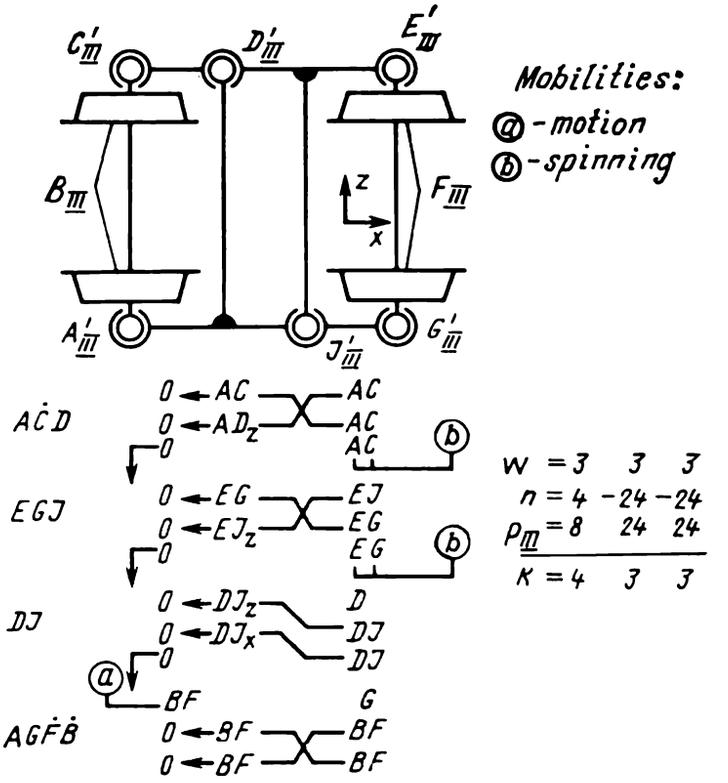


Fig. 6.81. Bogie of the Stockholm underground railway

in the mechanism $k = p - n$ which is obtained by calculation using the structural formulae given in the Table of Fig. 6.81. Therein are also shown the distribution of mobilities and redundant constraints in the loops. The bogie has two more linear redundant constraints—strains along the axles of wheel pairs. They are not, however, harmful as they are softened by the flexibility of the bushing assemblies. The bogie is, therefore, not bad from the point of view of redundant constraints. The situation is, however, worse with the strength. This follows from the comparison with a conventional *H*-shaped bogie in which moments caused by horizontal forces distorting the frame are taken-up by four assemblies of coupling between longitudinal and transverse girders, whereas there are only two such assemblies in the Stockholm bogie, which is disadvantageous.

**Proposed designs of two-axle bogies*.** Rational designs of bogie

*L.N. Reshetov. Two-Axle Locomotive Bogie with Independent Drive. Discoveries, Inventions, Industrial Designs, Trademarks, 1974, No. 33, USSR Inventor's Certificate No. 442104.

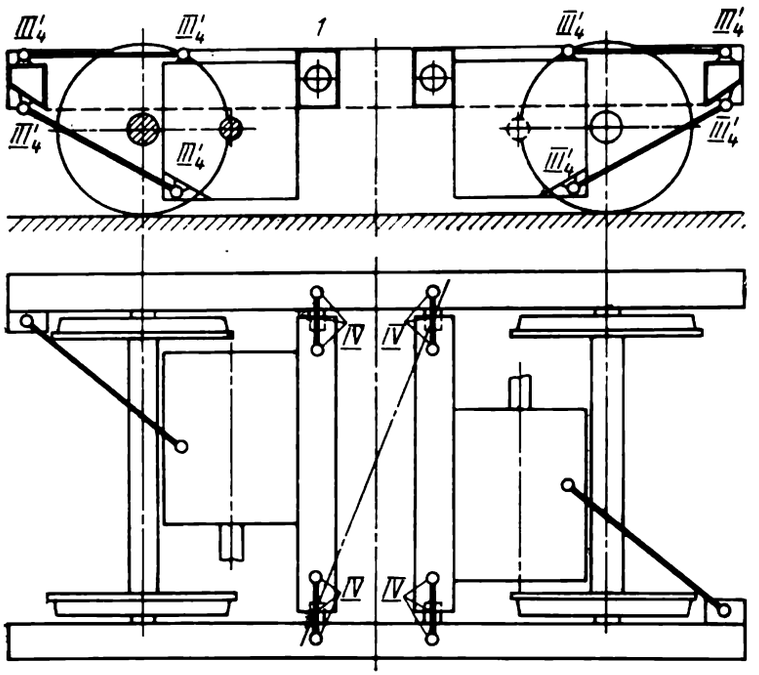


Fig. 6.82. Two-axle bogie with load-bearing framing of the traction motor

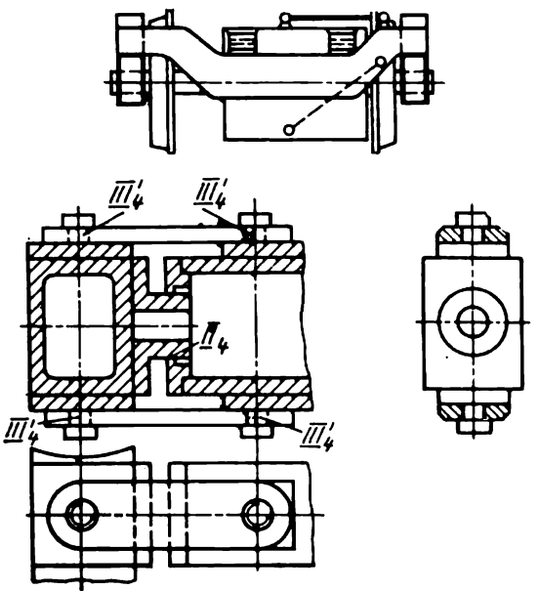


Fig. 6.83. Modifications of design of coupling between longitudinal and transverse girders

frames may be made with internal and external statical determinateness or only with the internal statical determinateness. In the former case all four wheels are uniformly loaded independent of the condition of the springs, but the bogie acquires a local mobility: it should bend near the inclined axis. When joints are made in the form of rubber blocks or flexible plates, a structure operating without wear and suitable for high-speed conditions may be obtained due to the absence of plays.

Let us first discuss this variant (see Fig. 6.82). Each bogie consists of two "halves" articulated to one another (similarly to the design of the Stockholm bogie).

The "half" consists of a longitudinal girder and a cross-piece which is pivotally ($IV_3$) connected to the girder. The transverse girder is rigidly secured to a traction motor which is, in turn, coupled to the longitudinal girder by means of two rods with spherical joints ($III'_4$) functioning as struts of a truss, one rod being installed horizontally and the other in an inclined position. A rigid structure is thus obtained which has only two local mobilities of rotation of the rods about their axes.

The coupling between the longitudinal and transverse girders is relieved from moment transmission by a joint. The truss is very sturdy with the height of the traction motor of 800 mm. There are no redundant constraints in the truss, and this may be checked-up using the structural formula (1.1). Assuming the longitudinal girder to be a fixed member, $q = 2—6 \times 3 + 4 \times 1 + 3 \times 4 = 0$.

The rod loads are not great. With the hourly current of the motor, the load on the upper horizontal rod is 944 kgf and on the lower rod is 1 250 kgf. If the couplings of the "halves" and those between the halves and the wheel pairs are made using the same kinematic pairs as shown on Fig. 6.83, then the bogie will have no redundant constraints. The kinematic pairs of the fourth class (see Fig. 6.83) may be made in the form of a ring pair imposing two restraints and two arms each imposing one restraint. For a third-class pair, one arm is needed. The second class pair does not have arms. The designs are, therefore, modular. It is preferred to make the bushing bearings different. Thrust bearings should be installed in the bushings under the trusses to take-up impacts against the flanges in both directions (*III'*). The other bushings ($II_3$) should have an axial mobility, and the longitudinal girder should be relieved of impacts against the flanges. In such case the end braces of the longitudinal girders become unnecessary, and the body is made still lighter in weight.

The two diagonal rods may be replaced by a bracket. It should be coupled to the motor by means of the pair $V_2$ and by means of the spherical pair $III_2'$ to the longitudinal girder. This bracket should be installed to extend along the diagonal line so as to function as a brace. This makes this design different from that proposed by A.I. Belyaev, where the bracket is installed in the longitudinal plane so that it cannot function as a strut in the truss.

In order to facilitate the manufacture, the mobilities in the couplings may be re-distributed (see Fig. 6.84). A complicated and heavyweight coupling between the motor and the transverse girder may be replaced by a pivotal coupling $V_2$ using stub shafts. In such case the coupling between the longitudinal and transverse girders should also be made in the form of the rotational pair $V_2$ which is simpler compared to the pair *IV*.

The bogie shown in Fig. 6.84 is also advantageous in that the couplings between the longitudinal and transverse girders are located closer to the plane of the wheel pairs in which the horizontal forces are applied, causing the wrenching moments. The only disadvantage resides in that the transverse girder is attached to the longitudi-

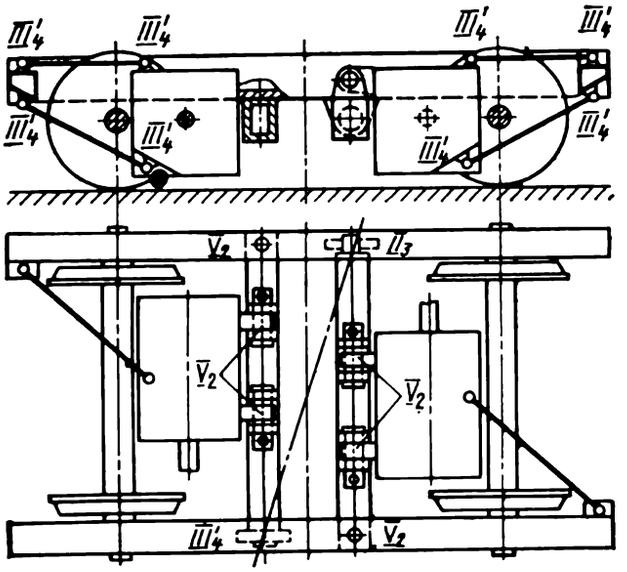

Fig. 6.84. Bogie with load-bearing framing of the motor with articulated coupling of the motor to the transverse girder

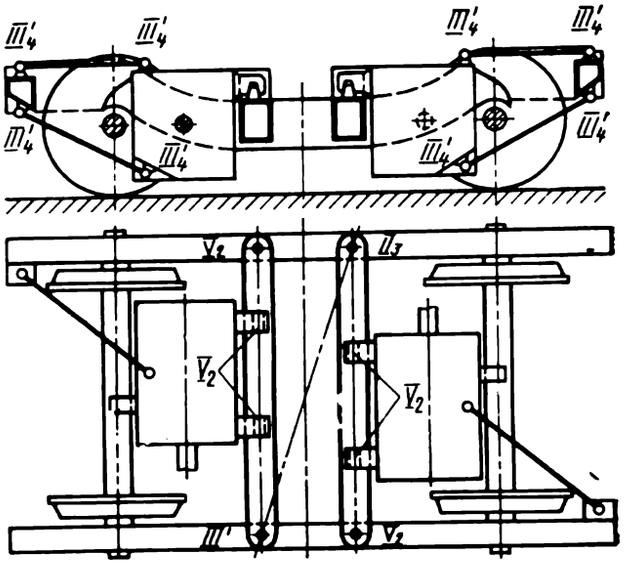

Fig. 6.85. Bogie with load-bearing framing of the motor with curved transverse girders

nal girder at the bottom. This may be avoided (see Fig. 6.85), but the girders have to be curved.

One of the rods securing the motor in the bogies extends under the axle of the wheel pair. The motors should be jacked apart for rolling out the wheel pair (e.g. for re-turning the rims). Then both rods may be readily removed.

Let us discuss a bogie with only internal statical determinateness (see Fig. 6.86). The bogie should be in the form of a rigid, three-dimensional and statically determinate truss. To obtain such a structure, both rods securing the motor should extend at the bottom and be fixed to both longitudinal girders. Loads in these rods are still smaller than in Fig. 6.82 and are only about 625 kgf with the hourly current.

## 6.14. Conclusions and Recommendations

A pulley should be installed on one rolling-contact bearing, rather than two.

The axes of rods in a double-jaw grab should not intersect at a point.

Wheels of crane carriages should be self-aligning both in the vertical and horizontal directions. The self alignment is especially important in building cranes where the accuracy of tracks is much lower.

The self-alignment prolonged the life of the wheels in travelling cranes from 2-3 months to several years. The folding boom mechanism should be made self-aligning as it is very difficult to manufacture it with desired accuracy owing to its large size.

In order to avoid rapid wear of rope pulley in elevators, a second equalizing mechanism should be installed on the counterweight. Guide shoes of the lift car should be self-aligning. The counterweight should be guided by three, rather than six shoes. The redundant constraints in the movable platform mechanism should be eliminated which is very important for children safety, otherwise the mechanism may not actuate owing to small load.

Self-alignment in roller supports of rotary kilns prolongs the life of lining of rollers, and their bearings and makes it possible to dis-

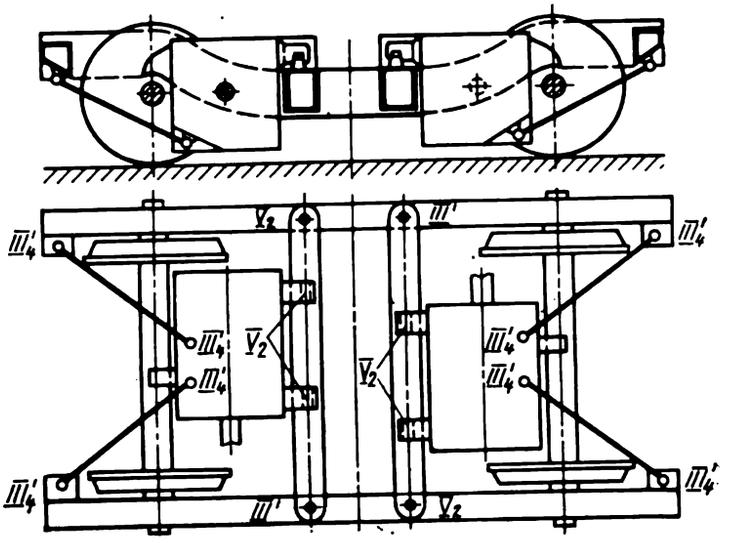

Fig. 6.86. Rigid bogie with load-bearing motor framing

pense with the gearing of enormous size by providing drive for rollers rather than for the drum. The equalizing mechanism may have a linkage, hydraulic or air pad. In the latter case, losses in the pipelines are proportional to $(\text{diameter})^{-5}$ and $(\text{pressure})^3$; this enables the pipelines to be made very small.

The elimination of redundant constraints in bridges makes it possible to avoid harmful stresses upon non-uniform settlement of piers and non-uniform heating of trusses and pavement by the sun.

The number of guide rollers, which is up to 12 in the vertical-lift bridges, may be reduced to three, and useless loads upsetting the piers can be avoided. The ropes may be loaded more uniformly by dividing the counterweight into several weights and by modifying the design of linkage.

Self-alignment in shoe brakes makes it possible to avoid unequal braking moments of the right-hand and left-hand wheels which may result in skidding of vehicle. The shoes no longer need finish turning when assembled with the axle; this reduces both labour and consumption of lining material.

The weak point in the locomotive bogies is the coupling between the longitudinal and transverse girders. Self-alignment makes it possible to eliminate this coupling by replacing it with a joint and by using a sturdy stator of traction motor as a load-bearing structure.

# REFERENCES


1. Aliev, Sh. N., Methods of Controlling Static Characteristics of Current Collectors of Rail Vehicles. Scientific Notes of Azerbaijan Polytechnical Institute, 1975, Series X, No. 3, pp. 142-151 (in Russian).

2. Bashta, T. M.. Hydraulic Actuators of Aircraft. 4th Edition, Moscow, Mashinostroenie Publishers, 1967 (in Russian).

3. Beschastnov, R. V., Approximation Profiling of Gear Tooth with Cogwheel Engagement. Works of MVTU, Problems of theory of machines and mechanisms, 1958, Vol. 77, pp. 62-97 (in Russian).

4. Bratukhin, I. P., Designing and Constructing Helicopters. Moscow, Oborongiz Publishers, 1955 (in Russian).

5. Budyka, E. Yu., Drawing Structural Formulas of Mechanisms in Logical Way. *Izvestiya Vysshikh Uchebnykh Zavedenii*, 1976, No. 8, pp. 71-73 (in Russian).

6. Bushuev, V. V., Naletov, S. P., Heavy-Duty Gear-Working Machines. Moscow, Mashinostroenie Publishers, 1976 (in Russian).

7. Volkov, D. P., Krainev, A. F., Transmissions of Construction and Road-Building Machines. Moscow, Mashinostroenie Publishers, 1974 (in Russian).

8. Gaipel, Ja. Ja., New Formula for Determining the Number of Loops in Mechanism. Methodological collection of Ministry of Higher Education on Theory of Machines and Mechanisms, 1975, Vol. 3, pp. 8-9 (in Russian).

9. Derzhavets, Y. A., On Distribution of Load Among Satellite Gears of Planetary Gearings, in book "Reliability and Quality of Toothed Gearings". Moscow, *NIIInformtyazhmash Publishers*, 1967, pp. 138-145 (in Russian).

10. Dolinski, P. A., Centering the Movement of Marine Diesels. Moscow, Morskoi Transport Publishers, 1958 (in Russian).

11. Evgrafov, G. K., Drawbridges. Moscow, Transzheldorizdat Publishers, Moscow, 1950 (in Russian).

12. Ermak, V. N., Kinematics and Kinetostatics of Twin-Path Gearing with Equalizing Mechanism. Works of MVTU, Theory of mechanisms, Moscow, 1973, No. 160, Vol. 6, pp. 126-129 (in Russian).

13. Zheligovski, A. V., Theory and Computation of Statically Determinate Mechanisms. *Mekhanizatsiya i elektrifikatsiya sotsialisticheskogo selskogo khozyaistva*", 1977, No. 1, p. 56 (in Russian).

14. Zhuravlev, G. A., Shakhbazov, N. A., Selecting Geometric Parameters of Spur Gears with Arcuate Teeth. "Avtomobilestroenie", 1970, No. 4, pp. 34-37.

15. Zablonski, K. I., Schuster, A. E., Built-In Reduction Gears. Kiev, Technika Publishers, 1969 (in Russian).

16. Zablonski, K. I., Shuster, A. E., Infinitely Adjustable Gearings. Kiev, Technika Publishers, 1975 (in Russian).

17. Zaporozhets, O. L., Kondrashov, Y. D. et al., Experimental Study of Planetary Reduction Gears. "Vestnik mashinostroeniya", 1976, No. 3, pp. 57-62

18. Kozhevnikov, S. N., Basis of Structural Synthesis of Mechanisms. Kiev, Naukova Dumka Publishers, 1979 (in Russian).

19. Kozhevnikov, S. N., Esipenko, J. I., Raskin, J. M., Mechanisms. Moscow, Mashinostroenie Publishers, 1976 (in Russian).

20. Kudin, V. V., To the Problem of Investigating Self-Aligning Motion of

Members of Quasi-Planar Leverages. "Teoriya mechanismov", 1973, Vol. 6, pp. 15-19 (in Russian).

21. Matveev, V. V. On the Problem of Design of Toothed Mechanisms Without Passive Constraints. "Vestnik mashinostroeniya", 1966, No. 10, pp. 5-7

22. Vavilov, V. V. et al., Modernization of Bridge Cranes. "Vestnik mashinostroeniya", 1969, No. 3 (in Russian).

23. Munteano, On Four-Member Mechanisms Without Passive Constraints, as Understood by Reshetov. "Bulletin of Yassy Polytechnical Institute", 1950, No. 4, pp. 31—42 (in Russian).

24. Odinokov, Y. G., Airplane Strength Analysis. Moscow, Mashinostroenie Publishers, 1973, pp. 325-327 (in Russian).

25. Ozol, O. G., On New Structural Formula "Izvestiya Vyshikh Uchebnykh Zavedeni", 1964, No. 4, pp. 49—58 (in Russian).

26. Pavlova, L. A., Graph Method in Structural Analysis of Three-Dimensional Mechanisms. Ufa, "Technologiya aviastroeniya", 1976, Vol. 1, pp. 182-190 (in Russian).

27. Planetary Gearings Edited by Kudryavtsev, V. N., Kudryavtsev Yu. N. Reference book, Leningrad, Mashinostroenie Publishers, 1977

28. Pozdnyakov, O. I., Mikhiev, V. P., Enhancing Current-Collection by Using Carriages with Increased Free Travel. Omsk, Western Siberia Publishers, 1960 (in Russian).

29. Popov, A. F., Fundamentals of Loop Structure of Kinematic Chains and Their Application to Determination of Freedoms. "Scientific notes of Lvov Polytechnical Institute", 1956, Vol. XLIII, Engineering Series, No. 8, pp. 158-166 (in Russian).

30. Reshetov, L. N., Legend on Control Levers of Feed and Speed Gear-Boxes. "Stanki i instrumenty", 1947, No. 3, pp. 5-7 (in Russian).

31. Reshetov, L. N., Designing Contacts of Control Circuitry for Heavy-Duty Operation. "Vestnik elektropromyshlennosti", 1948, No. 12, pp. 12-16

32. Reshetov, L. N. Designing Rational Mechanisms. "Vestnik mashinostroeniya", 1958, No. 5, pp. 3-10 (in Russian).

33. Reshetov, L. N. Rational Designs of Planetary Mechanisms. "Vestnik mashinostroeniya", 1960, No. 4, pp. 21-23 (in Russian).

34. Reshetov, L. N., Rational Design of Idlers and Satellite Gears. "Vestnik mashinostroeniya", 1964, No. 2, pp. 15-19 (in Russian).

35. Reshetov, L. N., Rational Patterns of Multiple and Closed Mechanisms. "Vestnik mashinostroeniya", 1964, No. 10, pp. 13-17 (in Russian).

36. Reshetov, L. N., Determining Mobilities and Redundant Constraints in Mechanisms. "Izvestiya Vysshikh Uchebnykh Zavedeni", Engineering Series, 1971, No. 8, 71-79 (in Russian).

37. Reshetov, L. N., Solomin, V. V., Designing Lift Spring Mechanism of Railway Vehicle Current Collectors. "Izvestiya Vysshikh Uchebnykh Zavedeni". Engineering Series, 1969, No. 5, pp. 15-20 (in Russian).

38. Reshetov, L. N., Pavlova, L. A., To Problem of Eliminating Redundant Constraints in Variable-Area Nozzle Control Mechanism. "Works of MVTU, Theory of mechanisms", 1975, Vol. 7, No. 227, pp. 33-37 (in Russian).

39. Reshetov, L. N., Shatsillo, A. A., On Terminology and Classification of Traction Drive of Electric Rail Vehicles and Locomotives. "Works of VELNII. Electric locomotive engineering", Novocherkassk, 1976, Vol. 16, pp. 145-149

40. Reshetov, L. N., Budyka, E. Y., To Problem of Determining Redundant Constraints in Mechanisms. "Izvestiya Vysshikh Uchebnykh Zavedeni", Engineering Series, 1976, No. 3, pp. 68-70 (in Russian).

41. Reshetov, L. N., Budyka, E. Y., Interaction of Constraints With Serial Connection of Kinematic Pairs. "Izvestiya Vysshikh Uchebnykh Zavedeni", Engineering Series, 1976, No. 4, pp. 56-59 (in Russian).

42. Reshetov, L. N., Gulida, I. I., Automatic Equalization of Load of Bearing Supports of Rotary Furnaces. "Mekhanizatsiya i avtomatizatsiya proizvodstva", 1976, No. 6, pp. 18-20 (in Russian).

43. Solomin, V. V., New Method of Selecting Rational Structural Designs of Mechanisms. "Izvestiya Vysshikh Uchebnykh Zavedeni", Engineering Series, 1967, No. 8, pp. 17-21 (in Russian).

44. Solomin, V. V., Synthesis of Guiding Mechanism of Electric Rail Vehicle Current Collectors. "Izvestiya Vysshikh Uchebnykh Zavedeni", Engineering Series, 1968, No. 11, pp. 5-7 (in Russian).

45. Statically Determinate Bridge Cranes, Catalog-Reference Book, Dnyepropetrovsk, Publishing Office of Aleksandriisk Load-Handling Machinery Works, 1969 (in Russian).

46. Fakhriev, M. A., Kinematics of Universal Joint with Spherical Pairs. "Izvestiya Vysshikh Uchebnykh Zavedeni", Engineering Series, 1966, No. 1, pp. 16-21 (in Russian).

47. Chernova, G. A., Structural Investigation of One Planetary Reduction Gear. "Izvestiya Vysshikh Uchebnykh Zavedeni", Engineering Series, 1978, No. 2, pp. 74-81 (in Russian).

48. Shamaidenko, N. E., On Using Kinematic Connections Instead of Kinematic Pairs at Rational Designing of Mechanisms. "Izvestiya Vysshikh Uchebnykh Zavedeni", Engineering Series, 1964, No. 6, pp. 26-31 (in Russian).

49. Shamaidenko, N. E., Experience of Plotting a Diagram of Formation of Mechanisms. "Works of VZMI", Research in Dynamics of mechanisms and machinery sets, 1969, Vol. IX, pp. 194-212 (in Russian).

50. Shatkus, D. I., On Rational Structures of Planetary Mechanisms. "Vestnik mashinostroitelya", 1968, No. 11, pp. 25-26 (in Russian).

51. Shatsillo, A. A., Traction Drives of Electric Rail Vehicles. Moscow, Transzheldorizdat Publishers, 1961 (in Russian).

52. Shulzhenko, M. N., Airplane Designs. Moscow, Mashinostroenie, 1971.

53. Boiko, L. S. et al. Experimental Studies of Types of Planetary Reduction Gears and Geared Motors; in book "Design and Production of Planetary Gearings". Alma-Ata, Publishing Office of Kazakh University, 1974, September, pp. 228-234 (in Russian).

54. "R9P Electric Train", Service Manual by Riga Rail Vehicle Engineering Works. Moscow, Transport Publishers, 1969, pp. 135-137 (in Russian).

55. Yakovlev, A. I., Design and Analysis of Electric Motor-Wheels. Moscow, Mashinostroenie Publishers, 1970 (in Russian).

56. Arnaudov, K., Sofia, Uber einige Crundlagen des Last ausgleiches bei Planetengetrieben. "Maschienenbau Technik", 1963, No. 12, H. 8, pp. 58-62.

57. Fritsch, F., Wien, Das Zwillings getriebe eine Neukonstruktion auf den Gebiet der Planetengetriebe. "Osterreichishe Ingenier Zeitschrift", 1960, No. 3, H. 3, pp. 11-17.

58. Fritsch, F., Wien, Planetengetriebe. "Osterreichische Ingenier Zeitschrift", 1960, H. 11, s. 73.

59. Göttinger, I., Berechnung der Seitenfestigkeit eines Scherenstromabnehnur. "Elektrotechnik und Maschinenbau", 1950, No. 4.

60. Shatkus, D. I., Leistungfähige Planetengetriebe. "Konstruktion", 1970, No. 22, H. 11, pp. 37-47.

# INDEX


**Air pads**
in equalizing device of roller supports, 478
Assur's structural groups, 145-149

**Bearings**
as kinematic pairs, 27
in grain harvesters, 302
of gears, 302-303
resistance to self-alignment, 79
Bogies, 506-530
Brakes
aircraft, 488-489
automotive vehicles, 479-480
dump trucks, 481-482
railway vehicles, 483, 494
self-boosting, 487-494
Bridges
arch, 497-498
bascule, 503
Herber, 496
suspension, 498-502
swing, 502
vertical-lift, 503
Wichert, 497

**Cam-and-follower** mechanisms, 275-278
Centrifugal governors, 163-170
Connecting rods in car engines, 132-133
Connections
flexible, 28
kinematic
electric and hydraulic, 38
in electric locomotives, 42-47
Counterweights
lifts, 460
vertical-lift bridges, 504
Cranes
gantry, 309
portal, 448-454
slewing gear in, 310-314
undercarriages of, 443-448

**Differential gear**, 324-326

**Equalizing mechanisms** in
gantry cranes, 309
motor vehicle differential gear, 325
multisatellite mechanisms, 379-382
planetary gearings, 355
planetary reduction gears, 387, 401
roller supports of rotary bodies, 470-477
toothed gearings, 304
variable-speed drives, 334
vertical-lift bridges, 504-506
wheel-motors, 405
Escalator drives, 433
Excavators
bucket-wheel, 302
gearing in, 309

**Flash tanks**, 144

**Gas turbine engines**
securing with spatial multiarm groups, 182
Gate valves, 172-173
Geared motors
in slewing mechanisms of cranes, 311
planetary reduction gears in, 396
Gears (*see also* Reduction gears)
bascule bridges, 503
bevel, 324-328
bucket-wheel excavator, 302
grain harvester, 302
load-handling machine, 309-311
self-aligning, in wheel-motors, 495-496
side gearings of tractor, 287-288
slewing mechanisms of crane, 311
spur, 284
Gimbals
general, 360
strain wave gearing, 426

**Handles**
securing, 91
Hooke joint (*see also* Universal joint), 205-222
connection mechanisms of planetary gearings, 353
electric locomotive traction drives, 217-218, 316-321
mixers, 219-222
rolling mills, 209
rope drum drives, 434
wobble plate mechanisms of helicopters, 197
Hydraulic mechanisms
as kinematic connections, 38
in equalizing devices of roller supports, 473-478

**Idlers**, 290-308
traction drives, 316
transmissions of automotive vehicles, 336

**Kinematic pairs**,
cylindrical, mounting of, 130
defined, 20-32

**Links**
flexible, 28
passive, 61
rigid, 28
Loops (in structural analysis), 51

**Oldham coupling**, 139
as Hooke joint, 206
in variable-speed drives, 333

**Planetary gearing**, 304
Pumps
aircraft systems, 187

**Reduction gears** (*see also* Gears, Teeth), 286, 303
cylindrical-bevel, 327-330
geared motor, 396
high-duty dump trucks, 396-397
planetary, 365-373, 387-394
excavator, 391-392
grain harvester, 367
rolling mills, 366
traction drives, 316-324
tractors, 398
wheel-motors, 401-410
winches, 434
with split second stage, 401, 404, 405, 431
Redundant constraints in
aircraft engines, 143
attachment of aircraft engines, 183
bevel gearings, 324-328
brakes, 479-475
bridges, 495-506
cam-and-follower mechanisms, 275-278
centrifugal governors, 163-170
compressors, 108
control circuitry, 280-281
crane slewing gears, 310-314
current collectors, 231-275
cylindrical-bevel reduction gears, 327-330
defined, 9
in diesels, 106
flush tanks, 144
friction variable-speed drives, 331-334
gate valves, 172-173
grabs, 438
guideways of machine tools and instruments, 109
gyration crushers, 199-205
harmonic gearings, 423-430
insulators of contact wire systems, 269-273
lift valves, 172
locomotive drives and suspensions, 222-231
locomotive transmissions, 137
multispindle drilling heads, 138
oil pumps, 143
paddle-wheel ships, 96
pillars of cranes and movable conveyers, 441-442
piston-type machines, 95
portal cranes, 448-454
power contacts of electric apparatus, 278-279
pumps, 188-192
rheostat controllers, 275-277

roller supports of rotating bodies, 468-479
rope drum drives, 433-435
screw hoists, 116
sheep steering, 143
steam boilers, 12
swinging-disk valves, 170-171
suspensions of lift cages, 455-465
toothed gearings, general, 282-290
undercarriages of cranes, 443-448
undercarriages of load-handling mechanisms, 439-441
wobble plate mechanisms of helicopters, 192-198
work tables of machine tools, 103
Resistance to self-alignment, defined, 68

Schtekicht planetary reduction gear, 368-369
with herringbone teeth, 370
Screw hoists, 116
Self-aligning planar structural groups (SAPS), 157-163
in planing machines, 161
Stephenson link gear, 155, 161
Structural blocks (for self-alignment of planetary mechanisms), 411-423
Structural diagrams
planar, 34
spherical, 35
Structural formula
Malyshev's, 17
non-planar, 65
Ozol's, 18
Somov's, 19
Supports for rotary motion, 97

**Teeth**
arch-shaped, 285, 310, 334, 340
barrel-shaped, 283
in planetary reduction gears, 370
herringbone, 289
in planetary reduction gears, 370-371
involute, 291, 294, 298
Traction drives
classification, 314-316
high-speed, 322-324
rational design of reduction gear in, 316-322
Traction gearing
electric locomotives, 339-341
ships, 339
Traction motors
suspension of (in electric locomotives), 91
Transmissions
automotive vehicles, 334-339
electric locomotives, 297, 300, 304
Trakt's mechanism, 208

**Universal joint** (*see also* Hooke joint)
double, 367-370
in planetary reduction gears, 378, 393, 396
multirow, 378
single-row, 361, 366
toothed, 355-359
with helical teeth, 373

Variable-speed drives
friction-type, 331-334

**Wheel-motors**, 401-411
Wobble plate mechanisms in helicopters, 192-198

*Printed in the Union of Soviet Socialist Republics*